Nuclei at HERA and Heavy Ion Physics

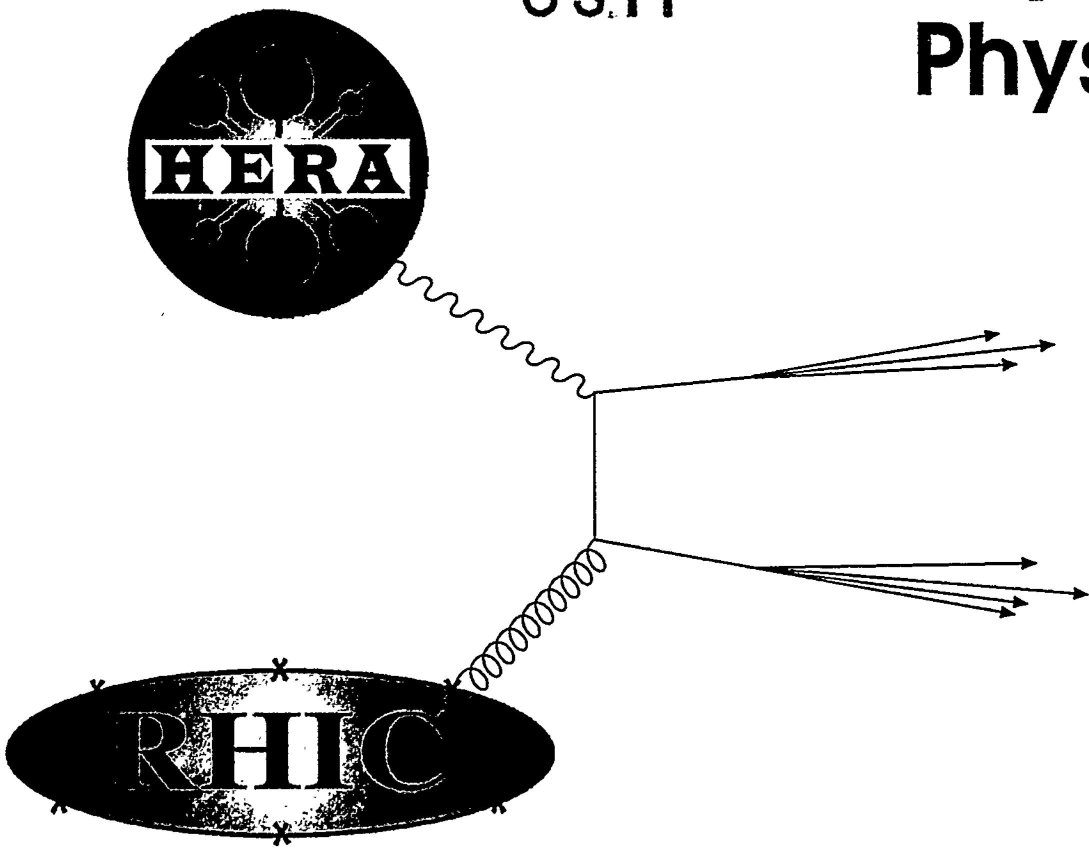

Brookhaven National Laboratory
17-18 November, 1995

Organizers:

Sean Gavin
BNL

Mark Strikman
Penn State

Transparencies shown at a Workshop held November 17–18, 1995 at Brookhaven National Laboratory

sponsored by
the Physics Department, BNL

This manuscript has been authored under contract number DE-AC02-76CH00016 with the U.S. Department of Energy. Accordingly, the U.S. Government retains a non-exclusive, royalty-free license to publish or reproduce the published form of this contribution, or allow others to do so, for U.S. Government purposes.

CONTENTS

HERA: The Present

Steven Ritz
Columbia University

S. RITZ
COLUMBIA U.

HERA: THE PRESENT

Workshop on the future of HERA
Nuclei at HERA & Heavy Ion Physics, BNL, 17 November 1993

- Caveats
- HERA in context, some kinematics, the machine
- Detectors: H1 & ZEUS
- Tools
- Some results:
  - High Q^2 DIS
  - F_2
  - Related topics: $g(x,Q^2)$, $\sigma_{tot}(\gamma^* p)$
  - The low Q^2 frontier
  - Large Rapidity Gap events (more kinematics)
  - F_2^D + related topics
  - LRG events in photoproduction : gluon content? gaps between jets
  - Exclusive vector meson production
  - The LPS
- Other topics
- Summary (+ questions)

References: http://zow00.desy.de:8000/ ZEUS
http://dice2.desy.de/ H1
+ references (links) therein

HERA IN CONTEXT

i) • compelling sequence of ep experiments

Hofstadter et al (ca 1956)

188 MeV e^- on protons → rms charge radius 0.74 ± 0.24 fm

↓

SLAC-MIT (late 1960's)

18 GeV e^- fixed target → charged partons!

• compelling sequence of other lepton-nucleon experiments

νN, μN, 2 neutrinos, neutral currents, ...

... all at $Q^2 \lesssim 300\,\mathrm{GeV}^2$

ii) unique opportunity

• early period of hadron physics: resonances, selection rules, diffractive scattering

Theoretical tools: vector dominance, Regge

• stunning results from earliest DIS experiments

→ Theory: Perturbative QCD successful at describing phenomena at large Q^2

→ physics partitioned into pert. and non-pert. domains
earlier phenomenology largely set aside

★ HERA: phenomena at low and high Q^2, perturbative and non-perturbative may be studied together in a single, clean, unique environment
(already some remarkable results...)

A VIEW OF WHAT HAPPENS IN AN ep COLLISION:

Kinematics: ("t-channel")

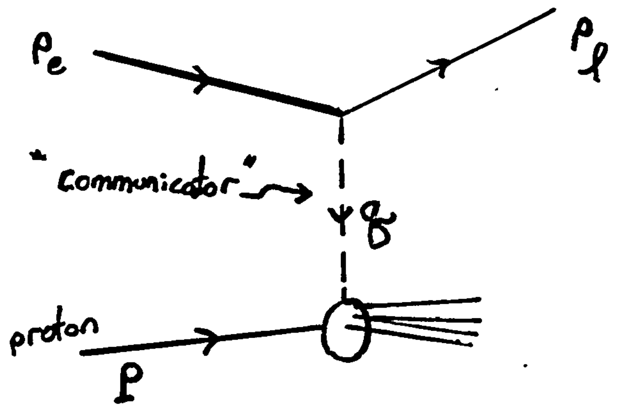

available cm energy:

$$s = (P + p_e)^2 \simeq 4E_e E_p$$

$$E_{cm} = \sqrt{s} : \left.\begin{array}{l} E_e = 30\,\text{GeV} \\ E_p = 820\,\text{GeV} \end{array}\right\} \Rightarrow \sqrt{s} = 314\,\text{GeV}$$

define variables:

1) $Q^2 \equiv -q^2 = -(p_e - p_\ell)^2$ (4-momentum transfer)^2

2) $x \equiv \dfrac{Q^2}{2P\cdot q}$ $\simeq$ fraction of proton momentum carried by struck constituent

"Bjorken x"

to see:

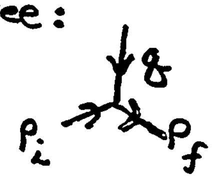

set $p_i = x\cdot(E_p, 0, 0, |\vec{P}_p|)$ and calculate

$$0 = p_f^2 = (p_i + q)^2$$

Two variables define kinematics; an alternative variable is

$$y \equiv \frac{P\cdot q}{P\cdot p_e} = \frac{Q^2}{xs}$$

Another kinematic variable: y

$$y = \frac{P\cdot q}{P\cdot p_e}$$

1) must be expressible in terms of x, Q^2

denominator: $P\cdot p_e \approx s/2$ $\quad [s = (P+p_e)^2]$

numerator: $P\cdot q \approx \frac{Q^2}{2x}$

$$\Rightarrow y = \frac{2Q^2}{2xs} = \frac{Q^2}{sx} \quad \text{or} \quad \boxed{Q^2 = sxy}$$

2) look in e-q c.m. system $(E = E_e')$

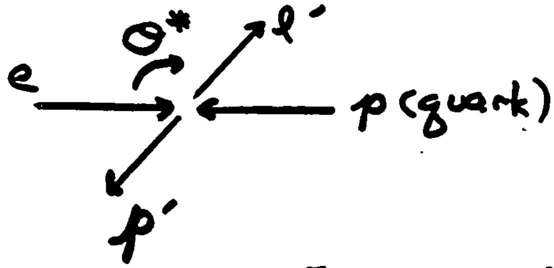

$$y = \frac{1+\cos\theta^*}{2}$$

[show this: $P\cdot q = P\cdot(p_e - p_l')$
$\approx E_p E_e(1+\cos\theta^*)$]

so: x chooses c.m. frame
y gives decay angle (scattering) in that frame

3) fixed target frame:

$P = (m_p, 0, 0, 0)$, $s = 2m_p E_e$

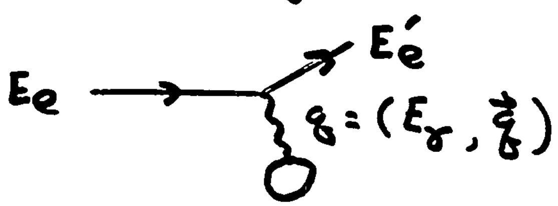

Energy transfer to proton:

$$\nu = \frac{q\cdot P}{m_p} = \frac{E_\gamma m_p}{m_p} = E_\gamma \checkmark$$

$$\nu_{max}: \frac{s}{2m_p} \quad (= E_e)$$

HERA : $\nu_{max} = 50$ TeV !!

ν is related to y:

$$\frac{\nu}{\nu_{max}} = \frac{q \cdot P}{m_p}\left[\frac{2m_p}{s}\right] = \frac{2q \cdot P}{s} = \frac{q \cdot P}{P \cdot p_e} = y$$

$\therefore$ y gives fraction of max possible energy transfer

x: $[0, 1]$

y: $[0, 1]$

Q^2: $[0, s]$

ep Collider kinematics

(NC case)

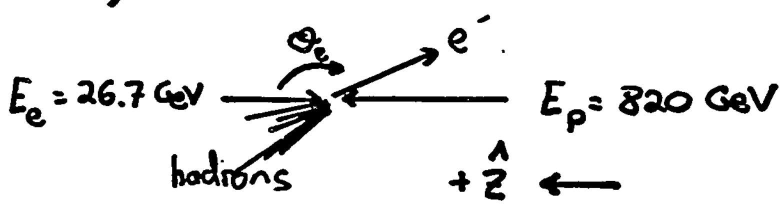

$$s = 4E_eE_p$$

$$Q^2 = sxy$$

$$W^2 = sy(1-x) + m_p^2 \simeq sy$$

(W is γ^*p c.m. energy)

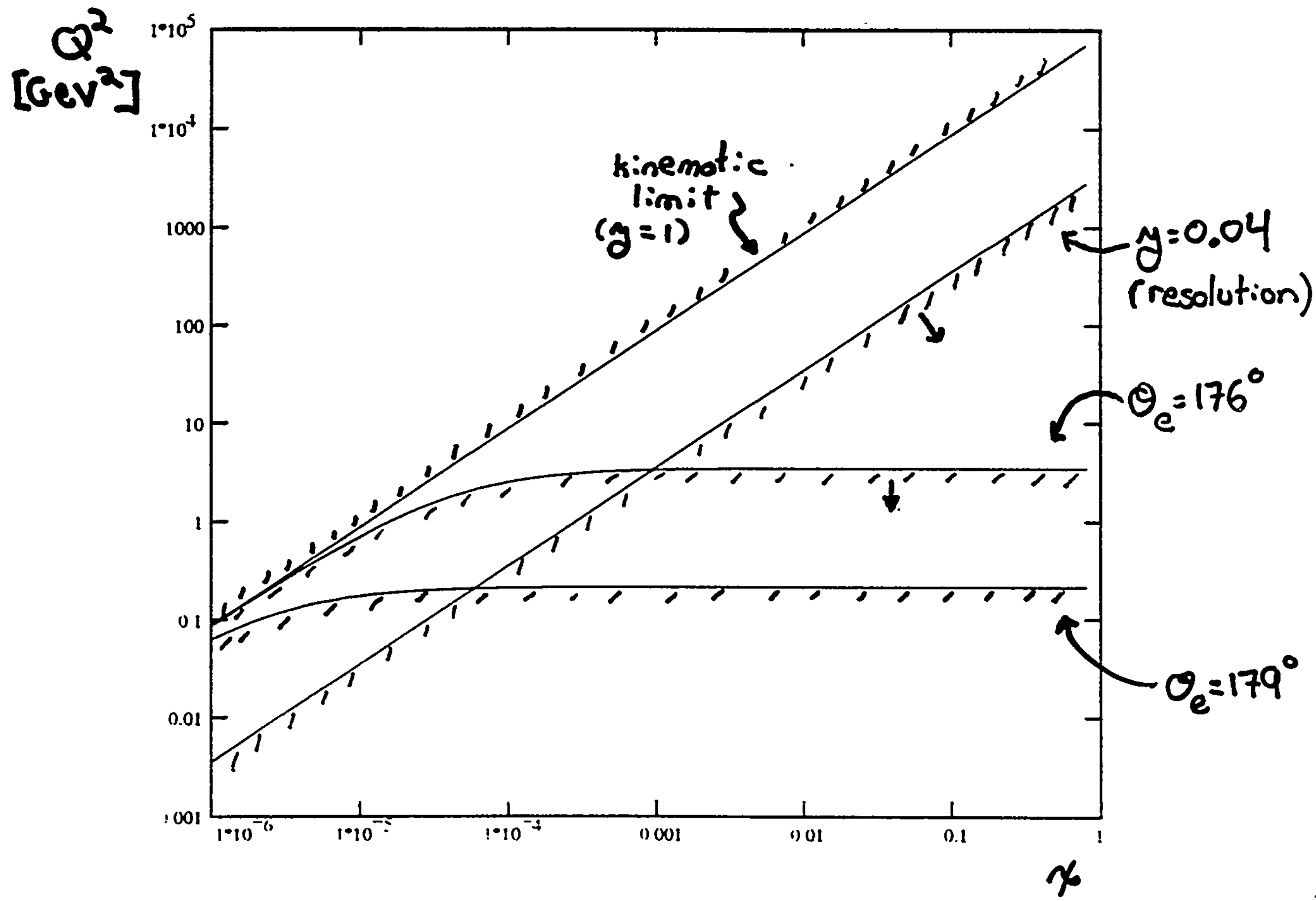

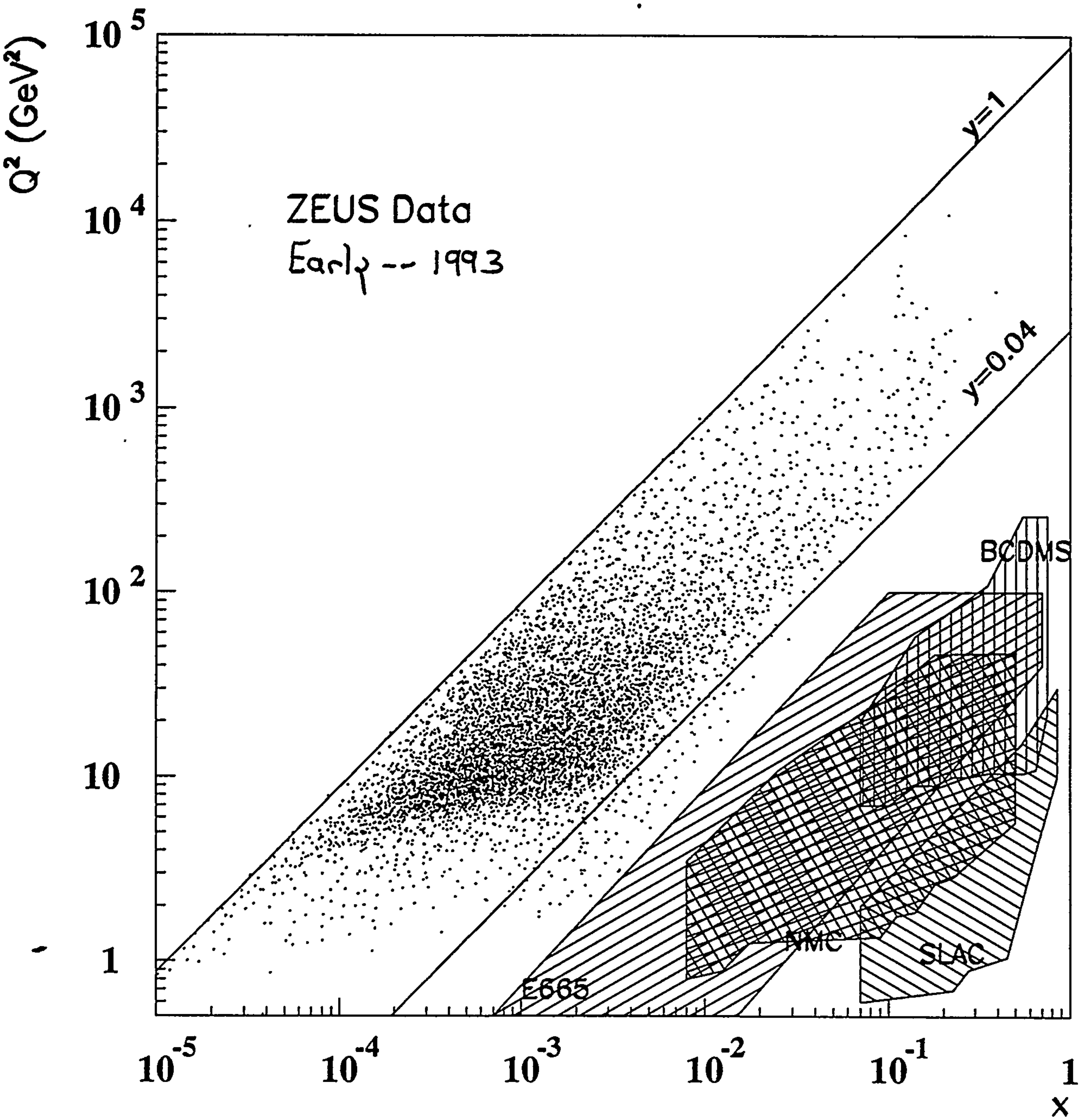

Q² (GeV²)
ZEUS Data
Early -- 1993
y=1
y=0.04
BCDMS
NMC
SLAC
E665
10 ⁵
10 ⁴
10 ³
10 ²
10
1
10⁻⁵
10⁻⁴
10⁻³
10⁻²
10⁻¹
1
x

KINEMATIC PEAK

Contours of constant electron energy

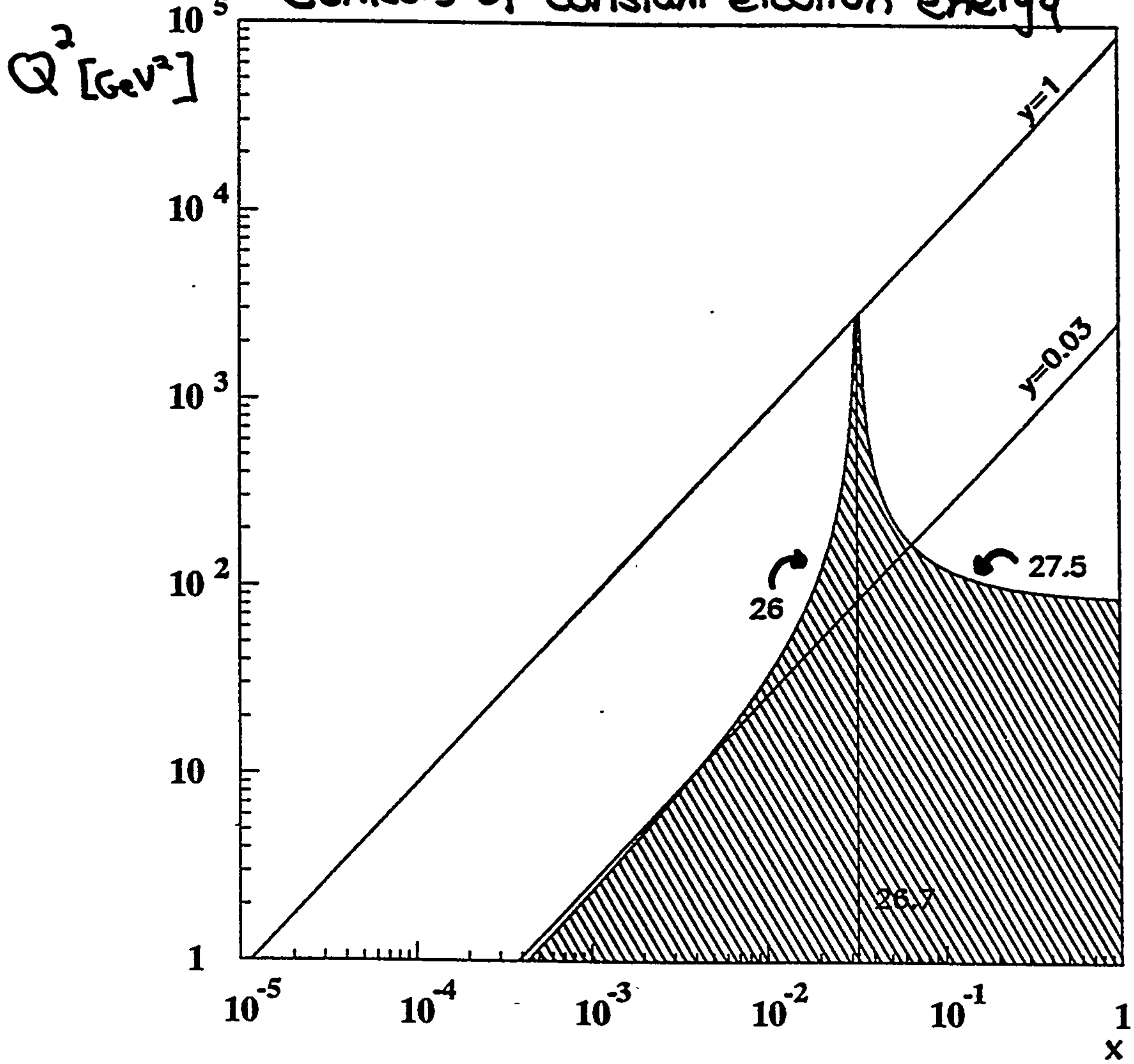

useful for calibration/checks

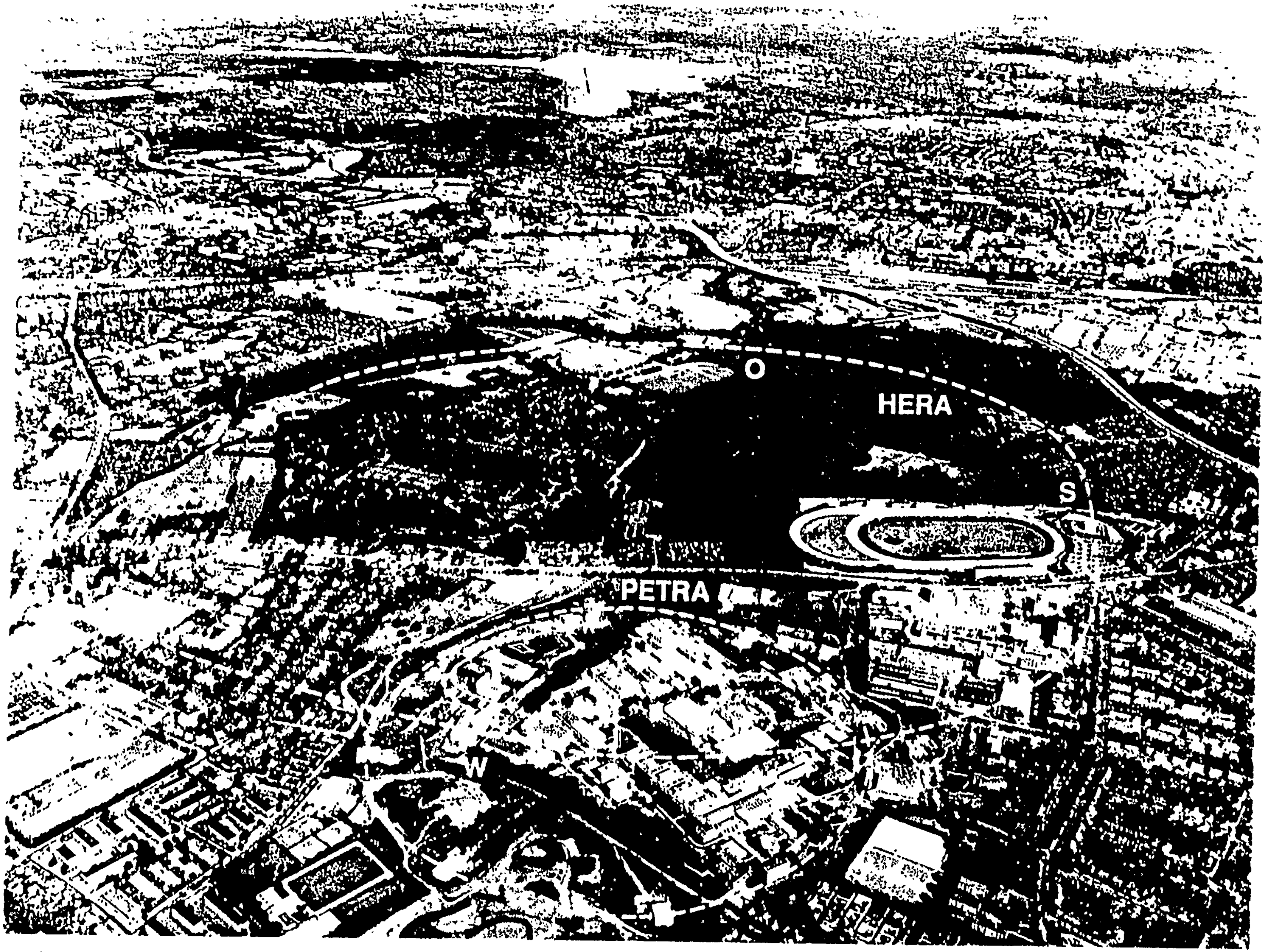
O
HERA
S
PETRA
W

HERA

Hadron - Elektron Ring Anlage

Historic Highlights

April 84 Construction starts

April 91 first protons stored @ 40 GeV

Oct 91 1 e bunch (12 GeV) + 1 proton bunch (480 GeV) collide

Nov 91 - March 92 Detectors roll in

May 31, 92 e (26.6 GeV) + p (820 GeV) collisions observed by detectors

"summer run" 1 month $\int \mathcal{L} dt = 2 nb^{-1}$

"fall run" Sept - Nov $\int \mathcal{L} dt = 30 nb^{-1}$

HERA

<u>Design:</u> 210 × 210 e × p bunches
⇒ time between crossings: 96 ns
$I_p = 160$ mA $I_e = 60$ mA
Luminosity 1.5×10^{31} cm$^{-2}\cdot$s^{-1}

<u>1993 operation:</u> 84 × 84 e × p bunches*
+ 10 e pilot + 6 p pilot unpaired bunches
$E_e = 26.7$ GeV $I_e \sim 10$ mA
$E_p = 820$ GeV $I_p \sim 10$ mA
IP $\sigma_z \simeq 20$ cm (proton RF 208 MHz)

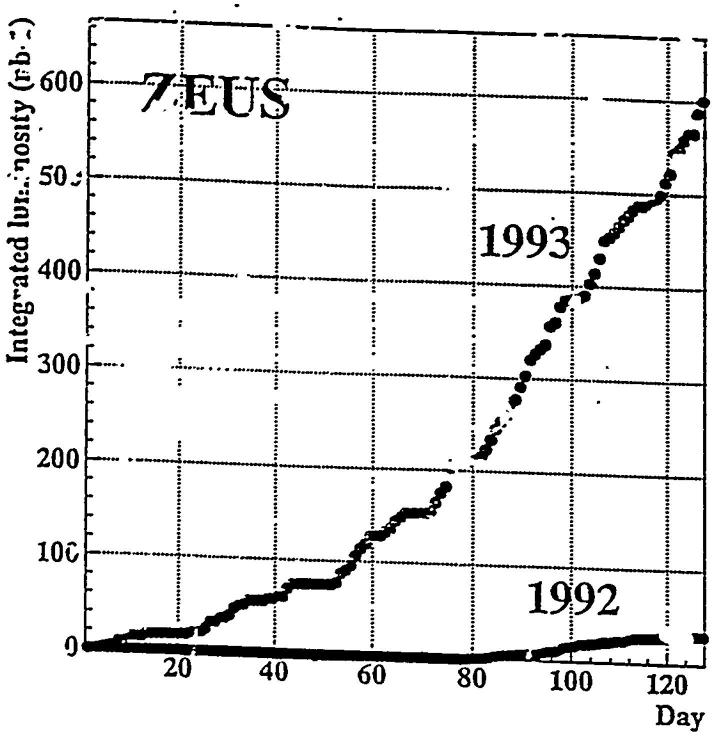

$\int \mathcal{L} dt = 550\,\text{nb}^{-1}$ (usable)

factor 20!

$\int \mathcal{L} dt = 24.7\,\text{nb}^{-1}$

Lum: measured via $ep \to e'p\gamma$

* adjacent bunches 96 ns apart!

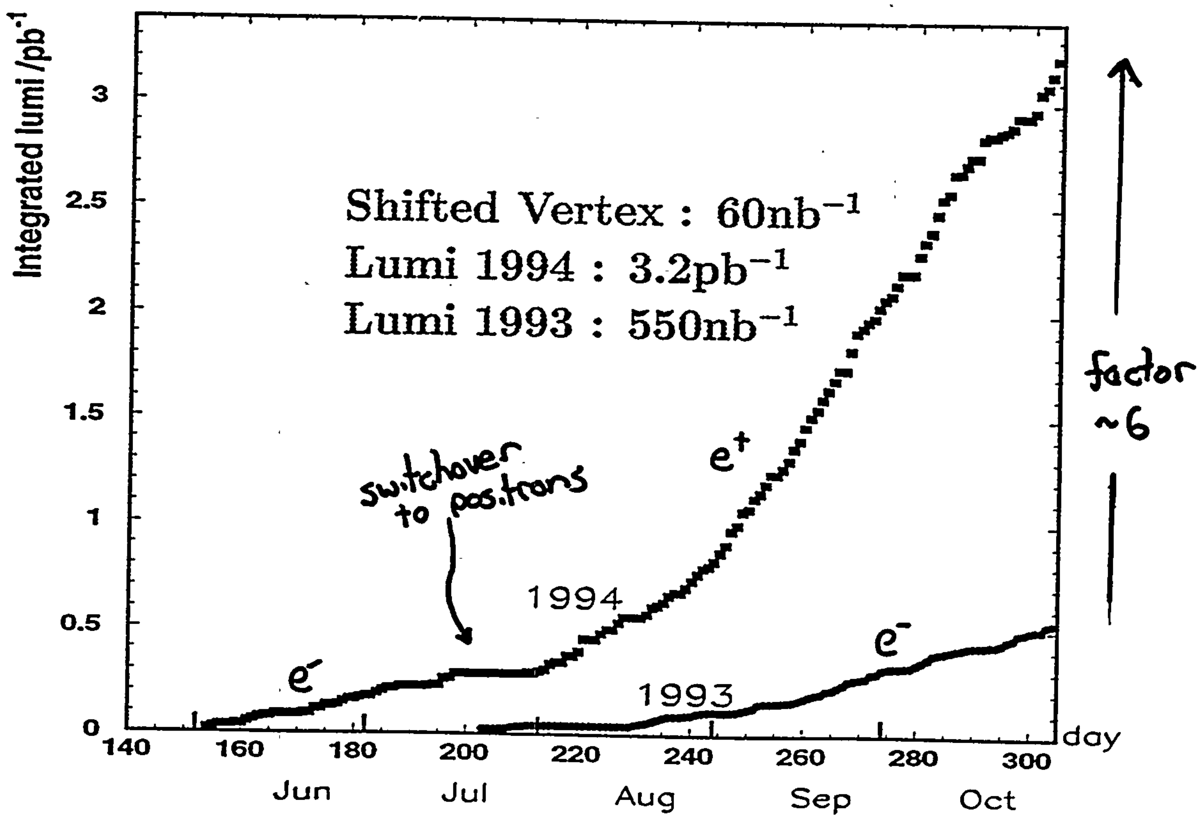

Integrated lumi /pb^{-1}
Shifted Vertex : 60nb^{-1}
Lumi 1994 : 3.2pb^{-1}
Lumi 1993 : 550nb^{-1}
switchover to positrons
1994
1993
e^+
e^-
e^-
factor ~6
day
Jun
Jul
Aug
Sep
Oct

e^- again in '97 ?

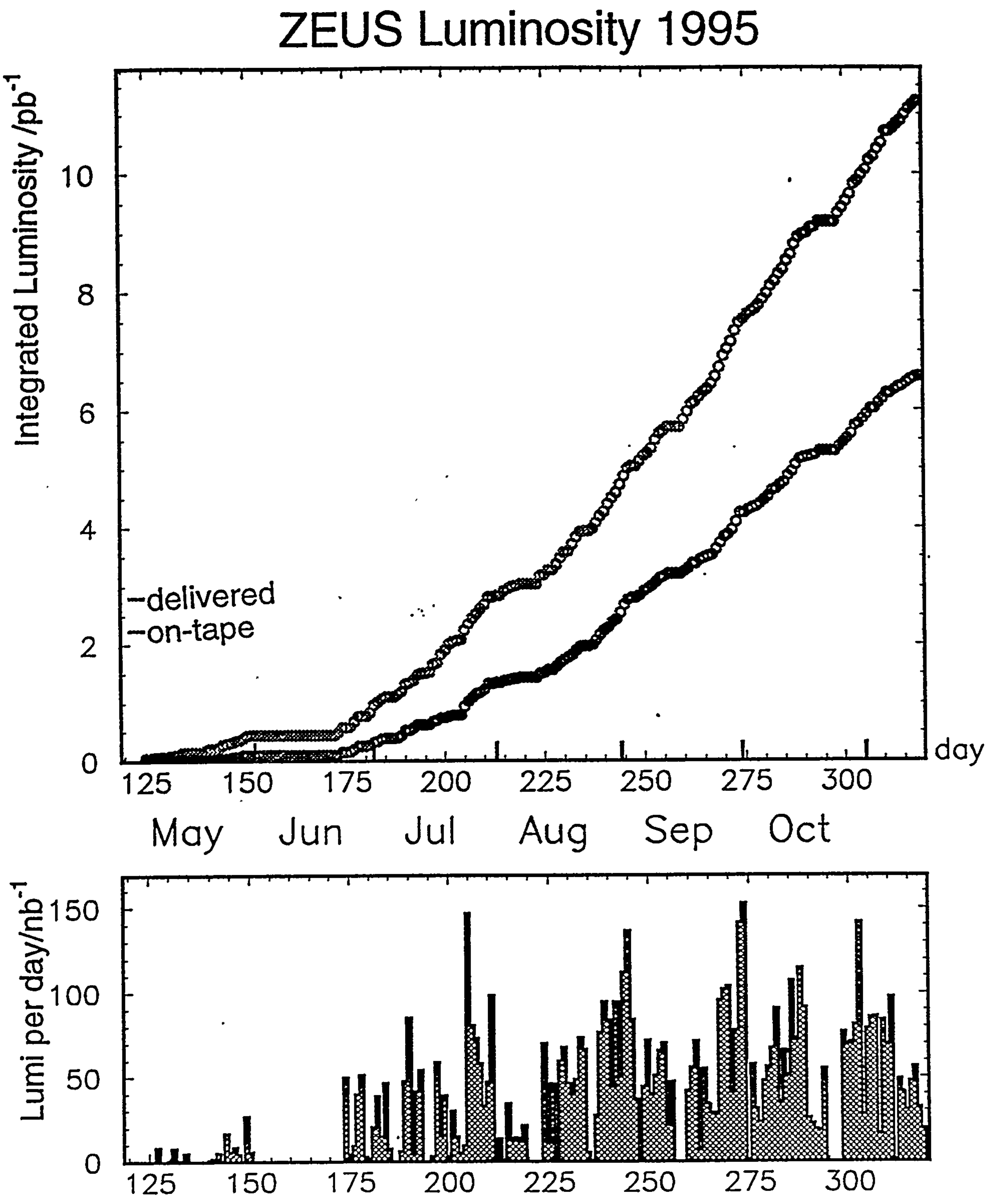

NOTE: YEAR INDICATED ON RESULTS
SIGNIFIES WHEN DATA WERE TAKEN
(AND NOT WHEN RESULTS WERE OBTAINED!)

Photoproduction

$\gamma p \longrightarrow$ anything

How?

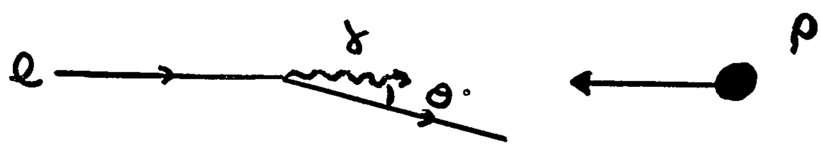

if θ small

$\Rightarrow q^2$ small $\Rightarrow \gamma$ "almost real" $(m_\gamma = 0)$

Rich phenomenology!

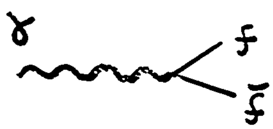

if f is a quark this gets interesting

q^2 small

$\Rightarrow$ a component looks like meson-p scattering

Signature

- may tag e^- in lumi counter $0.2 E_e^{beam} \lesssim E \lesssim 0.8 E_e^{beam}$

  $\Rightarrow \langle Q^2 \rangle \sim 6 \times 10^{-4}\ \mathrm{GeV}^2$

  BUT $W \simeq 200$ GeV!

  γp c.m. energy is huge

  $\hookrightarrow$ great opportunity!

- hadrons in central detector form bkgd to DIS

  (large σ ⊕ fake e^-)

BASIC EVENT TOPOLOGIES

DEEP INELASTIC SCATTERING ("DIS")

Neutral Current (NC) DIS

Charged Current (CC) DIS

"Boson-Gluon Fusion" (BGF)

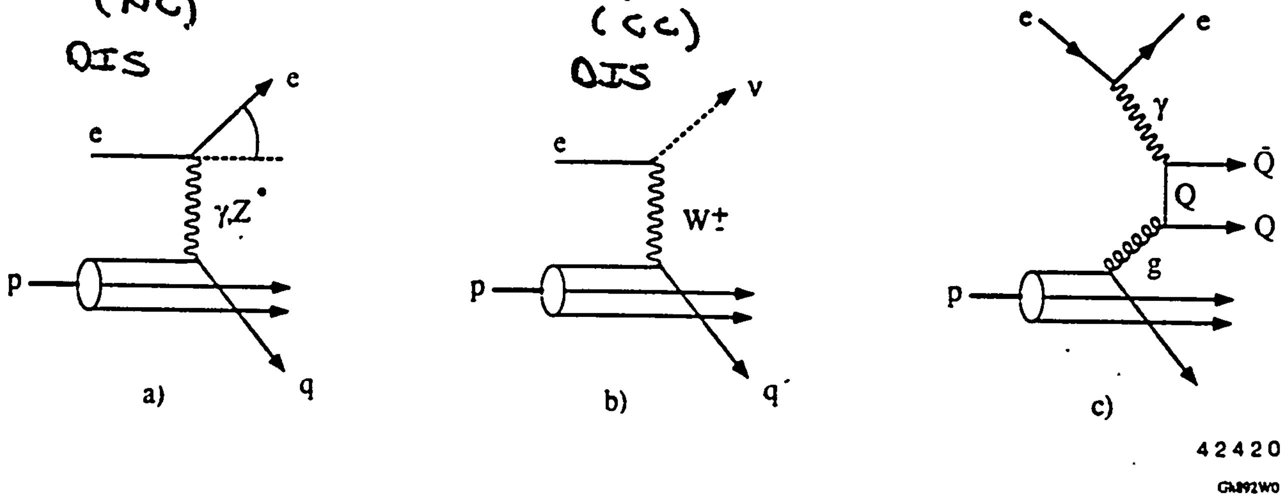

See in detector :

NC : scattered electron (energy E_e', angle Θ_e)
current jet
part of proton remnant (near FCAL beampipe)

CC : current jet
part of proton remnant

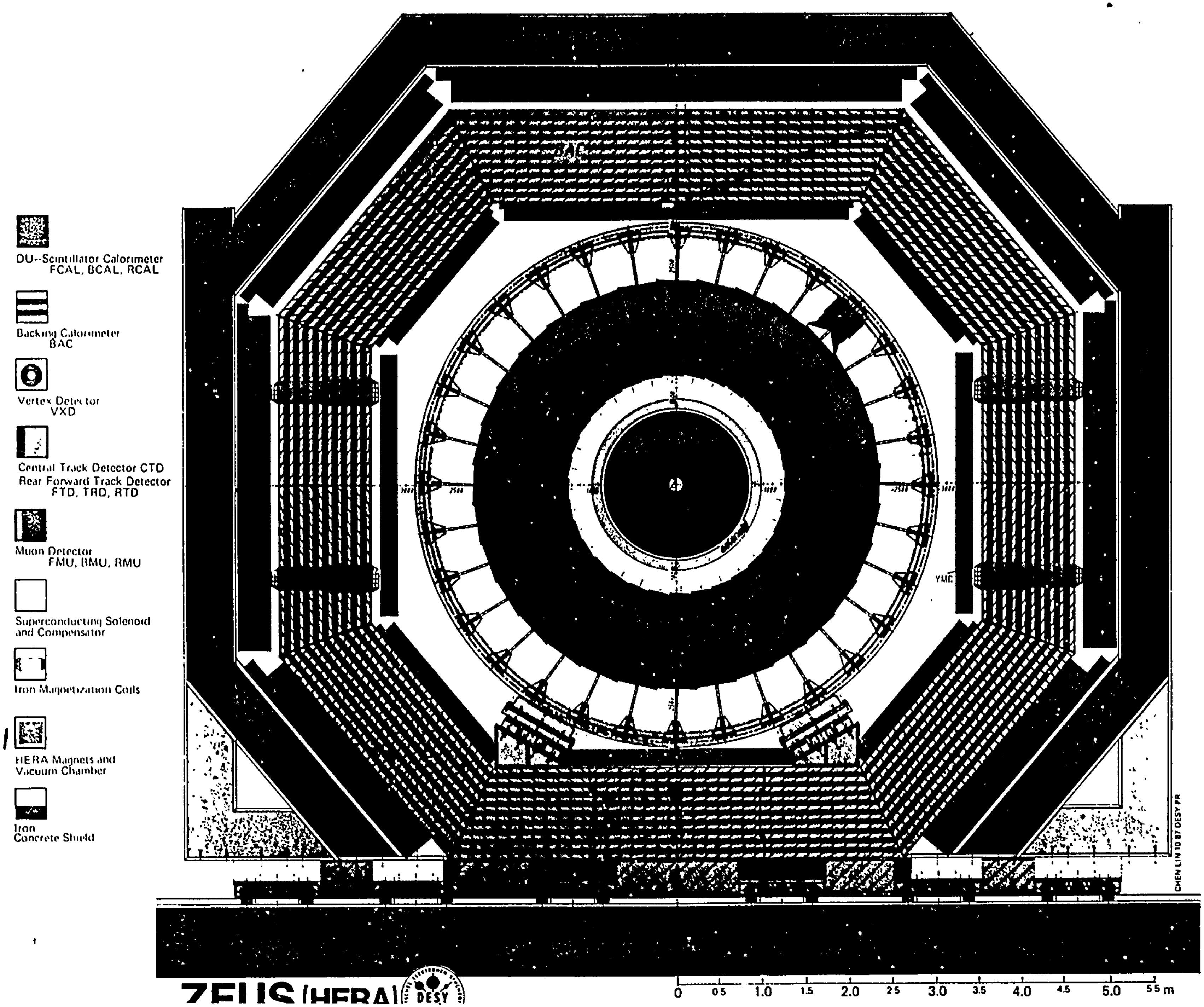
DU--Scintillator Calorimeter
FCAL, BCAL, RCAL
Backing Calorimeter
BAC
Vertex Detector
VXD
Central Track Detector CTD
Rear Forward Track Detector
FTD, TRD, RTD
Muon Detector
FMU, BMU, RMU
Superconducting Solenoid
and Compensator
Iron Magnetization Coils
HERA Magnets and
Vacuum Chamber
Iron
Concrete Shield
YMC
CHEN LIN 10 87 DESY PR
0
0.5
1.0
1.5
2.0
2.5
3.0
3.5
4.0
4.5
5.0
5.5 m
ZEUS (HERA)
DESY

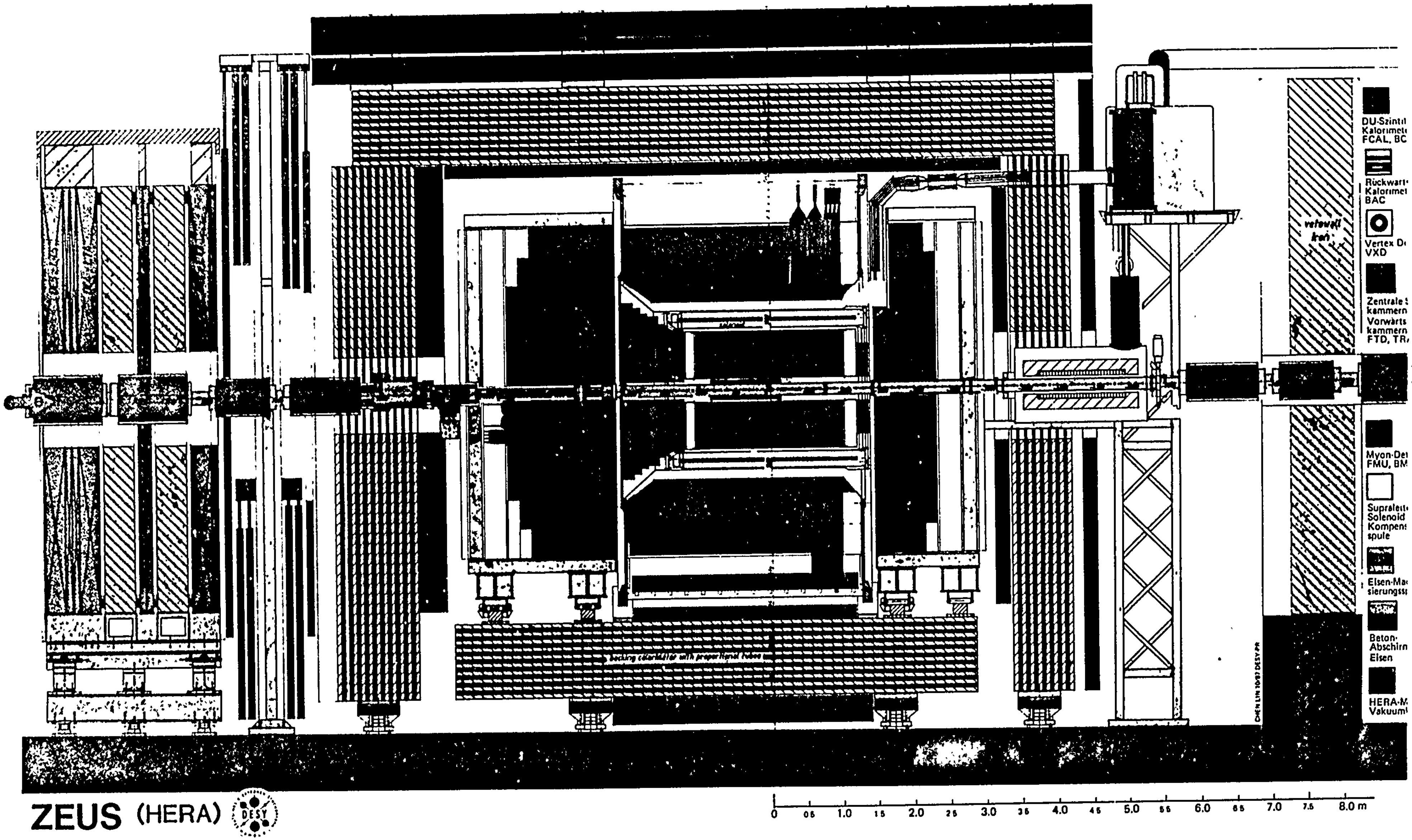

DU-Szintil Kalorimet FCAL, BC
Rückwärt Kalorimet BAC
Vertex D VXD
Zentrale kammern Vorwärts kammern FTD, TR
Myon-De FMU, BM
Supralei Solenoid Kompens spule
Eisen-Ma sierungs
Beton-Abschirn Eisen
HERA-M Vakuum
0 0.5 1.0 1.5 2.0 2.5 3.0 3.5 4.0 4.5 5.0 5.5 6.0 6.5 7.0 7.5 8.0 m
ZEUS (HERA)
DESY

ZEUS

51 institutes, 12 countries

Detector Unique Features

- Uranium-Scint. Calorimeter

Forward: $4.3 > \eta > 1.1$ (FCAL)
Barrel: $1.1 > \eta > -0.75$ (BCAL)
Rear: $-0.75 > \eta > -3.8$ (RCAL)

→ electrons: $\sigma_E / E = \frac{18\%}{\sqrt{E}}$

under testbeam* conditions

→ hadrons: $\sigma_E / E = \frac{35\%}{\sqrt{E}}$

→ timing $\sigma_t < 1\,\text{ns}$ $E > 4.5\,\text{GeV}$

BCAL testbeam at FNAL: E790

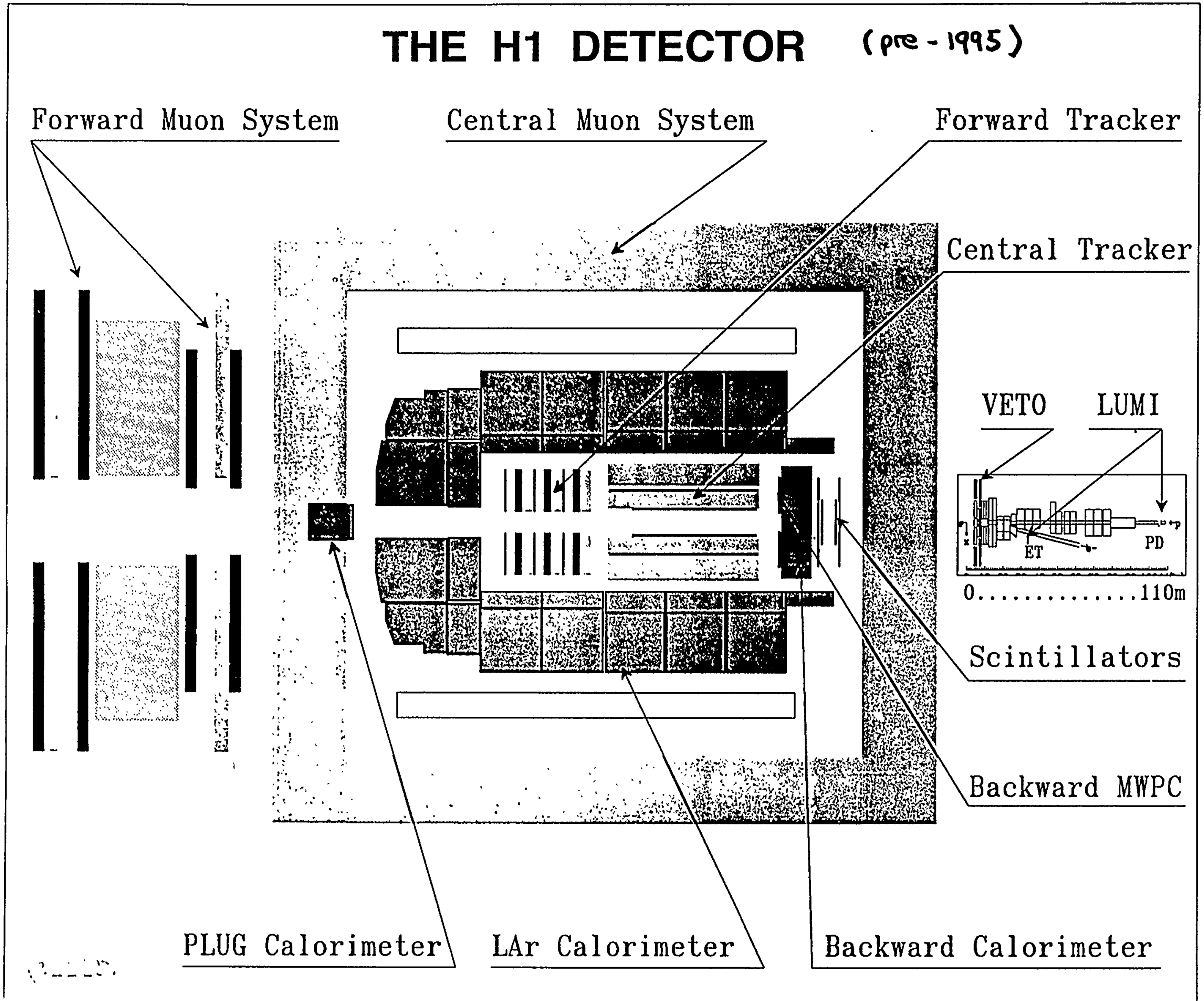

THE H1 DETECTOR (pre - 1995)
Forward Muon System
Central Muon System
Forward Tracker
Central Tracker
VETO
LUMI
ET
PD
0.............110m
Scintillators
Backward MWPC
PLUG Calorimeter
LAr Calorimeter
Backward Calorimeter

H1

32 institutes, 11 countries

Detector Unique Features

- Lead-Scint. Backward Electromagnetic CAL ("BEMC")

  electrons: $\sigma_E/E = \frac{10\%}{\sqrt{E}} \oplus \frac{42\%}{E} \oplus 3\%$ $160^\circ < \theta < 172.5$

- Liquid-Ar EM CAL

  electrons: $\sigma_E/E = \frac{12\%}{\sqrt{E}} \oplus 1\%$

- Liquid Ar Hadron CAL

  hadrons: $\sigma_E/E \simeq \frac{50\%}{\sqrt{E}} \oplus 2\%$ $4^\circ < \theta < 153^\circ$

- Backward Prop. Chamber $155^\circ - 174.5^\circ$

→ Major rear detector upgrade 1995

Run 59416 Event 3357 Run date 24/08/1993 17:04

$Q^2 = 2470\ \mathrm{GeV}^2 \quad x = 0.13 \quad y = 0.22$

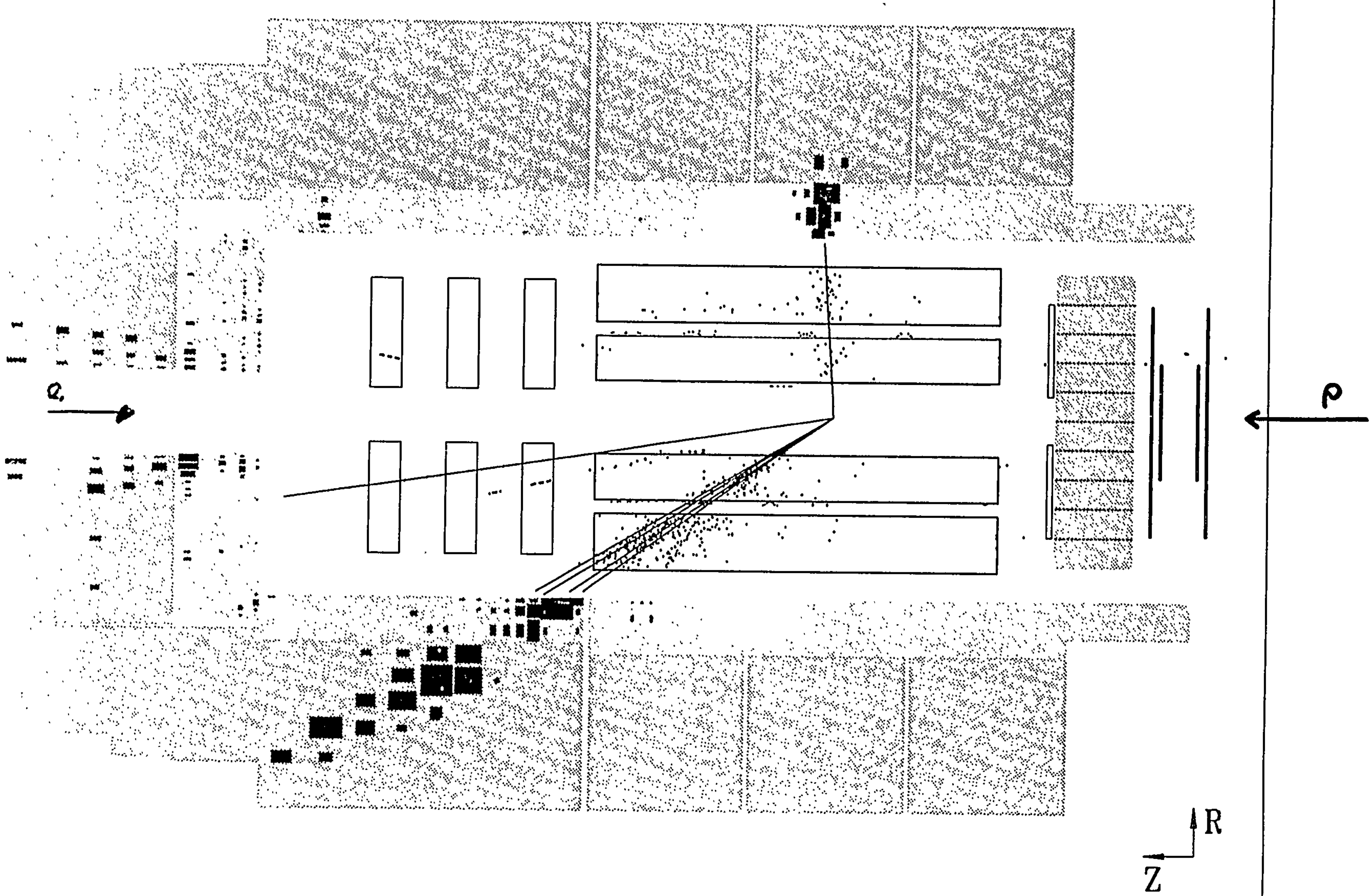

TOOLS

- RECONSTRUCTION METHODS

exploit hermetic detectors, fixed beam energies
NC case: x, Q^2 overconstrained by measurements
$\Rightarrow$ checks

I) Electron variables (Θ_e, E_e')

$$y = 1 - \frac{E_e'}{2E_e}(1-\cos\Theta_e) \qquad Q^2 = 2E_eE_e'(1+\cos\Theta_e)$$

$$x = Q^2/sy$$

- requires good knowledge of electron energy scale
- good at low x (high y) ; poor at high x
- sensitive to radiative corrections

II) Hadrons only $((E-p_z)_h, p_{T_h})$

Jacquet-Blondel (JB) method

$$y = \sum_h \frac{(E-p_z)}{2E_e} \qquad Q^2 = \sum_h \frac{p_T^2}{1-y} \qquad x = Q^2/sy$$

- insensitive to lost hadrons down forward beampipe!

(• necessary for charged-current events)

III) Double Angle Method (DA) (Θ_e, γ)

$$\cos\gamma = \frac{p_{t_h}^2 - (E-p_z)_h^2}{p_{t_h}^2 + (E-p_z)_h^2}$$

γ is angle of struck quark in QPM

- insensitive to energy scale
- better at low y ; worse at high x

IV) Mixed variables (Q_e^2, y_{JB})

$$x = \frac{Q_e^2}{s\, y_{JB}}$$

V) Σ Method

$$y_\Sigma = \frac{(E-P_z)_h}{(E-P_z)_{total}} \qquad Q_\Sigma^2 = \frac{P_{T_e}^2}{1-y_\Sigma}$$

- better at low y

- All methods using hadrons rely solely on energy-momentum conservation. No jet-finding required.

Method	ZEUS	H1
Electron	cross-check	✓
Double-Angle	✓	cross-check
Σ	—	✓

Comparing results from different methods is an important systematic check

High Q^2 Neutral & Charged Currents

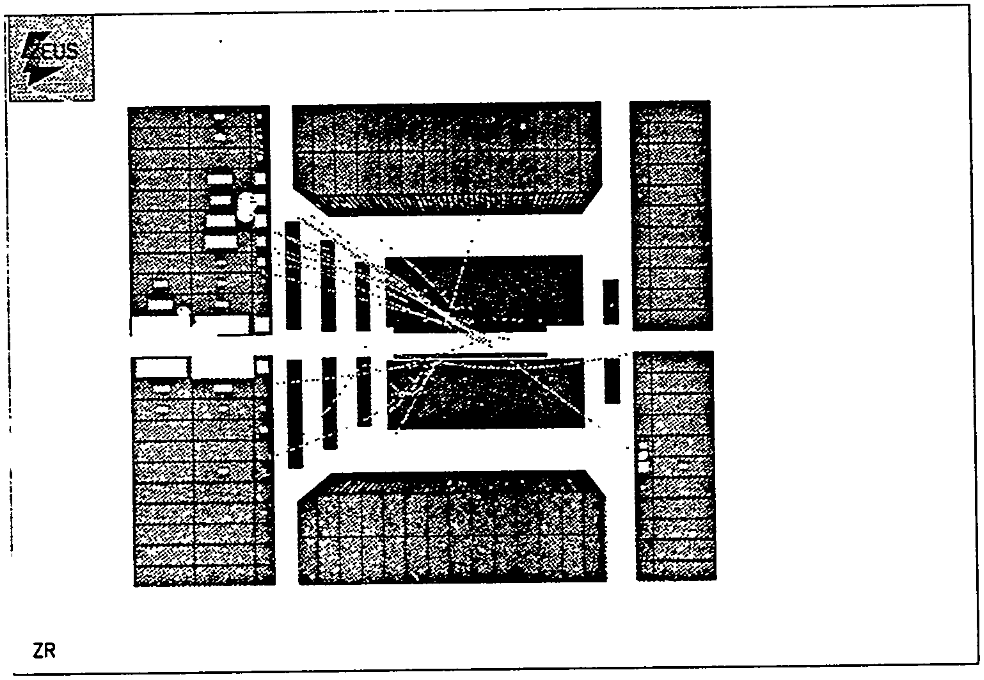

• [illegible]

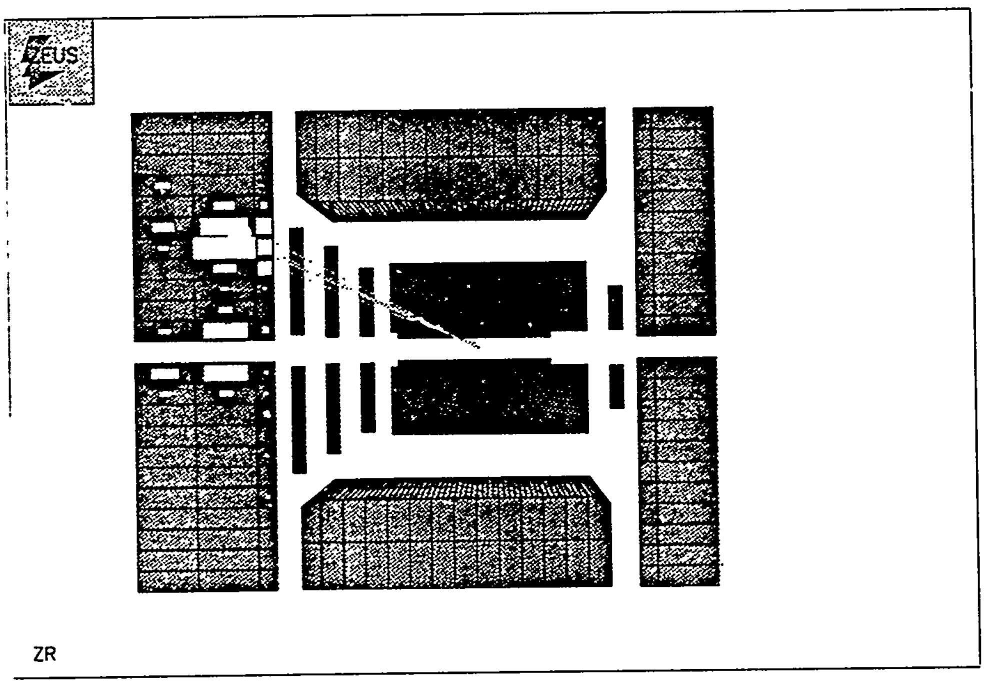

→ isolate NC/CC samples using $\not{p}_t$, electron i.d. from both e^+, e^- beams
1993 data sample: 136 NC events, 23 CC events ($Q^2 > 100$ GeV^2)

HERA High Q^2 DIS Data

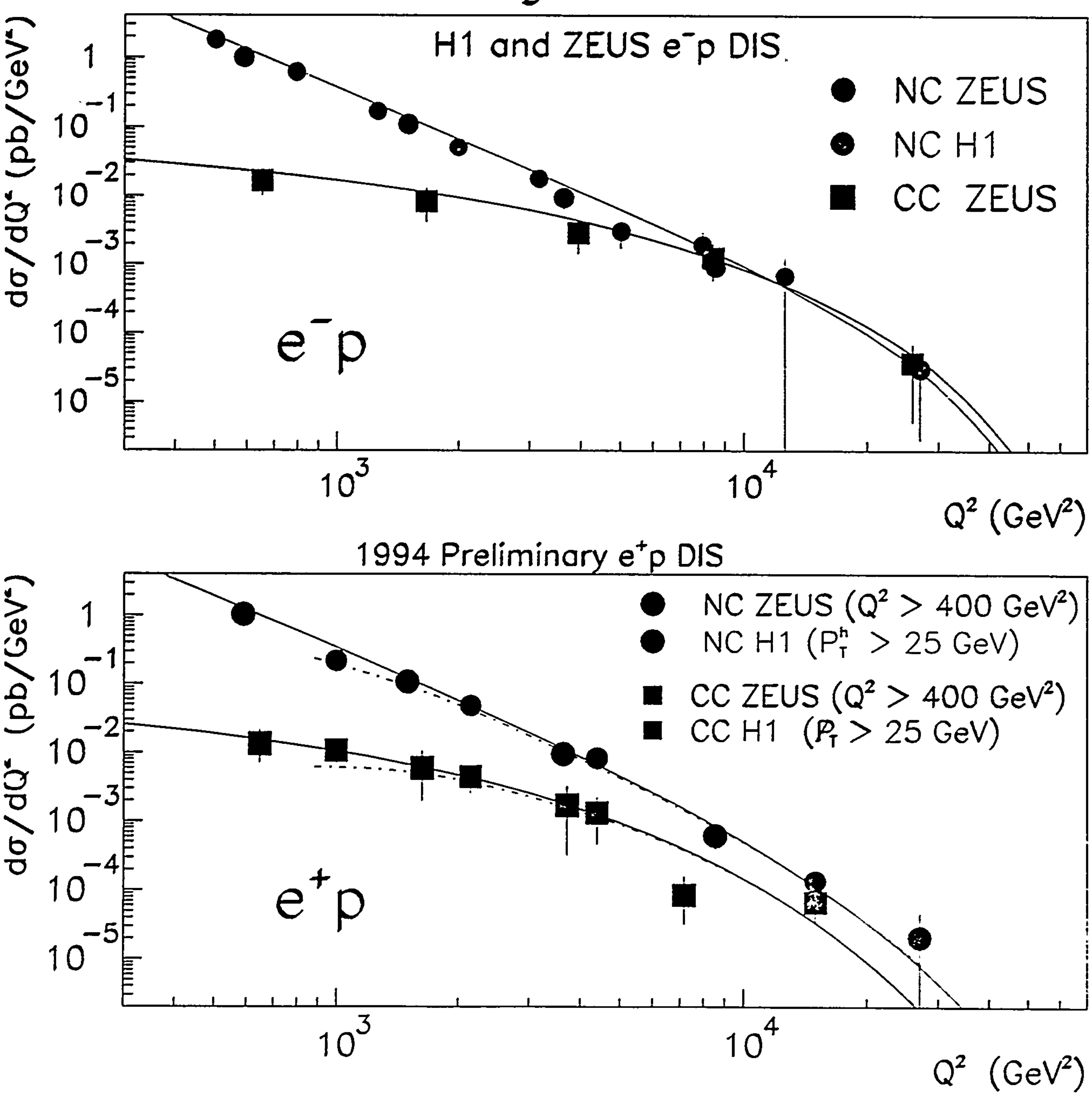

F2 Overview

$$\frac{d^2\sigma}{dx\,dQ^2} = \frac{2\pi\alpha^2}{xQ^4}\Big[\,Y_+ F_2(x,Q^2) - y^2 F_L(x,Q^2) + Y_- \, x F_3(x,Q^2)\Big]\big(1+\delta_r(x,Q^2)\big)$$

radiative corrections $\lesssim 5\%, 10\%$

with $Y_\pm = 1 \pm (1-y)^2$

$y = \frac{Q^2}{sx}$

- triggering & selections
- bin data
- subtract remaining bkgds statistically
- QCD for F_L
- Z^0, F_L corrections are small
  calculate & correct

Z_0: $Q^2 \gtrsim 4200\ \mathrm{GeV}^2$ ~20% correction
otherwise $\lesssim 6\%$ correction

F_L: biggest at high y $\lesssim 15\%$ correctio

$$\Rightarrow \boxed{\frac{d^2\sigma}{dx\,dQ^2} = \frac{2\pi\alpha^2}{xQ^4}\, Y_+ F_2(x,Q^2)\,(1-\delta_{F_L}+\delta_{Z_0})(1+\delta_r)}$$

thus, choose x,Q^2 reconstruction method
acceptance/migration from MC simulation
iterate/unfold to match data to MC
Systematic errors

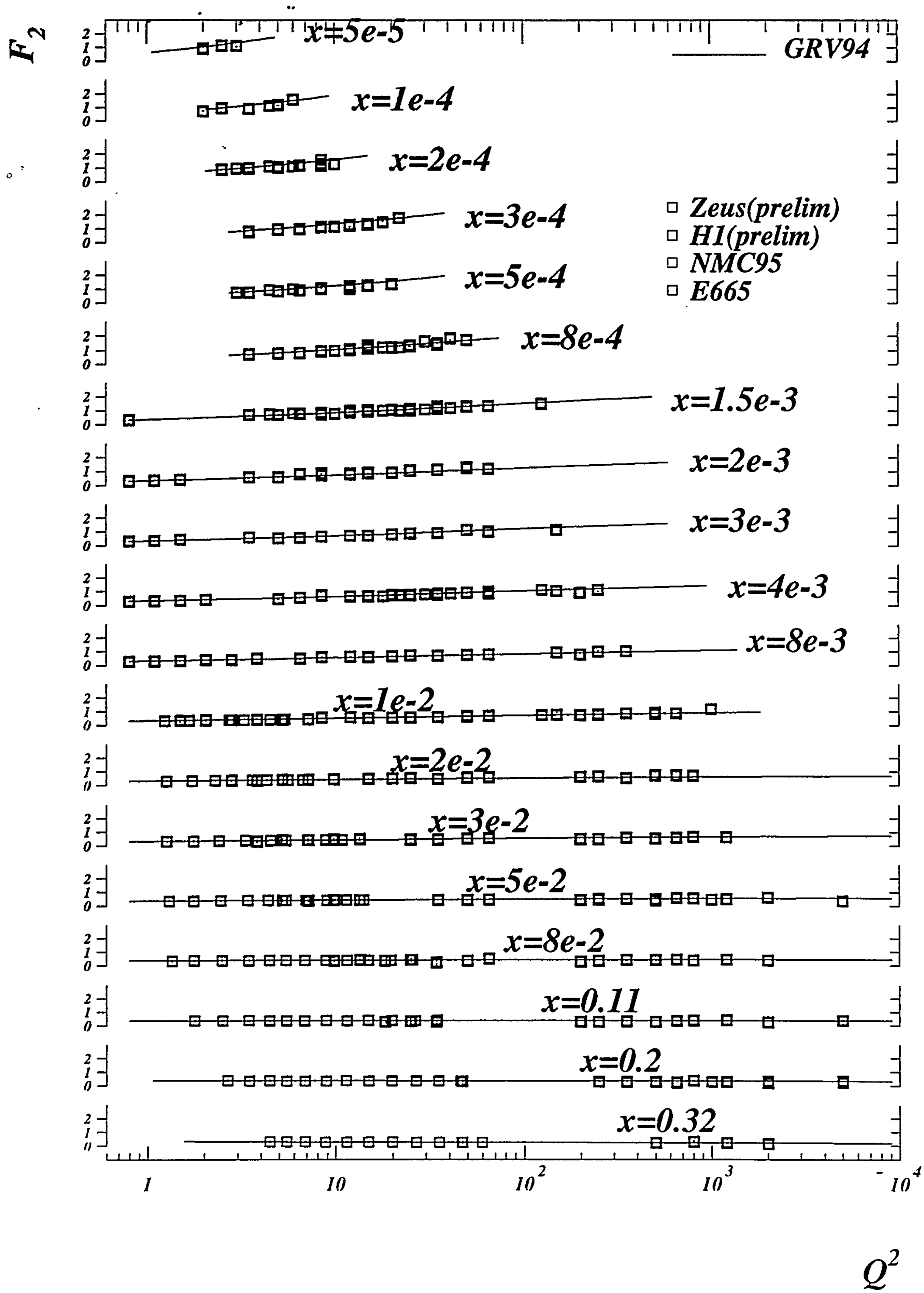

F_2
GRV94
Zeus(prelim)
H1(prelim)
NMC95
E665
x=5e-5
x=1e-4
x=2e-4
x=3e-4
x=5e-4
x=8e-4
x=1.5e-3
x=2e-3
x=3e-3
x=4e-3
x=8e-3
x=1e-2
x=2e-2
x=3e-2
x=5e-2
x=8e-2
x=0.11
x=0.2
x=0.32
Q^2

Q^2 Dependence with GRV94

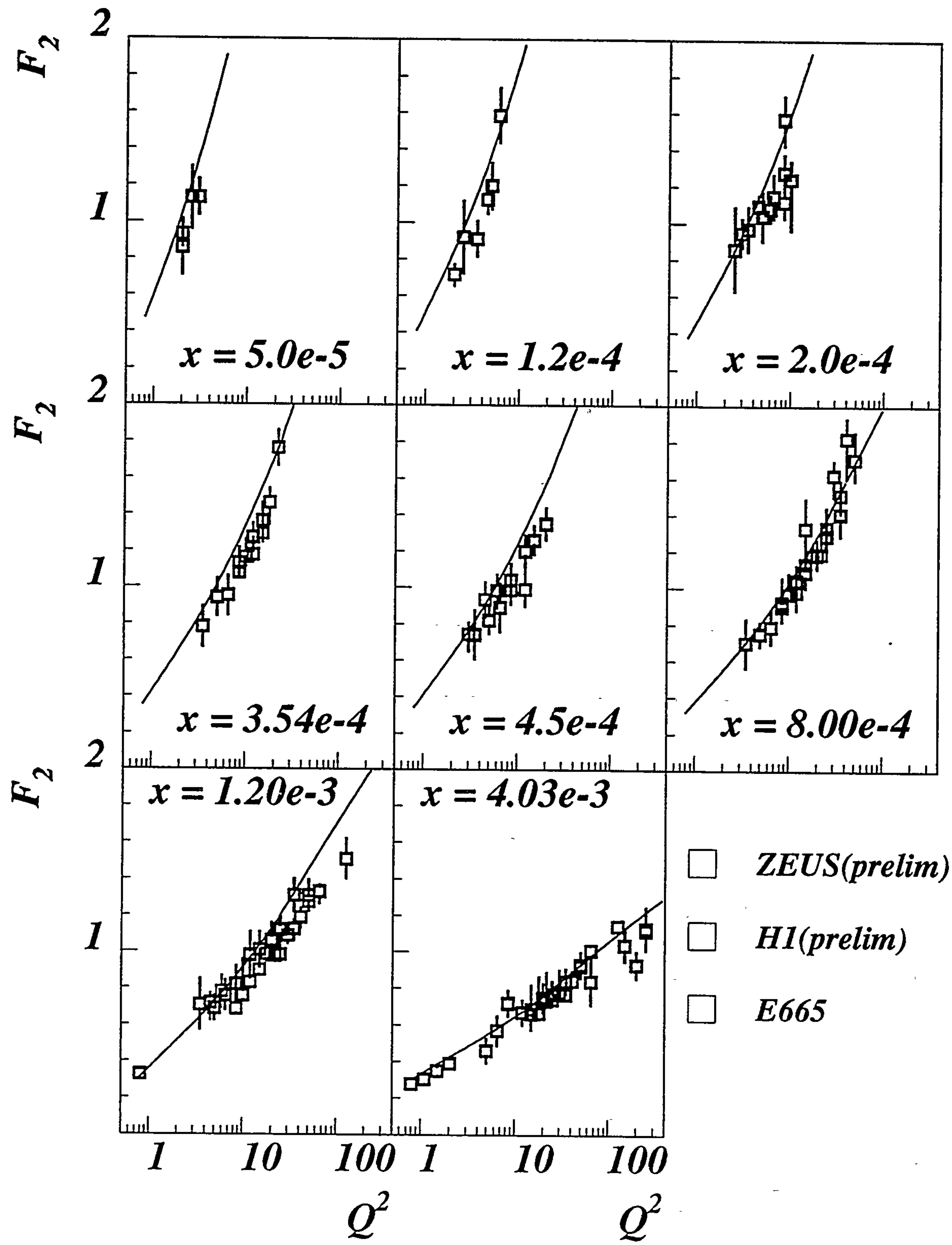

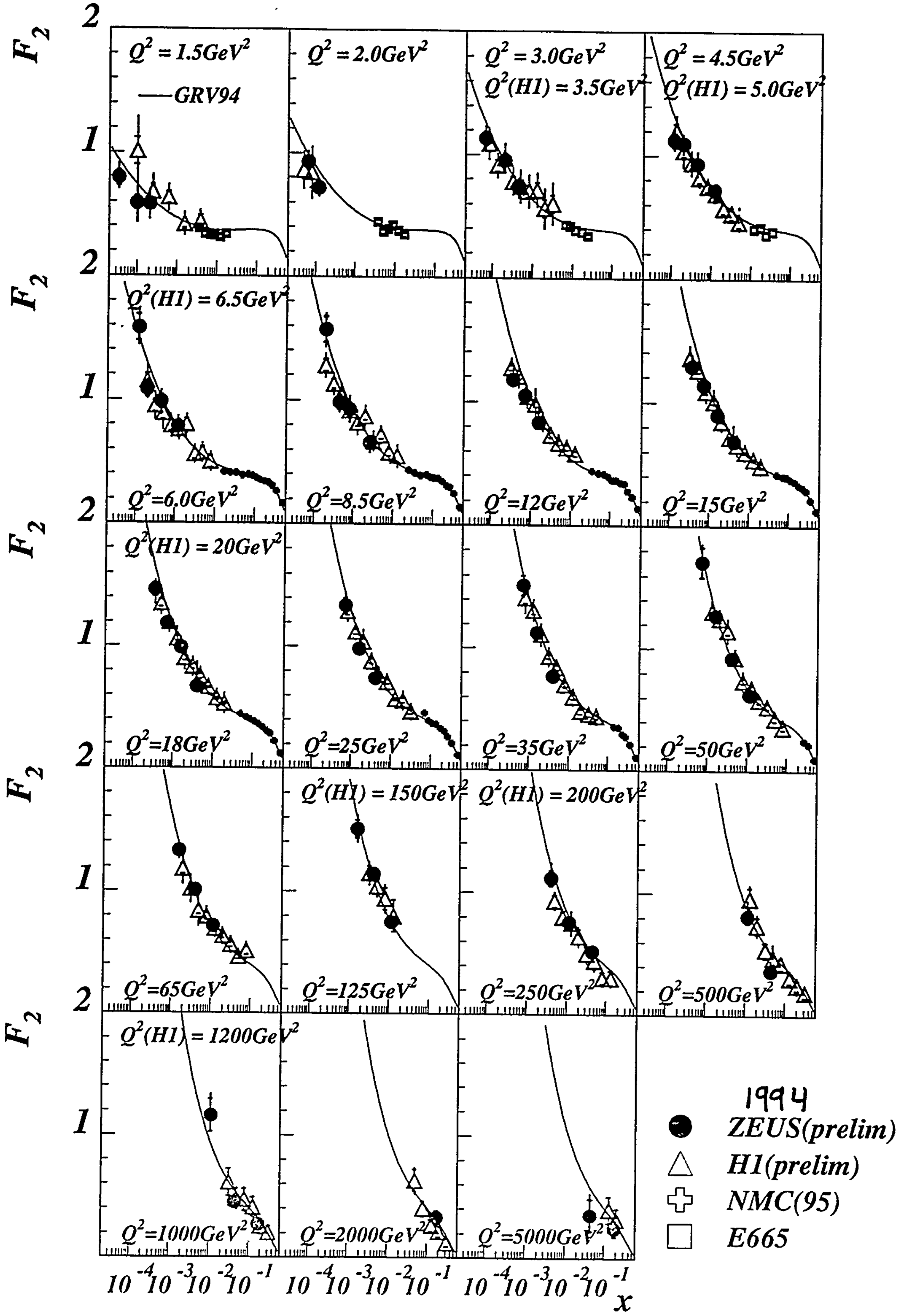

F2
Q² = 1.5GeV²
—GRV94
Q² = 2.0GeV²
Q² = 3.0GeV²
Q²(H1) = 3.5GeV²
Q² = 4.5GeV²
Q²(H1) = 5.0GeV²
Q²(H1) = 6.5GeV²
Q²=6.0GeV²
Q²=8.5GeV²
Q²=12GeV²
Q²=15GeV²
Q²(H1) = 20GeV²
Q²=18GeV²
Q²=25GeV²
Q²=35GeV²
Q²=50GeV²
Q²(H1) = 150GeV²
Q²(H1) = 200GeV²
Q²=65GeV²
Q²=125GeV²
Q²=250GeV²
Q²=500GeV²
Q²(H1) = 1200GeV²
Q²=1000GeV²
Q²=2000GeV²
Q²=5000GeV²
10⁻⁴ 10⁻³ 10⁻² 10⁻¹
x
1994
ZEUS(prelim)
H1(prelim)
NMC(95)
E665

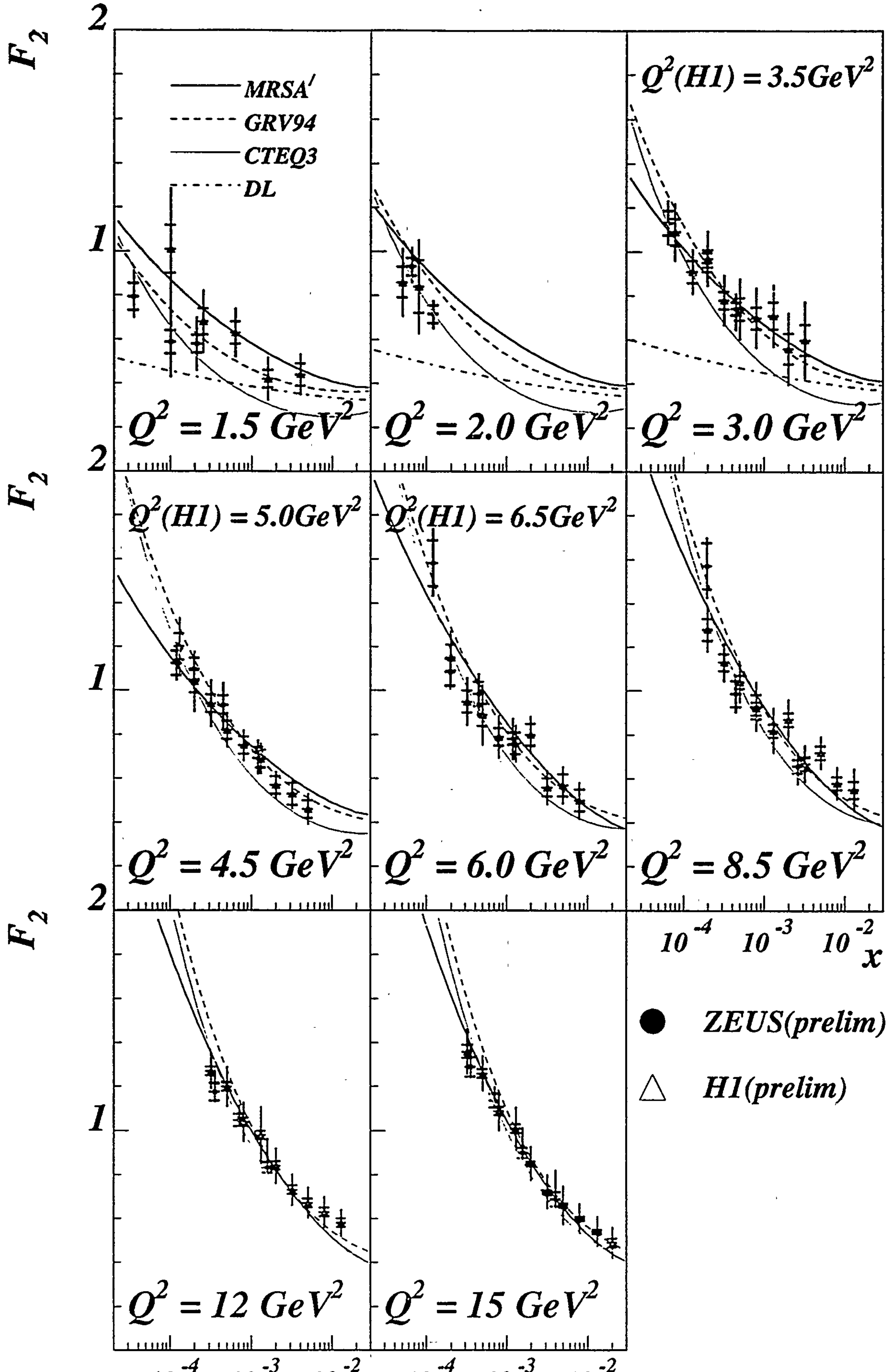

F2
MRSA'
GRV94
CTEQ3
DL
Q^2(H1) = 3.5GeV^2
Q^2 = 1.5 GeV^2
Q^2 = 2.0 GeV^2
Q^2 = 3.0 GeV^2
Q^2(H1) = 5.0GeV^2
Q^2(H1) = 6.5GeV^2
Q^2 = 4.5 GeV^2
Q^2 = 6.0 GeV^2
Q^2 = 8.5 GeV^2
Q^2 = 12 GeV^2
Q^2 = 15 GeV^2
10^-4 10^-3 10^-2
x
ZEUS(prelim)
H1(prelim)

ZEUS 1993

note

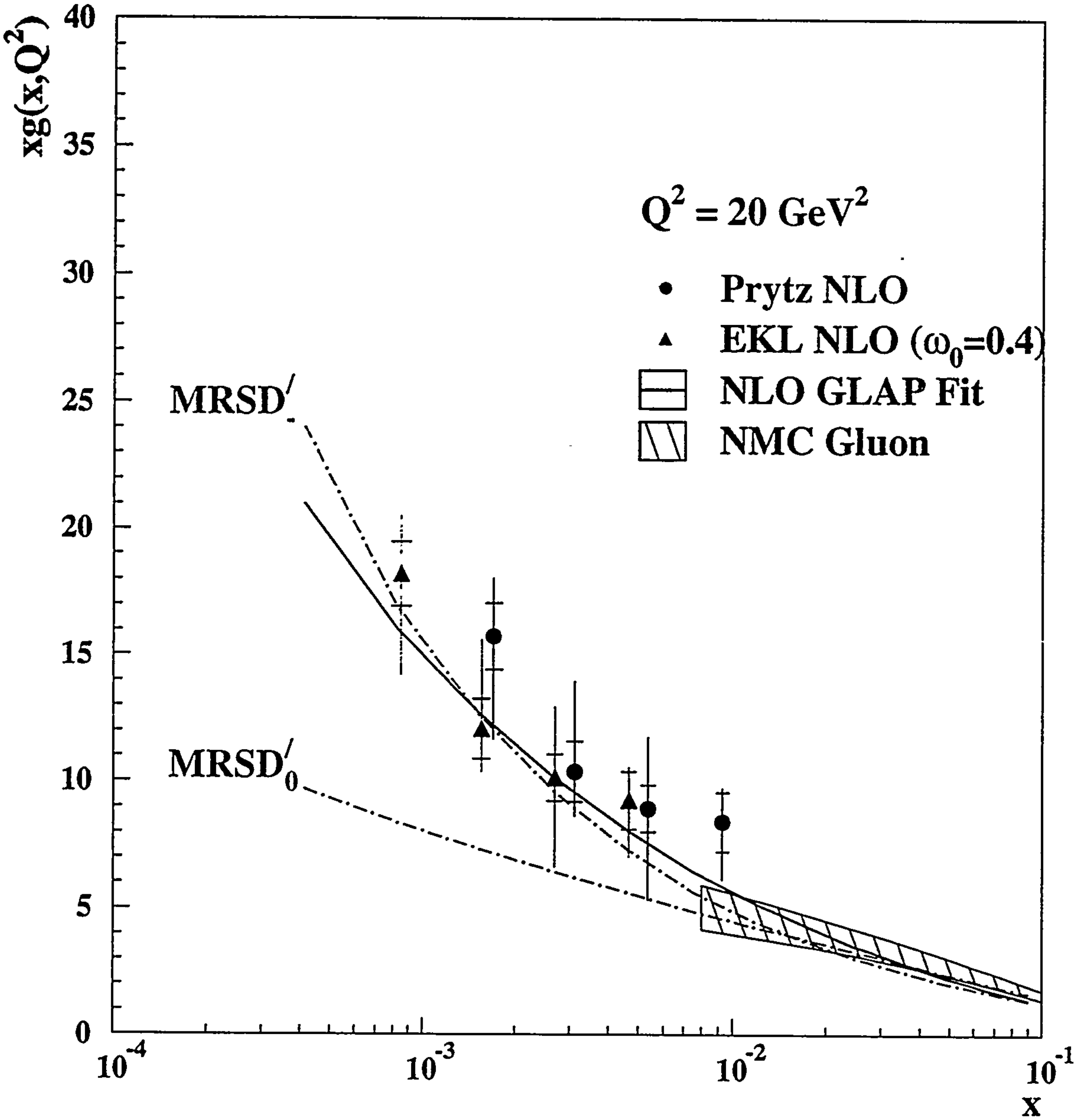

H1 also presents a "direct" determination of g via

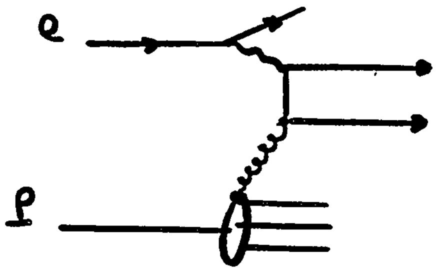

2 + 1 jet signature

subtract bkgds, unfold hadronization & detector effects, input α_s ....

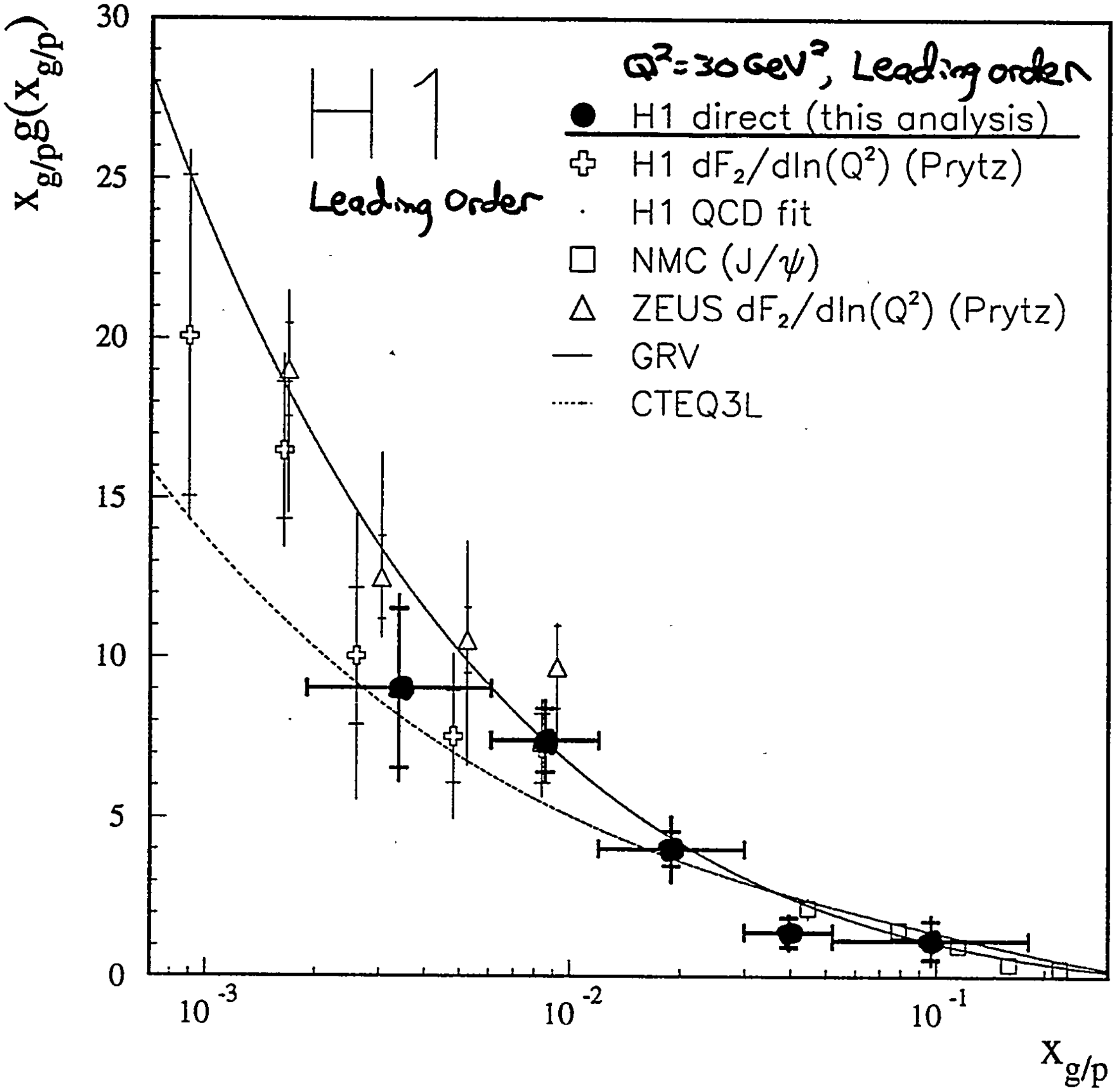

F_2 : $g(x,Q^2)$ Outlook

- Extraction of F_2 relied on R_{QCD} !

  Is it valid? Measure it!!

  recall $$\frac{d^2\sigma}{dx\,dQ^2} \approx \frac{2\pi\alpha^2}{xQ^4}\left[\left(1+(1-y)^2\right)F_2(x,Q^2) - y^2 F_L(x,Q^2)\right]$$

  $\Rightarrow$ measure $\frac{d^2\sigma}{dx\,dQ^2}$ (i.e., in bins of x, Q^2)

  at different y. recall $Q^2 = sxy \Rightarrow$ change $s = 4E_eE_p$

  It turns out most practical way is to lower E_p

  The measurement is not easy

  $\rightarrow$ try to run reduced $E_p = 500$ GeV in 1996 ? under discussion

- Measurement of $g(x,Q^2)$ in its infancy (we hope!)

  There are other methods:

  - ρ production in DIS (see later)
  - BGF processes:

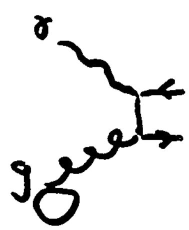

jets, heavy flavor production, ...

  - ⋮

Things to do with F_2

II) $\sigma_{tot}(\gamma^* p)$ (ZEUS)

flux of γ^* well-defined if $x \ll \frac{1}{2m_p R_p}$ $\quad R_p \simeq 4\,\text{GeV}^{-1}$

then lifetime of $\gamma^* \gg$ interaction time

$$F_2(x,Q^2) \simeq \frac{Q^2(1-x)}{4\pi^2\alpha}\left[\sigma_T(x,Q^2) + \sigma_L(x,Q^2)\right]$$

(taking $4m_p^2 x^2 \ll Q^2$)

write W is $\gamma^* p$ c.m. energy :

$$W^2 = m_p^2 + \frac{Q^2(1-x)}{x}$$

thus write

$$\boxed{\sigma_{tot} \simeq \frac{4\pi^2\alpha\, F_2(W,Q^2)}{Q^2}}$$

take bins w/ $Q^2 < 125\ \text{GeV}^2$ →

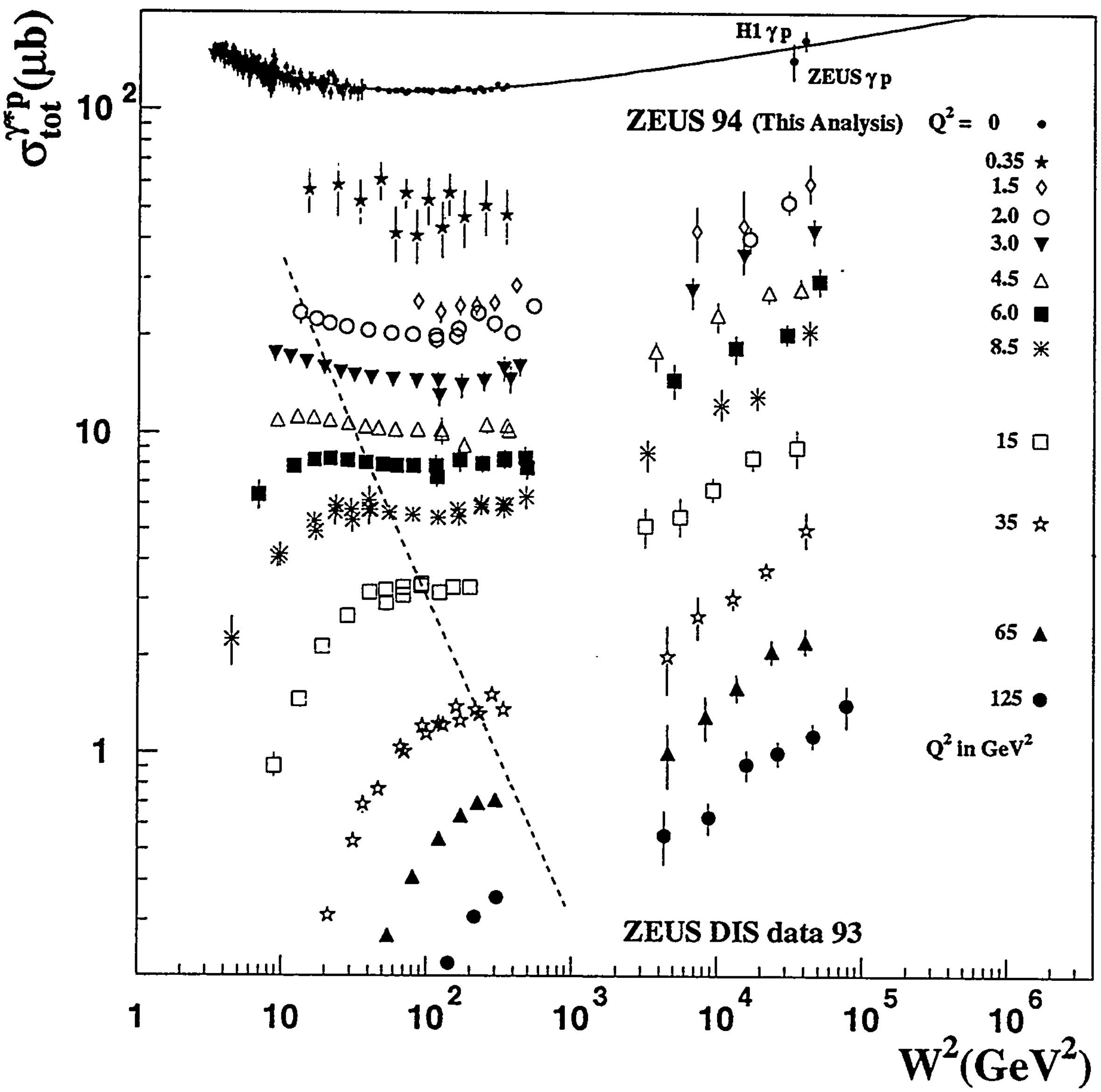

$\sigma_{tot}^{\gamma^* p}(\mu b)$
H1 γp
ZEUS γp
ZEUS 94 (This Analysis) Q^2 = 0
0.35
1.5
2.0
3.0
4.5
6.0
8.5
15
35
65
125
Q^2 in GeV^2
ZEUS DIS data 93
$W^2(GeV^2)$

The low Q^2 Frontier

- mechanism for large rise of F_2 at low x : driven by DGLAP?

- observed W dependence of $\sigma_{tot}(\gamma^* p)$ in DIS very different from photoproduction

How does photoproduction become DIS?

$\Rightarrow$ measure $\frac{d^2\sigma}{dx\,dQ^2}$ at lower Q^2

for 1995 RUN: (ZEUS)

- move RCAL closer to beamline
- install new beampipe
- install new beampipe calorimeter

$\rightarrow$ from now on, ZEUS will measure $\frac{d^2\sigma}{dx\,dQ^2}$ ~continuously from $\sim 0.1\ \mathrm{GeV}^2 \lesssim Q^2 \lesssim$ kinematic limit ($9 \times 10^4\ \mathrm{GeV}^2$)

Theorists: JUMP IN !!!

(e.g.: jets $\Rightarrow$ two scales Q^2, p_T^2 $\begin{cases} Q^2 > p_T^2 & \gamma^* \text{ probes } p \\ Q^2 < p_T^2 & p \text{ probes } \gamma^* \end{cases}$)

side view

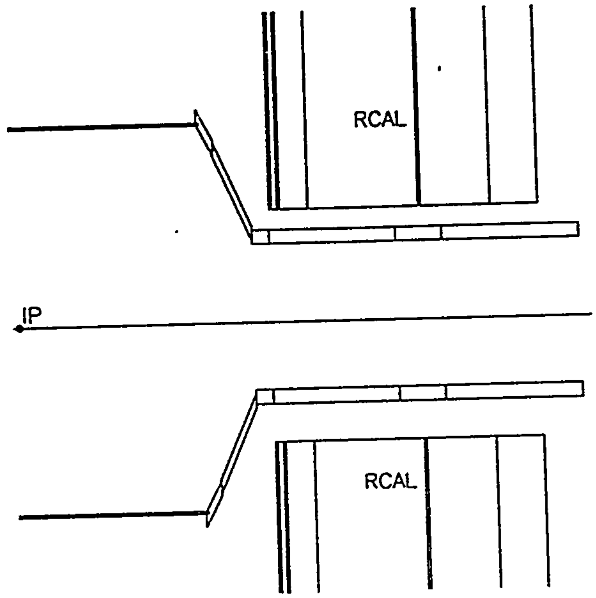

new beampipe for: lowered RCAL...

Figure 3: *A side view of the new beam pipe inside the RCAL. Note that different y and z scales are used.*

top view

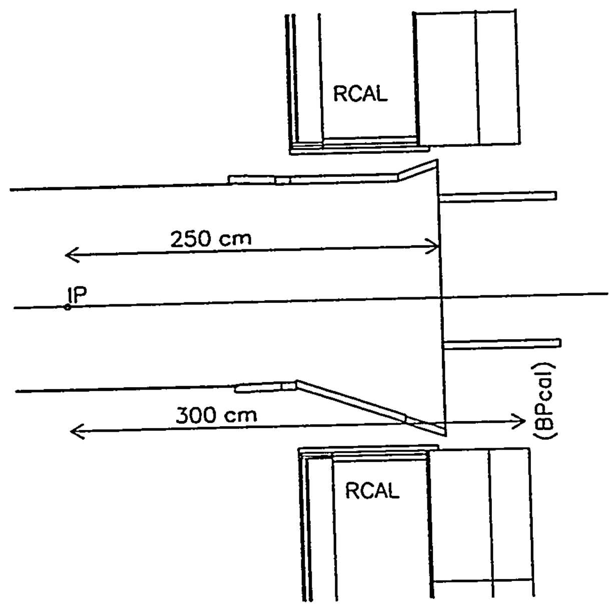

... and new beampipe calorimeter with ~zero dead material

Figure 4: *A top view of the new beam pipe inside the RCAL. Note that different x and z scales are used. The word 'BPcal' indicates the region for the new beam pipe calorimeter.*

W-Sci Calorimeters (8 mm x : y strips)

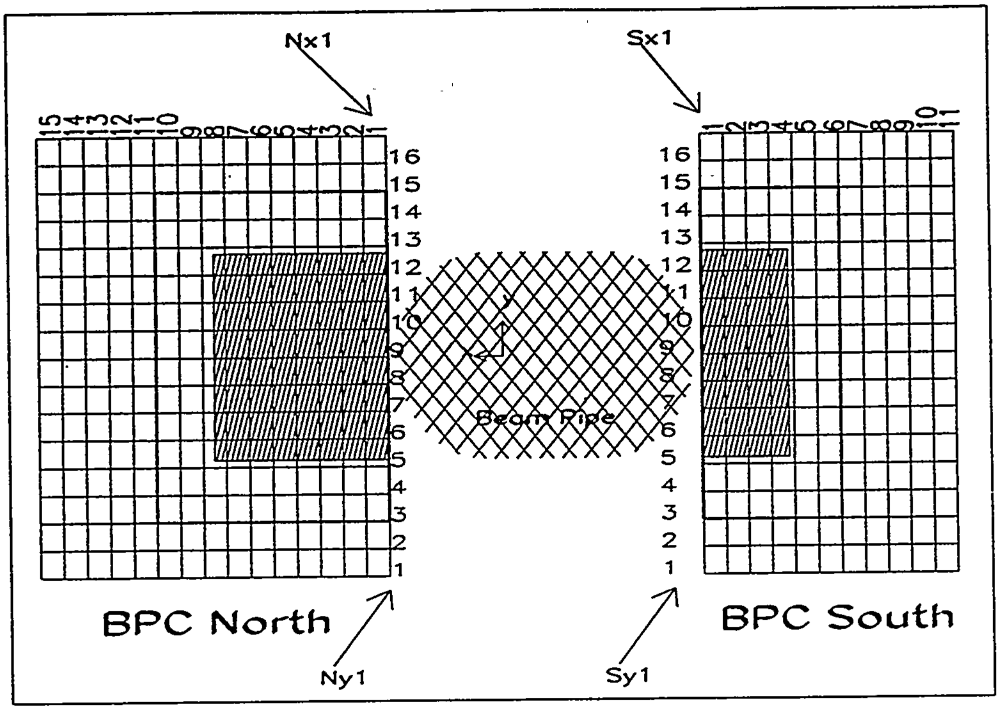

Figure 1: *Schematic of the BPC. The hashed areas on the detectors indicate the signal regions. The numbers along the top and side indicate the WLS readout of the vertical and horizontal strips. respectively. The dimensions are not to scale.*

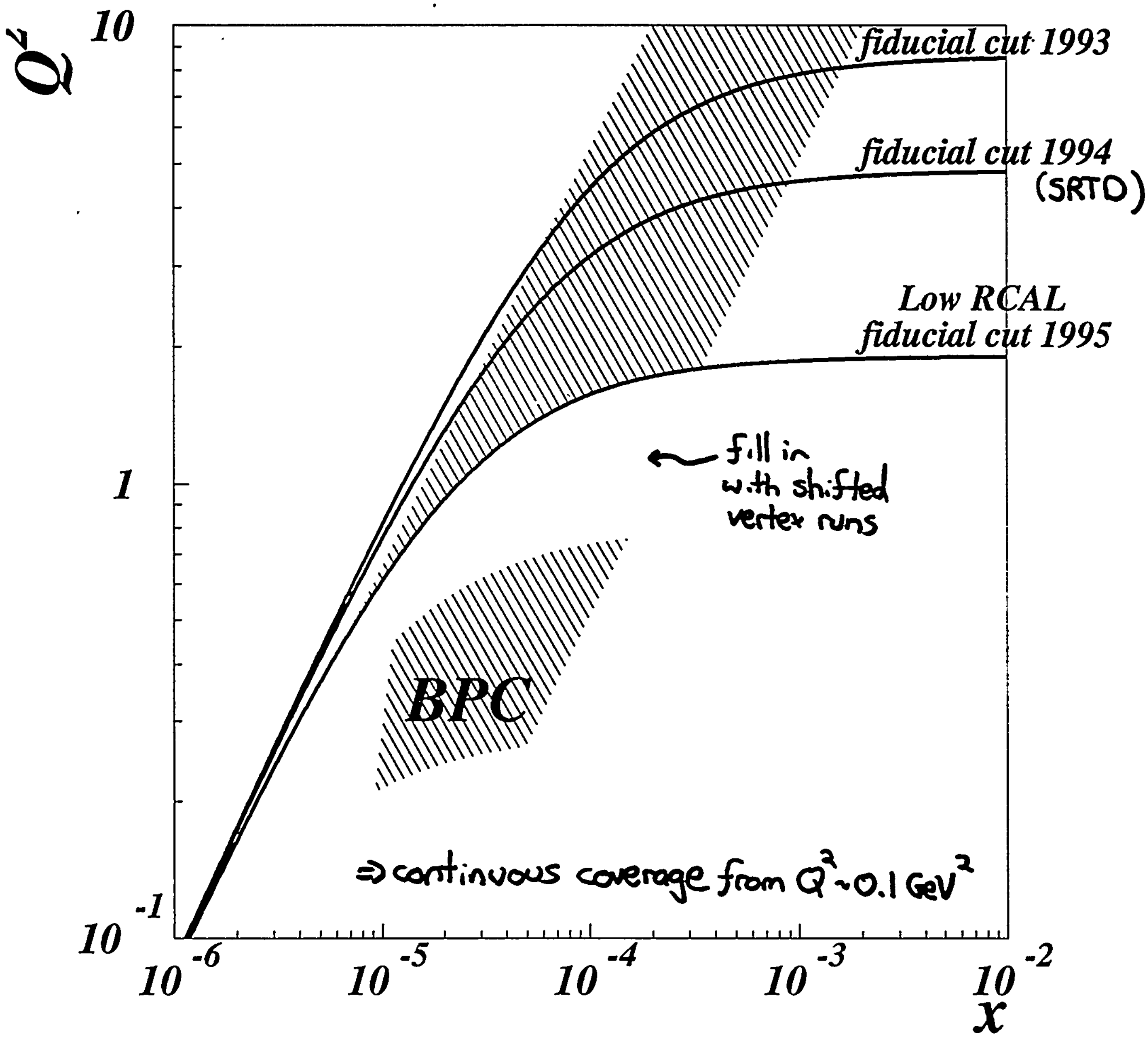

Q^2
10
1
10^{-1}
10^{-6}
10^{-5}
10^{-4}
10^{-3}
10^{-2}
x
fiducial cut 1993
fiducial cut 1994
(SRTD)
Low RCAL
fiducial cut 1995
fill in
with shifted
vertex runs
BPC
⇒ continuous coverage from $Q^2 \sim 0.1\ GeV^2$

 (11

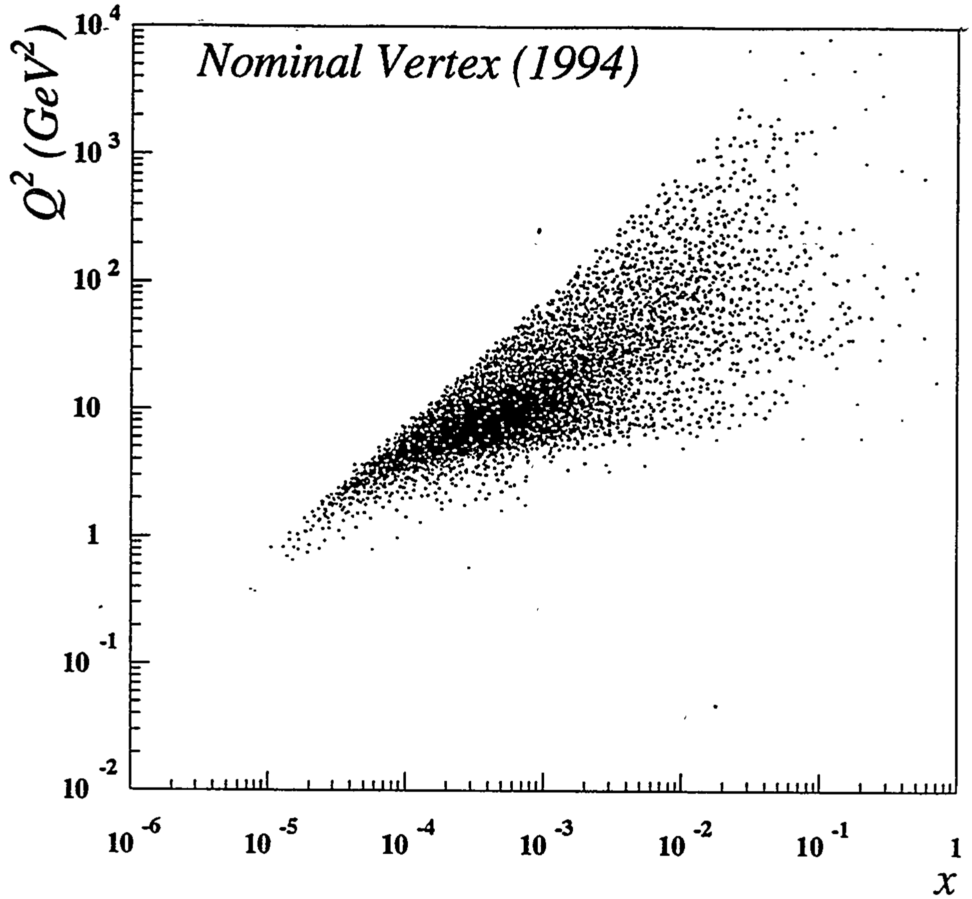
Nominal Vertex (1994)
$Q^2\ (GeV^2)$
10^4
10^3
10^2
10
1
10^{-1}
10^{-2}
10^{-6}
10^{-5}
10^{-4}
10^{-3}
10^{-2}
10^{-1}
1
x

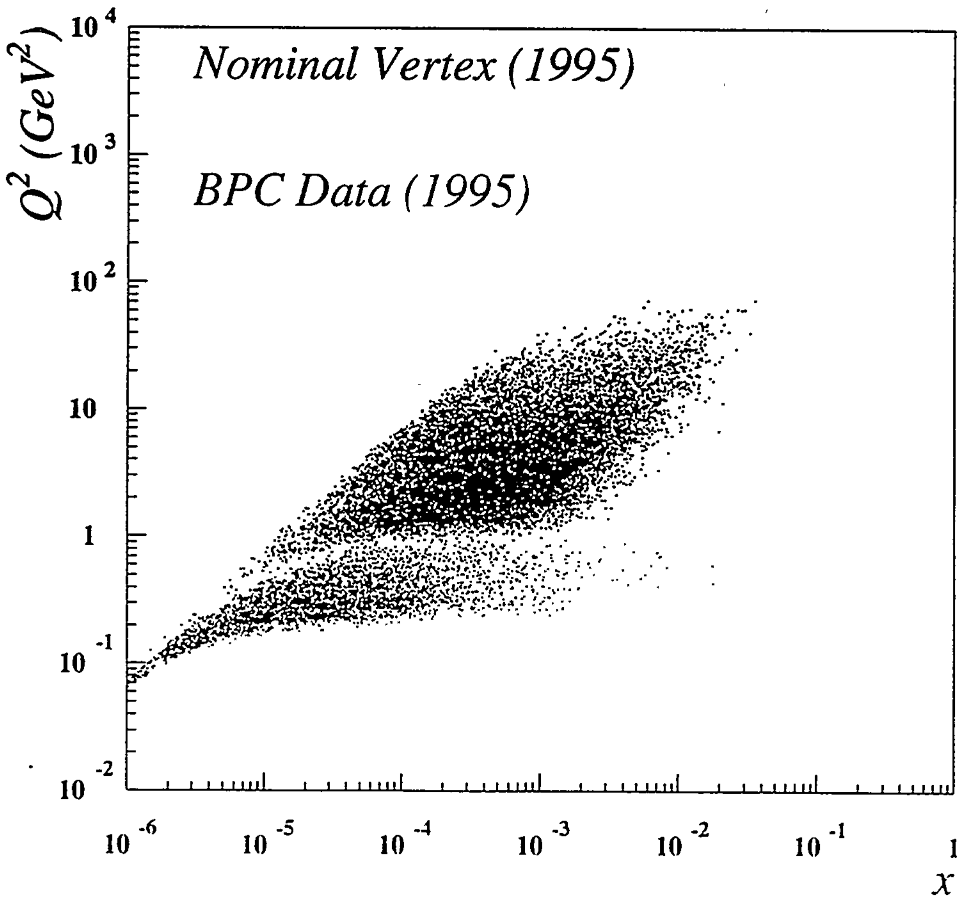
Nominal Vertex (1995)
BPC Data (1995)
$Q^2\ (GeV^2)$
10^4
10^3
10^2
10
1
10^{-1}
10^{-2}
10^{-6}
10^{-5}
10^{-4}
10^{-3}
10^{-2}
10^{-1}
1
x

Large Rapidity Gap Events

In the standard picture of DIS, color is "transferred" between the scattered quark and proton remnant

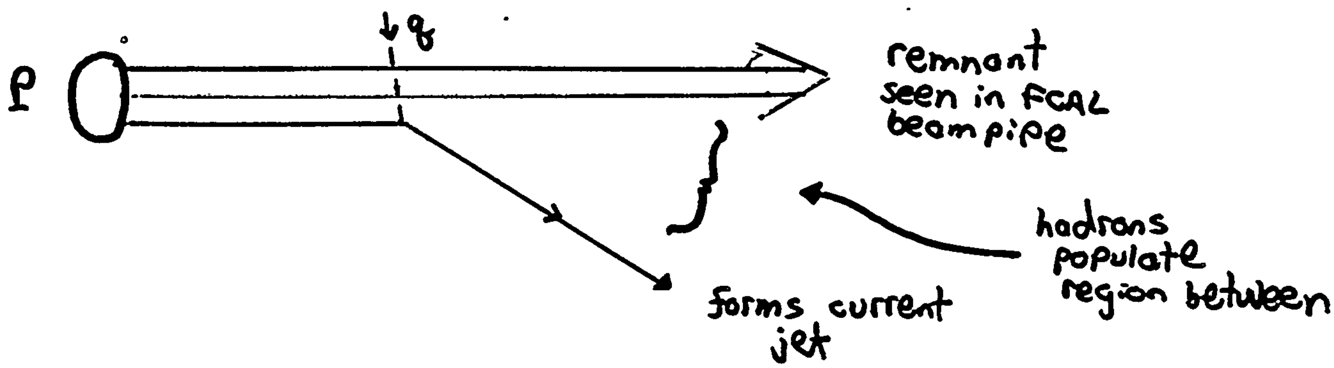

We see this:

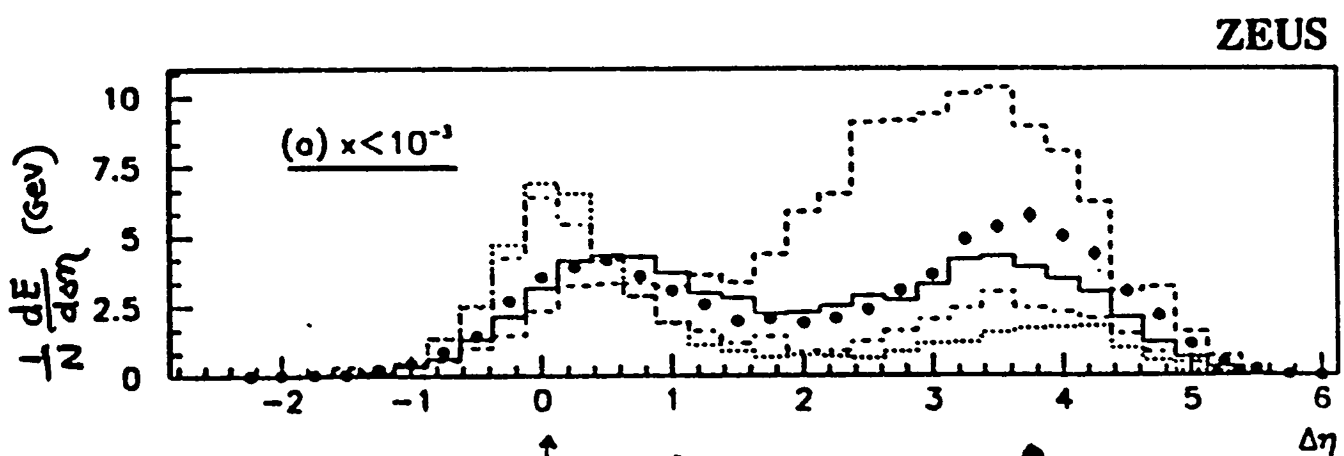

$\eta = -\ln\tan(\theta/2)$ ↑ current jet ↑ proton remnant

calculate γ (direction of "struck quark")
then $\Delta\eta$ is the energy-weighted pseudorapidity difference of the hadrons relative to struck quark

• = data
─┌ = ME + PS
--- = PS (W^2)
... = PS (Q^2)
-·- = ME

$\mathbb{P}$ content of proton and $\mathbb{P}$ structure

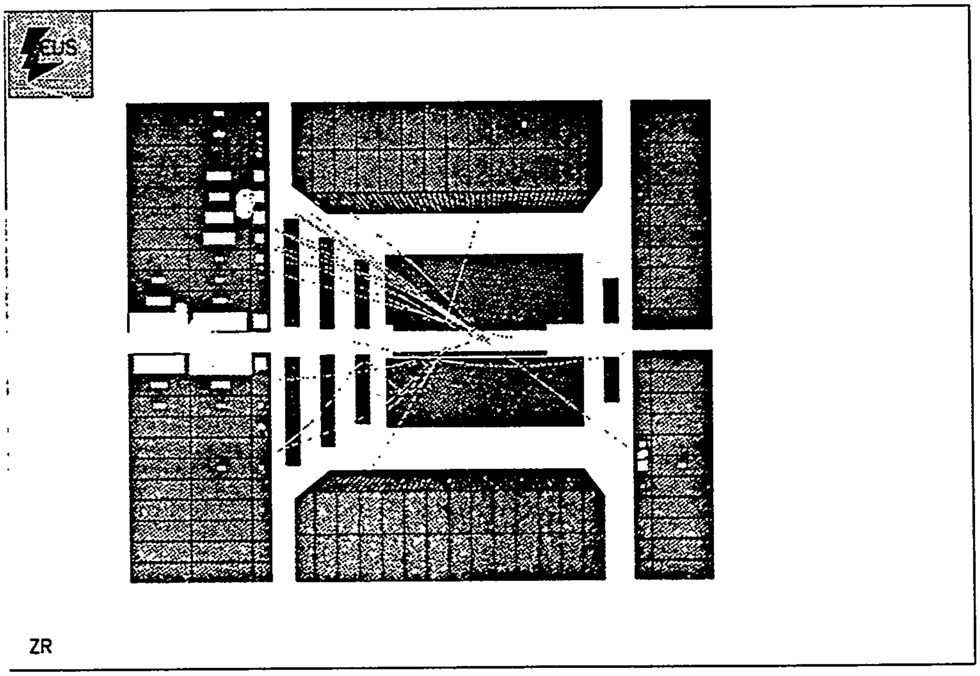

- Observation of DIS events with large rapidity gap in forward region

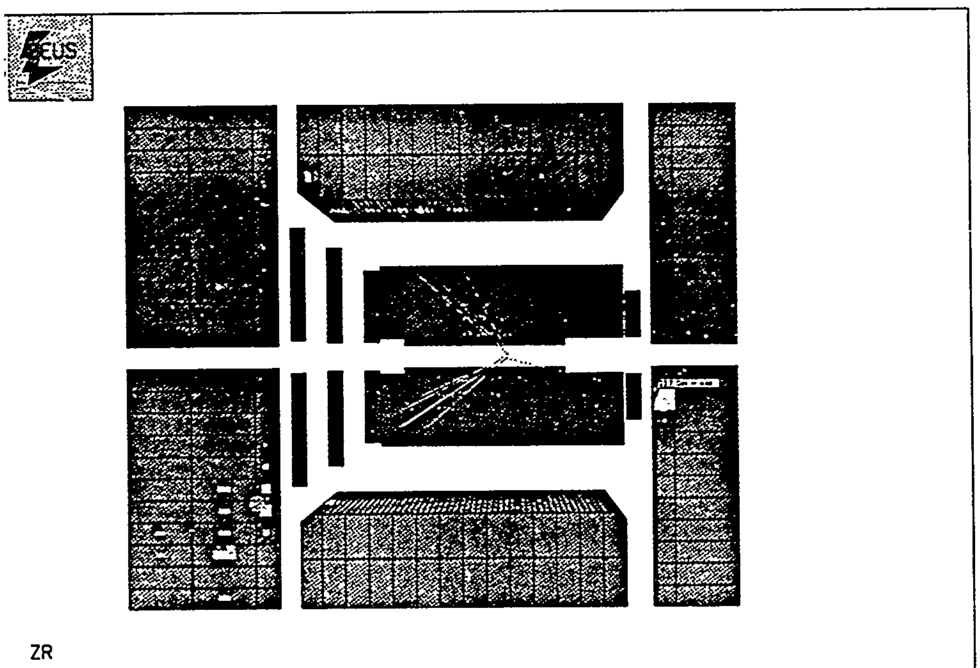

$\longrightarrow$ Exchange of a colorless object with vacuum quantum numbers - ($\mathbb{P}$) -

Surprise: early on we found a large number ($\gtrsim 5\%$) of DIS events with no remnant: there is a rapidity gap between the "current jet" and the particle(s) going through the beamhole.

Define: η_{max} is the η value of the most forward detected energy

- Standard DIS MC completely fails to describe low η_{max} tail
- Phenomenon is leading twist

(first measurement 1993)

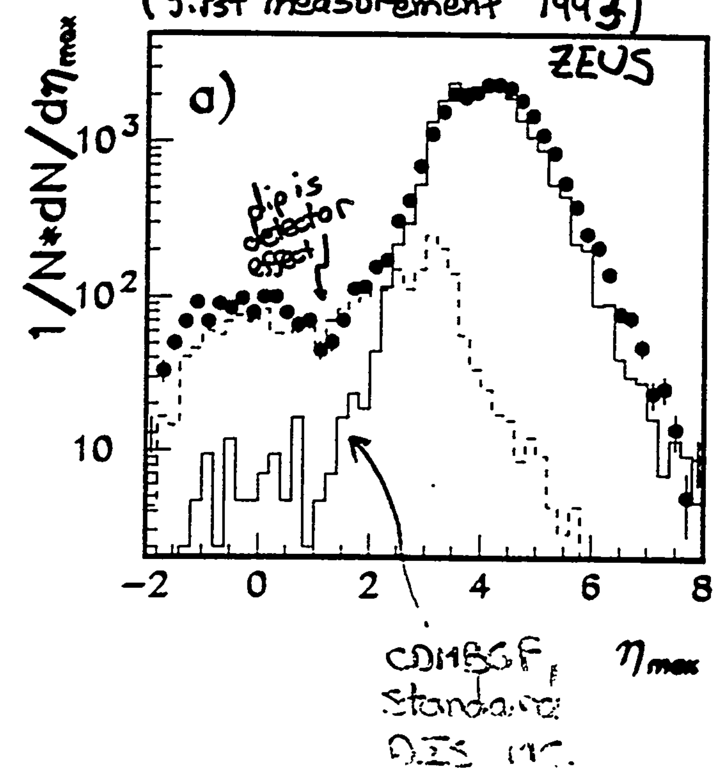

calorimeter covers $-3.8 < \eta < 4.3$

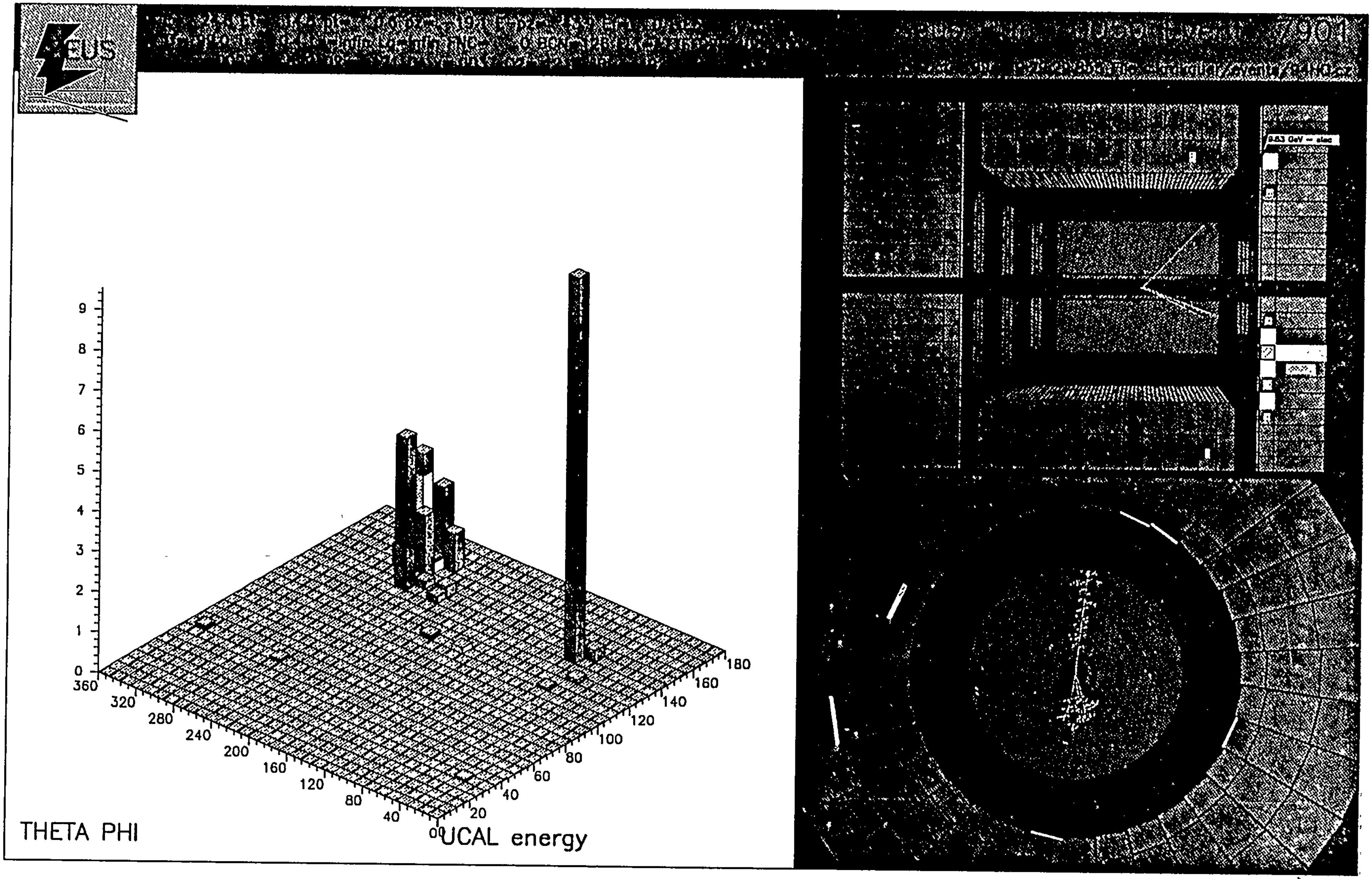
ZEUS
THETA PHI
UCAL energy
0
1
2
3
4
5
6
7
8
9
360
320
280
240
200
160
120
80
40
0
20
40
60
80
100
120
140
160
180

WHAT'S GOING ON ?

Interpret as scatter involving object with no net color

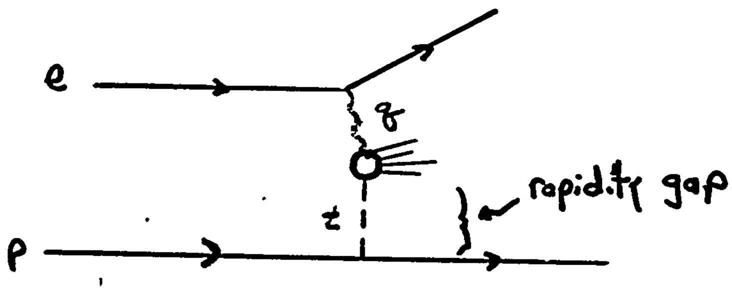

remarkable ! Electron energy is ~ 50 TeV in p rest frame !

What is - - - ?

Best candidate is Pomeron , agent of pp diffractive scattering

"diffractive dissociation of virtual photon"

What is Pomeron ? Does it "contain" partons ?

There are now MC models to compare with data →

Kinematic variables for diffraction

usual: $x = \dfrac{Q^2}{2p\cdot q}$

$Q^2 = -q^2$

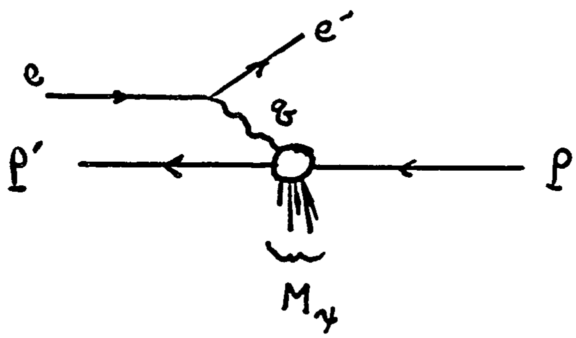

define $\quad x_{\mathbb{P}} = \dfrac{q\cdot(p-p')}{q\cdot p} \qquad \beta = \dfrac{-q^2}{2q\cdot(p-p')}$

then $\boxed{x = \beta\, x_{\mathbb{P}}}$

$x_{\mathbb{P}}$: fraction of p carried by "Pomeron" (∞ momentum frame)

β: fraction of q carried by struck parton

$t = (p-p')^2 \Rightarrow \quad x_{\mathbb{P}} = \dfrac{Q^2+M_x^2-t}{Q^2+W^2-M_p^2} \qquad \beta = \dfrac{Q^2}{Q^2+M_x^2-t}$

for $|t| \ll Q^2$, $|t| \ll M_x^2$,

$$\boxed{x_{\mathbb{P}} \simeq \frac{Q^2+M_x^2}{Q^2}\cdot x \qquad \beta \simeq \frac{Q^2}{Q^2+M_x^2}}$$

Diffractive Structure Function

$$\frac{d^4\sigma_{ep\to epx}}{dx\,dQ^2\,dx_{\mathbb{P}}\,dt} = \frac{2\pi\alpha^2}{xQ^4}\left[Y_+ F_2^{D(4)} - y^2 F_L^{D(4)}\right](1+\delta_r)(1+\delta_z)$$

$(x, Q^2, x_{\mathbb{P}}, t)$

no measure of t (yet) $\Rightarrow \int_{t_{min}}^{t_{max}} (\;)\,dt$; neglect F_L^D, δ_z

unknown! (ok for now)

$$\frac{d^3\sigma}{d\beta\,dQ^2\,dx_{\mathbb{P}}} = \frac{2\pi\alpha^2}{\beta Q^4}\left(Y_+ F_2^{D(3)}(\beta, Q^2, x_{\mathbb{P}})\right) \Rightarrow \text{extract } F_2^{D(3)}$$

Plot F_2^D in bins of β, Q^2 as a function of $x_{\mathbb{P}}$

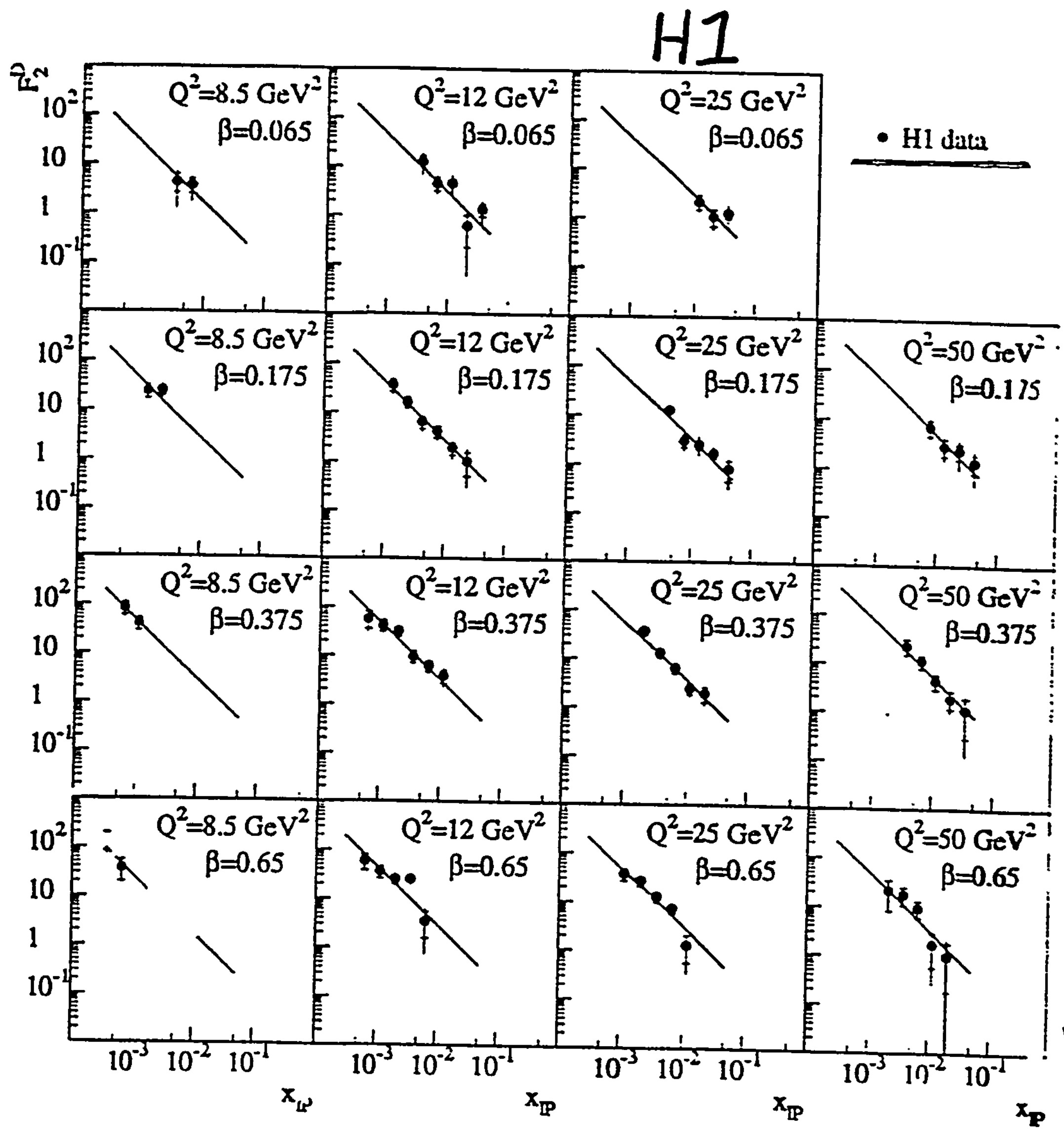

FACTORIZATION ?!!?

universal $x_{\mathbb{P}}^{-n}$ dependence $n = 1.19 \pm 0.06 \pm 0.07$ $\chi^2/dof = \frac{32}{46}$

Tempting to write $\dfrac{d^3\sigma}{d\beta\, dQ^2\, dx_{I\!P}} = \dfrac{d^2\sigma_{eI\!P \to ex}}{d\beta\, dQ^2} \cdot f_{I\!P}(x_{I\!P})$

Regge: $f \sim x_{I\!P}^{-(2\alpha(t)-1)} \Rightarrow \alpha(t) \simeq \alpha(t=0) = 1.10 \pm 0.03 \pm 0.04$

! The original pomeron: $\alpha(t) = 1.085 + 0.25t$!

$\tilde{F}_2^D$

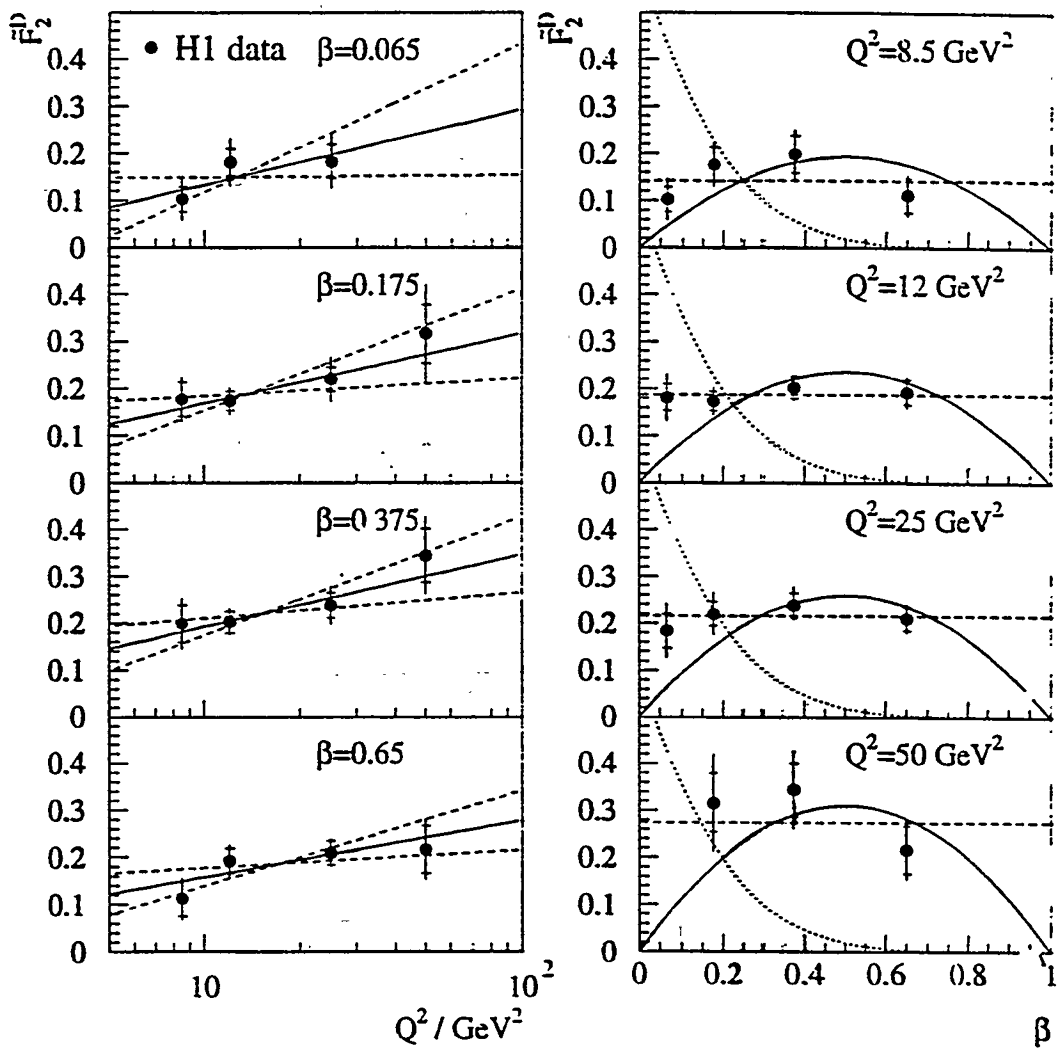

Pomeron Substructure ??

$$\tilde{F}_2^D(\beta, Q^2) = \int_{x_{I\!P_L}}^{x_{I\!P_H}} F_2^{D(3)}(\beta, Q^2, x_{I\!P})\, dx_{I\!P}$$

- ~ flat in Q^2 (pt-like interaction?)

Models + Interpretation

Some provide factorization:

- Ingelman & Schlein: p emits virtual $I\!P$
  γ^* probes structure of $I\!P$

$$F_2^{D(4)} = f(x_{I\!P}, t) \cdot F_2^{I\!P}(\beta, Q^2)$$

flux from UA4 data

Pomeron structure function

Implementation:

POMPYT MC with

HARD (HP) and SOFT (SF)

$\beta(1-\beta)$ $(1-\beta)^5$

structure functions

- Regge Inspired, e.g., Donnachie-Landshoff (DL)

$$f_{I\!P} \propto F_1^2(t)\, x_{I\!P}^{-[2\alpha(t)-1]}$$

steeply falling w/ t

pomeron trajectory $\alpha(t) = 1.085 + 0.25t$

(Goulianos: normalize $f_{I\!P}$ at each W)

$$\hookrightarrow f_{I\!P} = \frac{1}{N_0}\, 0.73\, e^{4.6t}\, x_{I\!P}^{1-2\alpha(t)} \;;\; \alpha(t) = 1.115 + 0.26t$$

integrating over t $\Rightarrow$ $\sim x_{I\!P}^{-0.93}$?

some models break factorization:

• Nikolaev-Zakharov:

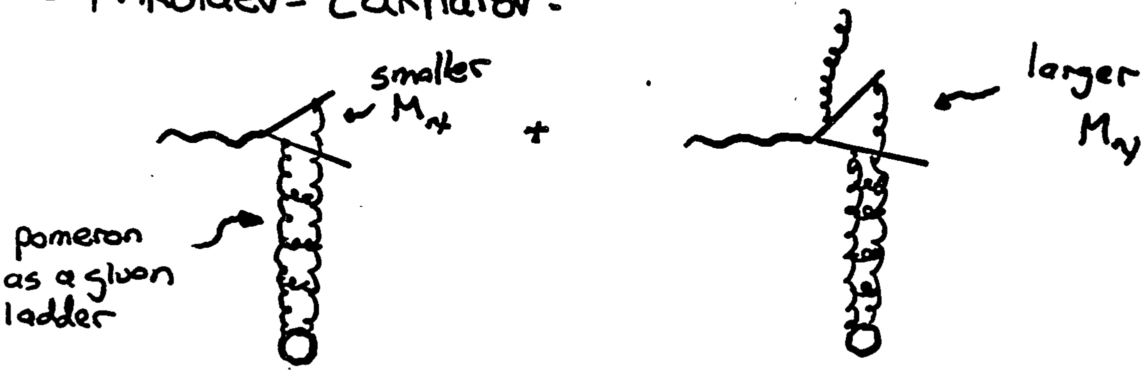

i.e., Fock state $|q\bar{q}\rangle$ and $|q\bar{q}g\rangle$

Diffractive cross-section ~ 2 component structure function, <u>each with its own flux factor</u>

$|q\bar{q}\rangle$ component looks like DL, HP (large $\beta \leftrightarrow$ small M_X)

$|q\bar{q}g\rangle$ component looks ~soft ← only visible factorization-breaking effects at smaller β

Data are consistent with factorization....

.... but not inconsistent with non-factorization! (yet)

can do more →
(use the models)

Compare rates

$$F_2^{D(4)} = \underset{\xi}{f}(x_{I\!P}, t)\, F_2^{I\!P}(\beta, Q^2)$$

can take flux from pp

but how to normalize $F_2^{I\!P}$? $\quad F_2^{I\!P}(\beta,Q^2) = \sum_i e_i^2\, \beta f_{q_i}(\beta,Q^2)$ quark density

try momentum sum rule: $\sum_i \int_0^1 N\beta f_i = 1$ quark density

for two light (u, d) quarks

Hard fn: $F_2^{I\!P}(\beta,Q^2) = \frac{10}{9}\cdot\frac{6}{4}\,\beta(1-\beta)$

Soft fn: $F_2^{I\!P}(\beta,Q^2) = \frac{10}{9}\cdot\frac{6}{4}(1-\beta)^5$

(can include s, c.f. Gehrmann & Stirling)

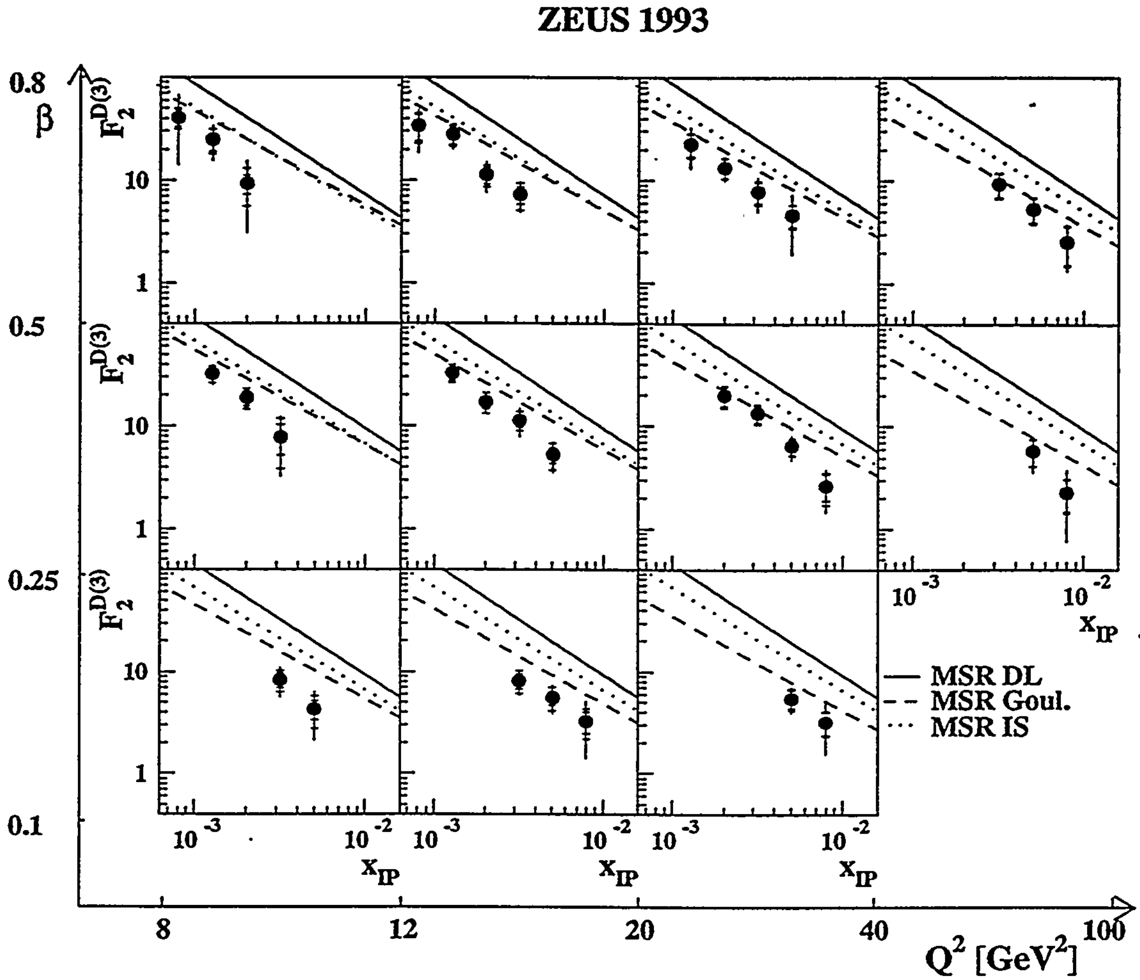

Figure 11: The results of $F_2^{D(3)}$ compared to an Ingelman-Schlein type model for which the momentum sum rule (MSR) for quarks within the pomeron is assumed. The β dependence is taken from the parametrisation discussed in the text. Note that the estimated 15% contribution due to double dissociation has been subtracted in order to compare with models for the single dissociation cross section. The inner error bars show the statistical errors, the outer bars correspond to the statistical and DIS event selection systematic errors added in quadrature, and the full line corresponds to the statistical and total systematic errors added in quadrature. The overall normalisation uncertainty of 3.5% due to the luminosity and 10% due to the subtraction of the double dissociation background is not included.

"conclude": large amount of IP momentum carried by glue

OR

there is no momentum sum rule

OR

⋮

(ZEUS: same ~ result in photoproduction)

Photoproduction complementary to DIS

look at jet sample in diffractive photoproduction
probes ~ similar scale

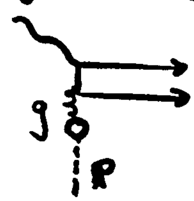

apparent total $\mathbb{P}$ momentum carried by constituents

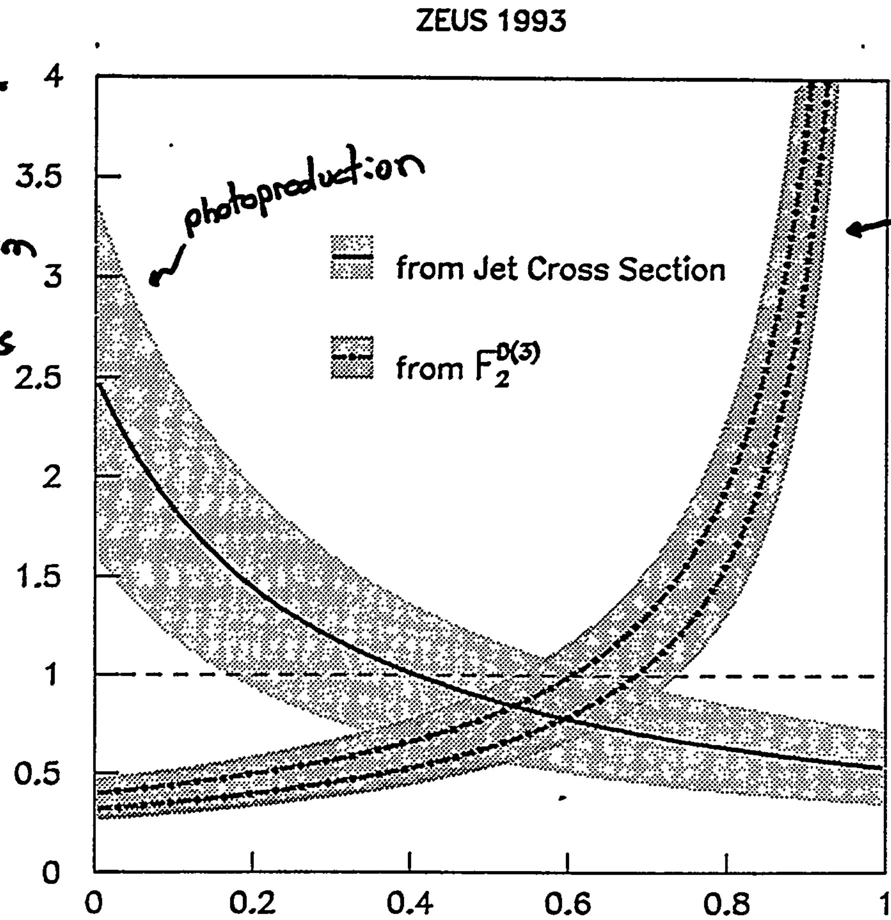

DIS

"all g"

"all q"

gluon fraction

Figure 4: The plane of the variables $\Sigma_{\boldsymbol{P}}$ (momentum sum) and c_g (relative contribution of hard gluons in the pomeron). The thick solid line displays the minimum for each value of c_g obtained from the χ^2 fit (the shaded area represents the 1 σ band around these minima) to the measured $d\sigma/d\eta^{jet}(\eta^{had}_{max} < 1.8)$ using the predictions of POMPYT. The constraint imposed in the $\Sigma_{\boldsymbol{P}} - c_g$ plane by the measurement of the diffractive structure function in DIS ($F_2^{D(3)}$) [10] for two choices of the number of flavours (upper dot-dashed line for $\Sigma_{\boldsymbol{P}q} = 0.40$ and lower dot-dashed line for $\Sigma_{\boldsymbol{P}q} = 0.32$) is also shown. The horizontal dashed line displays the relation $\Sigma_{\boldsymbol{P}} = 1$.

consistency between DIS & photoproduction ⇒ 30%-80% of the momentum of the pomeron carried by partons is due to hard gluons. (does not depend on validity of sum rule, but does depend on common flux factor)

Rapidity gaps between jets in photoproduction

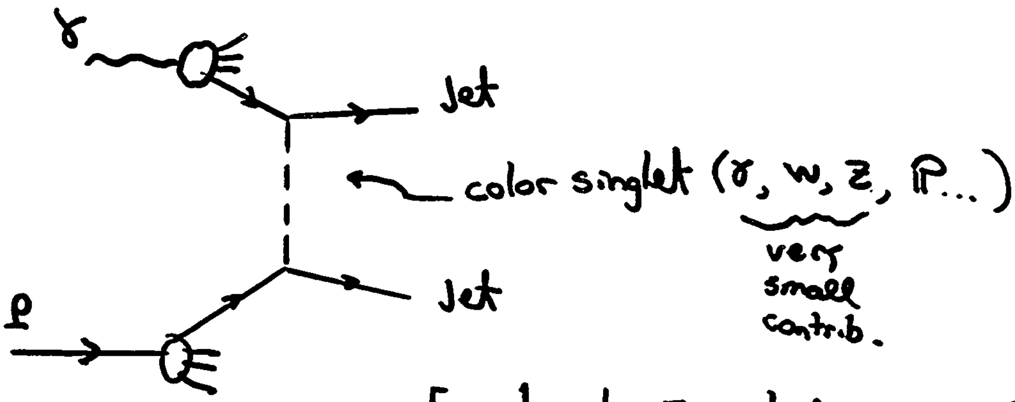

[similar to $\bar{p}p$ studies @ CDF, DØ]

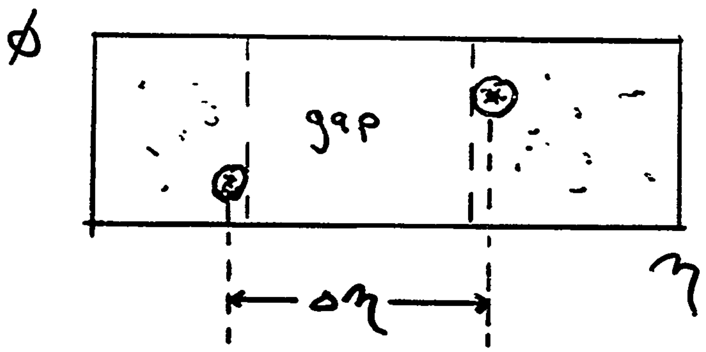

require $E_T^{Jet} > 6$ GeV

Expect gaps in color non-singlet exchange to be ~ exponentially suppressed w/ $\Delta\eta$

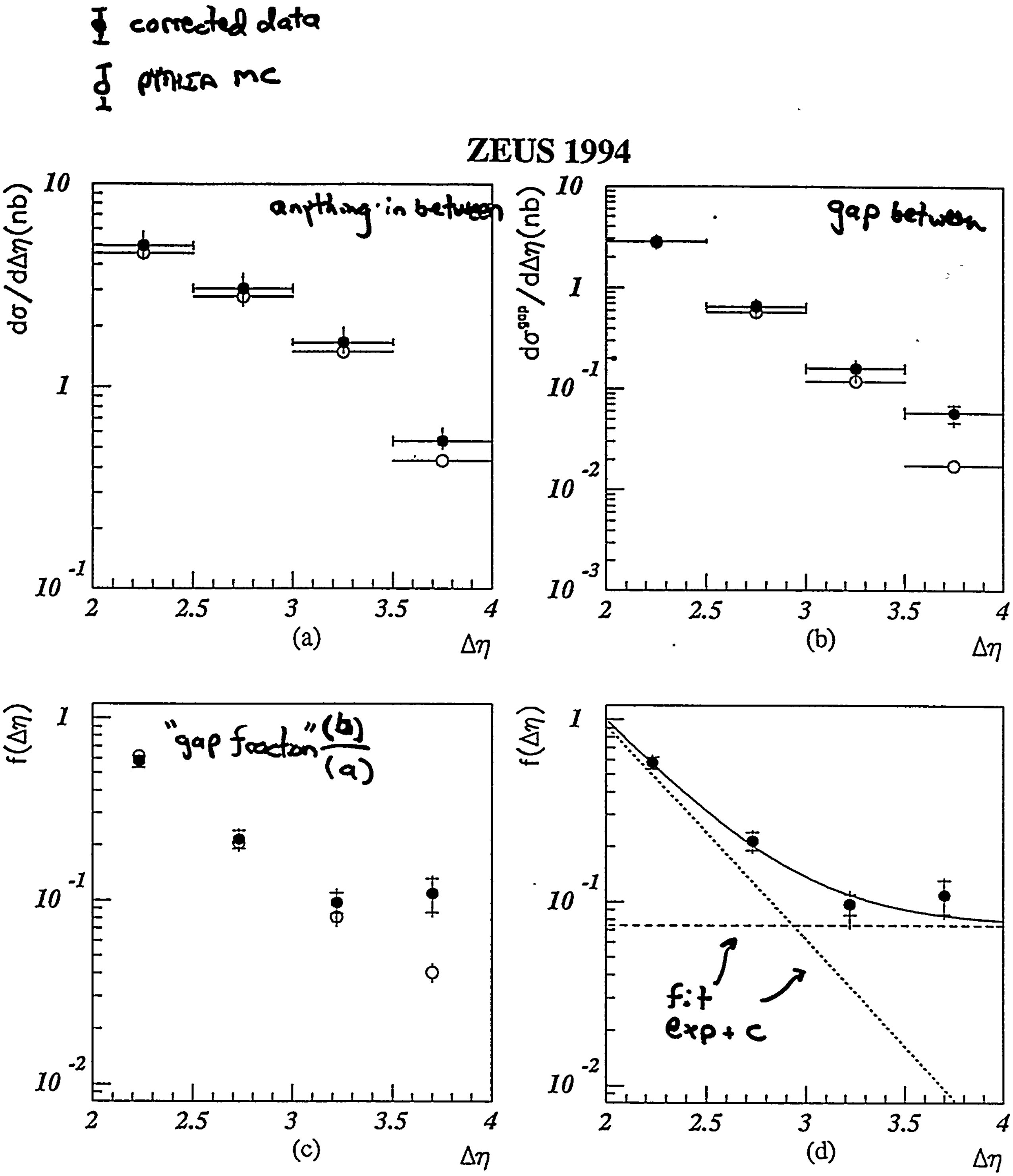

Figure 3: ZEUS data (black circles) corrected for detector effects. The inner error bars represent the statistical errors from the data and Monte Carlo samples, and the outer error bars include the systematic uncertainty, added in quadrature. In (a), (b) and (c) the PYTHIA prediction for non-singlet exchange events is shown as open circles. The inclusive cross section is shown in (a). The cross section for gap events is shown in (b) and the gap-fraction is shown in (c). The gap-fraction is redisplayed in (d) and compared with the result of a fit to an exponential plus a constant. In (c) and (d) the points are drawn at the mean $\Delta\eta$ of the inclusive distribution in the corresponding bin.

Exclusive Vector Meson Production in DIS

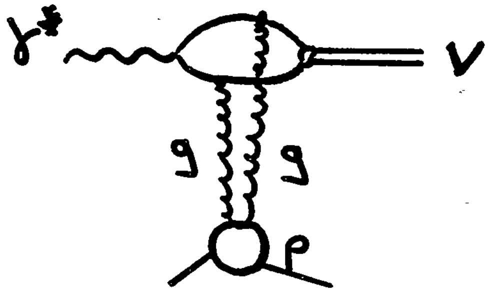

- perturbative QCD calculation of an exclusive process. A prediction! Brodsky - Frankfurt - Gunion - Mueller - Strickman
- probe $g(x,Q^2)$ directly
- good signature $ep \to ep\rho$

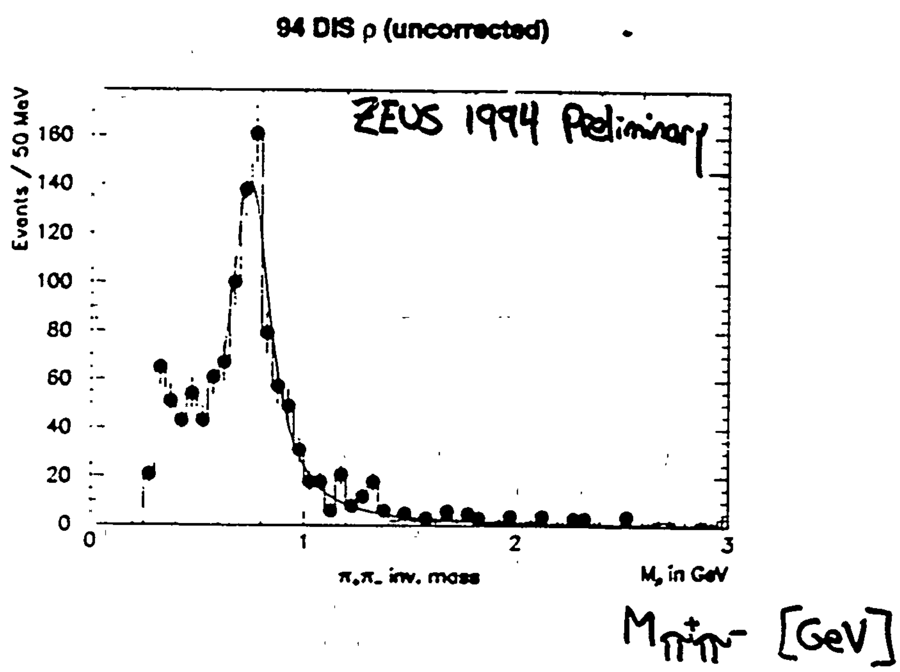

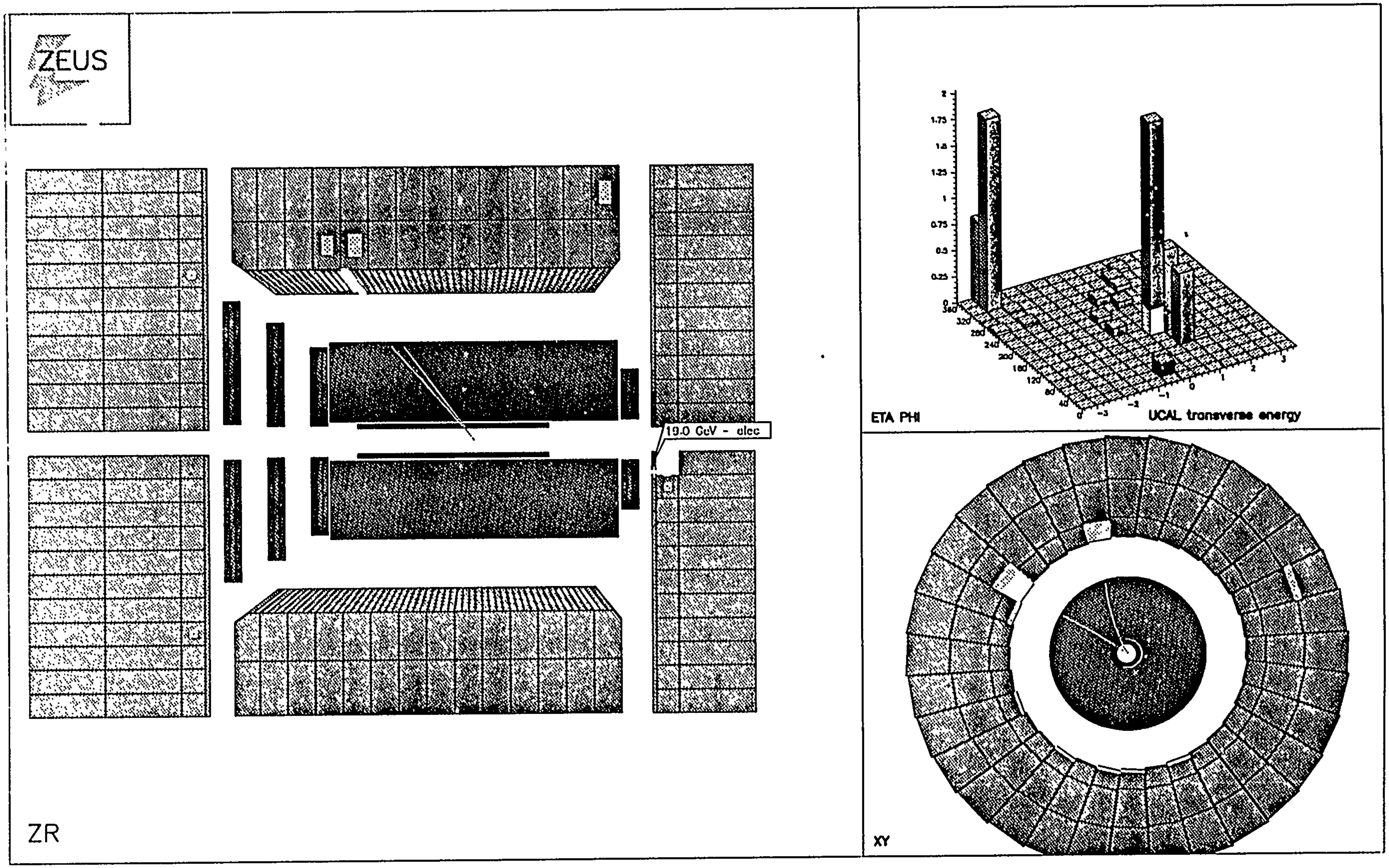
ZEUS
19.0 GeV - elec
ZR
ETA PHI
UCAL transverse energy
XY

ρ cross-sections at different Q^2: behavior w/ W (γ^*_p c.m. energy)

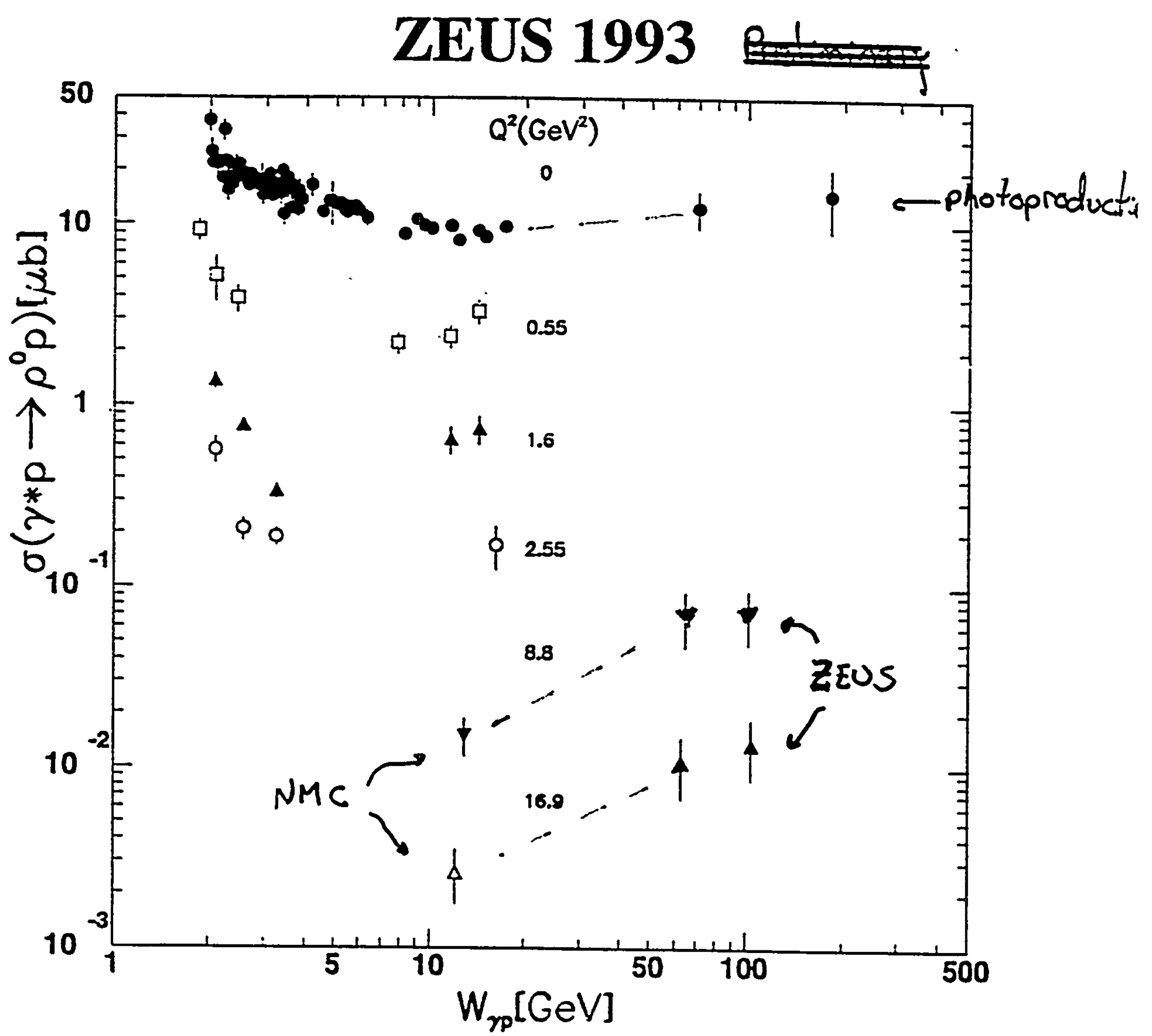

- In DIS regime, a rising cross-section for exclusive process; qualitatively different from photoproduction driven by glue?: $\sigma \sim [xg]^2 \sim [x^{-0.35}]^2 \sim W^{2(0.7)} = W^{1.4}$ at small x.
- Much more to come from 1994, 1995 data
  better statistics, ϕ, J/ψ, ω...

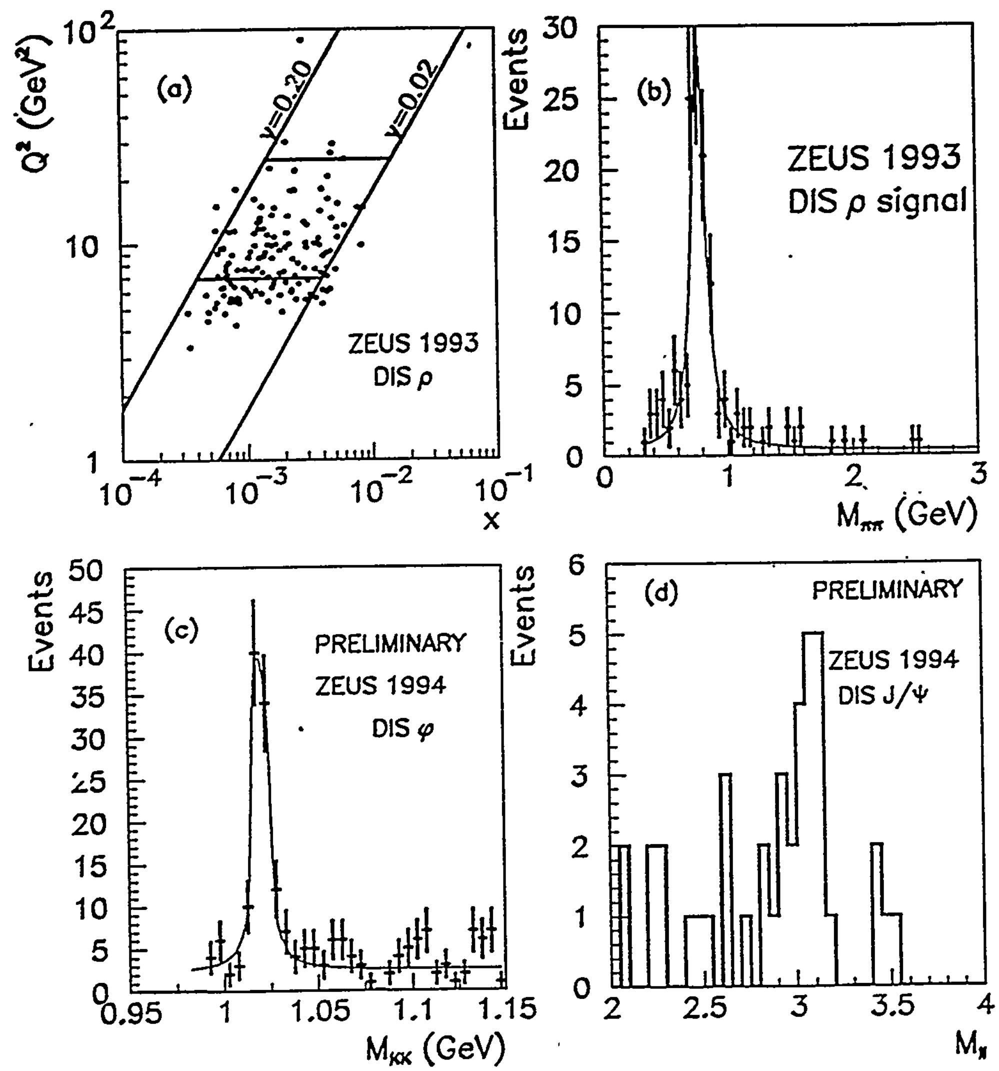

Figure 1: The phase space region covered by the 1993 DIS ρ sample is shown in Fig 1(a). Fig. 1(b) shows the $\pi^+\pi^-$ invariant mass spectrum from the 1993 data, with a clear signal for ρ production. Fig. 1(c) shows the φ signal in the K^+K^- mass spectrum for the 1994 data, and the 1994 J/ψ signal is shown in Fig 1(d).

ϕ cross-sections at different Q^2: behavior with W ($\gamma^* p$)

ZEUS 1994 PRELIMINARY

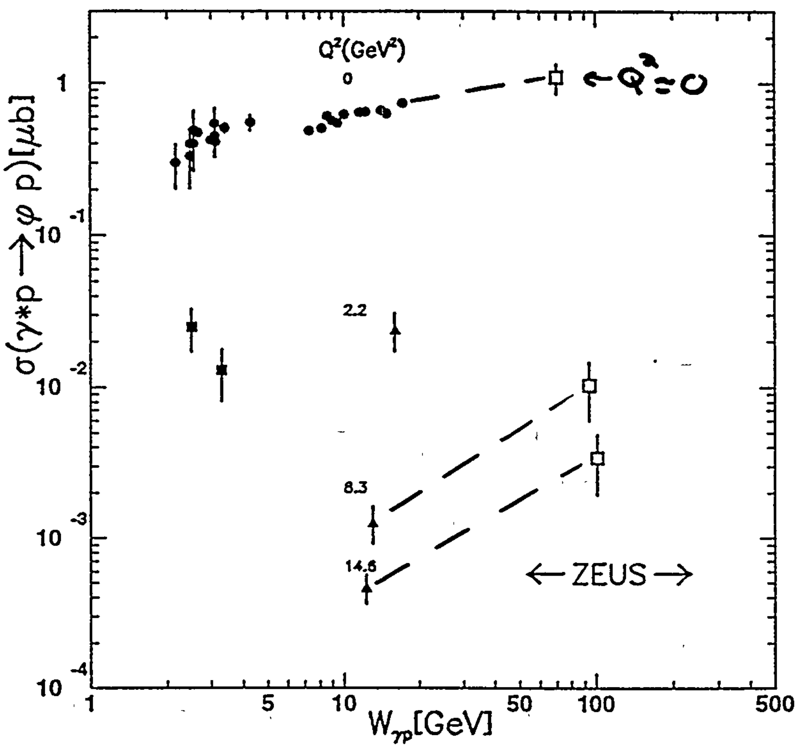

Figure 3: The $\gamma^* p \to \varphi p$ cross section (using the data collected in 1994 by ZEUS) as a function of W, the $\gamma^* p$ centre of mass energy, for several values of Q^2. The low energy data ($W < 20$ GeV) come from fixed target experiments. The high energy data ($W > 50$ GeV) come from the ZEUS experiment [1] and the present analysis. ZEUS data at $Q^2 = 8.3$ systematic normalisation uncertainty (not shown).

ρ, ϕ in photoproduction ($Q^2 \simeq 0$) well described by VDM,

but not J/ψ

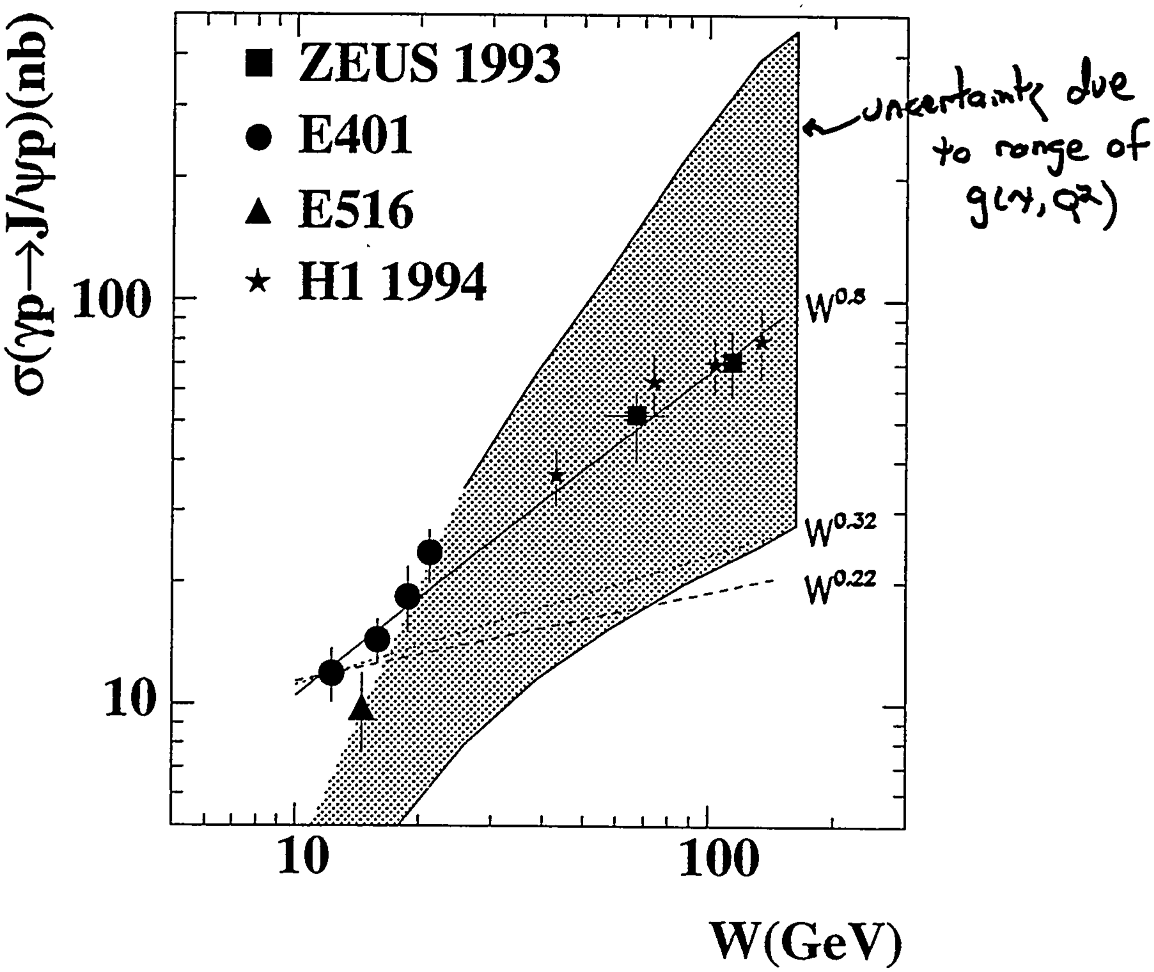

pert. calculations of exclusive ρ, ϕ, J/ψ production

→ promising technique to extract $g(x, Q^2)$

Summary

- Diffractive physics is important at HERA
- True underlying nature of the phenomena
  still unknown — join the fun!
- "Factorizing" flux + structure fn is

  Revealing the substructure* of the pomeron ???

  or

  just a way to present the data
- we need a set of tests to distinguish pictures
  (which are in different frames!)
- understanding this physics is important :

  IP plays a significant role in the life of the proton
  and it has the quantum numbers of the vacuum

* ok if no ∞-momentum frame ??

Leading Proton Spectrometer

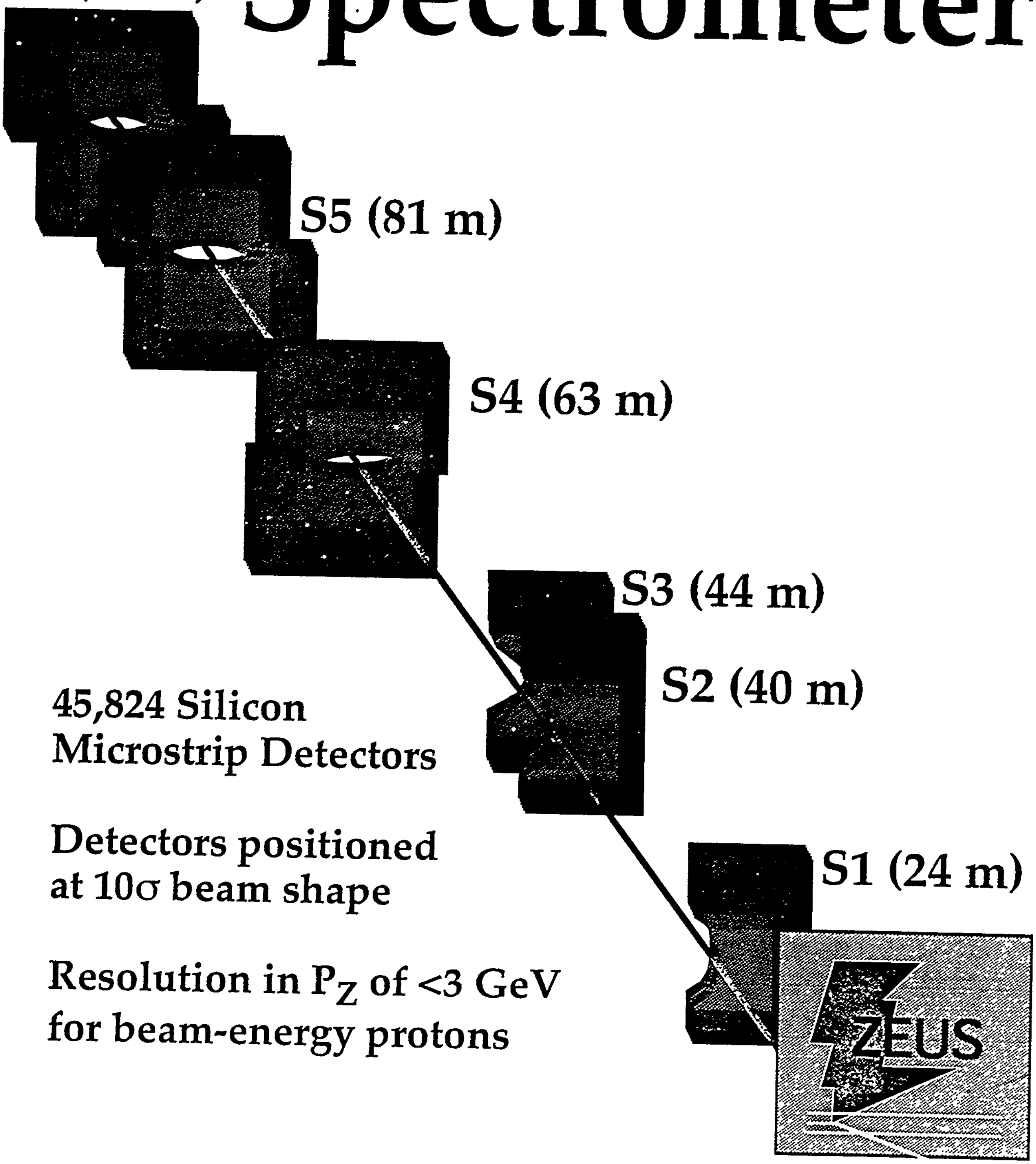

- 45,824 Silicon Microstrip Detectors
- Detectors positioned at 10σ beam shape
- Resolution in P_Z of <3 GeV for beam-energy protons

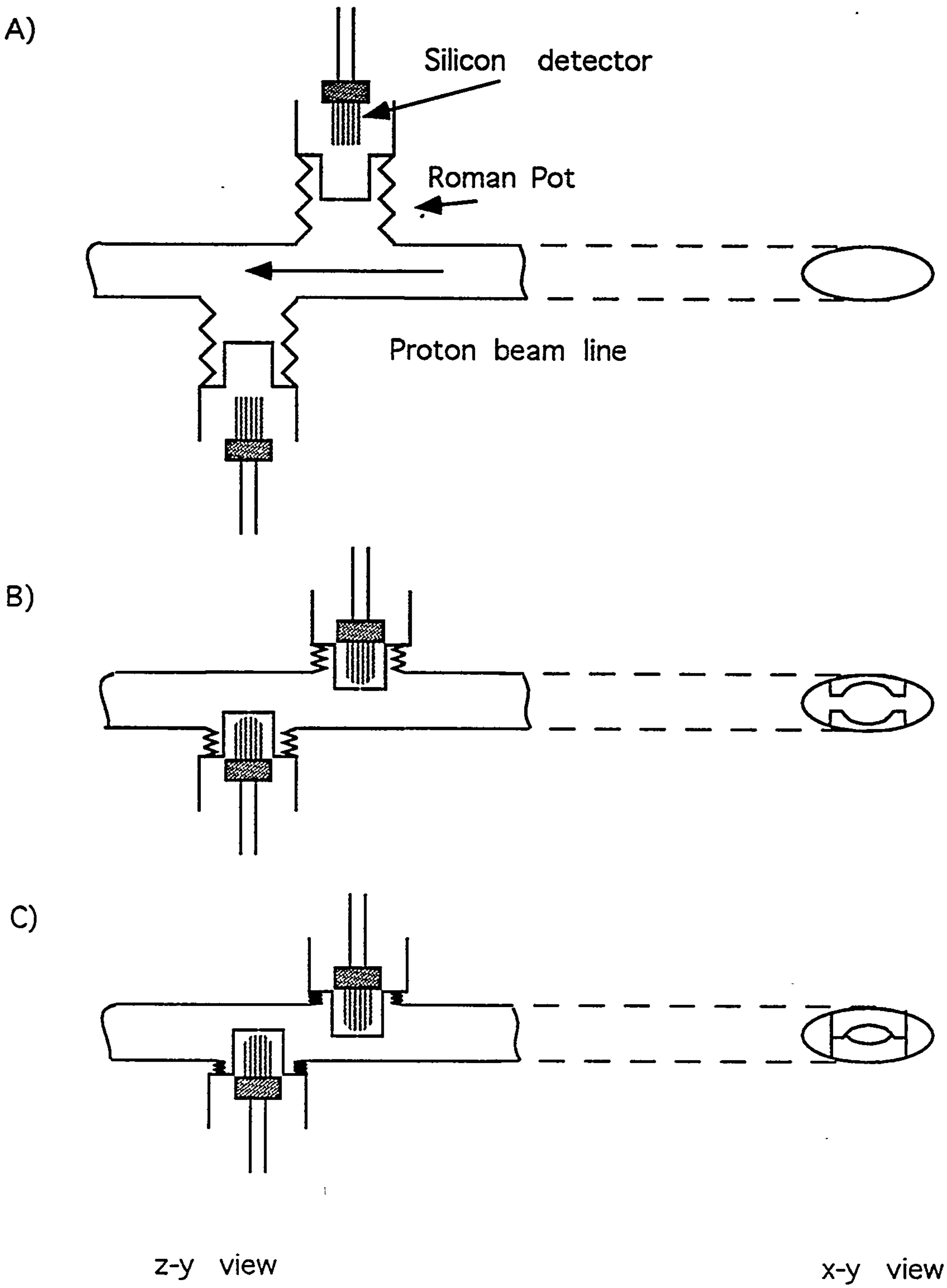
A)
Silicon detector
Roman Pot
Proton beam line
B)
C)
z-y view
x-y view

1994 ZEUS Preliminary (0.54 pb^{-1})

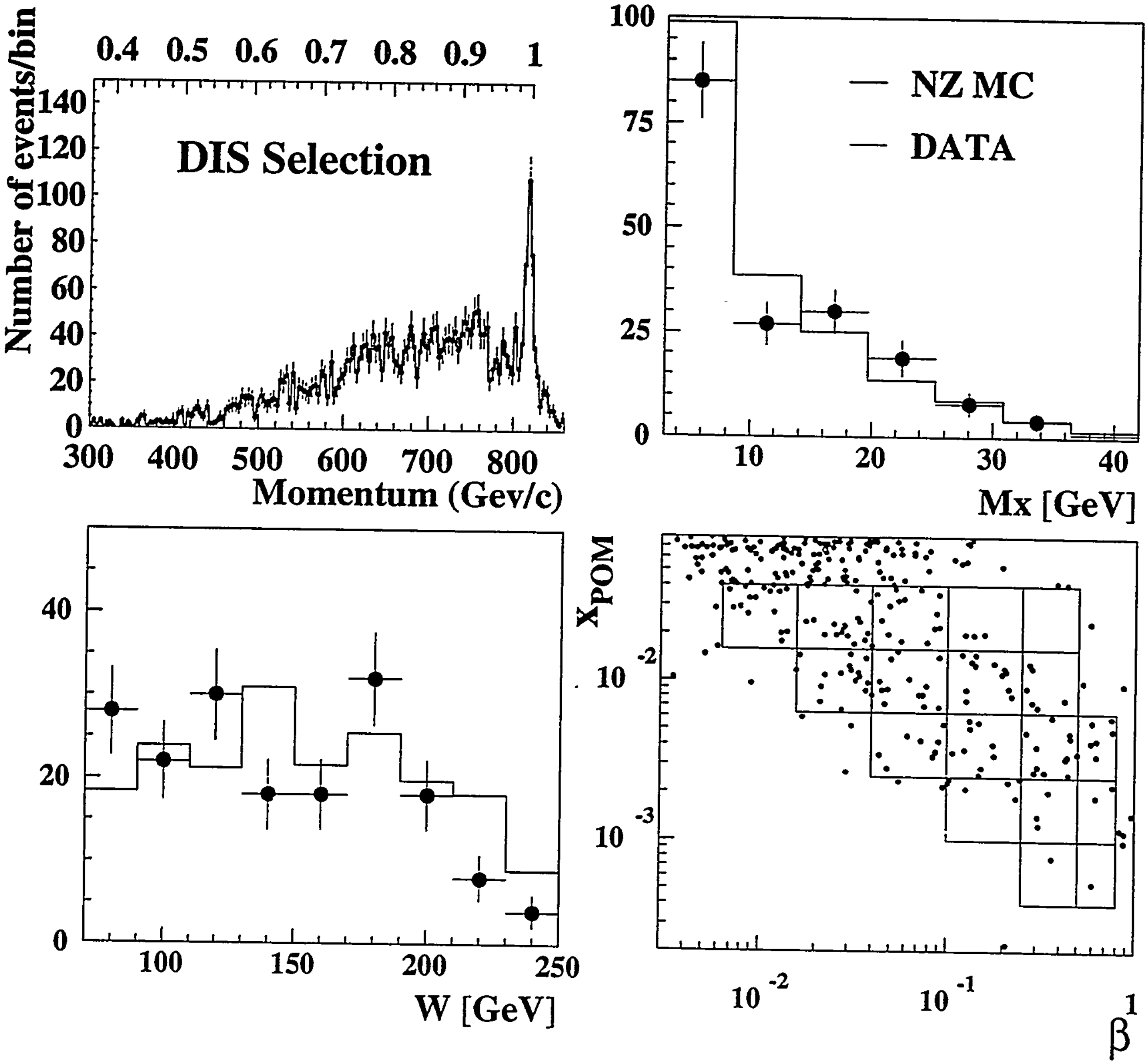

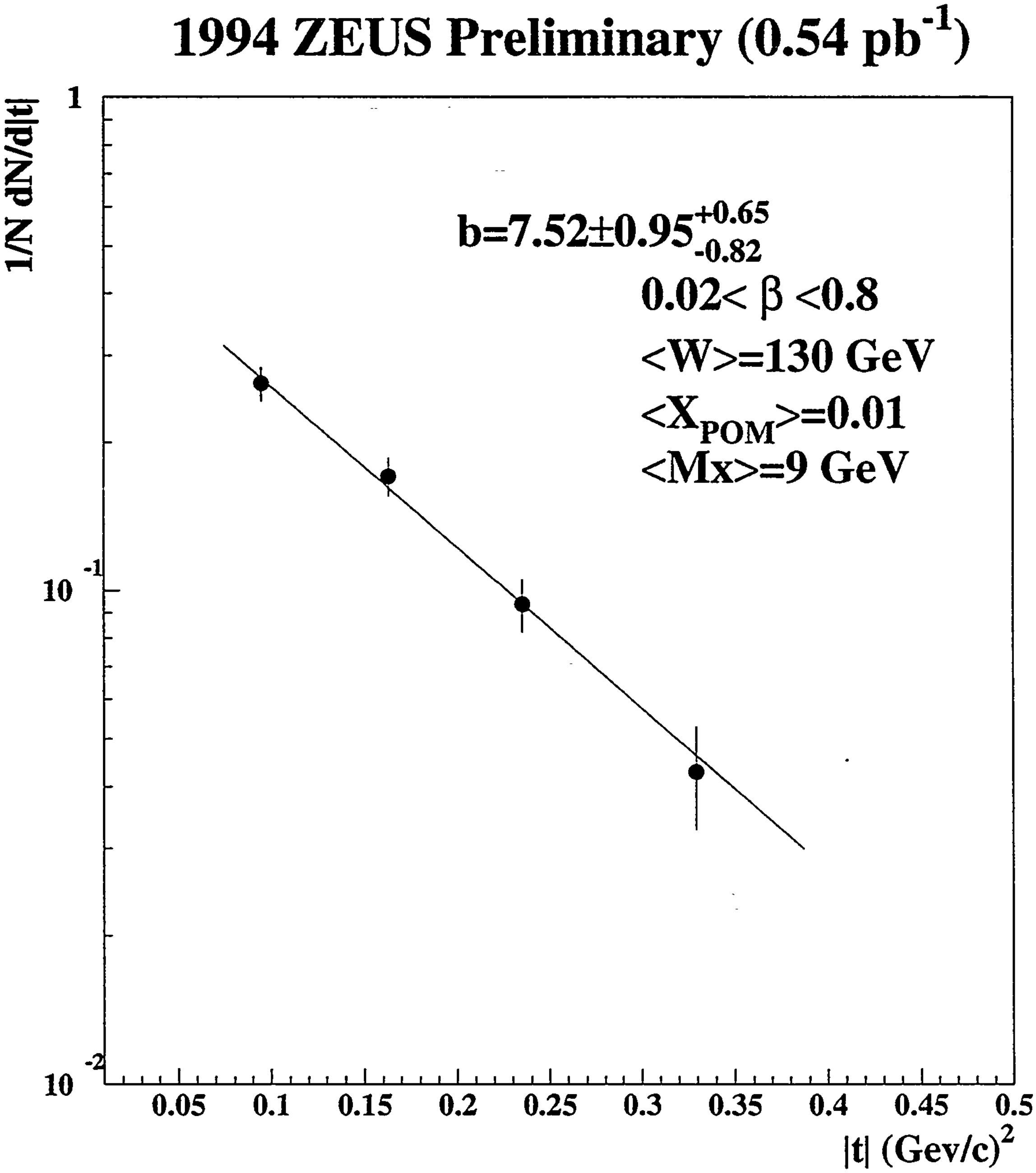

an advertisement for things to come: in bins of M_X

"hard" vs. "soft" processes

OTHER HERA ep PHYSICS THUS FAR (by Q^2)

photoproduction:

- jet cross-sections
- hard scattering
- J/ψ production
- photon remnant studies
- γp cross-section
- direct, resolved processes
- diffractive studies
- D^*
- inclusive charged particle production

DIS:

- jets
- multiplicity distributions
- Energy flows
- high x jets
- α_s

Exotica:

- Leptoquarks
- excited fermions
- heavy leptons
- squarks

much more to come from '94 data
'95 run underway

Diffractive eA/pA/AA Physics?

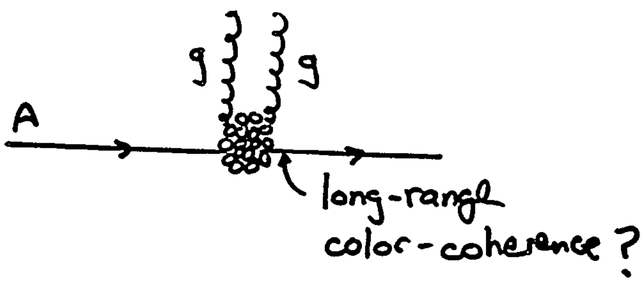

- nuclear diffractive excitations?
- nuclear diffractive dissociation (fission)?
- "ordinary" IP from single nucleon in A environment

dc at Hera

→ Useful to study "peripheral" interactions at RHIC in extreme forward-backward regions? (pA, AA)

Other physics?

Tachyphobia: the (irrational?) fear of large rapidity

GRAND SUMMARY

- rise of F_2 at low x exciting
  underlying dynamics needs clarification
  $\Rightarrow$ low Q^2 interesting?
- first extractions of $xg(x,Q^2)$ — rise at low x, long road ahead
- diffractive contribution to F_2 — "partonic pomeron"?? more study!
- exclusive vector meson production
- low + high Q^2 frontiers

"it is very difficult to remember that events now in the past were once far in the future"

- Frederic William Maitland

Longterm Program

this year factor ~ 3-~~5~~ ~ 2 data?
continued detector improvement, understanding (FNC, LPS, presampler, new BPC, HES, PRT, ...)
measure R next year?
e polarization
deuterium?
ρ polarization?
incremental lumi upgrades?
heavy ions?

Lots to keep us busy for many years!

HERA: Potential with Nuclei

Mark Strikman
Penn State University

WORKSHOP " FUTURE OF HERA "

SEPTEMBER 95 - MAY 96
VOLUME OF FINDINGS - SUMMER 96.

9 WORKING GROUPS

WORKING GROUP 8: "LIGHT AND HEAVY NUCLEI"

CONVENERS:
M.ARNEODO (ZEUS)
A.BIALAS (CRACOW NUCL.PHYS.INST.)
W.KRASNY (H1)
T.SLOAN (UNIV. OF LANCASTER)
G.VAN DER STEENHOVEN (HERMES)
M.STRIKMAN (PSU)

CHARGE: TO INVESTIGATE POTENTIAL OF HERA FOR eA PHYSICS
- HERMES (E_e=27 GEV, FIXED TARGET), COLLIDER MODE.

WORK OF THIS WORKING GROUP IS CONSIDERED AS A LONGER RANGE PROJECT - NUCLEAR WORKSHOP PLANNED FOR DECEMBER 96.

DESY CONSIDERS ALSO BUILDING CONTINUOUS ELECTRON BEAM FACILITY FOR NUCLEAR PHYSICS (E_e=27 GEV) AS A PART OF FUTURE LINEAR COLLIDER COMPLEX. SEPARATE STUDY.

The Future

Research based on the exploitation of an electron-positron linear collider facility

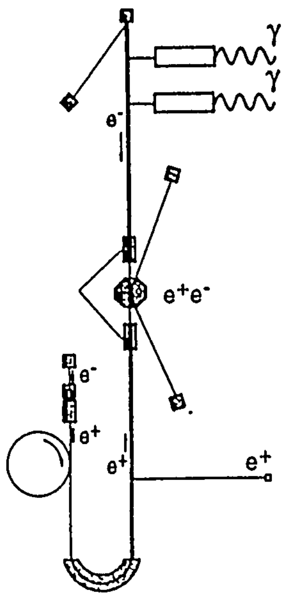

Highly intense source of coherent synchrotron radiation with wavelengths of order 1 Å

Particle physics (the universe 10^{-12} seconds after the „big bang")

Nuclear physics (NuPECC)

Development Program

Construction of a 500 - 1000 MeV superconducting linear collider

Construction of a bright coherent synchrotron radiation source with wavelengths of order 60 Å

Collaboration

D	Max Born Inst. Berlin, DESY, GH Wuppertal, Univ. Frankfurt, FZ Karlsruhe, TH Darmstadt, TU Berlin, TU Dresden
F	IPN Orsay, LAL Orsay, CEA Saclay
I	INFN Frascati, Milano, Roma,
PL	Polish Academy, Univ. Cracow, Univ. Warsaw
RUS	JINR Dubna, IHEP Protvino, Inst. of Nucl. Phys. Novosibirsk
SF	SEFT Helsinki
USA	Cornell Univ., Fermilab, UCLA
VR China	IHEP. Academia Sinica

From B. Wiik talk

Future Options.

- **Luminosity upgrade**

  Joint working group of accelerator and experimental Physicists

  Technical Proposal
  Cost / Schedule
  Physics Impact
  Report ~ spring -96

  $250\,pb^{-1} \longrightarrow 1000\,pb^{-1}$

- **Polarisation**

  Continue the feasibility study
  - if positive then set up a working group

  Workshop in Zeuthen

- **Store Nuclei in HERA**

  Define the physics issues.
  Involve the nuclear physics community.
  Small workshop ~ late 1996.

  Light nuclei: D, He^4, $_6C^{12}$ --

  Heavy nuclei

Kinematic range of HERA for eA scattering

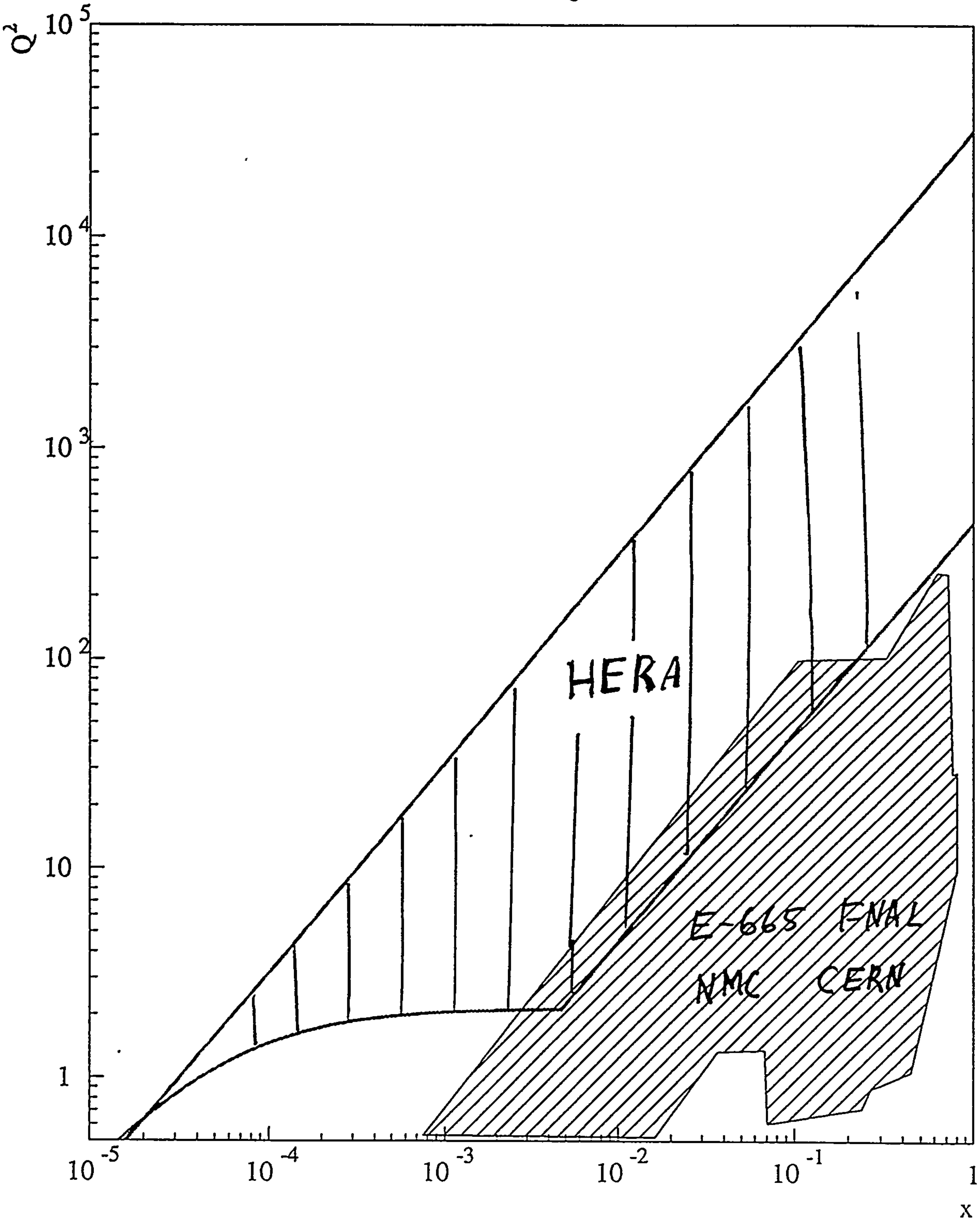

significant overlap with high precision NMC data

WILL DISCUSS ONLY COLLIDER PHYSICS.

PARAMETERS: E_{e^+}=27.5 GEV, E_A= 820 GEV/ A * (Z/A)

Equivalent lab energy $E_e \approx 20$ TEV ⇒ X RANGE $10^{-4} < x < 0.1$

FIG.1

INTENSITY (IF LUMINOSITY IS HIGH) DECREASES AS

$1/Z^2$ DUE TO INTERACTION WITH GAS IN THE BEAM PIPE

COUNTING RATE DECREASES AS

$$\frac{A}{Z^2}$$ (NEGLECTING SHADOWING EFFECTS)

(~ 1/3 FOR CARBON AND ~ 1/10 FOR CALCIUM)

FOR COHERENT PROCESSES REDUCTION EVEN LESS SIGNIFICANT

$$\frac{A^{4/3}}{Z^2}$$ (NEGLECTING SHADOWING EFFECTS)

(~ 0.8 FOR CARBON AND ~ 1/3 FOR CALCIUM)

cost of building ion source delivery system based on GSI experience

$\sim 15 \cdot 10^6$ D.M.

KEY ISSUES FOR INVESTIGATION

I) NONLINEAR HIGH DENSITY PHENOMENA IN QCD - nuclear shadowing of parton distributions

II) COLOR TRANSPARENCY AT ULTRA-HIGH ENERGIES -

When interaction of a small object becomes large (if ever). Interplay of soft and hard physics in diffraction.

III) QUARK AND COLOR DIPOLE PROPAGATION THROUGH THE NUCLEAR MATTER; HADRON FORMATION AND FINAL STATE INTERACTIONS

ALL THESE ISSUES HAVE IMPLICATIONS FOR HEAVY ION PHYSICS AT LHC & RHIC

In QCD parton densities increase at small x. Expect evolution equations break down when densities large enough.

- For proton target $x \sim 10^{-5} - 10^{-6}$

- For nucleus enhancement of parton densities <u>in impact parameter space</u> by the factor

$$A^{1/3}$$

$\Longrightarrow$ Nonlinear phenomena should start much earlier at

(*) $x \sim 10^{-3} - 10^{-4}$ for $Q^2 = 5\ GeV^2$

for σ_A. Based on unitarity.

(*) more optimistic than Mueller & Qiu which was based on GLR type model.

Questions to be studied at HERA:

i) How shadowing increases (?) for fixed Q^2 with decrease of x ?

Already real γ is interesting

ii) Rate of decrease of shadowing with increase of Q^2 at fixed x.

Nonlinear effects, leading twist vs higher twist shadowing.

iii) Gluon shadowing vs F_{2A} shadowing

No published data for G_A $\Rightarrow$ wide range of expectations.

Reminder: Shadowing $\equiv$

$$R_A = \frac{1}{A} \frac{F_{2A}(x,Q^2)}{F_{2p}(x,Q^2) + F_{2n}(x,Q^2)} < 1 .$$

for $x \le 0.05$

T. Sloan

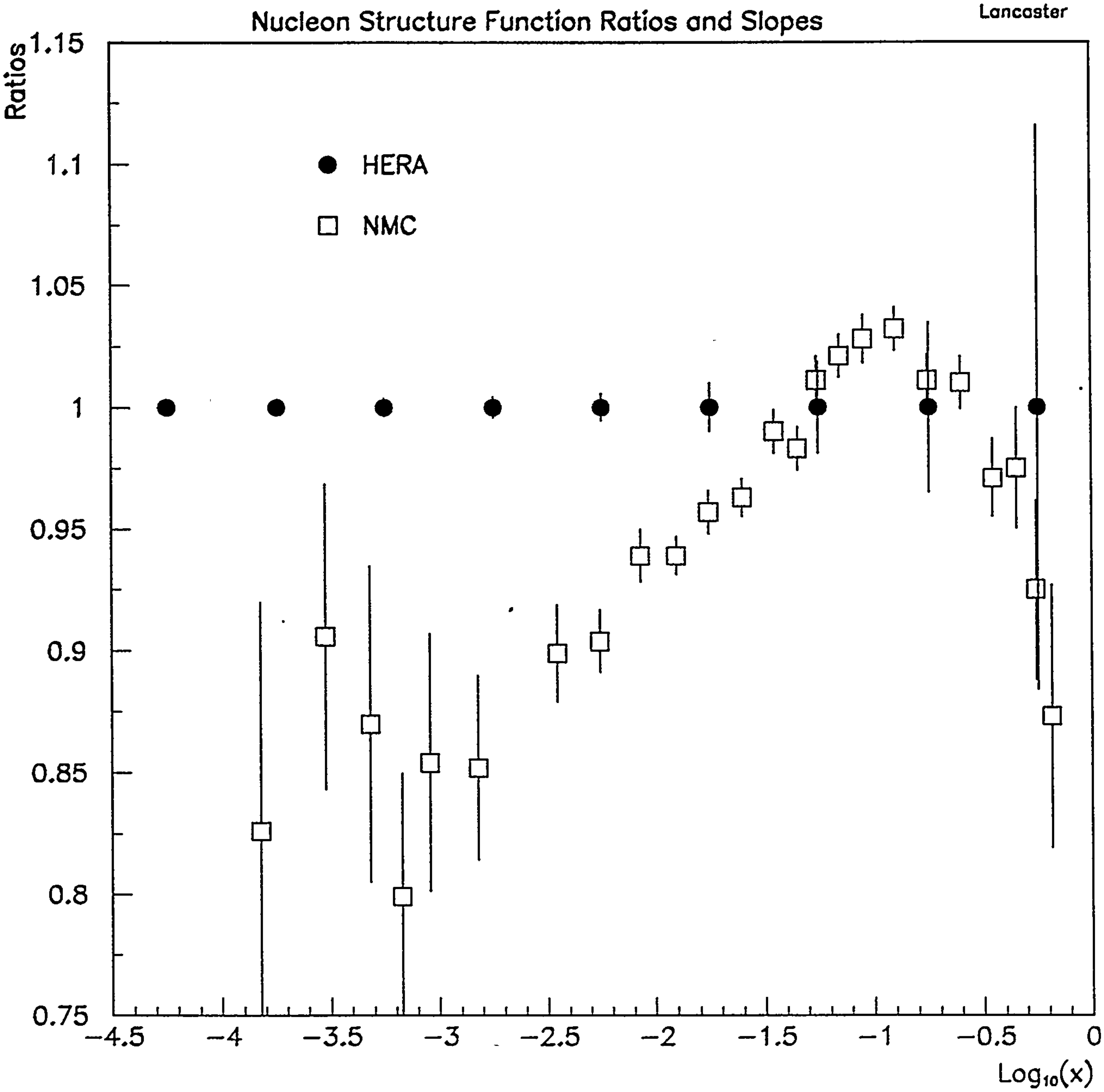

No systematic errors

Luminosity $(pb^{-1}/nucleon$ $\equiv \frac{1}{A}$ beam inten[s]
for protons
for 1 pb^{-1}

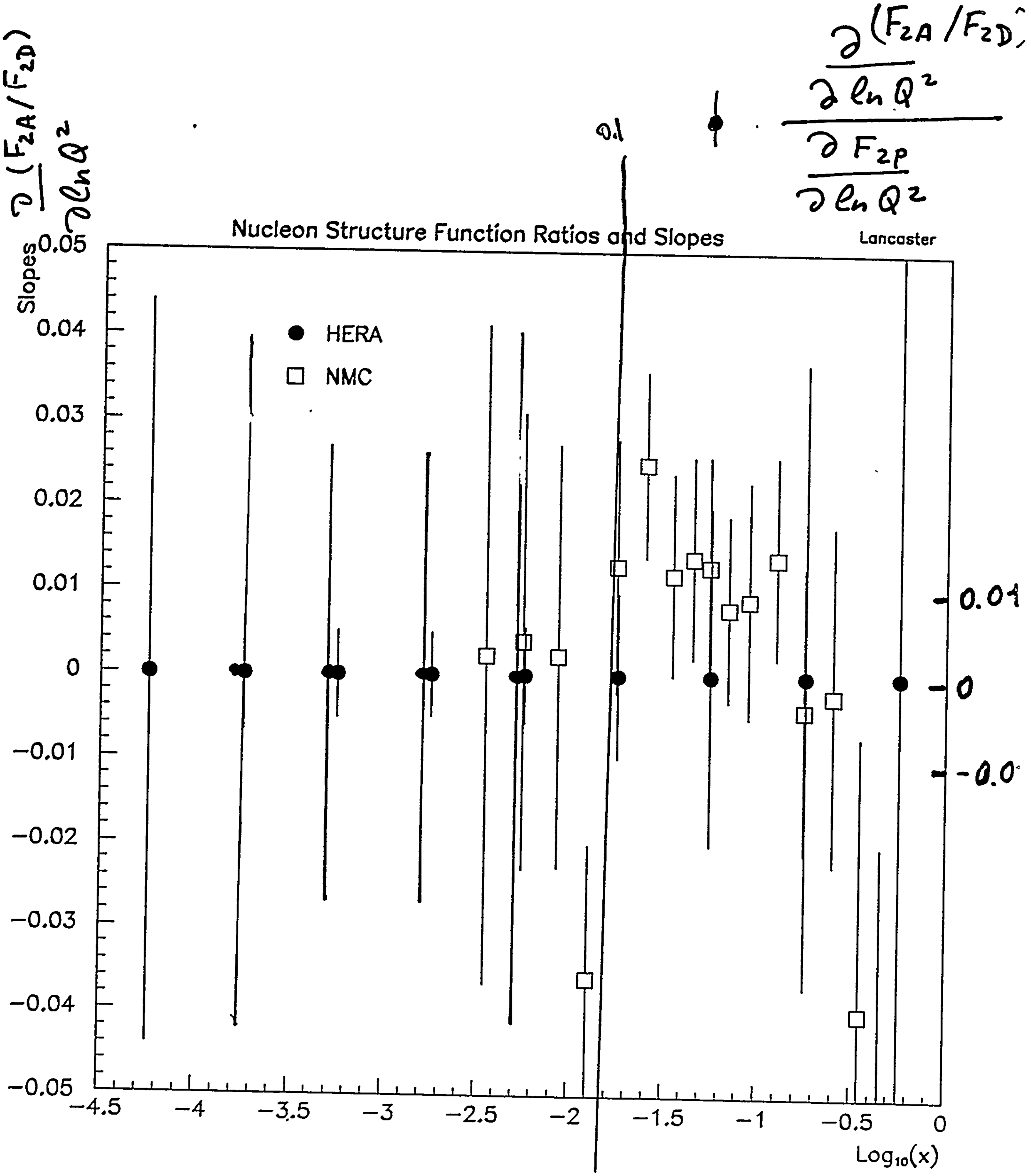

$\frac{\partial (F_{2A}/F_{2D})}{\partial \ln Q^2}$
0.1
$\dfrac{\frac{\partial (F_{2A}/F_{2D})}{\partial \ln Q^2}}{\frac{\partial F_{2p}}{\partial \ln Q^2}}$
Nucleon Structure Function Ratios and Slopes
Lancaster
Slopes
0.05
0.04
0.03
0.02
0.01
0
−0.01
−0.02
−0.03
−0.04
−0.05
HERA
NMC
0.01
0
−0.0
−4.5
−4
−3.5
−3
−2.5
−2
−1.5
−1
−0.5
0
$\mathrm{Log_{10}(x)}$

Dynamics of nuclear shadowing.

1) x, A - dependence at Q_0^2 -scale where QCD evolution starts

$$\bar{q}_A(x, Q_0^2)\,,\quad g_A(x, Q_0^2),\quad V_A(x, Q_0^2)$$

2) Q^2 - evolution - down to what x GLDAP evolution eq. works, at what x nonlinear effects are large.

At small x parton densities are large $\Rightarrow$ nonlinear effects possible

like

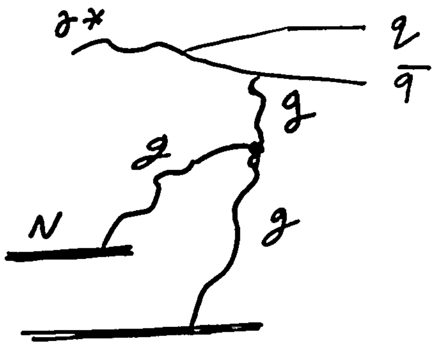

$\propto$ [parton density]^2

In the region of x, Q^2 studied so far effects are small

At smaller x effects should increase especially for gluon density: $xG \gg xq$, effective interaction is larger.

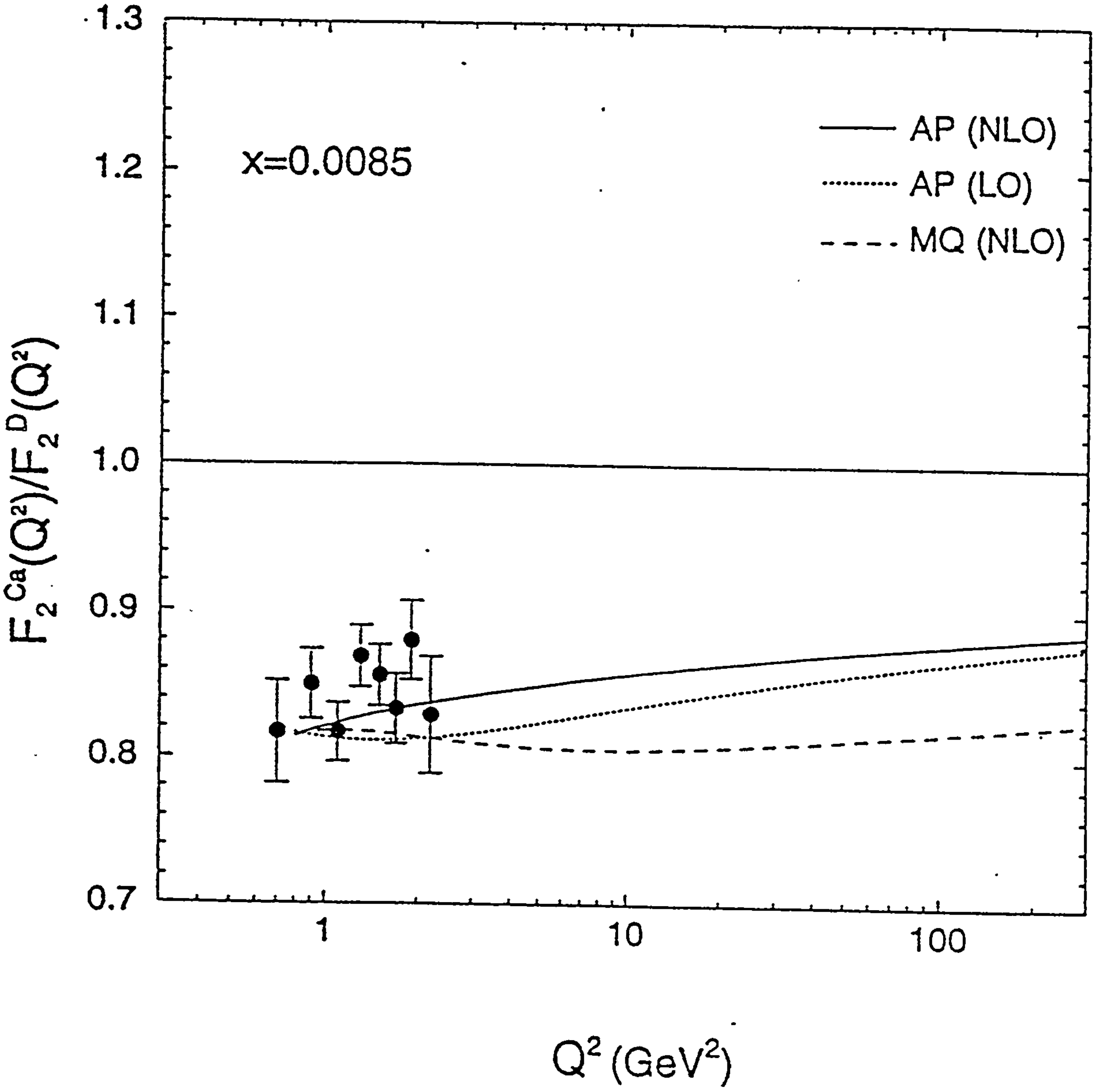
x=0.0085
AP (NLO)
AP (LO)
MQ (NLO)
$F_2^{Ca}(Q^2)/F_2^D(Q^2)$
1.3
1.2
1.1
1.0
0.9
0.8
0.7
1
10
100
Q^2 (GeV^2)

Kumano

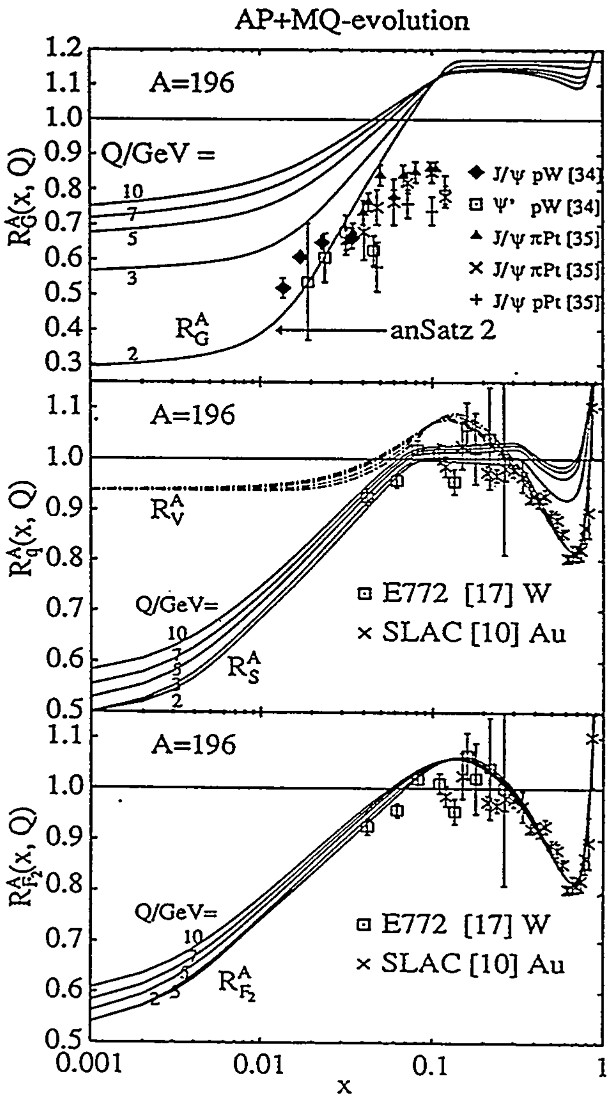

Fig. 3. The same as fig. 2 but with gluons in the *ansatz 2* at the initial scale $Q = 2$ GeV. Here the evolution of sea, and hence $R_{F_2}^A$ is clearly slower than with the gluons of 'Ansatz 1': the stronger shadowing of gluons is reflected to the behavior of R_S^A since the evolution eqs. (13) and (14) are coupled.

93

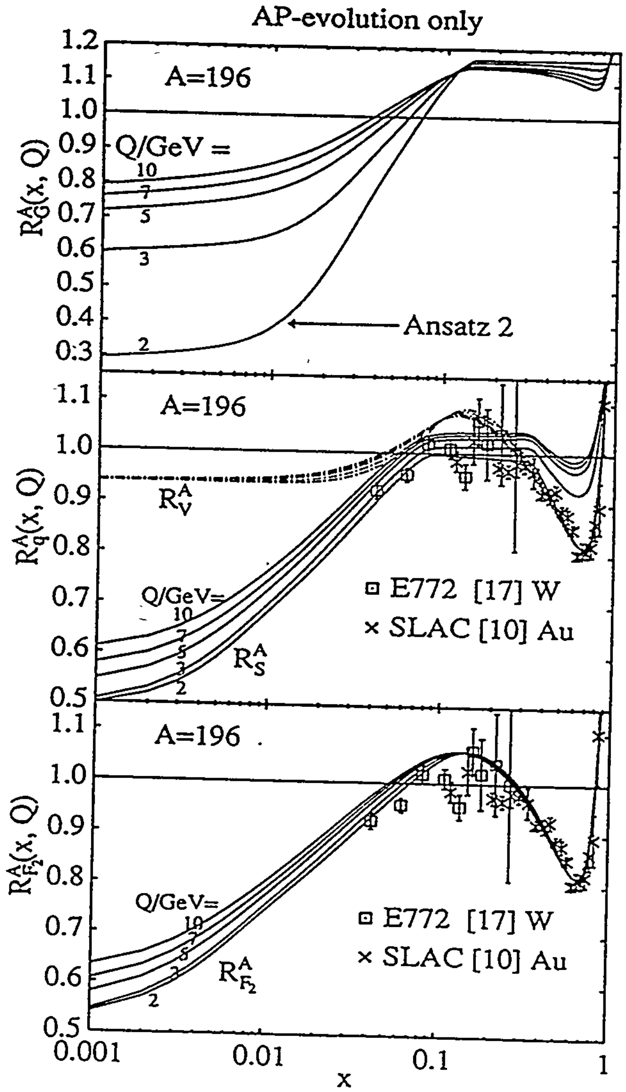

Fig. 4. The same as fig. 3 but with the scale evolution given by the traditional Altarelli–Parisi terms only (eqs. (12)–(14) without the modifications). By comparing figs. 3 and 4 we see that the mainline of QCD-evolution is determined by the unmodified Altarelli–Parisi equation; the Mueller–Qiu modifications then give the corrections to this evolution by slowing down the relative evolution of partons [15,16].

Nuclear shadowing at Q_0^2.

Physics: at small x large longitudinal distances are essential in $\gamma^* A$ interaction in the nucleus rest frame

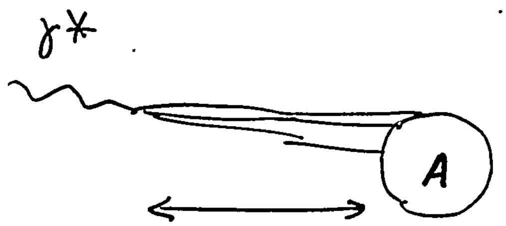

$$\ell \simeq \frac{1}{2 m_N x} \gg 2R_A$$

In frame where nucleus is fast:

wee $\frac{1}{\mu}$

$r_A \frac{m_A}{x p_A}$

: strong overlap of small x partons belonging to different nucleons.

fast partons

$\sim r_A \frac{m_A}{p_A}$

Two types of models:

Color singlet models

(white object exchange (Pomeron?)

leading twist QCD

Shadowing due to interaction of large size $q\bar{q}$ configurations which have small probability

Bj, FS, Brodsky & Liu, Nikolaev & Zakarov (91)

Kwiecinski, Kopeliovich & Povh

Generalized VDM (higher twist)

Interaction with small $\sigma \propto \frac{1}{Q^2}$, $\sigma(M^2) \sim \frac{1}{M^2}$, $M^2 \propto Q$

Shilknecht, Weise Piller, S.

[usually formulated in nucleus rest fran

Color octet models

Mueller & Qiu, Qiu, Close et al, Levin & Rys Eskola, Kumano

Generalized parton model

parton fusion mechanism.

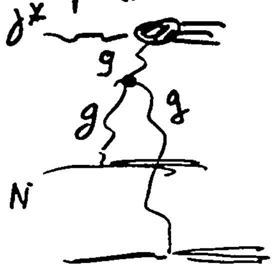

$\Downarrow$

qualitative difference for diffraction in DIS. (see below).

Nuclear shadowing in color singlet model:
[Discussion of color octet model, Qiu talk]

Main contribution in the x, Q^2 range probed at CERN, FNAL

Due to interaction of configurations in γ^* of large transverse size

$r \sim 1/\Lambda_{QCD}$ not $1/Q$

QCD Aligned Jet model FS88-89

Covariant model of Brodsky & Lin 90

2-gluon exchange model Zakharov & Nikolaev 90, Capella et al.

$\langle \sigma \rangle \simeq 15\text{-}17\,mb$ for $x \sim 10^{-2}$

- effects due to dispersion of σ
- small correction.

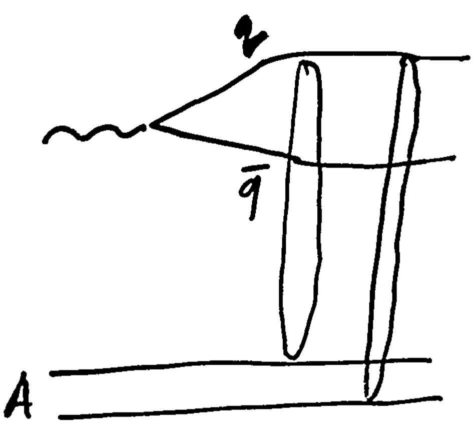

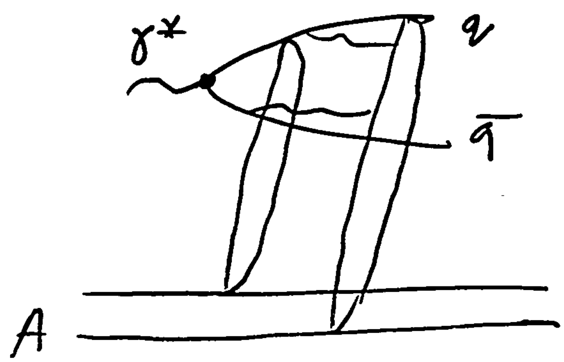

low Q^2 $\Longrightarrow$ large Q^2

x - dependence of shadowing is due to decrease of $q_{\parallel} = x m_N \left(1 + \frac{M^2}{Q^2}\right)$ with decrease of x. (increase of longitudinal distances $\ell \simeq \frac{1}{2 m_N x}$.

Reasonably reproduces

F_{2A}/F_{2D} , $\bar{q}_A/\bar{q}_N$

At small $x \le 10^{-3}$ one should include increase of $\langle \sigma \rangle$ - likely to be faster than for soft Pomeron.

Summary of experimental results.

Parton densities in nuclei at small $x < 0.2$.

Shadowing is observed (in DIS for $x \gtrsim 5\cdot 10^{-3}$)

*** F_{2A}

*** $\bar{q}_A$

** G_A (dijets)

* V_A (global analysis of $F_2, \bar{q}_A$ data + baryon charge sum rule)

For F_{2A} consistent with leading twist QCD predictions Fig.

Enhancement for $x \sim 0.1$

*** F_{2A}

*** $V_A(x)$

suppression → *** $\bar{q}_A$ (suppression from D-Y)

* G_A (from ψ production in DIS & sum rule analysis)

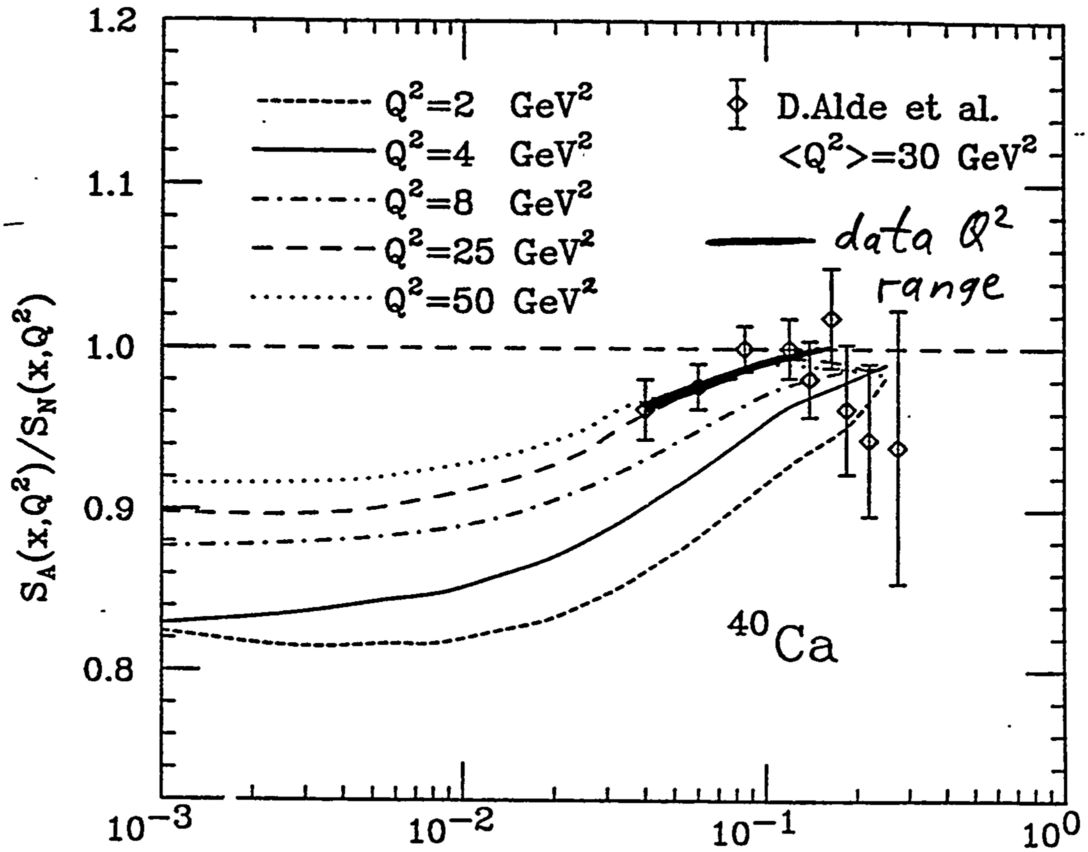

$\bar{q}_A$ suppression at nuclear Q^2 scale is much larger than at E-772 scale.

FS & Liuti

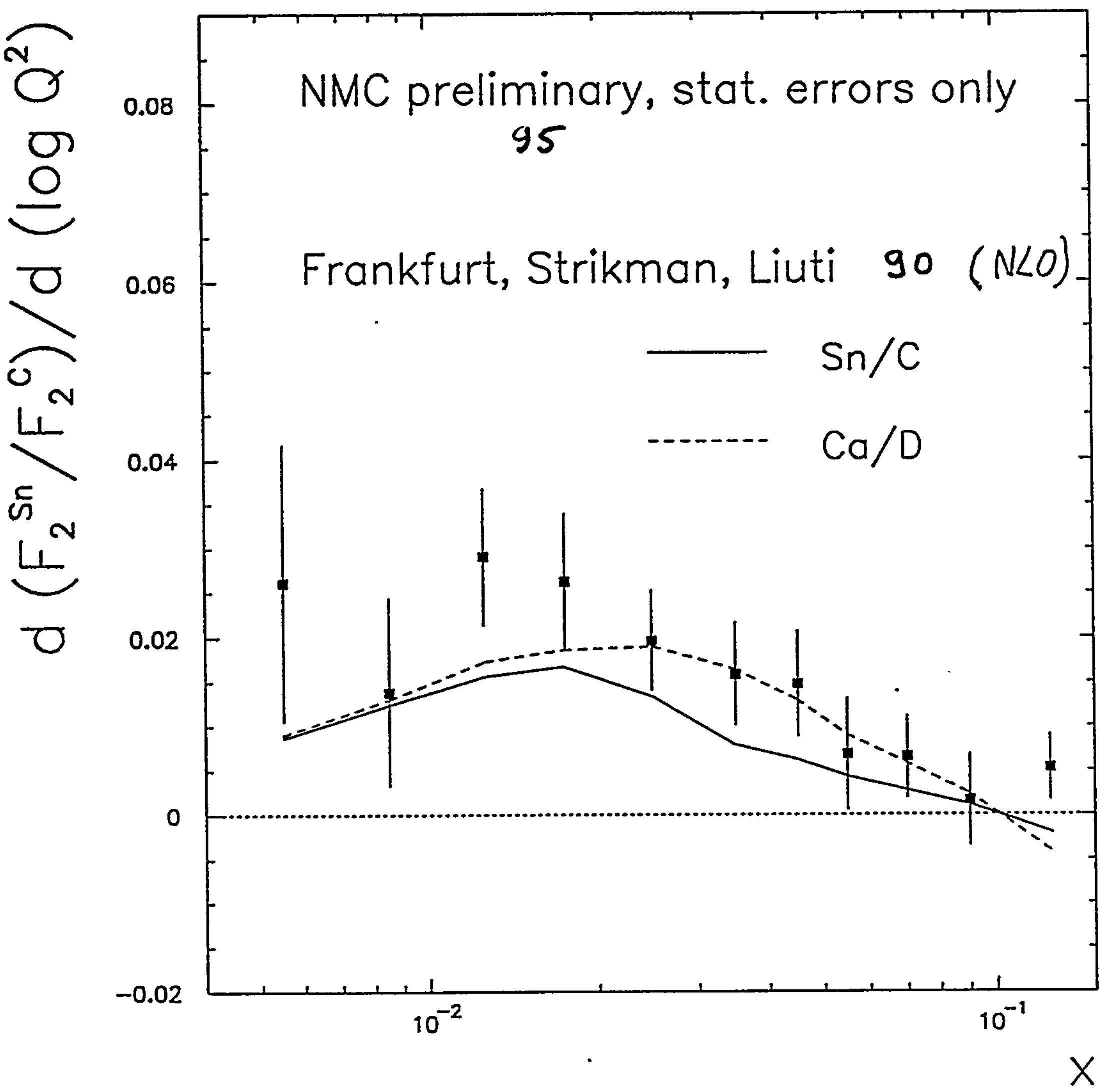
NMC preliminary, stat. errors only
95
Frankfurt, Strikman, Liuti 90 (NLO)
Sn/C
Ca/D
0.08
0.06
0.04
0.02
0
-0.02
10^{-2}
10^{-1}
X
$d\,(F_2^{Sn}/F_2^{C})/d\,(\log Q^2)$

STRIKMAN

FS, Liuti, 90

A = Ca

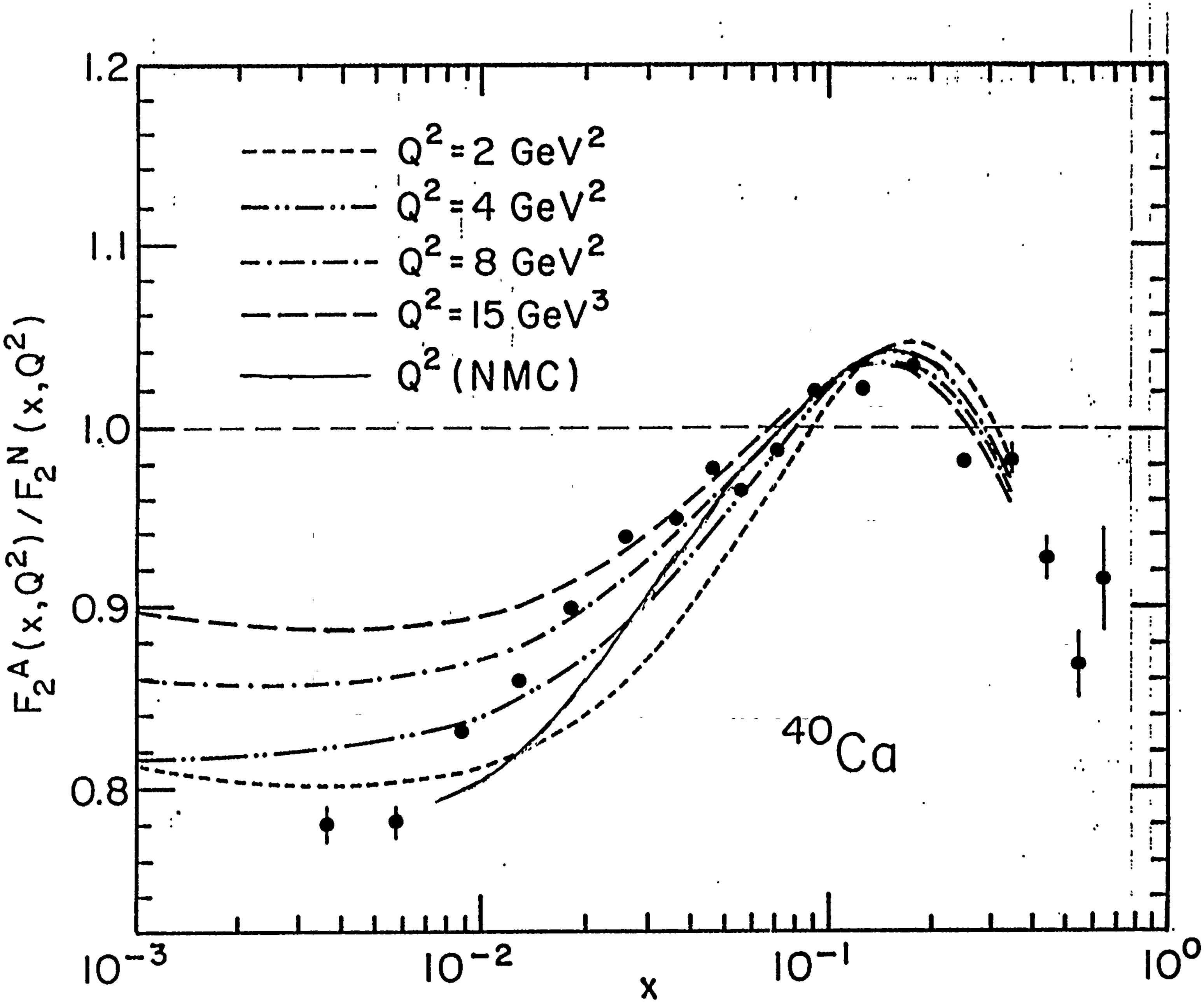

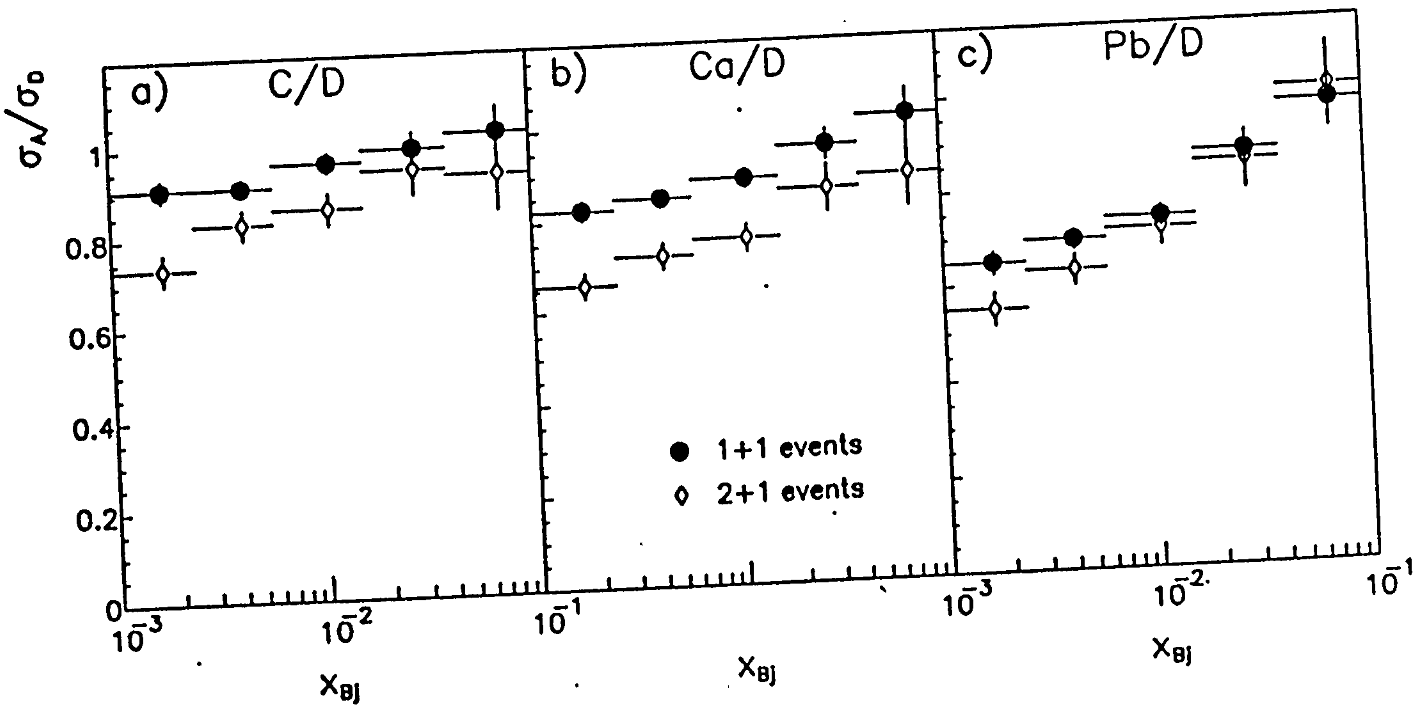

Figure 3: Per nucleon cross section ratios for events with 1+1 jets and 2+1 jets at $y_{cut} = 0.04$ vs x_{Bj} for C/D, Ca/D and Pb/D.

E-665

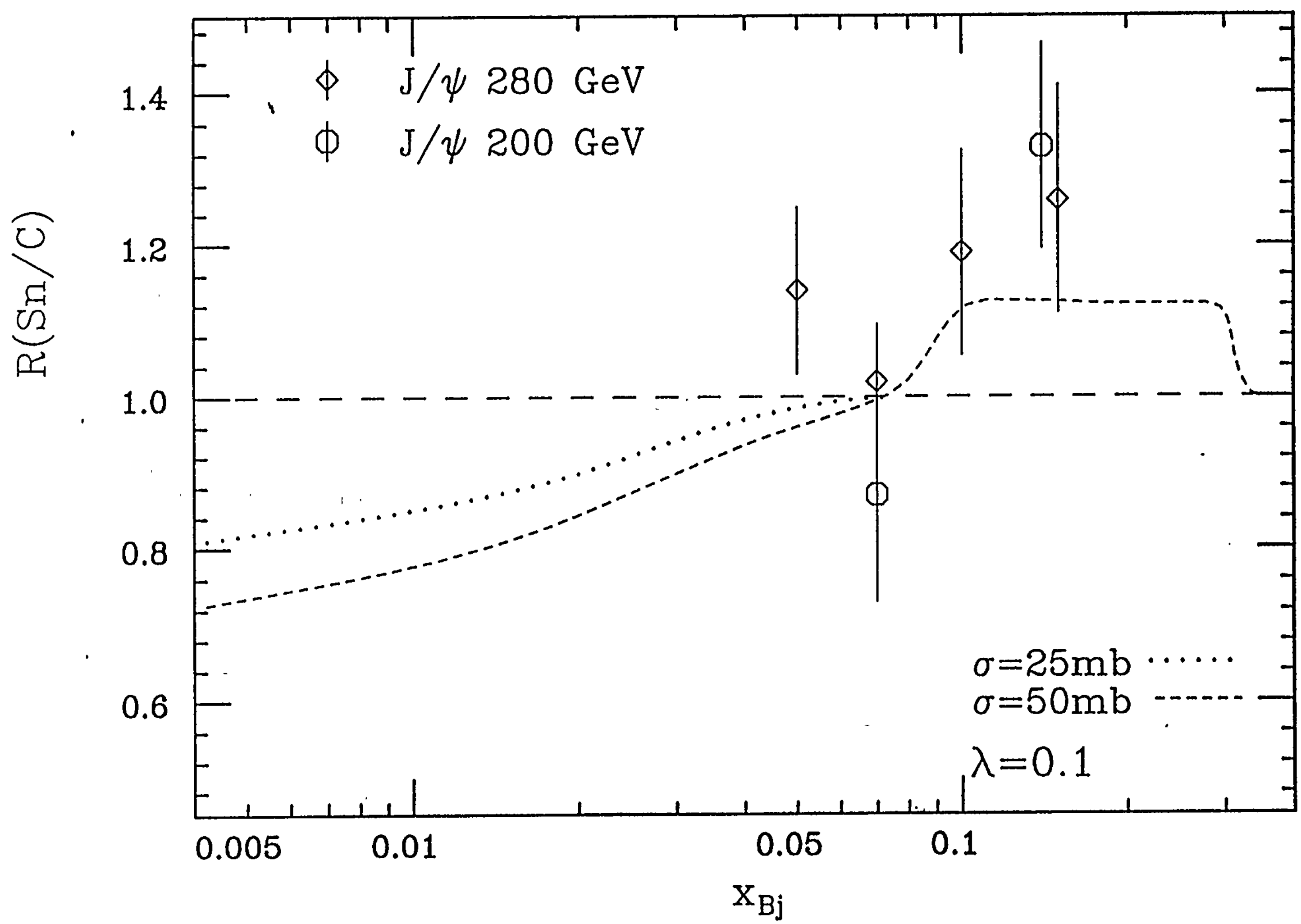
J/ψ 280 GeV
J/ψ 200 GeV
R(Sn/C)
1.4
1.2
1.0
0.8
0.6
0.005
0.01
0.05
0.1
x_Bj
σ=25mb
σ=50mb
λ=0.1

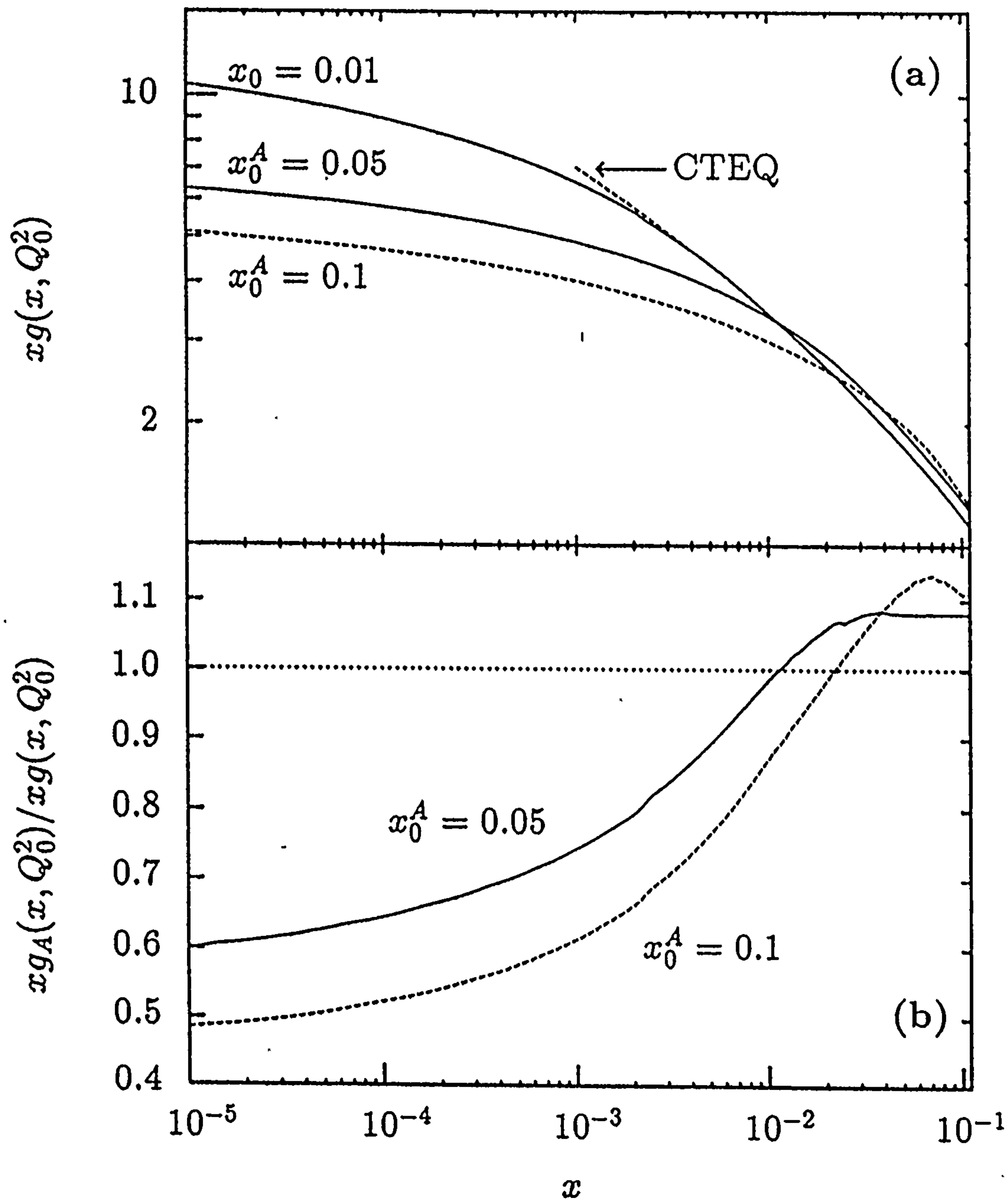

$Q_0^2 = 4 \ GeV^2$

$A = 200$

Eskola, Qiu & X-N. Wang 94

$\Sigma\Sigma$ Shadowing for $F_{2A}(x, Q^2)$ is large & weakly depends on Q^2 ($\simeq$ scaling). For $A \simeq 200$ reduction by a factor ~ 0.4.
Easy task for HERA.

For AA most important shadowing for G_A.

Several guesses for Q_0^2

i) $R_A^G \simeq R_A^q$ — Qiu 85, FS, FS & Ciuti 90, Eskola, Qiu & Wang 94 $\square$

ii) $R_A^G > 1$ — Nikolaev 91 $\square$

iii) $R_A^G < R_A^q$ — FS & Ciuti 92

Frankfort, Strikman and Liuti

Drell-Yan

$$\frac{x\,G(x)_{Ca}}{x\,G(x)_D}$$

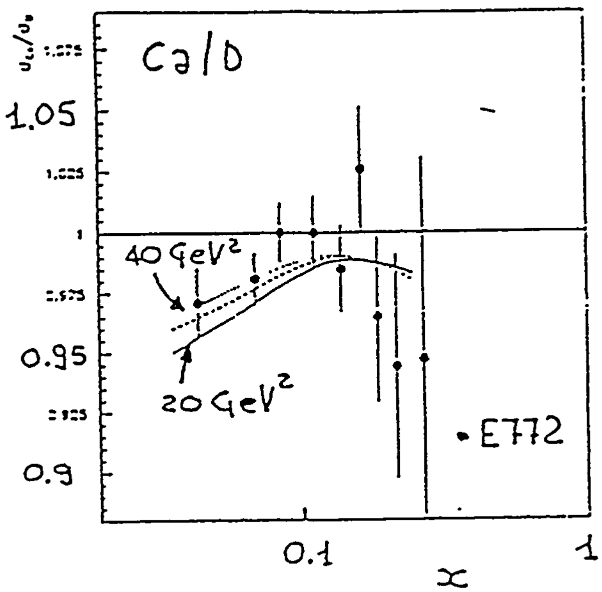

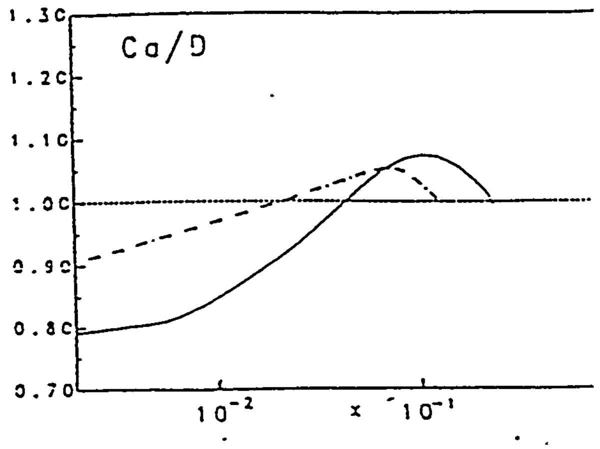

Drell-Yan

$$\frac{x\,G(x)_A}{x\,G(x)_D}$$

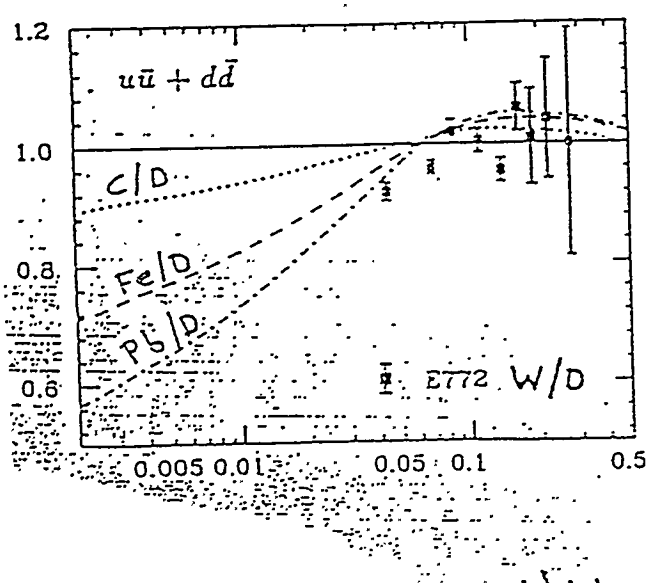

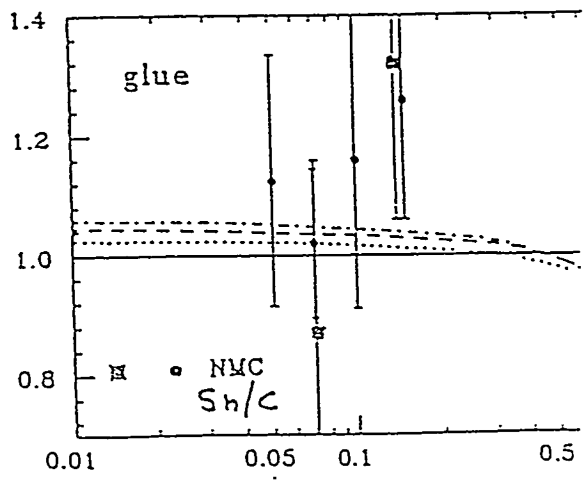

Nikolaev et al.

Reasoning of FSL :

Gluon shadowing is larger for

$Q^2 \sim$ few GeV^2

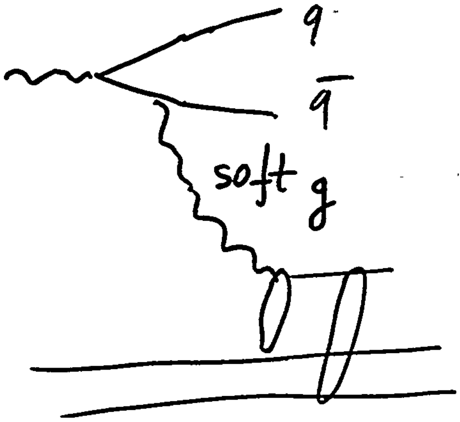

$\sigma_{eff} \sim \frac{9}{4} \langle \sigma_{q\bar{q}} \rangle$

but larger scaling violation for $\frac{\sigma_A}{\sigma_N}$

Higher twist effects may slower decrease of shadowing Mueller&...

Experimental strategies at HERA.

i) **Scaling** violation for small $x \ll 10^{-2}$

$$\frac{\partial F_{2A}(x,Q^2)}{\partial \ln Q^2} \propto \alpha_s G_A(x,Q^2)$$

$$\Rightarrow \quad \underbrace{\frac{\dfrac{\partial F_{2A}(x,Q^2)}{\partial \ln Q^2}}{\dfrac{\partial F_{2N}(x,Q^2)}{\partial \ln Q^2}}}_{\text{accuracy} \sim 4\%} \simeq \frac{G_A(x,Q^2)}{G_N(x,Q^2)}$$

problem - nonlinear effects
(may be good for $x > 10^{-3}$)

2) Charm production

3) Diffraction (see below).
to vector mesons.

Diffraction:

Unique feature of HERA (collider)

- easy to single out diffraction [rapidity gaps trigger]

α) $\gamma^* A \to X A$ at small t.

i) Color singlet models

$$\frac{F_{2A}}{F_{2D}} = R_A = 1 - f(A) \underbrace{\frac{\langle \gamma^* | \sigma^2(\rho, x) | \gamma^* \rangle}{\langle \gamma^* | \sigma(\rho, x) | \gamma^* \rangle}}_{\sigma_{eff}}$$

$$\frac{\sigma_{diff}}{\sigma_{tot}} \propto \tilde{f}(A) \cdot \sigma_{eff}$$

$\Rightarrow$ $\frac{\sigma_{diff}}{\sigma_{tot}}$ is predicted with small uncertainty

as soon as F_{2A}/F_{2N} fitted —

effect increases with A

and probably increases with decrease of x. Magnitude consistent with E-665

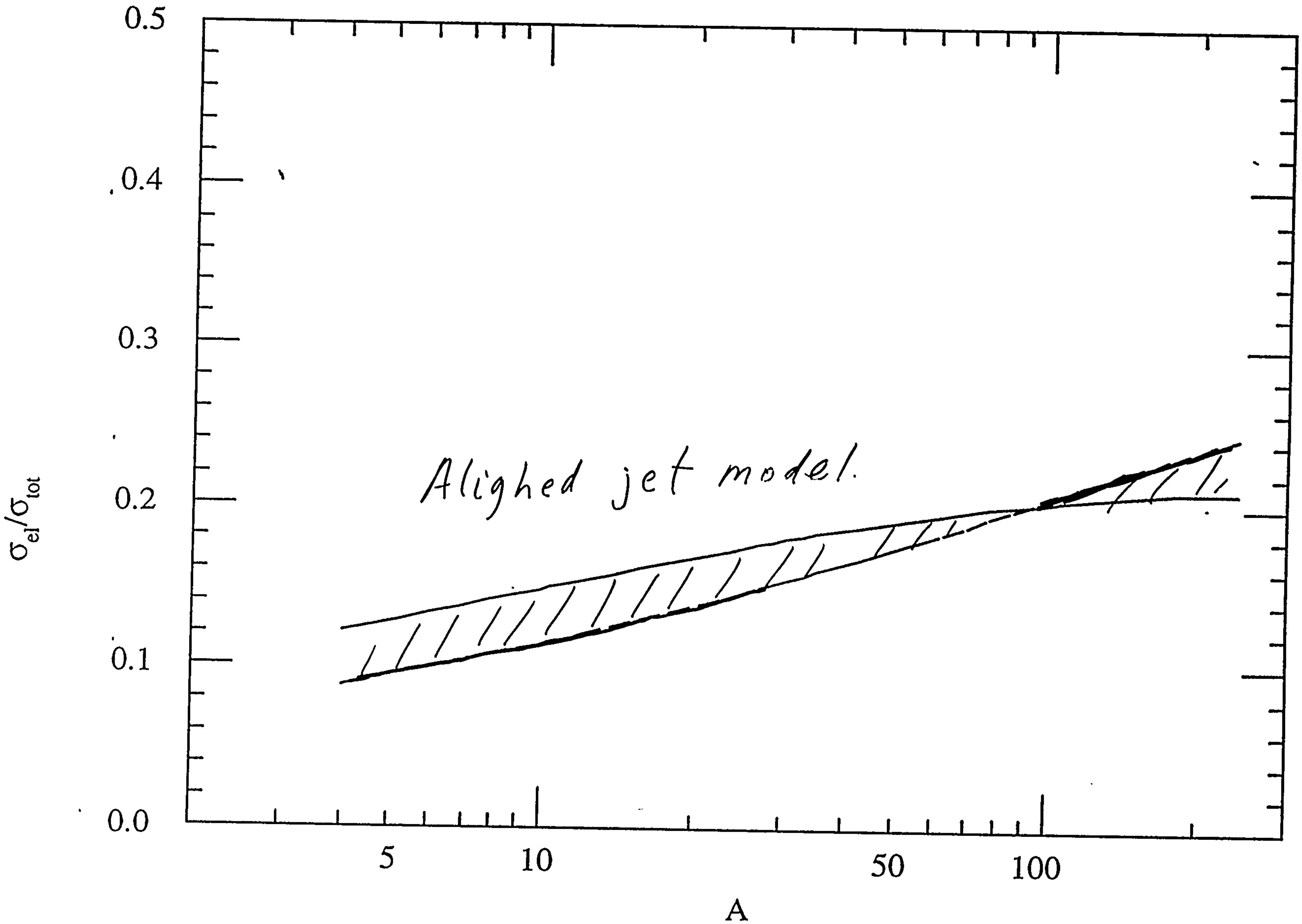

Alighed jet model.
0.5
0.4
0.3
0.2
0.1
0.0
σ_{el}/σ_{tot}
5
10
50
100
A

— ii) Charlror ~~petedudtiqnodelin diffryctsion~~ all

coherent diffraction - due to

— Relatrgd ~~qloestfdaw~~.

gap survival probability

$\Longrightarrow$ Coherent DIS diffraction off

γ nRclei $\to$ jet unique gap probe $+ jet$ $+ X$ of interplay (Bitz talk)

of soft p_t / large transverse size $-p_t$

if and hard $\gamma \to q\bar{q}$ / small of small transverse size size

color fluctuations in Pomeron weak A-dependence

— Possible lines of investigation:

if $b_{q\bar{q}} \sim b_{\rho\text{-meson}}$

A-dependence of diffraction to

2 jets decrease as a function with A of trust $\frac{1}{A^{0.3-0.5}}$

Aligned jet

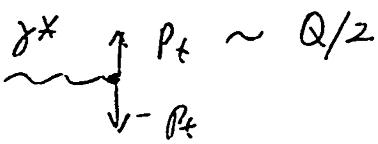

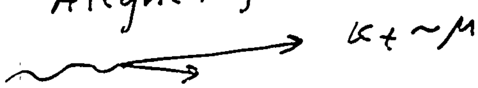

Small diffraction

Large diffraction

?

?

Diffractive production of vector states in DIS.

What one studies?

Propagation of small color dipole through nuclear matter.

Fascinating property: Interaction is small but fastly increases with energy

$$\sigma_{\bar{q}q\,T}(b^2, \nu) = \frac{\pi^2}{3} \alpha_s\left(\frac{\lambda}{b^2}\right) \times G_T\left(x, \frac{\lambda}{b^2}\right) b^2$$

$x = \frac{\lambda}{2 b^2 \nu}$, Baym et al 93

$\lambda \simeq 15$ FS & Koepf.

Origin of the increase of $\gamma^*_L + p \to \rho + p$ predicted by Brodsky et al.

Space-time picture

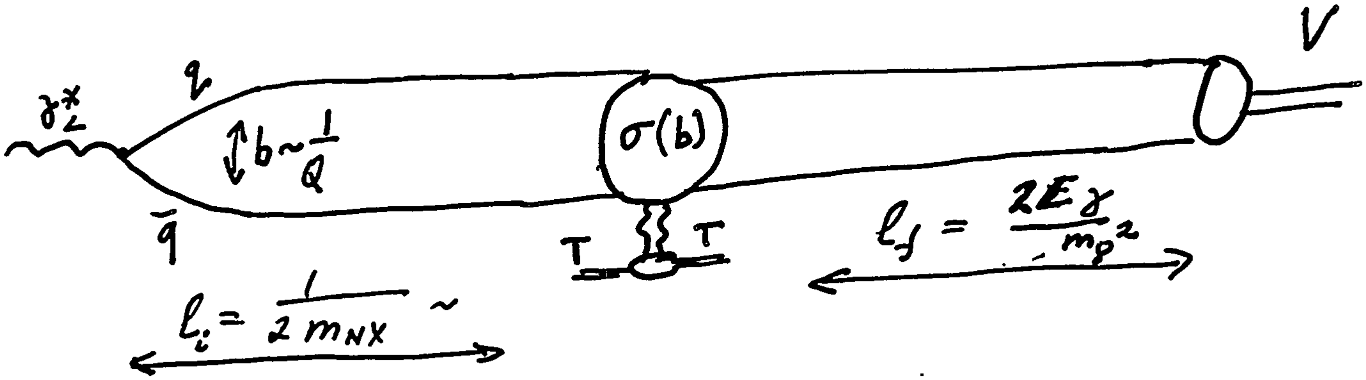

$\sim 1000 fm \quad x = 10^{-4}$

$$A^{\gamma^* T \to \rho T} = \Psi_{\gamma^*_L}(b) \otimes \sigma(b) \otimes \Psi_V(b)$$

$$\sigma_L^{\gamma^* T \to \rho T}(x, Q^2) \propto Q^2 \left[\frac{x G(x, Q^2)}{Q^2}\right]^2 \left[\frac{1}{Q^2}\right]^2$$

γ_L polarization

$\sigma(b)$

color screening.

$|\langle \Psi_{\gamma^*_L} | \Psi_V \rangle|$

probability of

PLC in V

FIGURES

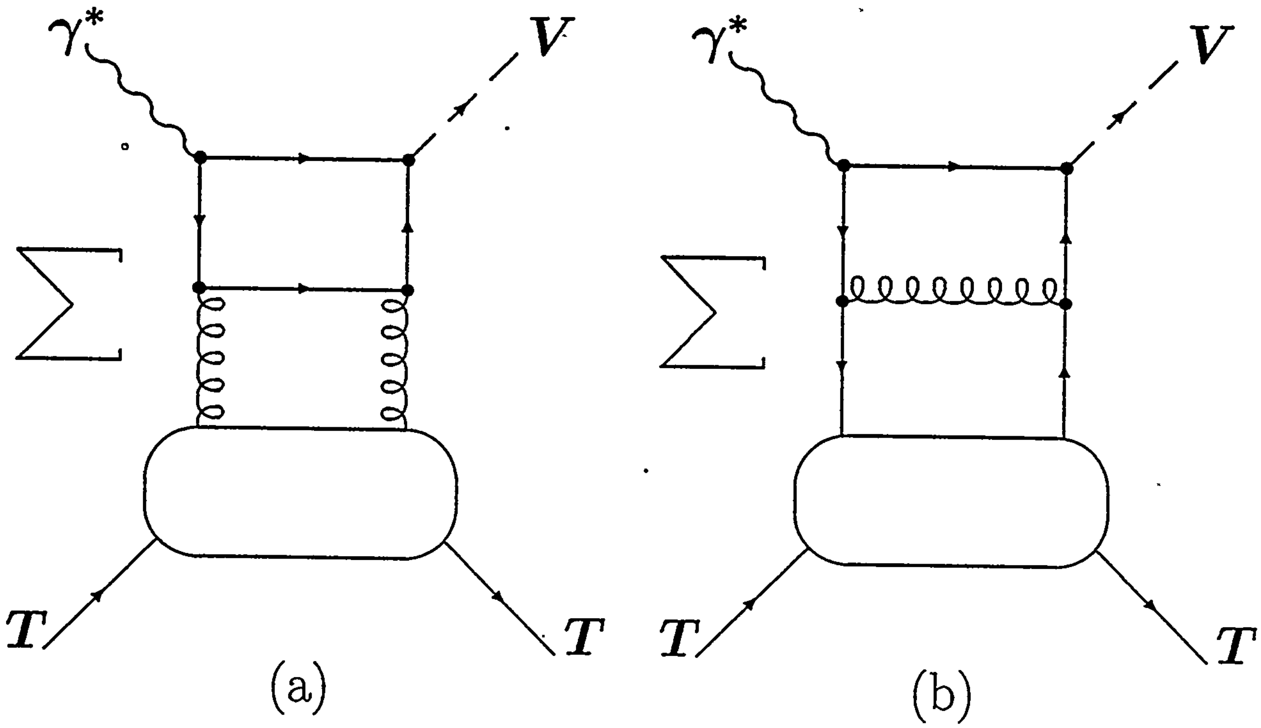

FIG. 1. Typical Feynman diagrams relevant for the evaluation of the cross section of diffractive electroproduction of vector mesons, i.e., the $\gamma^* + T \to V + T$ process, in leading $\alpha_s \ln \frac{Q^2}{\Lambda^2_{QCD}}$ approximation.

leading $\alpha_s \ln \frac{Q^2}{\Lambda^2_{QCD}}$ approximation.

Final answer in $\alpha_s \ln Q^2/\Lambda^2_{QCD}$ approx:

$$\boxed{\left.\frac{d\sigma^L_{\gamma^* N \to VN}}{dt}\right|_{t=0} = \frac{12\pi^3 \Gamma_{V\to e^+e^-} m_V \alpha_s^2(Q) T^2(Q^2)}{\alpha_{E.M.} Q^6 N_c^2} \cdot \left| \eta_V \left(1 + \frac{\pi}{2}\frac{d}{d\ln x}\right) x G_T(x,Q^2) + \frac{2}{3}\left(1 + i\frac{\pi}{2}\frac{d}{d\ln x}\right) x S_T(x,}$$

$$\eta_V = \frac{1}{2} \int \frac{\psi_V(z)\,dz}{z(1-z)} \Big/ \int \psi_V(z)\,dz \simeq 3$$

$T(Q)$ transverse overlap integral, $T(Q\to\infty) = 1$.

HERA data confirmed:

- fast increase of σ
- Absolute value of σ Fig.
- $\frac{1}{Q^n}$ with $n = 4.2 \pm 0.8$ ZEUS
  $n = 4.3 \pm 0.3$ pQCD
- $\sigma_L > \sigma_T$
- Increase of φ/ρ to $\simeq 0.2$ from ~ 0.05 ZEUS 95

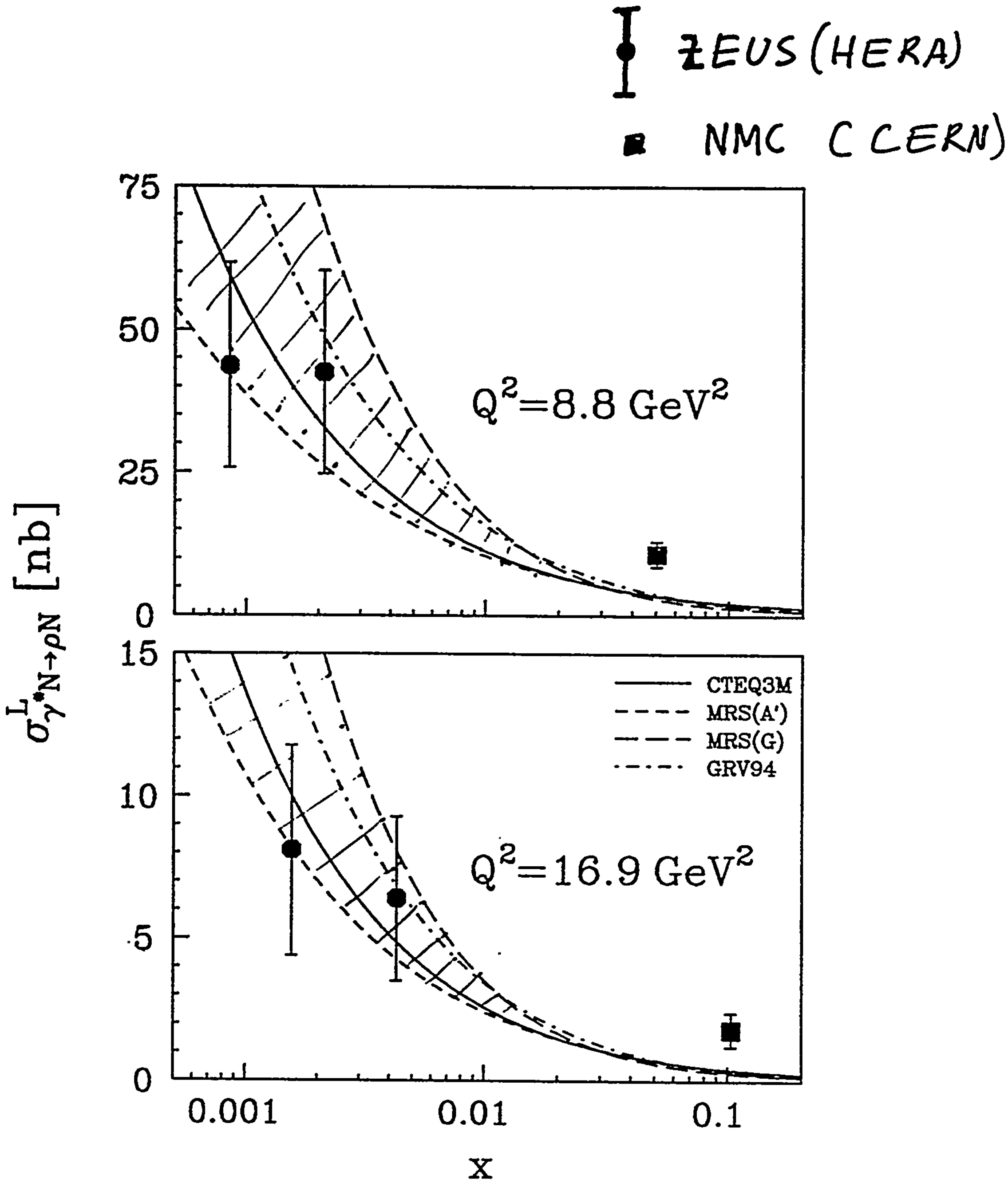

FIG. 6. The total longitudinal cross section, $\sigma^L_{\gamma^* N\to\rho N}$, calculated from Eq. (15) for several recent parametrizations of the gluon density in comparison with experimental data from ZEUS [3] (full circles) and NMC [12] (squares).

Probed transverse color separations

$b \leq 0.35\, fm$

$\Longrightarrow$ Confirmation of

- color screening
- presence of PLC in ρ-meson

For $Q^2 = 9\, GeV^2$ $\qquad b \simeq 0.35\, fm$

as compared to $\langle b \rangle \simeq 2 \cdot \sqrt{\frac{2}{3}}\, r_\rho = 1 f$

$\Longrightarrow$ CT effects in ρ-production are likely already for $Q^2 \gtrsim 2\, GeV^2$.

Some evidence from E-665
FNAL

$$\gamma^* + A \to \rho + A$$
$$\to \rho + A^*$$

In the case of nuclei

in the leading order in $1/Q^2$

$$\frac{d\sigma}{dt}^{\gamma_L^* + A \to \rho + A}\Big|_{t=0} \Big/ \frac{d\sigma}{dt}\Big|_{t=0}^{\gamma_L^* + p \to \rho + p} = \left[\frac{\sigma_A(x,Q^2)}{\sigma_N(x,Q^2)}\right]^2$$

$\Rightarrow$ for x, Q^2 where no shadowing in σ_A — color transparency effect.

For small x probes

- nuclear shadowing of σ_A
- •• Onset of nonlinear effects.

Nonlinear effects should stop/slow down increase of $\frac{d\sigma}{dt}^{\gamma_L^* + T}\Big|_{t=0}$ at $x \to 0$

Reason : <u>Unitarity</u>

$\sigma(q\bar{q}, T) \leq \pi r_T^2$ for small b

Effect is small for proton target for $x \gtrsim 10^{-4}$: for nuclei it is enhanced by a factor $A^{1/3}$ –

– starts at much smaller σ_N

We estimated minimal possible shadowing for

$\sigma_L(x, Q^2)$ & ρ-production

Effect is larger for ρ.

α) For $\rho \propto \sigma^2$, $\sigma_L \propto \sigma$

β) $\langle b(x,Q^2)\rangle_\rho > \langle b(x,Q^2)\rangle_{\sigma_L}$

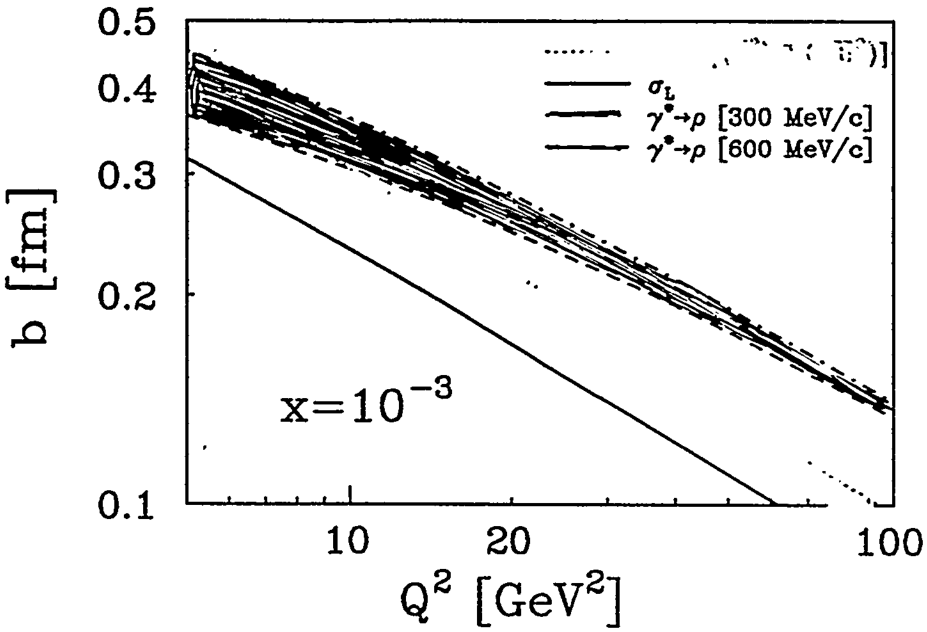

FIG. 2. Average transverse size of the $q\bar{q}$ components effective in $\sigma_{\gamma_L^* N \to VN}$ of Eq. (17) and $\sigma_{\gamma_L^* N}$ of Eq. (19).

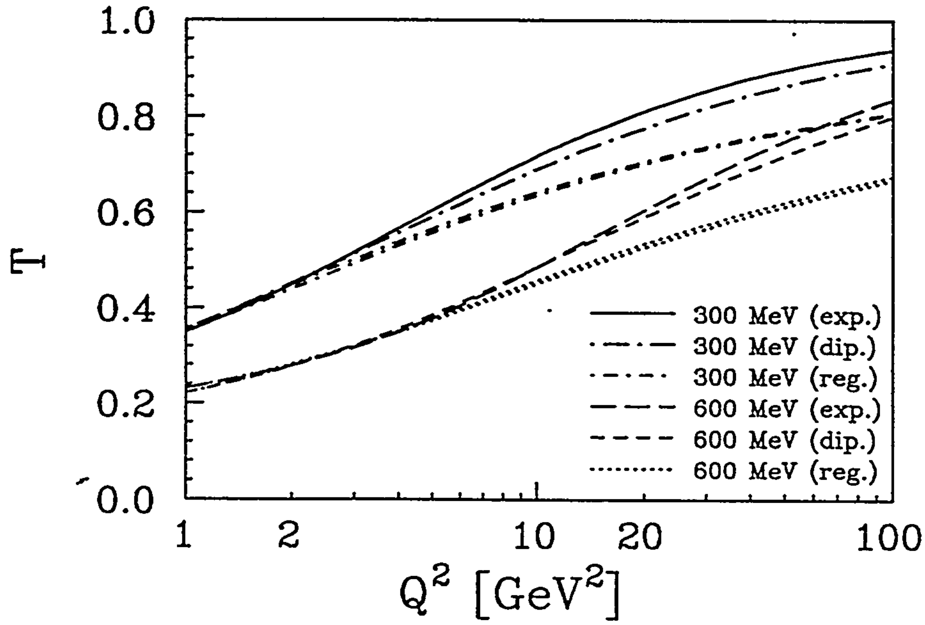

FIG. 3. Suppression factor, $T(Q^2)$ of Eq. (23), in $d\sigma_{\gamma_L^* N \to VN}/dt|_{t=0}$ due to transverse quark Fermi motion for diffractively produced vector mesons built of light quarks.

$$\left[\frac{1}{A^2} \frac{d\sigma^{\gamma^* A \to V+A}}{dt} \Big|_{t=0} \Big/ \frac{d\sigma^{\gamma^* p \to V+p}}{dt} \Big|_{t=0} \right]^{1/2}$$

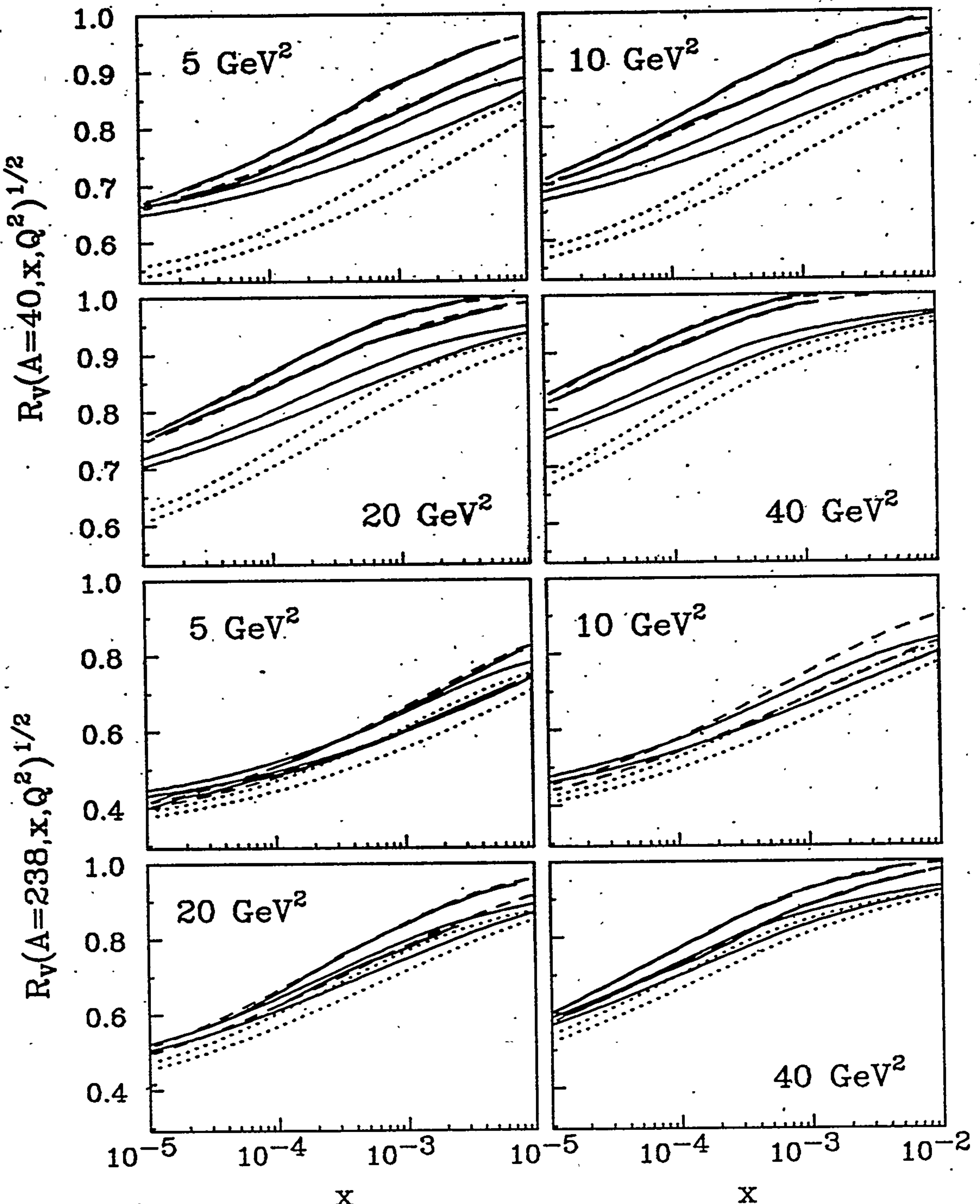

FIG. 11. Nuclear shadowing in diffractive electroproduction of vector mesons. The labeling is the same as in the previous figure. Note that in Figs. 10 and 11 the ordinates of the plots for different A are scaled $\propto A^{-1/3}$.

— Unitarity limit
— Eikonal model

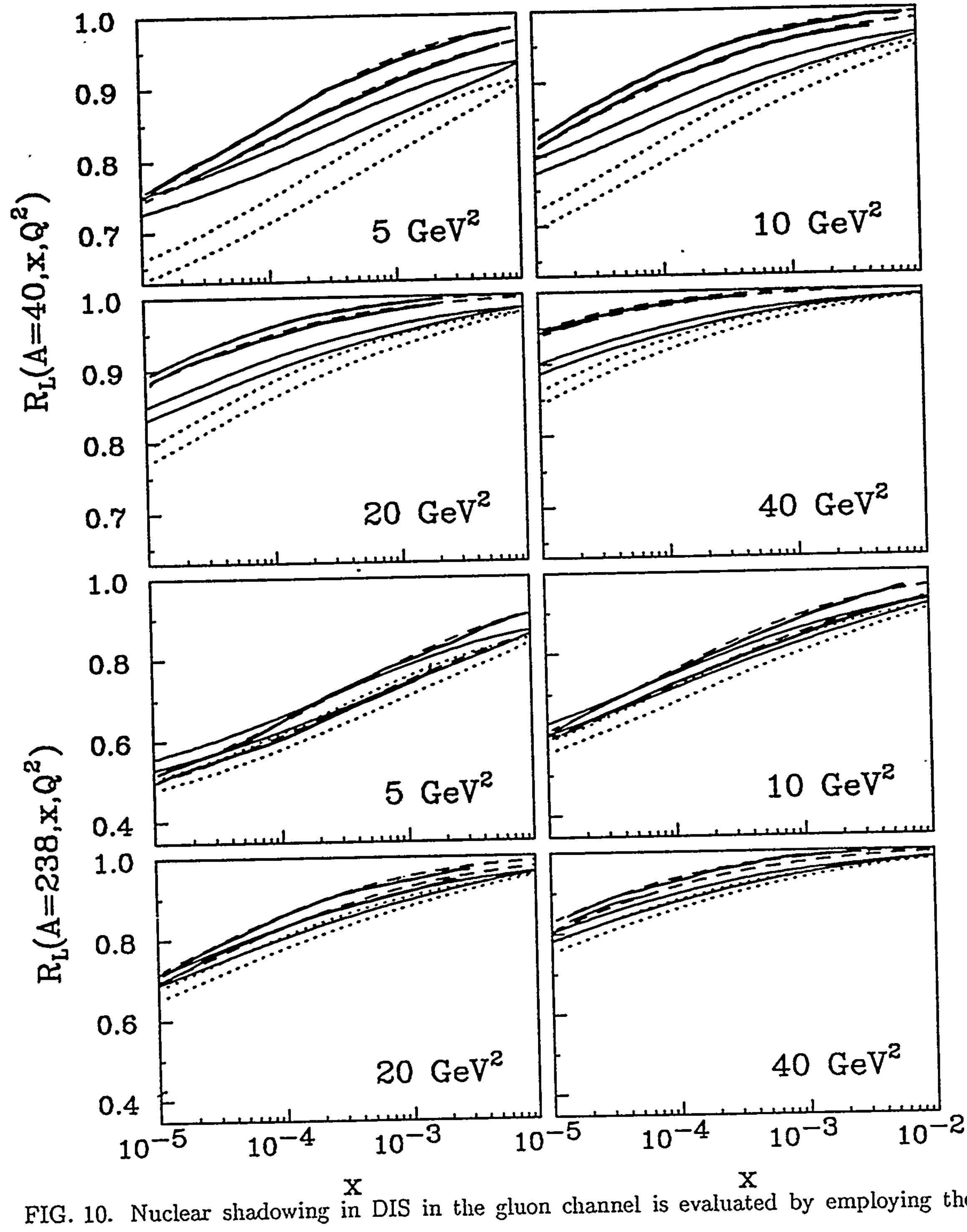

FIG. 10. Nuclear shadowing in DIS in the gluon channel is evaluated by employing the nuclear unitarity limit (dashed lines) and in b-space eikonal approximation using a realistic (solid lines) or infinitesimally sharp (dotted lines) nuclear density distribution.

Another strategy possible using light nuclei:

Observe onset of color transparency and (at even smaller x) nonlinear effects using double scattering kinematics. (Sargsyan talk)

The simplest model - QCD eikonal

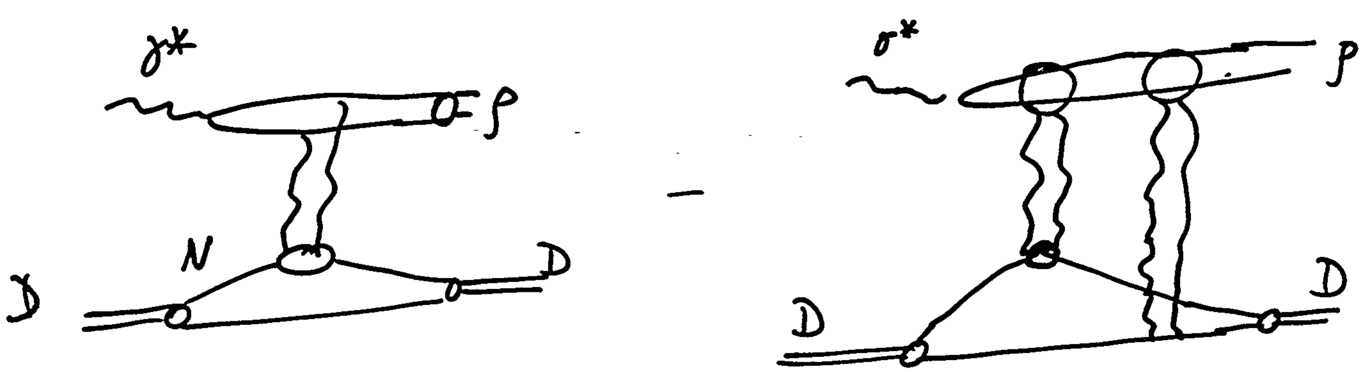

$$\frac{d\sigma^{\gamma^*_L + D \to V + D}}{dt}\Big|_{-t \geq t_0 \sim 0.5\,GeV^2} \Big/ \frac{d\sigma^{\gamma^*_L + D \to V + D}}{dt}\Big|_{t=0}$$

$$= \frac{1}{4}\left| \frac{\langle \sigma_{q\bar{q}N}(b) \rangle}{4\pi} \left\langle \frac{1}{R^2} \right\rangle^2 \right| \exp Bt$$

$$\propto \frac{x^2 G_N^2(x, Q^2)}{Q^4} \exp Bt$$

[Sargsyan talk

$\Rightarrow$ Strong suppression of secondary maximum, but fast increase of $\sigma(t > t_0) \propto G_N^4(x, Q^2)$ with $1/x$ increase.

Probably the best nucleus $A = 4$

spin zero, large 2 rescatterings

small ~~t~~triple rescatterings.

Quark propagation through ...

- inelastic processes. (Talks of Mueller, Ster

Questions : • Energy losses

• Hadron formation/Seconda interactions

Two kinematic regions

$x \gtrsim 0.05$ quark propagation

$x \ll 0.01$ color dipole propagatio

For quark propagation

- small energy losses

- p_t broadening for leading particles

- reinteraction for

$\Delta y \leq \ln A^{1/3}$

acceptance ?!

$\Delta y \sim 2-5$

Dipole case – interplay of soft and hard physics.

Practical question: How to probe energy loss at collider

longitudinal loss – too small

Δz – very small.

– Predictions for p_t-broadening

flavor dependence – charm

Rapidity correlations?

– Study hadron production in DIS of nuclei – will test models applied for AA.

$\Rightarrow$ Need codes applicable both to eA & AA. In our group K. Geiger works on this. Should be done for different AA models.

Few of the questions — I did not have time to cover

γA physics — color fluctions in "γ"

Nonfactorization — parton distributions in "A" "A" collisions depend on trigger.

"Nuclear Pomeron" — parton distribution in nuclear diffraction.

$\Sigma\Sigma\Sigma$ eA program at HERA

may provide for AA

- • parton distributions at small x
- •• parton interaction with nuclei
- ∴ Interplay of soft and hard interactions.
- ∴ Better understanding of Pomeron and overall high-energy QCD.

Review of Hadron–Lepton Nucleus Data

Wit Buzsa
Massachusetts Institute of Technology

REVIEW OF DATA RELATED TO OUR UNDERSTANDING OF THE ATTENUATION OF PHOTONS (REAL AND VIRTUAL) AND HADRONS AS THEY PASS THROUGH NUCLEAR MATTER

by: Wit Busza

Department of Physics and Laboratory for Nuclear Science
Massachusetts Institute of Technology
Cambridge Mass. 02139, USA

I was asked to review the most important aspects of hadron and lepton-nucleus data at high energies, in particular those aspects that may be most relevant to an understanding of relativistic heavy ion collisions. At the outset of preparing the talk I realized that, for a 20 minute presentation, this was a hopeless task. The literature on this subject is simply too extensive [1]. I have thus decided to limit my talk to a single general comment and a discussion of one body of data — that related to the attenuation of photons and hadrons as they pass through nuclear matter, which I find particularly interesting and instructive, and hopefully the understanding of which will prove useful in the interpretation of heavy ion data.

The general comment is this. In the last twenty years a very large quantity of data has been accumulated on the interactions of photons, leptons and hadrons with nuclear targets at energies ranging from a few GeV to over 800 GeV. A study of the literature [1] soon reveals that despite its extent there are very significant gaps in our knowledge of the phenomenology. What is even more apparent, in many cases the precision of the data is inadequate to give us a good picture of how the nuclear medium influences the interaction process. The difficulty is that frequently the main features of the A-dependence simply reflect the geometry of the nucleus, while the interesting part is often very subtle. A study of the literature also makes it all too apparent that there are many aspects of the A-dependence phenomenology for which we do not have a good understanding. This, of course, is not surprising since most of the A-dependence studies probe low P_t physics, the non- perturbative regime of QCD.

Why do I make these general remarks? The answer is simple — to warn those who are looking for fundamentally new physics in relativistic heavy ion collisions that signatures will be subtle and difficult to interpret, and that, in addition to studying the collision of heavy ions, it is absolutely

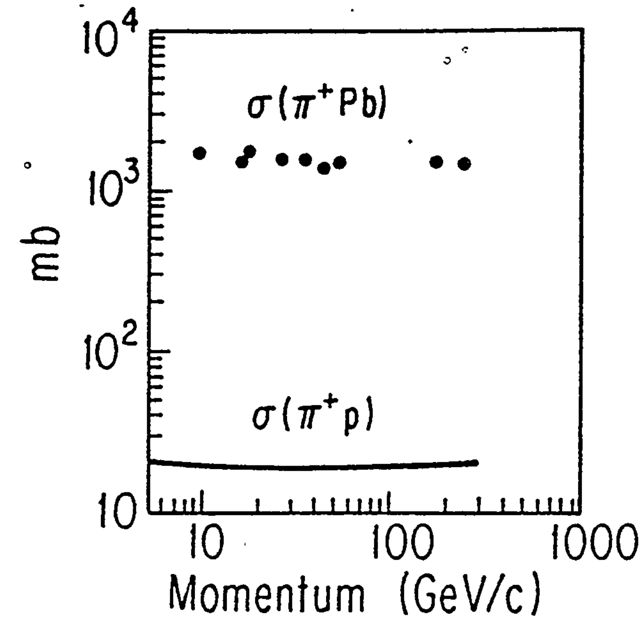

Fig. 1. Energy and A-dependence of π^+-nucleus absorption cross-sections [3].

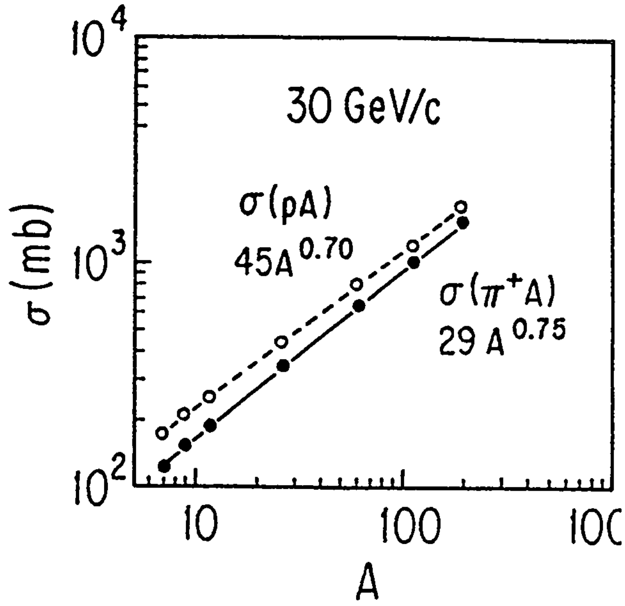

Fig. 2. A-dependence of π^+ and p - nucleus absorption cross-sections [3]. As can be seen the data can be well parametrized by $\sigma_A = \sigma_0 A^{\alpha}$.

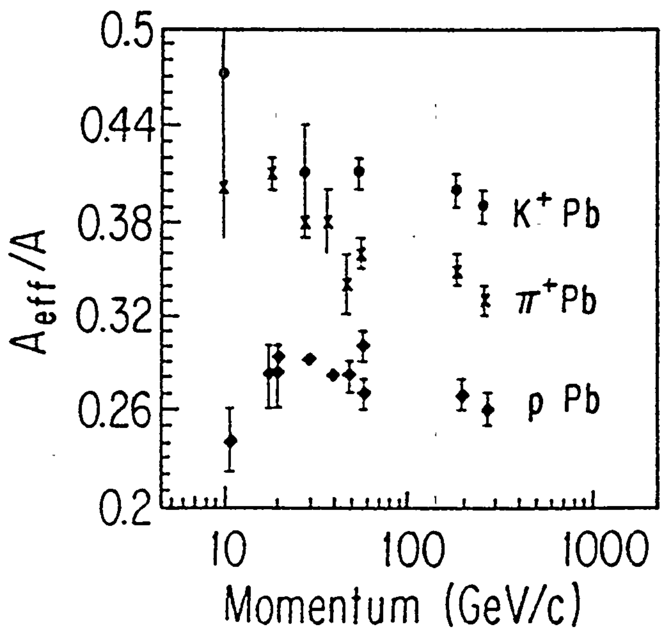

Fig. 3. Energy dependence of the effective number of nucleons in the nucleus for inelastic collisions. A_{eff} is defined as: $A_{eff}/A \equiv \sigma_A/A\sigma_p$. Data are from [3].

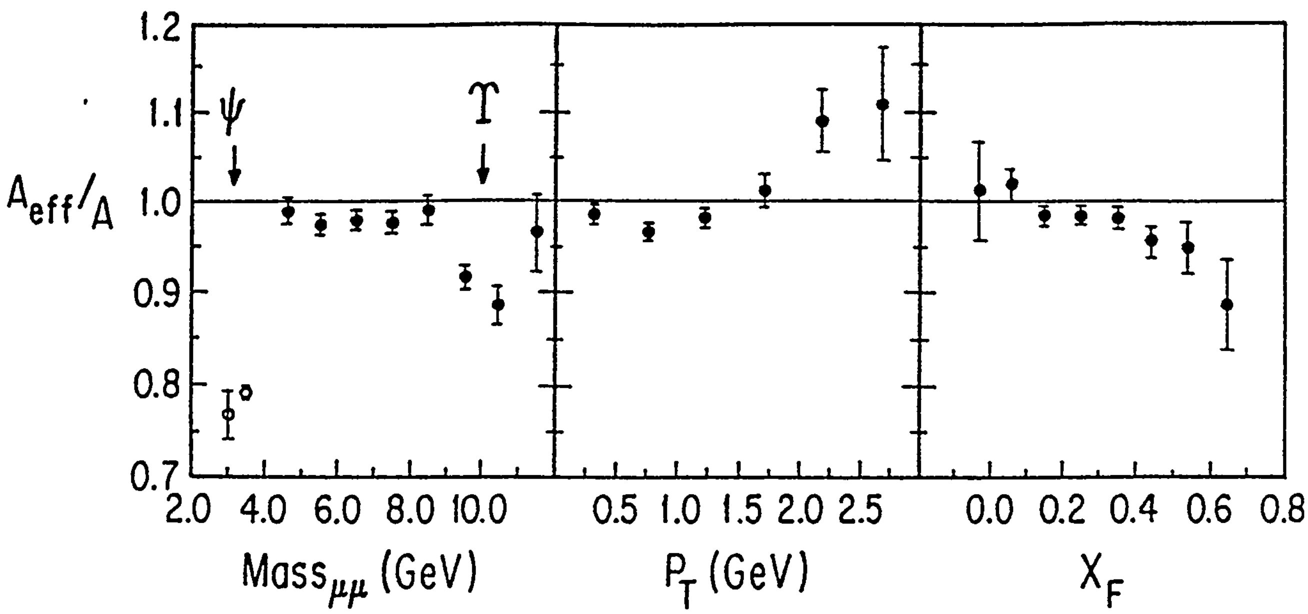

Fig. 4. Transparency of nucleus in Drell-Yan Process. $A_{eff}/A = 1$ corresponds to complete transparency. The data are for 800 GeV pA collisions [4].

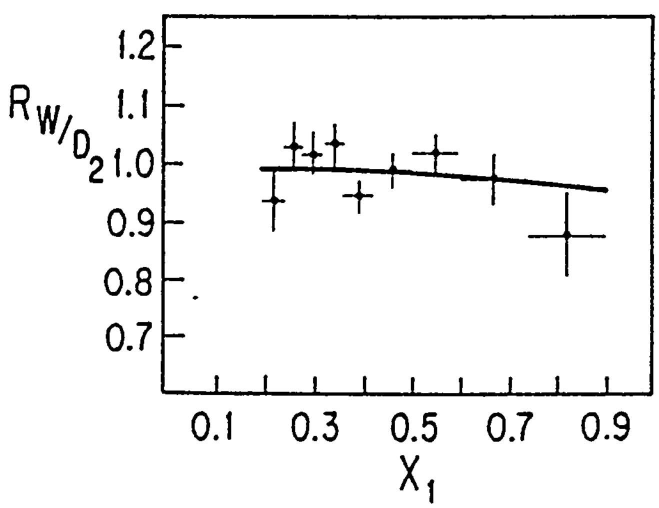

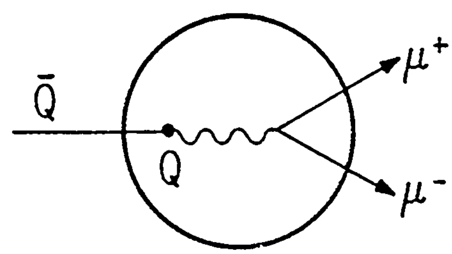

Fig. 5. Transparency of nucleus in π^- A Drell-Yan process at 140 and 286 GeV [5]. x1 is the fraction of the momentum carried by the incident quark. Data includes incident quarks of energy ≥ 30 GeV. It is consistent with complete transparency for such quarks.

Fig. 6. The Drell-Yan process. As can be seen, it probes simultaneously the nuclear transparency for quarks, photons and leptons.

crucial that equally precise and extensive measurements be made, using identical trigger and equipment conditions, for collisions of protons with protons and protons with nuclei. Without such comparisons it will be difficult, if not impossible, to disentangle new phenomena associated with the high energy and baryon densities produced in relativistic heavy ion collisions from phenomena which simply follow from multiple scattering in the nuclear medium or from simple space-time aspects of the collision process. I know that there are some who disagree with this point of view. They argue that in fact the interpretation of relativistic heavy ion data will be easier than that of pA collisions. If much larger nuclei existed so that the interaction volumes and times for every collision were similar and extensive enough to approximate the infinite limit, this point of view might be correct. However, for real colliding nuclei, I suspect it is far more likely that most of the phenomenology of nucleus-nucleus collisions will follow from the same physics that determines the phenomenology of proton-nucleus collisions. It must be well studied and understood if new physics is to be found in this background.

Now to the discussion of data related to the attenuation of photons and hadrons as they pass through ordinary nuclear matter. Since the interpretation of the data is often self-evident, I urge the reader to spend more time looking at the data than studying the text!

As is well known, hadronic matter has very low transparency for incident hadrons. For example, the center of a nucleon is only 6% transparent for incident protons, 18% for pions and 25% for kaons [2]. As a result nuclei are almost black for incident hadrons. This is apparent from the data shown in figs. 1-3. In figs. 2 and 3 I introduce two useful measures of the transparency of nuclei; the first is the parameter α in the parametrization of the cross-section on a nucleus of atomic number A in the form $\sigma_o A^{\alpha}$, and the second is the effective number of nucleons in the nucleus, A_{eff}, defined by $A_{eff}/A = \sigma_A/A\sigma_p$.

For comparison of nuclear transparencies for various processes, it is worth remembering that for "black" hadrons and large nuclei $\alpha \approx 2/3$ and $A_{eff}/A \approx 1/4$, while for total transparency both α and $A_{eff}/A = 1$.

In contrast to the opacity of nuclei to incident hadrons, they are almost completely transparent to high energy quarks, leptons and massive virtual photons. This can best be deduced from data on the Drell-Yan process (figs. 4&5) which, as is illustrated in fig. 6, probes all three transparencies simultaneously. Nuclear transparency to energetic quarks is also apparent from studies of the production of two jets with large P_t (see fig. 7).

The very different nuclear transparency for fast quarks and hadrons immediately suggests that fast quarks as compared to slow quarks or gluons have very different transparencies. If this is the whole story, and we accept the conventional picture that produced fast hadrons are the fragments of fast quarks, we would expect little attenuation of leading hadrons in processes of the type $hA \to h'X$. In fact, as can be seen in fig. 8, in such processes the faster is the leading hadron the more it is attenuated. Clearly the understanding of the attenuation of hadrons, in particular of newly created ones, is non-trivial. This becomes even more apparent when we look at the data in greater detail.

For example, for most produced particles, there is the unexpected result that the ratios of particles produced at a given value of x_{Feynmann} are independent of the target (e.g. see figs. 9 & 10). If this result is not an artifact of insufficiently precise measurements but follows from some general property related to the passage of constituents through nuclear matter, one is immediately faced with the dilemma why the A-dependence of the production of ϕ's, Ξ's, J/ψ's and perhaps $\bar{p}$'s is so very different from that of most of the other particles.

Looked at in its entirety, it is difficult to reconcile all these results with any multiple scattering picture, with or without attenuation, with or without a formation time for the produced hadrons.

As a digression, it is worth mentioning that the correctness of the observed momentum degradation of the leading baryon spectrum in $hA \to h'X$ is crucial for the prospect of interesting physics being produced in relativistic heavy ion collisions. It is this degradation which leads to the prediction that in such collisions large baryon densities are produced [10].

Since the passage through nuclei of hadrons is clearly very complicated, I will now consider the propagation through nuclear matter of much simpler partonic structures. The photon, both real and virtual, is an ideal tool for such studies. This can readily be seen through the following simplistic considerations [11].

As is well known, the photon has a hadronic nature [12]. It can fluctuate into partonic states of lesser or greater complexity depending on the kinematics of the process that produced the photon. Consider a photon with four-momentum $q \equiv (\vec{k}, \nu)$ which fluctuates into a partonic state of mass m illustrated below

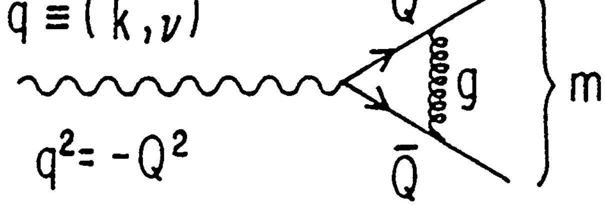

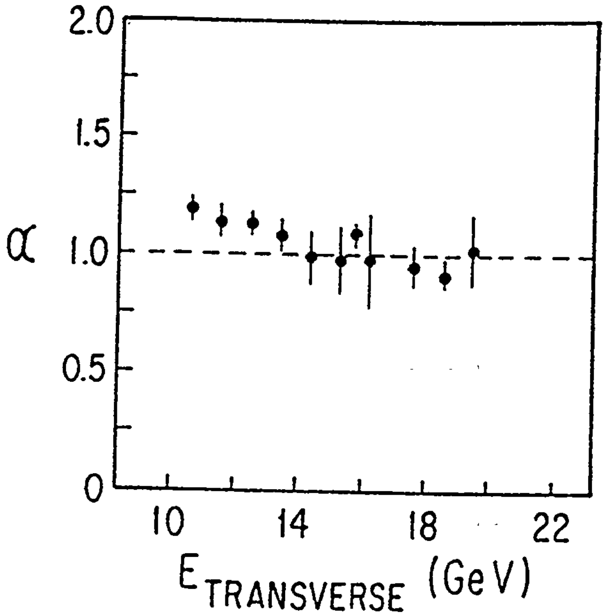

Fig. 7. A-dependence of the production of two jets as a function of the transverse energy of the jets, in pA collisions, at 800 GeV [6]. At the highest transverse energies, the data are consistent with complete transparency for the incident and outgoing quarks.

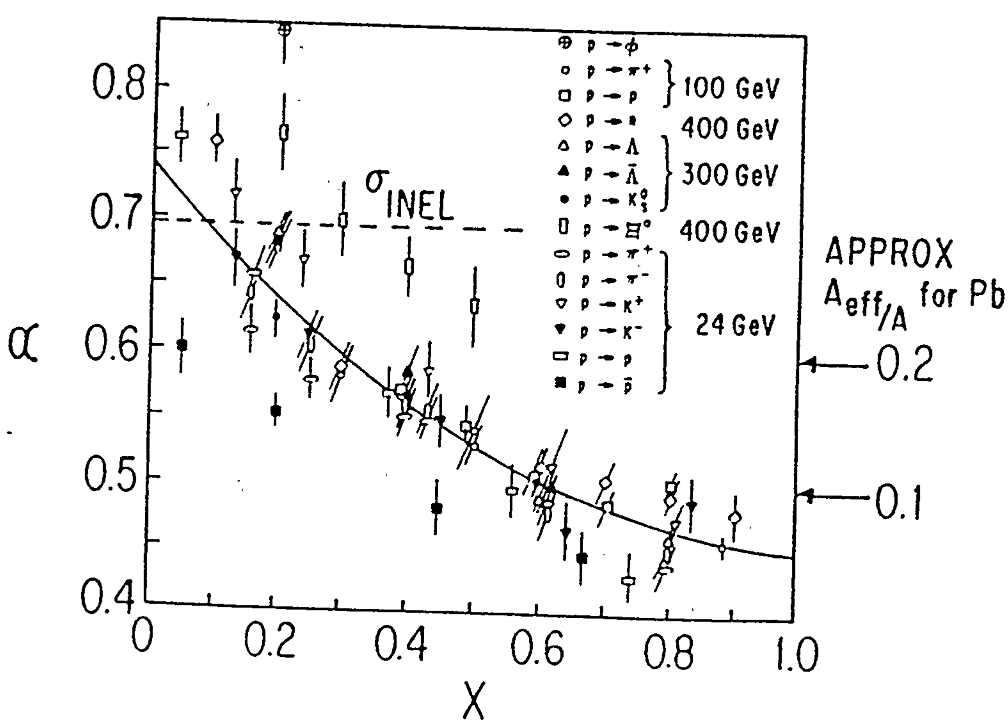

Fig. 8. Complilation of data on the A-dependence for processes of the type pA → hX. α is the exponent in the parametrization of the data in the form $\sigma A = \sigma_0 A^{\alpha}$. It is plotted as a function of x, the ratio of the momentum of the hadron, h, to the momentum of the incident proton. All the data are for low Pt (≤ 300 MeV/c) [7]. More and more attenuation is seen as the momentum of the produced hadron increases.

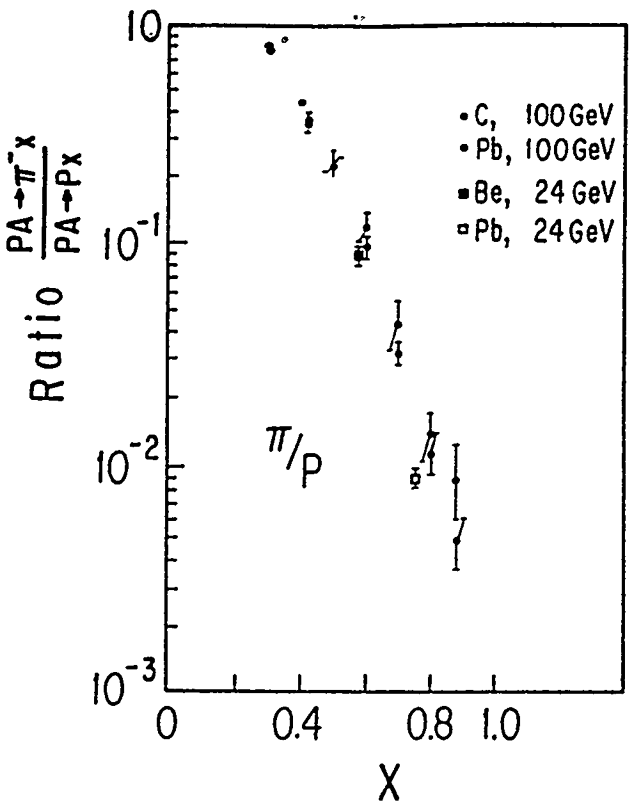

Fig. 9. Data [8] illustrating that in processes of the type pA → hX, for many varieties of produced particles, h, the ratios of the cross-sections are independent of the target nucleus.

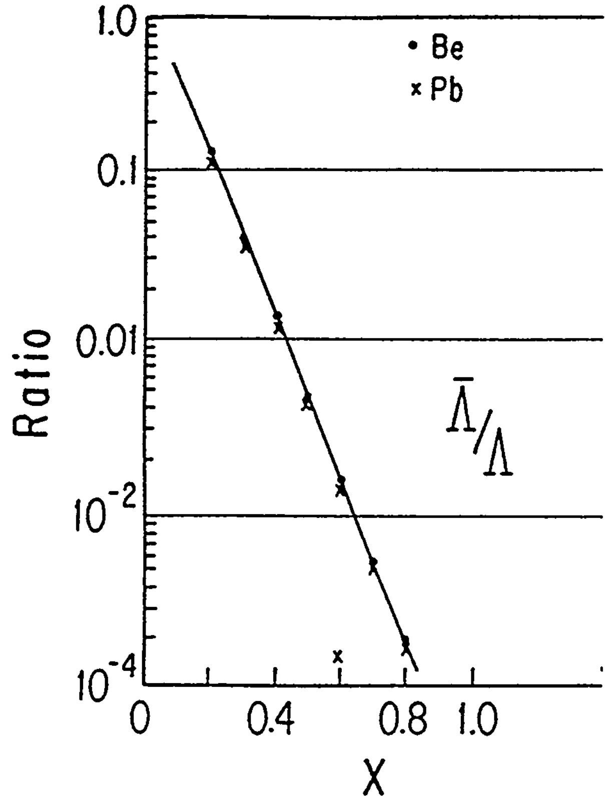

Fig. 10. Data [9] illustrating the unexpected result that the ratio of the cross-sections for the production of $\bar{\Lambda}$ and Λ in pA collisions is independent of the target nucleus A.

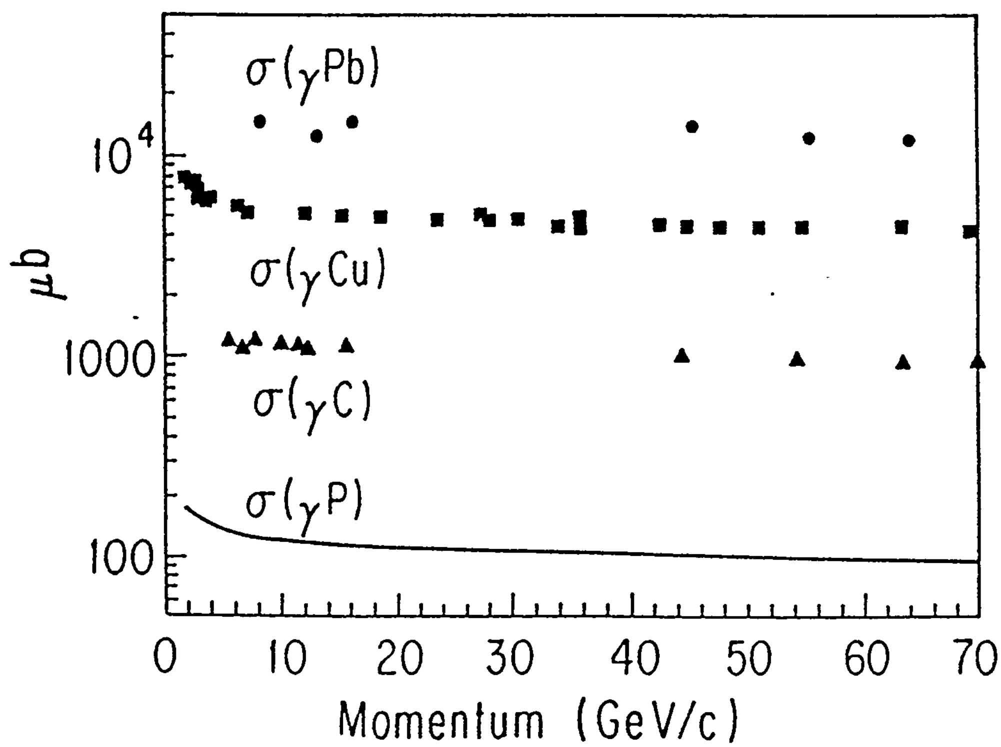

Fig. 11. Photon-nucleus total hadronic cross-sections [12,13,14].

$$\Delta E = \sqrt{m^2 + k^2} - \nu \approx \frac{m^2 + Q^2}{2\nu} \quad \text{for } \nu^2 >> m^2 + Q^2$$

It follows from the uncertainty relation that the longitudinal distance Δs_L over which the fluctuation lasts satisfies (with $\hbar = c = 1$):

$$\Delta S_L \geq \frac{2\nu}{m^2 + Q^2} \qquad (1)$$

In the distance ΔS_L there is a limit to how far the partonic system can grow in the transverse direction. It is straight forward to show that for the symmetric decays of the photon (quark-gluon fusion interaction) the maximum transverse size of the fluctuation $\Delta S_T \sim \frac{1}{\sqrt{Q^2}}$ and $m \sim \sqrt{Q^2}$. For asymmetric decays, where one of the quarks takes most of the momentum of the photon ("wee quark" or "naive parton picture" interaction), $\Delta S_T \sim \frac{1}{P_t}$, where P_t is the transverse momentum of the slower quark. Thus through $\vec{k}, \nu$ and Q^2 one can "dial" partonic structures of differing longitudinal and transverse dimensions, and study the propagation of such structures through nuclear matter.

Consider first real photons. $k = \nu$ and $Q^2 = 0$, and thus $\Delta S_L \sim \frac{2k}{m^2}$ and $\Delta S_T \sim \frac{1}{m}$. Taking into account the fact that the photon can couple to $Q\overline{Q}$ of every flavour and that the most likely value of m generated by a given $Q\overline{Q}$ is that of a vector meson with the appropriate quark composition (generalized vector dominance picture), it is amazing how well the photo-absorption data is reproduced. The value of $\sigma_{\gamma p}$ in fig. 11, A_{eff}/A and the difference of A_{eff}/A between γA and πA in fig. 12 are well accounted for by the magnitude of the coupling of the photon to the various $Q\overline{Q}$ states, the known ρ, ω and ϕ - nucleon cross-sections, and the expected smaller cross-section for the more massive vector mesons. Even the onset of shadowing at a few GeV is consistant with the estimate $k \geq \frac{m^2}{2}$ x nuclear size, based on the value of ΔS_L.

This spectacular agreement encourages us to look at virtual photon data. From equation (1), shadowing for virtual photons should become similar to that of real photons for $Q^2 << m^2$, i.e. for $x_{Bj} \leq \frac{m^2}{2\nu}$, and there should be no

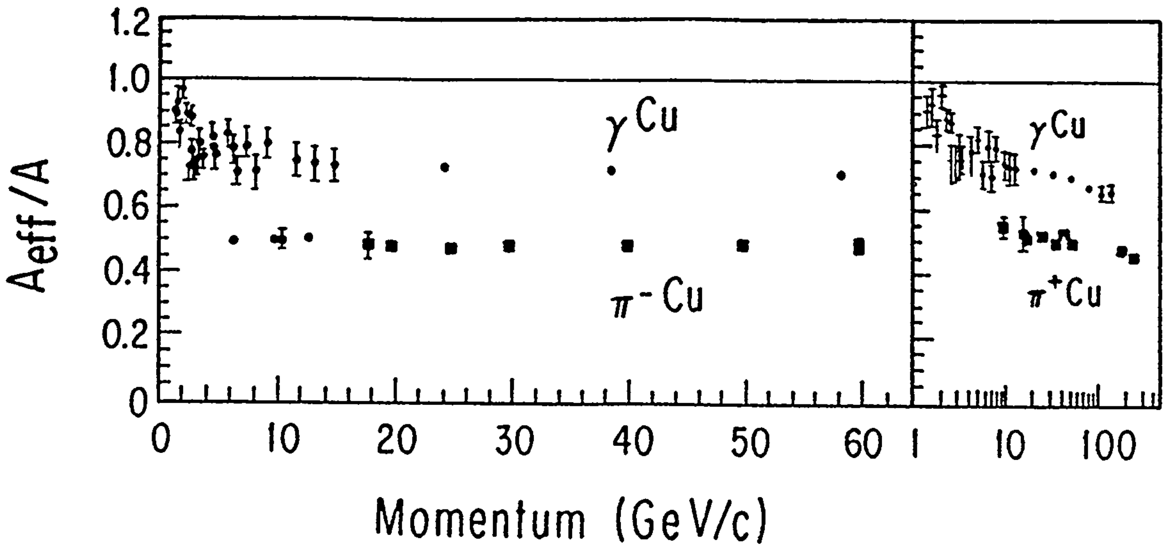

Fig. 12. Comparison of shadowing in photon-nucleus and hadron-nucleus interactions. The difference at the highest energies is a consequence of the small cross-section of high mass partonic structures, see text. Input data are from [3,12,13,14].

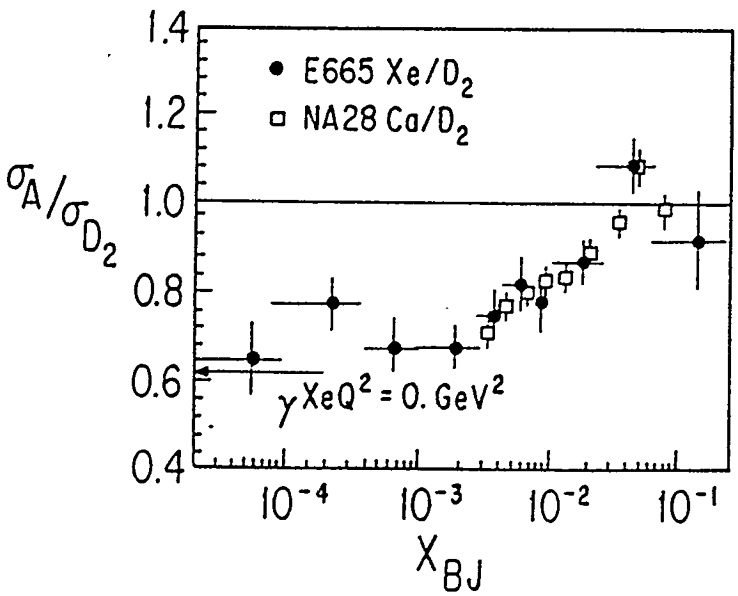

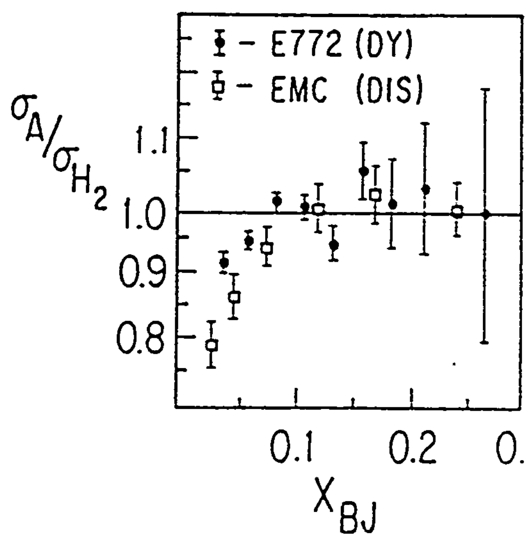

Fig. 13. Shadowing in inelastic μ-nucleus scattering. The E665 data [15] is for 0.01 < , Q^2 < , 60 GeV^2. The NA28 data [16] is for 0.3 < , Q^2 < 3.2 GeV^2. The cross-sections are quoted per nucleon. For $x_{Bj} > 0.1$ the data are consistent with complete transparency. For $x_{Bj} < 10^{-3}$ the same amount of shadowing is seen as for real photons.

Fig. 14. Comparison of shadowing of virtual photons in the Drell-Yan process and deep inelastic lepton scattering [17]. The cross-sections quoted are per nucleon.

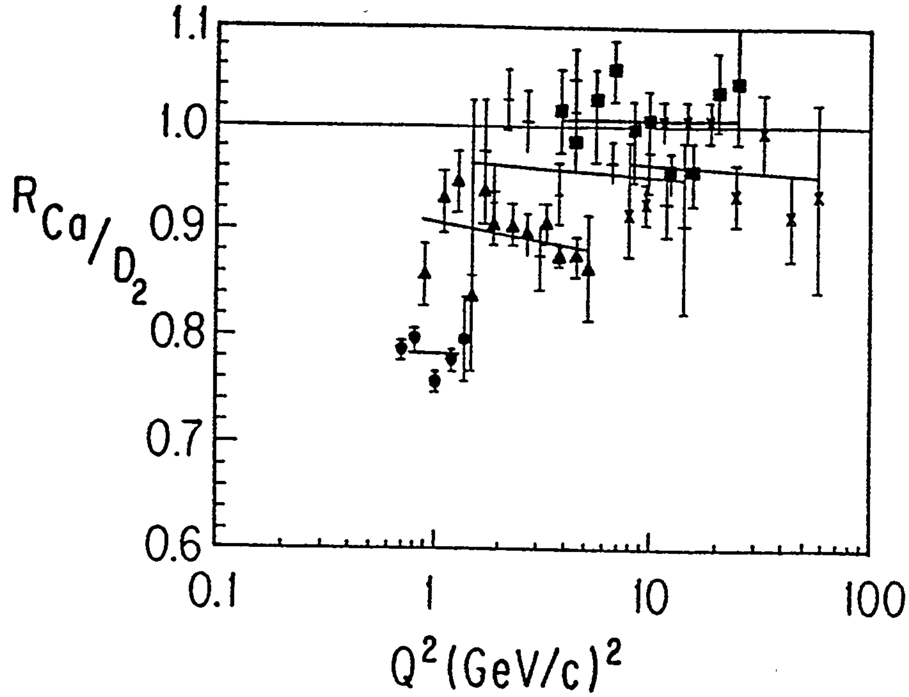

Fig. 15. Data showing that in deep inelastic muon scattering shadowing is independent of Q^2, but is a function of xBj [18]. The lines join data at the same value of xBj, to guide the eye. The circles, crosses and squares are for xBj = 0.0055, 0.045 and 0.25 respectively. R is the ratio of cross-sections per nucleon.

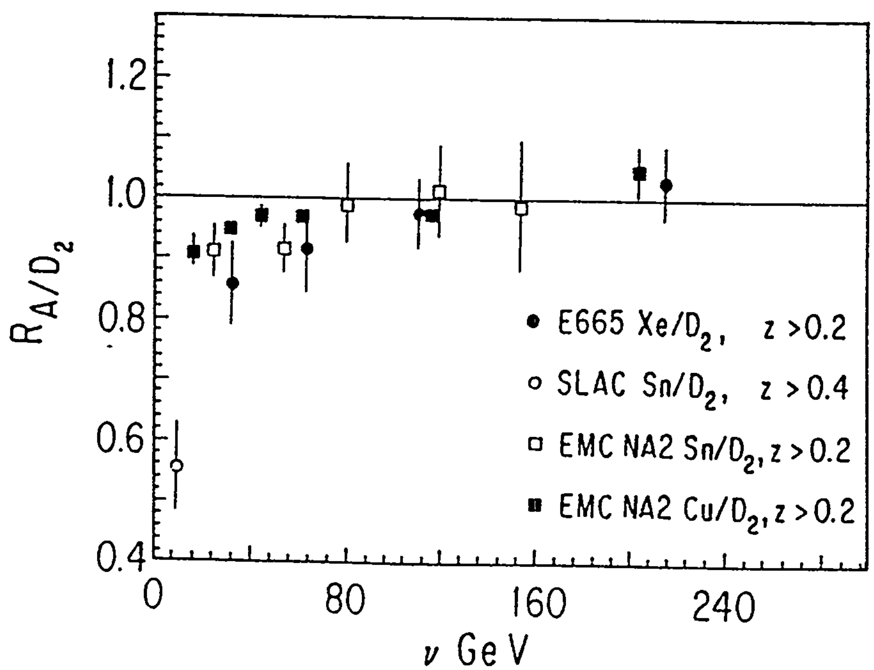

Fig. 17. Data [20] which suggests that slower hadrons produced in deep inelastic lepton scattering are attenuated as they pass through a nucleus. R is the ratio of the number of produced charged hadrons per nucleon for different nuclear targets. Z ≡ hadron energy / ν. ν = energy of virtual photon.

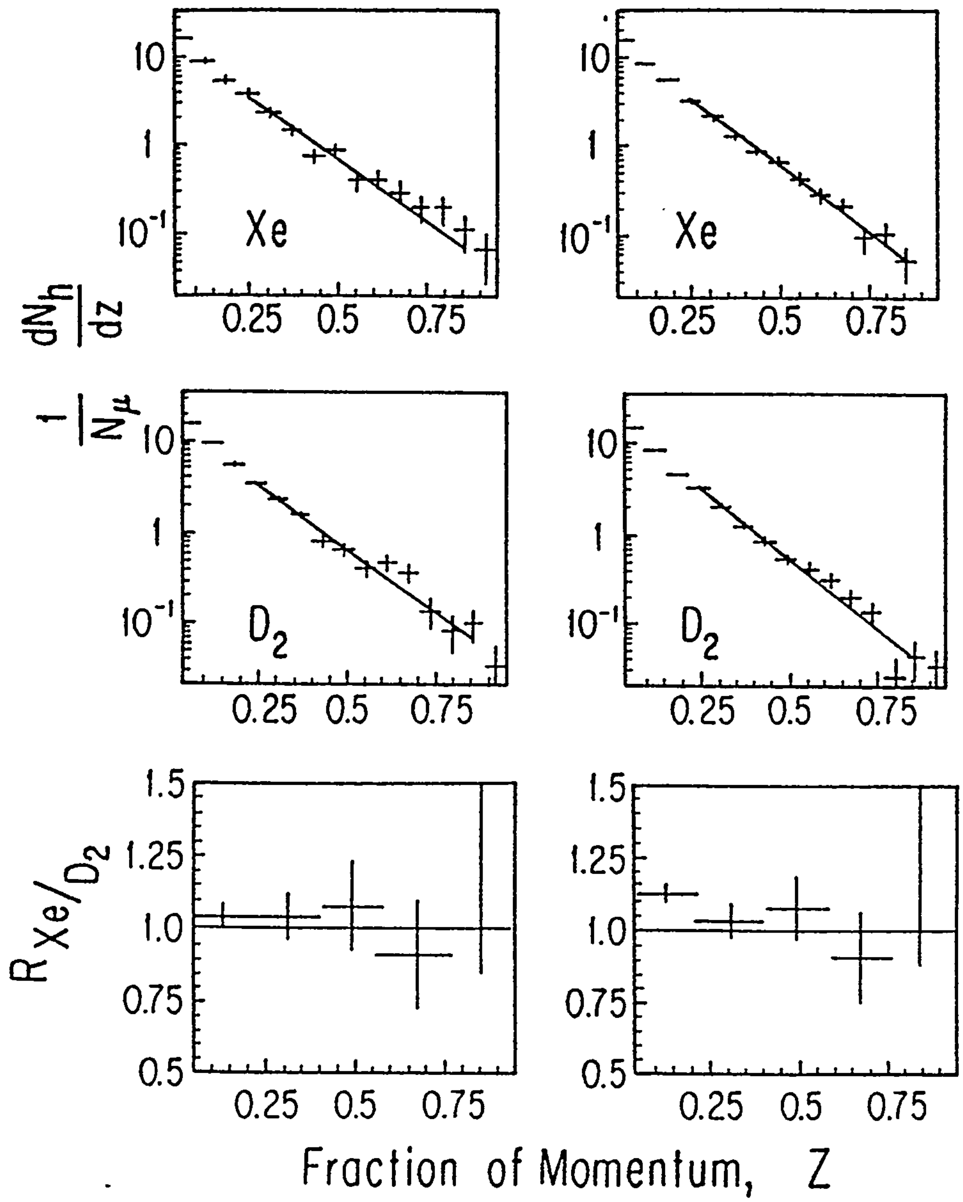

Fig. 16. Momentum spectra of charged hadrons produced in deep inelastic muon scattering for ν >. 100 GeV [19]. The cross-sections are per scattered muon. The data on the left are for $x_{Bj} < 0.005$ and $Q^2 < 1$, i.e. for the region where maximum shadowing is seen, see fig. 13. On the right they are for $x_{Bj} > 0.03$ and $Q^2 > 2$, i.e. for the region where no shadowing is seen. Z ≡ hadron energy / ν. ν = energy of virtual photon. The data suggests the surprising result that, from the point of view of the attenuation of produced hadrons, there is no difference in the two regions.

shadowing for $Q^2 >> m^2$ and $x_{Bj} \geq 0.1$. Once again this is in good agreement with the data, both for inelastic lepton scattering off nuclei (fig. 13) and for the Drell-Yan process (fig. 14).

For $\frac{m^2}{2\nu} \geq x_{Bj} \geq 0.1$ the photon fluctuates into a relatively simple $Q\overline{Q}$ system which lives long enough to be potentially interesting. As mentioned earlier, the transverse dimension of the system is either ~ $\frac{1}{\sqrt{Q^2}}$ or $\frac{1}{P_t}$ depending on whether the $Q\overline{Q}$ has a symmetric or asymmetric momentum division. As is evident from fig. 15, for a given x_{Bj}, shadowing is largely independent of Q^2. From this we can conclude that the asymmetric decays dominate the interaction. Thus the study of the A-dependence of the inelastic lepton scattering off nuclei can be viewed as the study of the production, evolution and propagation through nuclear matter of a $Q\overline{Q}$ system, where one quark is fast and the other slow. Based on our earlier discussion the manner in which such a system evolves and interacts with the nucleus should depend strongly on the kinematics of the virtual photon. In the non-shadowing kinematic regime ($x_{Bj} \geq 0.1$) the $Q\overline{Q}$ pair is produced within the volume of the nucleus. We would thus expect that the slower quark would strongly interact, leaving the fast quark to propagate through the nucleus. In the shadowing regime ($x_{Bj} \leq \frac{m^2}{2\nu}$) the $Q\overline{Q}$ pair is produced before the nucleus is encountered. It has time, as in the case of real photons, to evolve into a hadronic system. We thus would expect the A-dependence of the process to be very similar to that observed for incident hadrons. The surprising feature in the data is that the A-dependence of produced hadrons in lepton-nucleus scattering, to within the accuracy of the experiments, seems not to depend on the kinematics of the scattering. As can be seen in fig. 16, the spectra of produced high energy hadrons are the same in the shadowing and non-shadowing kinematic regimes. Furthermore, in both regimes, the spectra are at most very weakly dependent on the nuclear target. In the non-shadowing regime, this is exactly what we would expect. Here we are looking at the propagation of a fast quark through the nucleus and, from the A-dependence of the Drell-Yan process, we know that the nucleus is highly transparent to fast quarks. In the shadowing regime the data are surprising. If our overall analysis is correct, the incident state is basically a hadron. As in the case of incident hadrons, the produced fast hadrons should show strong nuclear attenuation. None seems to be seen. It points out, once again, the fact that we do not have a good understanding of the propagation and fragmentation of complicated hadronic systems as they pass through nuclear matter. It would be interesting to see if for real incident photons, the fast forward produced hadrons show transparency. I am not aware of any data on this subject.

We see that there is good reason to believe that very slow quarks are highly attenuated in the nuclear medium while fast ones are not. The final topic I wish to touch upon is the question: below what energy does the attenuation begin to be apparent? The compilation of data in fig. 17

summarizes everything that is known on this subject. For different reasons in the various experiments, the measurements at the lowest value of ν are difficult and, in my opinion, the data should be used with caution. Nevertheless, taking together the results of all the experiments, there is a clear indication that for virtual photons of energy below about 100 GeV, producing hadrons of energy greater than 20% of the photon's energy, there is observable attenuation. Since the formation distance of a 20 GeV pion is much larger than a nucleus, it is unlikely that these results are a consequence of the formation time of hadrons. It is also not known if the observed attenuation of the slower quarks is a reflection of an increase of cross-section with decrease of energy, or if it is a reflection of an energy loss which only becomes noticeable when its magnitude is significant compared to the energy of the quark [21].

To summarize and put it all together. I believe that we have a fairly coherent picture of the interaction with hadronic matter of photons, real and virtual. Depending on the energy and Q^2 of the photon, the interaction ranges from being that of an ordinary hadron to that of a simple pair of quarks, where one of the quarks carries almost the entire energy of the photon. The A-dependence of photon absorption, photo-production, the Drell-Yan process and lepto-production are thus a good starting point for the study of the space-time evolution and propagation through hadronic matter of various partonic structures. These A-dependences teach us, for example, that high energy quarks interact weakly, if at all, with nuclear matter (quark-nucleon cross-section $\leq$ a few mb). Furthermore, if quarks lose energy as they pass through nuclear matter, it is at most a few GeV/fermi.

This is to be contrasted with the passage of complex hadronic structures. When a hadron impinges on a nucleus it interacts strongly. Nuclei are almost "black" for incident hadrons. However, other than that the soft components of the hadrons interact strongly, little else is understood well about the propagation of complex hadronic structures through nuclear matter. The data from hadro-production or lepto-production, for the production of one type of particle or production of another type, at one P_t or another P_t (a subject I did not have time to cover), often give conflicting insights into the physics that is involved. Furthermore, the existing data is not systematic or precise enough to give reliable insights.

The fact that it has proven to be difficult to interpret existing data on the interaction with nuclear matter of complex partonic structures should not be overlooked by those searching for fundamentally new physics in the collisions of relativistic heavy ions. If photon, lepton and hadron-nuclear studies are a guide, interesting effects will be subtle. To understand them, it will be crucial to study systematically and with high precision a very wide range of phenomena in pp, pA and AA collisions.

REFERENCES

1. For reviews and compilations of data on hadron, photon and lepton-nucleus interactions see, for example: W. Busza, Acta. Phys. Pol. B8 (1977) 333; N. N. Nikolaev, Sov. J. Part. Nucl. 12 (1981) 63; S. Fredriksson, et al., Physics Reports 144 (1987) 187; T. Kanki, et al., Progress of Theoretical Physics, Supplement No. 97B (1989).

2. D. S. Ayres, et al., Phys. Rev. D15 (1974) 3105.

3. S. P. Denisov, et al., Nucl. Phys. B61 (1973) 62; A. S. Carroll, et al., Phys. Lett. 80B (1979) 319; W. Galbraith, et al., BNL preprint 11598 (1967); Particle data group, Phys. Lett. 204B (1988).

4. D. M. Alde, et al., Phys. Rev. Lett. 64 (1990) 2479.

5. P. Bordalo, et al., Phys. Lett. 193B (1987) 368.

6. C. Stewart, et al., Phys. Rev. D42 (1990) 1385.

7. R. Bailey, et al., Z. Phys. C22 (1984) 125; A. Beretvas, et al., Phys. Rev. D34 (1986) 53; and the compilation of D.S. Barton, et al., Phys. Rev. D27 (1983) 2580: For analogous πA results see W. Busza and M. Zielinski, Phys. Rev. D31 (1985) 192.

8. T. Eichten, et al., Nucl. Phys. B44 (1972) 333;D.S. Barton, et al., Phys. Rev. D27 (1983) 2580.

9. P. Skupic, et al., Phys. Rev. D18 (1978) 3115.

10. W. Busza and A.S. Goldhaber Phys. Lett. 139B (1984) 235.

11. This section is based to a large extent on discussions with A. H. Mueller and on J.D. Bjorken, Fermilab-Pub-86/16 (1986).

12. For a review of the data and a theoretical discussion of photo- and lepton-production see, for example: T.H. Bauer, et al., Rev. Mod. Phys. 50 (1978) 261; L. Frankfurt and M. Strikman, Phys. Reports 160 (1988) 235.

13. Particle data group, Phys. Lett. 204B (1988).

14. D.O. Caldwell, et al., Phys. Rev. Lett. 42 (1979) 553.

15. D.E. Jaffe, presented at the XXVI th Recontres de Moriond, Les Arcs, France (1991).

16. M Arneodo, et al., Phys. Lett. B333 (1990) 1; M. Arneodo, et al., Phys. Lett. B211 (1988) 493.

17. Figure taken from D.M. Alde, et al., op. cit. ref. 4.

18. P. Amaudruz, et al., CERN-PPE/91-52 (1991).

19. J.J. Ryan, Ph.D. Thesis, Massachusetts Institute of Technology (1990) E-665 data.

20. Compilation of data: A.F. Salvarani, Ph.D. Thesis, University of California at San Diego (1991). The reader should be warned that the E665 data is very preliminary, and that the ν-resolution and the normalization in the three experiments differ significantly.

21. See also M Gyulassy and M. Plumer, Preprint LBL-27605 (1989).

Acknowledgments

In preparing for this talk I have significantly profited from discussions with James Bjorken, Stan Brodsky, Clive Halliwell, Al Mueller, Jan Nassalski, John Ryan and Andrzej Zieminski. Without the dedicated help of Sandra Fowler and Anne Lees, this manuscript would never have been prepared in time for the proceedings. This work was supported in part by DOE Contract No. DE-AC02-76ER03069

Fermilab E665:

Results in Muon Scattering

John J. Ryan
Massachusetts Institute of Technology

Fermilab E665:
results in muon scattering

17-Nov-1995

Dr. John J. Ryan

Massachusetts Institute of Technology

The E665 Collaboration - 90/91

T. Dreyer, M. Erdmann, J. Haas, G. Siegert, H.E. Stier, M. Wilhelm
Albert-Ludwigs-Universität Freiburg i. Br., Germany

D.F. Geesaman, H.E. Jackson, S. Kaufman, E.R. Kinney,
T. Kirk, V. Papavassiliou, D.H. Potterveld, A. Zghiche
Argonne National Laboratory, Argonne IL USA

R.D. Kennedy, H.G.E. Kobrak, P. Madden, A. Salvarani, R.A. Swanson
University of California, San Diego, CA USA

B.R. Baller, H. Melanson,
H.E. Montgomery, J.G. Morfin, C.W. Salgado, S.A. Wolbers
Fermi National Accelerator Laboratory, Batavia, IL USA

J.M. Conrad, G.Y. Fang, A.V. Kotwal, D.G. Michael,
R.B. Nickerson, F.M. Pipkin, M. Schmitt, Richard Wilson
Harvard University, Cambridge, MA USA

M.R. Adams, D.A. Averill, R.S. Guo,
C. Halliwell, D.E. Jaffe, S.R. Magill, D.W. Mcleod
University of Illinois, Chicago, IL USA

J. Figiel, K. Olkiewics, B. Pawlik, P. Stopa
Institute for Nuclear Physics, Krakow, Poland

P.L. Anthony, F.S. Dietrich
Lawrence Livermore National Laboratory, Livermore, CA USA

S. Aïd, S. Kunori, S. O'Day, E.J. Ramberg
A. Skuja, G.A. Snow
University of Maryland, College Park, MD USA

M.D. Baker, W. Busza, L. Osborne, J.J. Ryan
Massachusetts Institute of Technology, Cambridge, MA USA

I. Derado, T.J. Carroll, V. Eckardt, H.J. Gebauer, D. Hantke, G. Jancso, A. Manz,
N. Schmitz, S. Söldner-Rembold, W. Wittek
Max-Planck-Institut für Physik, Munich, Germany

H.M. Schellman, P. Spentzouris
Northwestern University, Evanston, IL USA

H.L. Clark, R.W. Finlay, K.H. Hicks
Ohio University, Athens, OH USA

A. Banerjee, K.A. Griffioen
University of Pennsylvania, Philadelphia PA USA

A.A. Bhatti, U. Bratzler, R. Davisson, W. Dougherty, D.M. Jansen,
Z. Jin, J.J. Lord, H.J. Lubatti, T. Zhao
University of Washington, Seattle, WA USA

H.M. Braun, H. Breidung, U. Ecker, R.Otten, A. Röser
University of Wuppertal, Wuppertal, Germany

S.K. Dhawan, V. Hughes, K.P. Schüler, H. Venkataramania
Yale University, New Haven, CT USA

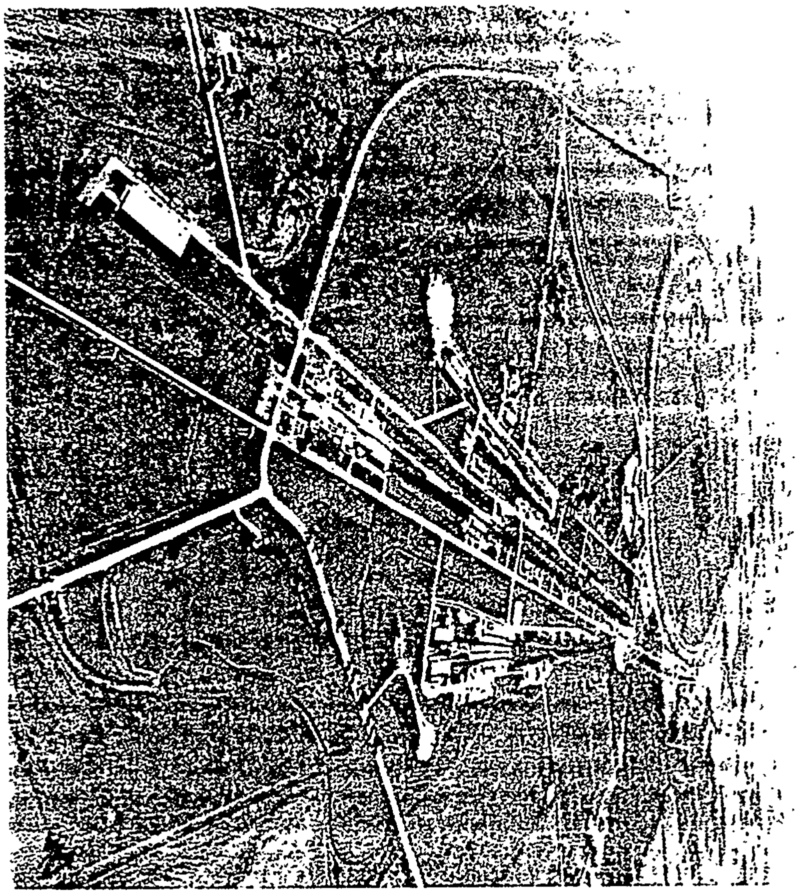

E665 Plan View

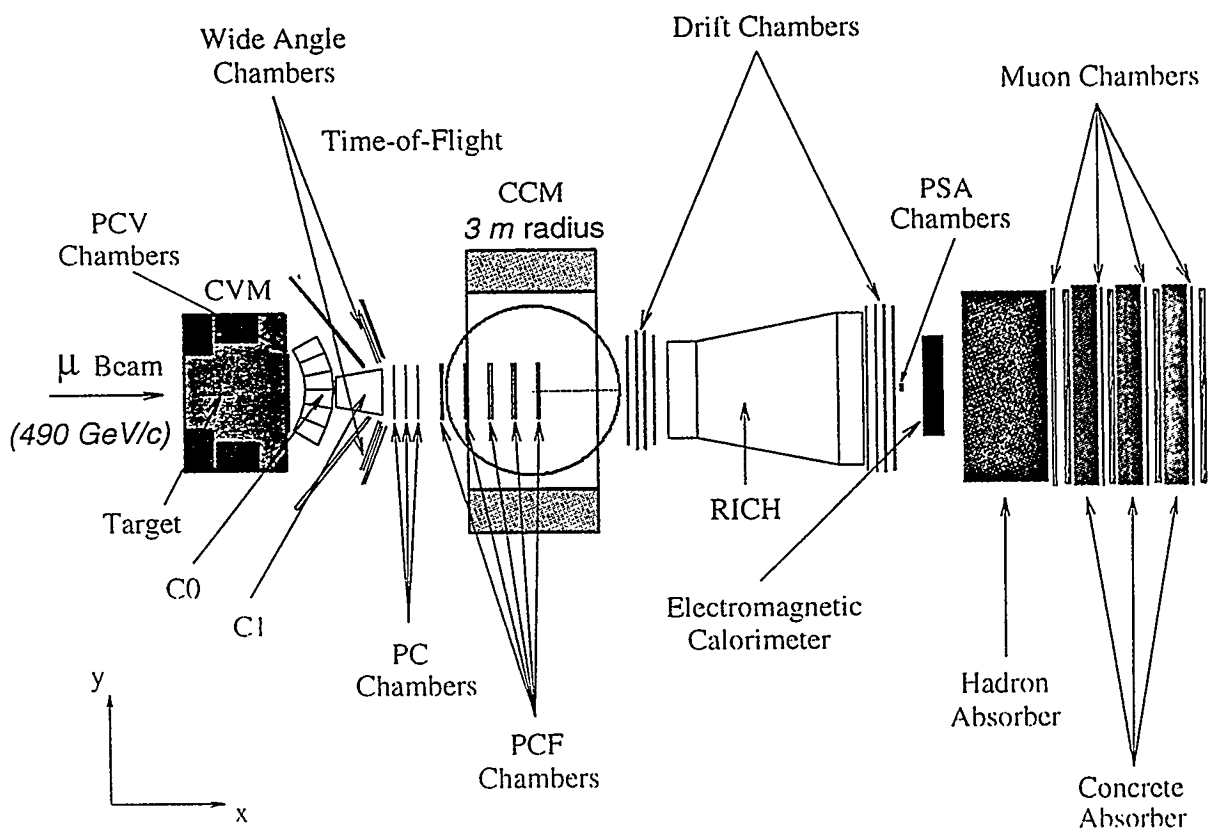

Deep Inelastic Scattering

Kinematic Variables:

Energy Transfer: ν.

4-Momentum Transfer: $Q^2 \equiv -q^2$.

$$Q^2 = -2m_\mu^2 + 2EE' - 2|\bar{k}||\bar{k}'|\cos\theta.$$

Bjorken Scaling variable:

$$x_{\mathrm{Bj}} \equiv \frac{Q^2}{2M\nu},$$

Mass of the Hadronic system: W.

$$Q^2 = 2M\nu + (M^2 - W^2).$$

Scaled Energy Transfer: $y = \nu/E$

Kinematic Ranges for DIS Experiments

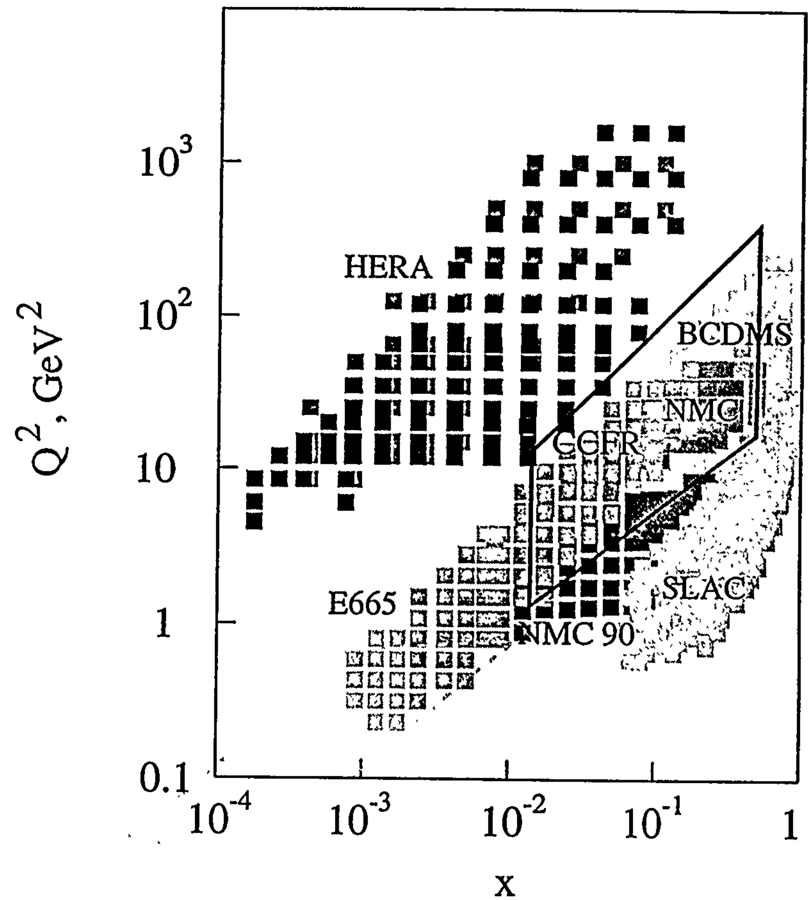

E665 n/p

Energy of the Beam: $\langle E_B \rangle = 490$ GeV

$100 \text{ GeV} < \nu < 500 \text{ GeV}$

$0.1 \text{ GeV}^2/c^2 < Q^2 < 150 \text{ GeV}^2/c^2$

$0.001 < x_{\text{Bj}} < 0.5$

Outline:

- A-dependent Shadowing of Total cross section:

  $$(\sigma_A / A) / \sigma_H < 1. \quad (\text{low } x_{Bj})$$

- Nuclear Effects in Forward (y*>0) Hemisphere for DIS events.
- Nuclear Effects in Backward (y*<0) Hemisphere for DIS events.
- A-dependence of ρ's in Forward (y*>0) Hemisphere for Diffractive events.
- A-dependence of Multiplicity for Diffractive events.

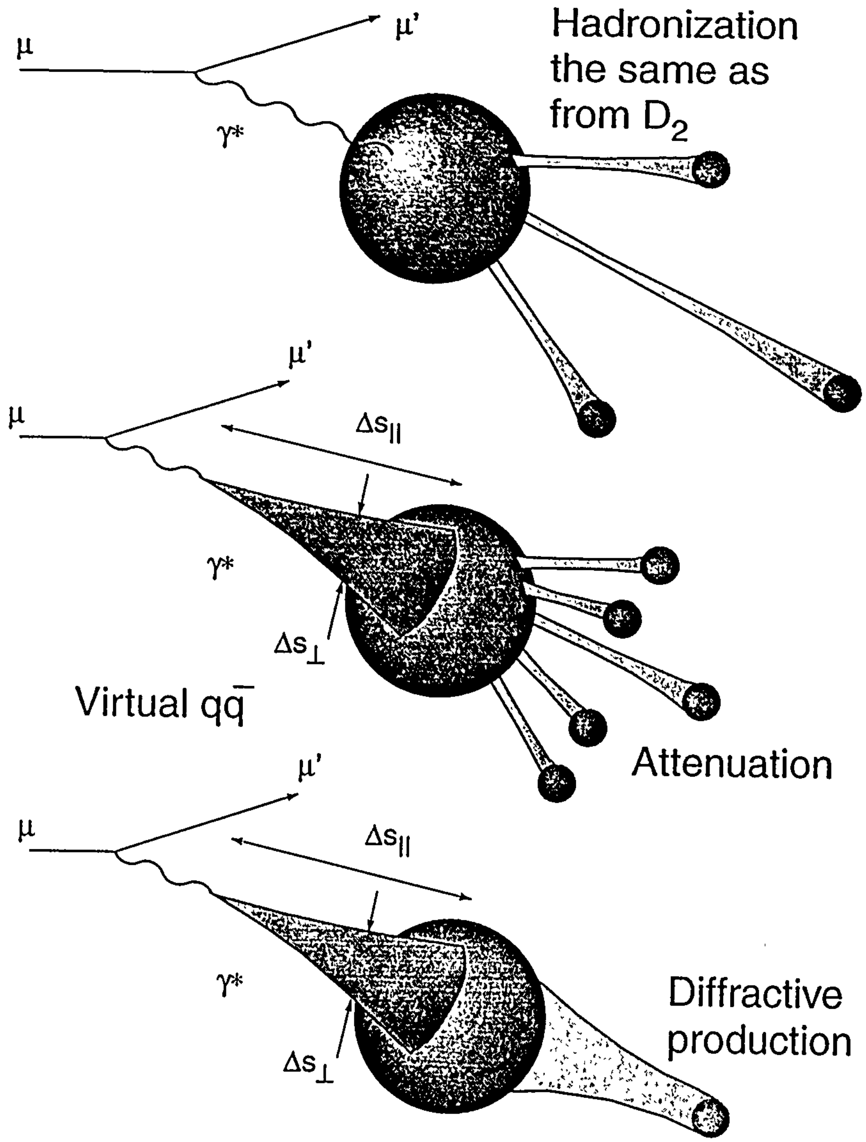

J.J.Ryan

Uncertainty Principle:

$$\Delta E = \sqrt{\nu^2 - q^2 + m^2} - \nu$$

$$\approx \frac{Q^2 + m^2}{2\nu},$$

gives the longitudinal extent of virtual state:

$$\Delta S_{\|} \approx c\Delta t \geq \frac{1}{x_{\mathrm{Bj}} M} \frac{Q^2}{Q^2 + m^2}.$$

and the transverse extent of virtual state:

$$\Delta S_{\perp} \approx 1/m \sim 1/\sqrt{Q^2}.$$

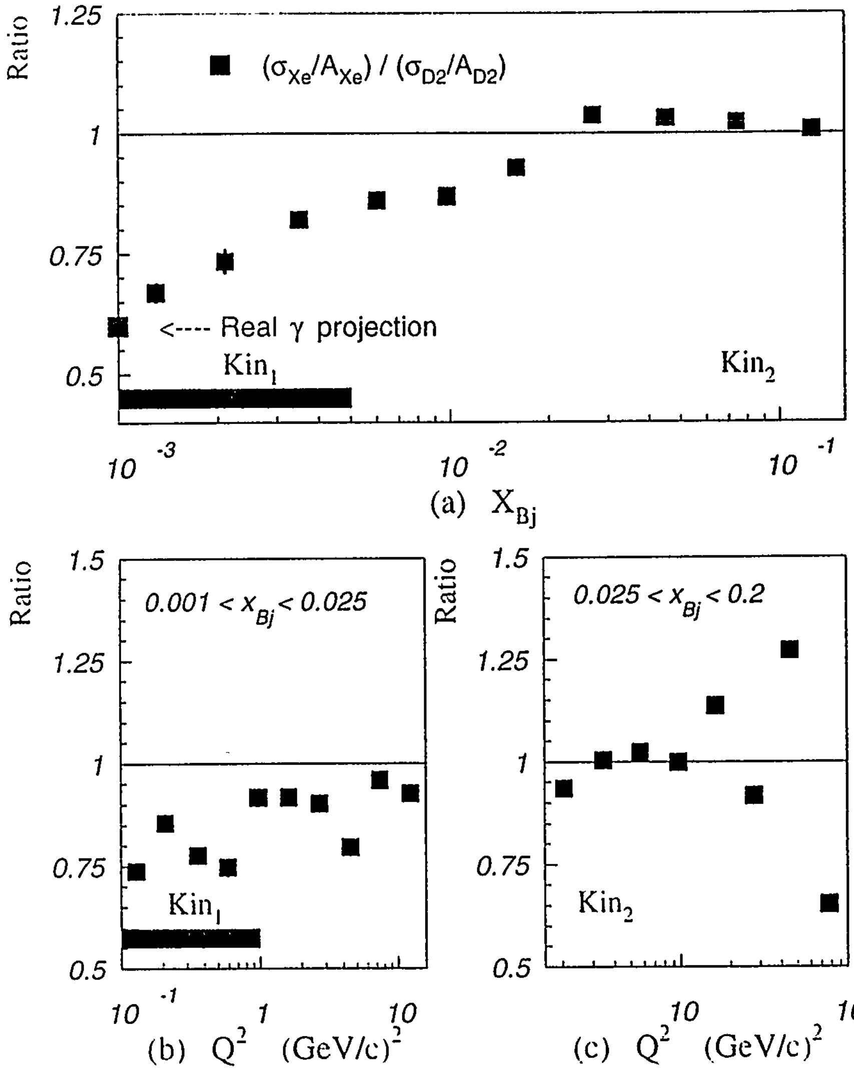

Phys. Lett. B287, (1992)

$$\text{Kin}_1 \equiv \begin{cases} x_{\rm Bj} < 0.005 & \text{and} \\ Q^2 < 1\ \text{GeV}^2/c^2 & \end{cases}$$

$$\text{Kin}_2 \equiv \begin{cases} x_{\rm Bj} > 0.03 & \text{and} \\ Q^2 > 2\ \text{GeV}^2/c^2 & \end{cases}$$

Phys. Rev. Lett. 68(22) (1992)

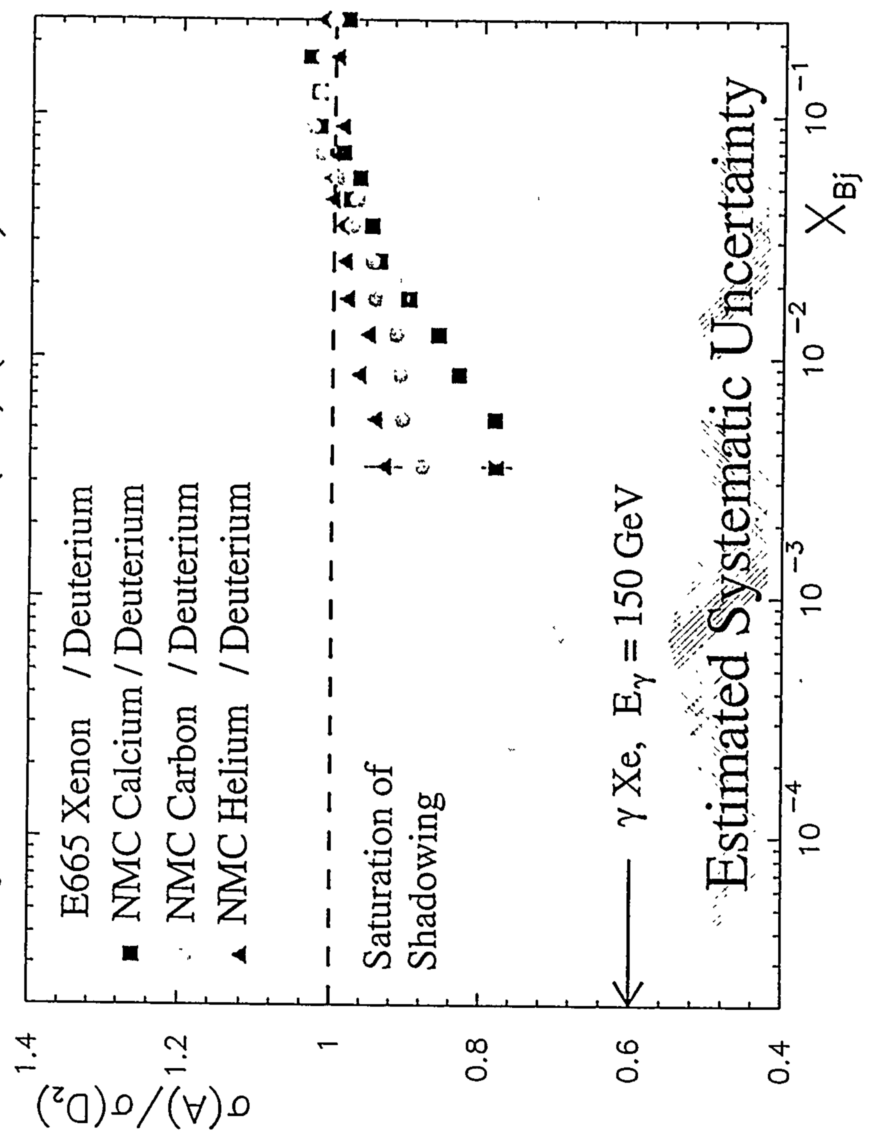

Differential Hadron Multiplicity:

$$D(z) \equiv \frac{1}{N_\mu}\,\frac{dN_h}{dz}.$$

Scaled Hadron Energy:

$$z \equiv \frac{P_{Target} \cdot P_{hadron}}{P_{Target} \cdot q}$$
$$= E_h/\nu \qquad \text{LabFrame}$$

Feynmann - x:

$$x_F \equiv \frac{P_{\|}^{cm}}{P_{\|max}^{cm}} \approx \frac{P_{\|}^{cm}}{W/2}$$

Partial Multiplicity:

$$R_{sample} \equiv \frac{\Sigma_{Z_{min}}^{Z_{max}} D_{sample}(z_i)\ \Delta z}{Z_{max} - Z_{min}}$$

$$\bar{R}_{Xe/D_2} = \frac{R_{Xe}}{R_{D_2}}$$

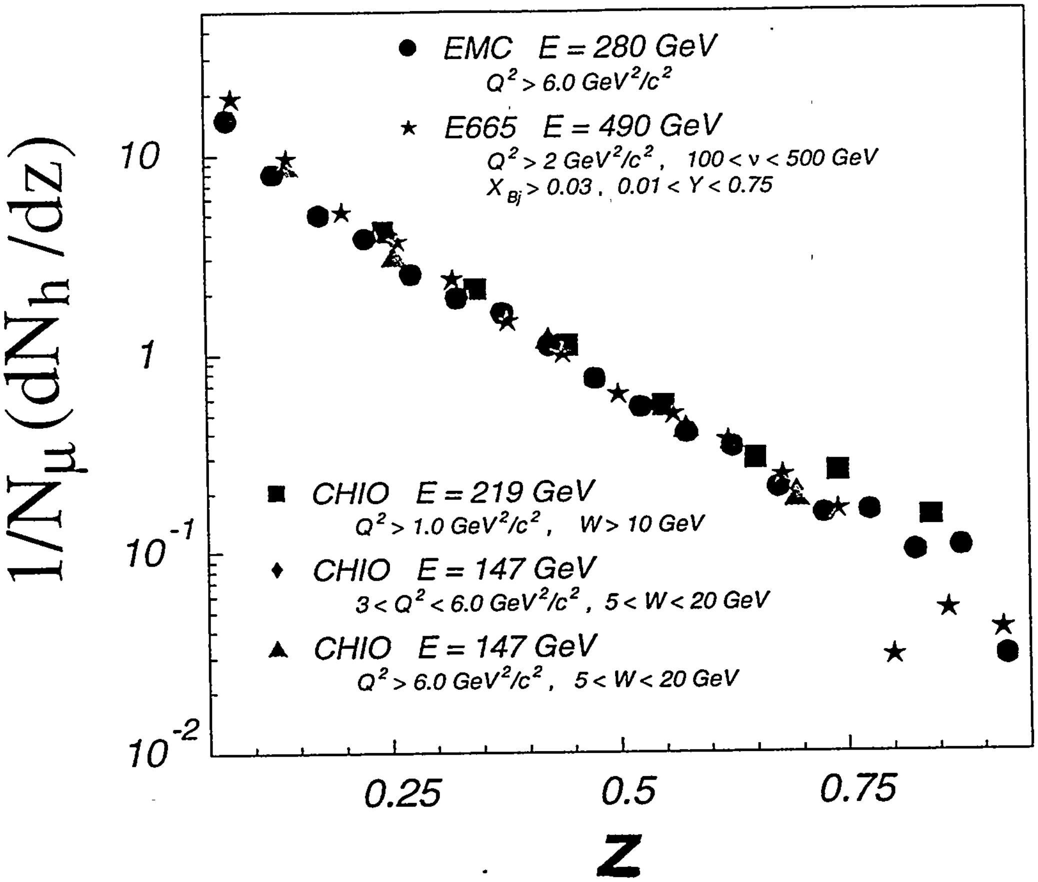

Phys. Rev. D50(3), (1-Aug-94)

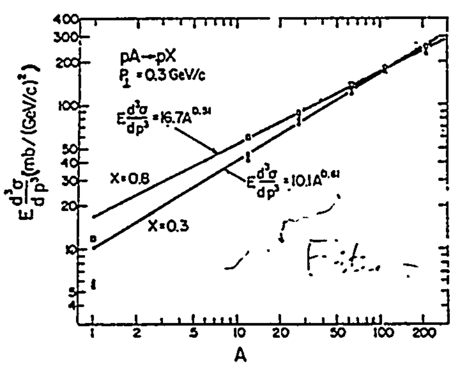

Hadron-Nucleus collisions,
forward hadron distributions.

Barton, *et al.*
Phys. Rev. D27(11), (1983)

Fit → $\sigma^h(x_F) = c_1 A^{\alpha(x_F)}$

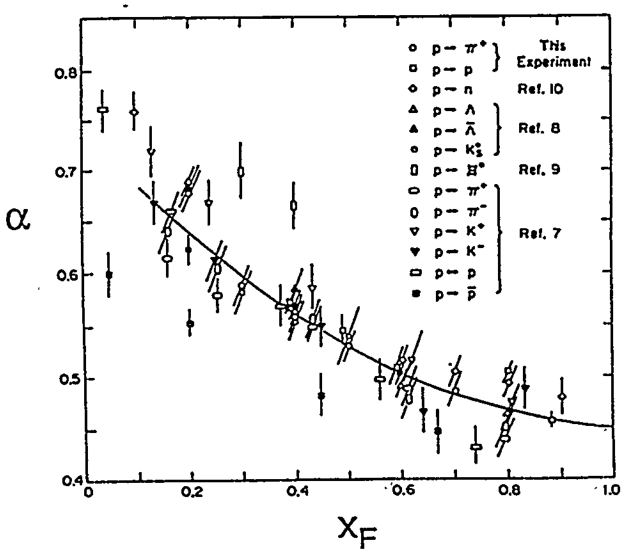

Predicted Ratio, then,
for xenon / deuterium
forward hadron distribution.

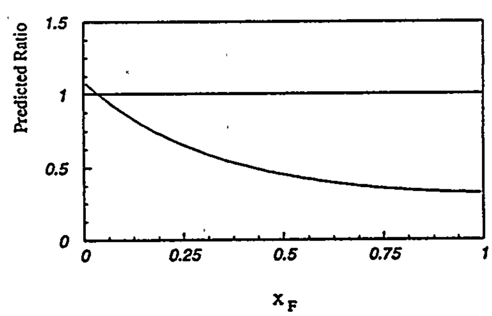

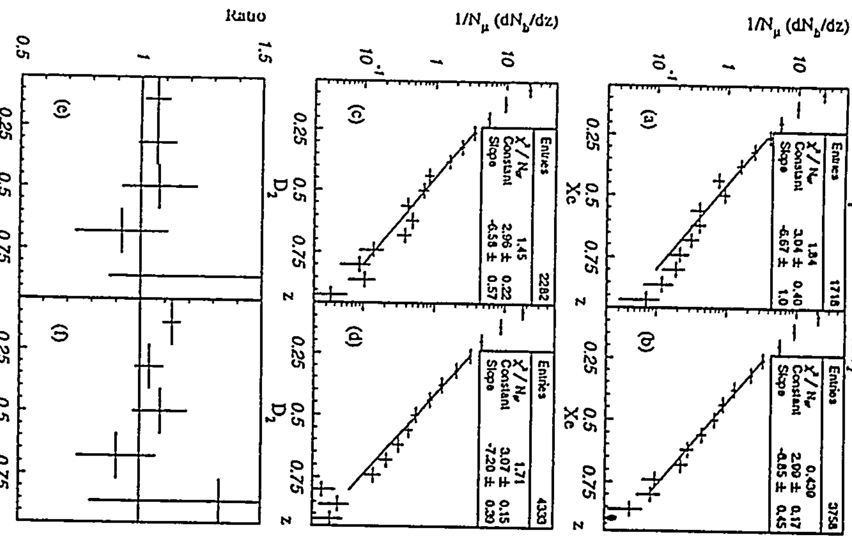

FIG. 7. z distributions: Xe and D_2. These plots show the z istributions from xenon and deuterium and the ratios of the istributions. The distributions on the left are from events n the low kinematic region: Kin_1, while those on the right re from events in the high kinematic region: Kin_2. The data ave been corrected for acceptance but not for target length ffects; they are tabulated in Tables XIX and XXX.

E665:
M.R. Adams, *et al.*
Phys. Rev. D50(3), (1994)

C. Corrected xenon and D_2

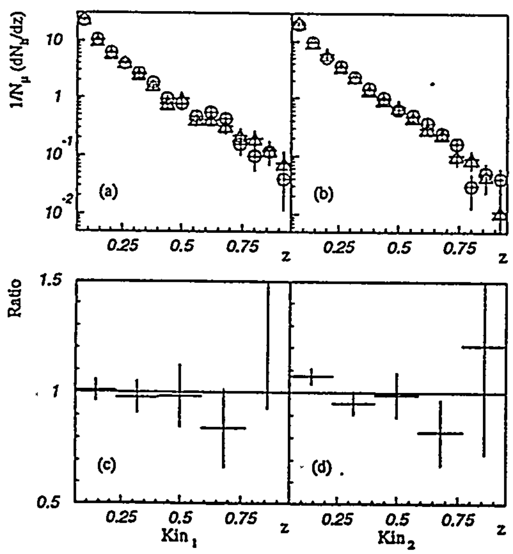

FIG. 13. Xe and D_2, corrected for rescattering. Plots (a) and (b) show the z distributions which have been corrected for rescattering in the targets. The circles represent the corrected deuterium distributions, while the triangles represent the corrected xenon distributions. The plots on the left are for the low kinematic region: Kin_1, while those on the right are for the high kinematic region: Kin_2. The ratio of these distributions is shown in (c) for Kin_1, and in (d) for Kin_2. These data are tabulated in Tables XX and XXXII.

TABLE V. Corrected $\overline{R}_A$ values. These values are from the comparison function of Eq. (28) for the listed comparisons; the comparisons used the distributions which were corrected for target length effects, except for the half-target samples.

	$\overline{R}_A$	$\pm$	$\sigma_{\overline{R}_A}$
Xe/D_2, (corrected Kin_1)	0.975	$\pm$	0.060
Xe/D_2, (corrected Kin_2)	0.957	$\pm$	0.044
Kin_1 / Kin_2 (corrected D_2)	1.134	$\pm$	0.058
Kin_1 / Kin_2 (corrected Xe)	1.156	$\pm$	0.066
Xe/D_2, (half) Kin_1	1.052	$\pm$	0.090
Xe/D_2, (half) Kin_2	0.990	$\pm$	0.064

E665:
M.R. Adams, *et al.*
Phys. Rev. D50(3), (1994)

Shadowing vs Non-Shadowing

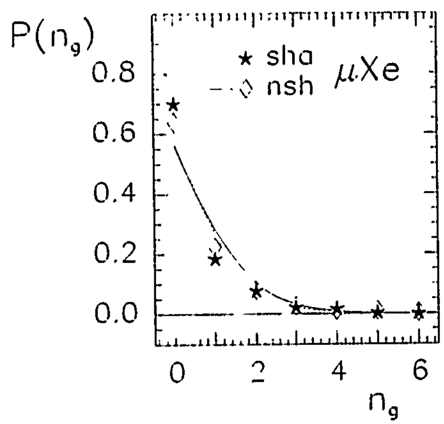

$$R(n_g) = \frac{<n(n_g)>_{\mu Xe}}{<n>_{\mu D}}$$

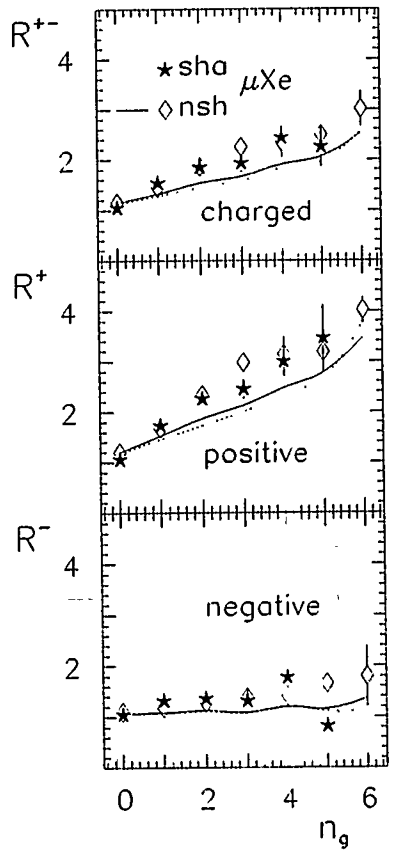

E665
Z. Phys. C65 (1995)

Shadowing:

$0.002 < x_{Bj} < 0.02$

$1 < Q^2 < 14$

Non-Shadowing:

$0.02 < x_{Bj} < 0.3$

$1 < Q^2 < 100$

Conclusions so far:

- A-dependent Shadowing of Total cross section:

  $(\sigma_A / A) / \sigma_H < 1.$ (low x_{Bj})

- No Nuclear Effects in Forward ($y^*>0$) Hemisphere for DIS events.

- Nuclear Cascading in Backward ($y^*<0$) Hemisphere for DIS events but NO difference between Shadowing and Non-Shadowing.

- Where is Shadowing dependence?

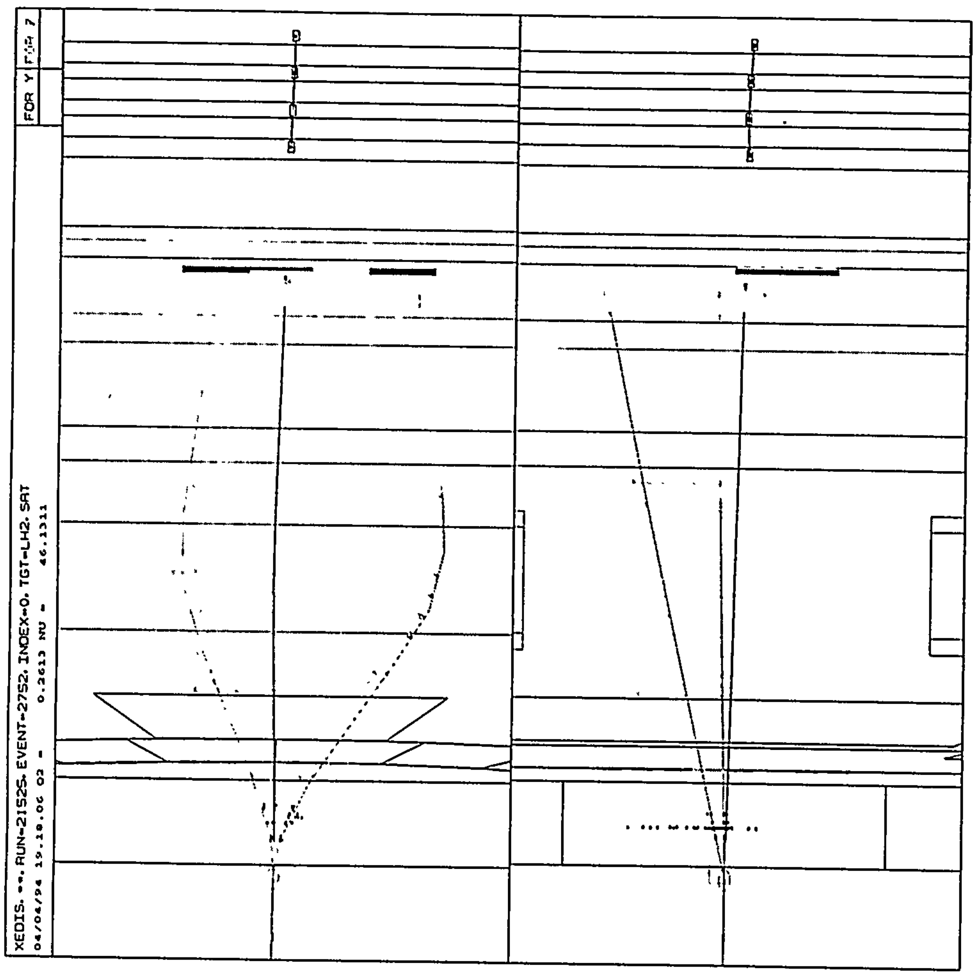

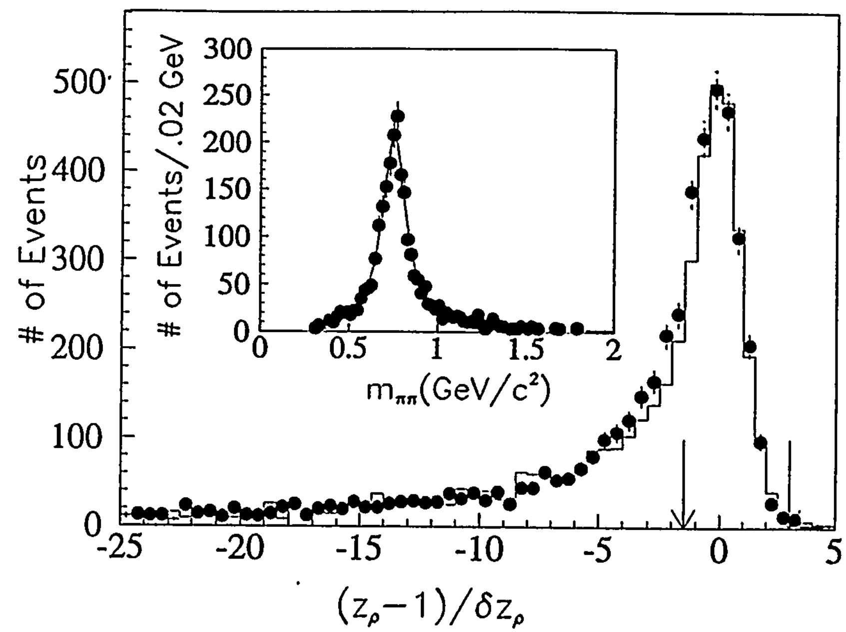

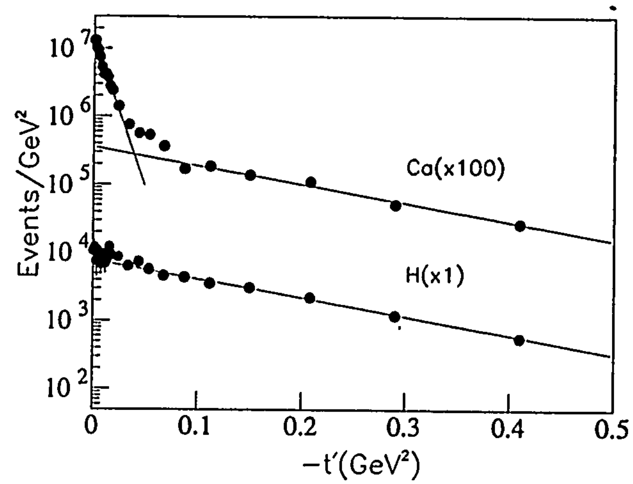

E665
Submitted to
Phys. Rev. Lett.
(1995)

A-dependence of diffractive ρ - scattering

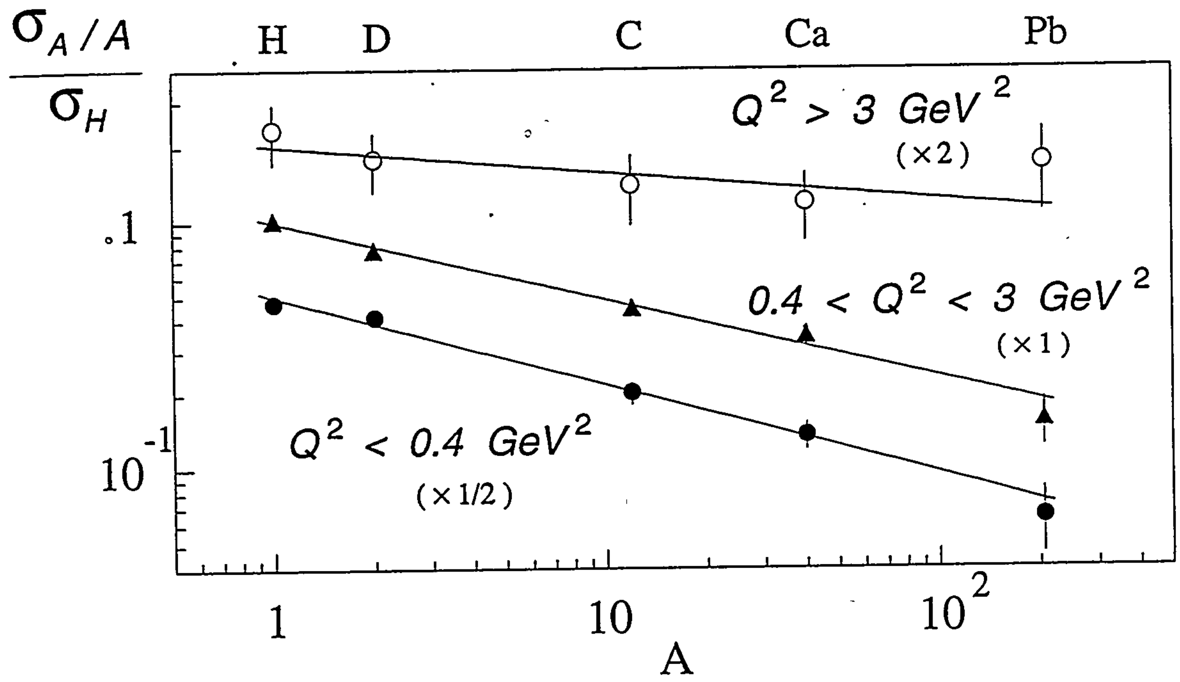

E665 Preliminary

Fraction of Events with Large Rapidity Gap

Use LRG to indicate Diffractive Scattering contamination.

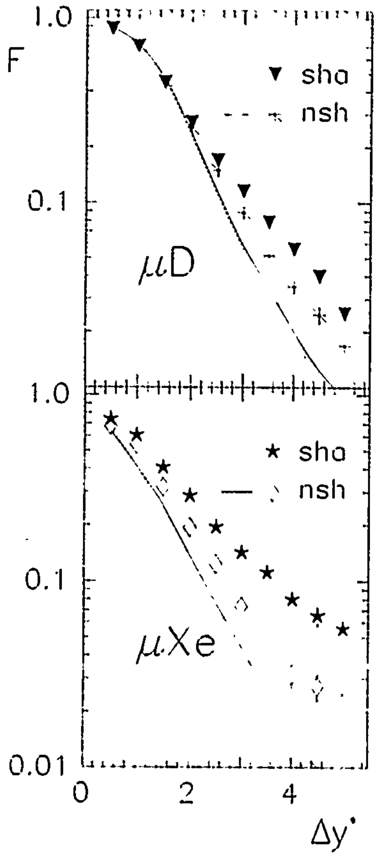

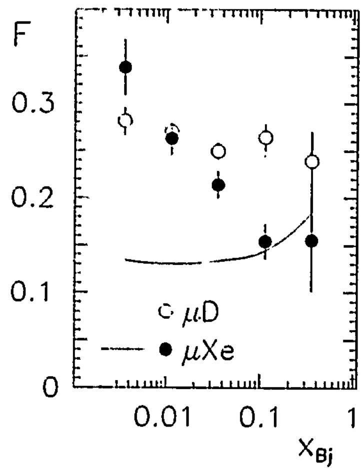

E665
Z. Phys. C65 (1995)

E665
Z. Phys. C65 (1995)

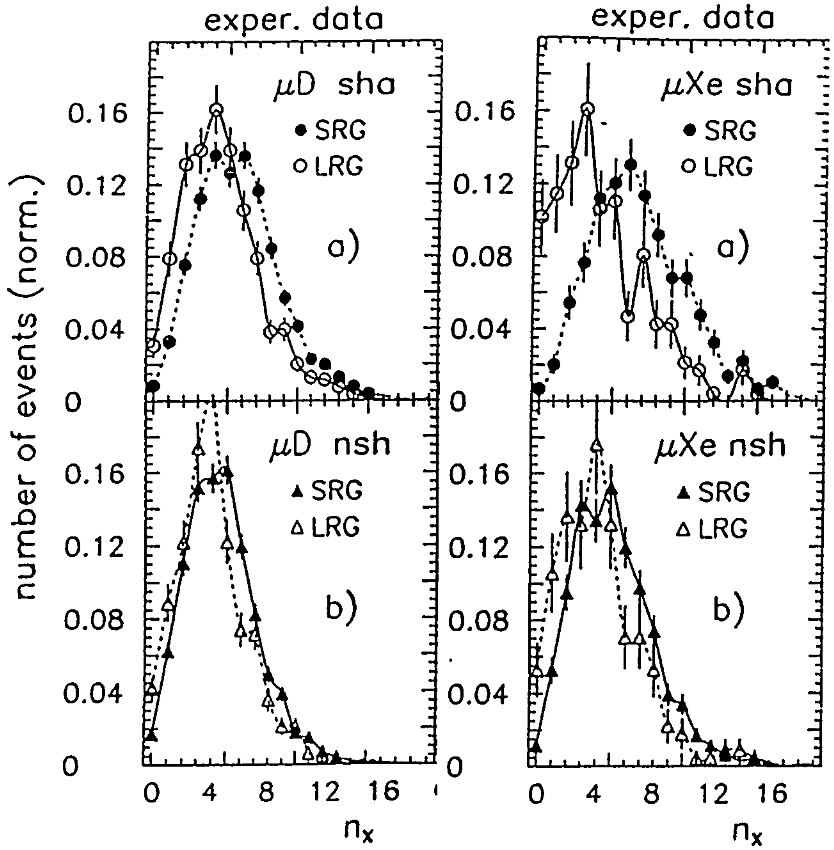

Table 9. Lower limits on the fraction of diffractive events in the LRG and total event sample, in the shadowing ($x_{Bj} < 0.02$) and non-shadowing ($x_{Bj} > 0.02$) region of μD and μXe scattering

	shadowing region A		non-shadowing region B	
	μD	μXe	μD	μXe
(diffractive/LRG)$_{min}$	0.44±0.06	0.61±0.07	0.32±0.09	0.49±0.13
(diffractive/total)$_{min}$	0.12±0.02	0.18±0.03	0.08±0.03	0.09±0.03

Conclusions:

- A-dependent Shadowing of
  Total cross section:

  $$(\sigma_A / A) / \sigma_H < 1. \quad (\text{low } x_{Bj})$$

- No Nuclear Effects in Forward ($y^*>0$)
  Hemisphere for DIS events.

- Nuclear Cascading in Backward ($y^*<0$)
  Hemisphere for DIS events.

- A-dependent Production of ρ's
  in Forward ($y^*>0$) Hemisphere
  for Diffractive events.

- A-dependence of Multiplicity (2 tracks only)
  for Diffractive events.

- Residual A-dependence for
  non-Diffractive events?

Interactions of Quarks and Gluons with Nuclear Matter

Al Mueller
Columbia University

Interactions of Quarks and Gluons with Nuclear Matter

Structure Functions at small x

νW_2 shows strong rise as x becomes small

Rise persists at least down to $Q^2 \approx 1.5\,\text{GeV}^2$

although total photoabsorption cross section shows much weaker growth with energy

At $Q^2 \sim 5\text{-}10\,\text{GeV}^2$

$$\left.\begin{array}{ll} x\sum_f (q_f + \bar{q}_f) & \sim 5\text{-}6 \\ xG & \sim 20\text{-}30 \end{array}\right\}$$

Very large numbers! but determination of xG unreliable?

What causes the rise?

Dokshitzer, Altarelli, Parisi, Gribov, Lipatov — DGLAP

Balitsky, Kuraev, Lipatov, Fadin — BFKL

Glück, Vogt, Reya — GRV

DGLAP is renormalization group

General formalism of anomalous dimensions and coefficient function evaluated to sufficiently order

GRV is 2^{nd} order DGLAP with $Q_0^2 = 0.3 - 0.35\,\text{GeV}^2$

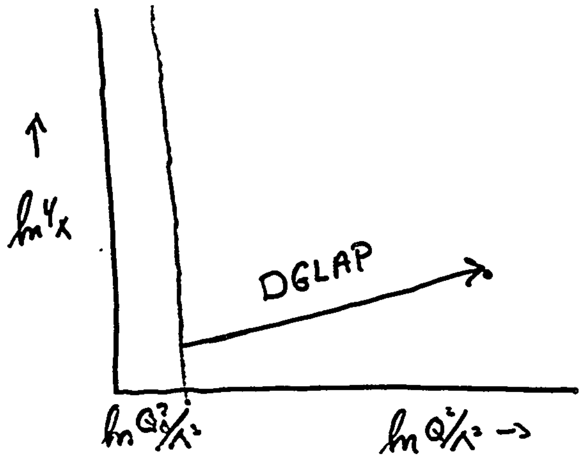

Normal x

2^{nd} order DGLAP good

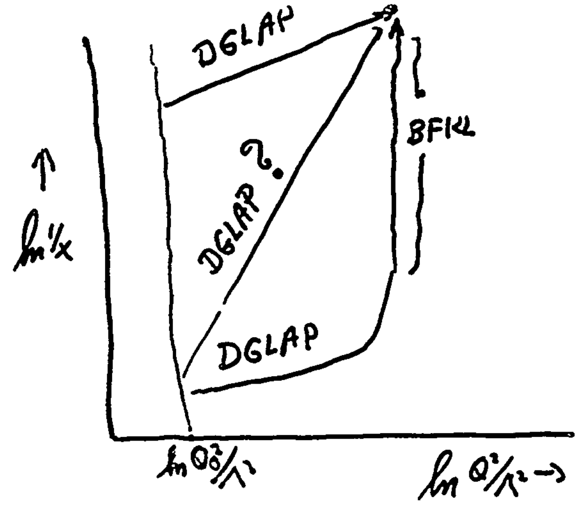

Small x

Situation somewhat confusing

GRV (2^{nd} order DGLAP with $Q_0^2 \sim 0.3\ GeV^2$ seems to fit the data well.

Resummation of higher order terms in anomalous dimension and coefficient function (BFKL) do not seem to be small.

Nuclear Structure Functions

shadowing apparent at CERN and Fermilab.

x-values not small enough to see strong rise in proton data.

Especially if there is truth in GRV for proton data the nuclear structure function should be quite different

Big Nucleus

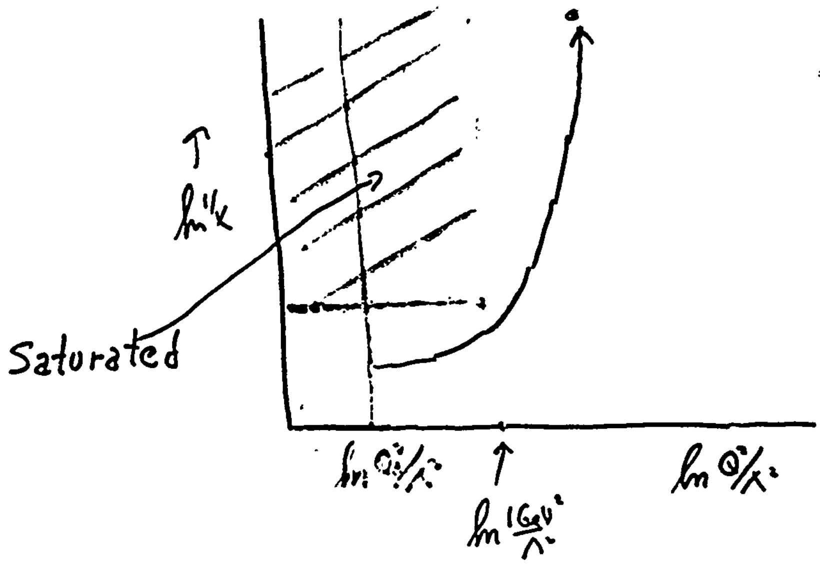

(a) For $Q^2 \lesssim 1\,GeV^2$ expect no growth in νW_2 as x goes between $2 \cdot 10^{-3}$ to $2 \cdot 10^{-5}$

(b) For $Q^2 \gtrsim 1\,GeV^2$ slower growth as $x \to$ small

(c) Enhancement of BFKL contribution by avoiding saturation region.

RHIC (LHC)

Dominant source of energy freed in heavy ion collision in central region likely(?) comes from "minijets" of $p_\perp \sim 1$ GeV. These "jets" are predominately gluons.

Important to measure $xG_A(x, Q^2)$!

Many ways to do this, but most reliable probably "direct" measurement

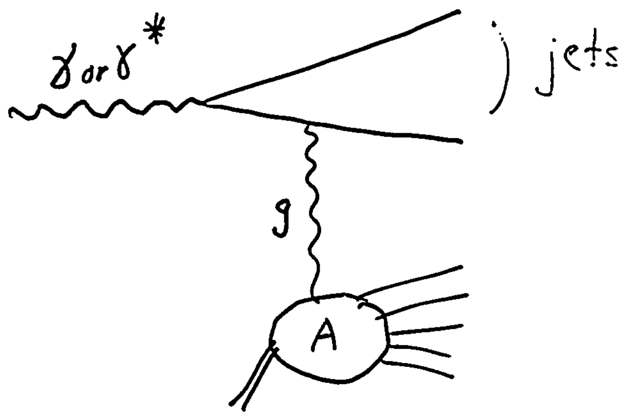

For $xG_A(x, Q^2)$ at not to large Q^2 will need to understand how jets propagate in nuclear medium.

Opportunity to study propagation of quarks in nuclear matter

Energy Loss of Quarks and Gluons in Hot and Cold Matter

New Calculations

Electrons in Atomic Matter

Drell - Blankenbecler

Baier, Dokshitzer, Peigné, Schiff

Quarks and Gluons in Hot Matter of Infinite Extent

Gyulassy - Wang

BDPS

Extension to Infinite Cold Matter

Levin

Finite and Infinite Length Hot and Cold Matter

BDMPS

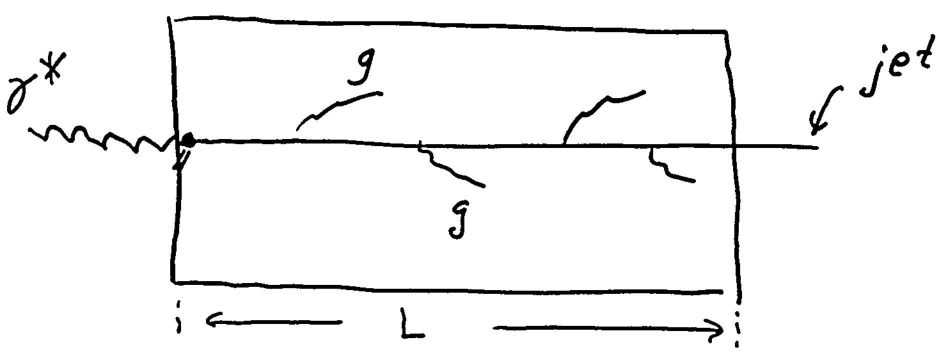

Energy loss due to gluon emission

$\Delta E \propto L^2$ already apparent in BDPS

Physical Picture

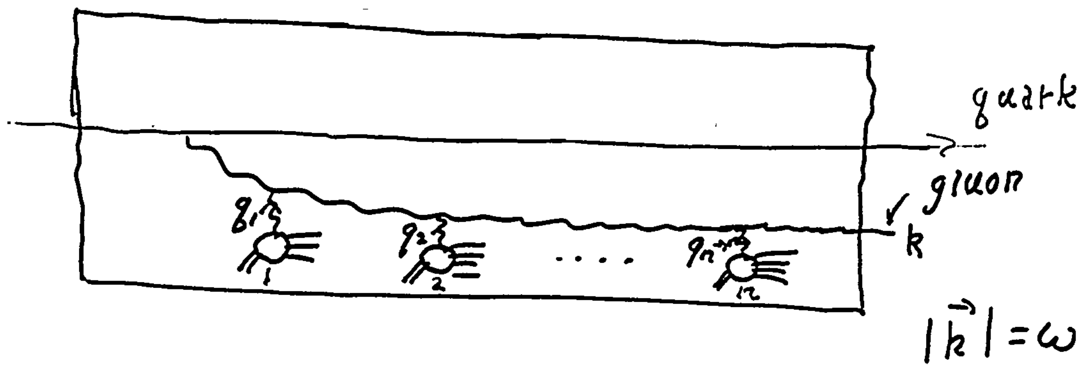

Need $\frac{2\omega}{k_\perp^2} \lesssim L$ in order to produce (and free) gluon in medium

take $\frac{2\omega}{k_\perp^2} = L$ for maximum energy loss

$k_\perp^2 \sim n\mu^2$ "typical" $q_\perp^2$ $\qquad n = L/\lambda \leftarrow$ mean free path

$$L = \frac{2\omega}{k_\perp^2} = \frac{2\omega}{n\mu^2} = \frac{2\omega}{L/\lambda\, \mu^2}$$

$$\Downarrow$$

$$\omega = \frac{1}{2} \mu^2/\lambda \; L^2$$

$$\Delta E \propto \mu^2/\lambda \; L^2$$

Preliminary numbers

Hot Matter

$$\Delta E = \frac{\alpha N_c}{4} L^2 \ln L/\lambda \;\; \mu^2/\lambda$$

$T = \frac{1}{4}$ GeV $\quad \alpha = 1/2$

$\mu^2 \approx 1/2$ GeV^2

$1/\lambda = 3/2 \; \frac{1}{fm}$

$L = 10$ fm $\Rightarrow \Delta E \approx 150$ GeV For $\alpha = 1/5$

Probably crazy!!!

Cold Matter

$$\Delta E = \frac{\alpha N_c}{4} L^2 \underbrace{\mu^2/\lambda \; 4\left(\frac{1-\tilde{N}(B^2)}{B^2}\right)}$$

$\frac{\alpha}{4} \pi^2 N_c \int xG \qquad\qquad \frac{16\alpha\pi^2}{9} \frac{A^{1/3}}{R} \lambda^2_{LQS}$

$\Delta E \sim$ A few GeV - 10 GeV $\qquad\qquad \sim 50$ GeV

$\lambda^2_{LQS} \sim \frac{1}{20}$ GeV^2 is large number!

Much to understand.

Likely ΔE much greater in hot matter than in cold matter

Rescattering in Nuclear Targets for Photoproduction and DIS

George Sterman
SUNY/Stony Brook

Rescattering in Nuclear Targets for Photoproduction and DIS

Xiaofeng Guo
Ma Luo
Jianwei Qiu
George Sterman

BNL Nov 17, 95

Outline

I. Parton (photon) nucleus scattering

II Single-jet γA

III Dijet mtm. imbalance

IV. Single-jet DIS

V. HERA & rapidity gaps

I. Parton / Nucleus Scattering

(A) Single Scattering ; $\sigma \propto A$

'rare' processes

$\nwarrow$ ('EMC' small correction)

DIS (target rest) (inclusive)

– large Q^2, x_B

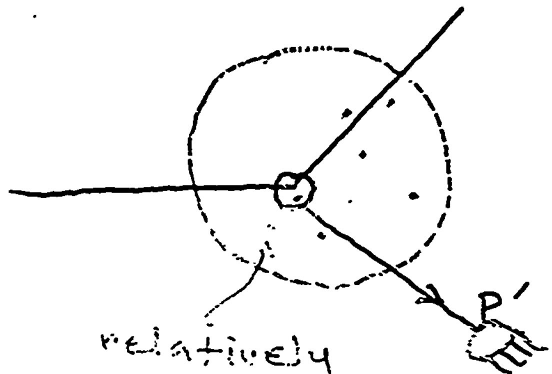

$1/k_T \sim 1/Q$

$1 > x \gg 0$

$1/Q$ $\overset{\downarrow}{\underset{\uparrow}{O}}$ = $q\bar{q}$

$\sigma \sim$ Volume

fate of scattered quark

$$\Delta t^{(p')} \sim \frac{1}{m_J} \quad m_J^2 \ll p_0' = E_J$$

$$\Delta t^{(\text{target})} \sim \frac{1}{m_J}\left(\frac{E_J}{m_J}\right) > R_A$$

for E_J large

further couplings at $\alpha_s(m_J^2)$

Hadronization outside nucleus!

(EM , E665)

II 2

(B) Double Scattering
→ Volumne Enhanced $\frac{d}{dA}\sigma(A) \sim \alpha\sigma(A$
since (Cronin et al, 1974
'doubly rare'

(a) Why pQCD

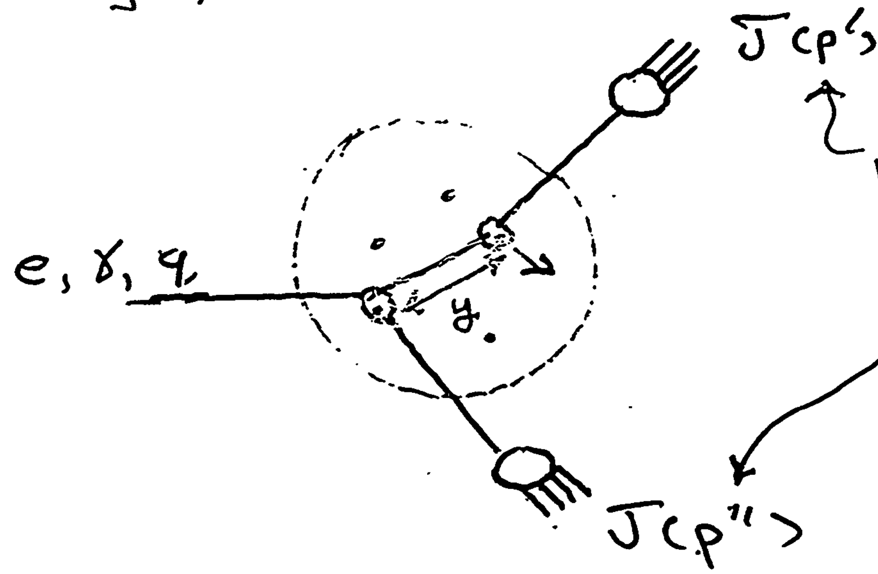

'Higher Twist'
Factorization theorem →

$\alpha_s(Q)$ ← 1/Q even if one of two scatterings is soft (Qiu, G.S. 91)

(see also: Bodwin, Brodsky, Lepage)

y above can give

$$\sigma \sim A\sigma' + \frac{\beta}{Q^2} A^{4/3}\sigma''$$

from y integral

Levin Ryskin 1981

(C) Leading Power Factorization Review

(1)

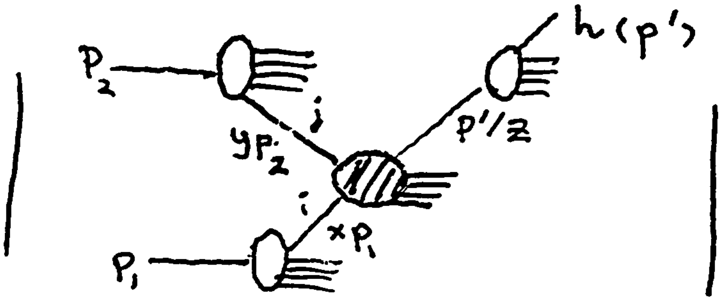

$$\Big|\ \cdots\ \Big|^2 \sim \sigma_{P_1+P_2 \to p'+X}$$

(2)

$$\omega \frac{d\sigma}{d^3p'} = \sum_{ijk} \int \frac{dx_2}{x_2} f_{j/P_2}(x_2) \int \frac{dx_1}{x_1} f_{i/P_1}(x_1)$$

$$\times \int \frac{dz}{z^2} D_{h/k}(z)\ \hat\sigma_{ij\to k}(x_1P_1, x_2P_2, p'/z)$$

(scale dependence implicit)

(3)

$$\sigma \sim \sum_n$$

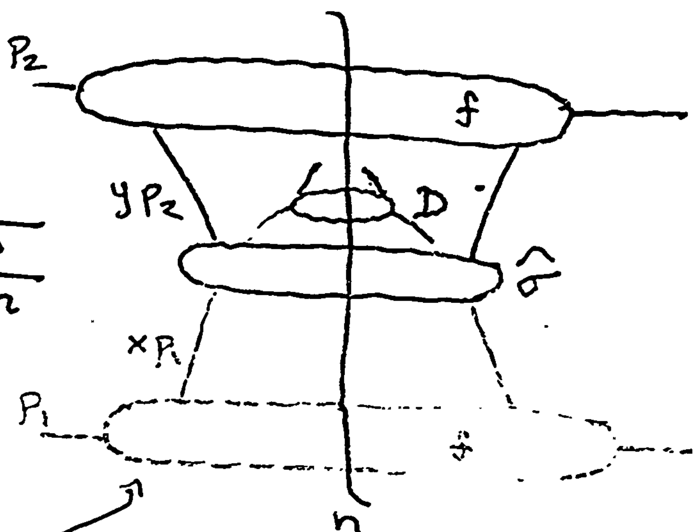

(4)

$$f_{q/p}(x, Q^2) = \int \frac{dy^-}{2\pi} e^{-ixp^+y^-} \langle P_1 | \bar q(0) \frac{\gamma^+}{2} q(y^-) | P_1 \rangle$$

(D) Factorization at Nonleading Power

(1)

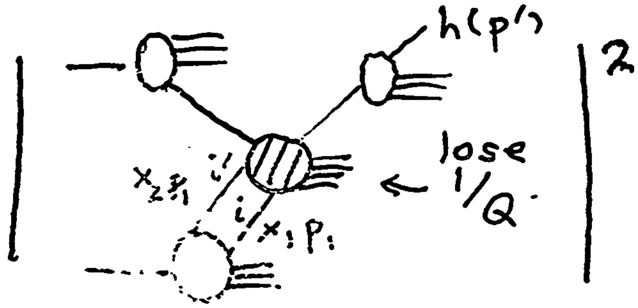

$\sim \quad \sigma_4$

(2)

$$\omega \frac{d\sigma_4}{d^3p'} = \sum_{(ii')jk} \int \frac{dx_2}{x_2} f_{j/p_2}(x_2) \int \frac{dz}{z^2} D_{h/k}(z)$$

$$\times \int dx_1\, dx_2\, dx_3\, T_{(ii')/p_1}(x_1, x_2, x_3) \times \hat{\sigma}^{(4)}_{(ii')+j\to k}$$

(3)

$\sigma \sim \sum_n$

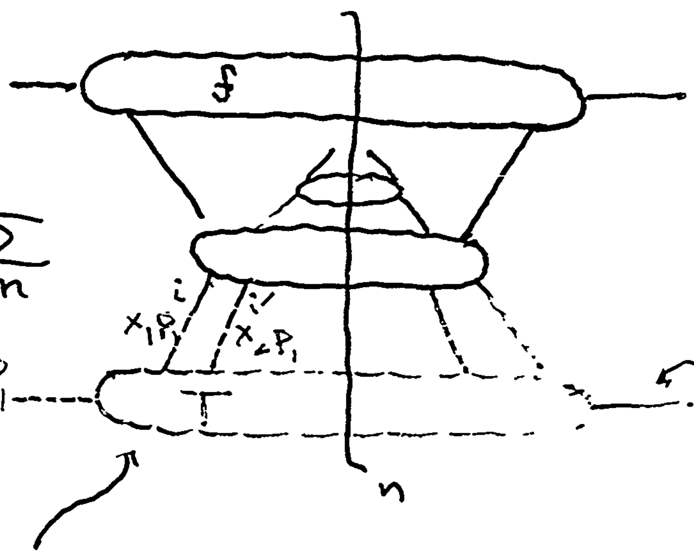

nucleus, for us

(4)

$$T(x_i) = \int \frac{dy_1^- \, dy_2^- \, dy_3^-}{(2\pi)^3} e^{ip^+(x_1 y_1^- + x_2 y_2^- + x_3 y_3^-)}$$

$$\times t_{\alpha\beta\gamma\delta} \langle p | B^+_{i\alpha}(0) \hat{B}^+_{i'\beta}(y_3) B_{i'\gamma}(y_2) B_{i\delta}(y_1) | p \rangle$$

R. Ellis, Furmanski, Petronzio (82)
R. Jaffe (82), J. Qiu (90) } DIS

(E). Why? (R. Basu, A. Ramalho + G.S. 1984)

(Formal arguments J. Qiu + G.S. 1991)

heuristic argument:

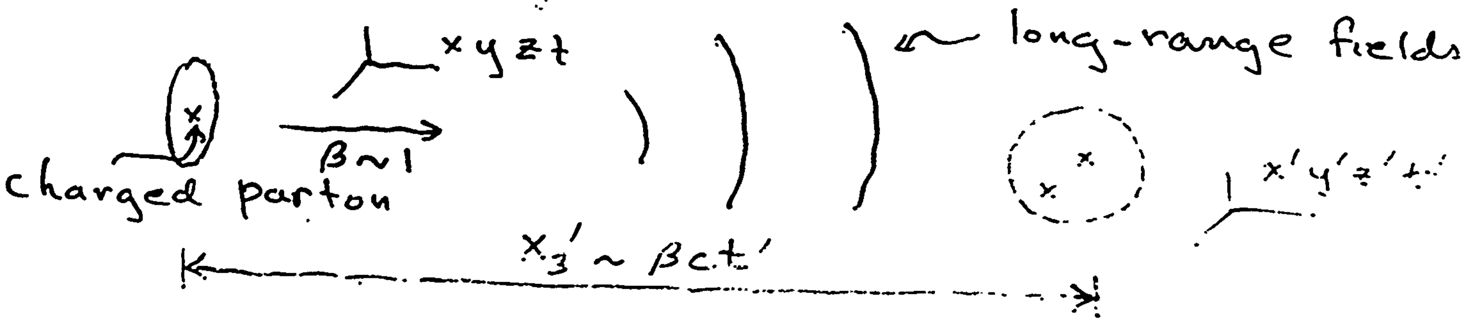

Lorentz Contractions $\boxed{\Delta \equiv \beta c t' - x_3'}$

field	x frame	x' frame
scalar	$V(x) = \dfrac{e}{\lvert\vec{x}\rvert}$	$V'(x') = \dfrac{e}{(x_T^2 + \gamma^2\Delta^2)^{1/2}}$ $\to 1/\gamma$ "like a ruler"
gauge	$A^-(x) = \dfrac{e}{\lvert\vec{x}\rvert}$	$A'^-(x') = \dfrac{e\gamma(1+\beta)}{(x_T^2 + \gamma^2\Delta^2}$ $\to 1$!!
field strength	$\mathcal{E}_3(x) = \dfrac{e}{\lvert\vec{x}\rvert^2}$	$E_3(x') = \dfrac{-e\gamma\Delta}{(x_T^2 + \gamma^2\Delta^2)^{3/2}}$ $\to \dfrac{1}{\gamma^2}$!!

suggests factorization to $\mathcal{O}(1/Q^2)$

(fails at $1/Q^4$: consistent w/
Doria, Frenkel, Taylor : noncancellation
of IR divergences in QCD)

(F.) A - Enhancement from matrix elements

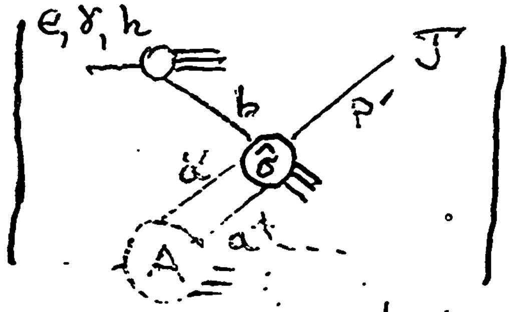

once more!

loose $1/Q^2$

$$\omega_{p'} \frac{d^3\sigma}{d^3p'} = \sum_{(aa')b} \int dx_b\, f_{b/h}(x_b)$$

$$\times \int dx_a\, dx_a'\, dx_a''\, T^{(4)}_{(aa')/A}(x_a, x_a', x_a'')\ \hat{\sigma}(\{x\}, p')$$

(twist-4) parton distribution

example:

$$T^{(4)}_{(qG)/A}(\{x\}) = \int \frac{dy\, dy'\, dy''}{(2\pi)^3}\, e^{ip_A^+(xy + x'y' + x''y'')}$$

$$\times \frac{1}{2} \langle A | \bar{q}(0)\, \gamma^+ F^{+\nu}(y')\, F^{+}{}_{\nu}(y'')\, q(y) | A \rangle$$

nucleon state

4 field operators
= 2 parton matrix element

'something new'

$$\boxed{A \text{ dependence in } T_{(q,G)}}$$

$x' = x'' = 0 \rightarrow \int_0^{A^{1/3}R_0} dy' \int_{y'-\epsilon}^{y'+\epsilon} dy''$ color $\times\, \epsilon$ cons.

Role of poles in hard scattering

Photoproduction at lowest order:

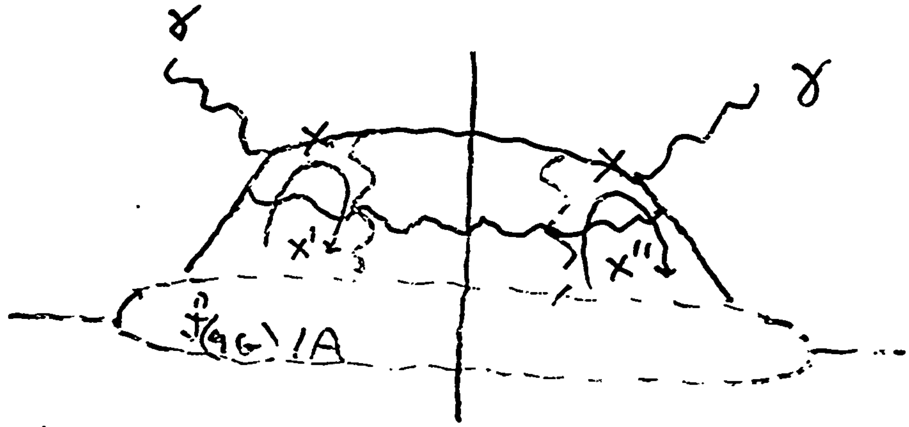

poles in x', x'' at $x' \cong x'' \cong 0$

$$\Rightarrow$$

$$f_{(qG)/A}(x, x', x'') \to f_{(qG)/A}(x, 0, 0)$$

$$\equiv T_q(x)$$

governs A dependence

A-enhanced Matrix elements !!

$$T_q(x,A) = \int \frac{dy_1^-}{2\pi}\, e^{i(n\cdot p)xy^-} \int \frac{dy_2^-\, dy_3^-}{2\pi}\, \theta(y_2^- - y_1^-)\,\theta($$

$$\times\ \frac{1}{2} \langle P_A |\, \bar{q}(0)\, \gamma^+ n_\nu F^{\alpha\nu}(y_3^-)\, n_\mu F^{\mu}{}_{\alpha}(y_2^-)\, q(y_1^-)\,|$$

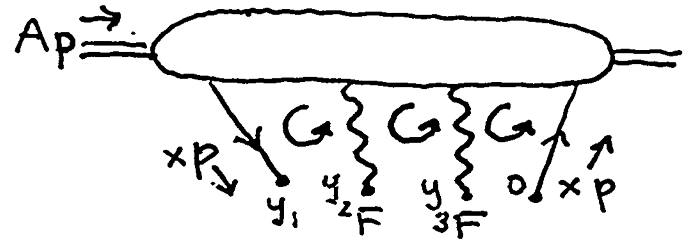

$$T_g(x,A) = \int \frac{dy_1^-}{2\pi}\, e^{i(n\cdot p)xy^-} \int \frac{dy_2^-\, dy_3^-}{2\pi}\, \theta(y_2^- - y_1^-)\,\theta(y$$

$$\times\ \frac{1}{x(n\cdot p)} \langle P_A |\, n_\xi F^{\beta\xi}(0)\, n_\nu F^{\alpha\nu}(y_3)\, n_\mu F^{\mu}{}_{\alpha}(y_2^-)\, n_\xi F^{\xi}{}_{\beta}(y_1^-)$$

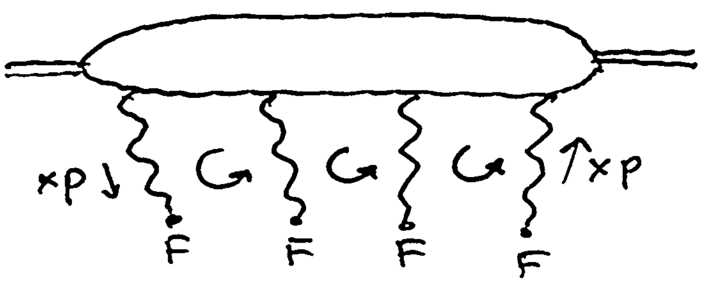

$\tilde{f}_{i/A}$ normaliz
to $f_{i/N}$
(weak A
dependen
for $x \neq$

Expected A-dependence $\quad \boxed{T_i(x,A) = A^{4/3}\, \lambda^2\, \tilde{f}_{i/A}(x)}$

to be determine
from experime

(G) Applications

– Jet photoproduction

$$\omega_\ell \frac{d^3\sigma}{d p_J'^3}$$ (Luo, Qiu, G.S.)

$\langle k_{t\phi} \rangle$ E683 (LQS in prep.)

– Jet DIS

$$\omega_\ell \frac{d^3\sigma}{d p_J'^3}$$ (LQS)

– Future:

$A^{1/3}$ in heavy quarkonium

pA, πA jet, dijet...

E557, E609

(d) Related Calculations

Levin - Ryskin

and evolution, energy loss

(dipole model of qN itn; all orders in rescattering)

Lev - Peterson ...

(multiple parton-model)

Bodwin Brodsky Lepage

? ⊥ struct.

(P_T distrib. in DY: QED model to all orders)

closely related to [illegible]

II8

II Single-Jet Photoproduction $P_T(A)$
(E609; FSI only)

Kinematics of Soft Rescatteri[ng]

Typical Photoproduction proces[s]

$$x = \frac{l_T^2 s}{(-t)(s+t)}$$

$$t \equiv -2p\cdot l$$

Extra soft rescattering:

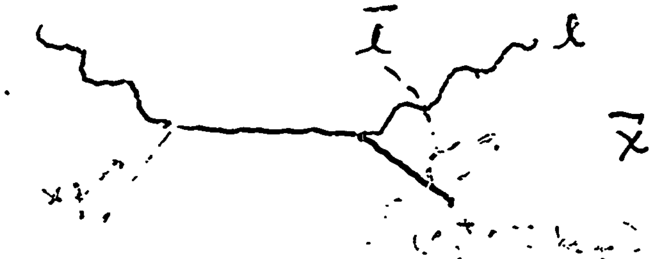

$$\bar{x} = \frac{(l_T - k_T)^2 s}{(-t)(s+t)}$$

$$\langle(\bar{x}-x)^2\rangle_{k_T} = \text{const}\langle k_T^2\rangle \frac{l_T^2 s^2}{(-t)^2(s+t)^2}$$

Expect correction like

[illegible]

[illegible]

$\boxed{\text{no energy loss: Hoyer Brodsky}}$

x "shift" due to soft rescatter

$$\omega_\ell \frac{d\sigma_{4/3}}{d^3\ell} = \frac{\alpha_{EM}(4\pi\alpha_s)^2}{s(s+t)}\Big[\sum_f e_f^2\, \Phi_f(x,A)\, H_q(x,\ell)$$

enhancement

$$+\Big(\sum_f e_f^2\Big)\Phi_g(x,A)\, H_g(x,\ell)\Big]$$

$$\Phi_i(x,A) = \left[\frac{\partial^2}{\partial x^2}\left(\frac{T_i(x,A)}{x}\right)\left(\frac{s}{-t(s+t)}\right)^2 \ell_T^2 + \frac{\partial}{\partial x}\left(\frac{T_i(x,A)}{x}\right)\left(\frac{s}{-t(s+t)}\right)\right]$$

$$H_q(x,\ell) = \frac{4}{9}\left[\frac{s}{s+t} + \frac{s+t}{s}\right] + \left[\frac{s}{-t} + \frac{-t}{s}\right]$$

$$H_g(x,\ell) = \frac{1}{6}\left[\frac{-t}{s+t} + \frac{s+t}{-t}\right]$$

LQS Define α by

σ Born

$$A\frac{d\sigma_1(A)}{d^3\ell} + \frac{d\sigma_{4/3}(A)}{d^3\ell} \equiv A^\alpha \frac{d\sigma_1(A)}{d^3\ell}$$

$\ln \alpha \approx \alpha^{1/3} \rightarrow \alpha$ not very A-dependent

Calculate samples with model T

II" $\rightarrow x_F, s, \ell_T$ dependence

II 12

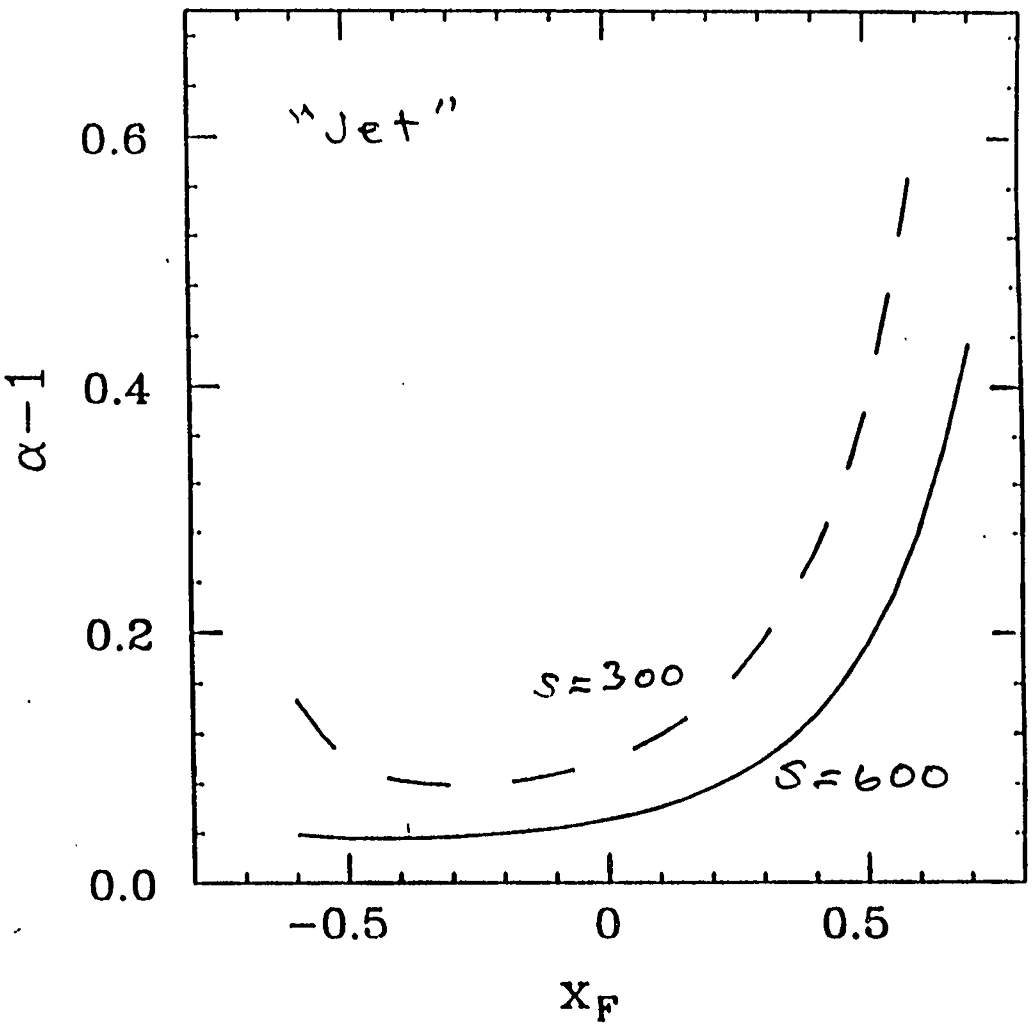

Model

$T_i = A^{1/3} \Lambda^2 q_i(x)$

$i = q, G$

Fig. 3(a)

(III) Dijets From Nuclear Targets

E683 pA

E609 γA, πA

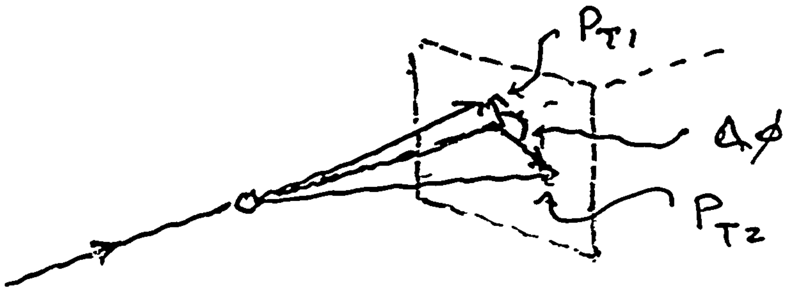

$$K_{t\phi} = \frac{P_{T1} + P_{T2}}{2} \sin \Delta\phi$$

Photoproduction:

$$\langle k_t^2 \rangle = 2 \langle k_{t\phi}^2 \rangle \sim C_0 + C_1 A^{1/3}$$

$$\sim 2(1.44 + 0.174 \ln A)\ \text{GeV}^2$$

$$\sim 2(1.44 + 0.174 A^{1/3})\ \text{GeV}^2$$

D. Naples et al to appear in PRL

$C_1 \sim 0.5$ GeV^2 for γA

($C_1 \sim 1$ GeV^2 for pA)

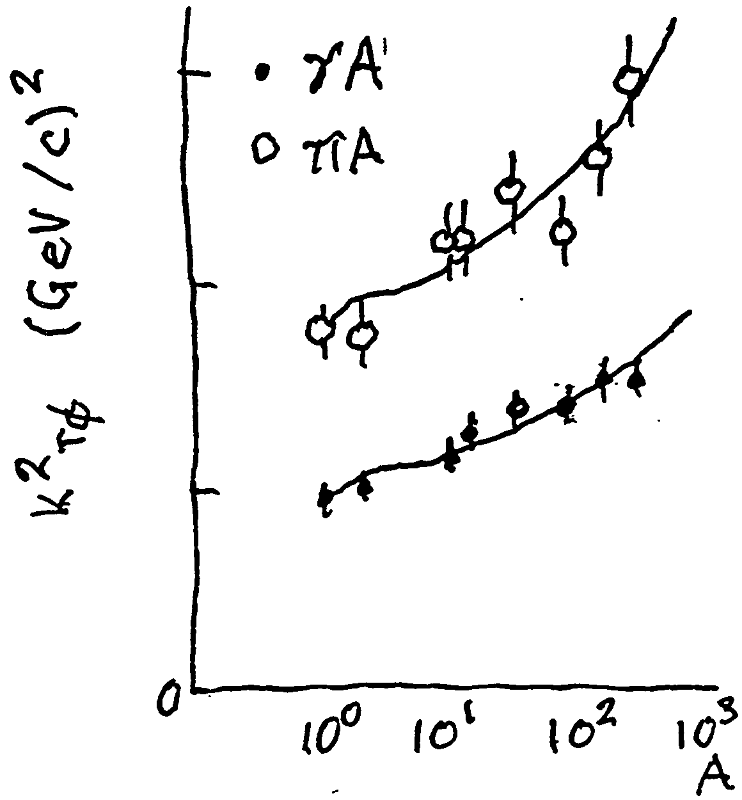

E683 PRL 72 2341
(1994)

D. Naples et al.
to appear in PRL 72 2337

$\langle k_T^2 \rangle$ as a twist-4 effect

$$\int_{PS} \hat{k}_T^2$$

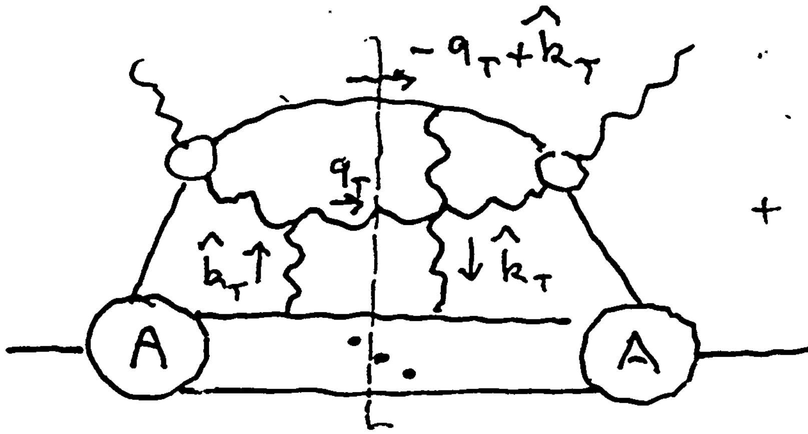

+ 3 more

Born approx : $\boxed{k_T^2 = \hat{k}_T^2}$

For fixed jet mta 'ℓ' let
$d\sigma^{\gamma a}(\ell, x, P_\gamma)$ be γ-a Born
cross section $(a = q, \bar{q}, G)$
Then

$$d\langle k_T^2 \sigma(\ell)\rangle^{\gamma A}_{4/3}$$

$$= \lambda^2 A^{4/3} \pi^2 \alpha_s \Big[\underset{4/3}{C_F} \sum_{f=q,\bar{q}} \int dx\, \tilde{f}_{f/A}(x)\, d\hat{\sigma}_1^{\gamma f}(\ell, x, P_\gamma)$$

$$+ \underset{3}{C_G} \int dx\, \tilde{f}_{G/A}(x)\, d\hat{\sigma}_1^{\gamma G}(\ell, x, P_\gamma) \Big]$$

(note: coherence of outgoing jets: $\to C_F$ $\rightleftarrows \to C_G$)

Estimate λ in valence quark approximation

integrate over some region R of dijet phase space

$$\langle k_T^2(R)\rangle_{1/3} \sim \frac{\int_R d\langle k_T^2 \sigma^{\gamma A}(\ell)\rangle_{4/3}}{\int_R d\sigma_1^{\gamma A}(\ell)}$$

"leading twis

$$= \frac{\pi^2 \alpha_s}{\sigma_1^{\gamma A}(R)} \lambda^2 A^{1/3} \left[C_F \sigma_{1,q}^{\gamma A}(R) + C_G \sigma_{1,G}^{\gamma A}(R) \right]$$

$$\sigma_1^{\gamma A}(R) = \sigma_{1,q}^{\gamma A}(R) + \sigma_{1,G}^{\gamma A}(R)$$

if drop $\sigma_{1,G}$ in 'valence' appro get

$$\langle k_T^2(R)\rangle_{1/3} \sim \pi^2 \alpha_s \lambda^2 A^{1/3}$$

$$\overset{\text{exp.}}{\sim} 0.2\, A^{1/3}\ \mathrm{GeV}^2$$

Include gluons

$\lambda^2 \sim 0.05 - 0.1$ GeV^2

$$\lambda^2 \sim \left(\frac{0.2}{\pi^2 \alpha_s}\right) \mathrm{GeV}^2$$

$\alpha_s(\langle \ell_T^2\rangle)$

$$\sim 0.1\ \mathrm{GeV}^2$$

Higher orders:

$\int_{PS} k_T^2$ 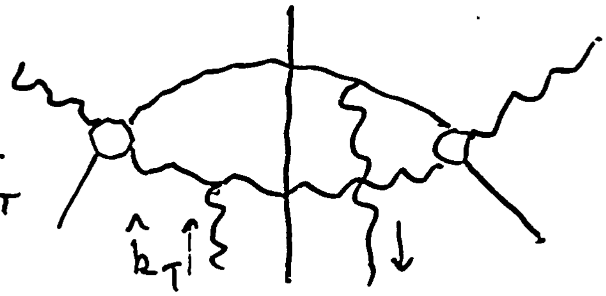

$\rightarrow \int_{PS} \hat{k}_T^2$ 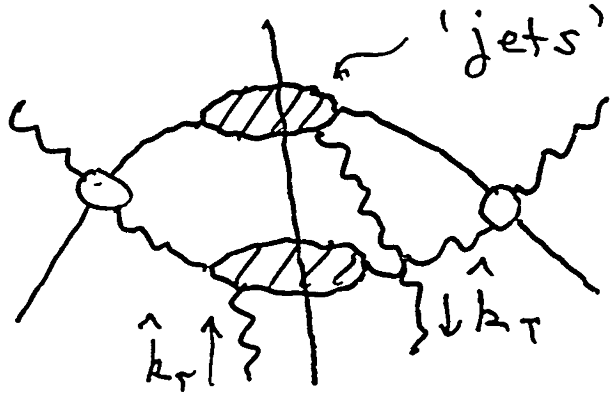

collinear emission doesn't change k_T

leading corrections stay in 'jets'

$$\hat{k}_T^2 = k_T^2$$

→ nuclear rescattering: factor from jets

$\rightarrow \int_{PS} \hat{k}_T^2$ 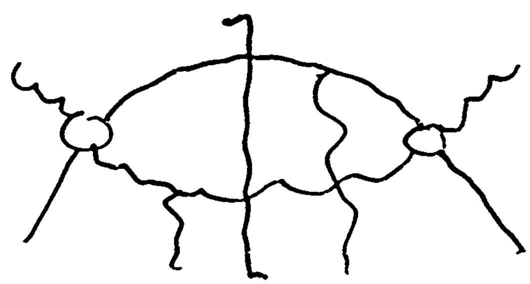 $\cdot$ 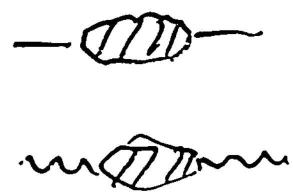

$(1+\mathcal{O}(\alpha_s(k_T^2)))$

Thus:

$\langle k_T^2 \rangle = A \langle k_T^2 \rangle_{A=1}$ + nuclear effect

(IV) Dilepton production and initial state interations

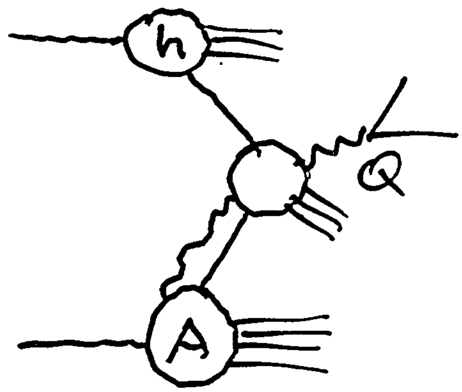

Would expect:

$$\langle Q_T^2 \rangle \sim A \langle Q_T^2 \rangle_1 + A\,\tilde{C}_{DY} A^{1/3}$$

from

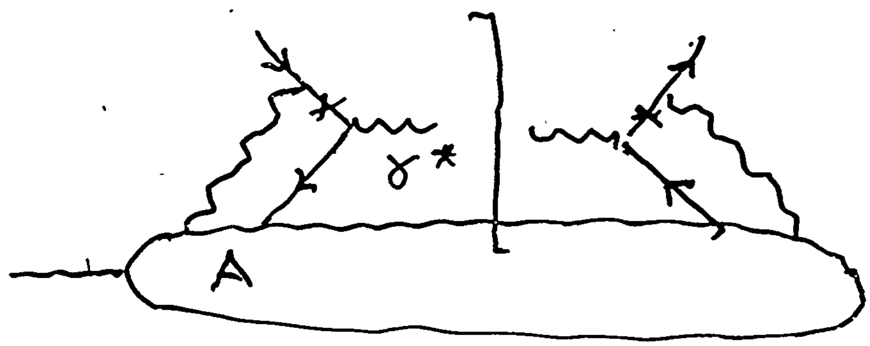

lowest order $\tilde{C}_{DY} \sim \tilde{C}_{\gamma A}$

experiment: $\hat{C}_{DY} \sim 0.02\ GeV^2$!

$\sim 0.1\,\hat{C}_{\gamma A}$!

can this suppression be understood in this language?

IV Jet Production in DIS

(PR D 50 1951 (94))

$$\gamma^*(q) + A \rightarrow \text{jet}(\ell) + X$$

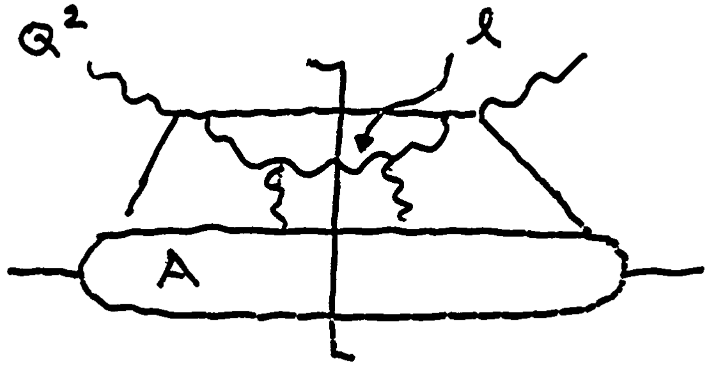

define α by

$$A \frac{d\sigma_1}{d^3\ell} + \frac{d\sigma_{4/3}(A)}{d^3\ell} = A^{\alpha} \frac{d\sigma_1}{d^3\ell}$$

for $A = 200$

estimate:

$$T_q(x) = A^{4/3} \lambda^2 q(x)$$

$$\frac{M_q(x)}{x} = A^{4/3} \lambda^2 \left(G(x)/x\right)$$

$E_e = 470$ GeV

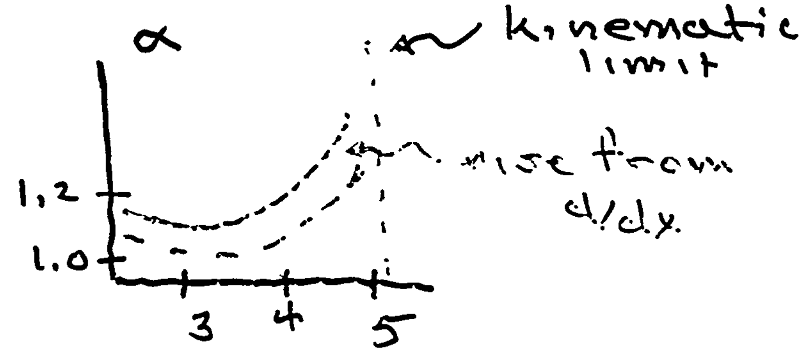

V. HERA

- Geometrical, Energy Advantage
- Complementarity to pA at RHIC (LHC?): new era for hard scattering in nuclear media
- Special interest: $A^{4/3}$ in rapidity-gap jet production? (Zeus, H1...)
  well established in ep
- Yesterday's k_T smearing
  → today's higher twist
  (Huston et al for pp γprod.

Multiple scattering and rapidity gap. jets

Compact pomeron (no $A^{4/3}$?)

interference?

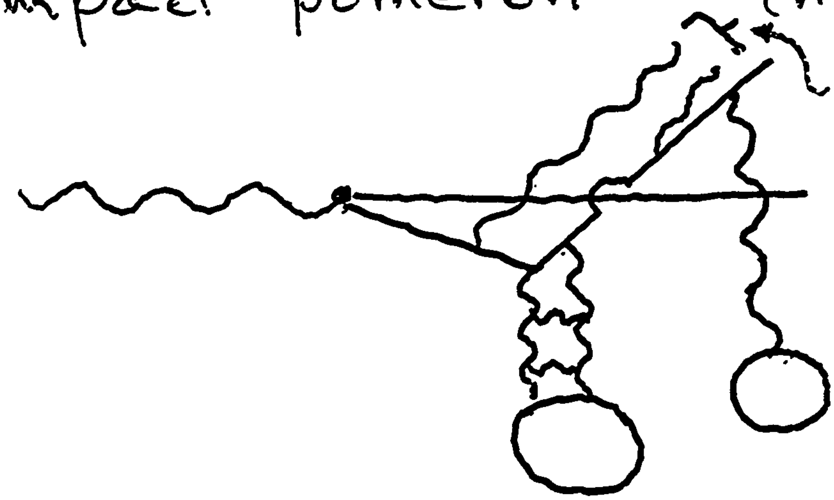

Extended pomeron ($A^{4/3}$?)

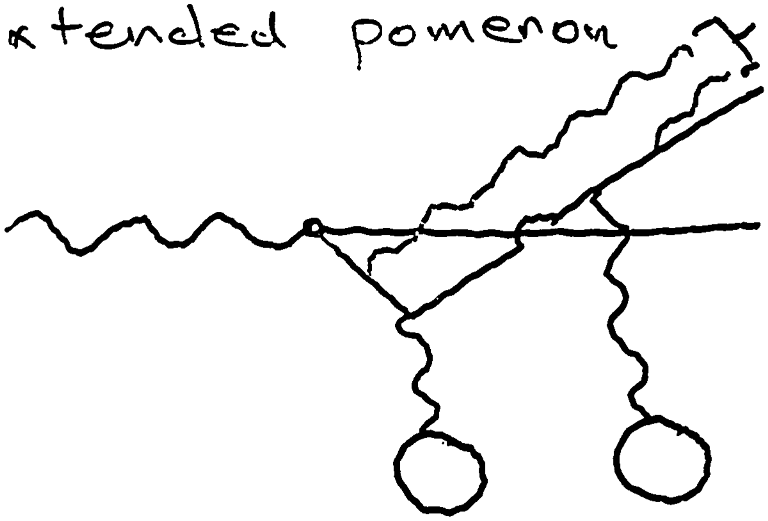

Reln. to Φ_g ?

Parton distributions for diffraction

- Collins et al
- Berera & Soper

Structure Functions and Nuclear Effects at PHENIX

Mike Leitch
Los Alamos National Laboratory

STRUCTURE FUNCTIONS AND NUCLEAR EFFECTS AT PHENIX

- Mike Leitch, LANL -

- NUCLEAR EFFECTS
- SELECTED p-A RESULTS
- EVOLUTION TO RHIC
- PHENIX CAPABILITIES + COVERAGE
- PHENIX SPIN

Theoretical Phenomenology of Nuclear Dependences

- **Shadowing of small x quarks and gluons in nuclei** - $x_T < 0.1$ quarks are suppressed in nuclei; gluons probably also suppressed. Can explain DY at low x, but not the large suppression for J/Ψ and Υ.
  - J/Ψ and Υ suppressed at all x?
  - does not scale with x_T?
  - D's not suppressed.
- **Parton energy loss and multiple scattering in nuclei** - multiple scattering explains p_T broadening of DY and resonances. Energy loss can explain the x_F dependencies, but values may be too large. (quarks - 1.5 GeV/fm, gluons - 3.4 GeV/fm).
- **Nuclear absorption and co-mover interactions** - before hadronization, resonances can be broken up by interactions with nucleons or co-movers. Can explain suppression at low x_F, and is consistent with lack of suppression of *D*.

- **Intrinsic charm & beauty** - At large x_F (>0.5), intrinsic $c\bar{c}$ or $b\bar{b}$ states in the projectile can dominate the production of heavy-quark pairs. Can explain x_F dependence of J/Ψ and Υ; but E789 set very low limit on amount of intrinsic charm.
- **Broken nucleons** - Low x components of projectile stripped off by nuclear surface.
- **$q\bar{q}$ formation time** - $c\bar{c}$ and $b\bar{b}$ formed compact and evolve over time to form resonances. Effective cross sections vary over time. Gives $\sqrt{S}$-dependendent absorption effects; and x_F dependence.
- **Feeding of resonances from χ decays and excited states** - e.g. only about ~2/3 of J/Ψ's are formed directly.
- **Nucleon sea asymmetric in $\bar{u}$ & $\bar{d}$** - Gottfried Sum Rule.

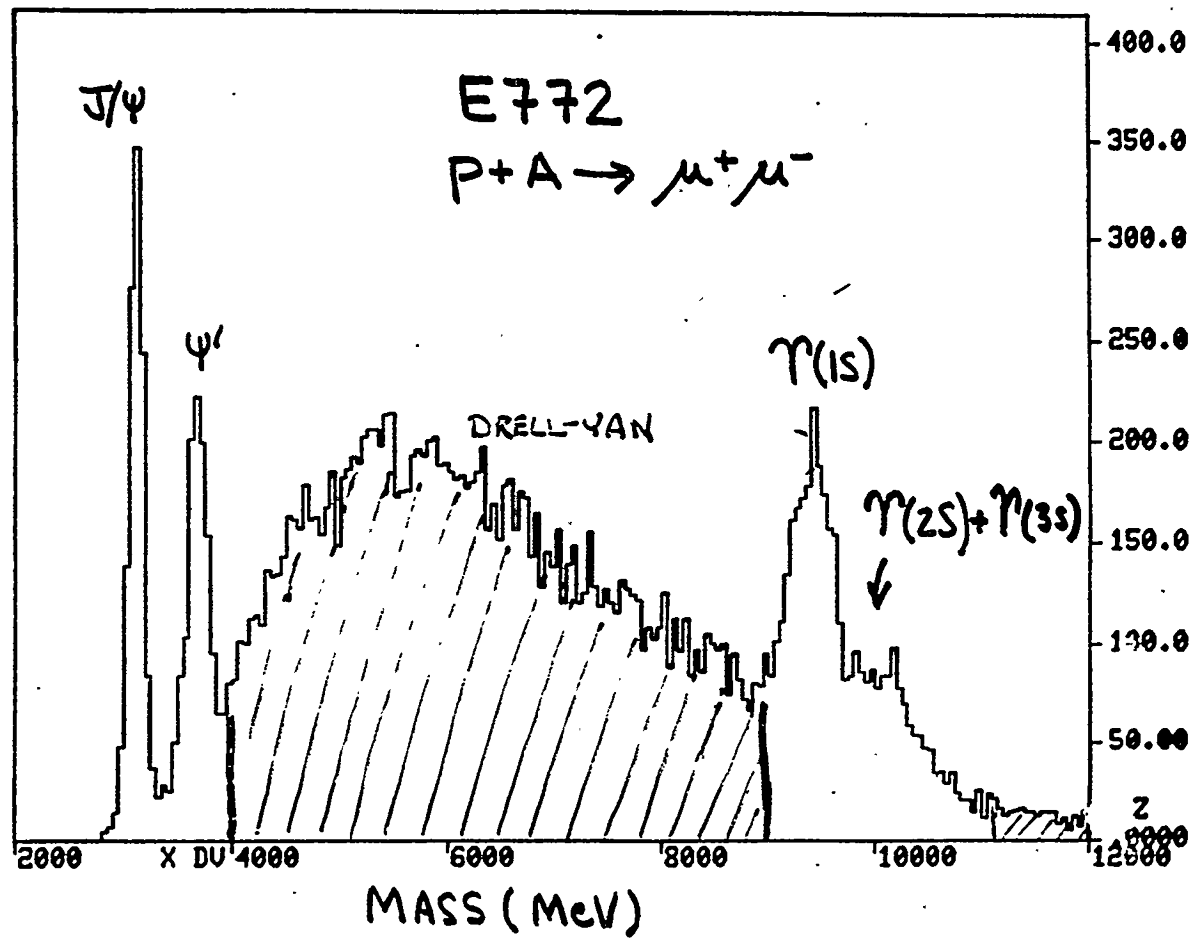

~450,000 Drell-Yan
~100,000 J/ψ + 12,000 ψ'
~ 27,000 ϒ

≥ 1½ % systematic errors.

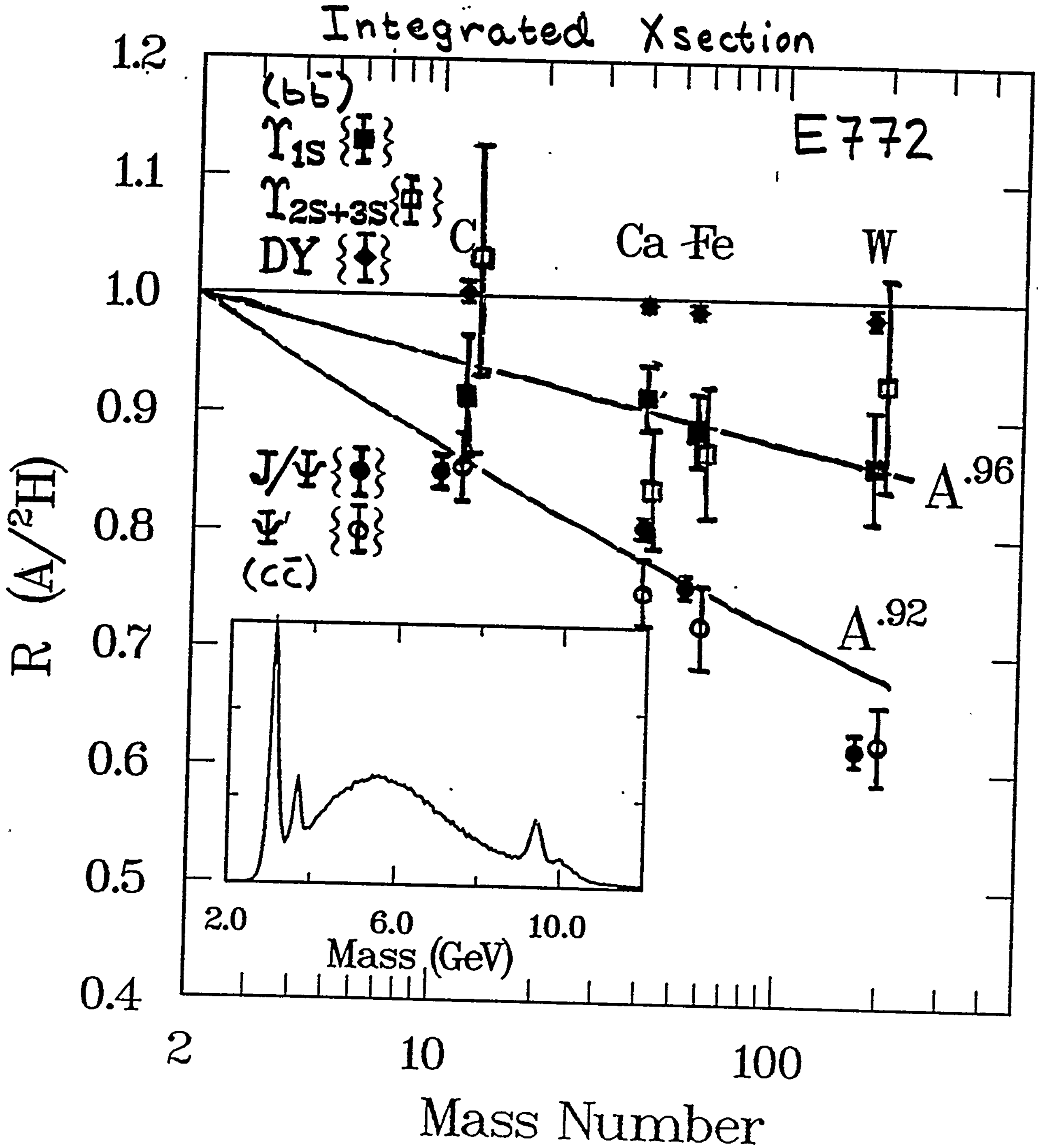

VM	r_{RMS} (fm)
Υ	0.13
Υ′	0.18
J/ψ	0.29
ψ′	0.56

P_T DEPENDENCE

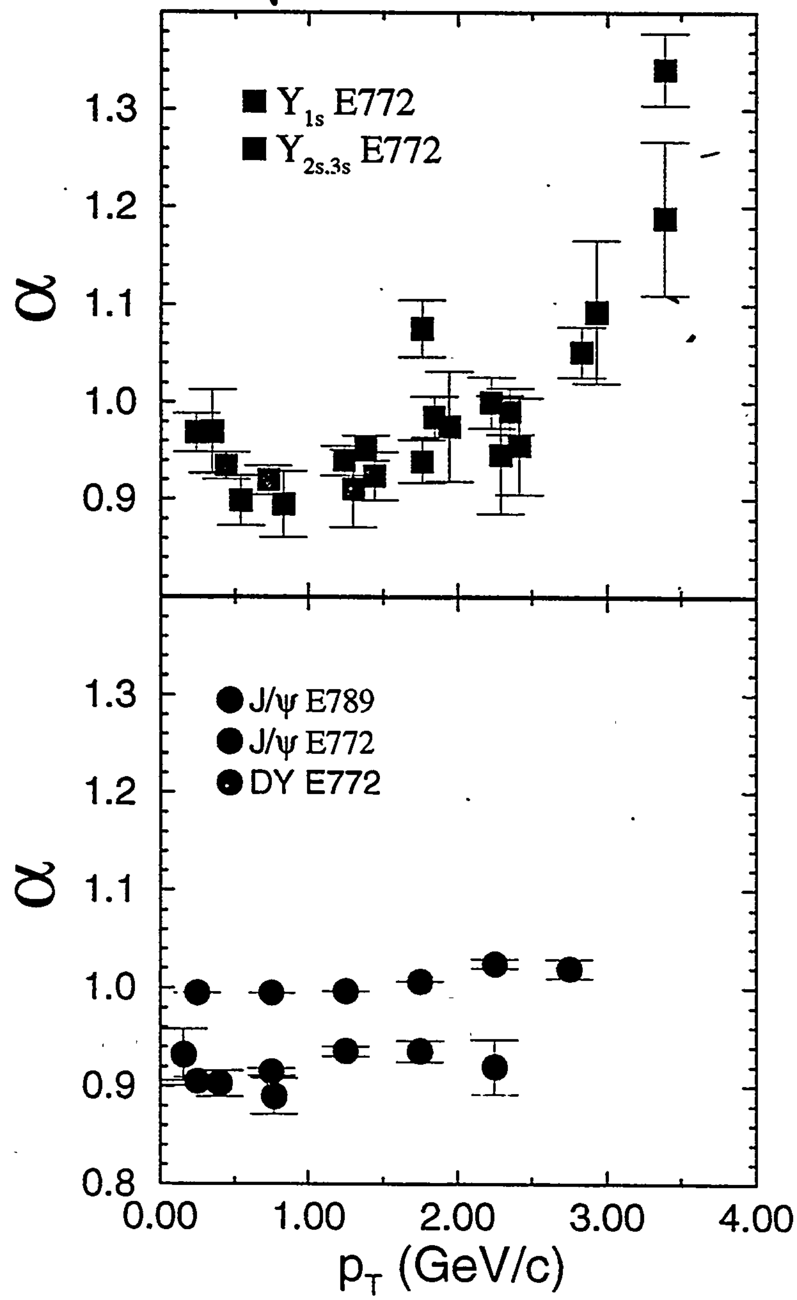

Where does x_F dependence come from?

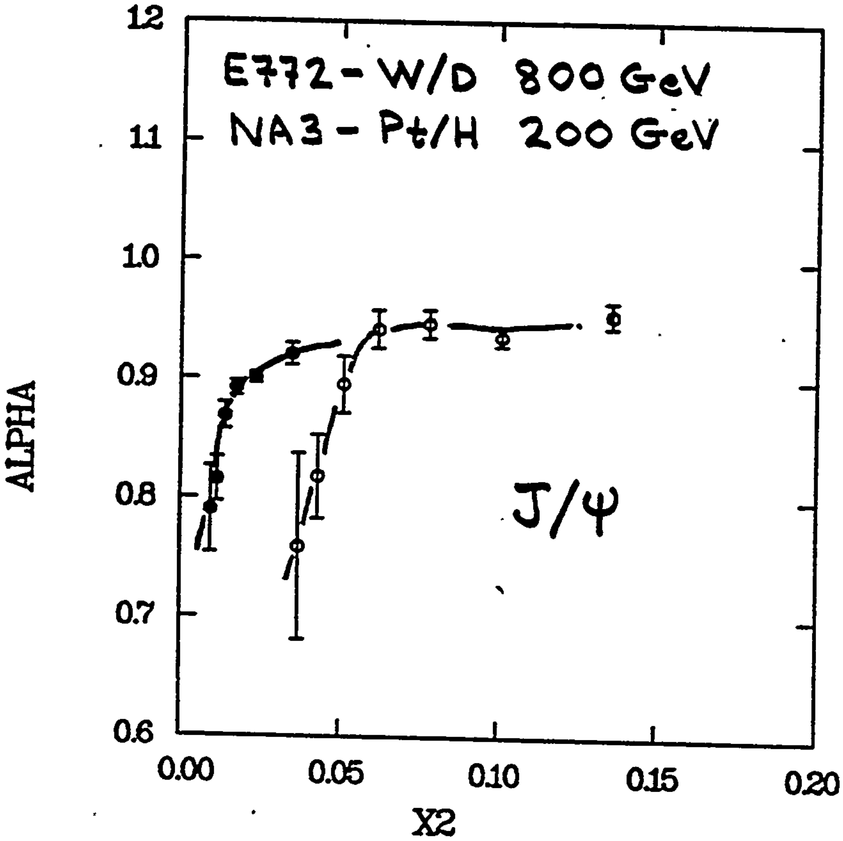

Not from x_2.
(i.e. not intrinsic property of struck parton)

Shift in x_F ?

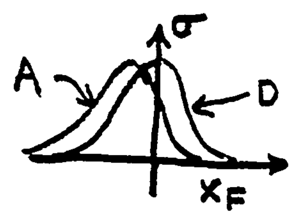

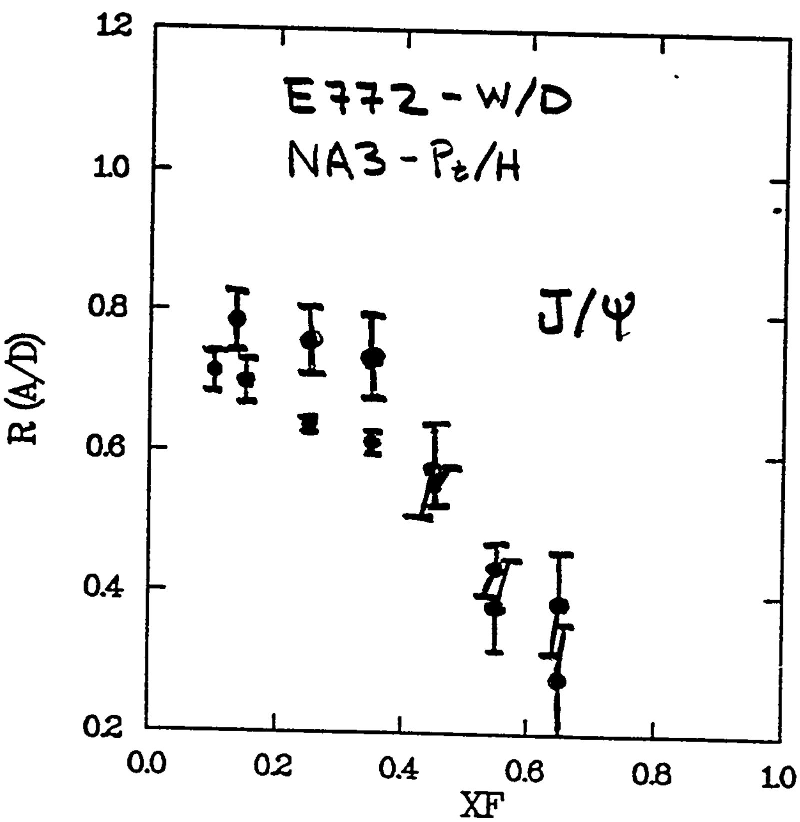

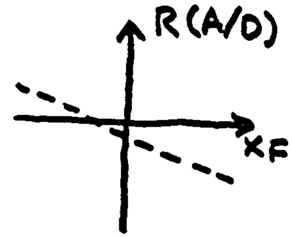

Need data for $x_F < 0$!

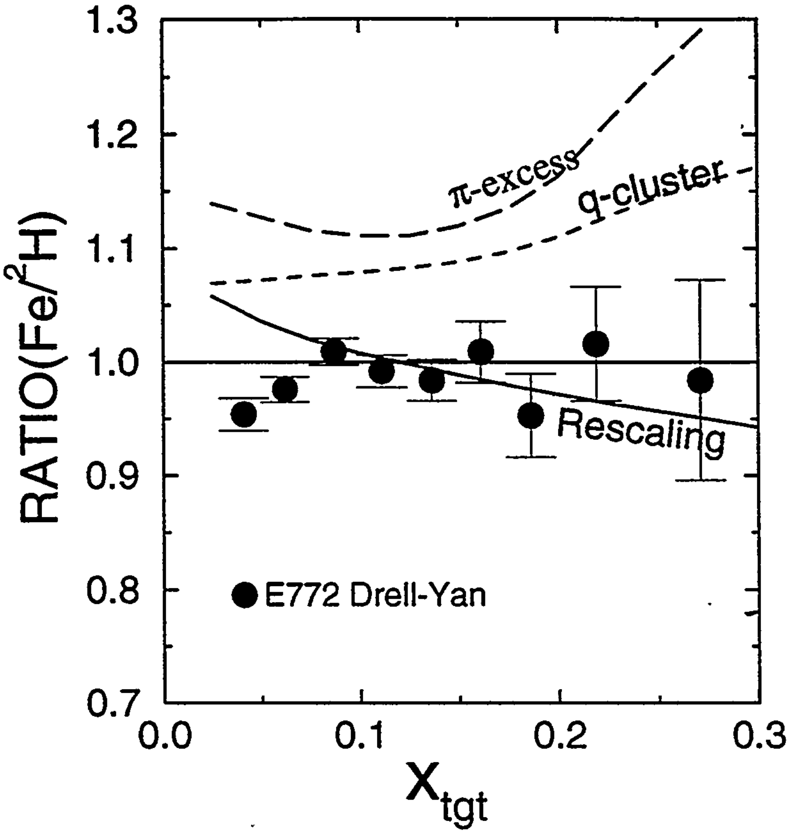

RATIO(Fe/^{2}H)
π-excess
q-cluster
Rescaling
E772 Drell-Yan
X_{tgt}

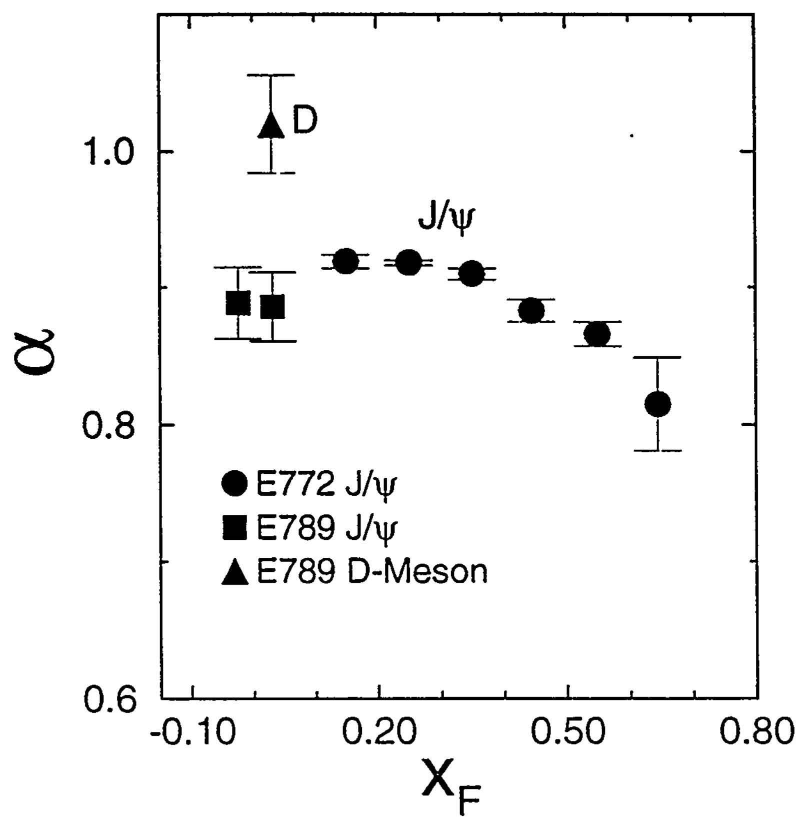

D
J/ψ
α
E772 J/ψ
E789 J/ψ
E789 D-Meson
X_F

INTRINSIC CHARM?

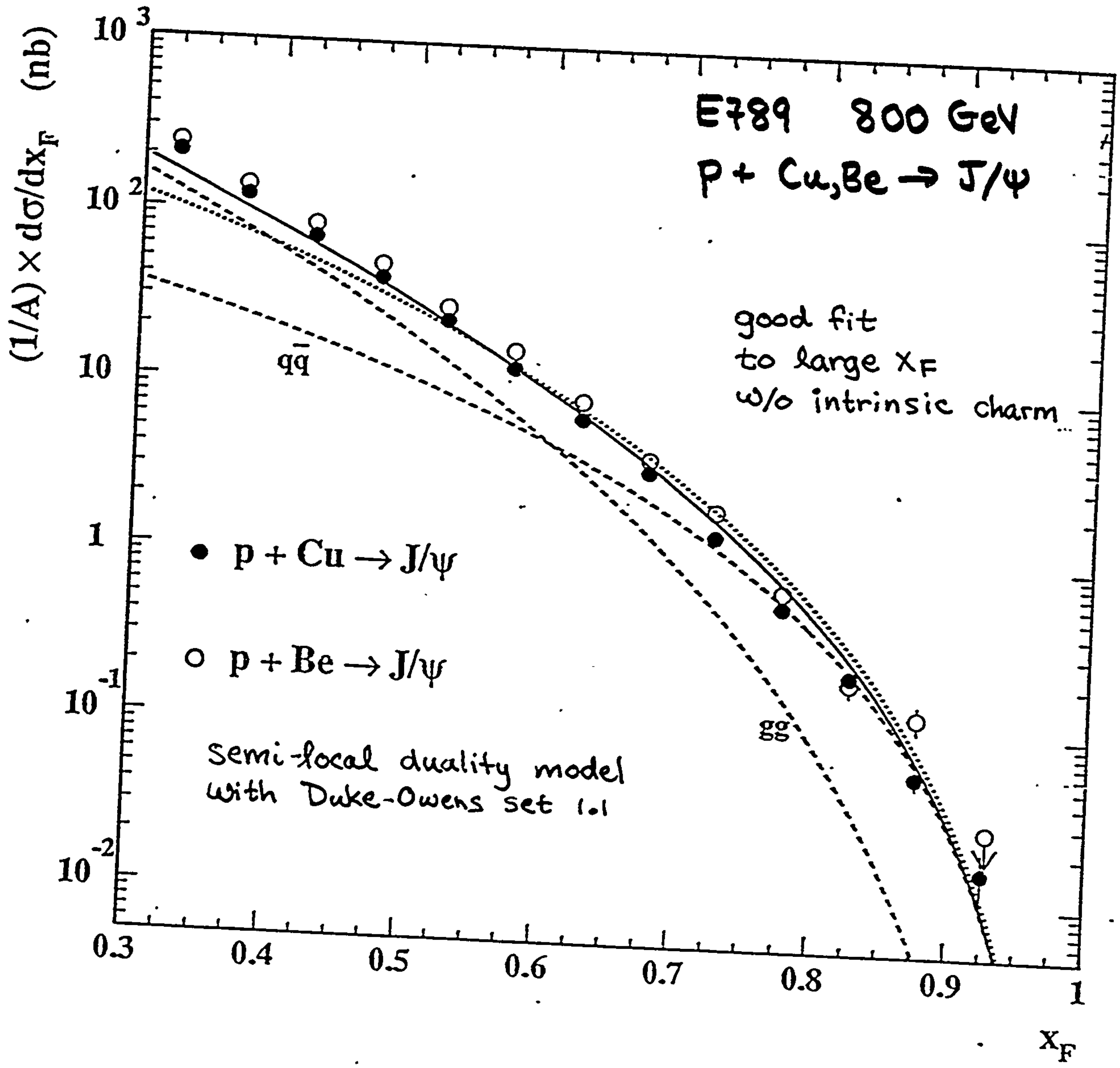

Figure 2

PARTON ENERGY LOSS?

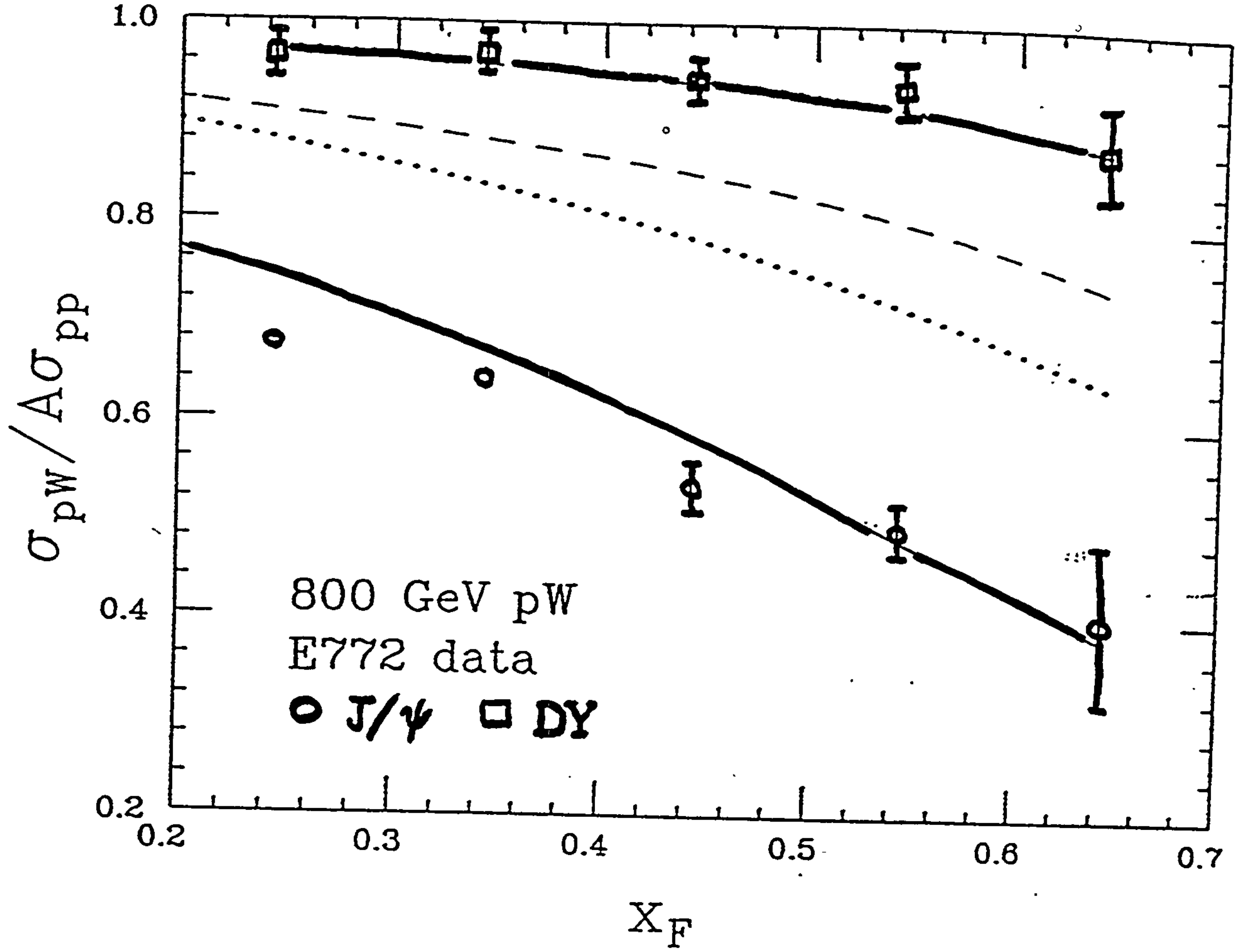

from Gavin + Milana, Phys. Rev. Lett. 68, 1834 (1992).

$\Delta E_q \sim 1.5$ GeV/fm } too
$\Delta E_g \sim 3.4$ GeV/fm } large?

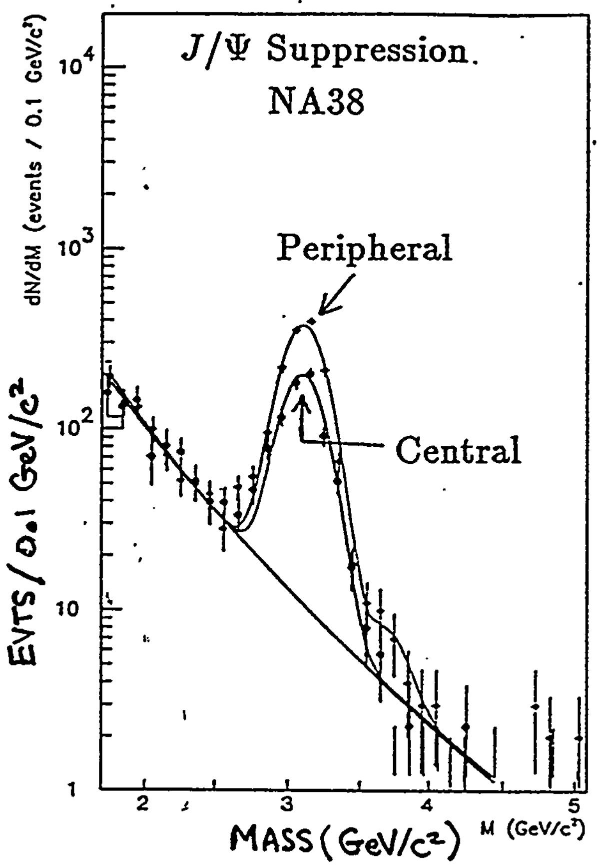

J/ψ Suppression
in Heavy-Ion Collisions

Evidence for
Quark-Gluon Plasma ??

Can be explained by
same effects seen
in p-A.

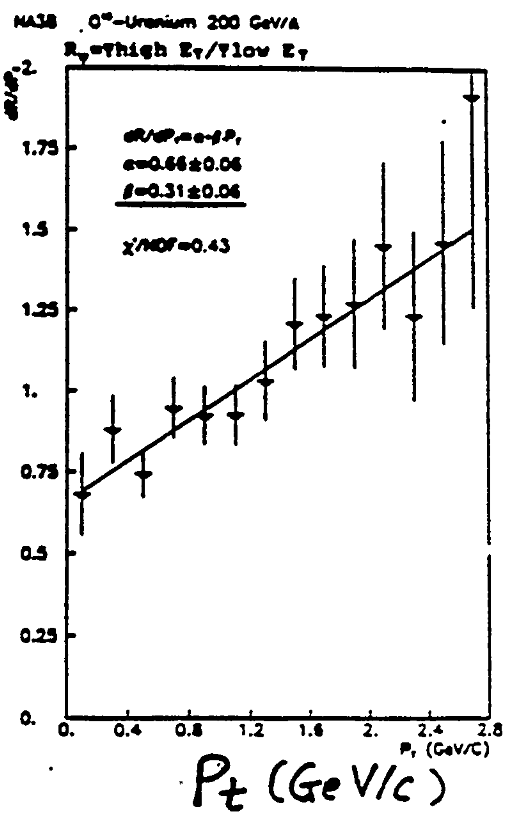

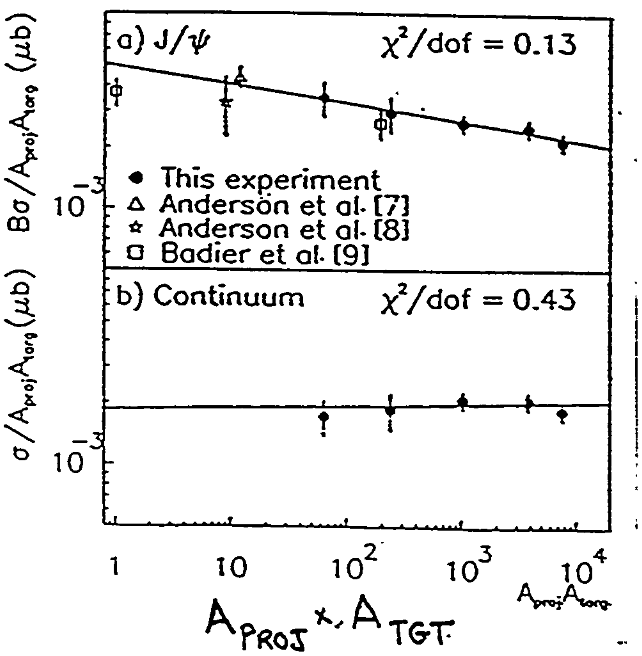

Evolution Toward RHIC Energies

- Quark-gluon-plasma signals visible via high-mass dileptons:
  - J/Ψ suppression by Debye screening in the plasma.
  - Thermal dileptons from $q\bar{q}$ annihilation in the plasma.
  - Enhanced charm from fusion of hot plasma gluons.
- Expected evolution of nuclear effects to $\sqrt{S} = 200$ GeV:
  - Shadowing - becomes dominant effect as $x_t \sim 0.02$ at 4 GeV mass, and structure functions are not well known at low x.
  - Intrinsic charm and beauty - not important for low x_F collider measurements.
  - Energy loss and multiple scattering - become less important at low x_F and as $<p_T>$ increases with $\sqrt{S}$.

- Nuclear absorption and co-movers - expect large effects due to ~1000 charged particles per unit rapidity at small x_F.
- Broken nucleons - would eliminate J/Psi production except from near the nuclear surface; $\alpha \rightarrow 2/3$.
- Finite formation times - less important for $x_F \sim 0$.
- Feeding of resonances - [redacted] large effects due to increase in $\sqrt{S}$.

• Other issues:
  - As $\sqrt{S}$ and number of participant nucleons increase, high mass pair production from secondary interactions may become important and could give $\alpha > 1$.
  - Hot glue models of QGP also give $\alpha > 1$.
  - $\bar{u} / \bar{d} \neq 1$ causes $\alpha \neq 1$ for Drell-Yan.

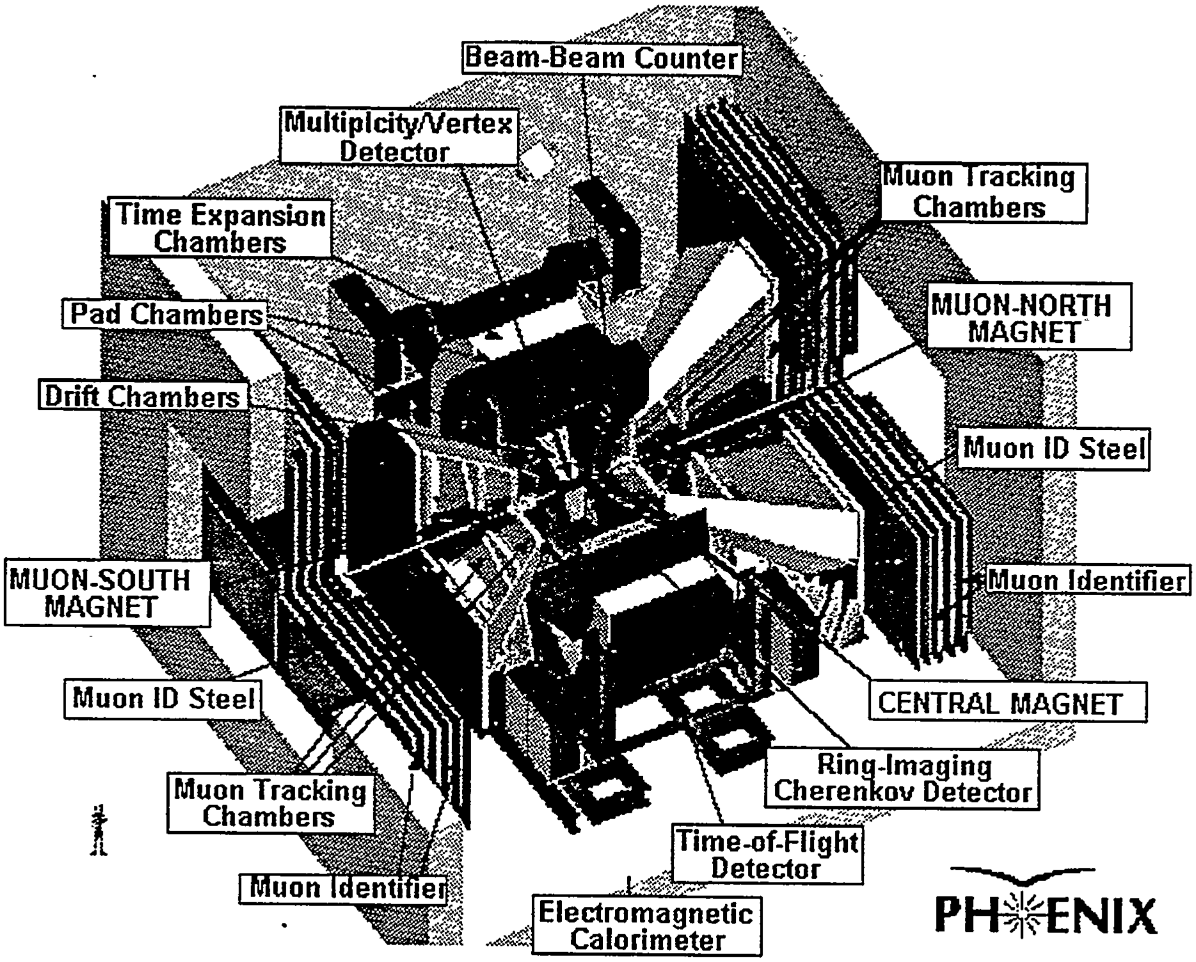

PHENIX Detector

Spokesman : S. Nagamiya, Project Director : S. Aronson

[Probes]

Electrons (2 sr, $|y|<0.35$) **Photons** (2 sr, $|y|<0.35$)
Muons ($1.2<|y|<2.4$) **Identified Hadrons** (0.36 sr)
Event Multiplicity ($d^2N/d\eta d\varphi$) ($-2.7<y<2.7$)

[Physics Highlights]

J/ψ, ψ', ϒ: Debye screening.
ω/φ mesons ($\Delta m \leq 4$ MeV): Chiral symmetry restoration.
Direct γ ($p_T > 1$ GeV/c) : Radiation from a hot gas.
Identified hadrons Order of phase transition.
eμ Coincidence: Open charm enhancement.
γ, e, μ: Studies on the nucleon spin with polarized p's.

[Others]

396 collaborators from 10 countries (45 institutions)
All detector elements are funded

Phenix Muon Arm Accepted events per RHIC Year

good rates from ρ to Υ for both p-Au and Au-Au

resonances	Central Au + Au	Min. bias Au + Au	Min. bias p + Au
$\rho \rightarrow \mu^+ + \mu^-$	309,000 ± 10,000	1,100,000	920,000
$\phi \rightarrow \mu^+ + \mu^-$	139,000 ± 8,000	500,000	420,000
$J/\psi \rightarrow \mu^+ + \mu^-$	390,000 ± 1,100	1,730,000	1,060,000
$\psi' \rightarrow \mu^+ + \mu^-$	5700 ± 350	24,200	14,700
$\Upsilon \rightarrow \mu^+ + \mu^-$	1180 ± 60	4920	1400
Drell-Yan $\rightarrow \mu^+ + \mu^-$			
2 GeV	49,000	216,000	87,000
3 GeV	15,000	67,000	26,000
4 GeV	6800	30,000	12,000
5 GeV	2900	13,000	5400
6 GeV	1500	6600	6600
7 GeV	790	3500	1400
8 GeV	400	1800	740
DD $\rightarrow \mu^+ + \mu^- + X$			
2 GeV	81,000	360,000	215,000
3 GeV	26,000	115,000	73,000
4 GeV	7200	32,000	20,000
5 GeV	1800	8000	5000
6 GeV	590	2600	1600
DD $\rightarrow e + \mu + X$	140,000	620,000	370,000

assumptions 3000 hours $L(\mathrm{Au\,Au}) = 2 \times 10^{27}$, $(p+\mathrm{Au})$ 1.5×10^{29}

no detector frames. Θ = 10 - 35° : $P_{min}(\mu) = 2$ GeV

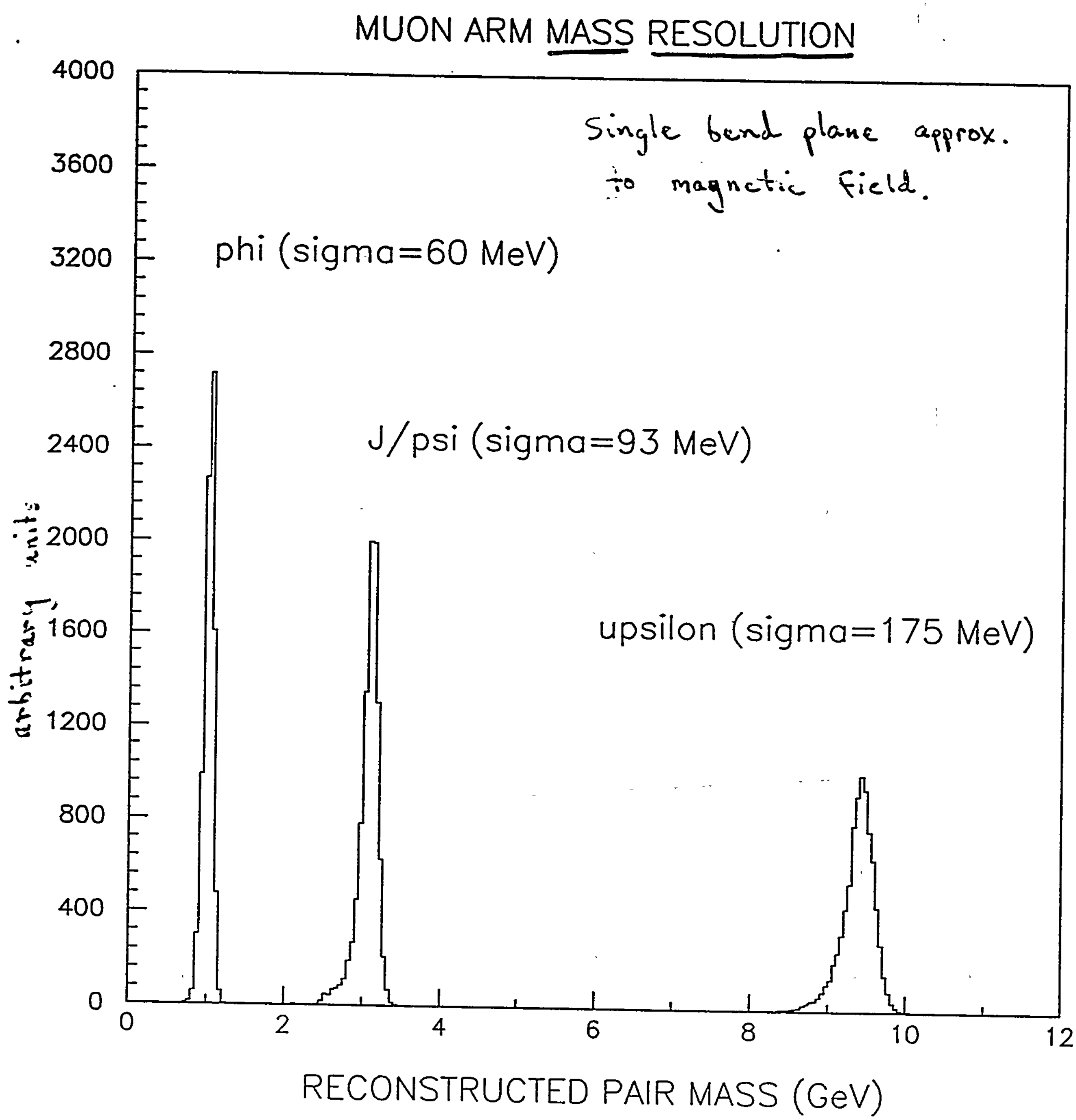

adequate resolution at all masses!

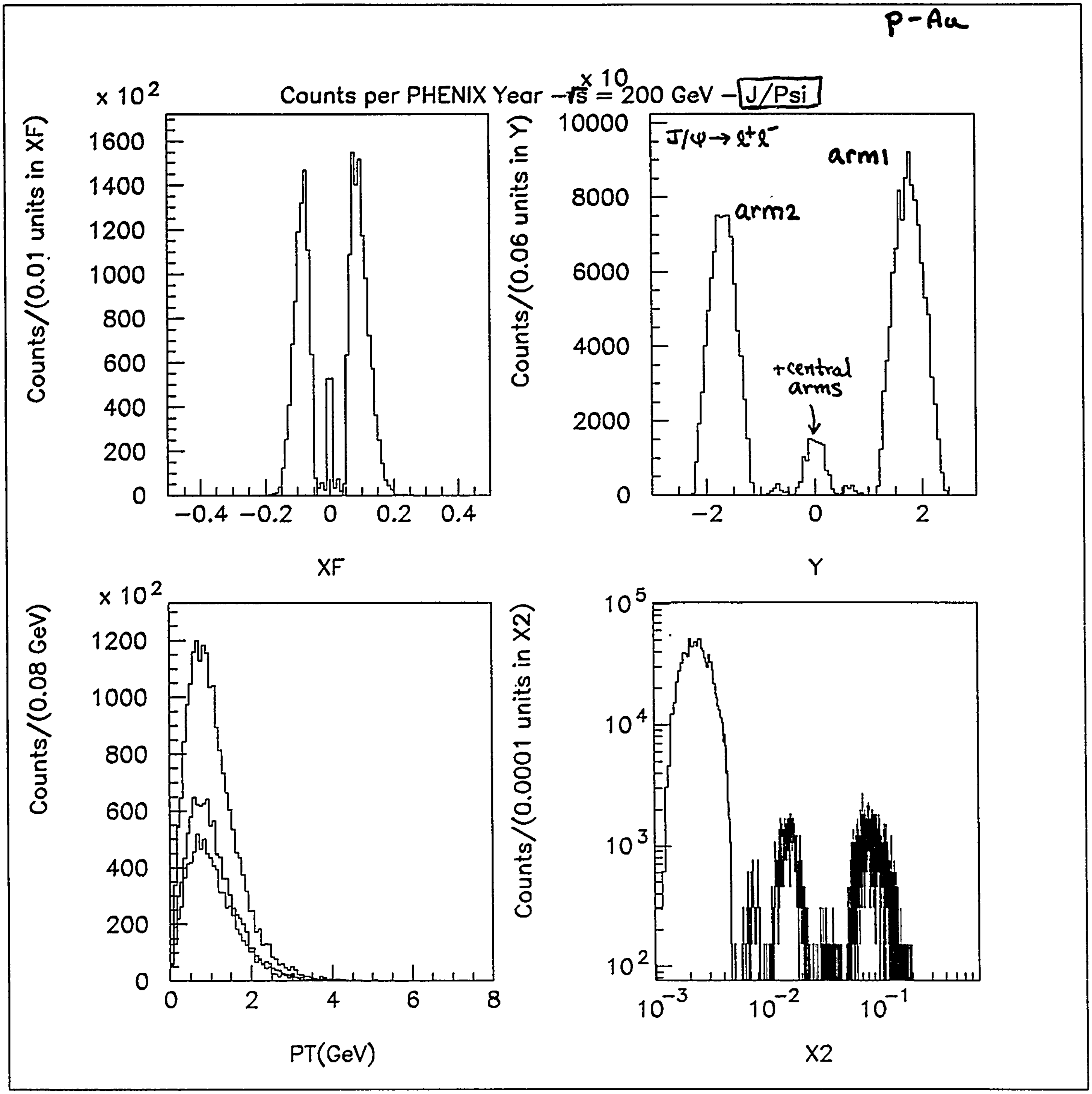

p-Au
Counts per PHENIX Year – √s = 200 GeV – J/Psi
x 10²
Counts/(0.01 units in XF)
XF
x 10
Counts/(0.06 units in Y)
J/ψ → ℓ⁺ℓ⁻
arm1
arm2
+central arms
Y
x 10²
Counts/(0.08 GeV)
PT(GeV)
Counts/(0.0001 units in X2)
X2

p-Au

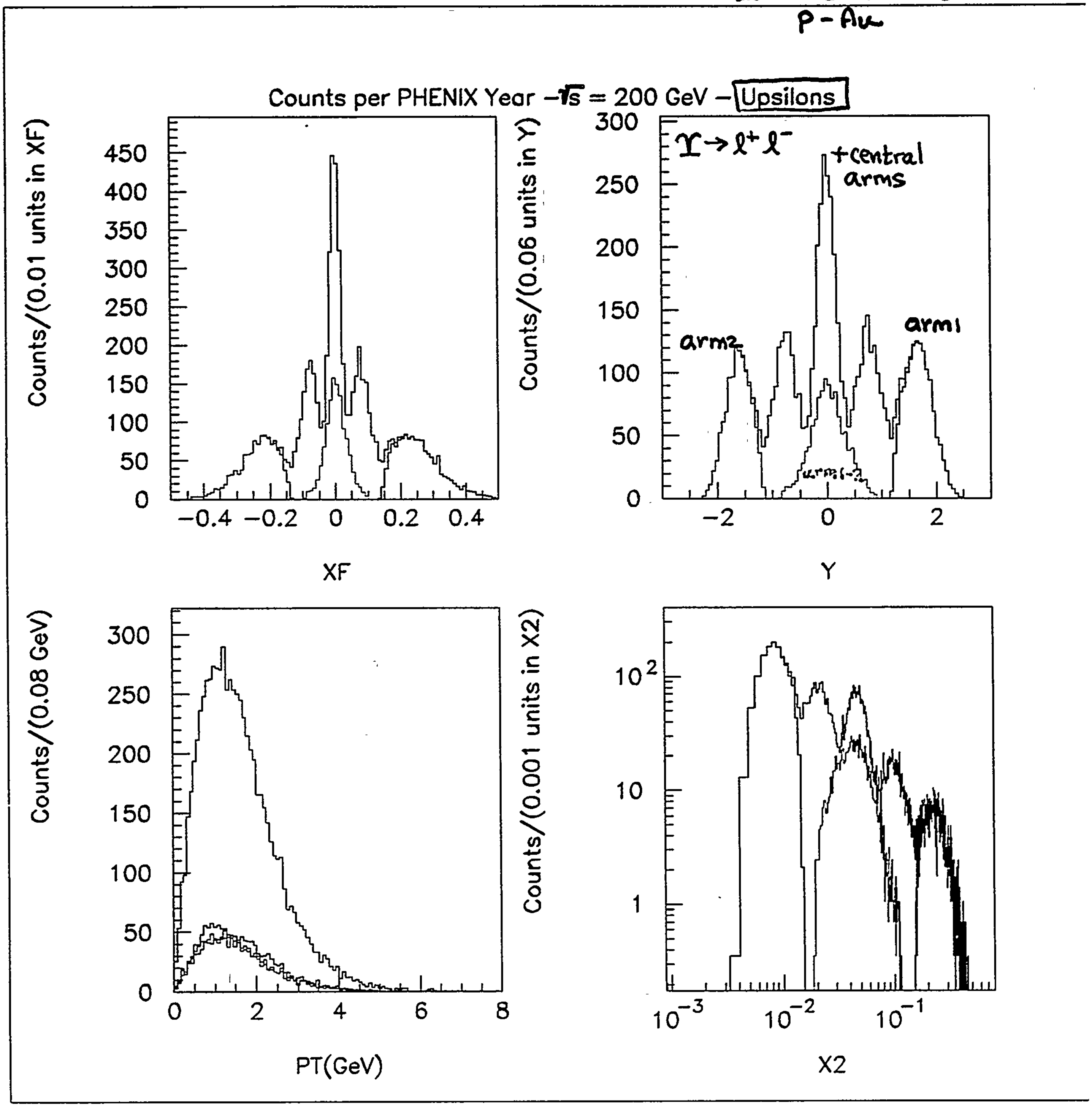

Counts per PHENIX Year – $\sqrt{s}$ = 200 GeV – Upsilons
Counts/(0.01 units in XF)
XF
Counts/(0.06 units in Y)
Y
$\Upsilon \to l^+ l^-$
+central arms
arm2
arm1
arm1-2
Counts/(0.08 GeV)
PT(GeV)
Counts/(0.001 units in X2)
X2

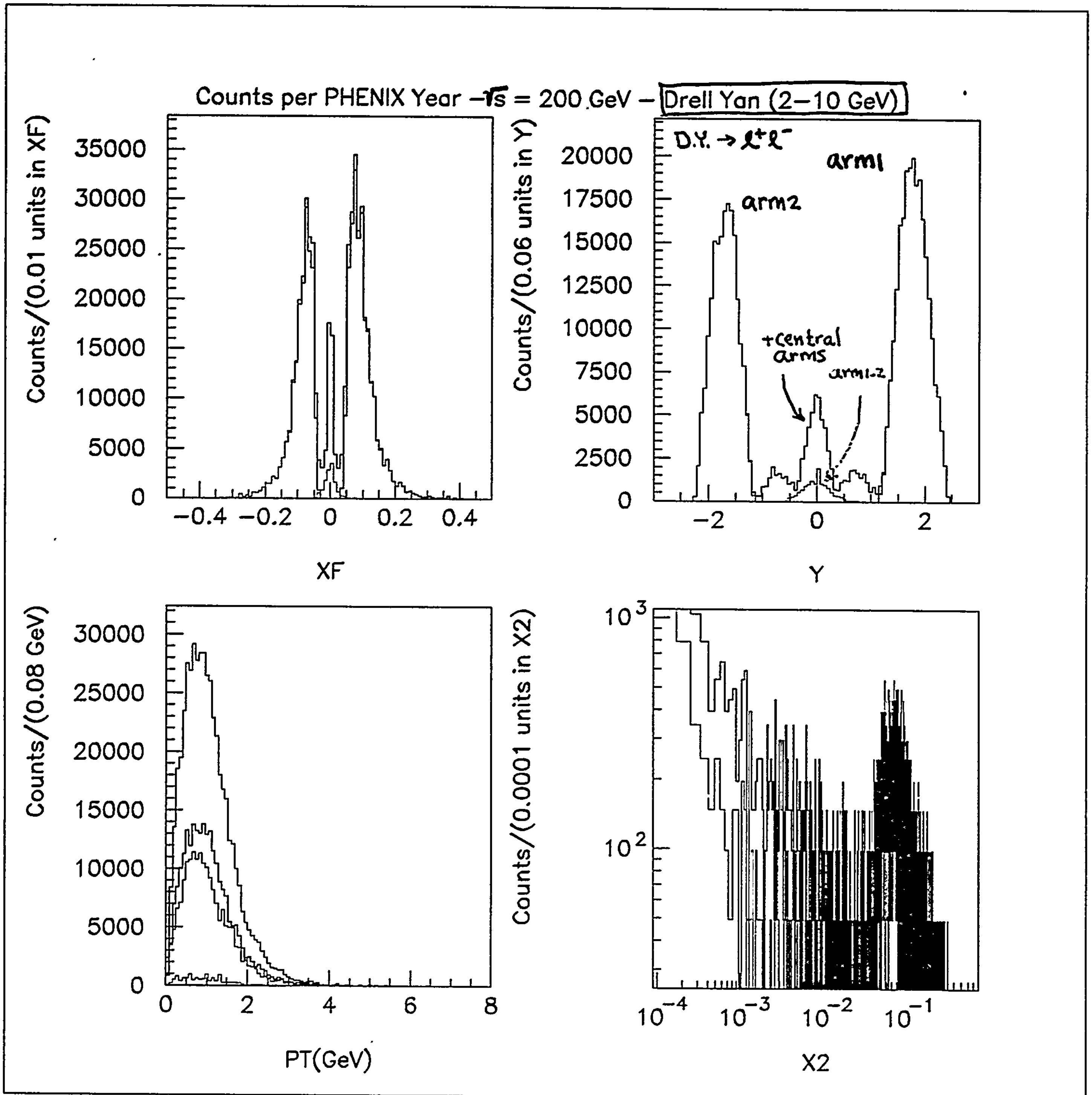

Counts per PHENIX Year – $\sqrt{s}$ = 200 GeV – Drell Yan (2–10 GeV)
Counts/(0.01 units in XF)
XF
Counts/(0.06 units in Y)
D.Y. → $\ell^+\ell^-$
arm1
arm2
+central arms
arm1-2
Y
Counts/(0.08 GeV)
PT(GeV)
Counts/(0.0001 units in X2)
X2

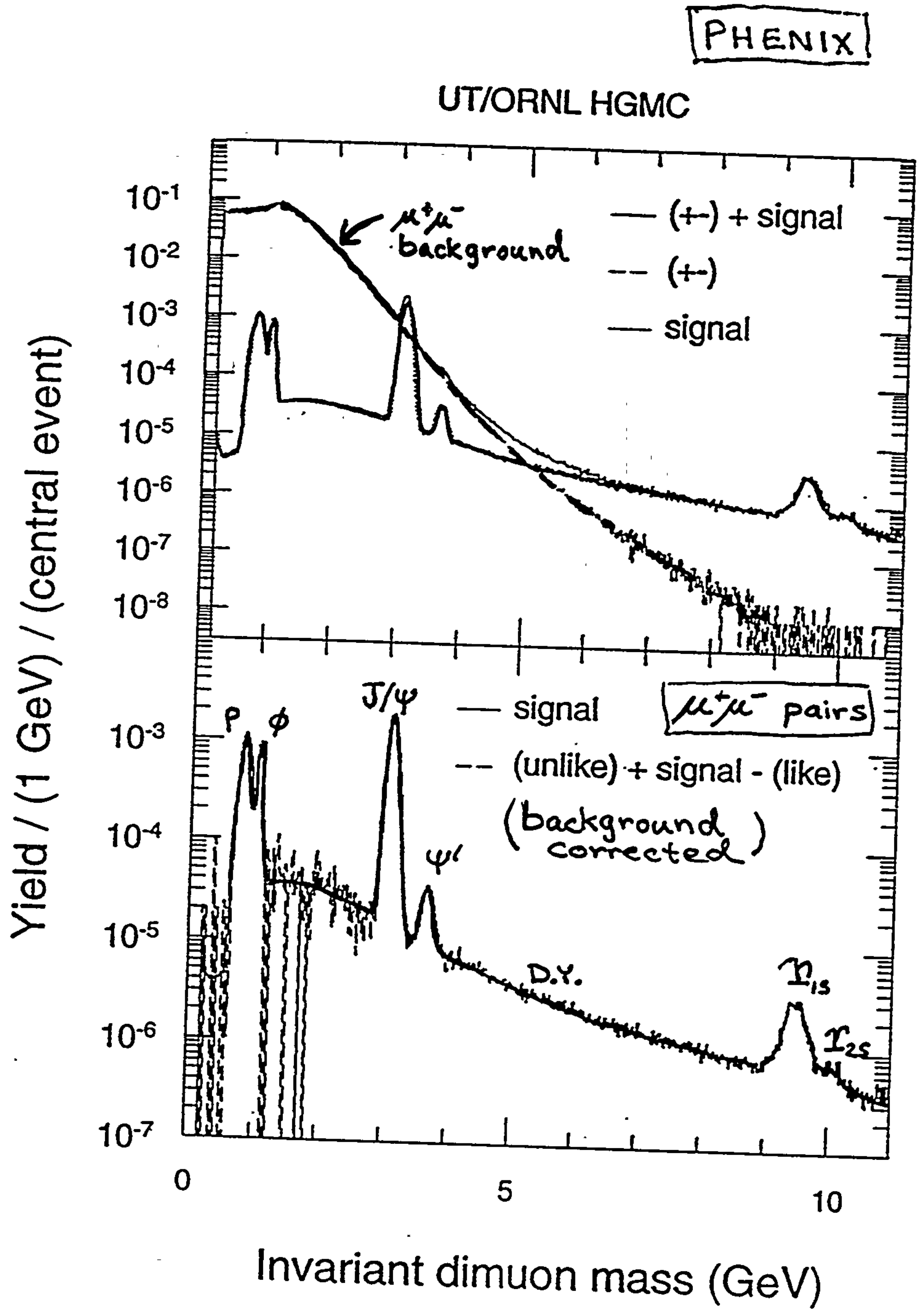

Figure 3.6: Top: Contributions to the unlike-sign dimuon yield per central event as function of the invariant mass. The dashed line shows the combinatoric background, the dotted line shows the signal and the solid line their sum. Bottom: Results from a like-sign subtraction. The solid line is the assumed signal; the dashed line is constructed by subtracting the like-sign combinatoric background from the total unlike sign distribution.

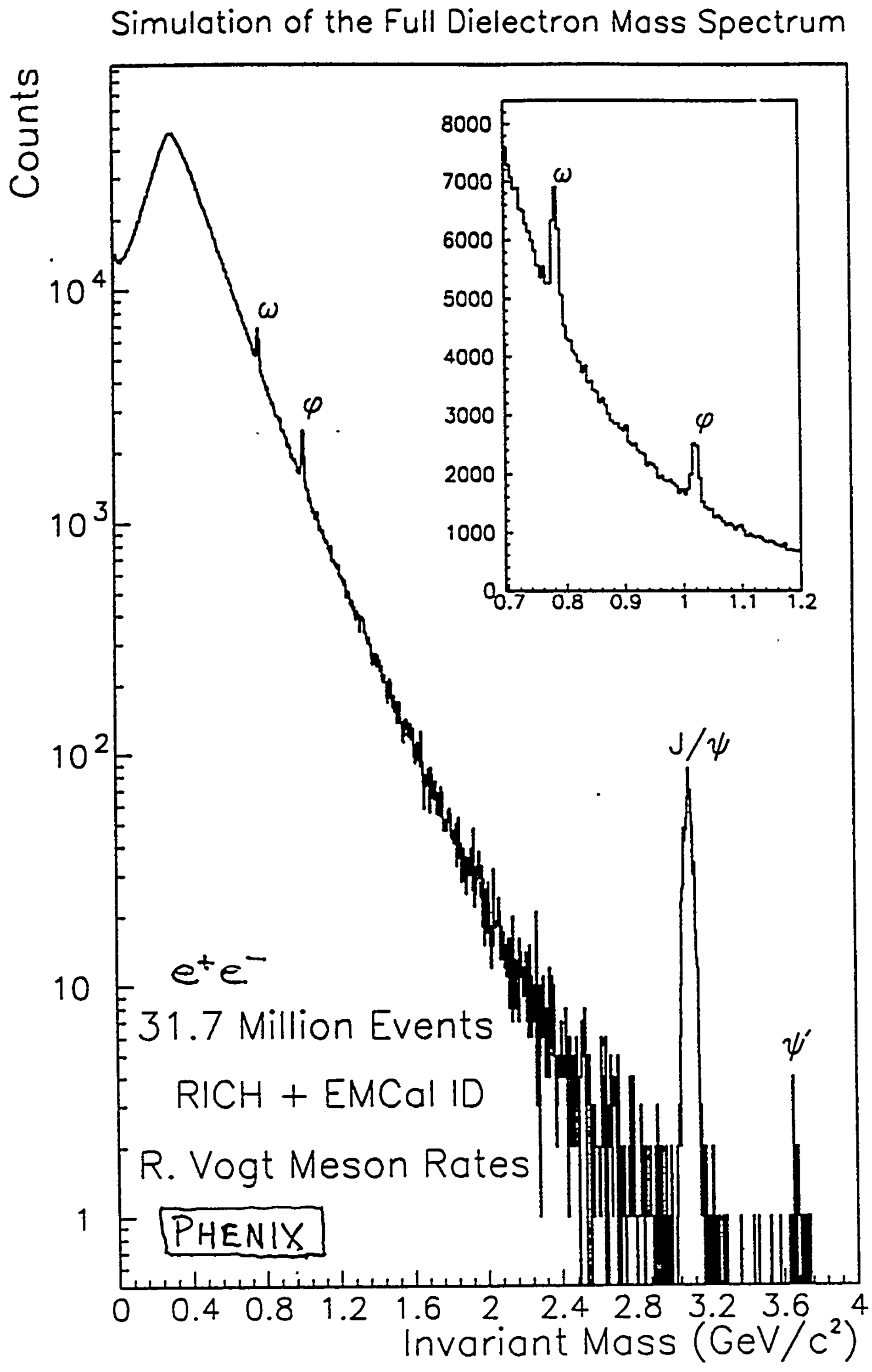

Simulation of the Full Dielectron Mass Spectrum
Counts
10^4
10^3
10^2
10
1
ω
φ
J/ψ
ψ'
e^+e^-
31.7 Million Events
RICH + EMCal ID
R. Vogt Meson Rates
PHENIX
0 0.4 0.8 1.2 1.6 2 2.4 2.8 3.2 3.6 4
Invariant Mass (GeV/c²)
8000
7000
6000
5000
4000
3000
2000
1000
0
0.7 0.8 0.9 1 1.1 1.2

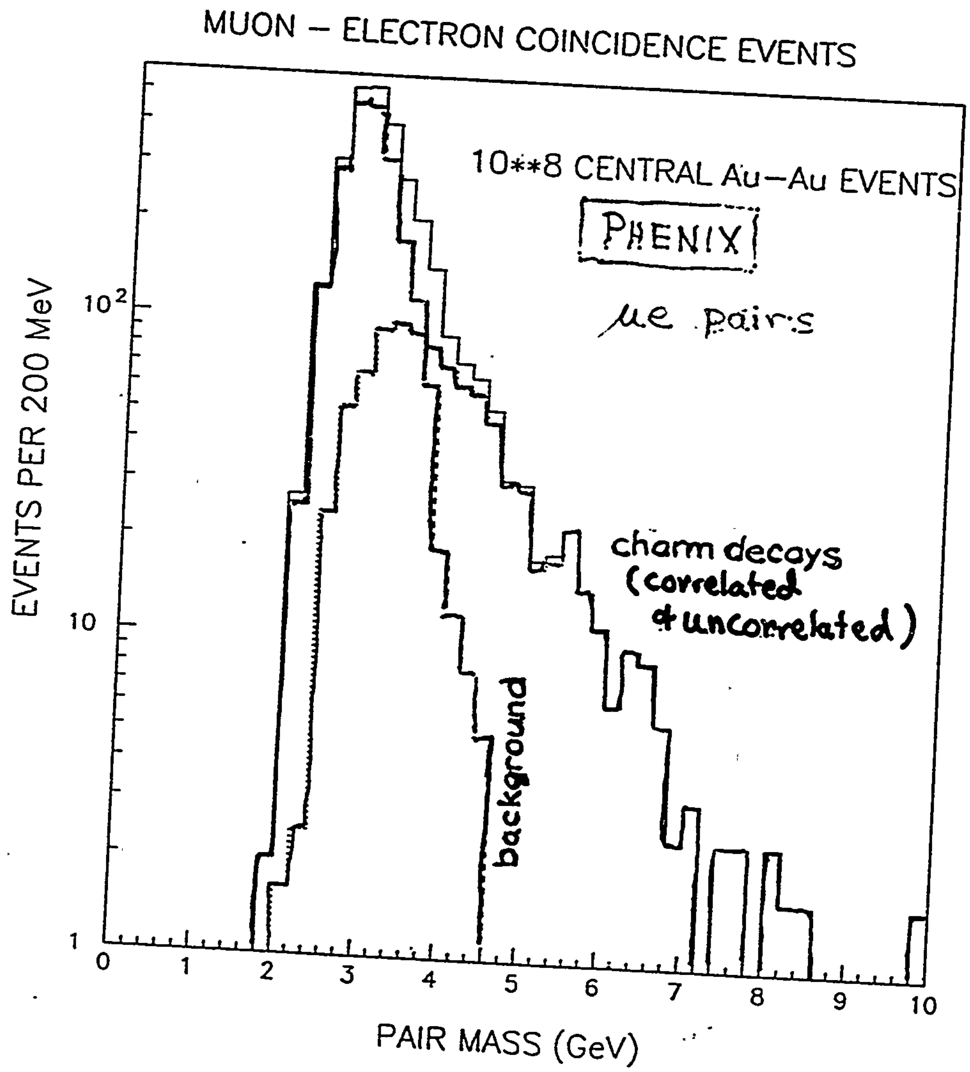

Figure 3.8: The mass spectrum for $e\mu$ pairs from 10^8 central Au + Au events, with $\phi_{e-\mu} > 90°$ and $\theta_\mu > 25°$. The dotted line is the charm pair signal, while the dashed line is the background from pion decays. The solid line is the sum of both. A Dalitz pair cut has been applied to the electron background signal.

RHIC/SPIN Facility overview

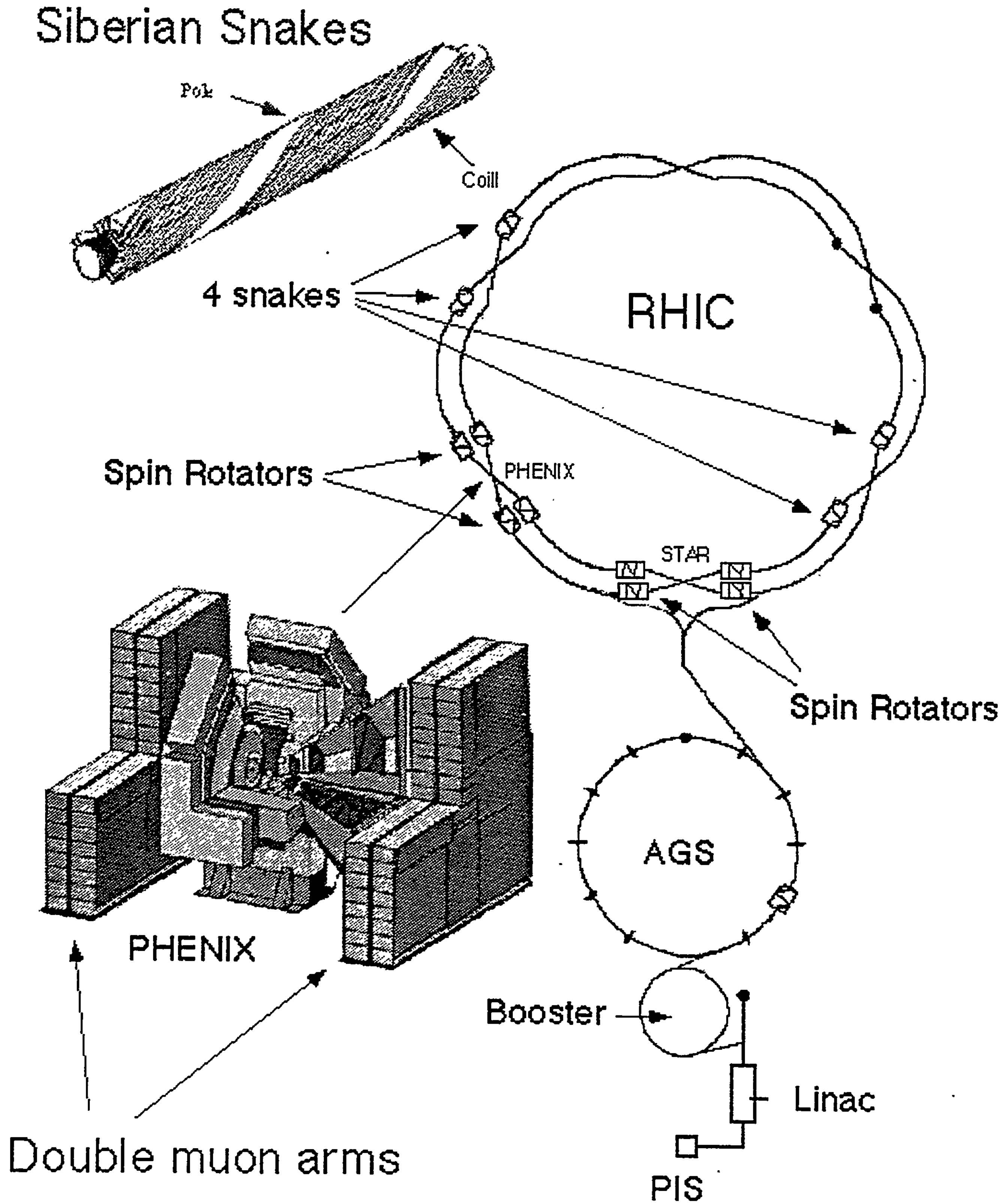

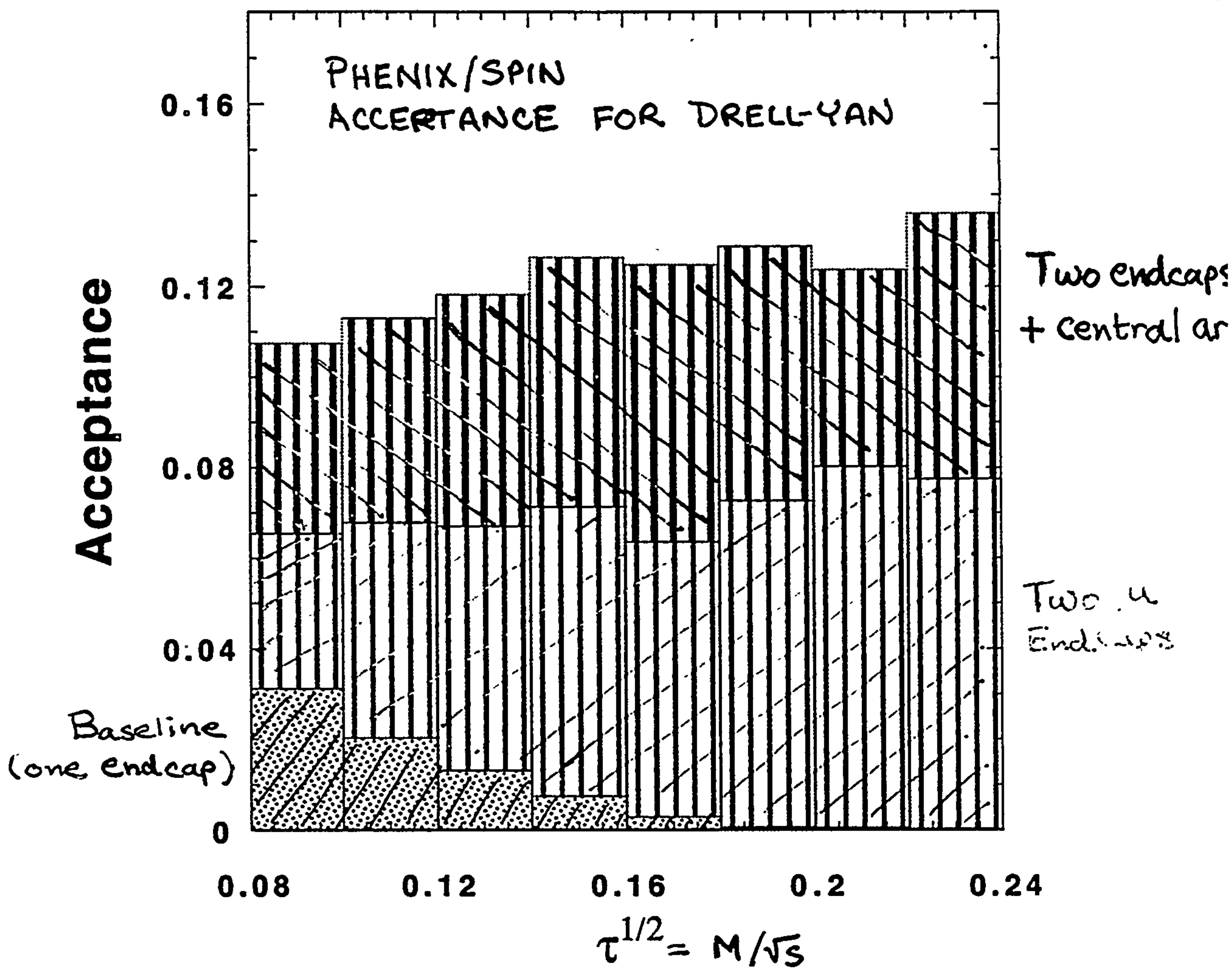

Figure 3. Acceptance for three version of the PHENIX muon subsystem; baseline (dotted), 2 endcaps (hatched), 2 endcaps plus central arm muon identification (solid). The calculations were performed at $\sqrt{s} = 50$ GeV, but are approximately valid at higher energies as well due to $\sqrt{\tau}$ scaling.

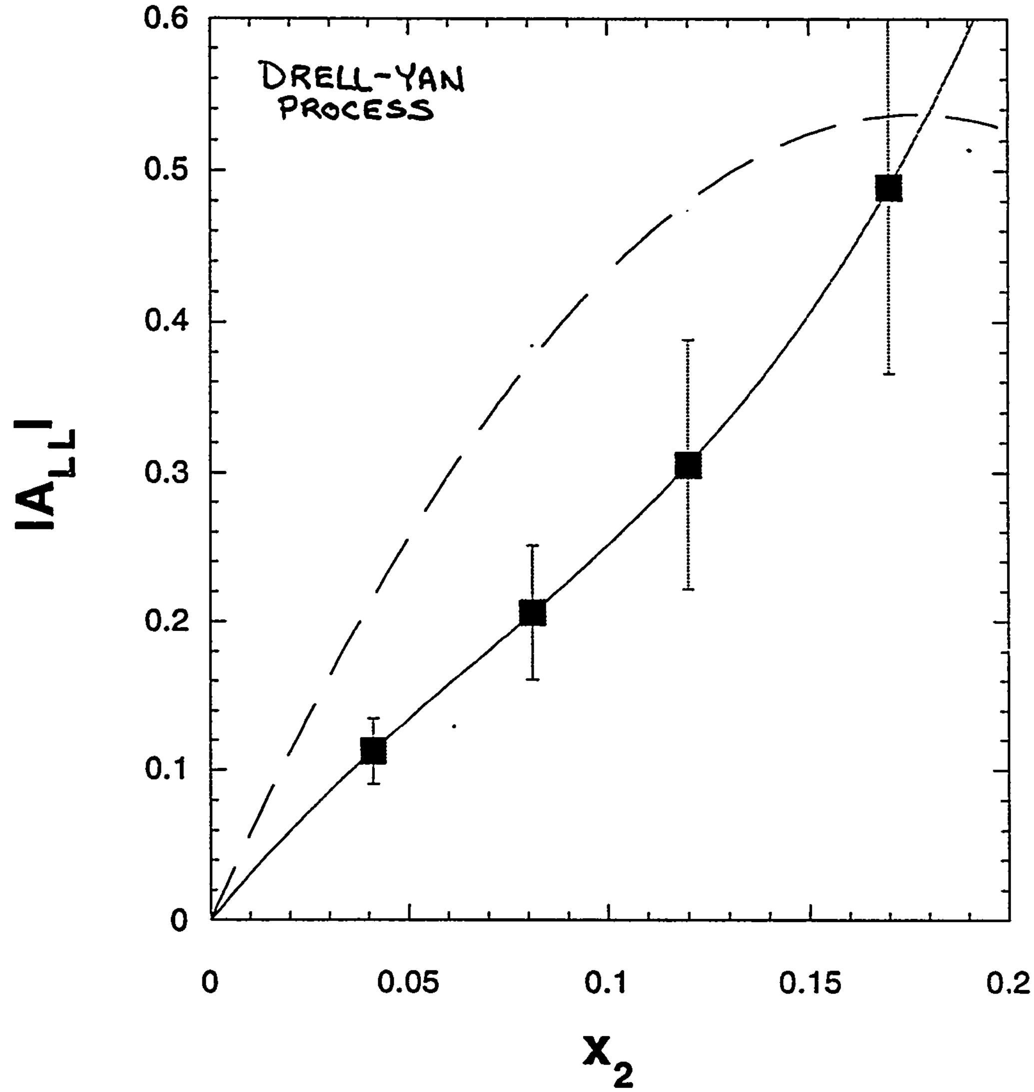

Figure 6. Helicity asymmetry using Eq. 5 and the model of Bourrely and Soffer[19]. Two extrapolations consistent with the experimental results from CERN NA51[21] yield the two curves. Error bars (shown on the lower curve) are based on an integrated luminosity of $2\times10^{38}cm^{-2}$ at $\sqrt{s}$ = 50 GeV; beam polarizations are taken to be 0.7

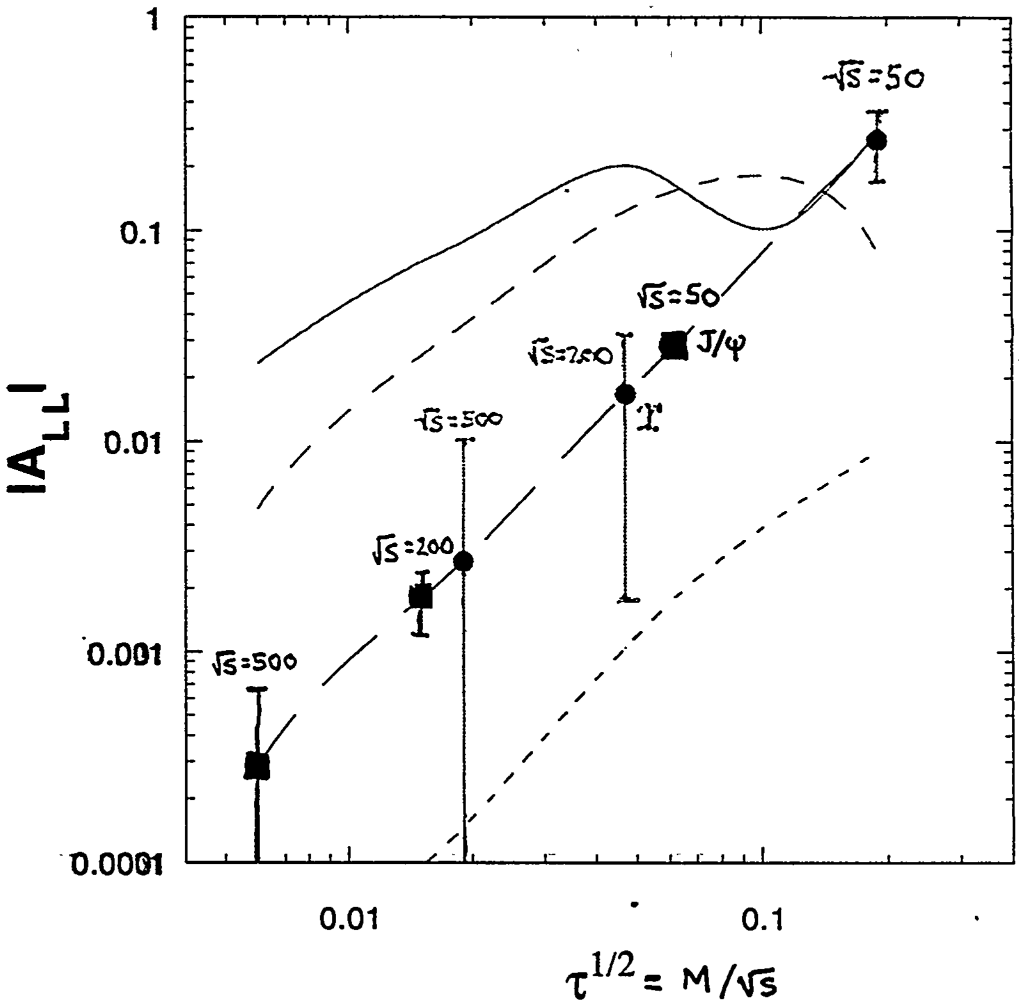

Figure 11. Asymmetries from the polarized gluon structure functions of Ref. [31] solid, Ref. [33], medium dash, Ref. [32] long dash, and Ref. [31] short dash. A parton-level asymmetry, $|\hat{a}_{LL}| = 0.3$ was assumed. The points show error estimates for J/ψ and Υ (circles) production at $\sqrt{s}$ = 50, 200, and 500 GeV (right to left on the graph).

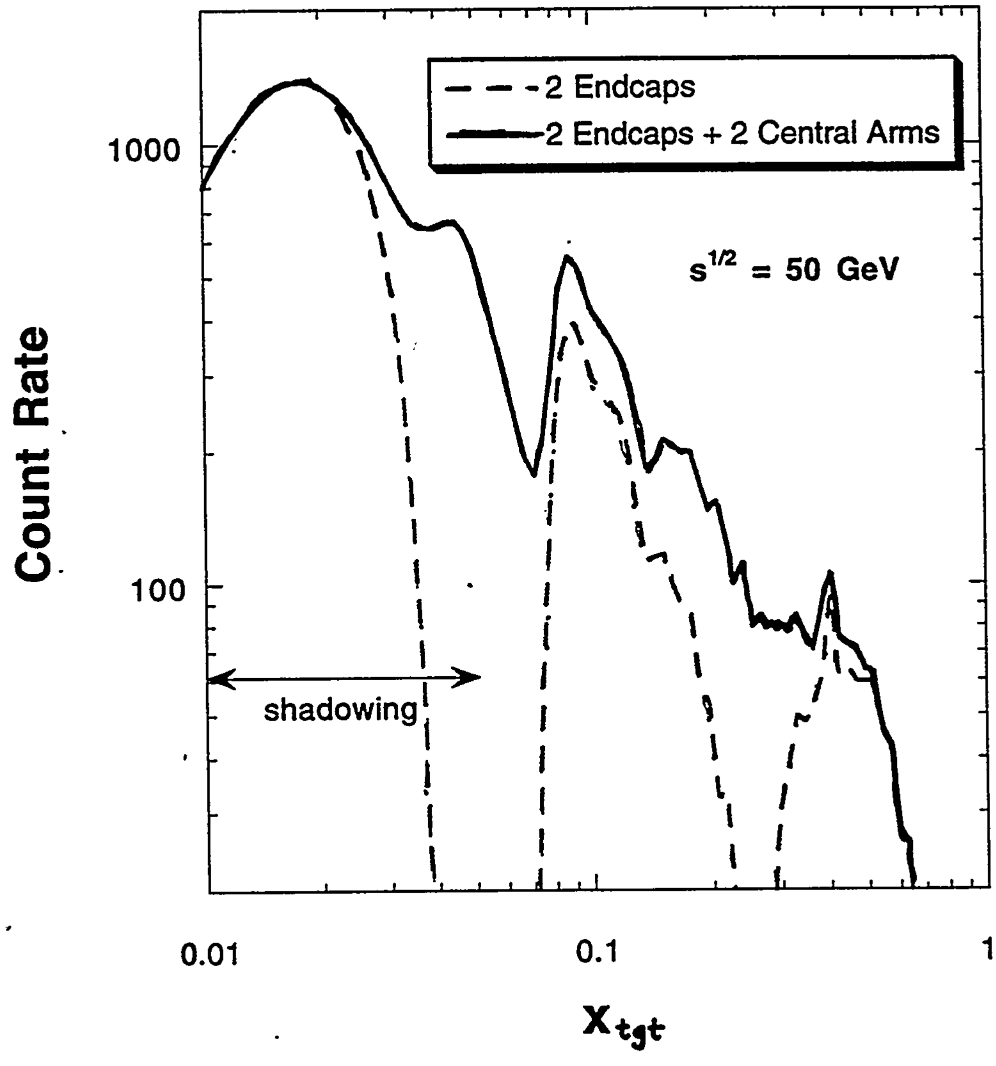

Figure 13. Acceptance of the upgraded PHENIX muon spectrometer for Drell-Yan pairs with $M \geq 4$ GeV versus x, with and without muon detection in the central magnet arms. The arrow show the region of nuclear shadowing expected in pA and AA collisions.

Probing Spin-Averaged and Spin-Dependent Parton Distributions Using the Solenoidal Tracker at RHIC (STAR)

Tim Hallman
Brookhaven National Laboratory

Probing Spin-Averaged and Spin-Dependent Parton Distributions Using The Solenoidal Tracker At RHIC (STAR)

T. Hallman

Nuclei at HERA and Heavy Ion Physics Workshop

November 17-18, 1995
Brookhaven National Laboratory
Upton, NY

The Role of Hard-Parton Scattering in the STAR Physics Program

- **Determining the initial conditions in AA collisions**

  Compton QCD diagram in pp and pA

- **Studying the effects of "jet-quenching" in AA interactions**

  Jets, γ + Jet events, and inclusive high p_t particle spectra

- **Searching for evidence of a change in parton energy loss in "special" event samples possibly indicating new physics**

  Jets, γ + Jet events, and inclusive high p_t particle spectra

- **Determining the contribution from gluons to the proton spin**

  QCD Compton diagram

- **Determining the polarization of the valence and sea quarks in the proton**

  $W^{\pm}$ production

- **Measuring the transversity distribution $h_1(x)$ of quarks in the proton**

  Z^{o} , Jet-Jet production

- **Searching for new physics (parity violating asymmetries)**

  Jet-Jet production

STAR DETECTOR

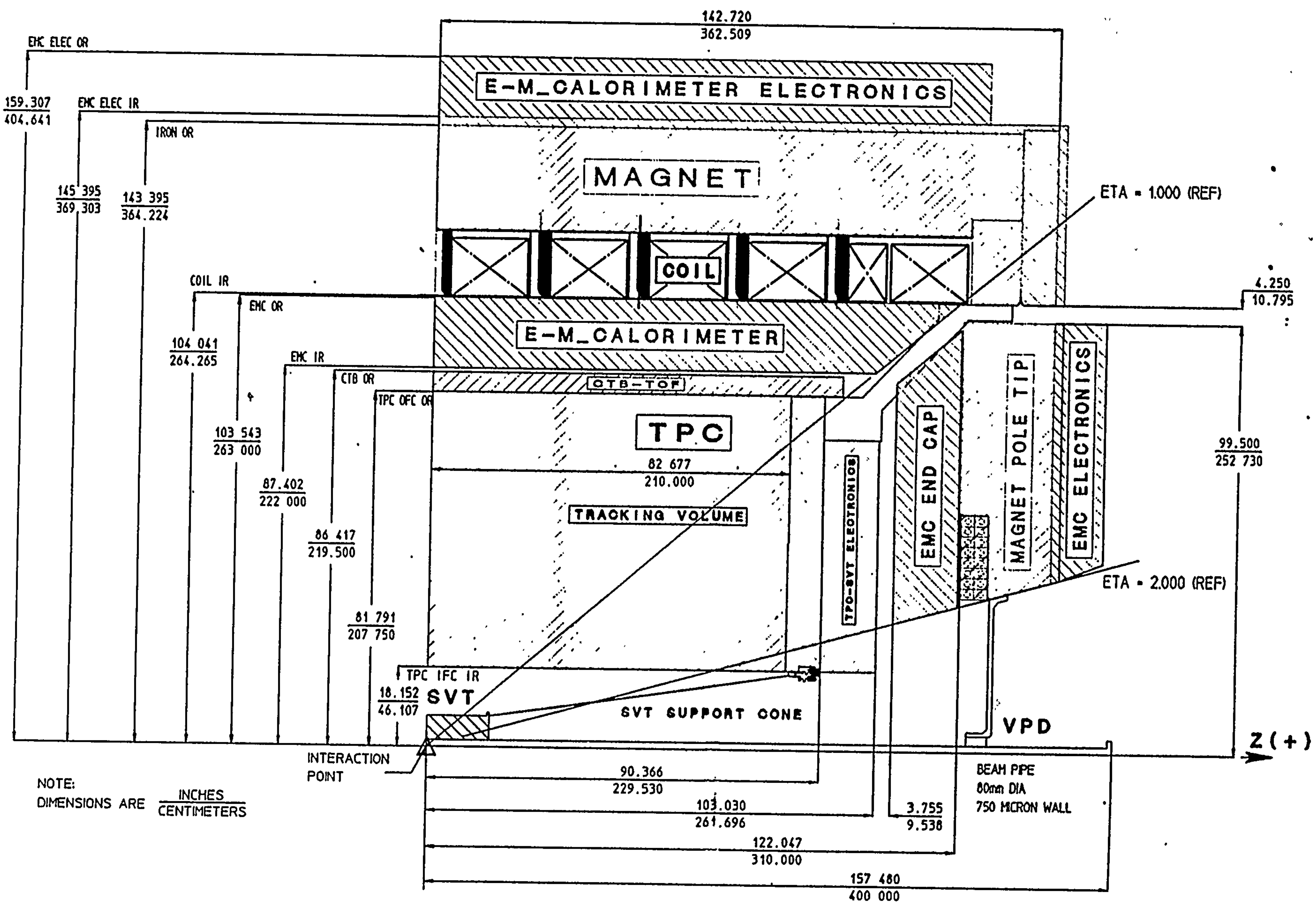

NOTE:
DIMENSIONS ARE INCHES / CENTIMETERS

/fritz/star/STAR-ENVELOPE/24A1401-3_envlp_Q-SECTION_w_dims....11-May-94

Phys Rev D 50 (1994) 6734

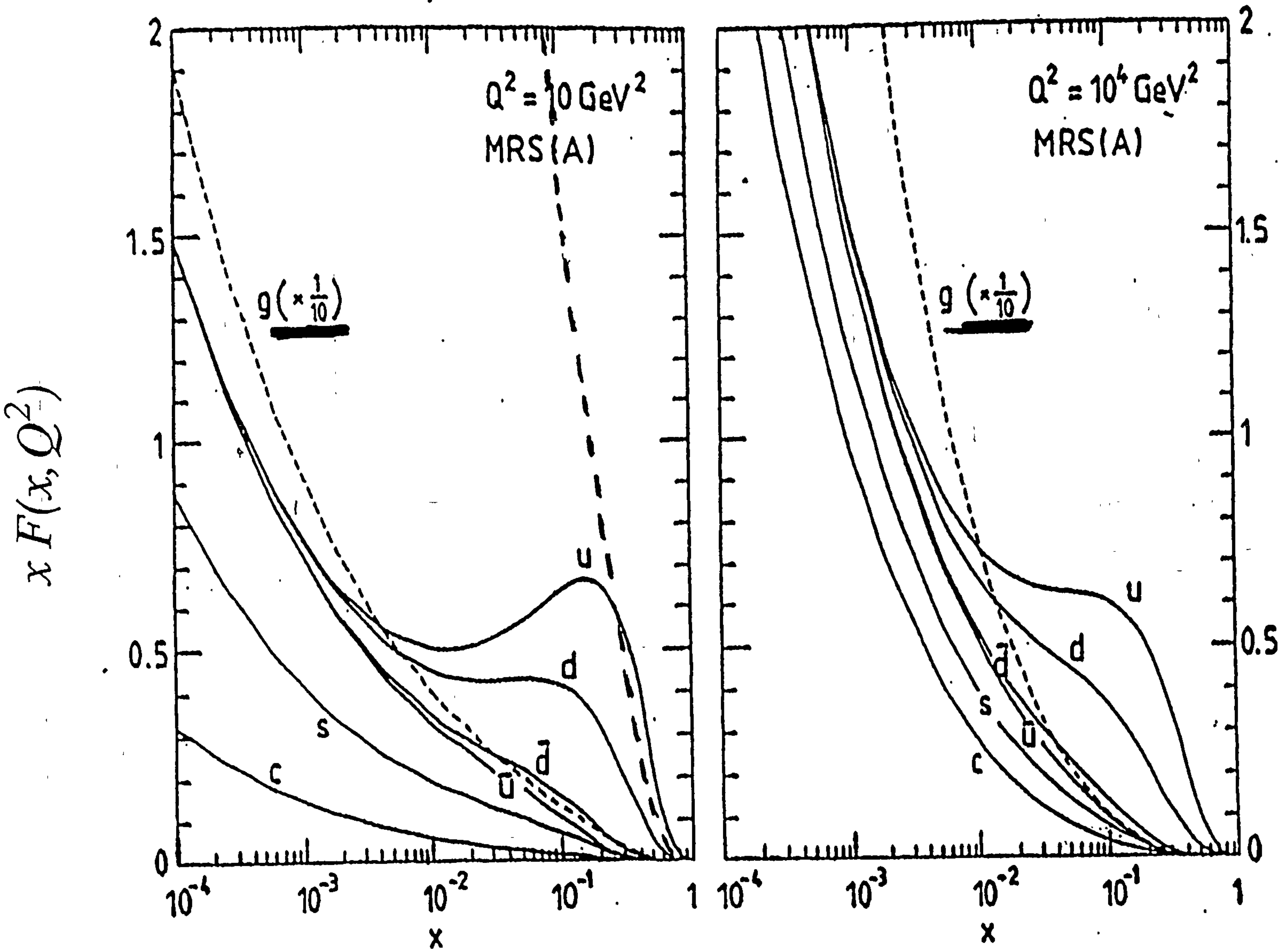

FIG. 9. MRS(A) partons shown as a function of x at $Q^2 = 10$ and 10^4 GeV^2.

Measuring the Gluon Structure Function in the Nucleus

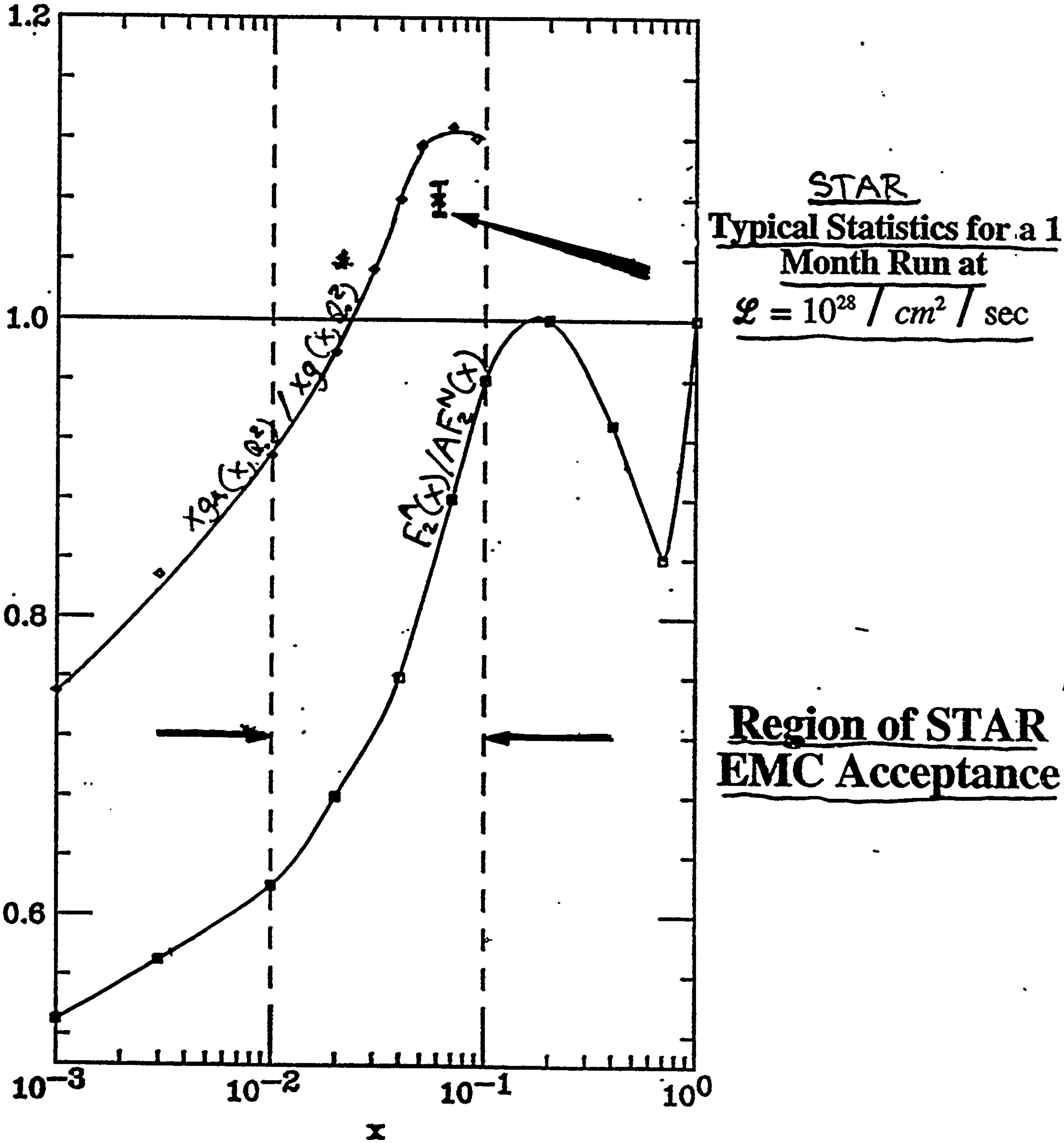

The normalized ratio of the quark and gluon structure functions in Au^{197} to those in the proton.

*Ref. K. Eskola, et. al PRL 72 (1994) 36.

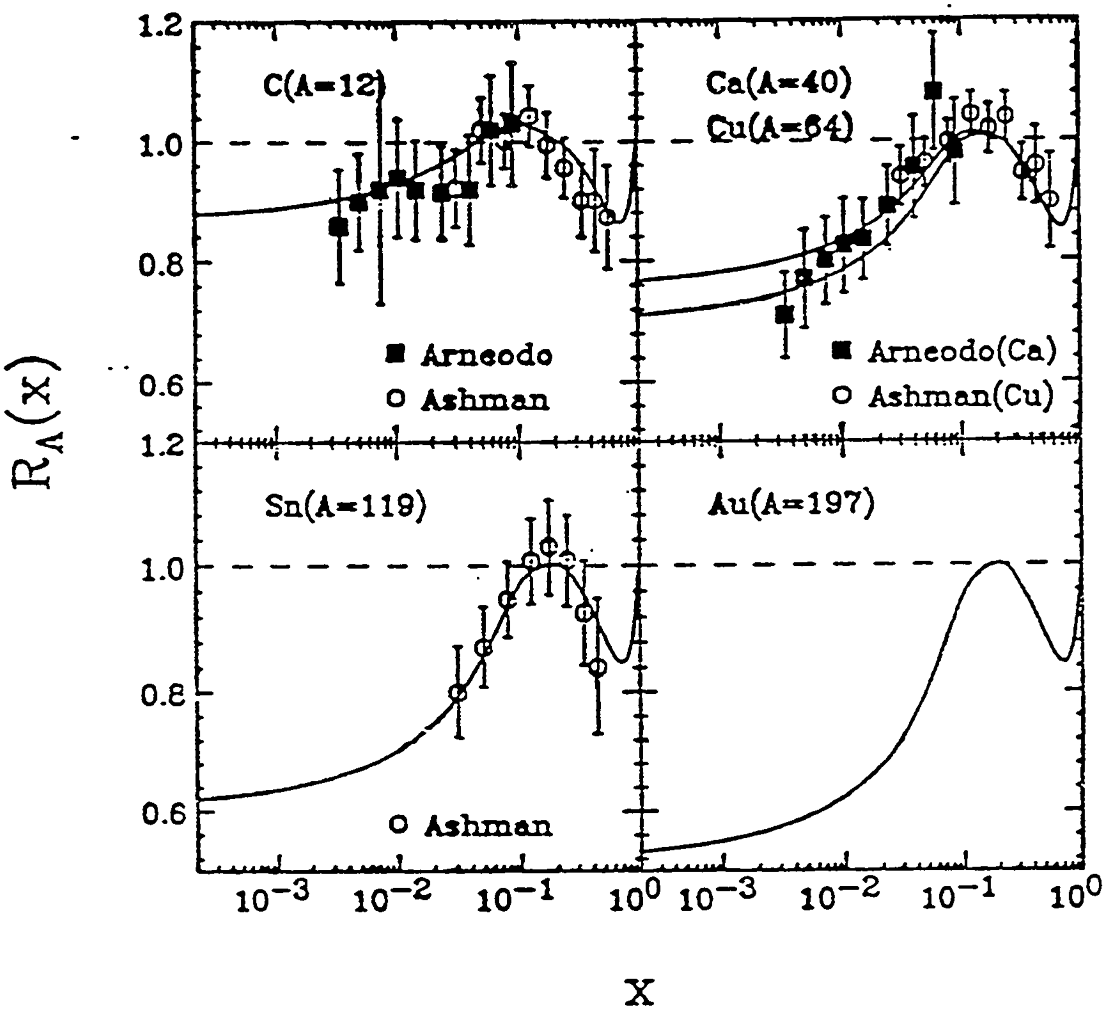

Fig. 14 The ratio of quark structure functions $R_A(x) \equiv F_2^A(x)/AF_2^N(x)$ as a function of x in small and medium x region for different nuclear mass number A. The data are from Ref. [47] and curves are the parametrization in Eqs. 36 and 37.

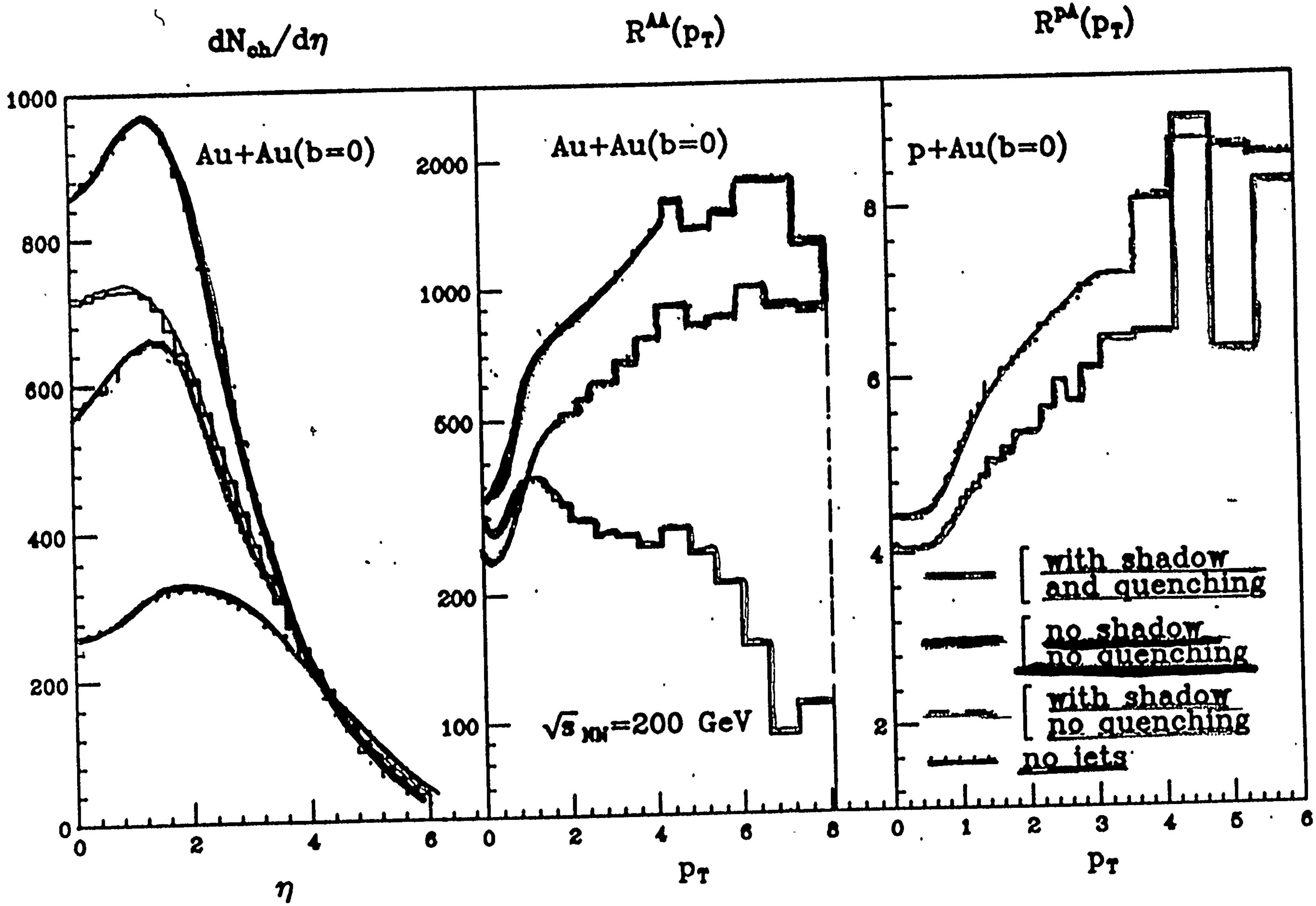

X.N. Wang, M. Gyulassy, Phys. Rev. Lett 68 (1992) 1480

The STAR EMC

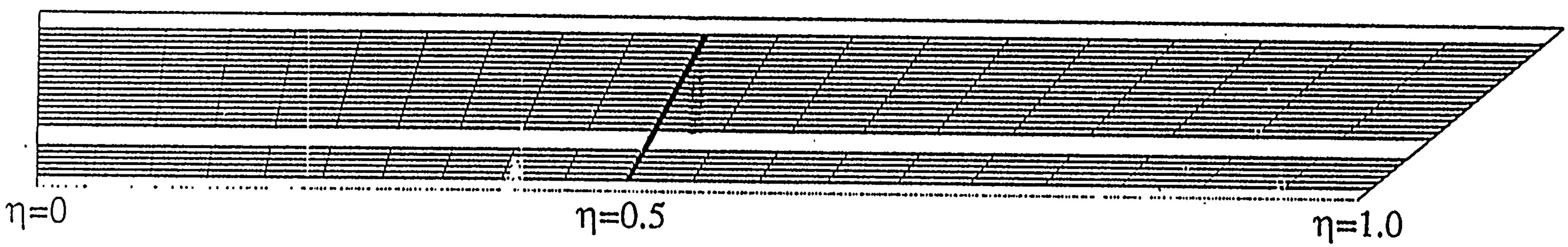

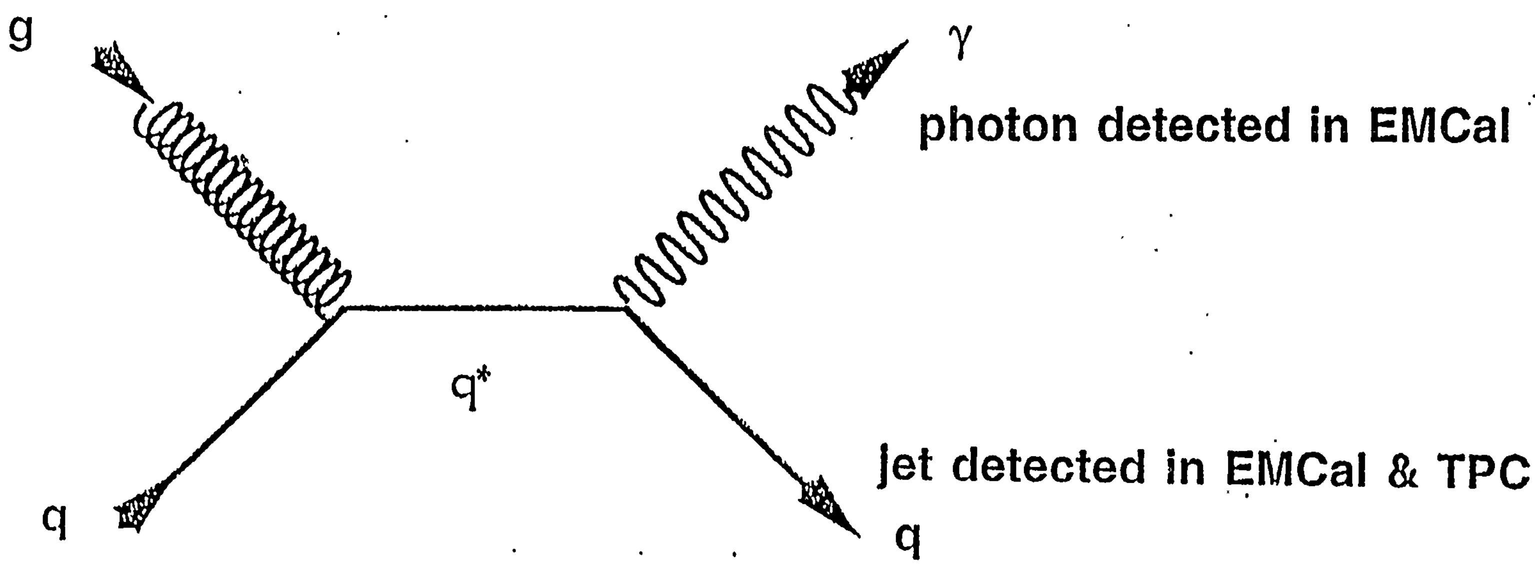

- The gluon distribution in pp interactions
- Modification of the gluon distribution (shadowing) in the nucleus in pA interactions to determine the initial conditions in AA collisions

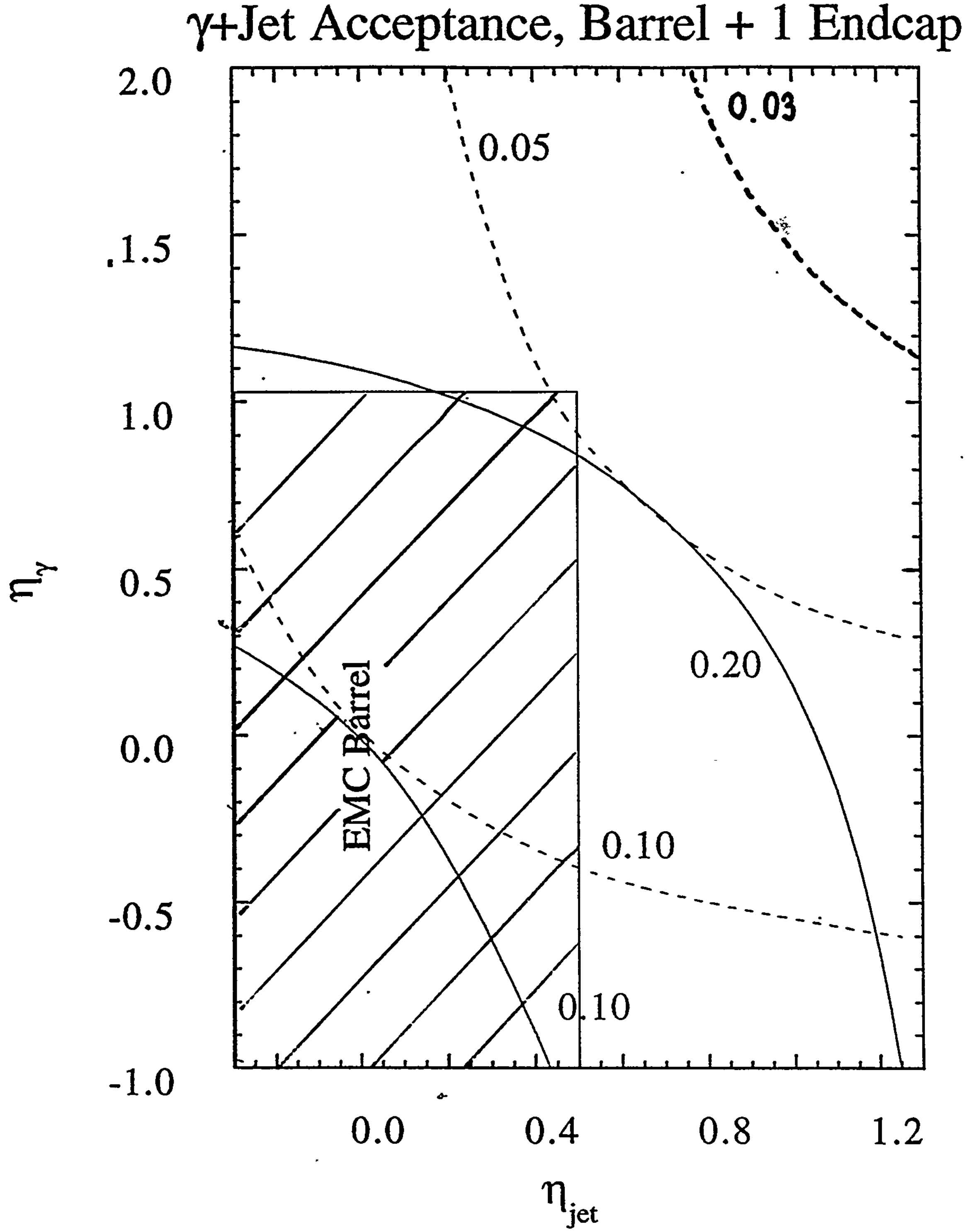

γ+Jet Acceptance, Barrel + 1 Endcap
2.0
1.5
1.0
0.5
0.0
-0.5
-1.0
η_γ
0.0
0.4
0.8
1.2
η_{jet}
0.03
0.05
0.20
0.10
0.10
EMC Barrel

$p + Au \rightarrow \gamma + jet$

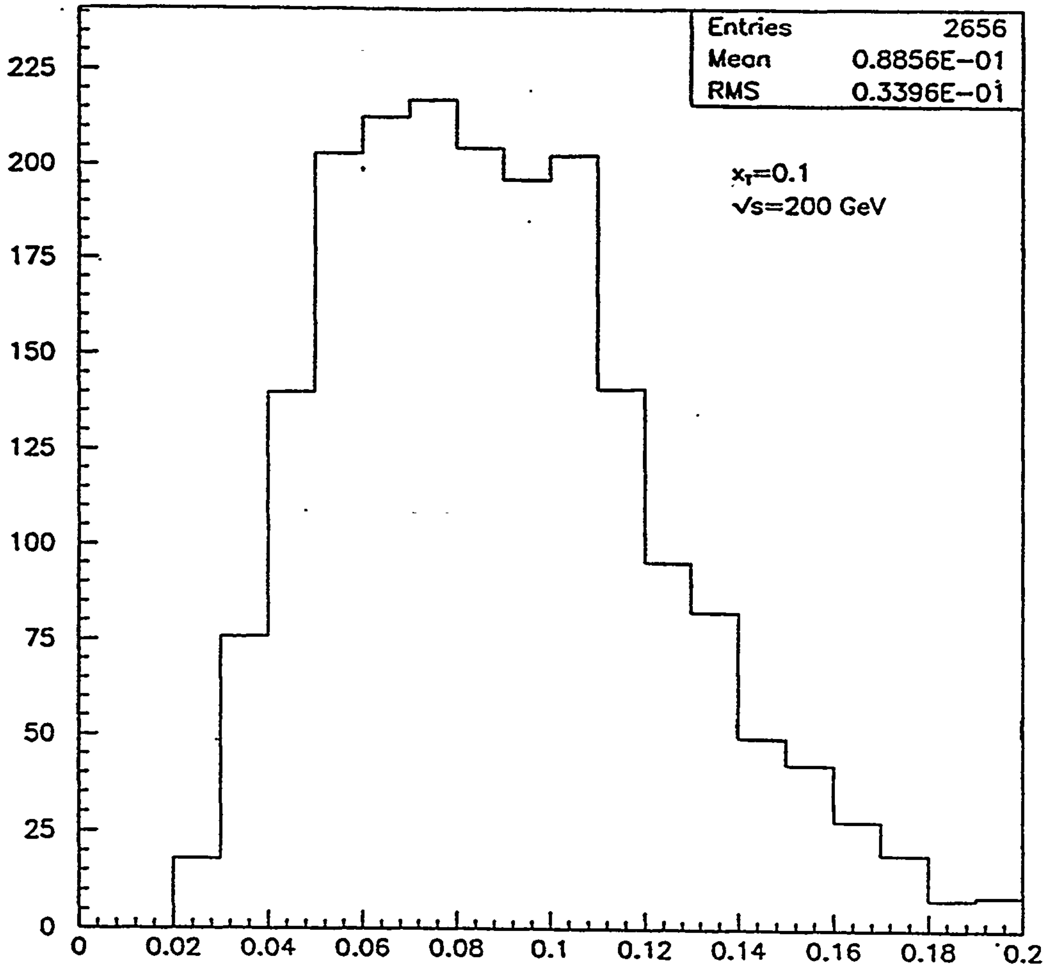

min(x1,x2)

"Useful" Events in 5 RHIC Days

- $-1 \leq \eta_\gamma \leq 2$
- $-0.3 \leq \eta_{jet} \leq 0.9$

  $1.1 \leq \eta_{jet} \leq 1.3$
- $\mathcal{L}^\circ = 10^{28}\ \mathrm{cm}^{-2}\,\mathrm{sec}^{-1}$
- **Jet and γ efficiencies not included.**

STAR barrel, $\sqrt{s}$=200GeV, Pt jet=30GeV

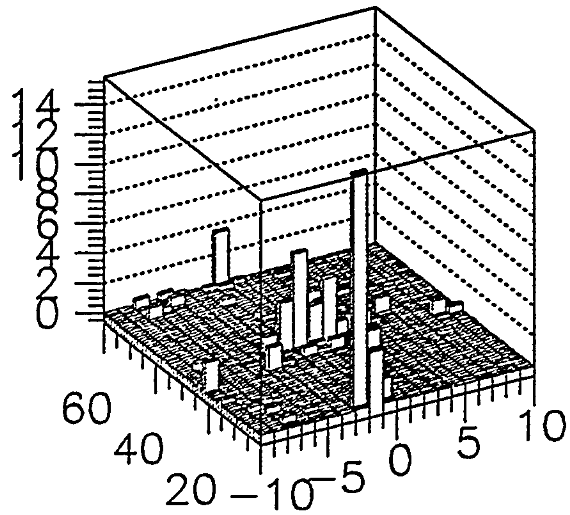

Proton on Proton

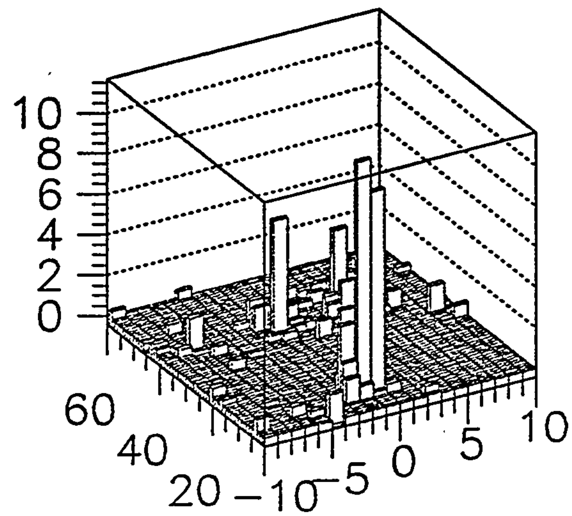

p on Au

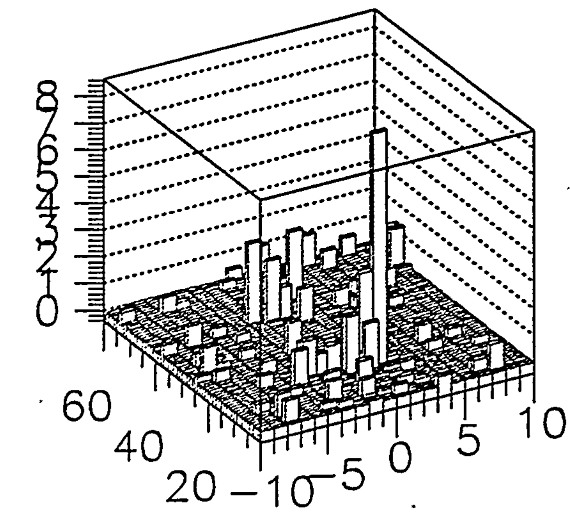

Carbon on Carbon

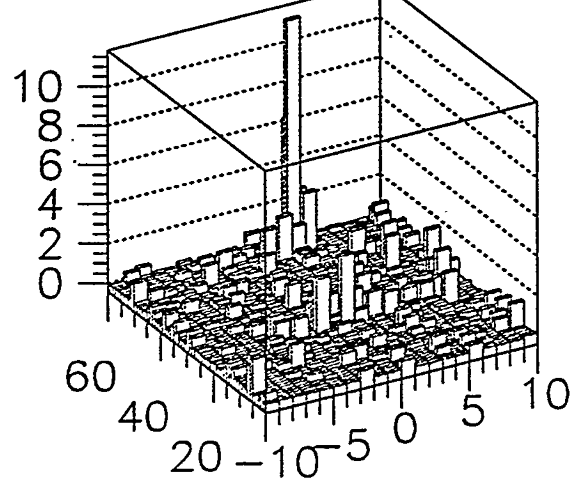

Silicon on Silicon

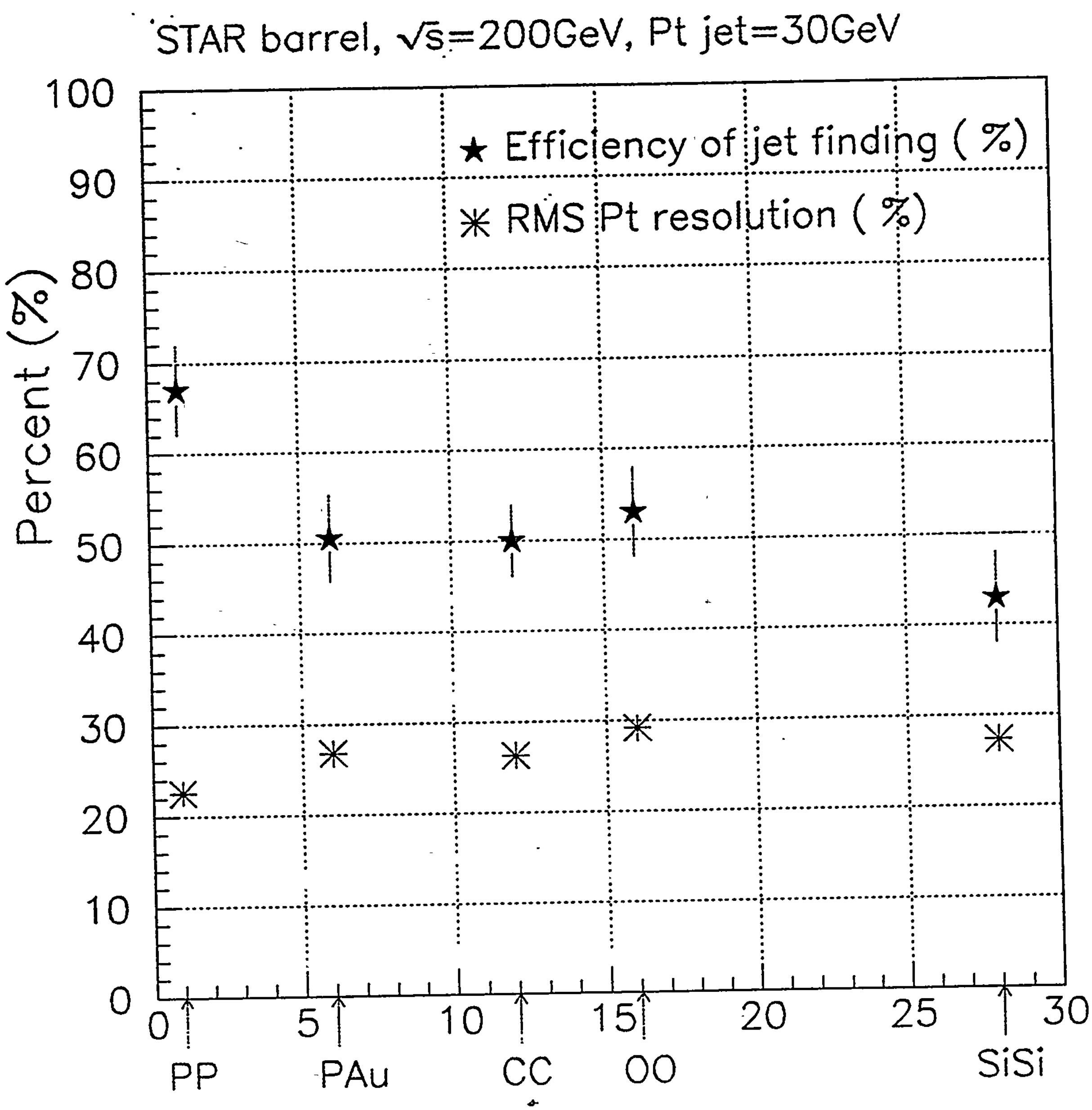

STAR barrel, √s=200GeV, Pt jet=30GeV
Percent (%)
★ Efficiency of jet finding (%)
✳ RMS Pt resolution (%)
0
10
20
30
40
50
60
70
80
90
100
0
5
10
15
20
25
30
PP
PAu
CC
OO
SiSi

CDF Shower Maximum Cuts

(Abe et al, Phys. Rev. D48 (1993) 2998

For direct γ candidate events having $p_t \geq$ 14 GeV/c :

Cut	Prompt γ Efficiency
$E_{cone} \leq 2$ GeV	0.89
$\lvert x \rvert$ and $\lvert z \rvert$ fiducial cuts	0.64
extra strip/wire clusters	0.95
associated track	0.97
E_t balance	0.99
$\lvert z_{vertex} \rvert \leq 50$cm	0.88
shower profile	0.80

Total Prompt γ Efficiency 0.37

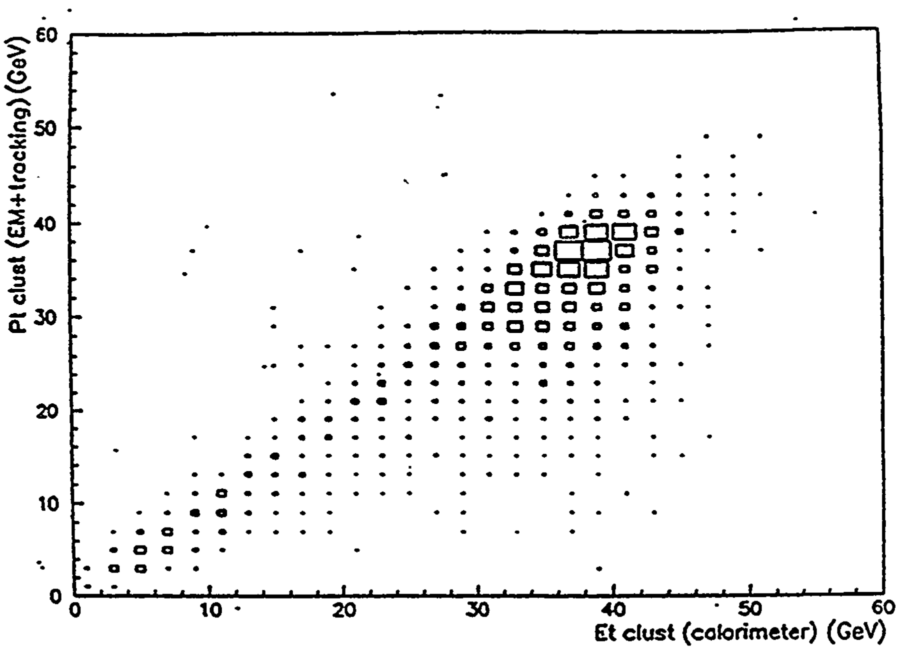

Figure 4A-6. A scatterplot of the energy of clusters found using electromagnetic energy from the STAR EMC plus tracking and momentum information from the TPC versus EM plus hadronic calorimetry. Data shown are for 40 GeV jet events from pp collisions at $\sqrt{s} = 200$ GeV. The asymmetry in the distribution is due primarily to the transverse energy of neutrons and K^0_L mesons which are detected using EM plus hadronic calorimetry but are detected in the EMC alone with low probability.

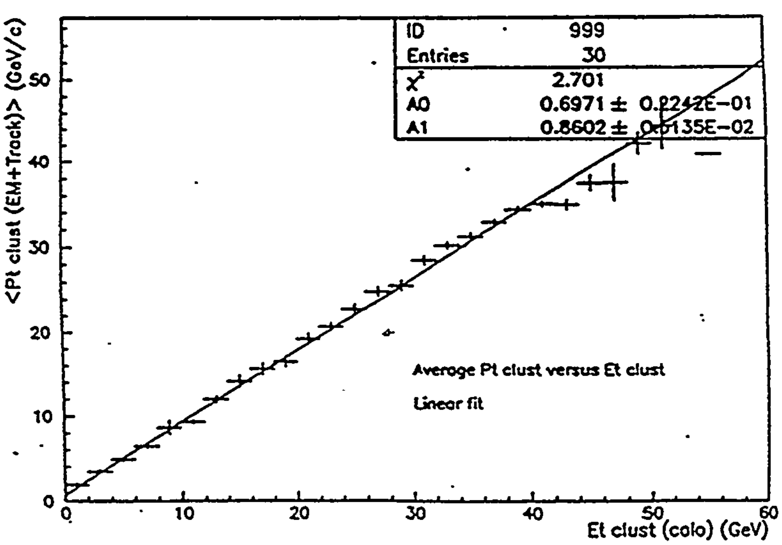

Figure 4A-7. A plot of the average energy of clusters found using EM plus tracking versus the average energy found using EM plus hadronic calorimetry for 40 GeV jet events from pp collisions at $\sqrt{s} = 200$ GeV.

- **Direct measurement of the spin-dependent gluon structure function of the proton, $\Delta G(x)$**

  inclusive jets, inclusive direct photons, jet-direct photon coincidences

- **Direct measurement of the spin-dependent distribution of sea quarks and sea anti-quarks in the proton**

  $W^{\pm}$ Production

- **Direct measurement of the transversity distribution of valence and sea quarks in the proton**

  Z° Production, JETS (JET-JET)

- **Search for small parity-violating asymmetries as possible indications of quark compositeness or new physics beyond the Standard Model**

"SPIN EMC EFFECT"

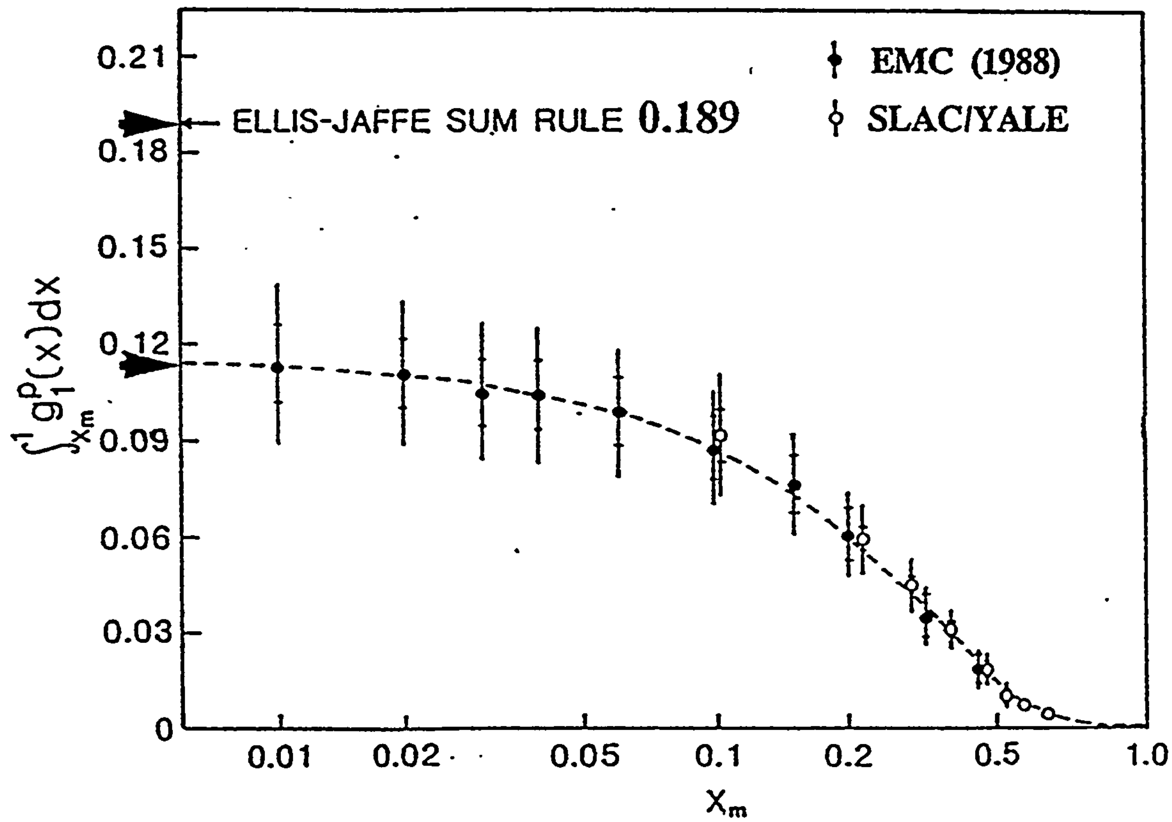

- ELLIS JAFFE SUM RULE VIOLATED:

$$\Gamma_1^p = \int_0^1 g_1^p(x)dx = 0.189$$

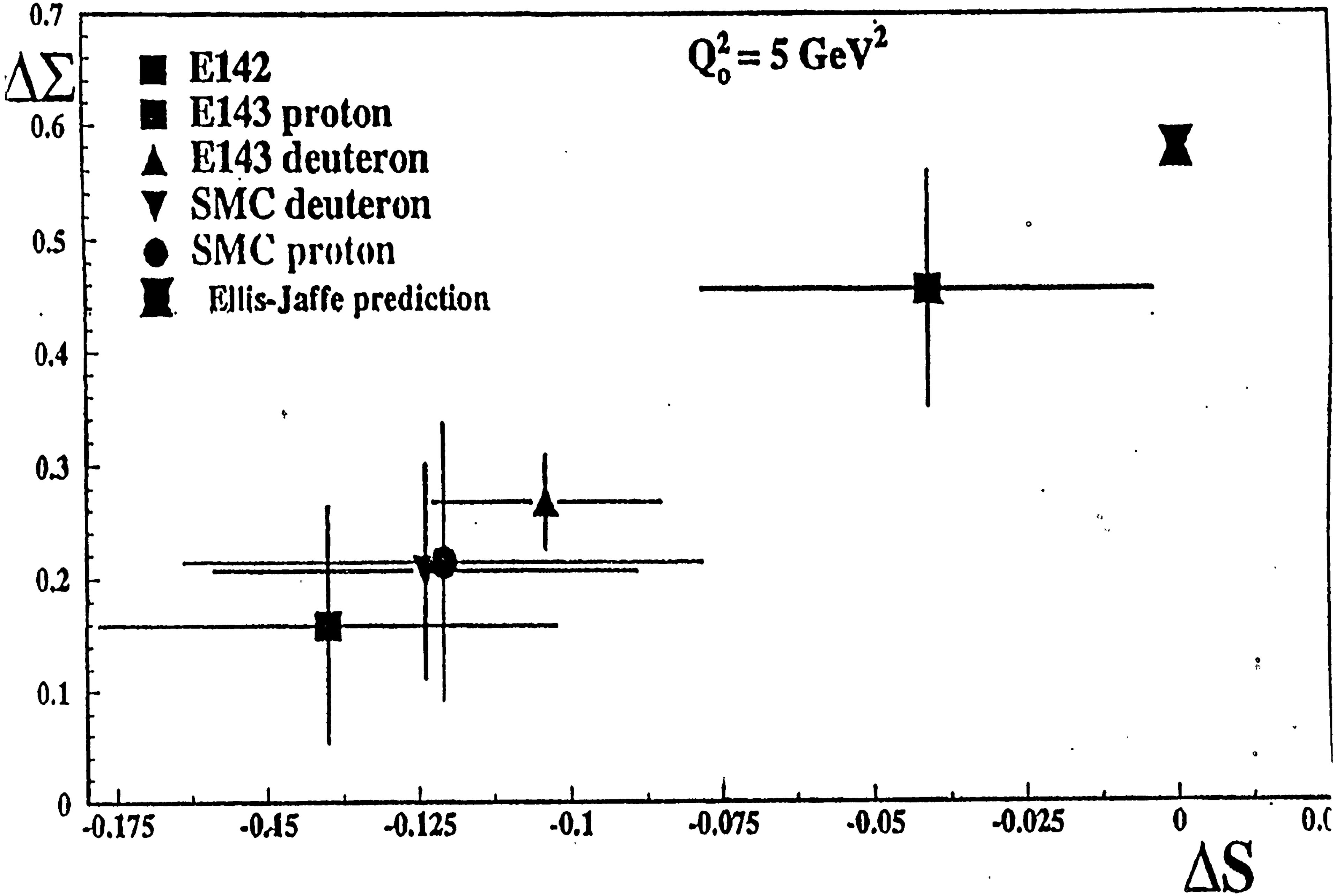
$\Delta\Sigma$
$Q_o^2 = 5\ GeV^2$
E142
E143 proton
E143 deuteron
SMC deuteron
SMC proton
Ellis-Jaffe prediction
0.7
0.6
0.5
0.4
0.3
0.2
0.1
0
-0.175
-0.15
-0.125
-0.1
-0.075
-0.05
-0.025
0
ΔS

$$\int_0^1 dx\{g_1^p(x) - g_1^n(x)\} = \frac{1}{6} g_A \bullet QCD_{corr}$$

CONCLUSIONS FROM CURRENT DATA

- BJ sum rule confirmed to about 10%.

- $\Delta\Sigma = 0.27 \pm 0.05$

$$\Delta s = -0.10 \pm 0.03$$

$$\Delta u_v > 0$$

$$\Delta d_v < 0$$

- Theoretical understanding of nucleon spin structure has progressed, but is still limited.

Current Data on Spin Structure Functions

- **In Scaling Approximation**

$$F_1(x) = \frac{1}{2} \sum_{u,d,s} e_q^2 \left(q^{\uparrow}(x) + q^{\downarrow}(x)\right)$$

$$g_1(x) = \frac{1}{2} \sum_{u,d,s} e_q^2 \left(q^{\uparrow}(x) - q^{\downarrow}(x)\right)$$

$$\Delta\Sigma = \sum_{u,d,s} \int_0^1 dx \Delta q(x) [\equiv \Delta u + \Delta d + \Delta s]$$

$$\frac{1}{2} = \frac{1}{2} \Delta\Sigma + \Delta G + \langle L_z \rangle$$

- **First moment must strictly obey Bjorken Sum Rule:**

The Asymmetry Predicted for Inclusive Direct Photon Production

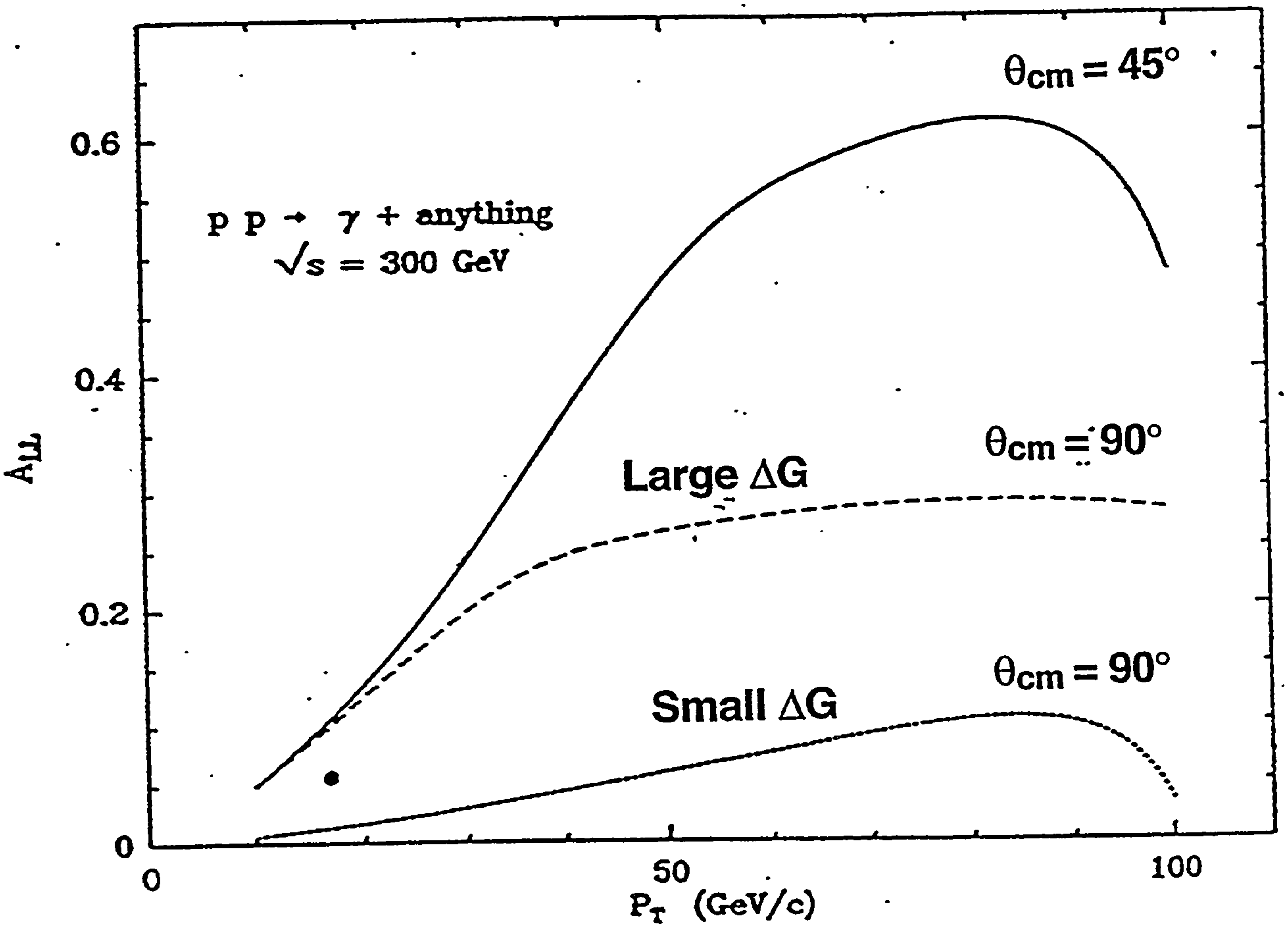

$$A_{LL} d\sigma \approx \int dx_a dx_b g_1(x_a) \Delta G(x_b) a_{LL}^{qg} \sigma^{qg}$$

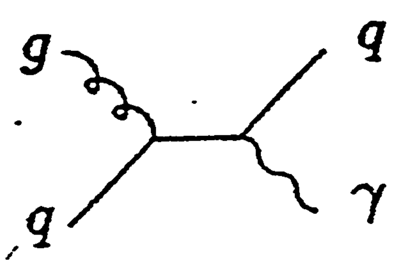

$$\delta\left(\frac{\Delta G}{G}\right) \approx 5 \times \delta A_{LL} \approx 0.03$$

Bourrely, Guillet and Soffer, Nuc. Phys. B361 (1991) 72

Bourrely, Guillet and Soffer, Nuc. Phys. B361 (1991) 72

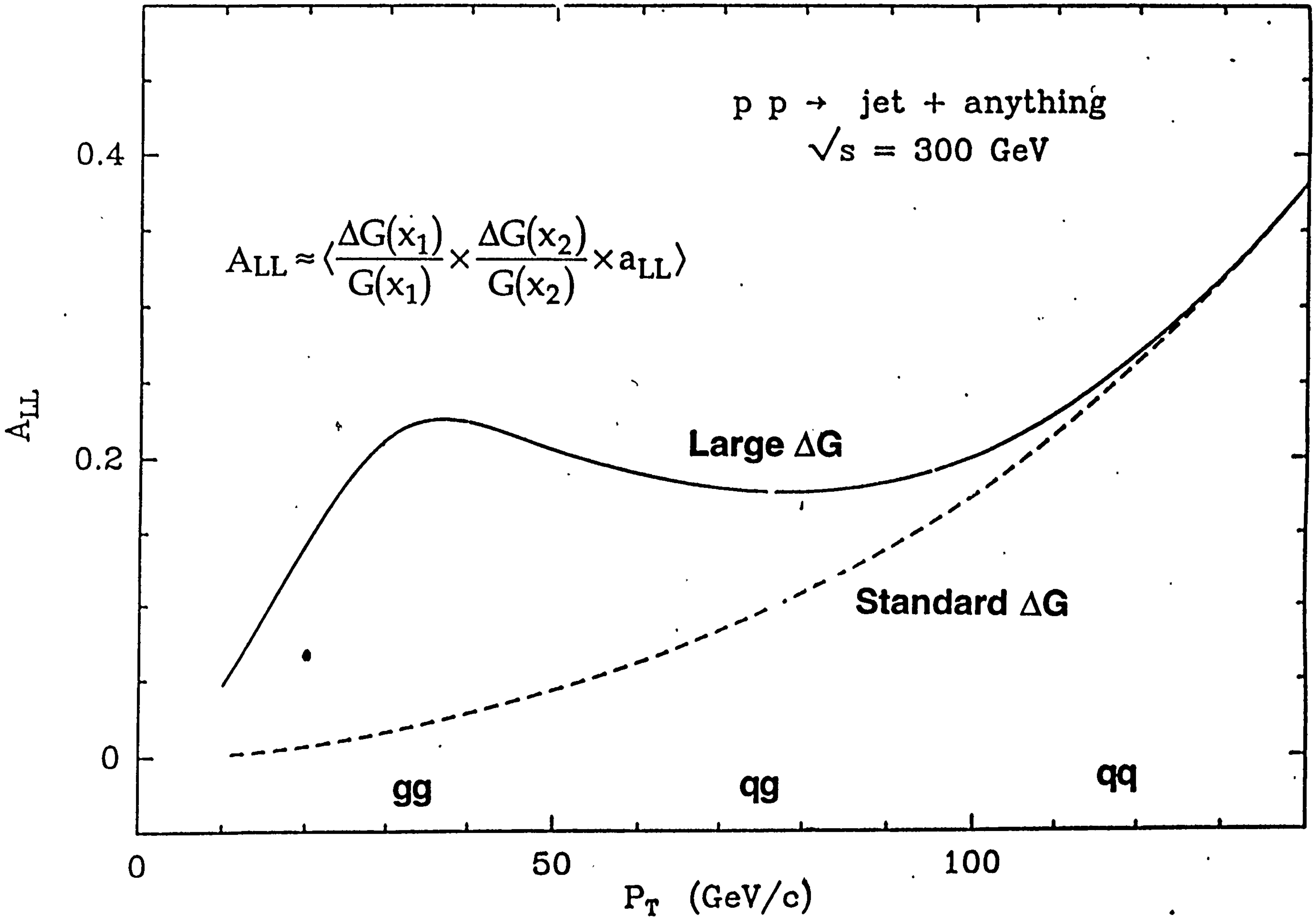

STAR Spin Physics in Perspective

- **EMC/SMC/SLAC data — revived interest in spin physics: tests fundamental sum rules and models of nucleon structure.**
  - Expts underway at CERN, SLAC, HERA on spin structure functions.
  - New acceleration projects at BNL, FNAL, HERA.

- **More spin data on proton's constituents are necessary to complete the picture of nucleon structure.**
  - Both *longitudinal* (Δq,ΔG)and *transverse* (h_1)spin distributions
  - Separately for *valence* (Δu,Δd) and *sea* ($\Delta\bar{u}$,$\Delta\bar{d}$) *quarks* and for *gluons* (ΔG).
  - Using the measured spin distributions, asymmetries in $\vec{p}\,\vec{p} \rightarrow$ (jets, $W^{\pm}$, Z^{0}, ...) are calculable and test standard model in new domain.

- **Ideal place to make these measurements: STAR at RHIC with the $\vec{p}\,\vec{p}$ option.**

Working Assumptions

40 Weeks of Heavy Ion Running

(Including Maintenance)

10 Weeks for pp Spin Running

At $\sqrt{s}$ = 500 GeV,

$$L = 2\times10^{32}\, cm^{-2}\, \sec^{-1}$$

For $4 \times 10^{6} sec$

(~ 100 days, 50% efficiency)

$$\int L dt = 800\, pb^{-1}$$

At $\sqrt{s}$ = 200 GeV,

$$L = 8\times10^{31} cm^{-2} \sec^{-1}$$

For $4 \times 10^{6} sec$

$$\int L dt = 320\, pb^{-1}$$

For These Working Assumptions:

For These Working Assumptions:

Type	Barrel	Barrel & 1 Endcap
W^+	69k	72k
W^-	15k	21k
Z^o	3k	4.2k
γ^*	224k	~ 300k
$\gamma - \mathrm{Jet}$ *		100k
Jet^{**}	~10^9	
$Jet-Jet$	~10^7	

Can these signals be triggered upon and measured with an acceptable signal to noise ?

Is a significant measurement possible in the available running time?

* $p_t \geq 10$ GeV/c

* $|\eta_\gamma| \leq 2$, $|\eta_{Jet}| \leq 0.3$, $10 \leq p_t \leq 20$ GeV/c, $x_q \geq 0.2$

** $|\eta_{Jet}| \leq 0.3$, $p_t \geq 10$ GeV/c

$W^{\pm}$ Background Study

Backgrounds Considered	W^{+}, W^{-}
Z° with missing electron (positron)	2%, 10%
π° Dalitz electrons	~0
Mis-identified high p_t charged hadrons	5%, 20%
Overlap of γ from π° with charged hadron	

Cuts to minimize background

Energy-Momentum matching

Isolation Criterion

Shower Width

P_t^e Cut

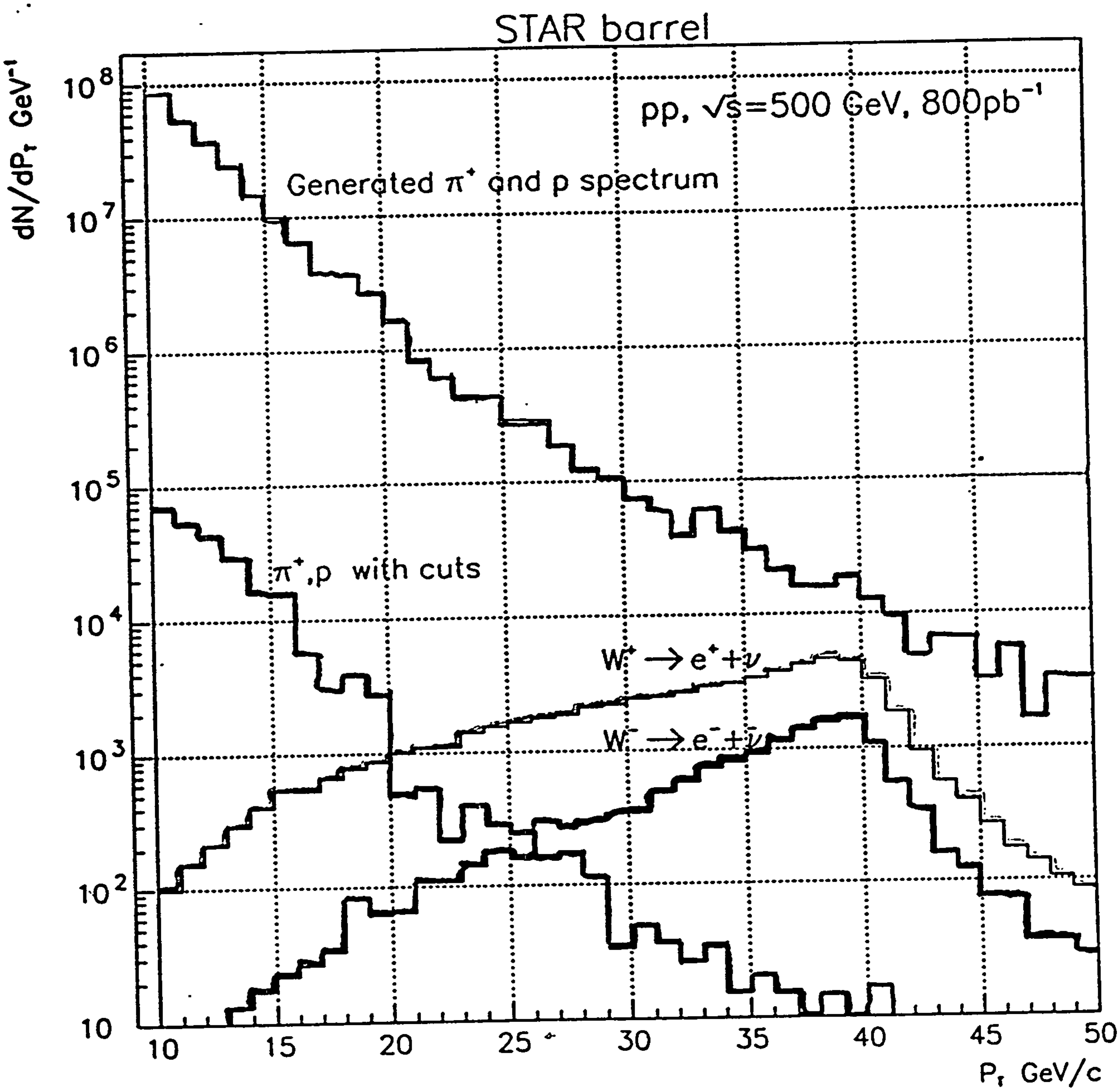

With P_t^e cut ≥ 25 GeV/c

Efficiency for W^+ ~ 80%, Background ~ 5%

Efficiency for W^- ~ 85%, Background ~ 20%

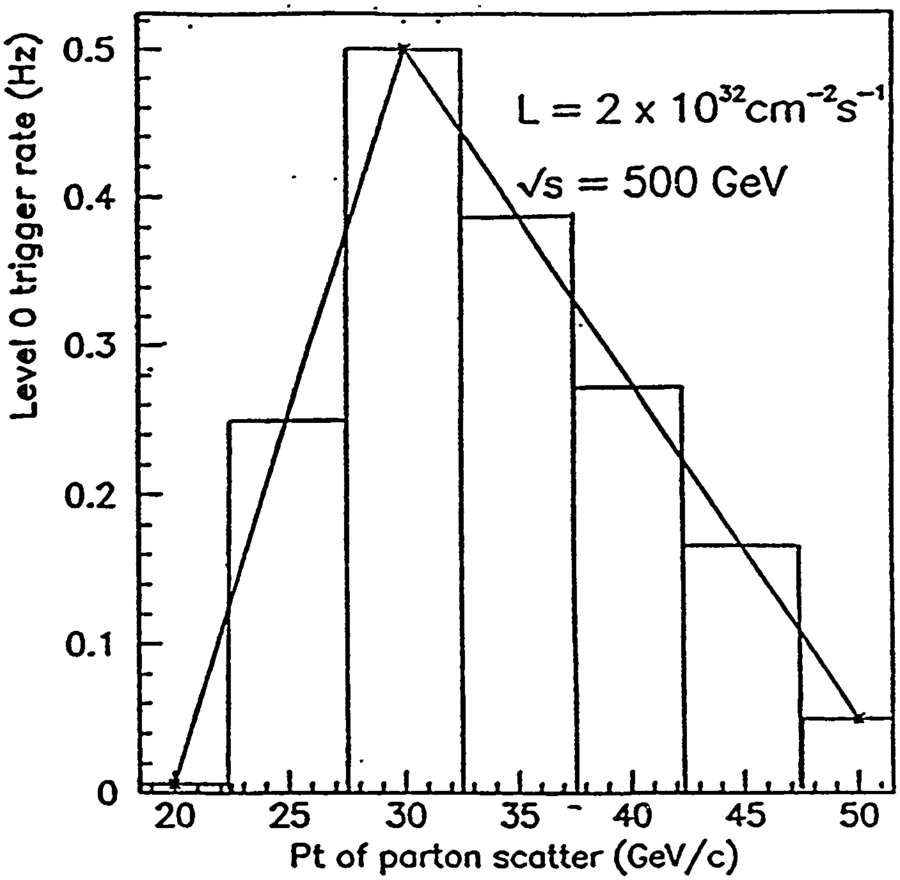

Jet Pt	dσ/dηdpt	No. per sec (Barrel, 1 EC)	Level 0 per sec (20 GeV Tower)
(GeV)	(μb/ GeV)	(Hz)	(Hz)
20	0.8	480	0.006
30	0.08	48	0.5
50	0.003	1.5	0.05

Total Level 0 Trigger rate (20 GeV High Tower)	3.5 Hz
Trigger rate for W+/- and Z	.03 Hz

Effective Yields

Type	Yield (STAR)	ε	Background	Effective Yield
W^+	72k	0.8	5%	58k
W^+	21k	0.85	20%	18k
Z^0	4.2k	1.0	~ 0%	4.2k
γ^*	300k	0.5	$\leq 50\%$	150k
$\gamma + \text{Jet}^*$	100k	0.35	~ 0%	35k
Jet^{**}	10^9	0.01 **	~ 0%	10^7
$\text{Jet} + \text{Jet}^{**}$	10^7	1.0 **	~ 0%	10^7

* $p_t \geq 10$ GeV/c

* $|\eta_\gamma| \leq 2$, $|\eta_{Jet}| \leq 0.3$, $10 \leq p_t \leq 20$ GeV/c, $x_q \geq 0.2$

** $|\eta_{Jet}| \leq 0.7$, $p_t \geq 10$ GeV/c

** DAQ/Trigger limited

$W^{\pm}$ and Z° Production at 500 GeV

1) Parity-Violating Asymmetry

The observable A_L (PV) is defined as, $A_L = (N^- - N^+)/(N^- + N^+)$, where -(+) are minus (plus) helicity. For W^+,

$$A_L = \frac{\Delta u(x_1)\bar{d}(x_2) - (u \leftrightarrow \bar{d})}{u(x_1)\bar{d}(x_2) + \bar{d}(x_1)u(x_2)}.$$

When the helicities of both beams are the same, we define another observable as:

$$A_{LL}^{PV}(y) = \frac{\left[\Delta u(x_1)\bar{d}(x_2) - \Delta\bar{d}(x_2)u(x_1)\right] - (u \leftrightarrow \bar{d})}{\left[u(x_1)\bar{d}(x_2) - \Delta u(x_1)\Delta\bar{d}(x_2)\right] + (u \leftrightarrow \bar{d})}.$$

For $y = 0$, $A_L^{W^+} = 1/2\left(\Delta u/u - \Delta\bar{d}/\bar{d}\right)$, $A_L^{W^-} = 1/2\left(\Delta d/d - \Delta\bar{u}/\bar{u}\right)$

$$A_{LL}^{PV}(y) = A_L(y) + A_L(-y)$$

2) Parity-Conserving Asymmetry

For W^+,

$$A_{LL} \sim \frac{\Delta u(x_1)\Delta\bar{d}(x_2)}{u(x_1)\bar{d}(x_2)}$$

A similar expression for W^- production by permuting u and d.

Tests of SU(2) Flavor-Breaking of the Quark Sea in Unpolarized pp Interactions

$$\bar{d}(x) > \bar{u}(x) \quad ?$$

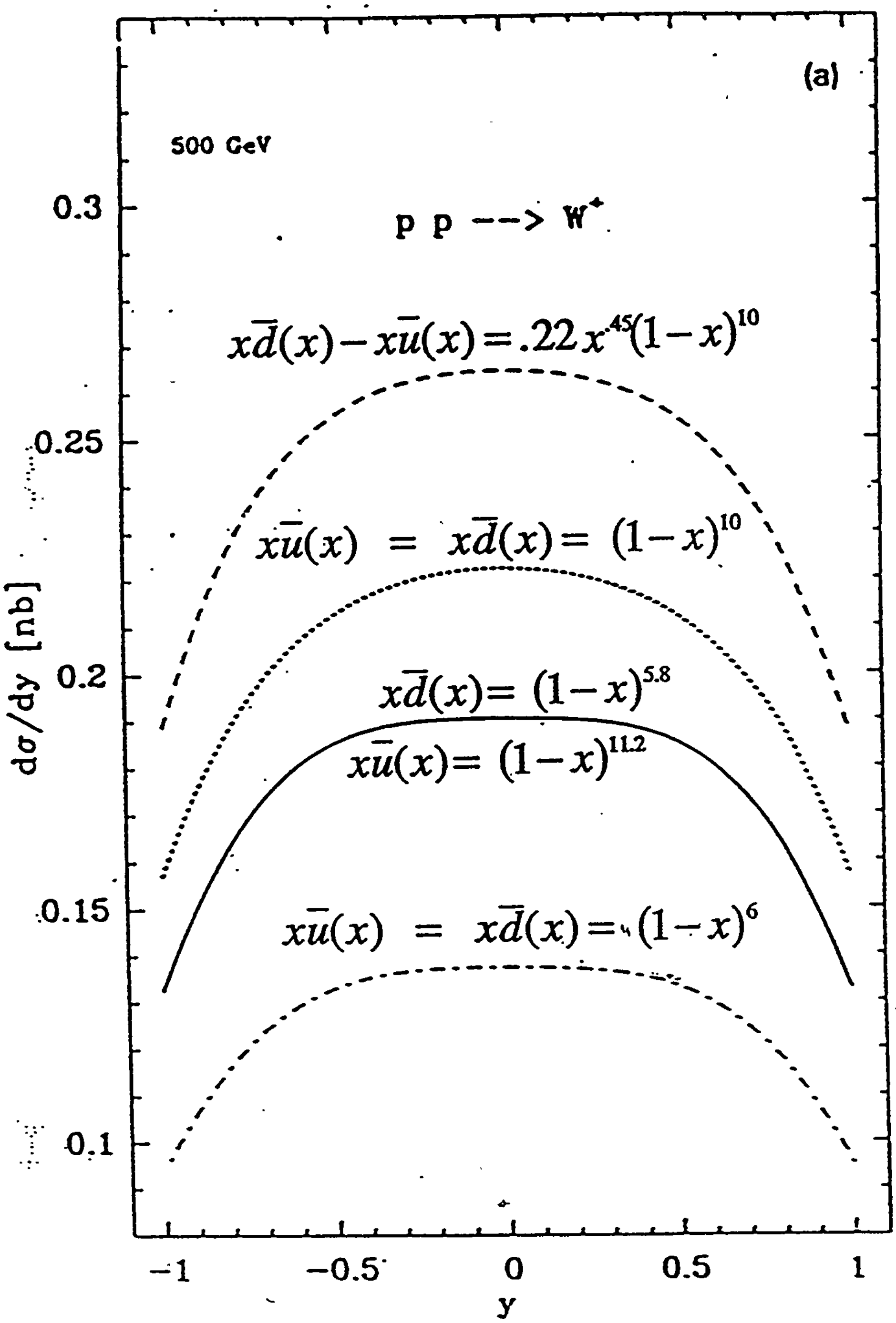

$$\frac{d\sigma^{W^+}}{dy} = G_F \pi \sqrt{2\tau} \times \frac{1}{3}\left[u\left(x_a, M_W^2\right)\overline{d}\left(x_b, M_W^2\right) + (u \leftrightarrow \bar{d})\right]$$

$$G_F = \frac{\pi\alpha}{\sqrt{2} M_W^2 (\sin^2\theta_W)} \qquad x_a = \sqrt{\tau}\, e^{y},\ \ x_b = \sqrt{\tau}\, e^{-y},\ \ \tau = M_W^2$$

Tests of Sea Quark Polarization in Polarized pp Interactions

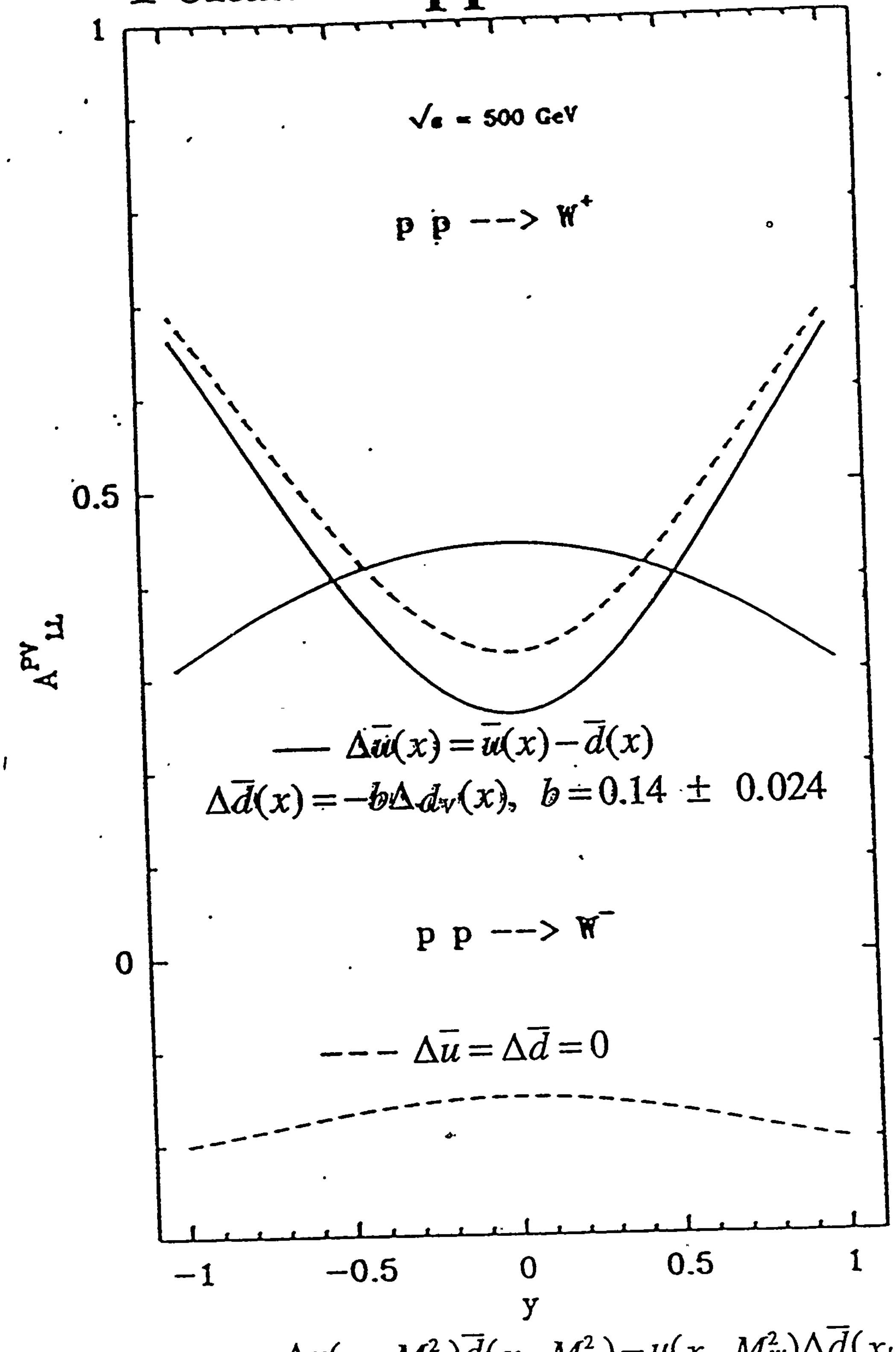

$$A^{PV}_{LL}(y) = \frac{\sigma_{--} - \sigma_{++}}{\sigma_{--} + \sigma_{++}} = \frac{\Delta u(x_a, M_W^2)\bar{d}(x_b, M_W^2) - u(x_a, M_W^2)\Delta\bar{d}(x_b, M_W^2) - (u \leftrightarrow \bar{d}}{u(x_a, M_W^2)\bar{d}(x_b, M_W^2) - \Delta u(x_a, M_W^2)\Delta\bar{d}(x_b, M_W^2) - (u \leftrightarrow \bar{d}}$$

Transversity Structure Function h_1

- h_1 decouples from DIS, even with QCD corrections

- In STAR, h_1 can be measured from $q\bar{q}$ annihilation in $pp \rightarrow Z^\circ \rightarrow e^+e^-$

$$A_{TT} = \frac{a_{TT} \; \sum_a e_a^2 h_1^a(x_1) h_1^{\bar{a}}(x_2)}{\sum_a e_a^2 f_1^a(x_1) f_1^{\bar{a}}(x_2)}$$

- h_1 can also be measured in $pp \rightarrow$ jet + jet

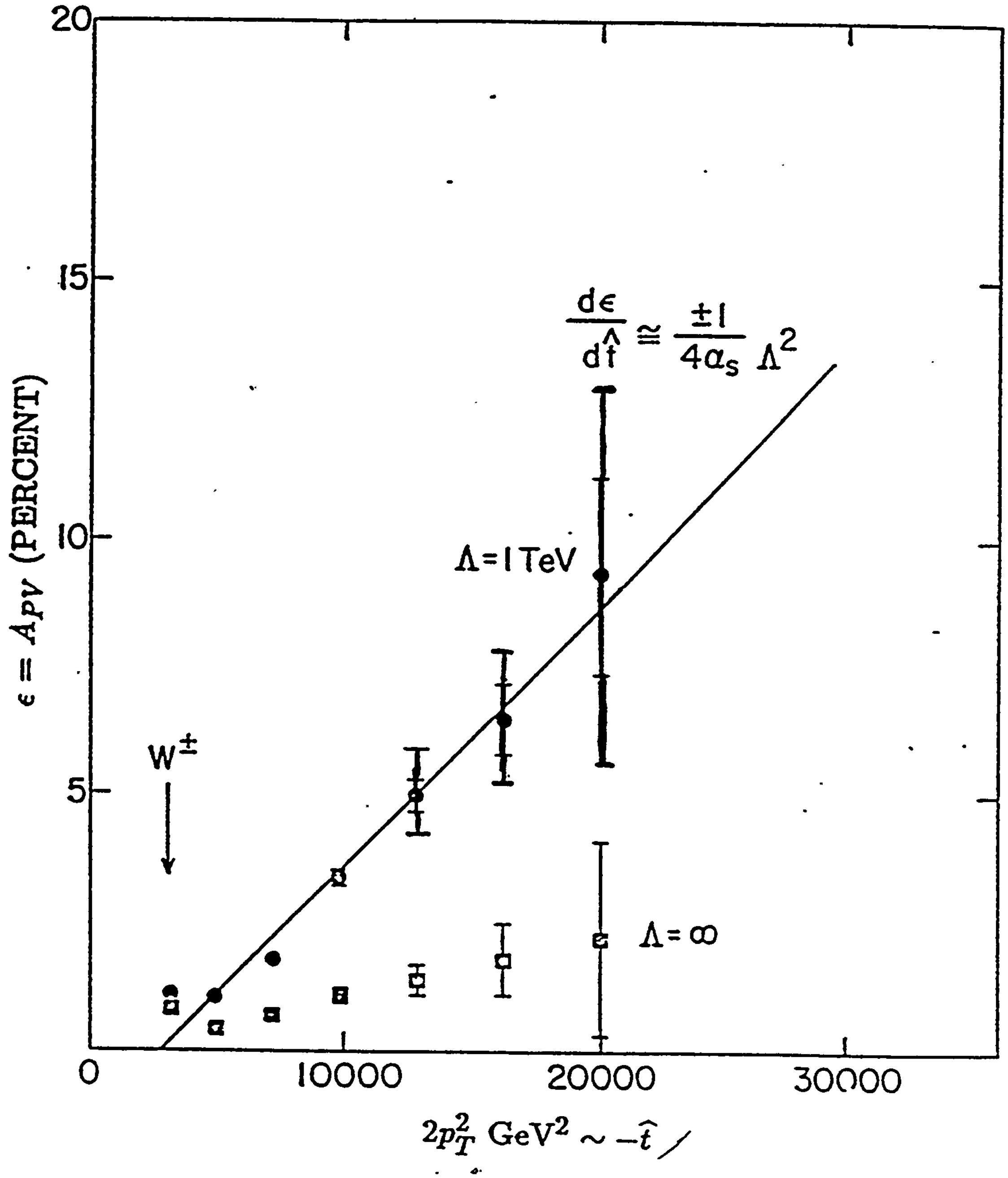

Figure 4.3: Predicted single jet PVA (A_{PV}) for quark substructure model[6] with parameters $\Lambda = 1$ TeV and $A = -1$. The A_{PV} is plotted in percent as a function of the quantity $2p_T^2$ which is a good estimator of $-\hat{t}$, the invariant-four-momentum-transfer-squared of the constituent scattering. The value of Λ can be derived from the observed linear slope, as illustrated. The error bars are calculated assuming an integrated luminosity of 2×10^{39} cm^{-2}, corresponding to 10 months running, and a "nominal" collider detector covering $\Delta\phi = 2\pi$, $\Delta y = \pm 2.5$. This figure indicates that the sensitivity of PVA measurements at RHIC can be much larger than the c.m. energy of the $p - p$ collisions, with sufficient integrated luminosity.

Complimentary Studies Possible in Principal at HERA with Nuclear and Longitudinally Polarized Proton Targets

- **Study of jet quenching in nuclei**
- **Extension of gluon shadowing measurements to low x_{BJ}**
- **Study of gluon shadowing in the proton**
- **Study of gluon contribution to the proton spin (photon-gluon fusion)**

H1 DESY Rpt ISSN 0418-9833
MAY '95

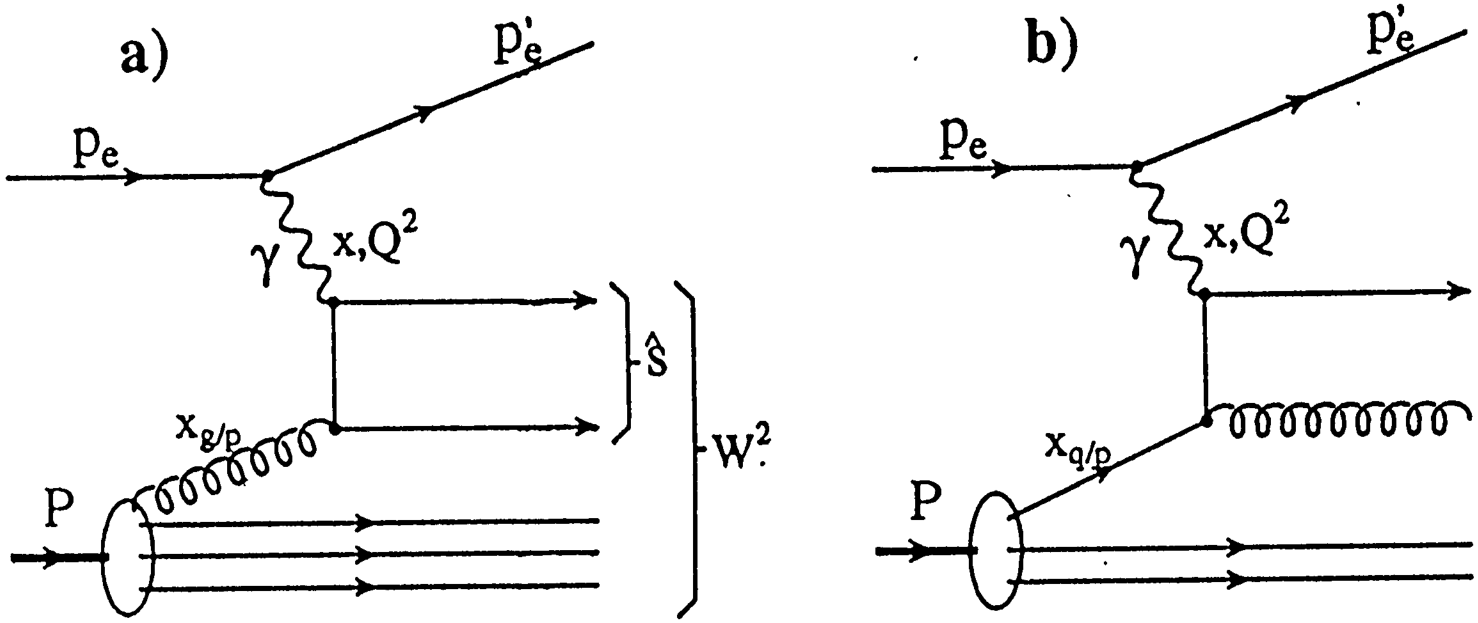

gure 1: *Generic Feynman diagrams for a) the boson-gluon fusion process and,* *CD-Compton process*

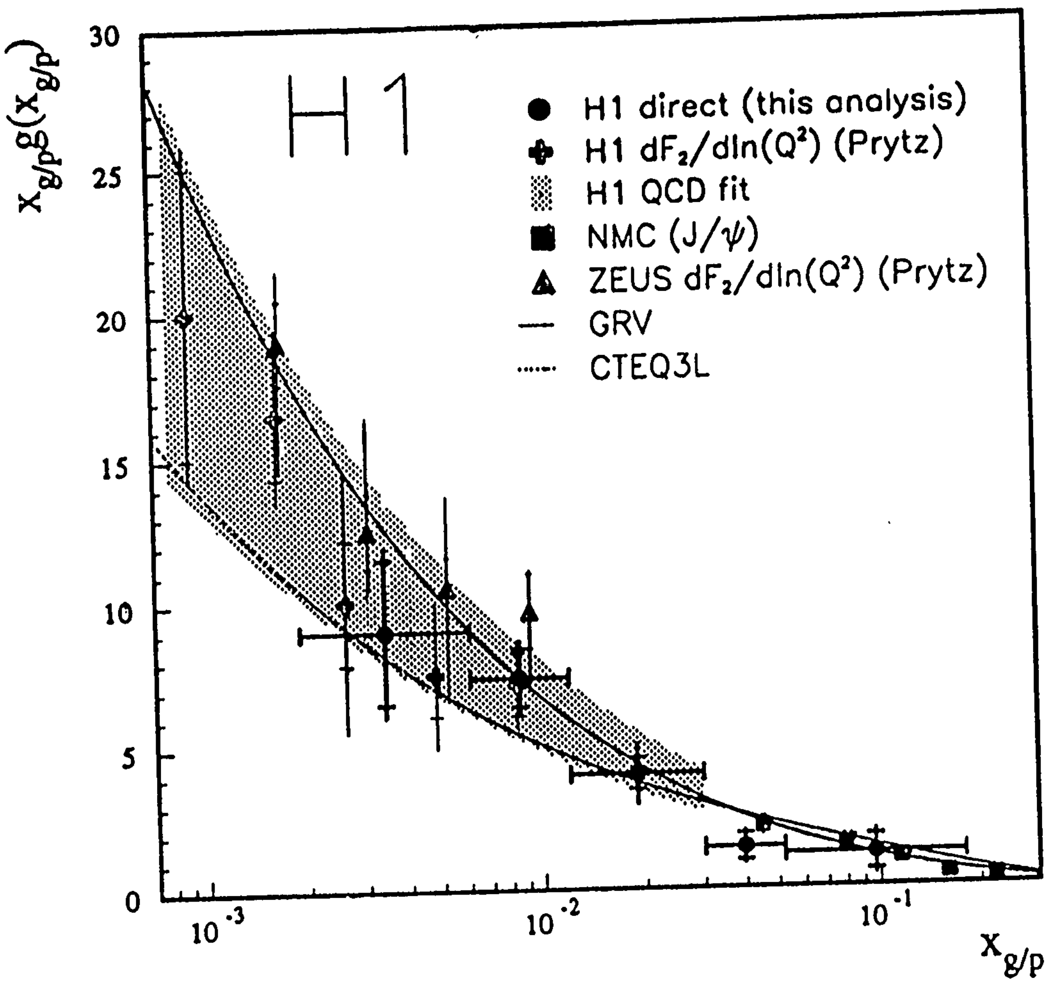

Figure 5: *The measured gluon density at an average Q^2 of 30 GeV^2 as a function of the fractional gluon momentum compared with indirect determinations by H1 [23] and ZEUS [24] at $Q^2 = 20$ GeV^2 as well as with a determination from J/Ψ production by NMC [27] evolved to $Q^2 = 30$ GeV^2 (see text).*

H1, DESY Rpt ISSN 0418-9833

Conclusions

- The STAR Collaboration looks forward to an exciting period of discovery in the nucleus-nucleus and polarized proton programs at RHIC.
- The use of hard-parton scattering as a penetrating probe in AA interactions is an integral part of the STAR physics program
- The use of hard parton scattering to determine the initial conditions in AA interactions, and probe the spin-dependent parton distributions of the proton is a key element of the STAR physics program
- The use of nuclear targets in HERA can in principal provide some complimentary studies of jet quenching, gluon shadowing in the proton, and spin-dependent parton distributions of the proton
- The level of interest in future nuclear and spin studies at HERA is to some extent dependent on the projected time scale for upgrading the accelerator.

Jet Quenching in eA, pA, AA

Miklos Gyulassy
Columbia University

11/18/95

Jet Quenching in eA, pA, AA

M. Gyulassy (Columbia)

1. We need $xg_A(x\,Q^2)$ $x \sim 10^{-2}$ $Q^2 \sim 1-10\ \mathrm{GeV}^2$
   from HERA to fix initial conditions
   in A + A at RHIC

2. Thermalization time scales in AA
   depend on $dE_g/dx \sim L\left(\frac{\mu^2}{\lambda}\right)_T$
   Need eA → jets at HERA to fix $\left(\frac{\mu^2}{\lambda}\right)_{T=0}$

   a) Estimate of $\left(\frac{\mu^2}{\lambda}\right)_{T=0} \approx \Lambda^3_{QCD}$ from $pA \to J/\psi + X$

   b) why $eA \to \pi (x_F > 0)$ is insensitive to $\frac{dE}{dx}$
      need $\nu \lesssim 50\,\mathrm{GeV}$

   c) $eA \to h\,(x_F < 0)$ most sensitive to $\frac{dE_q}{dx}$

3. Jets in AA : huge effects from $\left(\frac{dE_g}{dx}\right)_{T>T_c}$

4. Why pA → jets at fixed target energies
   is so insensitive to $(\mu^2/\lambda)_{T=0}$?

For $\sqrt{s} \gtrsim 100$ AGeV Mini-Jet production determines initial conditions

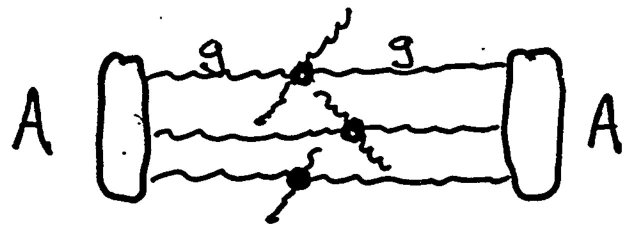

Capella, Kajantie, Mueller, ...

$$\frac{dn^g}{dy_1 dy_2 d^2p_\perp} = \underbrace{x_+ g(x_+, p_\perp^2)\, x_- g(x_-, p_\perp^2)}_{\text{structure}} \underbrace{\frac{d\sigma^{gg}}{d\hat{t}}}_{\text{pQCD}} \underbrace{R_A(x_+) R_A(x_-)}_{\text{shadow}} \underbrace{T_{AA}(\cdots}_{\text{geo}\cdots}$$

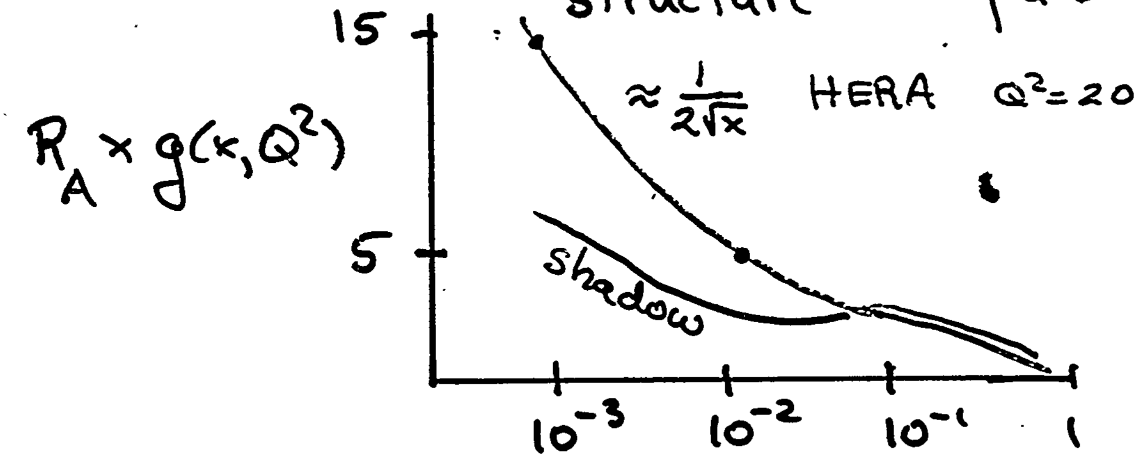

$$x_\pm = \frac{p_\perp}{\sqrt{s}}(e^{\pm y_1} + e^{\pm y_2}) \sim \begin{matrix} 0.01 \text{ RHIC} \\ 0.001 \text{ LHC} \end{matrix}$$

Geometry:

$$T_{AB}(b) = \int d^2b_1\, dz_1\, dz_2\, \rho_A(z_1, \vec{b}_1)\, \rho_A(z_2, \vec{b} - \vec{b}_1) \sim \frac{A^{4/3}}{40\,\text{mb}}$$

$$N^{AuAu}_{glue}(b=0) \approx \frac{30}{\text{mb}} \times 2\sigma_{jet}(p_0) \times \underbrace{2.5}_{\substack{\text{radiation} \\ gg \to gggg}} \approx 1500$$

$p_0 \sim 2$ GeV

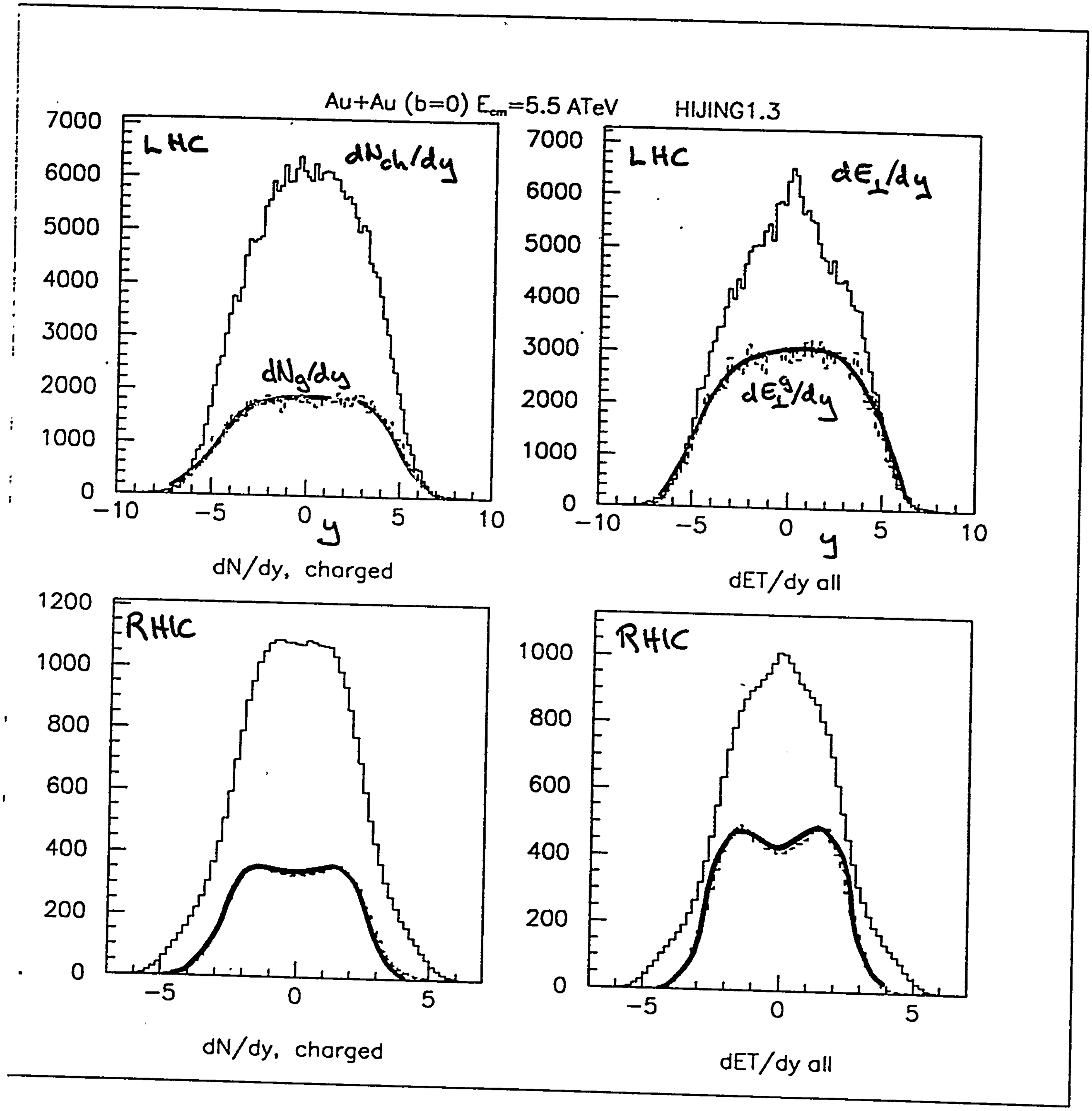

Au+Au (b=0) E$_{cm}$=5.5 ATeV
HIJING1.3
LHC
dN$_{ch}$/dy
dN$_g$/dy
y
dN/dy, charged
LHC
dE$_\perp$/dy
dE$_\perp^g$/dy
y
dET/dy all
RHIC
dN/dy, charged
RHIC
dET/dy all

Local energy density: $z=0,\ \vec{x}_\perp,\ t$

$$\epsilon(\vec{x}_\perp, z=0, t)$$

HIJING

$$= \underbrace{\int_{p_0}}_{\text{mini jet scale}} d^2\vec{p}_\perp \ \frac{p_\perp}{t} \ \frac{dN^{glue}}{dy\, d^2p_\perp\, d^2x_\perp}\left(y=0, \vec{p}_\perp ; z=0, \vec{x}_\perp - \hat{p}_\perp t\right) \otimes \underbrace{\frac{1}{1+\left(\frac{\hbar}{p_\perp t}\right)^2}}_{\text{Formation probability}}$$

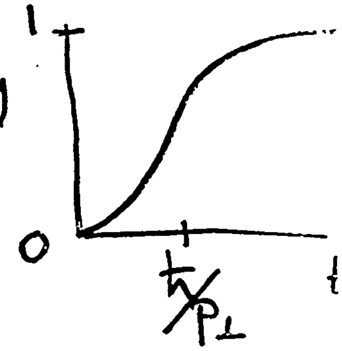

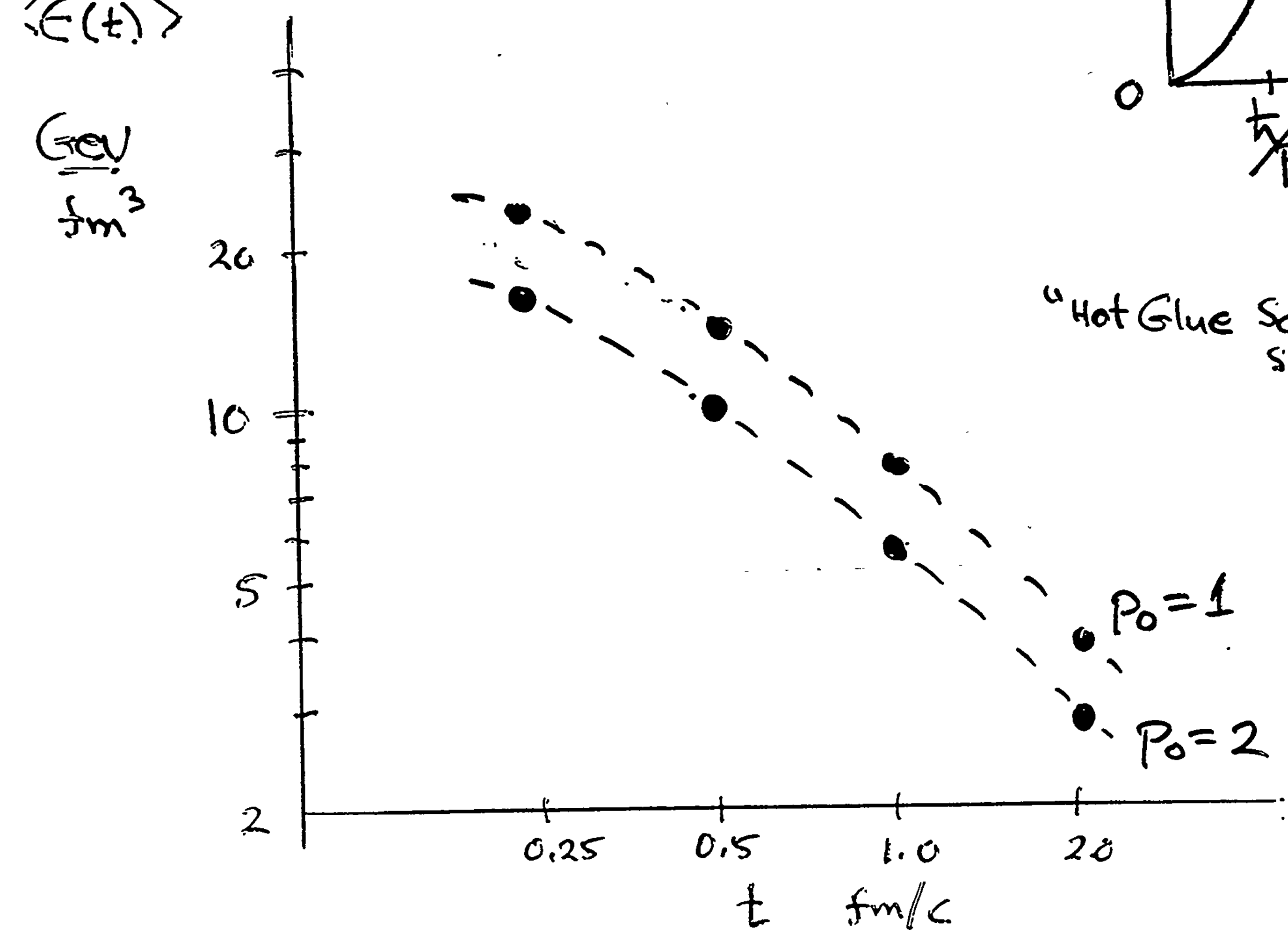

"Hot Glue Scenario"
Shuryak
(9

Thermalization Time Scales:

1) Elastic Scattering  Debye screening $\mu \sim 2T$

$$\tau_{el} = \frac{T}{dE^{el}/dx} \approx \frac{1}{4\alpha^2 \log\frac{1}{\alpha}\, T} \approx \frac{2}{T} > \text{fm}$$

Baym, etal Thoma, MG, Selikhou

2) Soft radiative $\frac{dE}{dx}^{soft}$ $(k_\perp \lesssim \mu)$

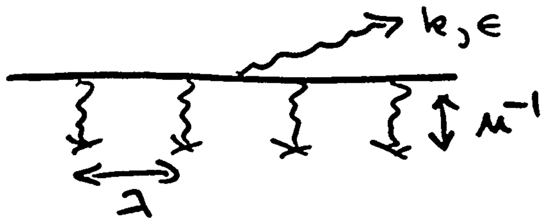

$\mu^2 \lambda \sim 10T$

$$\frac{dE^{soft}}{dx} \approx \alpha\, \mu^2 \log^2 E/T \approx \underline{1\,\text{GeV/fm}} \quad \Big\{ \begin{matrix} E = 2\,\text{GeV} \\ T = 0.3\,\text{GeV} \end{matrix}$$

XN Wang, M Plümer, MG PRD51 (95) 3436

3) Hard radiative $\frac{dE}{dx}$ $(k_\perp \gg \mu)$

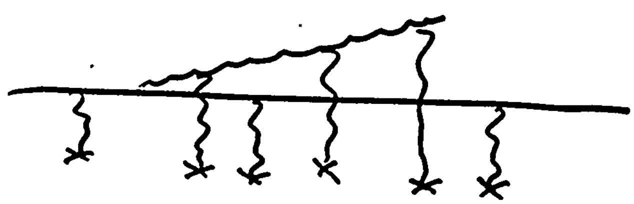

$\langle k_\perp^2 \rangle \approx \left(\frac{\ell}{\lambda}\right) \mu^2$ gluon random walk

Dokshitzer et.al. PLB345 (95) 277

$$\frac{dE}{dx} \approx \sqrt{\frac{E\mu^2}{\lambda}} \ln \frac{E}{\mu^2 \lambda} \sim \underline{2\,\text{GeV/fm}} \quad !$$

Uncertainty Principle Bound

Brodsky, Hoyer

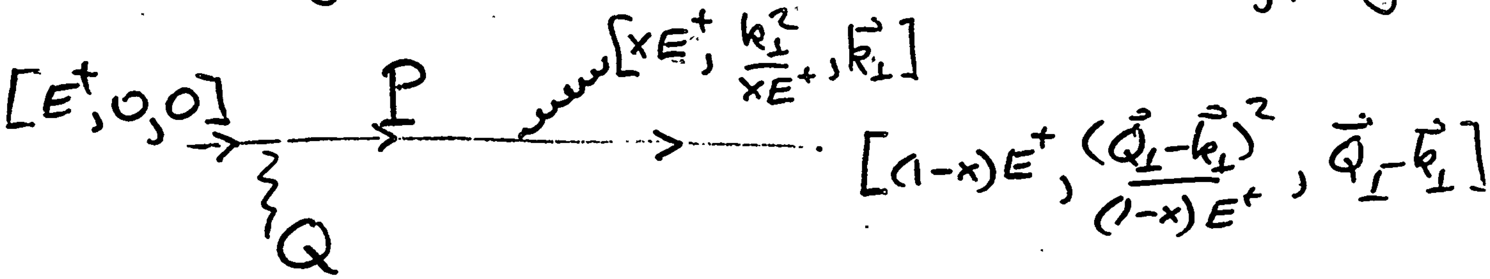

Propagator is coherent for

$$\boxed{\Delta L^{\pm} \gtrsim \frac{\hbar}{P^{\mp}}}$$

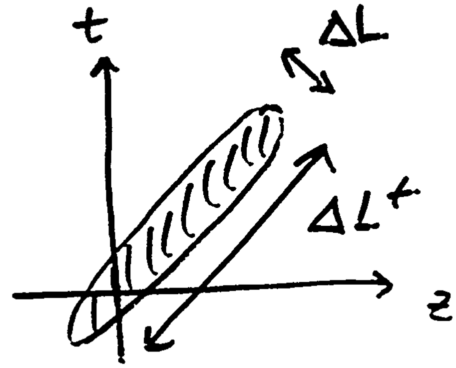

$$\Delta L^- \sim \frac{\hbar}{xE^+} \longrightarrow 0$$

$$\text{but } \Delta L^+ \gtrsim \frac{1}{k_\perp^2/xE^+} = \frac{xE^+}{k_\perp^2} = \frac{\Delta E^+}{k_\perp^2} \approx \frac{E^+}{P^2}$$

$$\boxed{\frac{dE}{dx} \equiv \frac{\Delta E^+}{\Delta L^+} \leq \langle k_\perp^2 \rangle}$$

For 1 glue only!

However, for multiple gluon emission

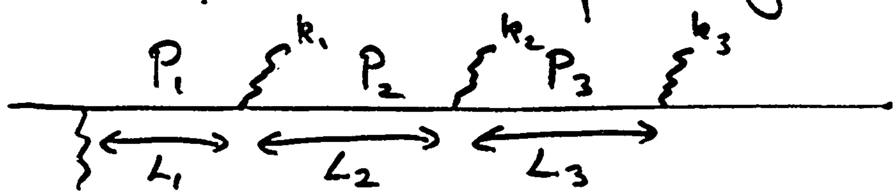

$$\Delta L_i^+ \gtrsim \frac{1}{P_i^-} \approx \frac{E^+}{\sum_{j \geq i} k_i^2/x_j} \approx \frac{x_i E^+}{k_\perp^2 \bar{\rho}}$$

$$\sum_{j \geq i} 1/x_j \approx \int_{x_i}^{1} dx \, \frac{dN_g}{dx} \frac{1}{x} \approx \bar{\rho}/x_i \qquad \bar{\rho} \equiv \frac{dN_g}{dy}$$

$$\boxed{\frac{dE}{dx} = \frac{\sum \Delta E_i^+}{\sum \Delta L_i^+} \lesssim \bar{\rho} \langle k_\perp^2 \rangle}$$

Random Walk in $\vec{p}_\perp$ shortens formation time

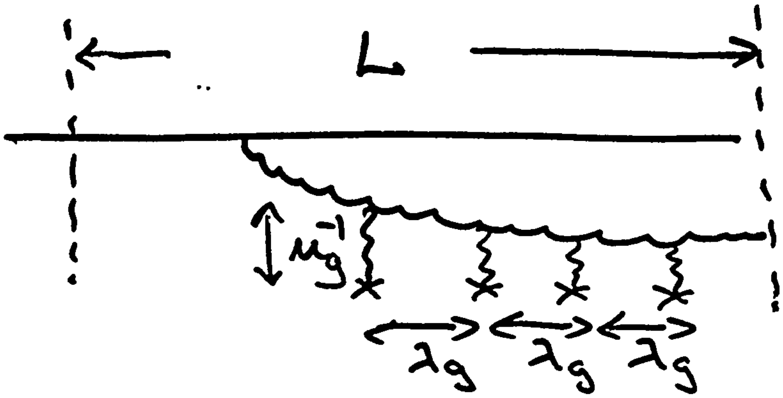

$$\langle k_\perp^2 \rangle_L \approx \frac{L}{\lambda_g} \mu_g^2$$

$$\frac{dE}{dx} \lesssim \bar{\rho}\, L \left(\frac{\mu^2}{\lambda}\right)_g$$

Mueller, BDPS

$$\bar{\rho} = \frac{\alpha N_c}{2} \log\frac{L}{\lambda} \sim 1$$

In QGP $\quad \mu = \mu_{Debye} \approx gT \approx 2T \sim 0.6\,\text{GeV}$

$$\lambda_g^{-1} = \sigma_g \rho_T \approx \frac{4\pi\alpha^2}{\mu^2}(2T^3)$$

$$\left(\frac{\mu^2}{\lambda}\right)_{QGP} \approx 4\pi\alpha^2 \rho_T \approx 3T^3 \underset{T=300\,\text{MeV}}{\sim} 0.4\ \frac{\text{GeV}^2}{\text{fm}}$$

In cold nuclei use $\quad p+A \to J/\psi + X$

$$\langle p_\perp^2 \rangle_A = p_0^2 + \nu_A \lambda_N (\mu_g^2/\lambda_g)_{T=0} \qquad \nu_A \lambda_N \approx 1.8 A^{1/3}\,\text{fm}$$

Badier et al $\quad \langle p_\perp^2 \rangle_{Pt} - \langle p_\perp^2 \rangle_p \approx 0.36\,\text{GeV}^2$

$$\left(\frac{\mu_g^2}{\lambda_g}\right)_{T=0} \approx 0.05\ \text{GeV}^2/\text{fm} \approx \Lambda_{QCD}^3 \approx \frac{1}{10}\left(\frac{\mu_g^2}{\lambda_g}\right)_{QGP}$$

IN NUCLEAR COLLISIONS ☆

S. GAVIN and M. GYULASSY   PLB 214 (88) 241

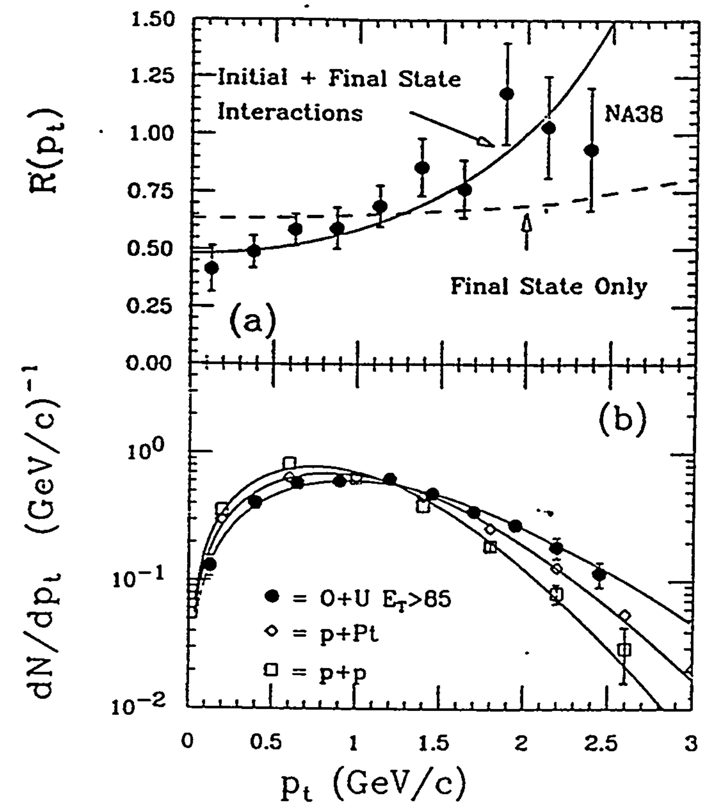

Fig. 1. (a) The preliminary NA 38 data [1] on the relative J/ψ-to-continuum yield (1) with $E_T^> > 85$ GeV and $E_T^< < 34$ GeV are compared to our calculations for the analogous LUND model values E_T=60 and 15 GeV including both quasielastic initial-state scattering and final-state inelastic J/ψ–hadron scattering for $\bar{\sigma}$=5 mb. The dashed curve shows the suppression factor in the absence of initial-state interactions. (b) Transverse momentum distributions of p+A→ψ+X at 200 GeV for ^{195}Pt (diamonds) and p (squares) targets from ref. [11] are compared to those measured in O+U (dots) for E_T>85 GeV [1]. We use (6) and the measured values of $\langle p_\perp^2 \rangle$ [11] to obtain the p+A curves. The O+U curve is calculated using (4) for E_T=60 GeV.

$$\langle p_\perp^2\rangle_g = [1.2 + 0.12(\nu_A - 1)]\ \mathrm{GeV}^2$$

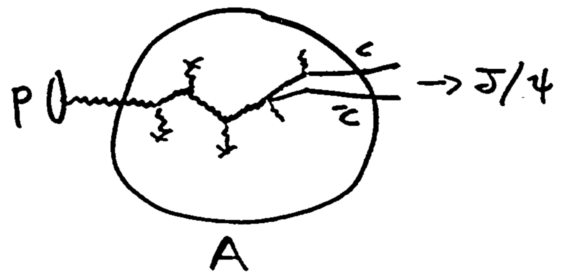

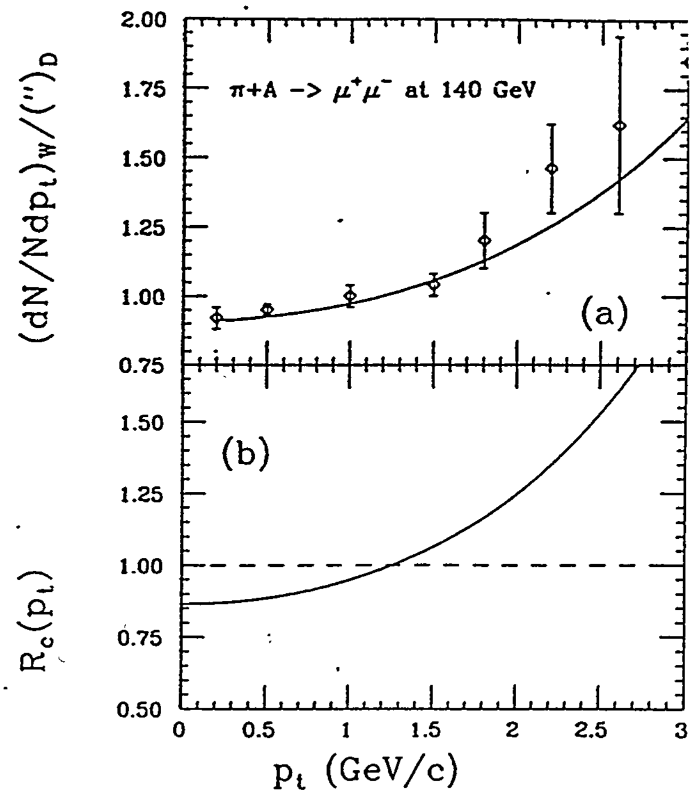

Fig. 2. (a) Measured [13] ratio of Drell–Yan yields as a function of transverse momentum for a 140 GeV π^- beam on ^{184}W and deuterium targets are compared to the gaussian fit (solid curve) with $\langle p_\perp^2 \rangle$ taken from refs. [13,15]. (b) Shown is the expected $p_\perp$ variation of the Drell–Yan continuum ratio for the same E_T cuts as in fig. 1a.

$$\langle p_\perp^2\rangle_q = (1.4 + 0.06(\nu_A - 1))\ \mathrm{GeV}$$

$$\nu_A = 0.8 A^{1/3} \approx 3.7 \quad \mathrm{Pt, W}$$

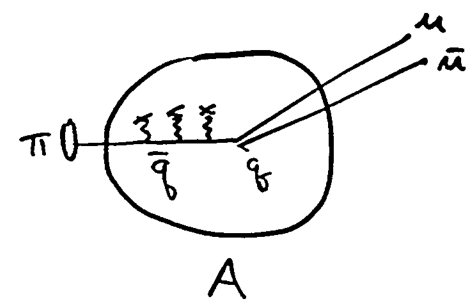

Energy loss of quark jets in eA

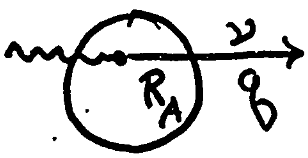

$$\Delta E_A = \frac{1}{2} R_A^2 \left(\frac{\mu_q^2}{\lambda_q}\right)_{T=0} \approx \frac{1}{4} R_A^2 \left(\frac{\mu_g^2}{\lambda_g}\right)_{T=0}.$$

$$\Delta E_{A\sim 200} \approx \frac{(7\,\mathrm{fm})^2}{4}\, 0.05\, \frac{\mathrm{GeV}^2}{\mathrm{fm}}\, \frac{1}{0.2\,\mathrm{GeV\,fm}}$$

$\approx 3\ \mathrm{GeV}$ ← small compared to $\nu \sim 100\ \mathrm{GeV}$

Expect only small modification in fragmentation

$$f_{\pi/A}(z) = f_{\pi/A}(E_\pi/\nu) \xrightarrow[\Delta E]{} f_{\pi/N}\left(\frac{E_\pi}{\nu - \Delta E_A}\right)$$

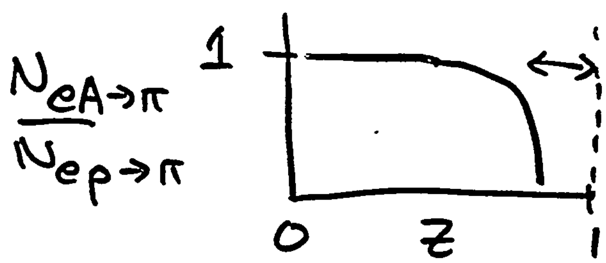

$$\Delta z \approx \frac{\Delta E_A}{\nu} \approx \frac{3\ \mathrm{GeV}}{\nu} << 1$$

Energy Loss of gluon jets in A+A

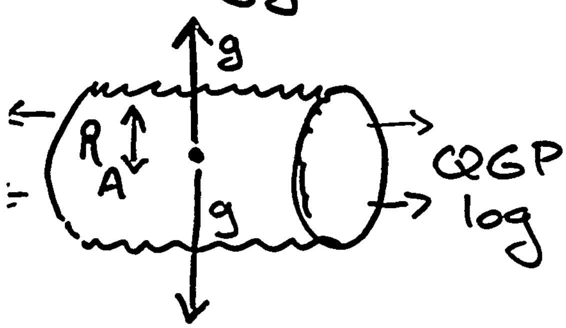

$$\Delta E_A \approx \frac{1}{2} R_A^2 \left(\frac{\mu_g^2}{\lambda_g}\right)_{QGP} \approx \frac{3}{2} R_A^2 T^3$$

$R \approx 7\,\mathrm{fm}$ $\quad T \approx 300\ \mathrm{MeV}$

$\Delta E_{Au} \approx 50\ \mathrm{GeV}$ ← Astonishing huge

Also $T^4 \propto \frac{dE_\perp}{dy} \propto A^{4/3} \Rightarrow \Delta E_A \propto A^1$ ← highly non-linear in $R_A \propto A^{1/3}$

H.L. Melanson / E665

$$R_{A/D} = \frac{N_{\ell A}(z > 0.2)}{N_{\ell D}(z > 0.2)}$$

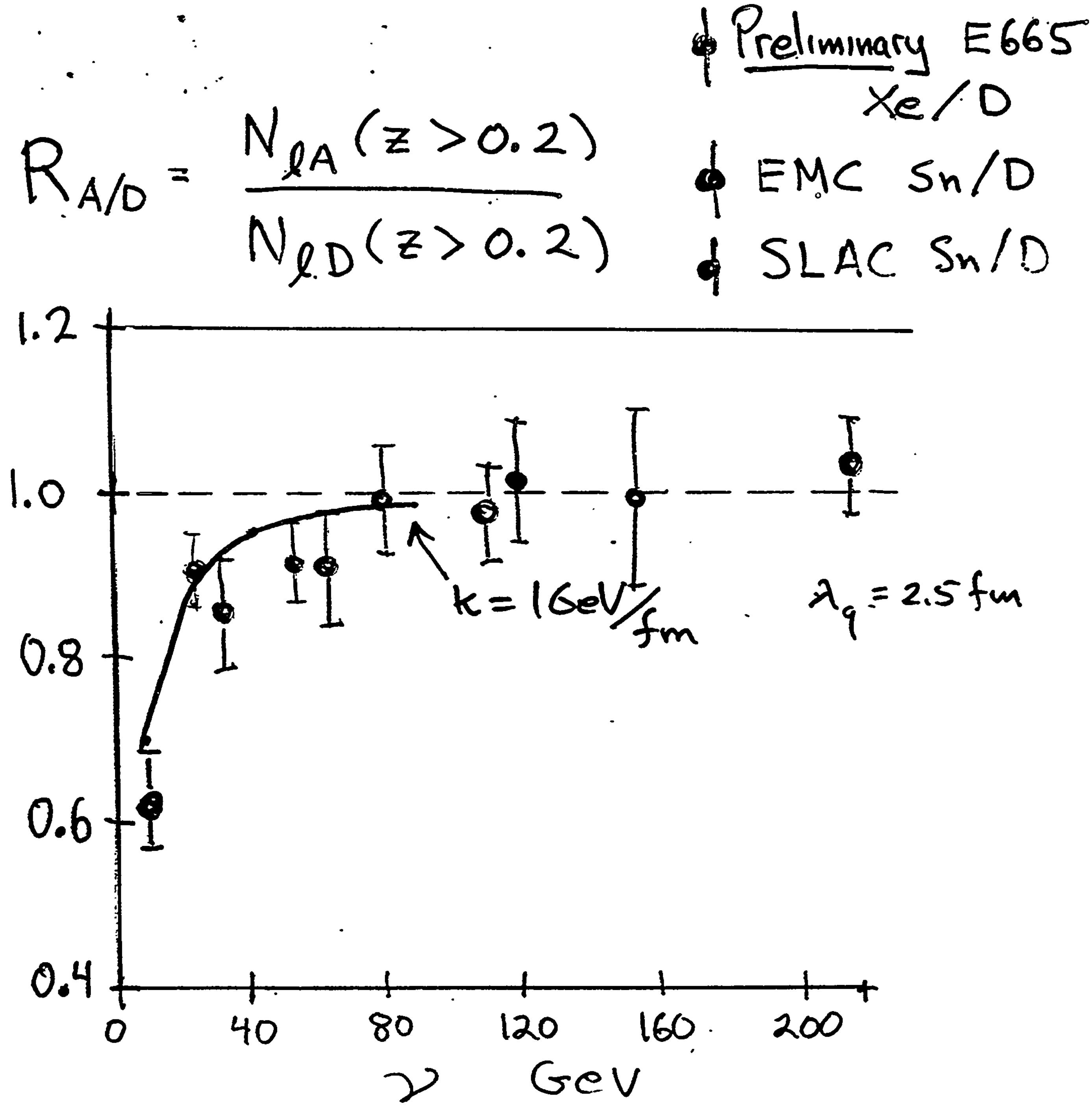

EMC : CERN-PPE-91-60

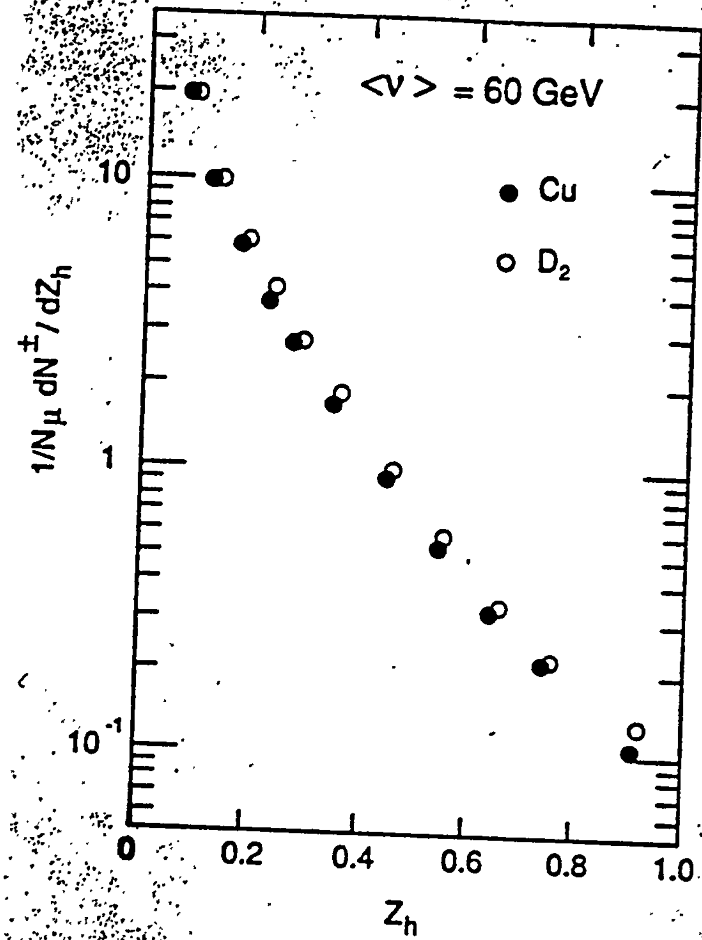

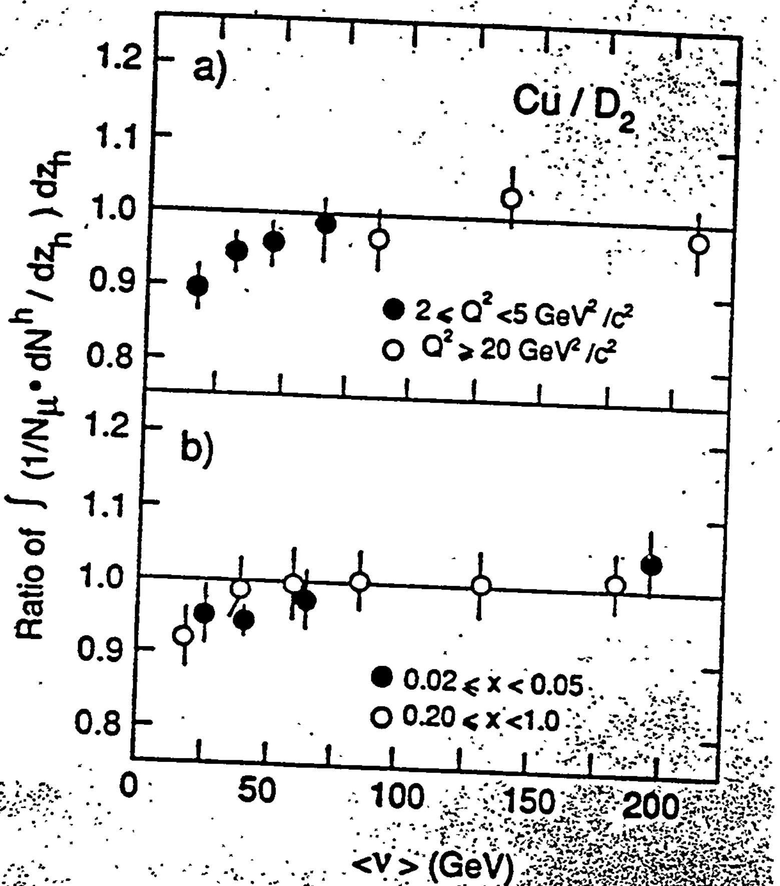

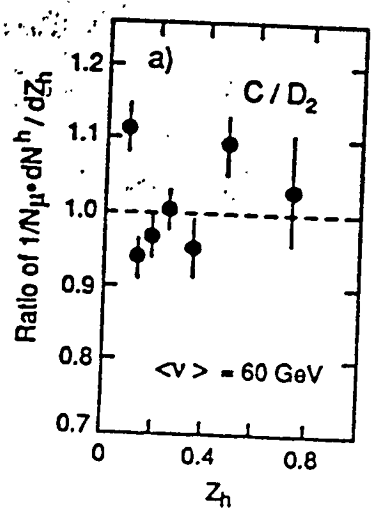

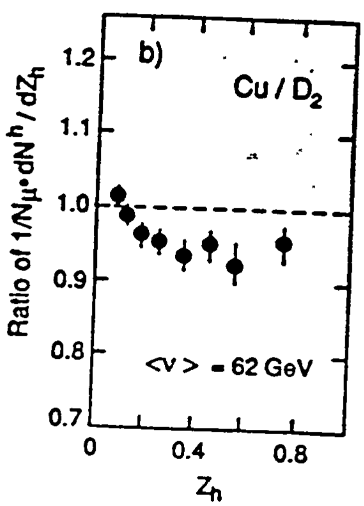

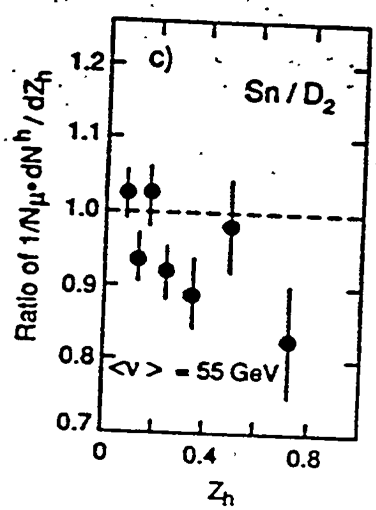

E665 MPI-PhE/93-17 Geesaman et al.

$E_\mu = 490\,\mathrm{GeV}\ (\pm 60)$

$\nu \gtrsim 50$ GeV $\quad Q^2 > 1 \quad x_{Bj} = \frac{Q^2}{2m\nu} > 0.002$

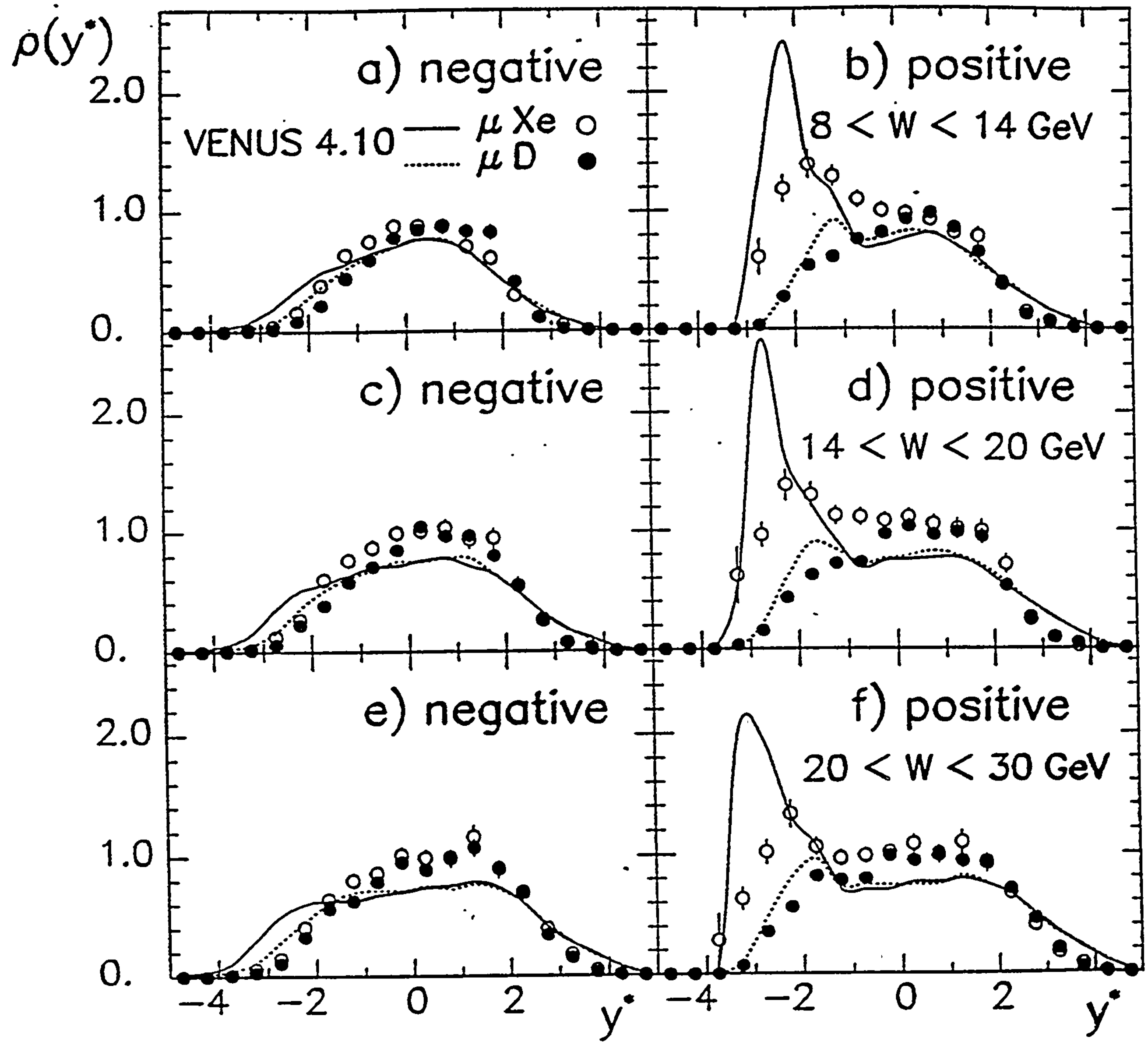

Fig. 22: Normalized cms-rapidity distribution of negative and positive hadrons, for μD (full circles) and μXe scattering (open circles), in three bins of W. The lines represent the predictions of the VENUS model for μD (dotted lines) and μXe scattering (solid lines). It should be noted that the distribution for positive hadrons in μXe scattering has a systematic error, the size of which can be estimated from the distributions in Fig. 23.

$W^2 = -Q^2 + 2m\nu + m^2$

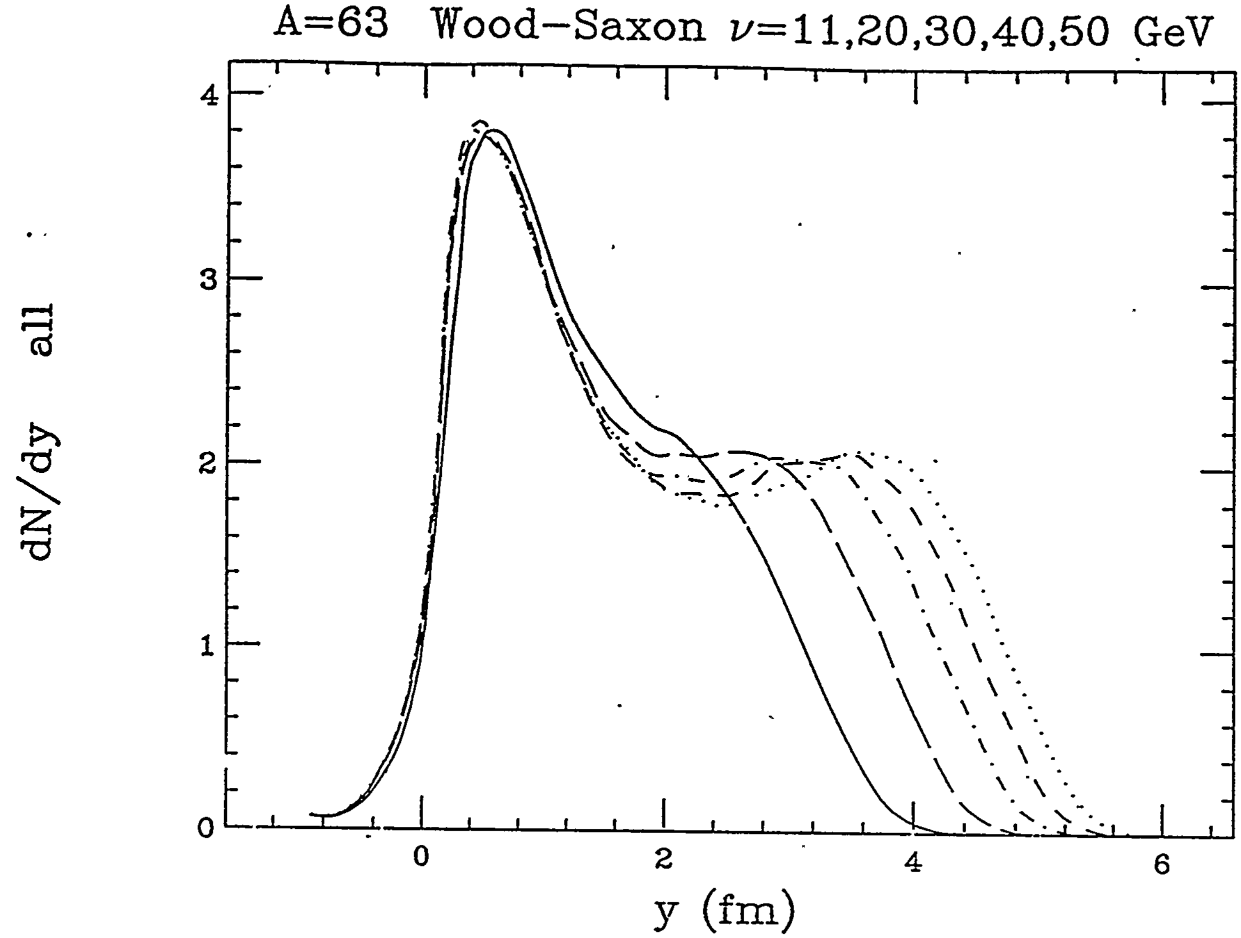
A=63 Wood–Saxon ν=11,20,30,40,50 GeV
dN/dy all
y (fm)
0
1
2
3
4
0
2
4
6

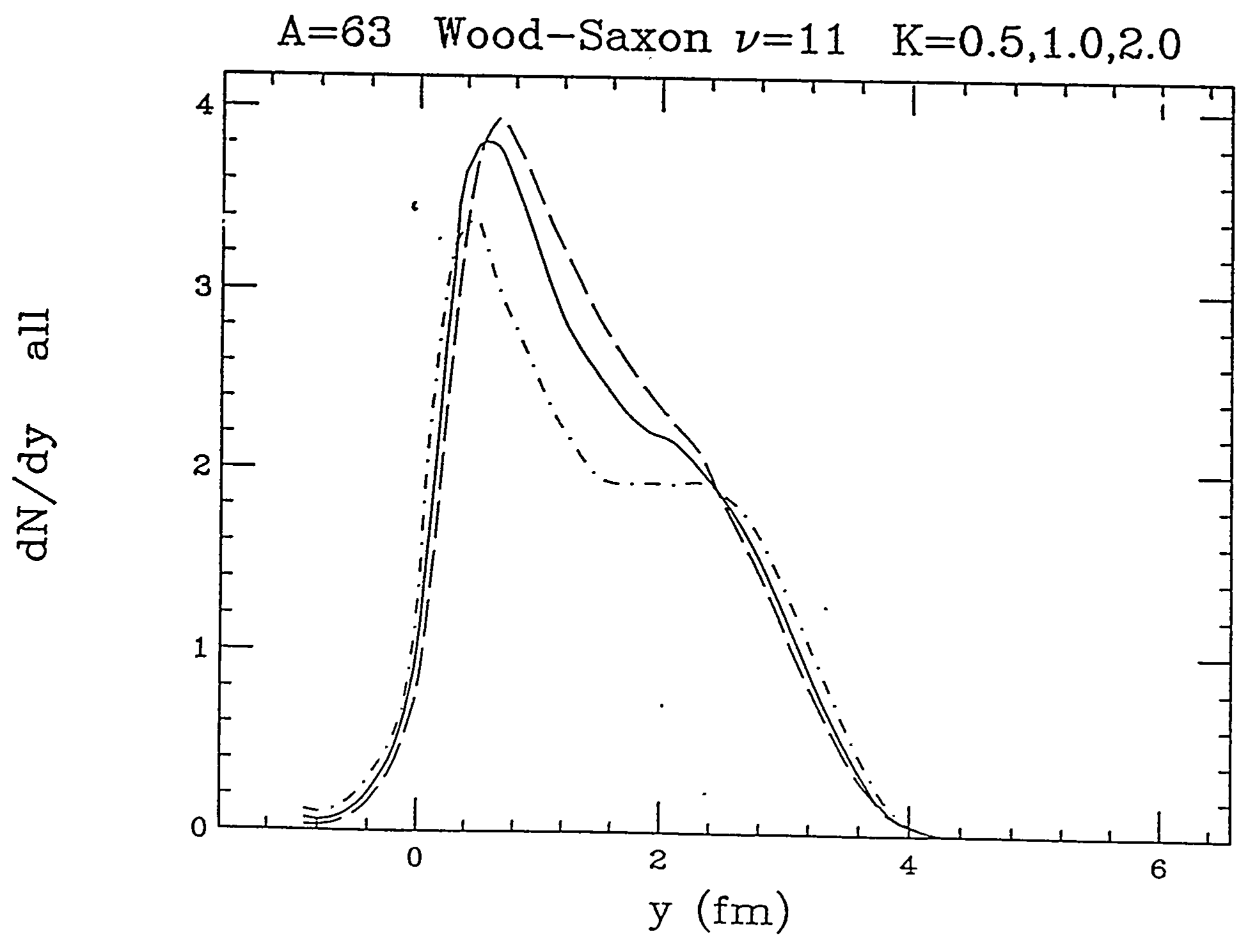
A=63 Wood–Saxon ν=11 K=0.5,1.0,2.0
dN/dy all
y (fm)
0
1
2
3
4
0
2
4
6

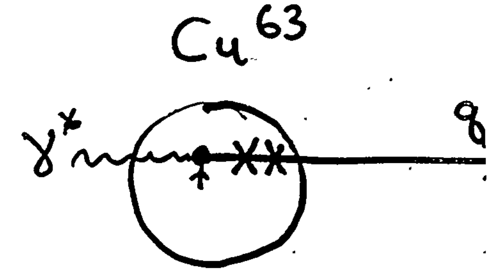

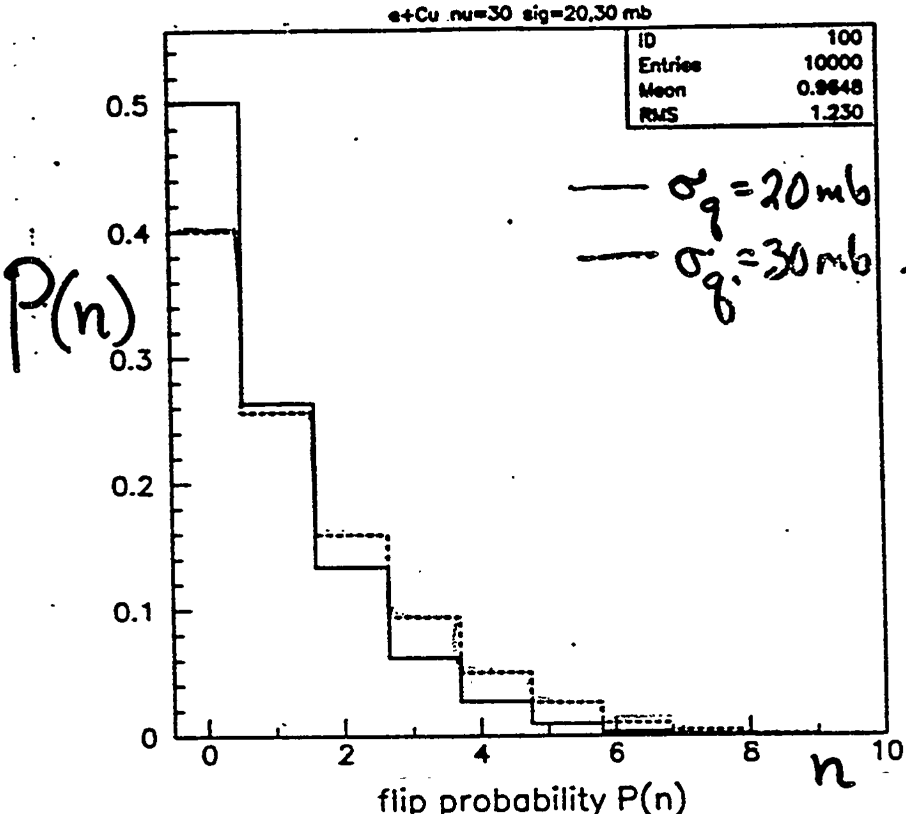

* large prob P(0)
that no final st
interactions occ

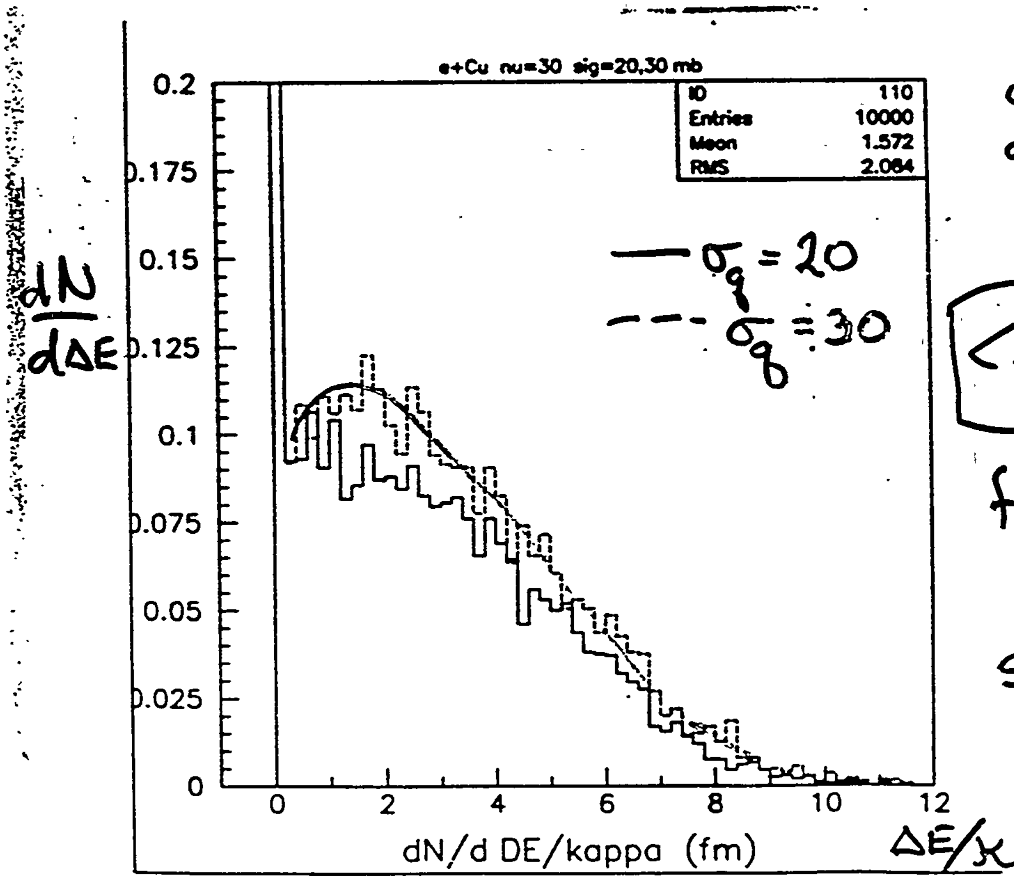

$$\frac{dN}{d\Delta E} = P(0)\,\delta(\Delta E) + (1 - P(0))\, f(\Delta E)$$

$$\boxed{\langle \Delta E \rangle_{Cu} \sim 1.5 \text{ GeV}}$$

for $\kappa \approx 1$ GeV/fm

Small effective energy loss in nuclei !

$\nu = 30$ $\ell + Cu^{63} \rightarrow$ hadrons

1+1 Nambu

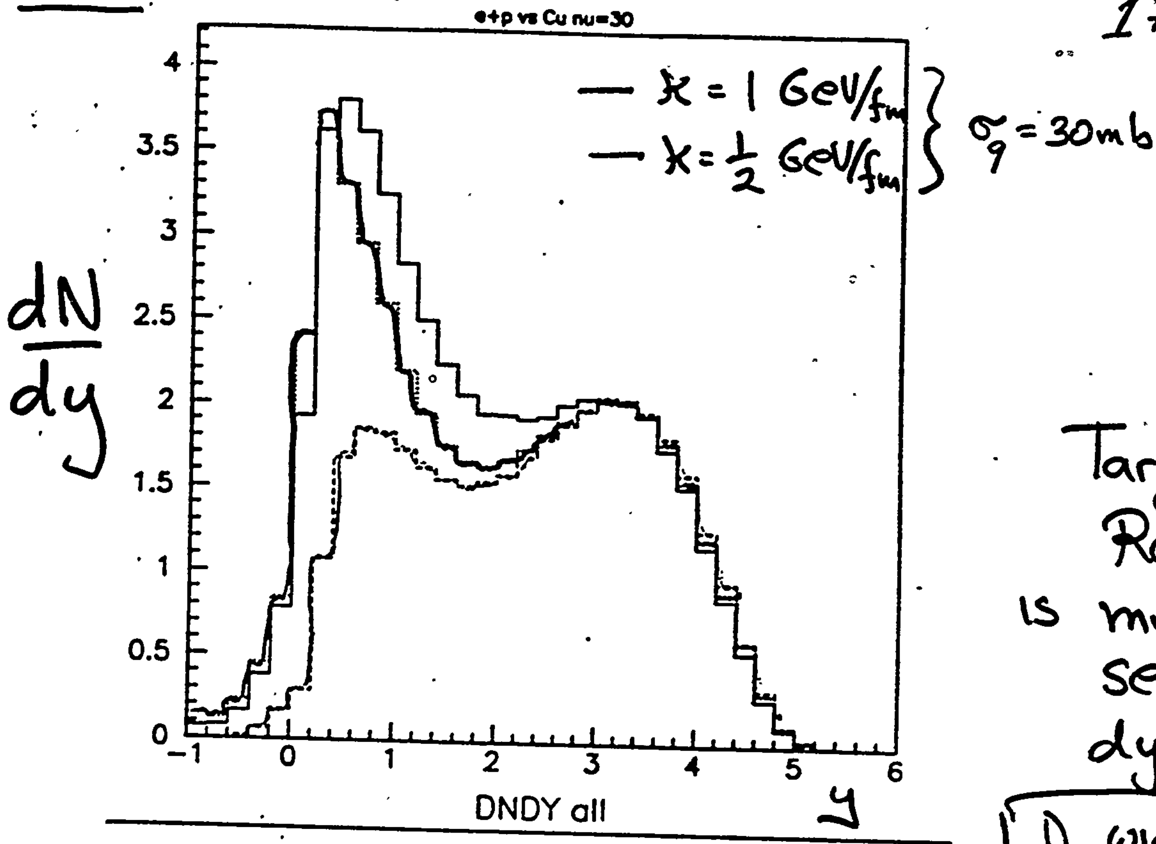

Target Frag. Region ($x_F < 0$) is much more sensitive to dynamics:

1) width $\frac{dN}{dy} \propto \kappa$
2) height $\frac{dN}{dy} \propto \sigma_q$

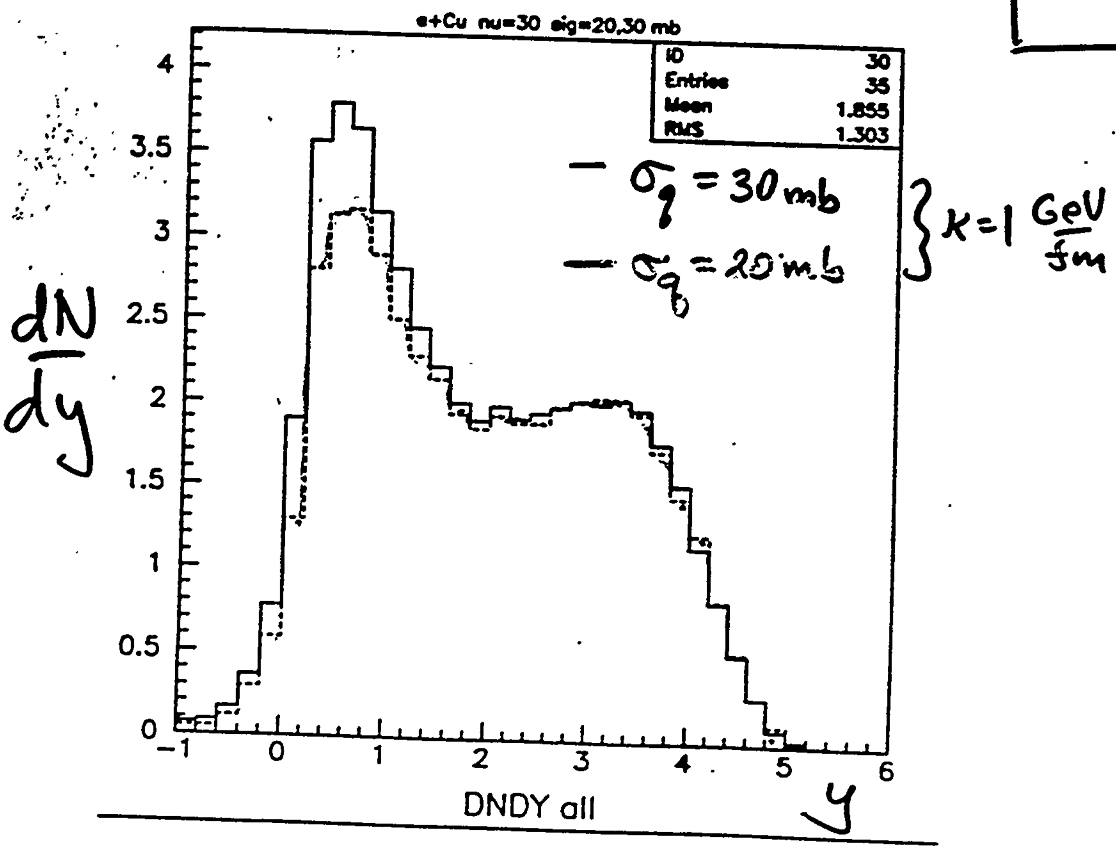

Hard jets in U+U

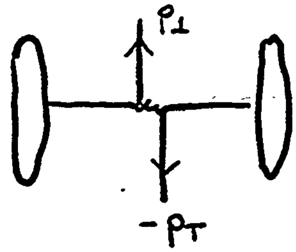

number of jets at $y_1 = y_2 = 0$ in $b=0$ U+U collisi

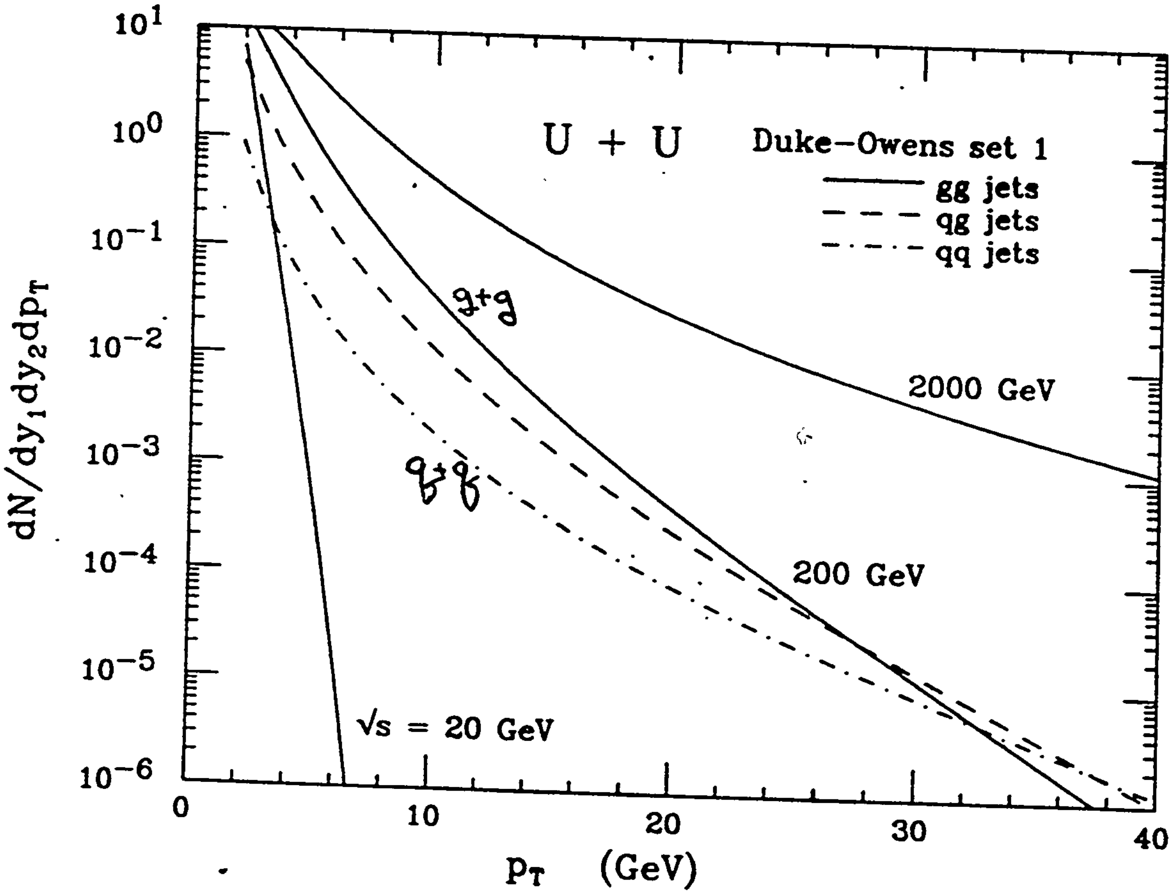

$$dN = T_{uu}(0)\, d\sigma_{pp} \qquad T_{uu}(0) \simeq 38/mb$$

$$\Rightarrow N_{pp} \sim 1500$$

binary

$$\frac{d\sigma^{pp}}{dp_\perp^2 dy_1 dy_2} = \sum_{ab} x_1 f_a(x_1)\, x_2 f_b(x_2)\, \frac{d\sigma^{ab}}{dt}$$

$$y_1 = y_2 = 0 \qquad x_1 = x_2 = p_\perp / \sqrt{s}$$

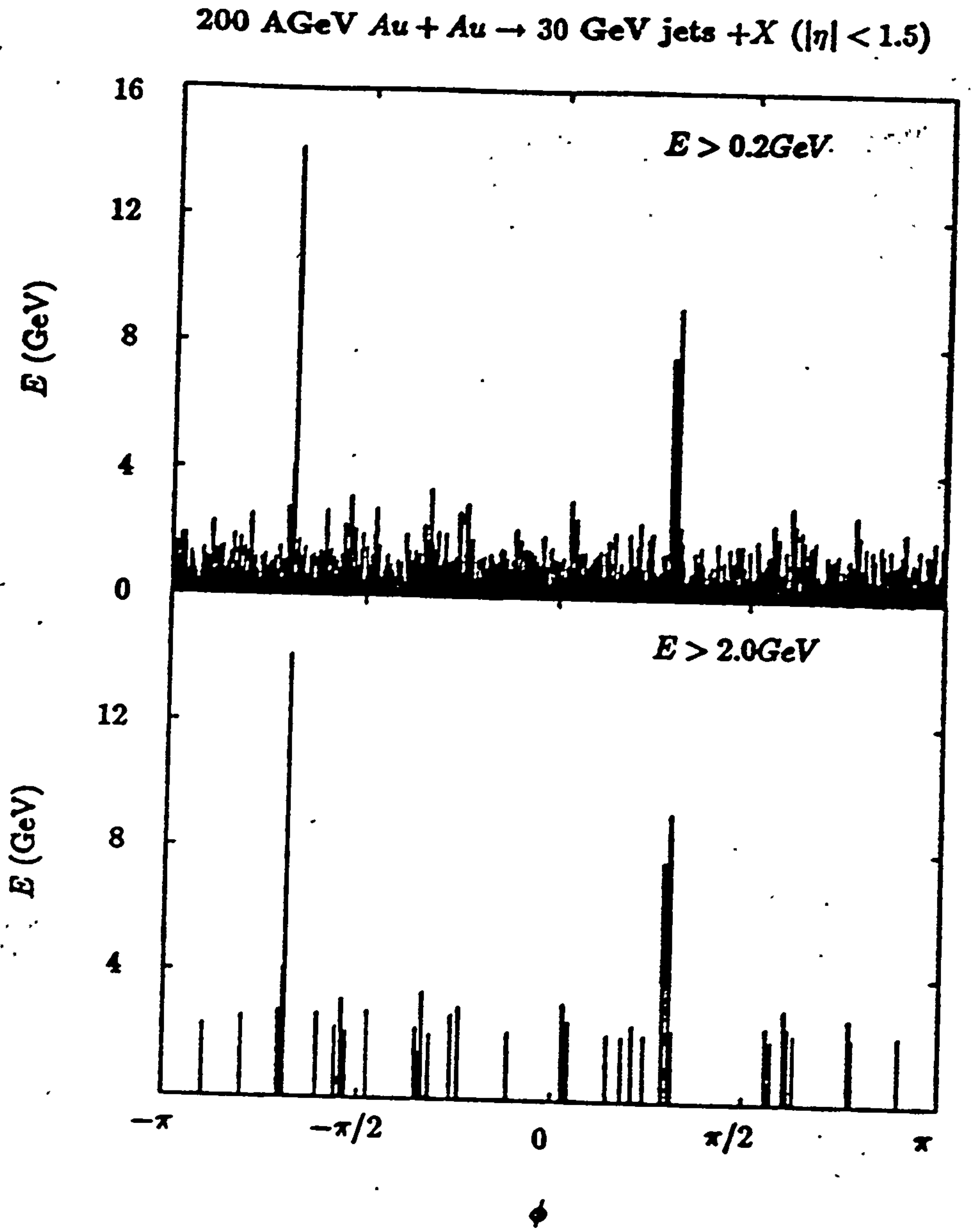
200 AGeV $Au + Au \to$ 30 GeV jets $+X$ ($|\eta| < 1.5$)
$E > 0.2GeV$
$E > 2.0GeV$
E (GeV)
E (GeV)
16
12
8
4
0
12
8
4
$-\pi$
$-\pi/2$
0
$\pi/2$
π
ϕ

Figure 4

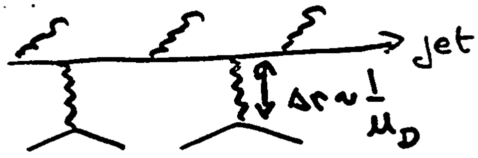

$$\frac{dE}{dx} \approx \alpha_s \mu_D^2 \log^2 s/4\mu_D^2 \quad \text{energy loss}$$
$$\sim 1-2 \text{ GeV/fm}$$

Effects of Energy Loss

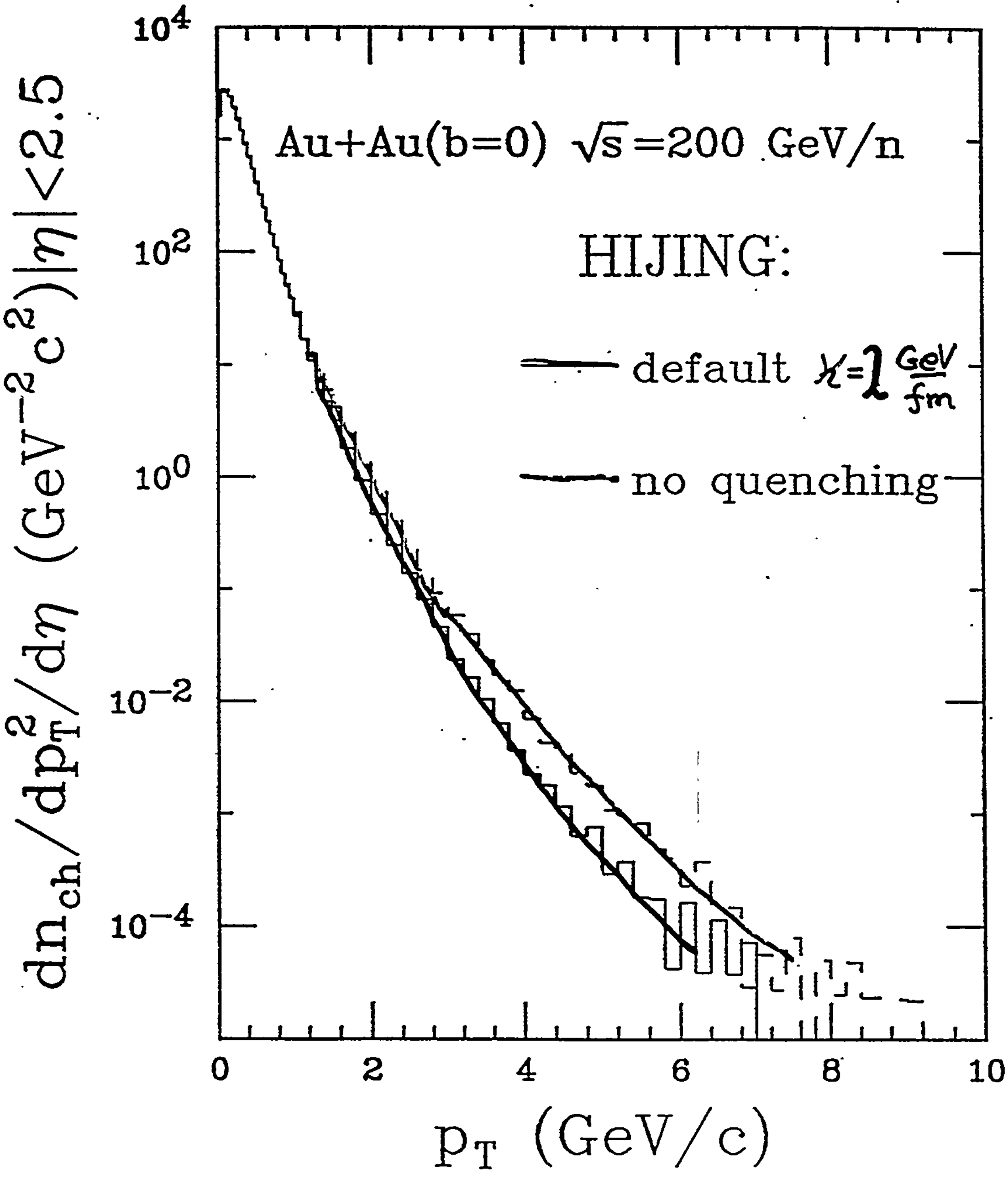

Jet quenching provides info on color screening μ_D

$$R = \frac{dN_{AA}/dp_\perp}{dN_{pp}/dp_\perp}$$

Au+Au (RHIC)

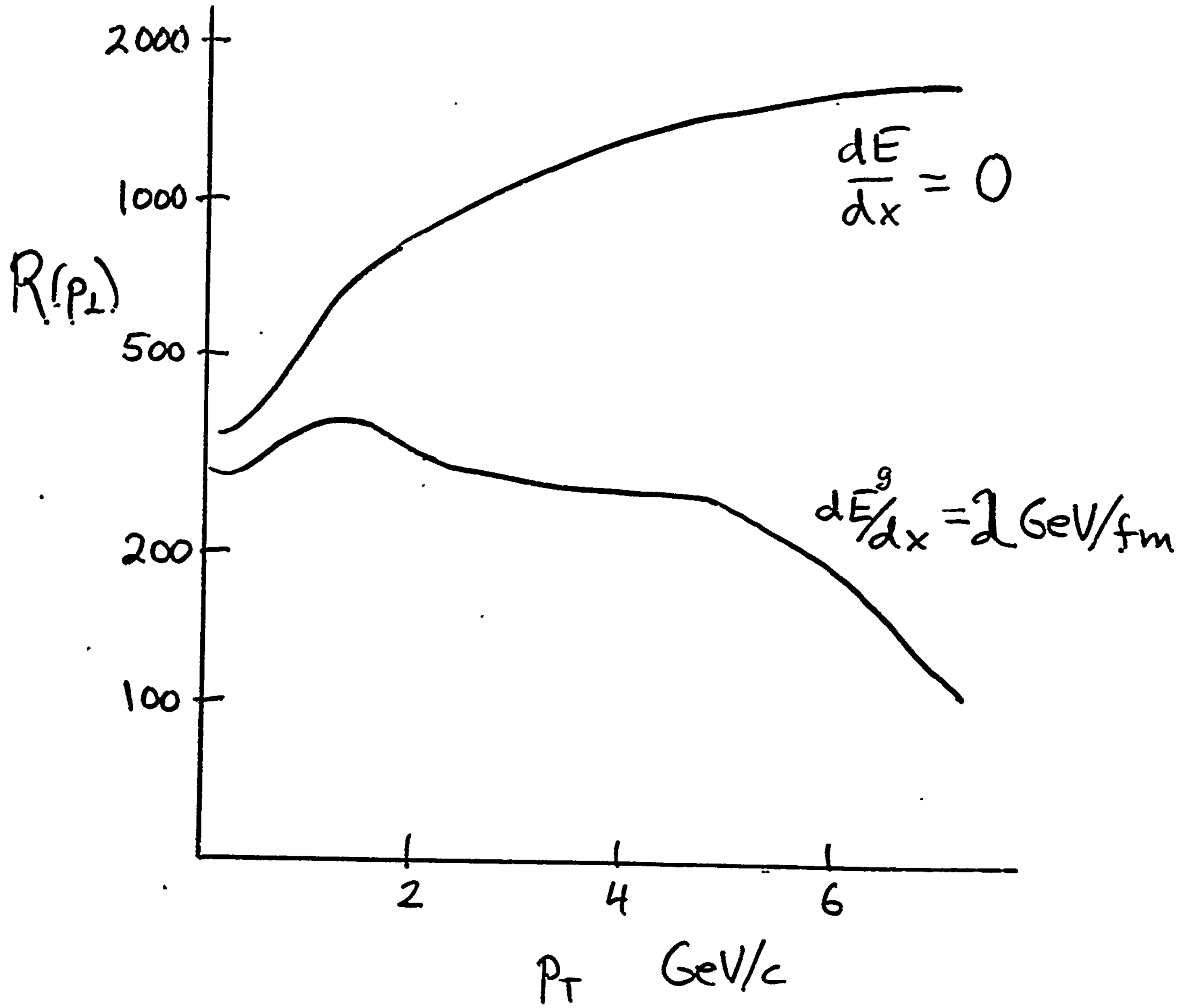

Number of y1=y2=0 pt=30GeV jets in b=0 U+U from gg, qg, qq scatt vs Ecm per nucleon

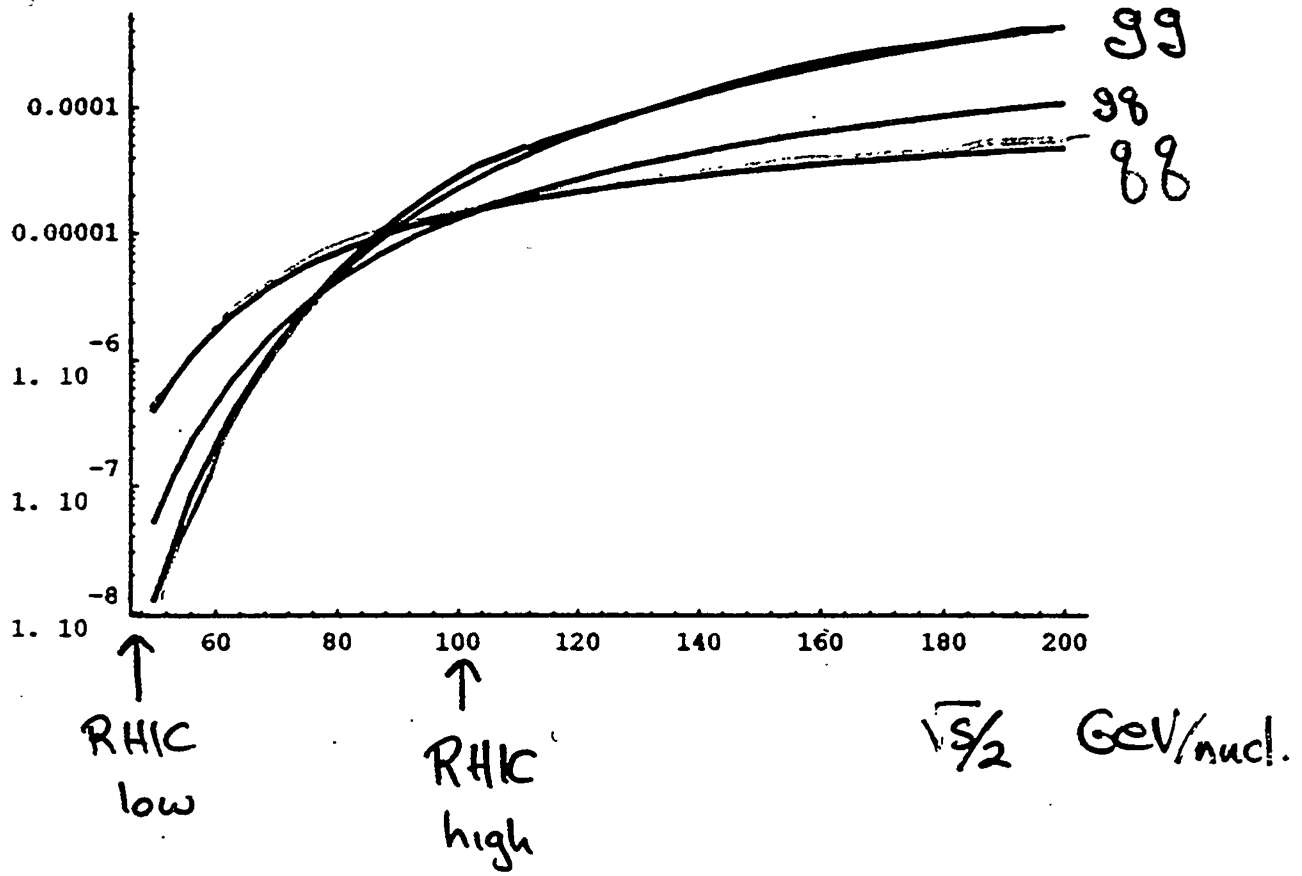

$$\text{rate} \propto f_i\left(x=\frac{p_\perp}{\sqrt{s}/2}, p_\perp^2\right) f_j\left(x=\frac{p_\perp}{\sqrt{s}/2}, p_\perp^2\right)$$

for $p_\perp \sim 30$ GeV $\sqrt{s}/2 \sim 100$ GeV
rate explores $x \sim 1/3$ region

decrease $\sqrt{s}$ => increase x => far less g

Dijet Quench excitation fn. as signature of color interactions

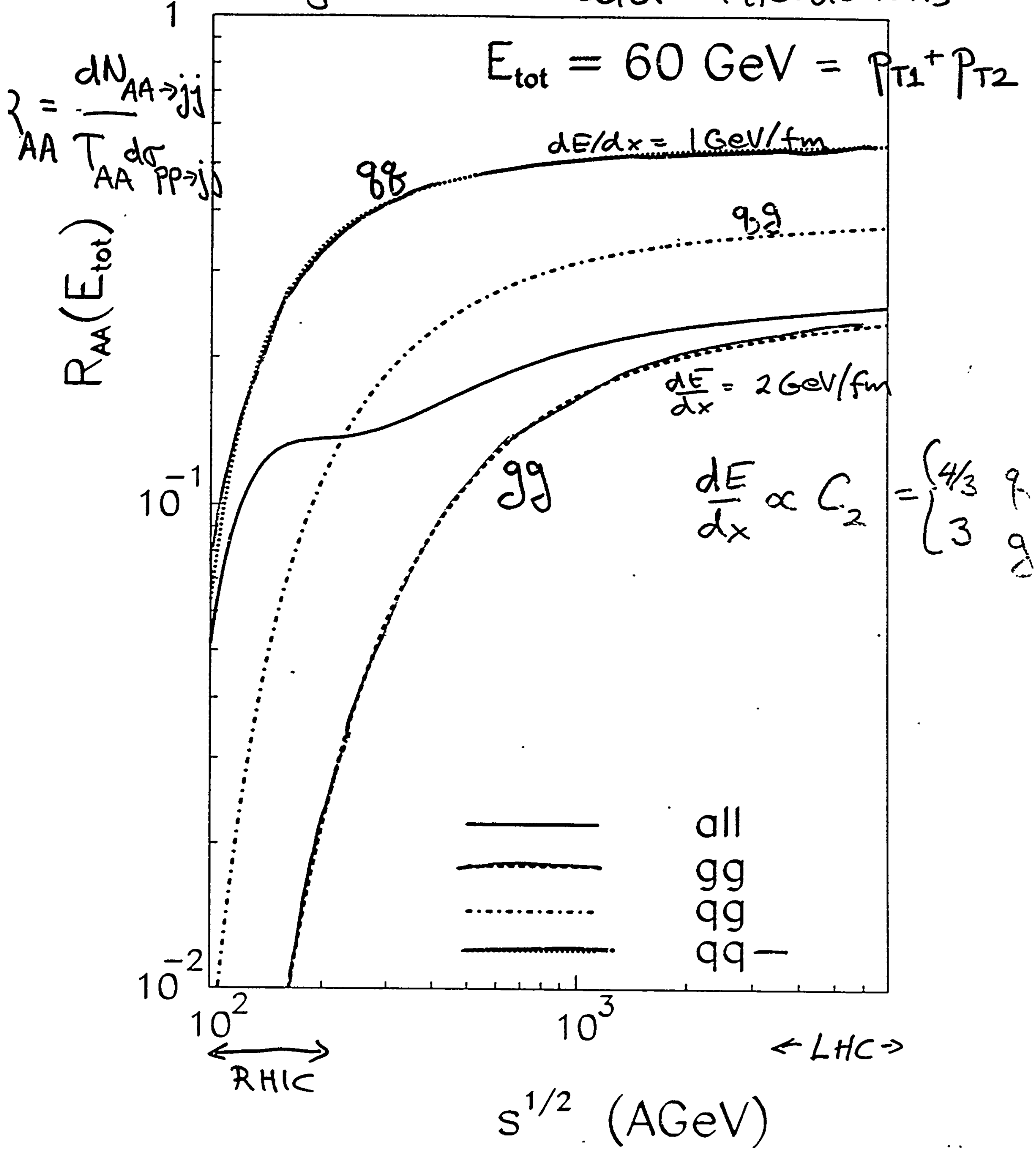

Plümer, Wang, M.G. (94)

Is there any effect of $\frac{dE}{dx}$ in pA?

Gavin Milana

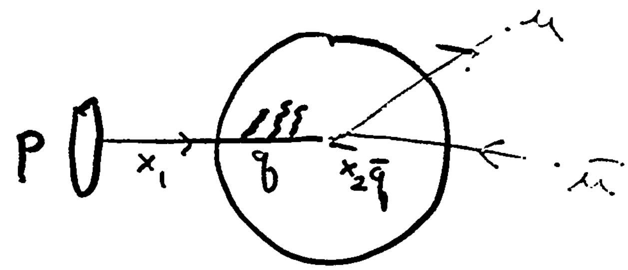

$x_F = x_1 - x_2 - \Delta x_q$

Δx_q due to initial state energy lo[ss]

$R \propto q(x_1 + \Delta x_q)\,\bar{q}(x_2)$

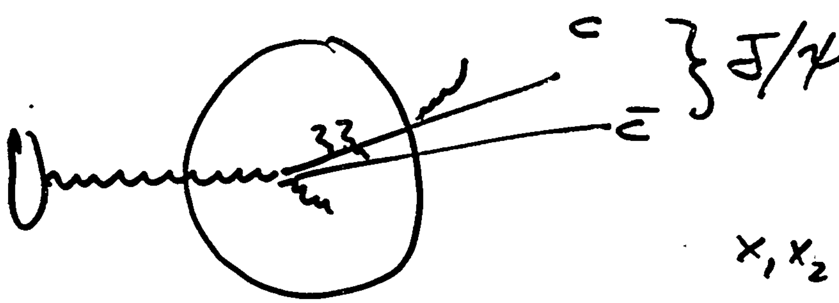

$x_1 x_2 s = M_\psi^2$

$x_1 \to x_1 - \Delta x_g$

Both initial and final contribute to $\Delta x_g \sim 2\Delta x_q$

$R \propto g(x_1 + \Delta x_g)\,g(x_2)$

Gavin + Milana 72

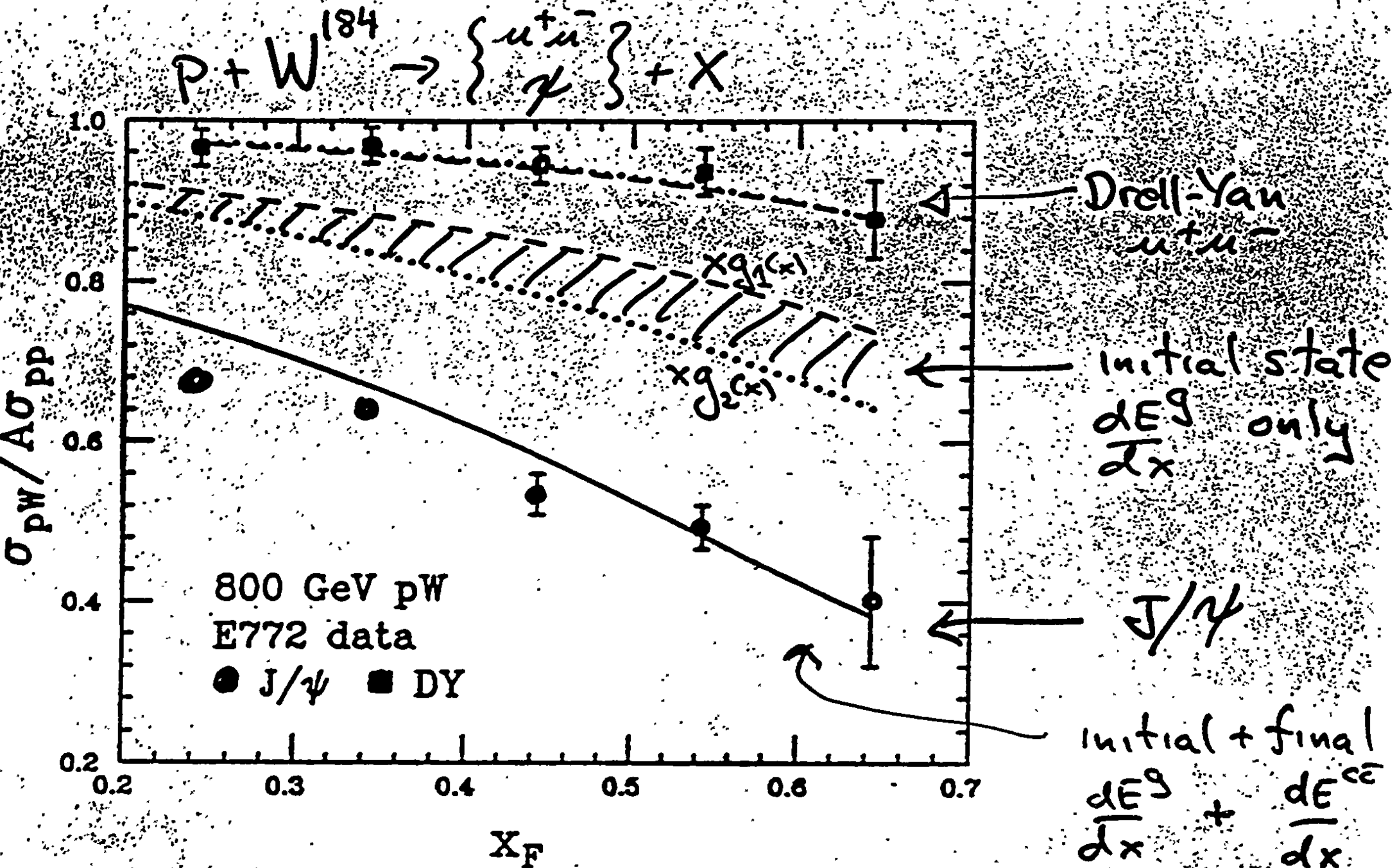

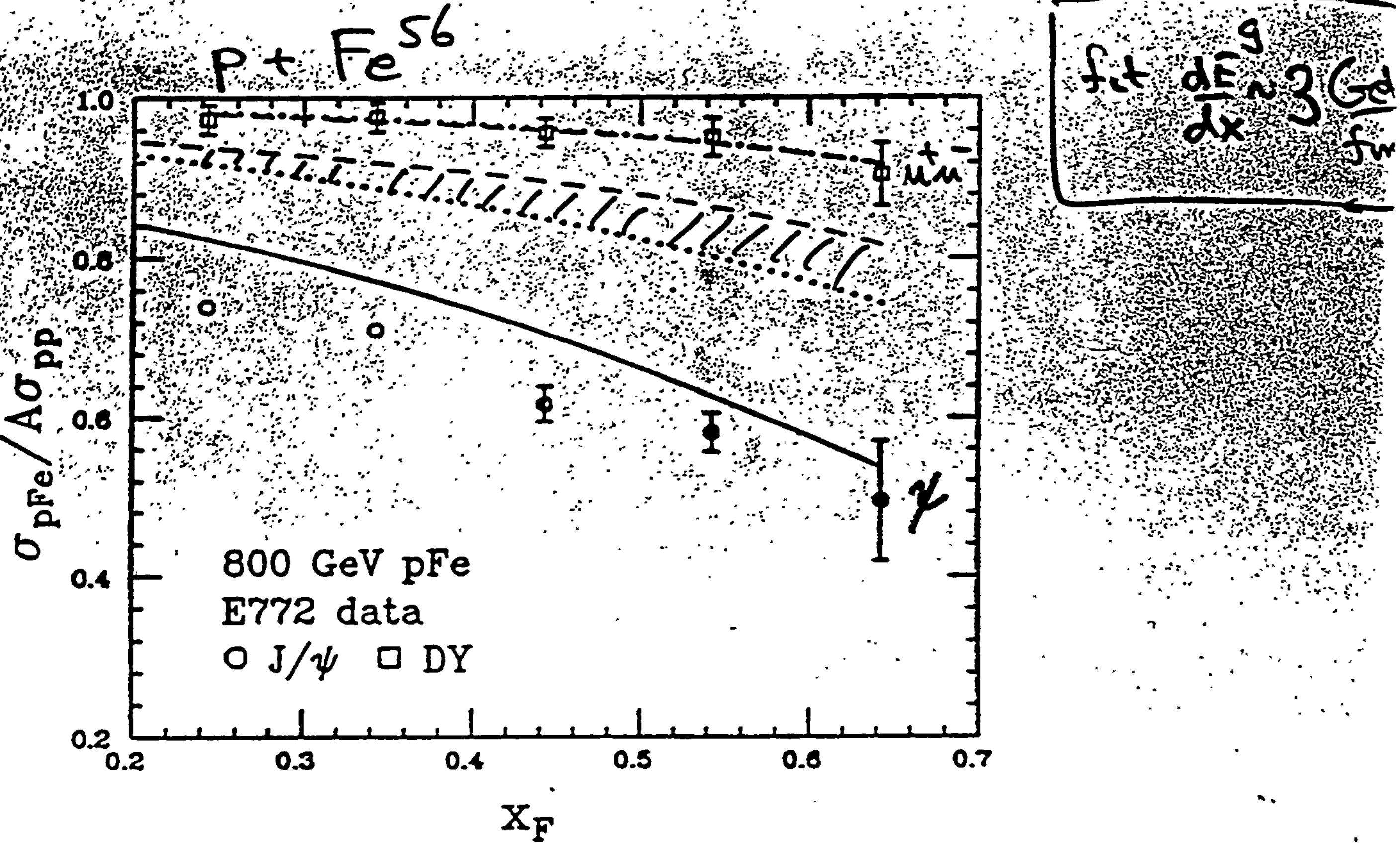

800 GeV $p + (p, Be, C, Cu, Pb) \rightarrow$ dijet

FNAL E557
PRD 42 (90) 1385

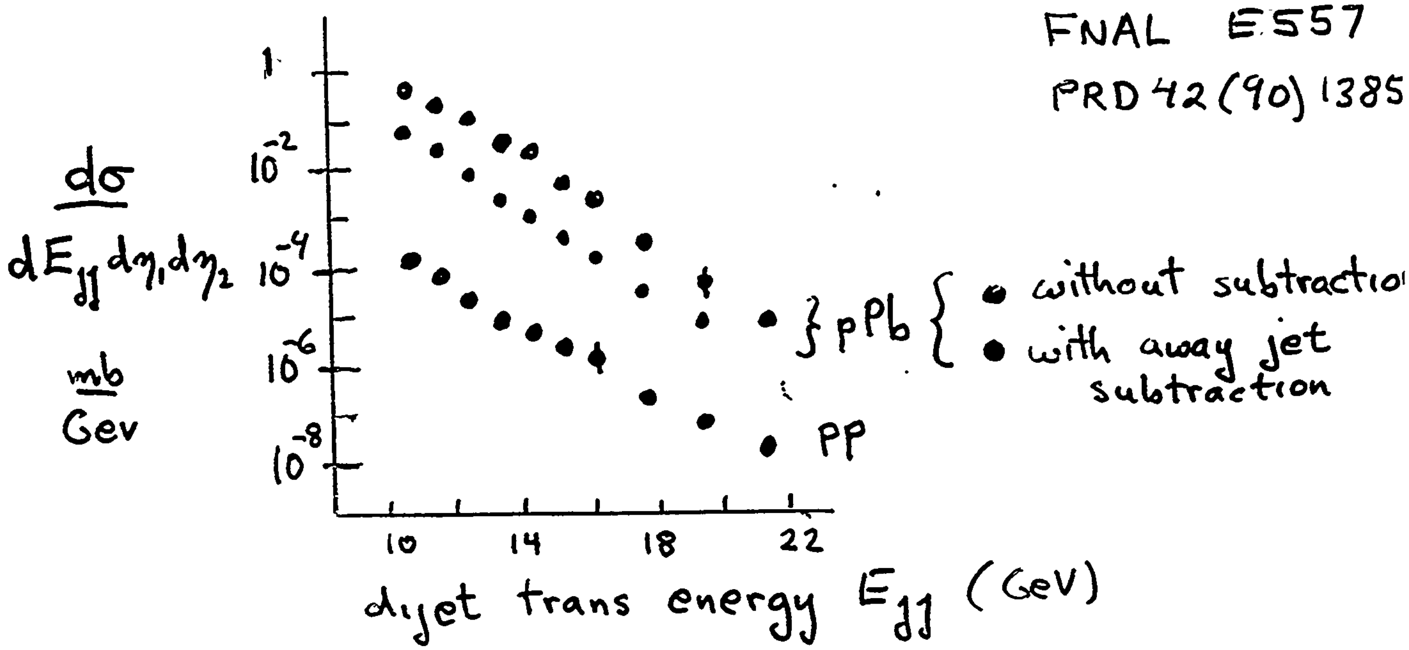

$$d\sigma^{pA} = A^{\alpha}\, d\sigma^{pp}$$

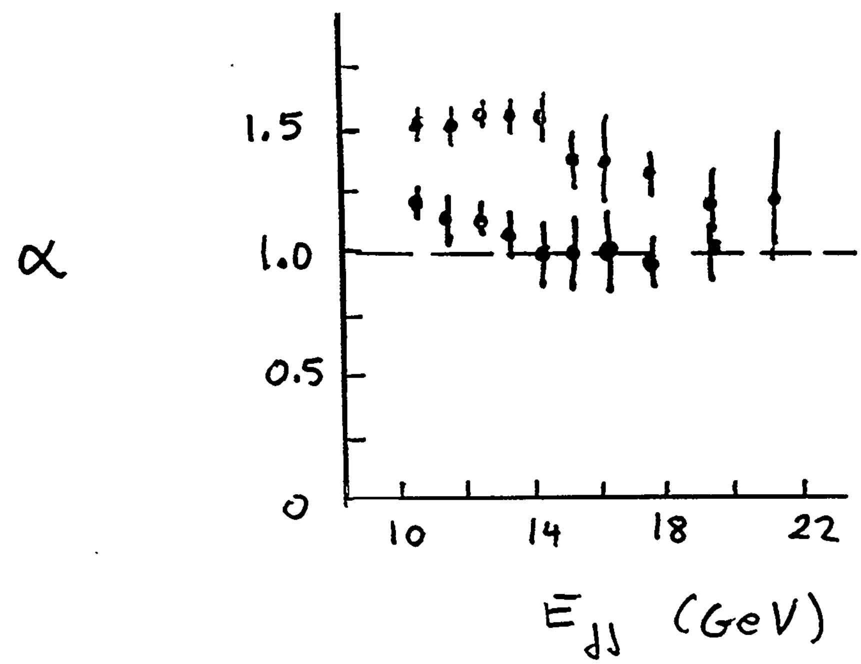

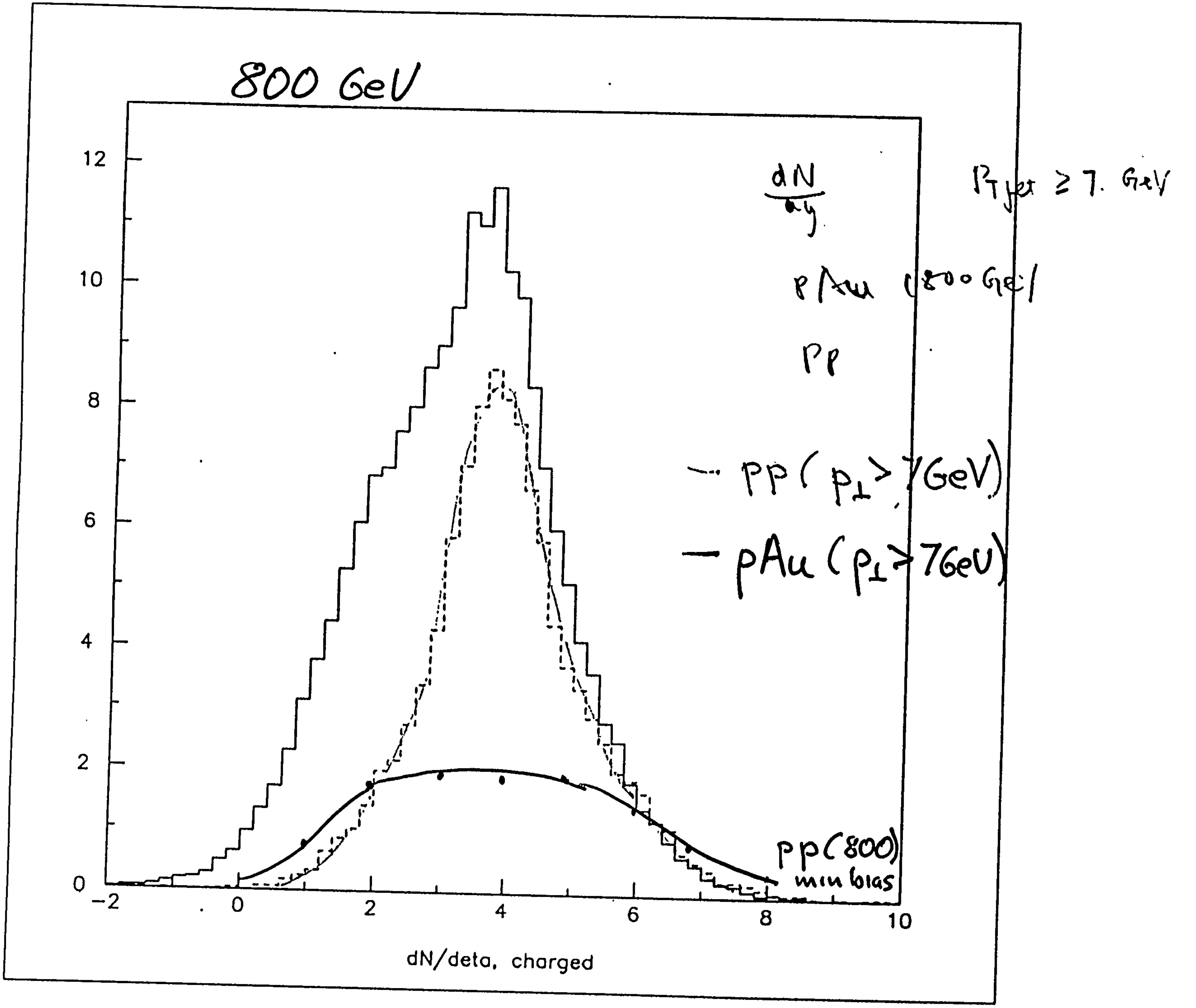

800 GeV
12
10
8
6
4
2
0
−2
0
2
4
6
8
10
dN/deta, charged
dN/dy
pAu (800 GeV)
pp
$P_{T\,jet} \geq 7.$ GeV
pp ($p_\perp$ > 7GeV)
pAu ($p_\perp$ > 7GeV)
pp(800) min bias

Why Jet Quenching is so small in p+A ?

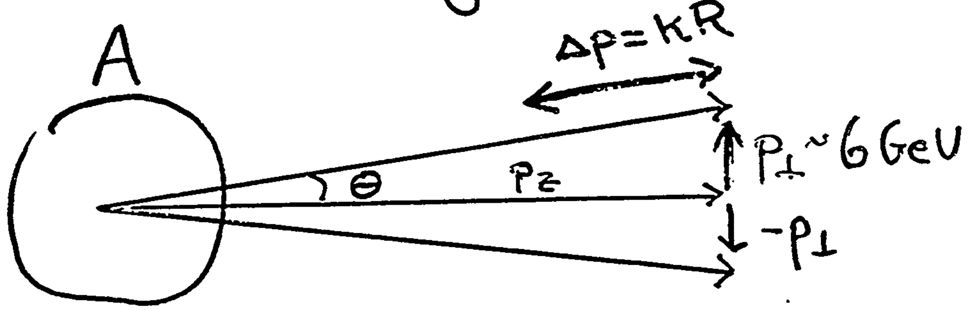

$P_z = P_\perp \gamma^*$

E_{lab}	γ^*
400	14
800	20

$\theta \sim \frac{1}{\gamma^*} \sim \frac{1}{20}$ rad

$$\Delta p \approx KR < 10 \text{ GeV}$$

$$\Delta p_\perp \approx \theta \Delta p = \frac{KR}{\gamma^*} < 2 \text{ GeV}$$

$$\text{If } \frac{d\sigma^{pp}}{dp_\perp} \propto \frac{1}{p_\perp^{q\sim 6}} \Rightarrow \frac{d\sigma^{pA}}{dp_{\perp f}} \propto \frac{A}{(p_{\perp f} + \Delta p_\perp)^q}$$

$$R^A = A\left(1 - q\frac{\Delta p_\perp}{p_\perp}\right) \equiv A^\alpha$$

$$-(\alpha - 1) \approx +q\frac{\Delta p_\perp}{p_\perp}\frac{1}{\log A} \approx +\frac{q\cancel{KR}}{p_\perp \gamma^*}\frac{1}{\cancel{\log} A}$$

$$< \underline{0.1}$$

Nuclear Dependence of High-x_t Hadron and High-τ Hadron-Pair Production in p-A Interactions at $\sqrt{s}=38.8$ GeV

P. B. Straub,[9] D. E. Jaffe,[8),(a] H. D. Glass,[8),(b] M. R. Adams,[8),(a] C. N. Brown,[4] G. Charpak,[2] W. E. Cooper,[4] J. A. Crittenden,[3),(c] D. A. Finley,[4] R. Gray,[9),(d] Y. Hemmi,[7] Y. B. Hsiung,[3),(b] J. R. Hubbard,[1] A. M. Jonckheere,[4] H. Jöstlein,[4] D. M. Kaplan,[5),(e] L. M. Lederman,[4),(f] K. B. Luk,[9),(g] A. Maki,[6] Ph. Mangeot,[1] R. L. McCarthy,[8] K. Miyake,[7] R. E. Plaag,[9),(h] J. P. Rutherfoord,[9),(i] Y. Sakai,[6] J. C. Santiard,[2] F. Sauli,[2] S. R. Smith,[3),(j] T. Yoshida,[7),(k] and K. K. Young[9]

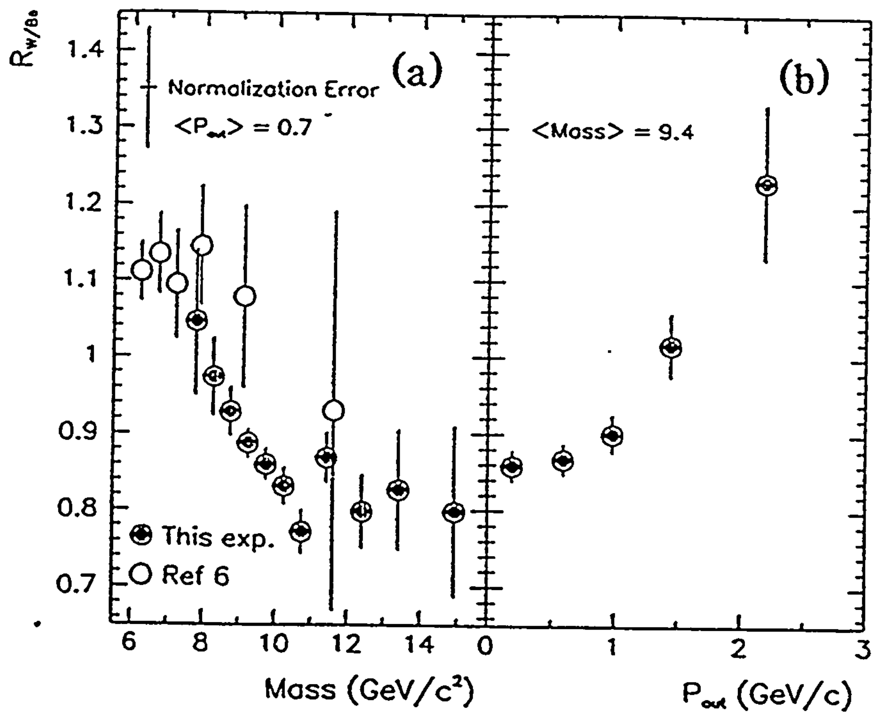

FIG. 3. W-to-Be ratio of per-nucleon cross section, $R_{W/Be}$, vs (a) mass and (b) p_{out} for h^+h^- pairs.

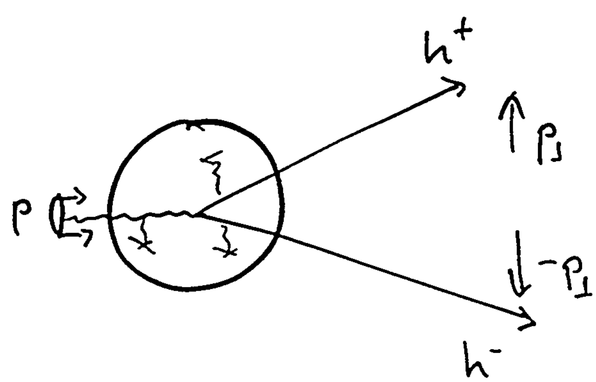

$M \simeq 2p_\perp \qquad y_{cm} \simeq 0$

Nuclear Gluon Shadowing via
Continuum Lepton Pairs

Ziwei Lin
Columbia University

Nuclear Gluon Shadowing via Continuum Lepton Pairs in $p-A$ at $\sqrt{s}=200$ AGeV

Ziwei Lin

[a]

HERA

11/18, 95

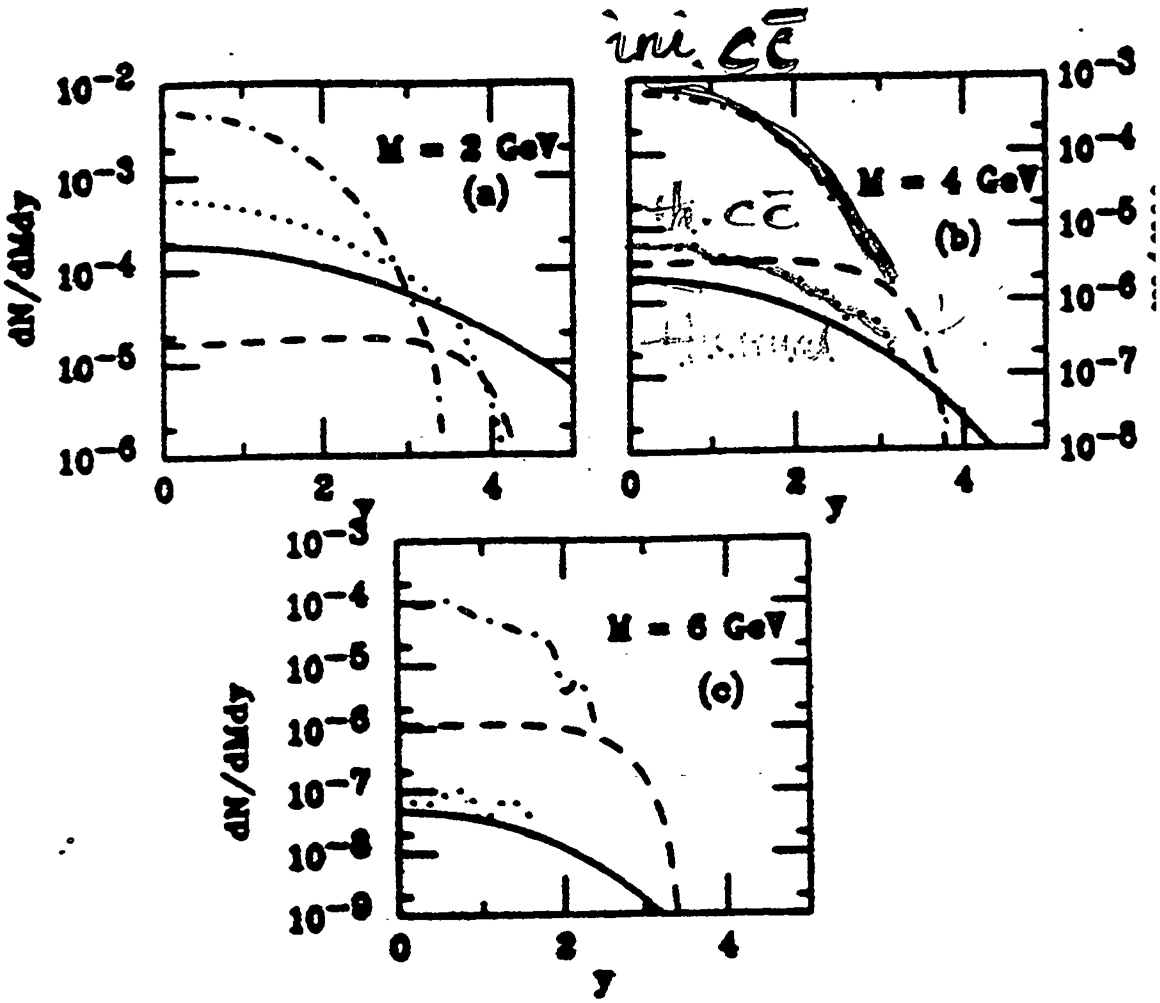

FIG. 5. We compare the contributions to the dilepton spe trum at RHIC for (a) $M=2$ GeV, (b) $M=4$ GeV, and (c) $M=$ GeV. Drell-Yan (dashed), direct thermal dileptons with $C=$ (solid), thermal (dotted) and initial (dot-dashed) charm produ tion are included.

PRD49, 3345

3

 NPS400

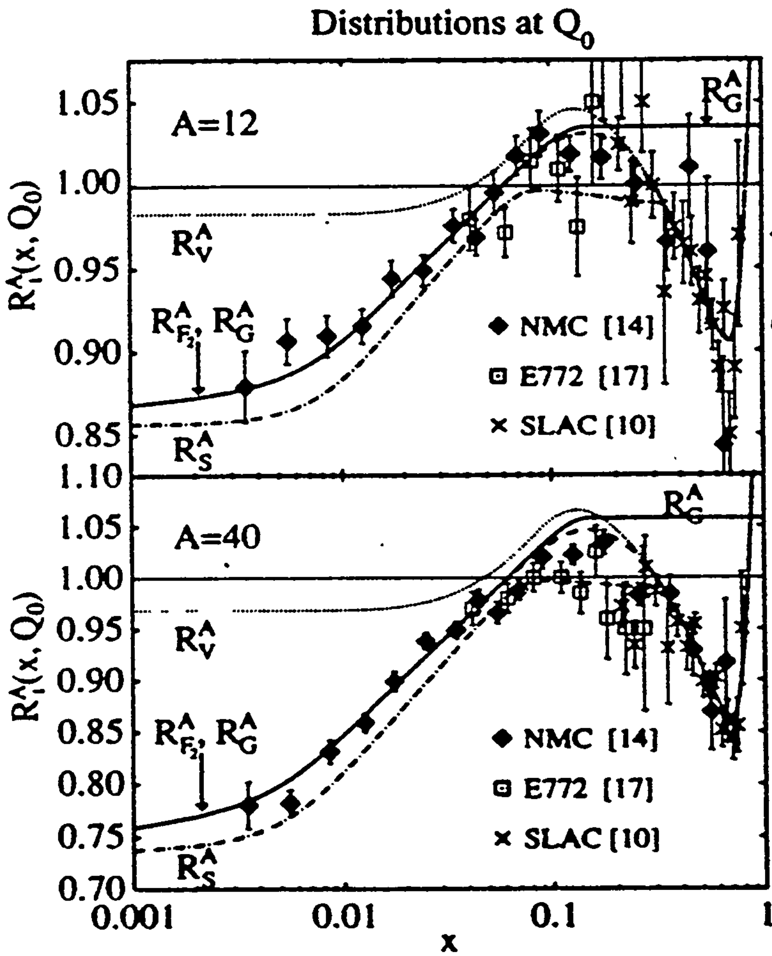

Data on gu
No data on gluons

Fig. 1. The ratios of the parton distributions in a nucleus A to the ones in deuteron (a): ^{12}C, (b): ^{40} at an initial scale $Q = Q_0 = 2$ GeV, as defined in eqs. (5) and (8). Only our 'ansatz 1' is shown for gl ratio R_G^A (solid line). The data points shown are the deep inelastic NMC 200 GeV μA data (diamonds) and the SLAC 8–24.5 GeV eA data [10] for the ratio $R_{F_2}^A$ (crosses), and the E772 800 C pA Drell–Yan data [17] corresponding to the ratio R_S^A (boxes). The parametrization (A.1) of R_F^A plotted with a dashed line. Valence quarks, R_V^A, are shown by the dotted line, and seaquarks, R_S^A the dotted-dashed line.

4

Leading order:

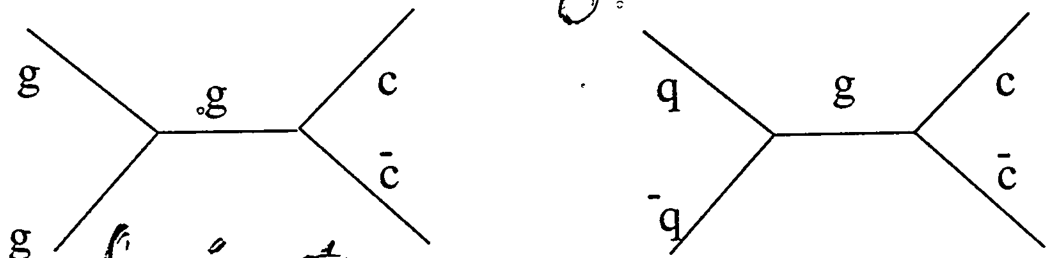

dominates

pre-equilibrium charm production

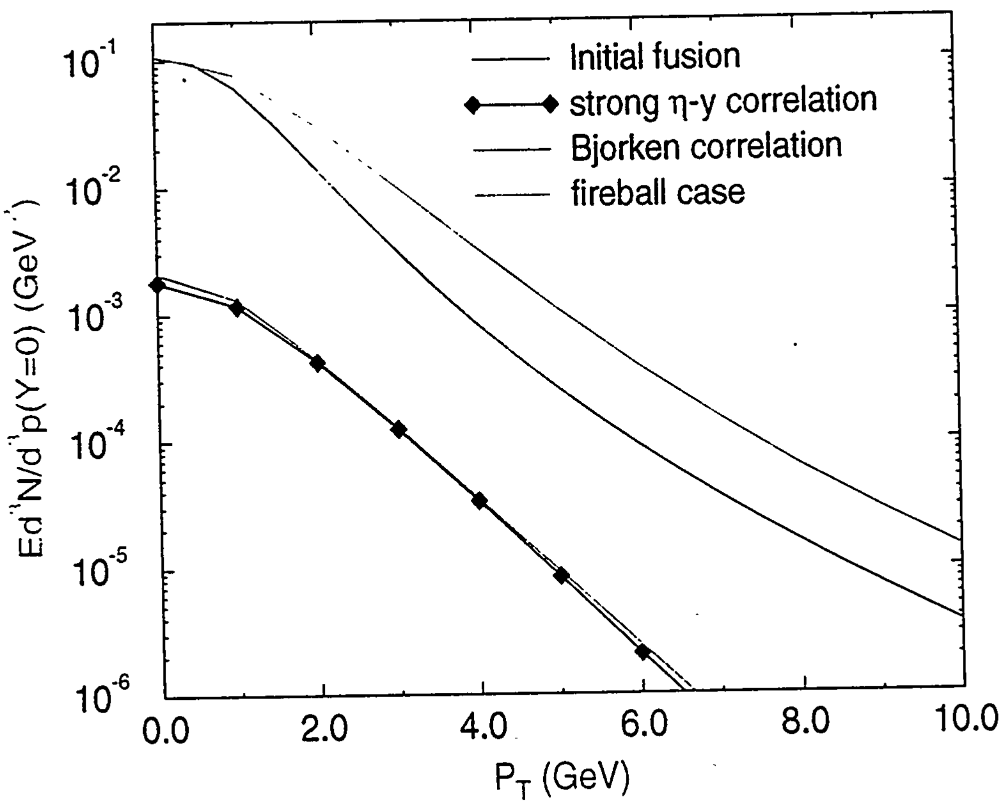

Z. Lin and M. Gyulassy, Phys. Rev. C51, 2177 (1995).

Unknown...

Two gluon shadowing functions

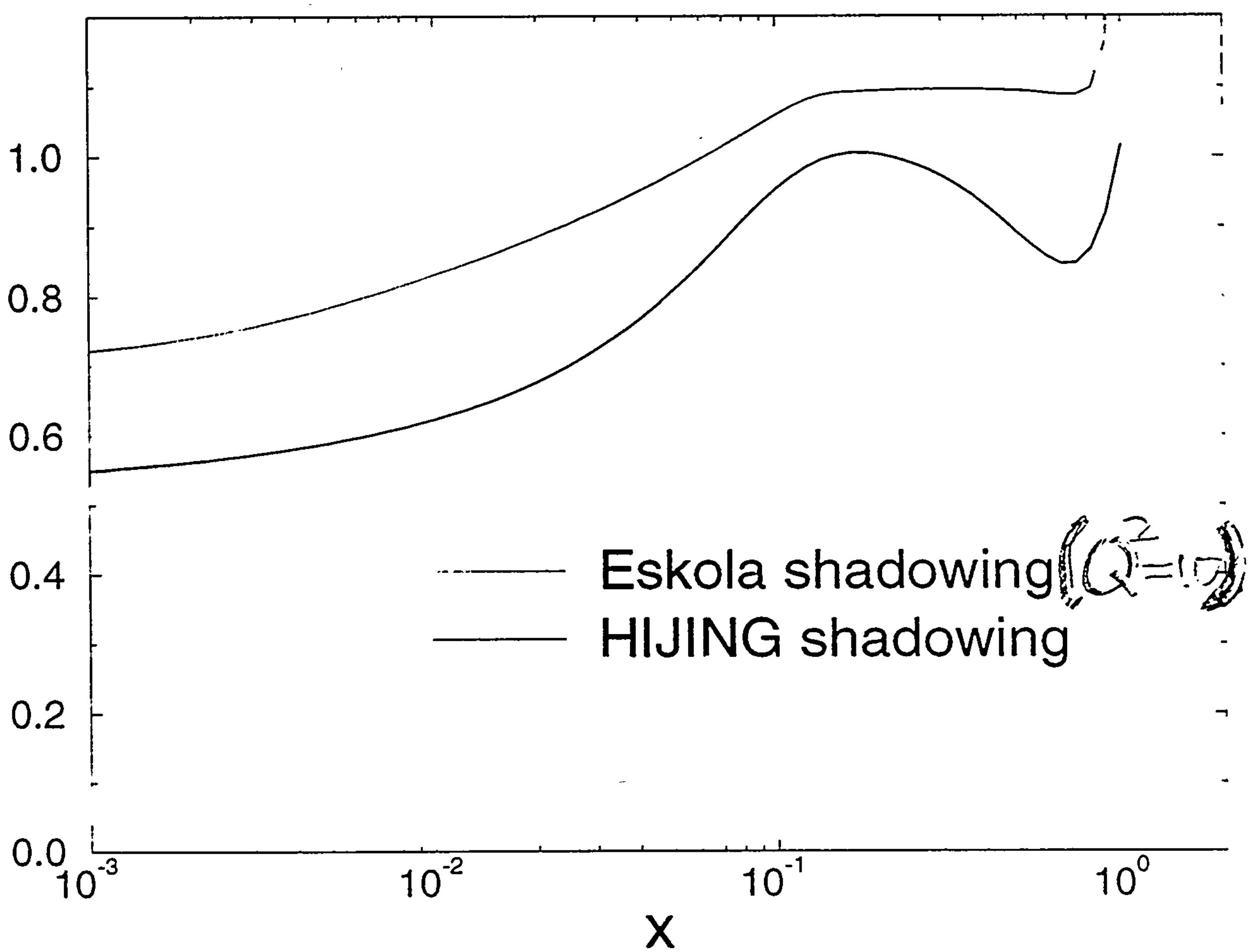

1. Lepton pair spectrum ($ee.e\mu.\mu\mu$)
from open charm decay

Two commonly used shadowing scenarios:
a: independent of scale or component[a].
b: scale and component-dependent shadowing[b].
Dilepton signals with different invariant masses scale approximately to the shadowing curve :
— a sensitive probe for nuclear shadowing.

2. Estimate signal-to-background in detector

Consider:

detector suppression of background leptons.

RHIC detector geometry, kinematical cut.

The signal-to-background ratio is promising.

---

[a] [illegible]

Shadowing in $D/\bar{D}$ production

{ delta-function fragmentation: $D(z) = \delta(1-z)$
Lund string fragmentation, etc.

$$\frac{dN^{p-Au}}{dp_\perp^2 dy_3 dy_4} \propto \sum_{a,b} x_a f_a(x_a, Q^2) x_b f_b(x_b, Q^2)$$

$$\times \quad R^{p-Au}_{b/Au}(x_b, Q^2) \frac{d\sigma_{ab}}{d\hat{t}} \frac{E_3 E_4}{E_1 E_2}$$

where $R^{p-Au}_{b/Au}(x_b, Q^2)$ is the shadowing for parton b in Au nucleus.

$\frac{dN}{dp_\perp{}^2 dy_3 dy_4} \Rightarrow D/\bar{D}$ events

$\Rightarrow D \rightarrow e + X$,$D \rightarrow \mu + X$ (BR:$\sim$ 12%)

$\Rightarrow \frac{dN}{dMdy}$[a] for ee, $e\mu$,$\mu\mu$

---

[a] $M = (p_e + p_\mu)^2$, $y = \tanh^{-1}[(p_e^{\parallel} + p_\mu^{\parallel})/(E_e + E_\mu)]$

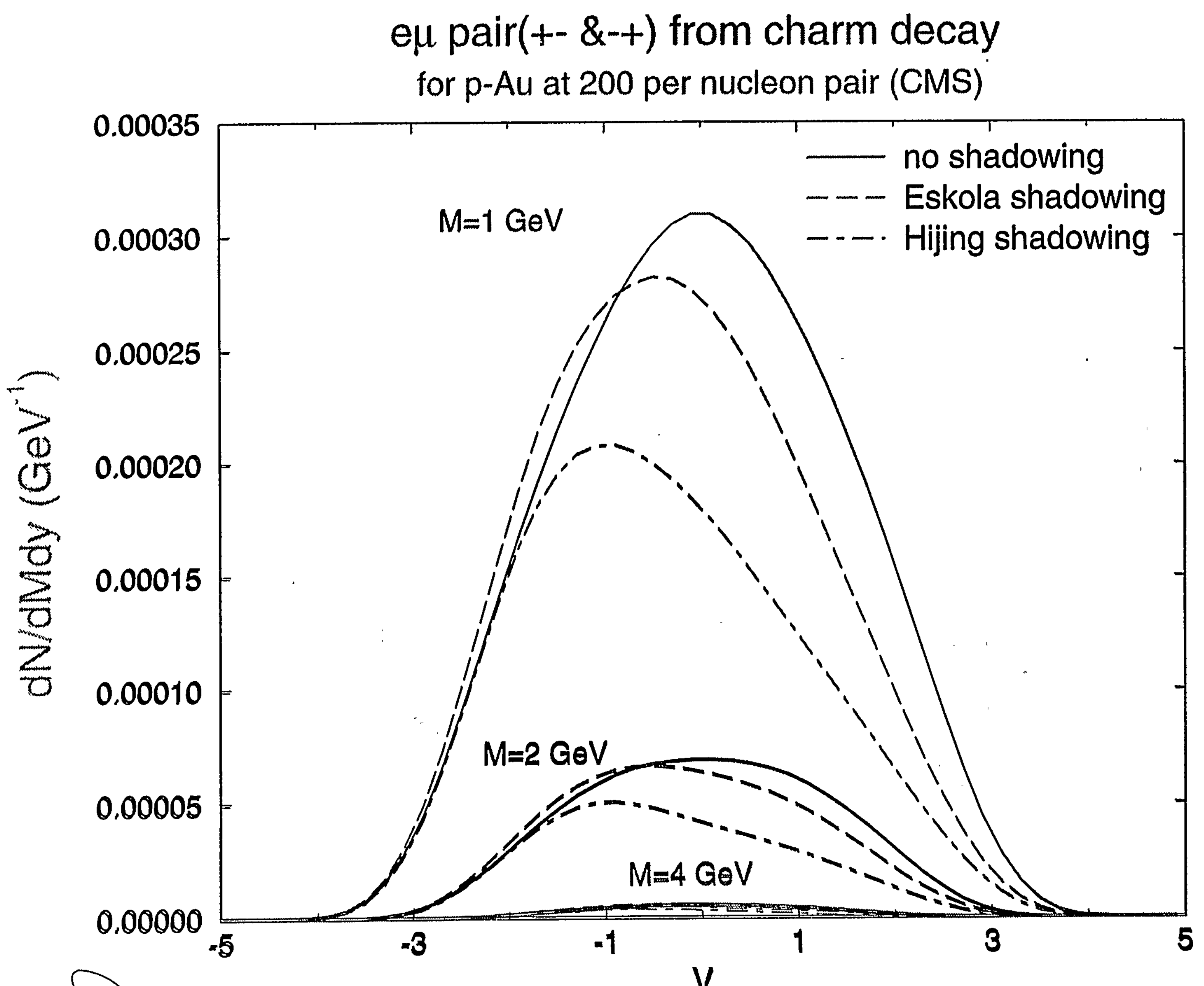
eμ pair(+- &-+) from charm decay
for p-Au at 200 per nucleon pair (CMS)
no shadowing
Eskola shadowing
Hijing shadowing
M=1 GeV
M=2 GeV
M=4 GeV
dN/dMdy (GeV^{-1})
0.00035
0.00030
0.00025
0.00020
0.00015
0.00010
0.00005
0.00000
-5
-3
-1
1
3
5
y

6

$$\frac{\frac{dN^{pA}}{dMdy}}{\nu \frac{dN^{pp}}{dMdy}} \; ; \quad \nu \equiv \frac{A\,\sigma^{pp}_{in.}}{\sigma^{pA}_{in.}}$$

dilepton dN/dMdy ratio as a function of rapidity

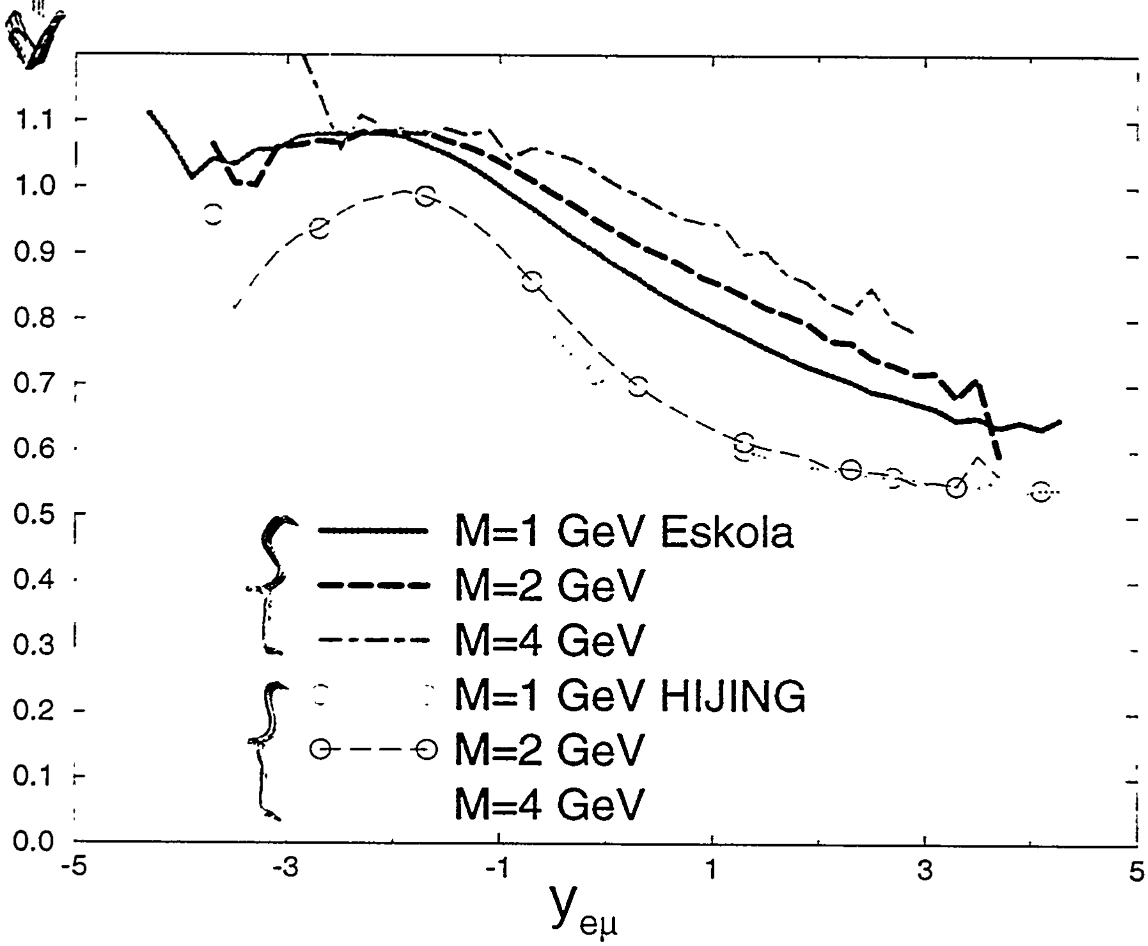

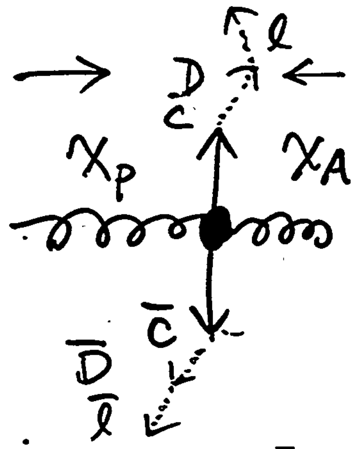

Scaling

For gluon fusion $gg \to c\bar{c}$:

$$
\begin{aligned}
x_A &= \frac{M_{c\bar{c}}}{\sqrt{s}} e^{-y_{c\bar{c}}} \\
\Rightarrow \ln x_A &= -y_{c\bar{c}} + \ln(M_{c\bar{c}}/\sqrt{s}) \\
&\approx -y_{e\mu} + \ln[\beta(M_{e\mu} + \Delta)/\sqrt{s}]
\end{aligned}
$$

$\Rightarrow$ approximate scaling among the observables $M_{e\mu}, y_{e\mu}$ and the shadowing variable x_A.

$\Rightarrow$

$$R^{pA}_{e\mu}(M_{e\mu}, y_{e\mu} \simeq -\ln x_A + \ln[\beta(M_{e\mu} + \Delta)/\sqrt{s}])$$
$$\equiv \frac{dN^{pA}_{e\mu}(shadowing)}{dN^{pA}_{e\mu}(no-shadowing)}$$
$$\approx R_{g/A}(x_A, Q^2 \sim [\beta(M_{e\mu} + \Delta)]^2/2)$$

mass mapping between eμ and c$\bar{c}$

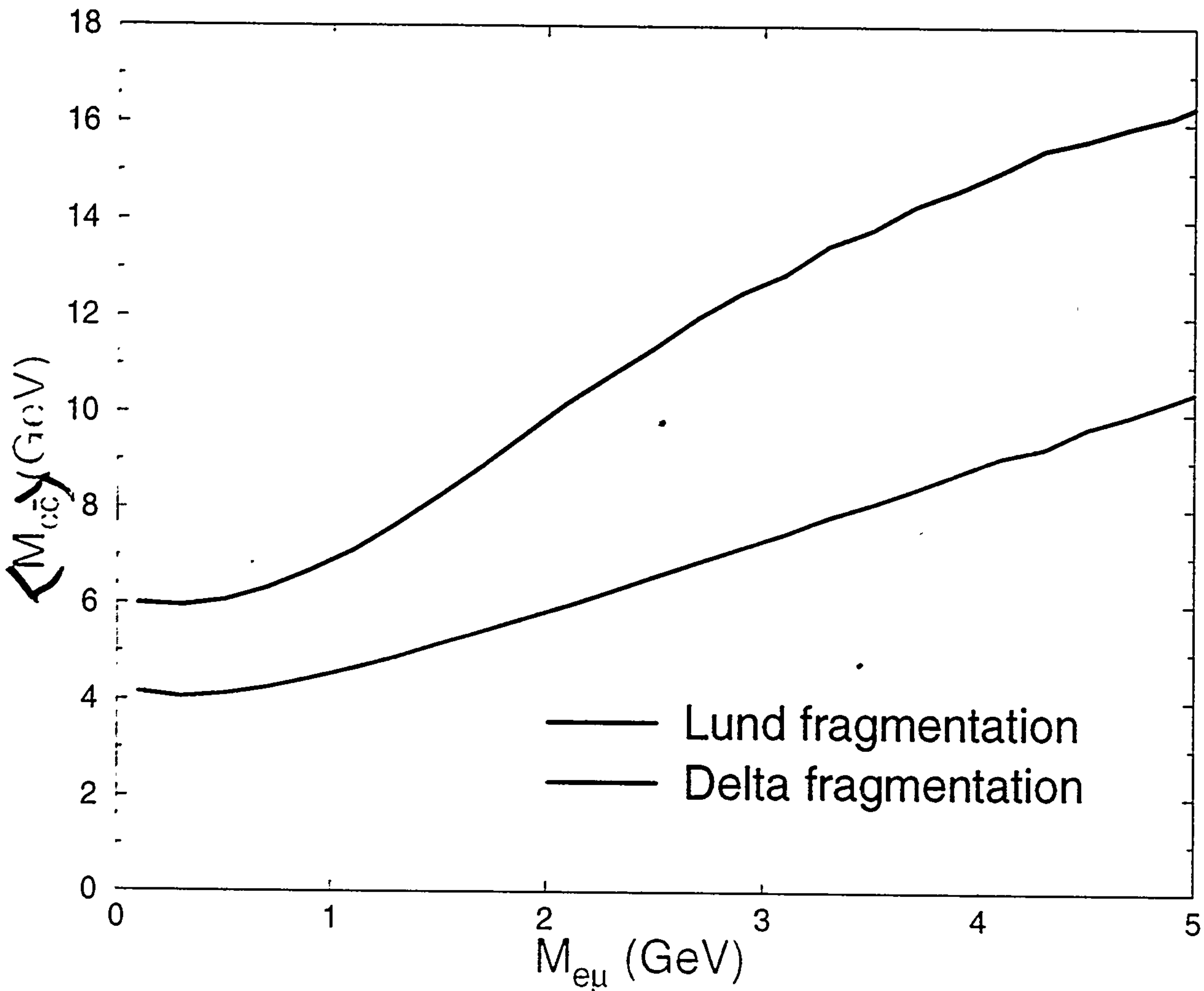

almost linear.

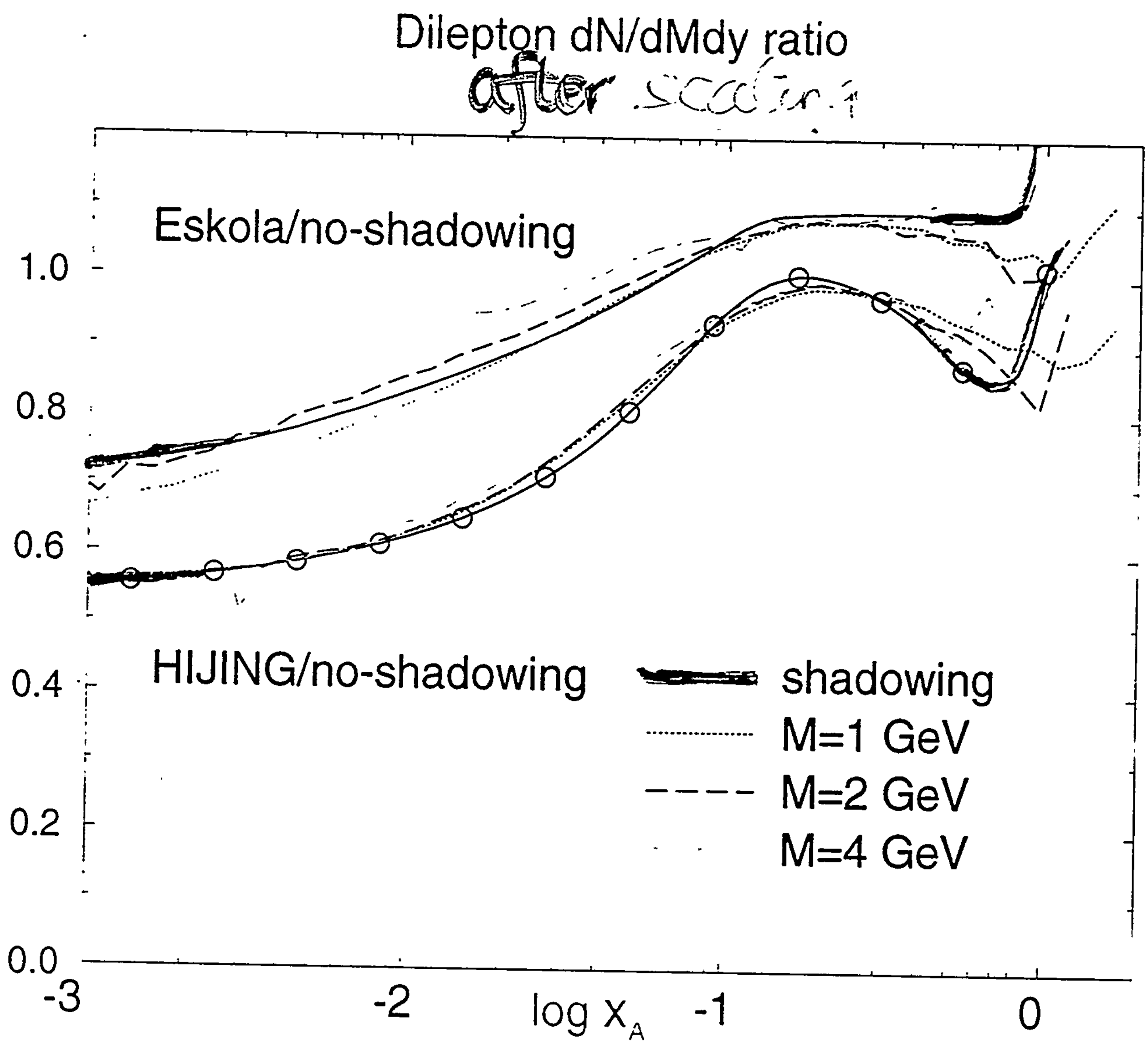
Dilepton dN/dMdy ratio
after scaling
Eskola/no-shadowing
HIJING/no-shadowing
shadowing
M=1 GeV
M=2 GeV
M=4 GeV
1.0
0.8
0.6
0.4
0.2
0.0
-3
-2
log x_A
-1
0

Background Estimates

electron background:

Dalitz decay (π^0, η, etc.), photon conversion.

muon background: random decays (π, K. etc.)

decay in the free space

before the hadron absorber.

decay from hadron leakage and

shower particles in muon arm.

generate background e and μ from the e and μ spectrums $dN/dp_\perp dy$ (produced from HIJING)

How many? We have to estimate:

1 RHIC detector geometry

2 a specific kinematical cut

3 detector suppression of background leptons

PHENIX

1 [redacted] detector geometry:

$-0.35 < \eta_e < 0.35$, $\phi_e \in \pm(22.5°, 112.5°)$

$1.15 < \eta_\mu < 2.44$ (Now we have second ar

2 a specific kinematical cut:

$E_e > 1$ GeV, $E_\mu > 2$ GeV, $\phi_{l^+l^-} > 90°$.

Due to detector geometry and kinematical cuts, the pair rapidity region covered by ee, $e\mu$ and $\mu\mu$ spectrums is 0. 1 and 2, respectively.

3 detector suppression of background leptons:

for electrons: suppression factor 5.

for muons: suppression factor 100.

4 Finally, Signal-to-Noise Ratio:

large (~ 200) for ee; ~ 2.5 for $e\mu$; $\sim 1/4$ for $\mu\mu$.

(like-sign subtraction?)

(DY for ...

Dilepton in detector: Signal to Noise

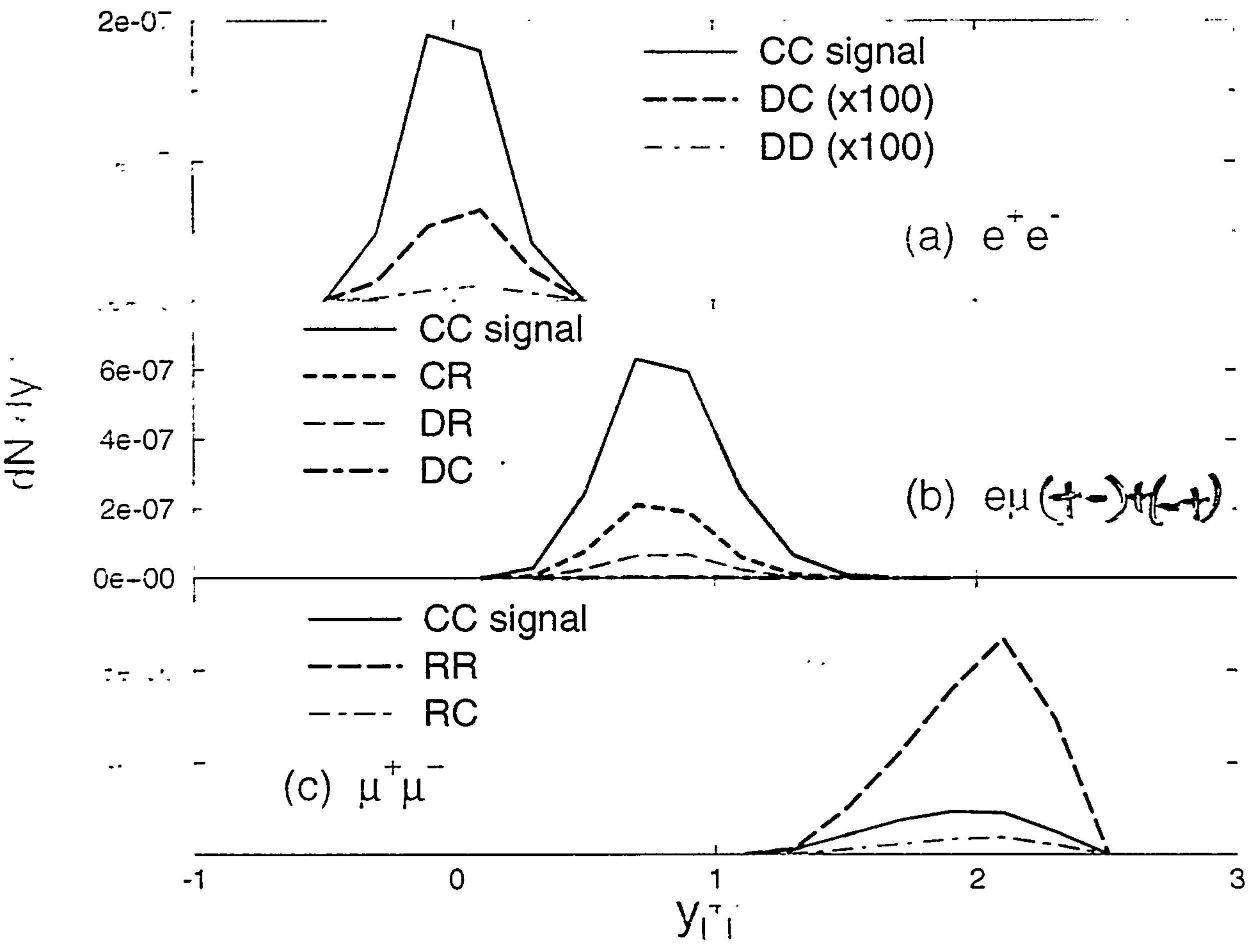

[illegible] C : from Charm (D/D̄)

D : π° Dalitz, photon conv.

R : Random decay

Summary:

Lepton pair (ee, $e\mu$ and $\mu\mu$) spectrums from open charm decay in two different shadowing scenarios have clear differences.

Nuclear shadowing effects is reflected nicely in the scaled ratios of lepton pair $dN/dMdy(M)$ spectra.

The charm decay signal can be seen in $p - Au$ collisions, some even before using like-sign subtraction.

HERA: ideal for xg from eA,

but when?

STAR: $D/\bar{D}$ directly.

D, K: $|y| \leq (\pm 1)$, $p_t > (0.5-1)$ GeV;

What can we learn from HERA with a colliding heavy ion beam?

Jianwei Qiu
Iowa State University

What can we learn from HERA with a colliding heavy ion beam?

Jianwei Qiu
Iowa State Univ.

1, Inclusive Process:

Nuclear Shadowing at small x

2, Semi-inclusive Process:

Multiple Scattering and Anomalous Nuclear dependence [large x only]

BNL Workshop
Nov. 18, 95

Nuclear Dependence at High Energy

* Scattering processes:

$$\begin{pmatrix} \text{lepton} \\ \text{hadron} \end{pmatrix} + A \Rightarrow \begin{pmatrix} \text{lepton} \\ \text{hadron} \\ \text{jet} \\ \vdots \end{pmatrix} + X$$

* Nucleus: A collection of A nucleons with the binding energy ~ 8 MeV/nucleon

* High Energy: energy exchange in the collision is much larger than a few GeV >> Nuclear binding energy

* Naive Expectation:

Any physical observable : $\frac{\sigma^A}{A}$

Would have very small A-dependence due to Nuclear density

* Experimental Results:

$$\text{Anomalous Nuclear dependence} \begin{cases} \text{Suppression} \\ \text{Enhancement!} \end{cases}$$

Nuclear Shadowing — suppression

NMC Collaboration: P. Amaudruz et al.

Z. Phys. C51, 387 (1991)

C57, 221 (1992)

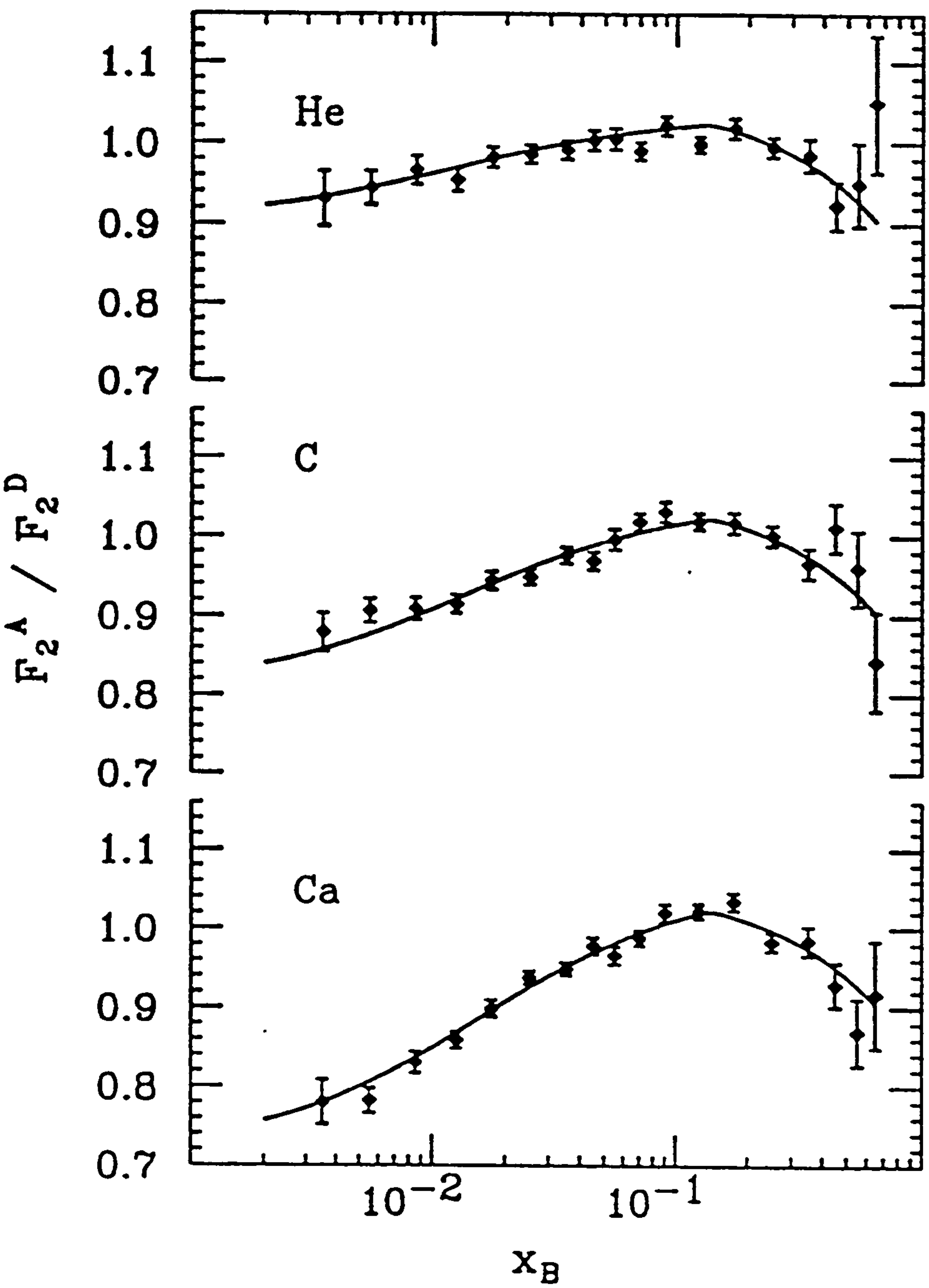

Figure 3

Cronin Effect :

P.B. Straub, et al. PRL. 68. 452 (1992)

$\alpha \approx 1.14 \quad \sigma_A = A^{\alpha}\sigma_0$

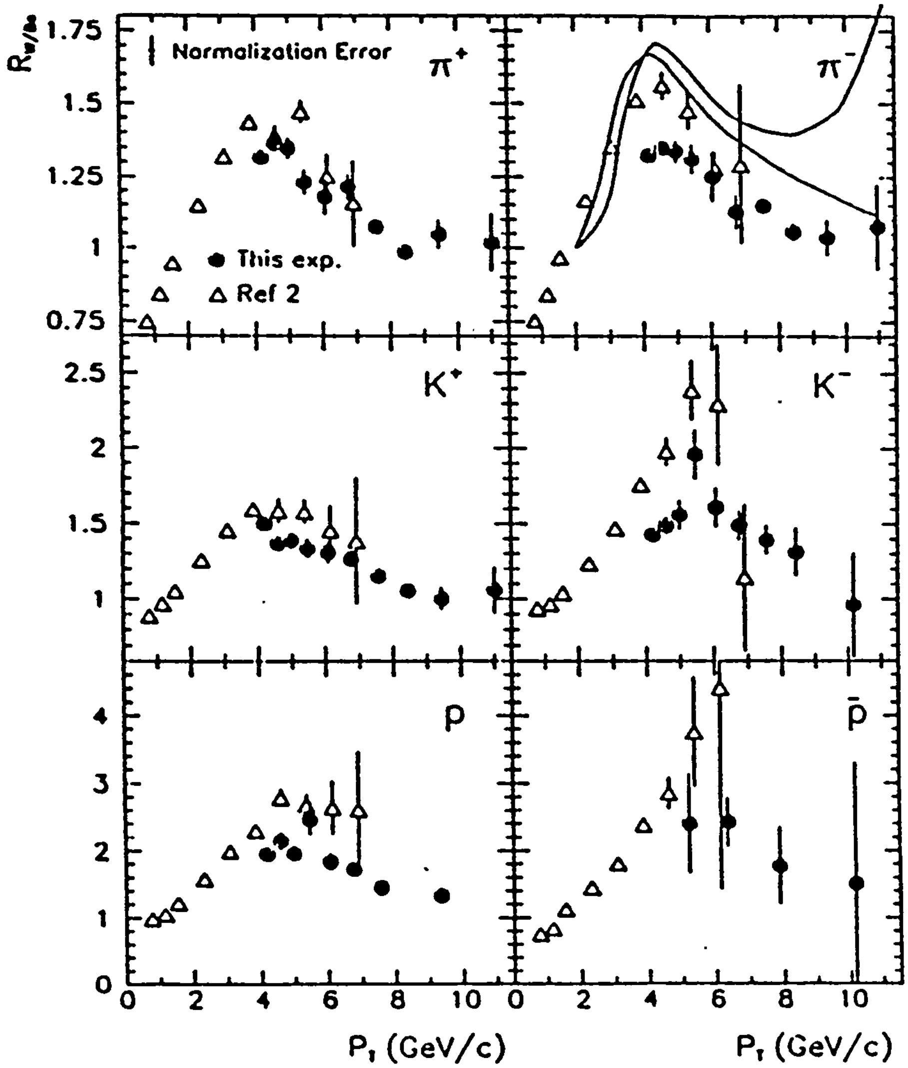

FIG. 1. W-to-Be ratio of per-nucleon cross sections, $R_{W/Be}$, vs p_t for each hadron species. Also shown are results [2] at $\sqrt{s}=27.4$ GeV and model calculations [12] for π^- at $\sqrt{s}=27.4$ GeV (upper curve) and $\sqrt{s}=51.3$ GeV (lower curve).

* Possible Interpretations :

— binding energy should have very little effect on observed anomalous nuclear dependence

— key in any explanation is the fact "Nucleons in a nucleus are very close to each other"

* Large x vs. small x :

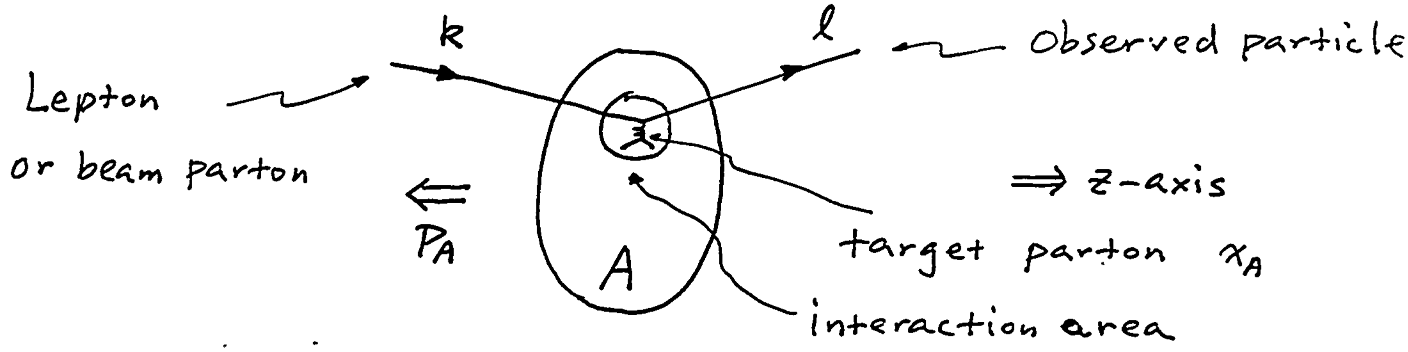

- Size of interaction area :

— Transverse Size $\sim 1/Q \ll 1\,\text{fm}$ "Localized"

— Longitudinal Size $\sim \Delta z_x \sim \frac{1}{x_A P}$

Longitudinal Size of a nucleon : $\Delta z_n \sim 2r\left(\frac{m}{P}\right)$

- Nuclear dependence :

— $\Delta z_x > \Delta z_n \Leftrightarrow x_A < x_c \sim \frac{1}{2mr} \sim 0.1$ } Small x

More than one nucleon involved in Collision

— $\Delta z_x < \Delta z_n \Leftrightarrow x_A > 0.1$ } large x

Single scattering is Localized

* Conclusions without detail calculation:

— Small-x region:

Anomalous nuclear dependence <u>due to coherence</u> of multi-nucleons (or partons from multi-nucleo involved <u>in the interaction area</u>.

Coherence $\Rightarrow$ Suppression

— Large-x region:

Anomalous nuclear dependence <u>due to multiple scattering</u> covering different nucleons.

Note:

- Anomalous nuclear dependence

  $\sim$ power dependence of A

- Multiple scattering can also take place in small-x region (Not to discuss today)

Nuclear Shadowing at Small x

* What data try to tell us ?

— small Q^2-dependence at fixed value of x

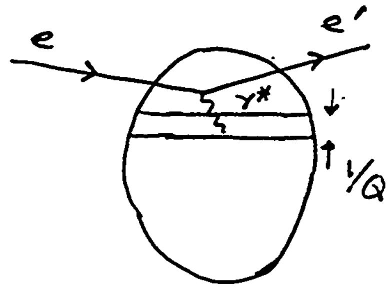

Not much dependence on transverse size

$\Rightarrow$ Shadowing due to <u>coherence in Longitudinal direction</u>.

— Smaller value of x, Stronger shadowing

$\left\{ \begin{array}{l} \text{more nucleons involved} \\ \text{more partons are overlap} \end{array} \right.$

$\Rightarrow$ shadowing proportional to number of partons overlapped at the same impact parameter

$\Rightarrow$ Parton recombination at small x

Note :

- Recombination can decrease # of Partons at x by

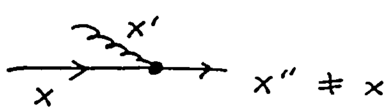

- Recombination can also increase # of Partons at x

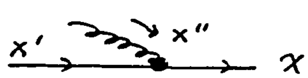

* Parton Recombination to shadowing:

Mueller, Qiu
Close, Qiu, Rober
Eskola, Qiu, Wan

— $\sigma^{\gamma^* A} \sim \mathrm{Im}\,(F_{\underbrace{\gamma^* A \to \gamma^* A}_{\text{Forward scattering amplitude}}})$

- Single parton:

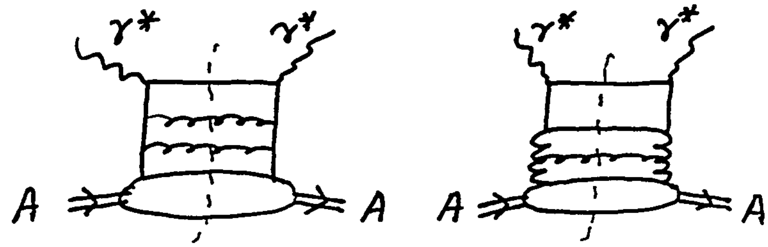

- Two partons:

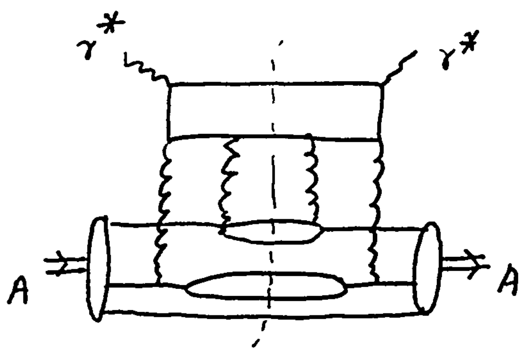

\+

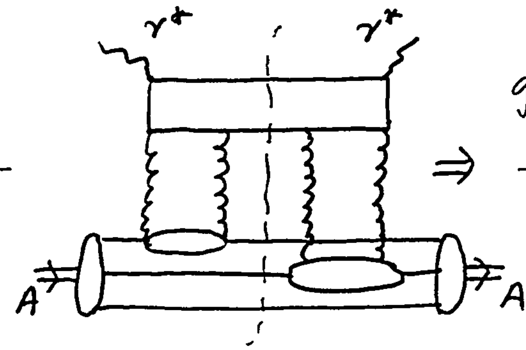

$\Rightarrow$ give <u>positive</u> contribu

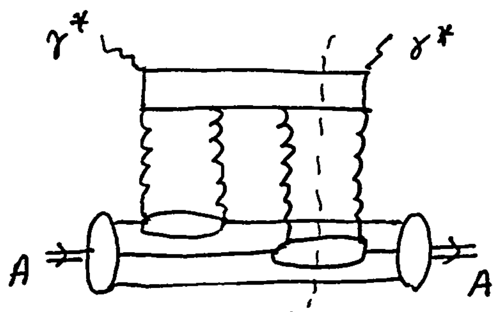

\+ c.c. $\Rightarrow$ give <u>Negative</u> contribution

Net contribution at small-x is negative

$\Rightarrow$ shadowing

* Two type of Contribution to shadowing :

— Directly contribute to structure Functions ($\sim \sigma^{\gamma^* A}$):

$$F_2^A(x_B, Q^2) = \sum_f \Big\{ \underbrace{C_2^f(x_B, Q^2/\mu^2, \alpha_s)}_{\text{twist-2 Coef. functions}} \otimes \overbrace{\Phi_{f/A}(x, \mu^2)}^{\text{Twist-2 Parton distribution}}$$

$$+ \frac{1}{Q^2} \underbrace{C_4^f(x_B, Q^2/\mu^2, \alpha_s)}_{\text{twist-4 Coef. func.}} \otimes T_{f/A}\underbrace{(x_1, x_2, x_3, \mu^2)}_{\text{twist-4 Matrix-element}} \Big\}$$

from parton recombination

Vanish as $1/Q^2$

— Contribute to the evolution of Structure Functions :

$$\frac{\partial}{\partial \ln Q^2} F_2^A(x_B, Q^2) = \frac{\alpha_s}{2\pi} \gamma(x_B) \otimes F_2^A(x, Q^2) + \cdots$$

$$- \underbrace{\frac{\alpha_s^2}{Q^2 R^2} \cdot C \cdot \bar{\gamma}_f(x_B) \otimes T_{f/A}(x, Q^2)}_{\text{from parton recombination}} + \cdots$$

Vanish as $\frac{1}{Q^2}$ for the "slope".

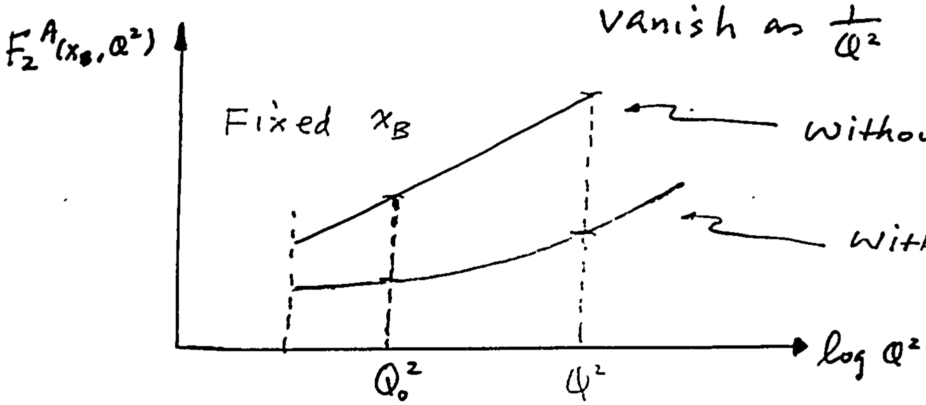

without shadowing & Normal evolution

with shadowing & GLR type Evolution

$\frac{1}{Q^2}$ term in evolution generates shadowing at Low Q_0^2.

$\Rightarrow$ Ratio of F_2^A should have weak Q^2 dependence.

* Explicit example to show "Parton Recombination generates shadowing not vanish as $\frac{1}{Q^2}$"

by direct integration of the Modified evolution equation (GLR equation) from Q_0^2 to Q^2

$$F_2(x_B,Q^2) = \underbrace{\int_{Q_0^2}^{Q^2} \frac{d\bar{Q}^2}{\bar{Q}^2}\left[\frac{\alpha_s}{2\pi}\,\gamma(x_B)\otimes F_2^A(x,\bar{Q}^2)+\cdots\right] + F_2^A(x_B,Q_0^2)}_{F_2^A(x_B,Q^2)_{DGLAP}}$$

$$-\int_{Q_0^2}^{Q^2} \frac{d\bar{Q}^2}{\bar{Q}^4}\left[\frac{\alpha_s}{R^2}\cdot c\cdot \bar{\gamma}_f(x_B)\otimes T_{f/A}(x,\bar{Q}^2)+\cdots\right]$$

$$= F_2^A(x_B,Q^2)_{DGLAP}$$

$$-\underbrace{\int_{Q_0^2}^{\infty} \frac{d\bar{Q}^2}{\bar{Q}^4}\left[\frac{\alpha_s}{R^2}\cdot c\cdot \bar{\gamma}_f(x_B)\otimes T_{f/A}(x,\bar{Q}^2)+\cdots\right]}_{F_2^A(x_B,Q_0^2)_{GLR}} \rightarrow \text{Finite as } Q^2 \rightarrow$$

$$+\underbrace{\int_{Q^2}^{\infty} \frac{d\bar{Q}^2}{\bar{Q}^4}\left[\frac{\alpha_s}{R^2}\, c\cdot \bar{\gamma}_f(x_B)\otimes T_{f/A}(x,\bar{Q}^2)+\cdots\right]}_{\frac{1}{Q^2}\tilde{F}_2^A(x_B,Q^2)_{H.T.}} \rightarrow \text{Vanish as } \frac{1}{Q^2}$$

arbitary cho

$$\Rightarrow F_2(x_B,Q^2) = \underbrace{F_2^A(x_B,Q^2)_{DGLAP} - F_2^A(x_B,Q_0^2)_{GLR}}_{F_2^A(x_B,Q^2)_{L.T.}}$$

$$+\frac{1}{Q^2}\tilde{F}_2^A(x_B,Q^2)_{H.T.}$$

* Solution of GLR (Eskola, Qiu, Wang)

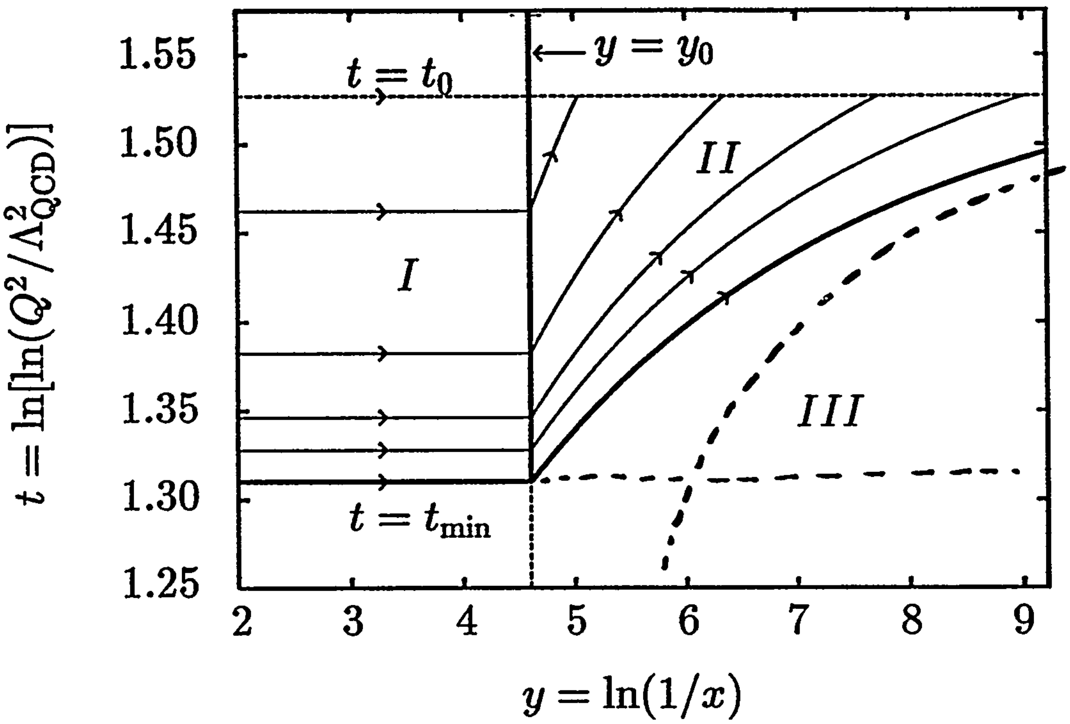

Fig. 1

Figs. 2 a,b

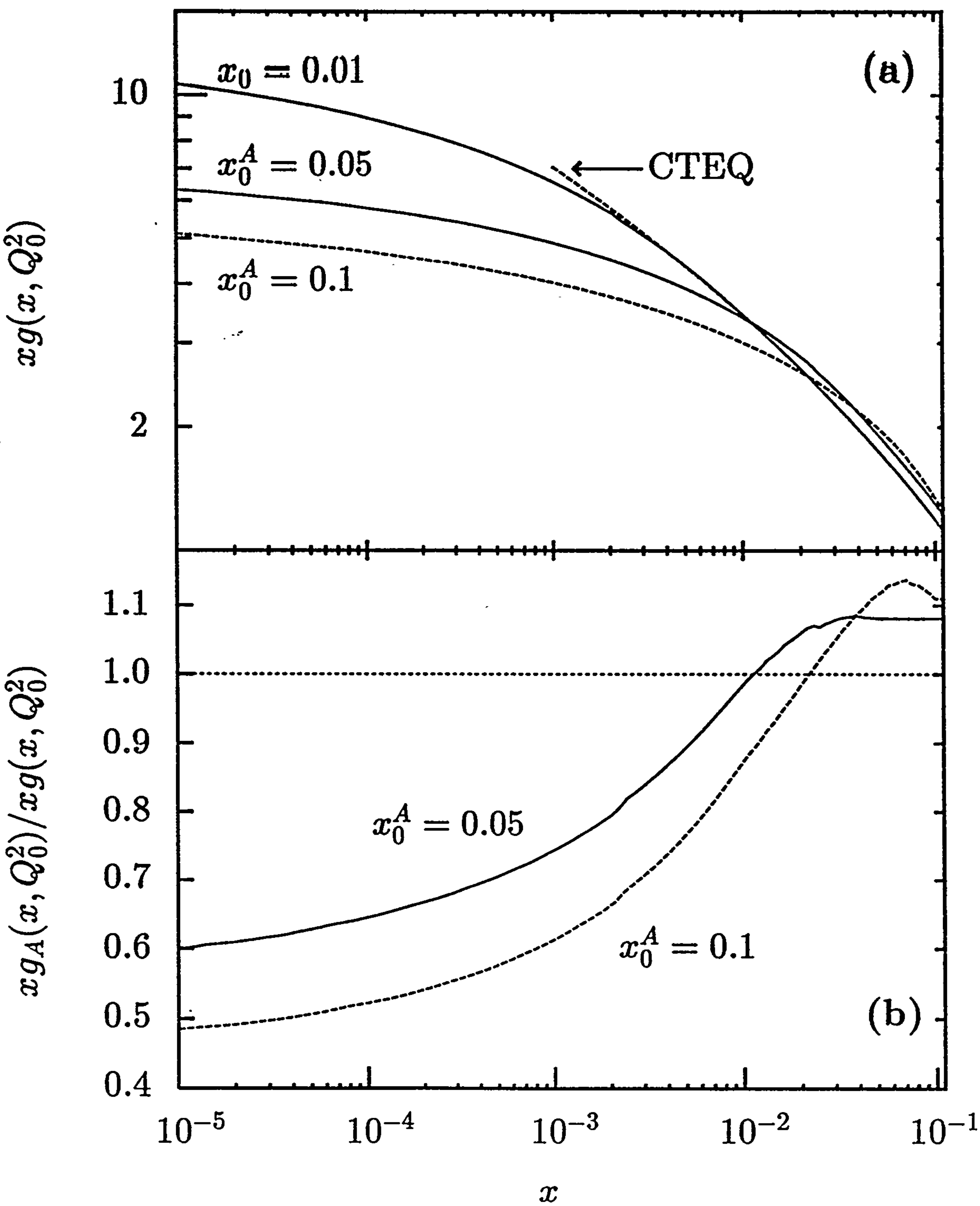

(a)
$x_0 = 0.01$
$x_0^A = 0.05$
$x_0^A = 0.1$
CTEQ
10
2
$xg(x, Q_0^2)$
(b)
$x_0^A = 0.05$
$x_0^A = 0.1$
1.1
1.0
0.9
0.8
0.7
0.6
0.5
0.4
$xg_A(x, Q_0^2)/xg(x, Q_0^2)$
10^{-5}
10^{-4}
10^{-3}
10^{-2}
10^{-1}
x

Nuclear Enhancement at Large x

* For semi-inclusive process, $x_{Bj} \neq x_{parton}$

— Kinematics :

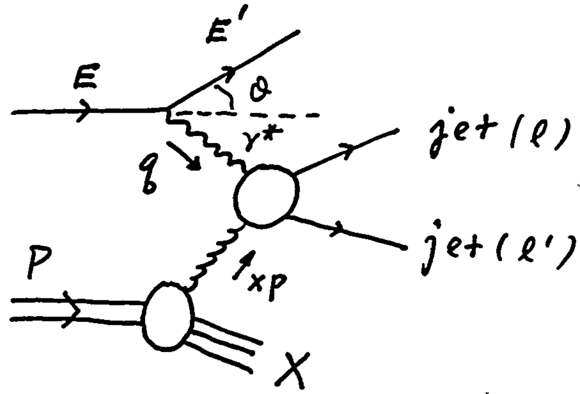

— photon–nucleon frame :

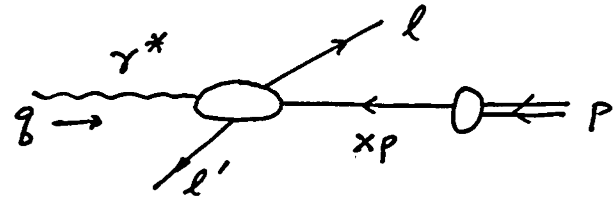

$\bar{n}^\mu = (1, 0, 0_\perp)$ (components $+$, $-$, $\perp$)

$n^\mu = (0, 1, 0_\perp)$

$$p^\mu = P\bar{n}^\mu, \quad q^\mu = -x_B p^\mu + \frac{Q^2}{2x_B P} n^\mu$$

$$\Rightarrow \quad q^2 = -Q^2, \quad x_B = \frac{Q^2}{2p\cdot q}$$

— "$\sqrt{s}$" for photon - nucleon scattering :

$$W = \sqrt{(p+q)^2} \simeq \sqrt{Q^2\left(\frac{1}{x_B}-1\right)}$$

— "$\hat{s}$" for the photon-parton scattering :

$$\hat{s} = (xp+q)^2 = Q^2\left[\frac{x-x_B}{x_B}\right]$$

$$\Leftrightarrow \quad x_{parton} = x_B\left(1+\frac{\hat{s}}{Q^2}\right) > x_B \quad \text{for } \hat{s} \neq 0$$

(

* Two-jet events in DIS (or 2+1 Jets including beam Jet)

$$\hat{S} \gtrsim (\ell+\ell')^2 \geqslant 4\ell_T^2 \quad \text{or } x_{parton} \geqslant x_B\left(1+\frac{4\ell_T^2}{Q^2}\right)$$

— DIS with fixed nuclear target (e.g. E665 Kinematic

$W \sim 20$ GeV, $x_B \sim 0.01 \sim 0.03$, $Q^2 \approx 4\,\text{GeV}^2$

$\Rightarrow x_{parton} \gtrsim 0.17$ if $\ell_T = 4$ GeV

out of shadowing region!

$\Rightarrow$ Nuclear dependence in Jets ~ Large-x physic

(Multiple scatteri

— DIS with colliding heavy ion beam (HERA ?)

$Q^2 \approx 4\,\text{GeV}^2$, $x_B \gtrsim 10^{-5}$

$\Rightarrow x_{parton} \geqslant x_B\left(1+\frac{4\ell_T^2}{Q^2}\right) \sim 1.7\times10^{-4}$ if $\ell_T = 4$ GeV

in shadowing region!

$\Rightarrow$ Measure gluon <u>shadowing</u> to very small x.

But, final state interaction between Jet and nuclear matter <u>enhance</u> the cross section.

Who wins? Shadowing or multiple scattering

(even at $\ell_T \gtrsim 10$ GeV, $x_{parton} \sim 10^{-3}$

* How well we understand the multiple Scattering?

Luo, Qiu, Sterman

—. Hard - Soft vs. hard - hard double scattering

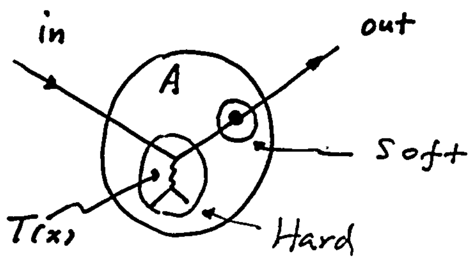

Soft Scattering effectively Change the partonic flux.

$$\frac{1}{k_T^2}\frac{\partial^2}{\partial x^2}\left(\frac{T^A(x)}{x}\right), \quad \frac{1}{k_T^2}\frac{\partial}{\partial x}\left(\frac{T^A(x)}{x}\right), \; \frac{}{k}$$

↳ dominate if x is Large

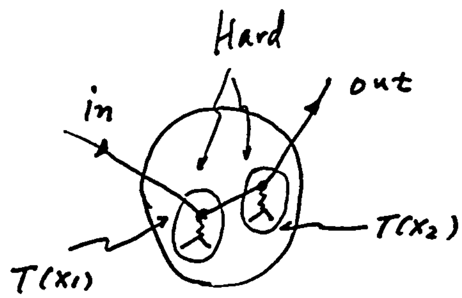

Double hard scattering

change k_T-spectrum directly

example:

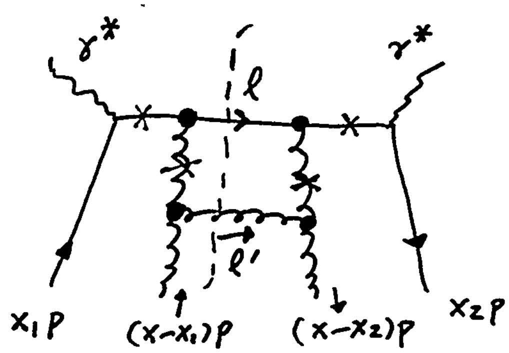

$P \sim (+)$, com.
$\gamma^* \sim (+,-)$
$\sim (-)$
$\sim (+)$

x-x poles ⇒ double Hard scattering

x-x poles ⇒ Hard-soft scattering

— Independent Scattering picture is infrared sensitive.

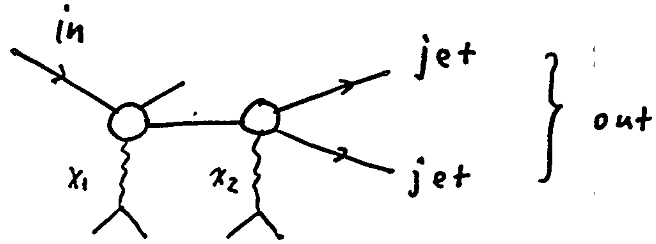

Kinematics fix only $x_1 + x_2$ = finite,

potential Infrared divergence when $x_1 =$
or $x_2 =$

— Interference takes care of all infra sensitivity.

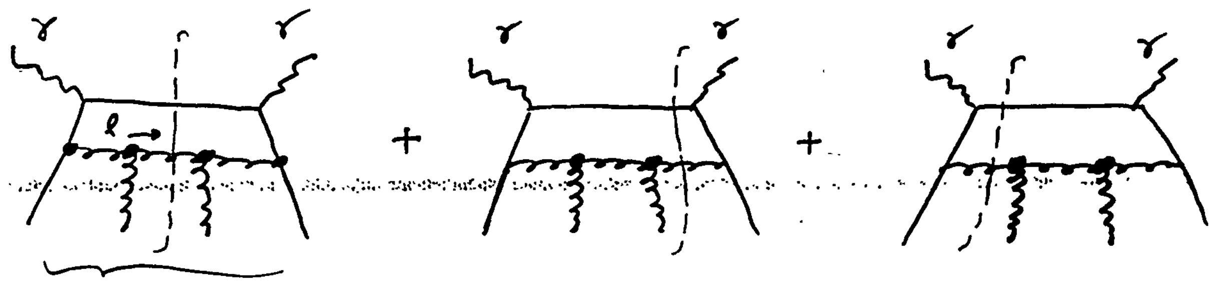

3 - independent momentum fractions

- 2 of 3 momentum fractions integrated by Contour integration, No pinch singularity
- 3^{rd} momentum fraction treated in the same way as the case single scattering

— Only real diagram ("symmetric") contribute to nuclear enhancement.

$\Longrightarrow$ Double scattering picture preserved.

— Leading pole contribution to anomalous nuclear dependence is important only when effective x_A is large.

double scattering $\sim \quad \frac{1}{k_T^2}\, x^2 \frac{\partial^2}{\partial x^2}\left(\frac{T(x)}{x}\right),\ \frac{1}{k^2}\, x \frac{\partial}{\partial x}\left(\frac{T(x)}{x}\right),\ \frac{1}{k_T^2}$

Single Scattering $\sim \quad \frac{T(x)}{x}$

$$T(x) \sim (1-x)^n \quad \text{as } x \to 1$$

$$\left|\frac{\partial^2}{\partial x^2}\left(\frac{T(x)}{x}\right)\right| \gg \left|\frac{\partial}{\partial x}\left(\frac{T(x)}{x}\right)\right| \gg \left|\frac{T(x)}{x}\right|$$

— example : Nuclear dependence in direct photon production.

* Nuclear Dependence in Direct Photon Production

X. Guo, J. Qiu, G. St

- $h(p') + A(p) \longrightarrow \gamma(\ell) + X$.

- Only initial state double scattering:

e.g.

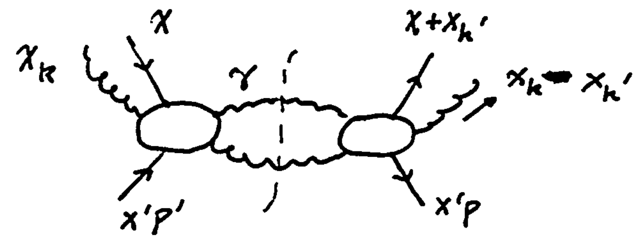

x large

x_k & x_k' Contour integratio

Since the final state gluon is not observed, double scattering on this gluon has No effect

- $\alpha(\ell)$:

$$\sigma_{hA}(\ell) \equiv \sigma^{(S)}_{h\cdot N}(\ell)\, A^{\alpha(\ell)}$$

$$\approx A\, \sigma^{(S)}_{h\cdot N}(\ell) + \sigma^{(D)}_{hA}(\ell)$$

$$\Rightarrow \quad \alpha(\ell) = 1 + \frac{1}{\ln A} \ln\left[1 + \frac{1}{A} \frac{\sigma^{(D)}_{hA}(\ell)}{\sigma^{(S)}_{hN}(\ell)} \right]$$

— $\sigma^{(D)}_{hA}(\ell) \sim A^{4/3}$, and much larger than $\sigma^{(S)}_{hN}$

$\Rightarrow \quad \alpha(\ell) \longrightarrow 4/3$

— $\sigma^{(D)}_{hA}(\ell)$ Could be negative at certain value of ℓ

$\Rightarrow \quad \alpha(\ell) < 1 \quad$ if $\sigma^{(D)}_{hA}(\ell) < 0$

— $\sigma^{(D)}_{hA}(\ell) > 0$ at large ℓ_T.

$\Rightarrow \quad 1 < \alpha(\ell) < 4/3$

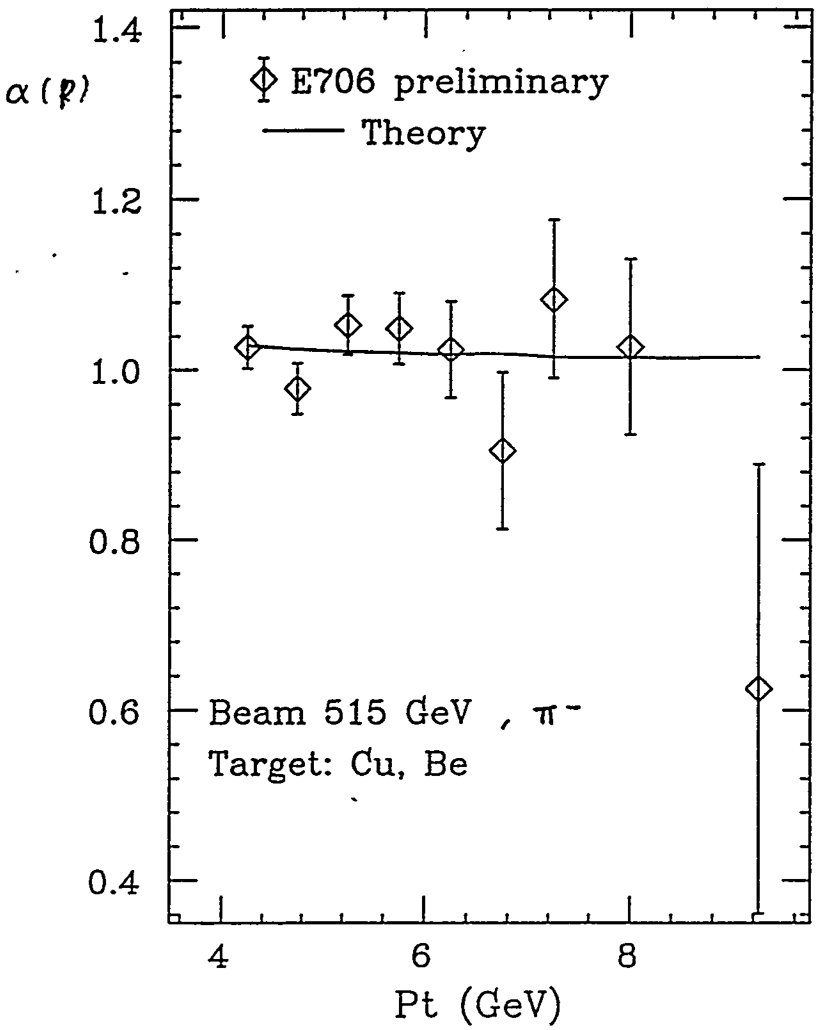

$x_F = 0$

$T_q(x, A)$, $T_g(x, A)$ extracted from γ-A experiment.

No free parameter for theory curve.

Why $\alpha_\gamma(p)$ is much smaller than $\alpha_\pi(p) \sim 1.1$?

Same experiment.

α_Lt

$$(x_A)_{eff} \approx x_T = \frac{2P_T}{\sqrt{s}} < \frac{18}{30} = 0.6$$

→ Final state interaction.

• Convolution with $\Gamma_{g\to\pi}(z) \Longrightarrow$ enhance $(x_A)_{eff}$.

Summary

- Nuclear beam at HERA provide a unique mechine to study shadowing at large Q^2 (but very small x).

- Two-jet events at HERA can be a very good probe to measure gluon shadowing. However, potential anhancement from the final state multiple scattering may alternate the signal.

The Limiting Curve of Leading Particles at Infinite A

Mark Strikman
Penn State University

Strikman

The limiting curve of leading particles at infinite A.

A. Berera, MS, B. Toothtaker, J. Whitmore

Experimental data (D-Y) &

pQCD (see A. Mueller talk) indicate

that leading parton propagating through

nuclei looses tiny fraction of longitudinal

momentum.

Where from "absorption" of hadrons

comes from in this case?

Partons get substatial transverse

momenta

$\langle k_t^2 \rangle \propto A^{1/3} \, k_0^2$

- Observed in DY

If $A \gg 1$ this leads to

$\langle k_{t_q}^2 \rangle \gg \langle k_t^2 \rangle_h$ for leading partons

of the projectile $\Rightarrow$

coherence is lost, fusion (recombinati

impossible

$\Downarrow$

Independent fragmentation for sufficiently large z say $z \gtrsim 0.2$.

$\Downarrow$

Would look as absorption for

leading hadrons

$$z \frac{dN^{h/a}(z)}{dz} = \sum_{i=q,\bar{q},g} \int_z^1 dx \, \frac{z}{x} \, D^{a/i}\left(\frac{z}{x}, Q^2\right) F_h^i(x, Q^2)$$

$\boxed{h + A \to a + X}$.

where

$F_h^i(x, Q^2)$ – parton distribution function

$D^{a/i}(\beta, Q^2)$ fragmentation function of parton i going to "a."

$$z \frac{dN^{h/a}(z)}{dz} = z \frac{1}{\sigma_{inel}^{hA}} \frac{d\sigma^{h+A \to a+X}(z)}{dz}$$

$D^{a/i}(\beta, Q^2) \, d\beta$ – # of hadrons of kind a produced per event between β and $\beta + d\beta$

How much is $\langle k_t^2 \rangle$ for $A \sim 200$

& $E_{inc} = 800$ GeV — use D-Y

$\langle p_t^2 \rangle$ broadening

In average number of nucleons on impact parameter is n

$$\langle p_t^2 \rangle = \frac{2n}{n-1} \left[\langle k_A^2 \rangle_{D.Y.} - \langle k^2 \rangle_{proton} \right]$$

"2" due half of nucleons in D.Y. case

"$-\frac{1}{2}$" because nucleon in "hp" scattering does not contribute to broadening as measured in D.Y.

$\Rightarrow$ $p_t \sim 0.6$ GeV/c for $A \sim 200$

Relative $\langle p_{t_{1,2}} \rangle \sim \sqrt{2}\, p_t \sim 0.8$ GeV/c $\overset{?}{\gg}$ 0.4 Ge

May be preasymptotic...

At higher energies situation may be better since $\langle k_t^2 \rangle \propto \sigma_p(x, Q^2)$

$x \sim \frac{Q^2}{s}$

Correction terms $\sim \frac{1}{A^{2/3}}$ from fusion mechanism

$\sim \frac{1}{A^{1/3}}$ from small size $q\bar{q}$ in projectile for pion production (actually a bit faster)

$\sim \frac{1}{A^{2/3}}$ from small size $qqq \to N$

For numerical estimates in realistic situation need (i) parton distributions at $Q_0^2 \sim k_t^2 \sim 1\ GeV^2$, (ii) $q \to h$ fragmentation functions for Q_0^2 — D

D not well known [good data for $Q^2 \sim 10\ GeV^2$ — but large scaling violatio

We used Quark-gluon string model D (Kaidalov et al) — it is close to ν data for small Q^2. Uncertainty in Q_0^2 $\Rightarrow$ uncertainty in absolute predictions

Parton Distribution Function

GRV $Q^2 = 1\,GeV^2$

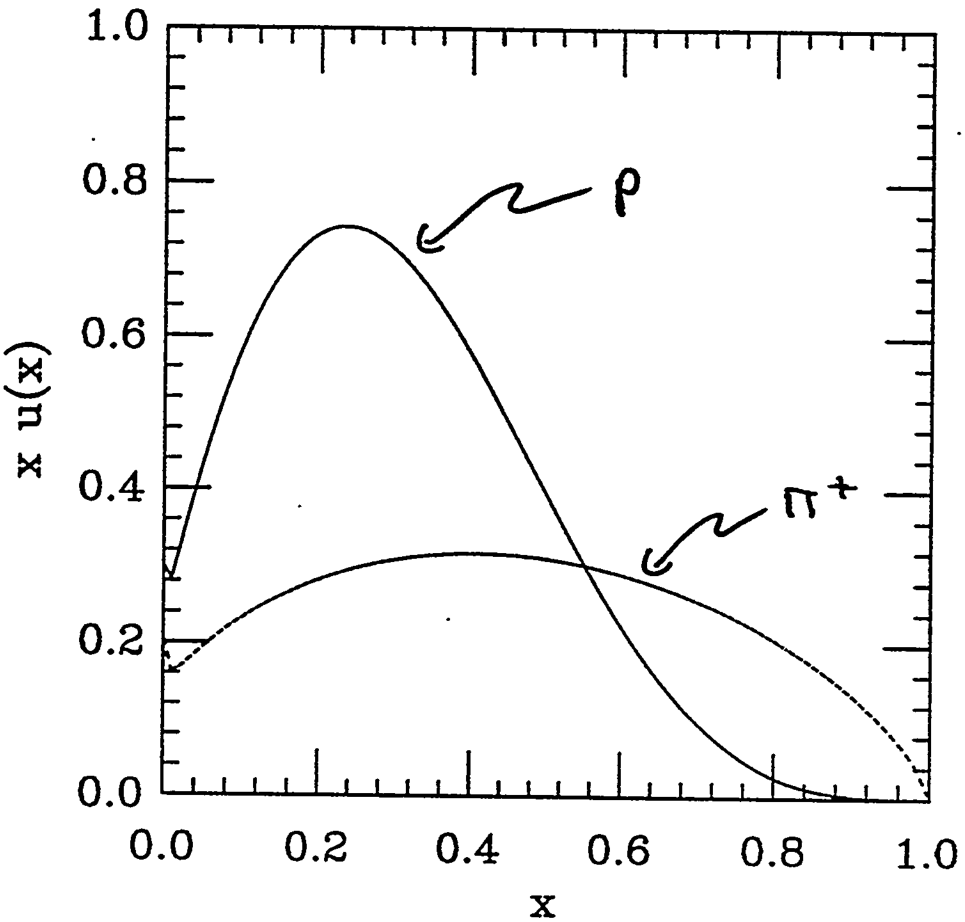

Limiting Curves of
Leading Particle Multiplicities

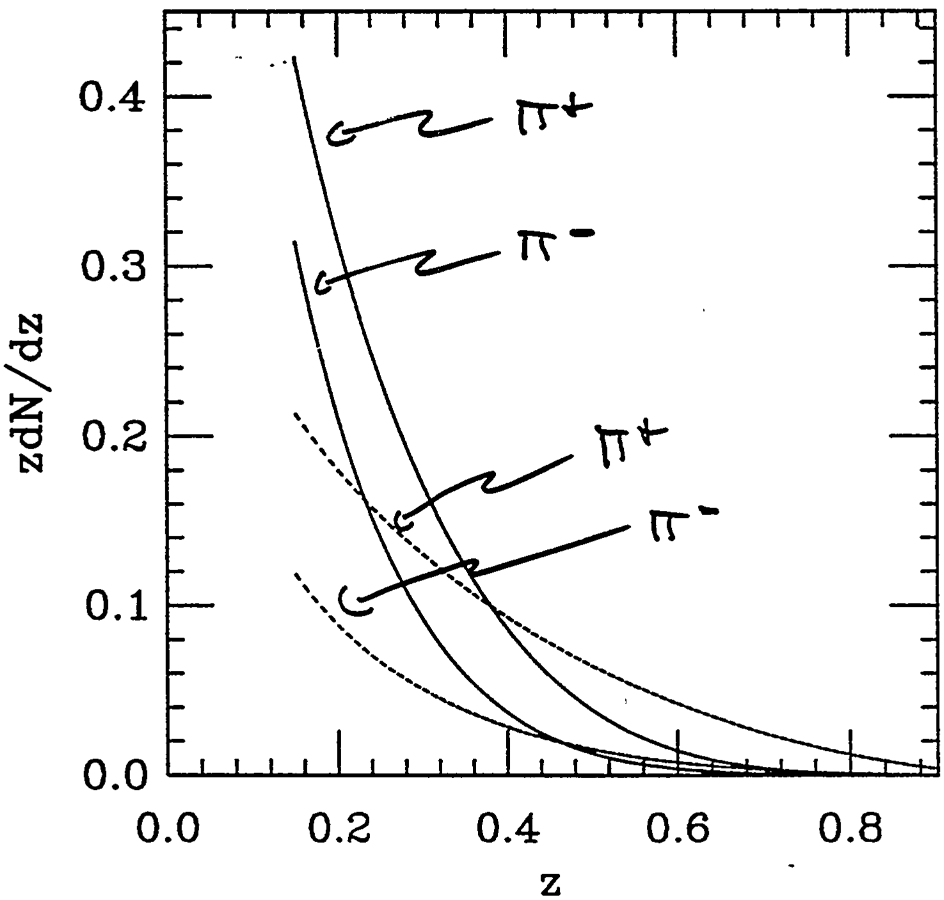

— proton projectile
--- pi+ projectile

GRU+QGSM

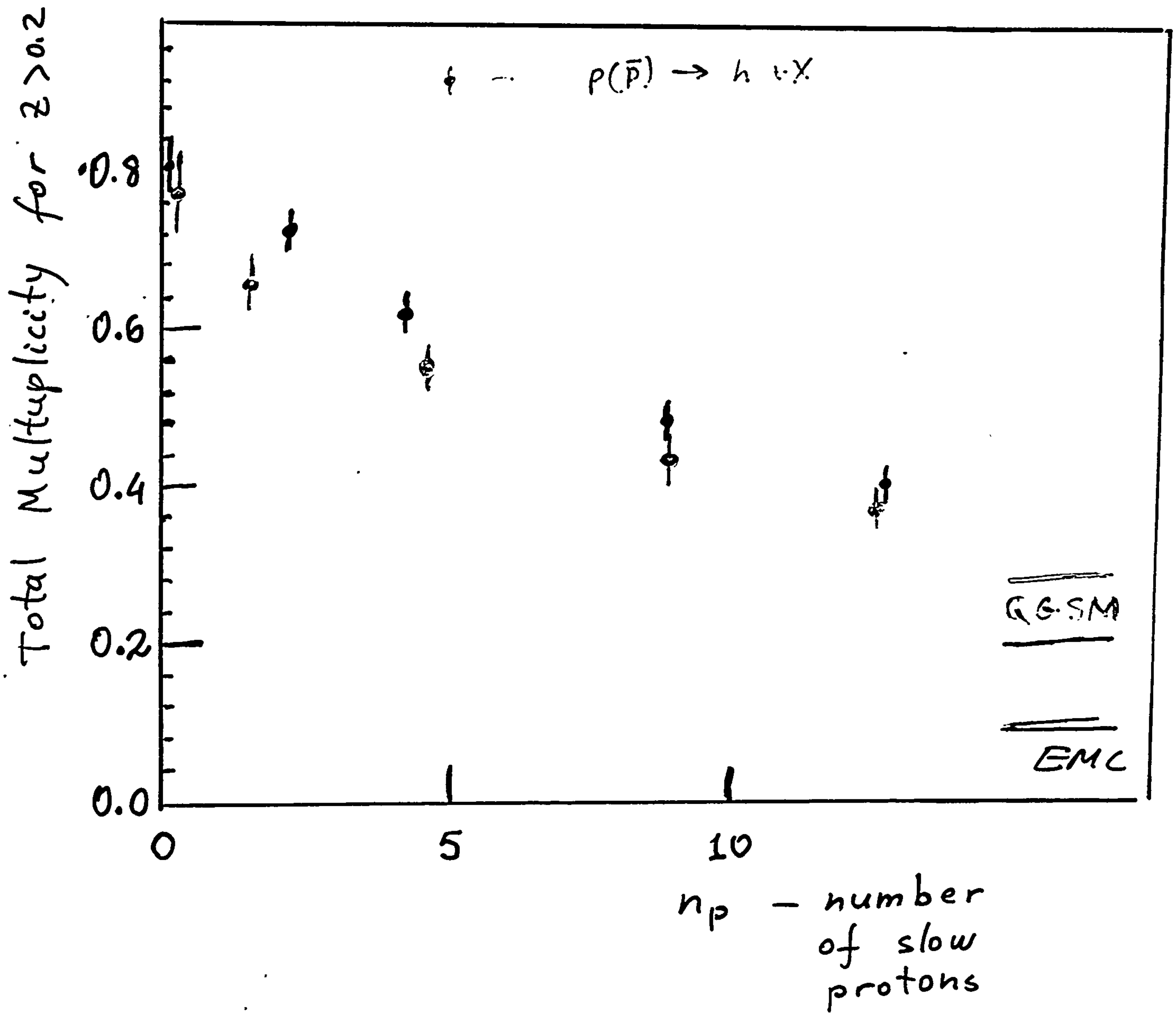

Total Multiplicity for z > 0.2
p(p̄) → h + X
0.8
0.6
0.4
0.2
0.0
GGSM
EMC
0
5
10
n_p – number of slow protons

Powers

$$z\frac{dN}{dz} \propto (1-z)^n$$

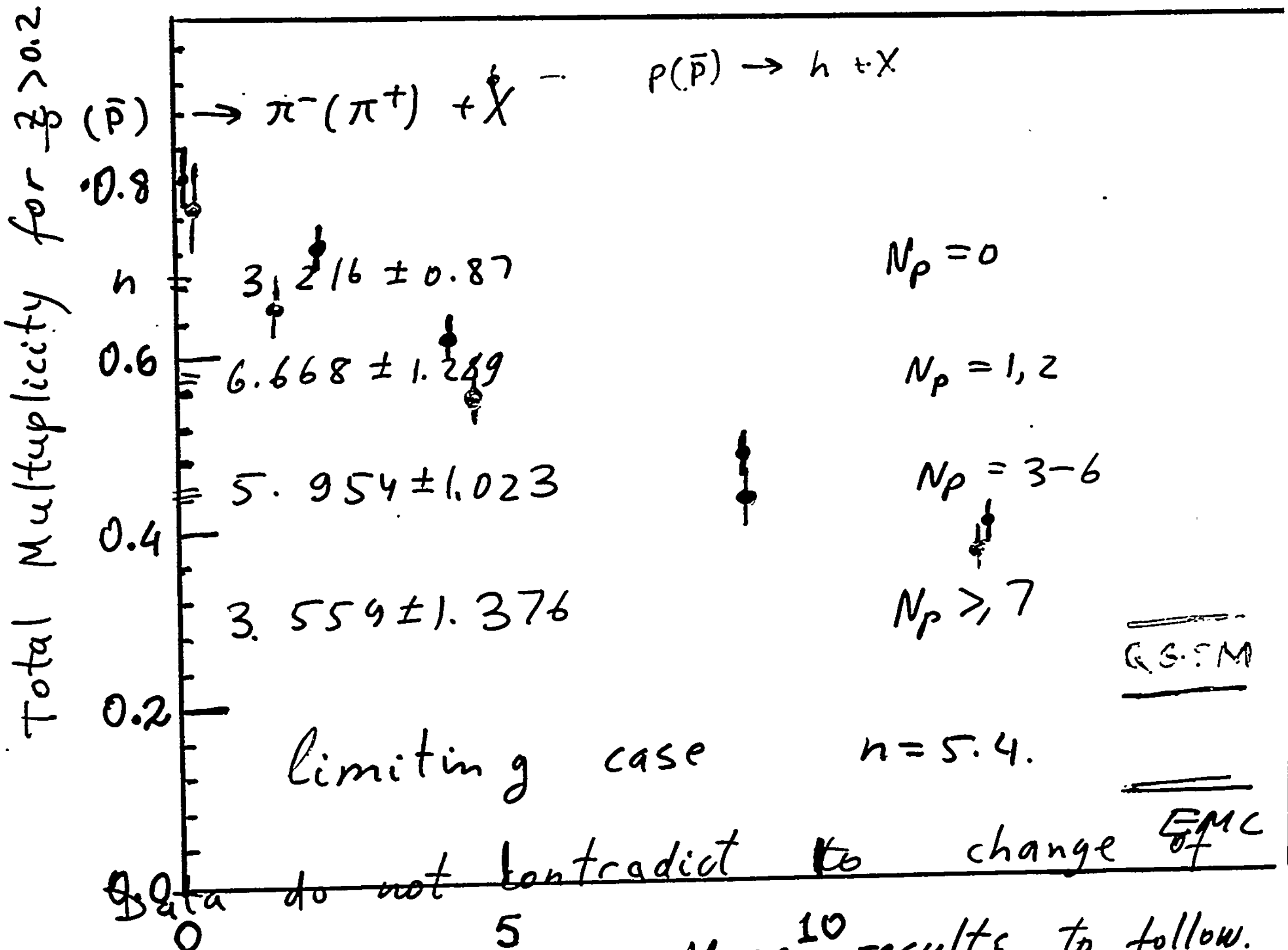

n = 3.216 ± 0.87 $N_p = 0$

6.668 ± 1.249 $N_p = 1, 2$

5.954 ± 1.023 $N_p = 3-6$

3.559 ± 1.376 $N_p \geq 7$

limiting case $n = 5.4$.

Data do not contradict to change of power with N_p. More results to follow.

n_p – number of slow protons

⇒ Would be nice to look at this problem at RHIC. and in more sofisticated hA fixed target experiments.

Coherent Production of Vector Mesons off Light Nuclei in DIS

Misak Sargsyan
Tel Aviv University

Coherent production of vector mesons off light nuclei in DIS

Nuclei at HERA and Heavy Ion Physics. 199
BNL, 17-18-NO

Misak Sargsyan

L. Frankfurt, W. Koepf, M. S. — Tel Aviv Univ.

M. Strikman, V. Guzey — Penn State Univ.

- we are interested in reactions

$$\gamma^* + A \longrightarrow V + A'$$

$A = d, {}^4He$

$V = \rho, \rho', \varphi, \omega \ldots$

- why deuteron?

→ the deuteron target is a simplest bound object

→ at the case of internal momenta ≤ 350 MeV/c it is also best understood nucleus ~ accuracy ...

→ in average configurations very small shadowing ≤ few %, average radius ~ 4 fm

→ in rescattering diagrams internucleon distances are important in deuteron ~ 1.5

→ shadowings in deuteron in kinematics dominated by rescatterings could be as large as for any heavy nuclei.

- why coherent production?

→ simplest structure for final stat[e]
  - form factors of nucleus

→ more degree of Freedom, inclusive x, Q^2; exclusive x, Q^2, t

→ the deuteron is the isoscalar partic[le]
once we detected the deuteron and J
in final state, the contribution from isospin exchange diagrams is suppress[ed]

→ there is a clear experimental evidence for coherent productions, for dominance of rescatterings.

two message

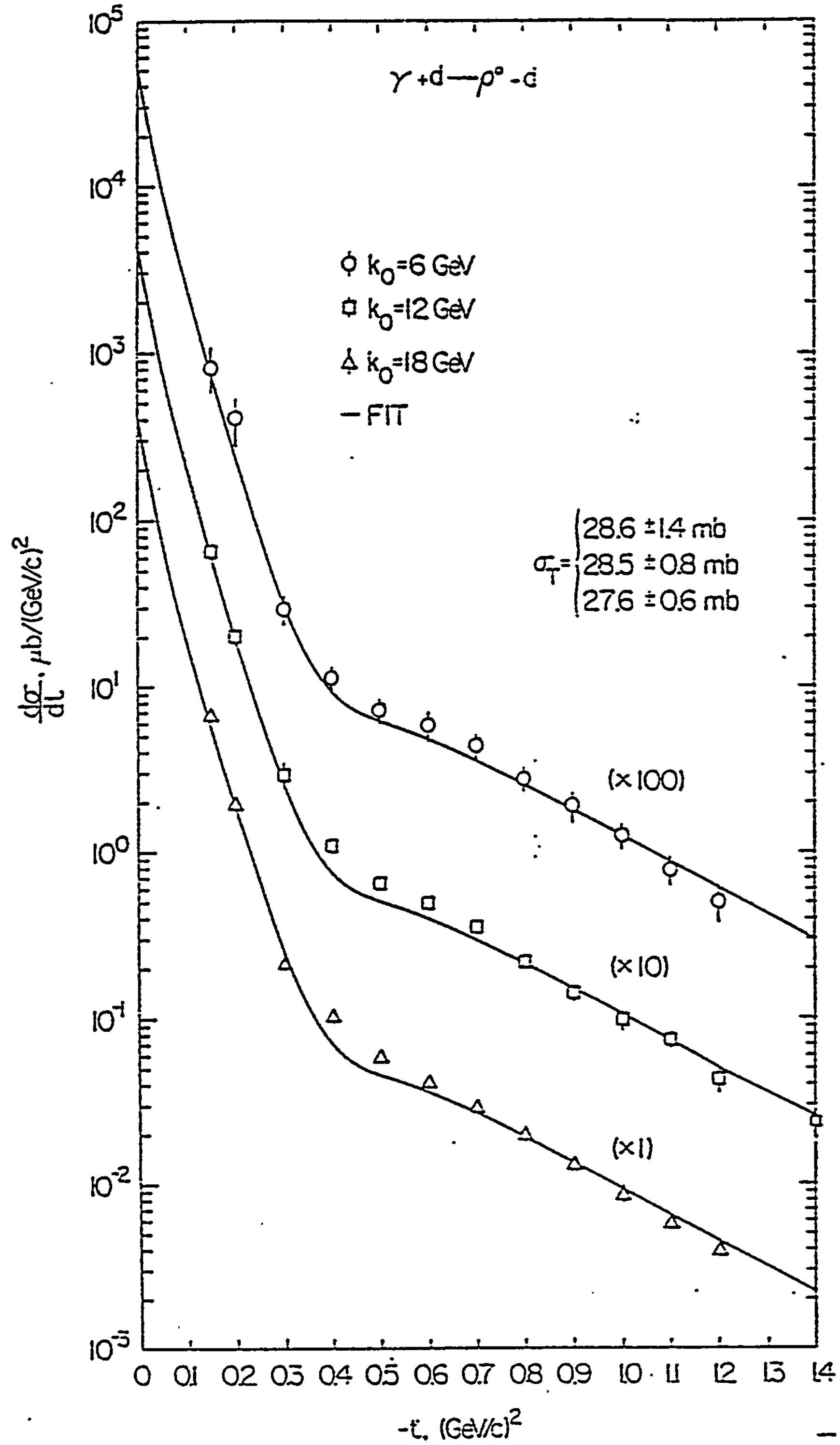

FIG. 20: Differential cross section.

Anderson et al
Phys. Rev. D 4, 3245, 1971

3

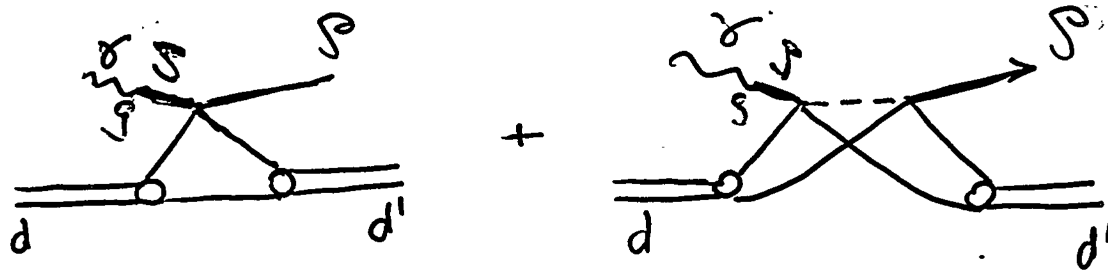
γ
ρ
ρ
d
d'
+
γ
ρ
ρ
d
d'

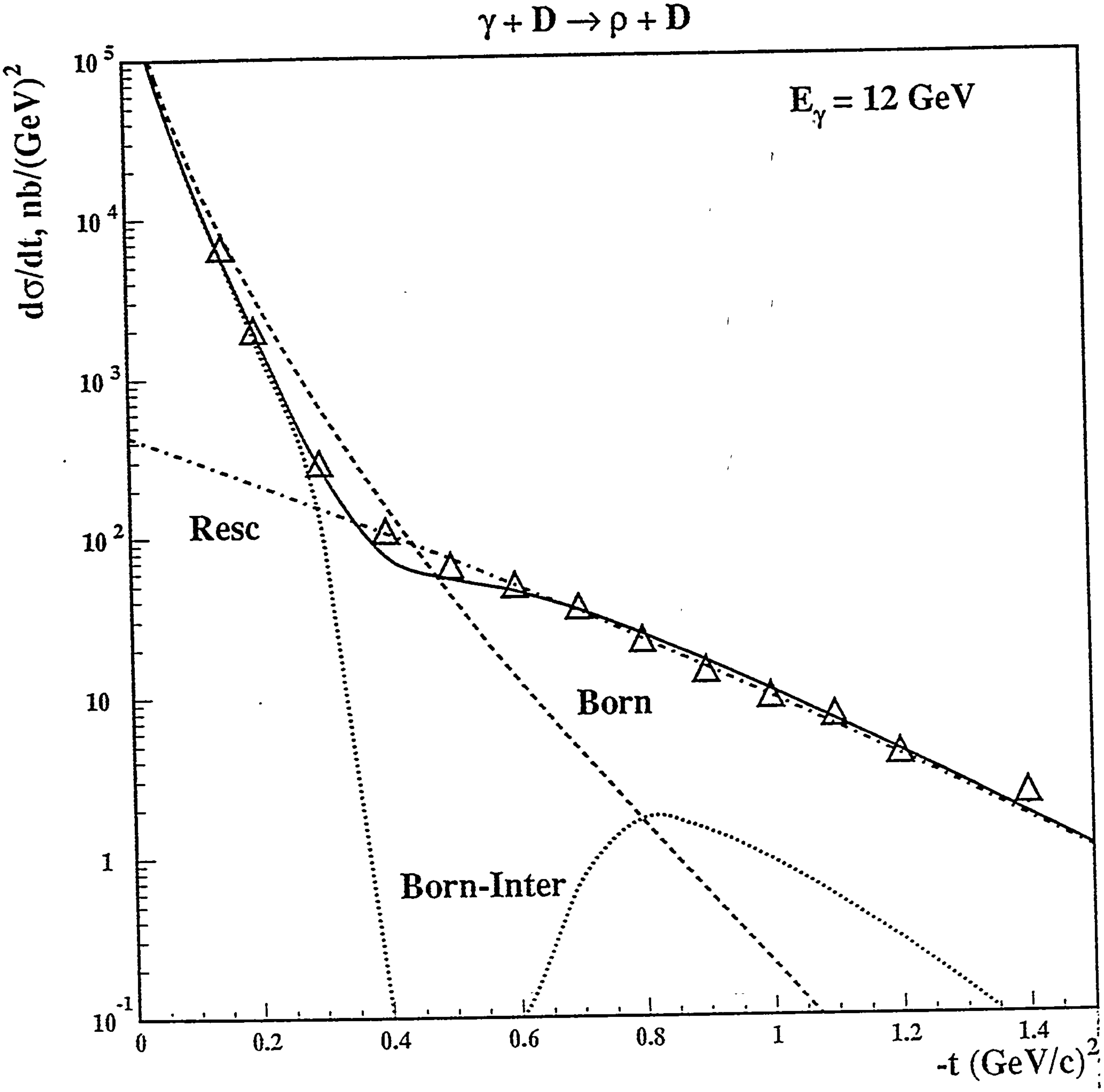
γ + D → ρ + D
dσ/dt, nb/(GeV)^2
E_γ = 12 GeV
Resc
Born
Born-Inter
-t (GeV/c)^2
10^5
10^4
10^3
10^2
10
1
10^-1
0
0.2
0.4
0.6
0.8
1
1.2
1.4

rho.2

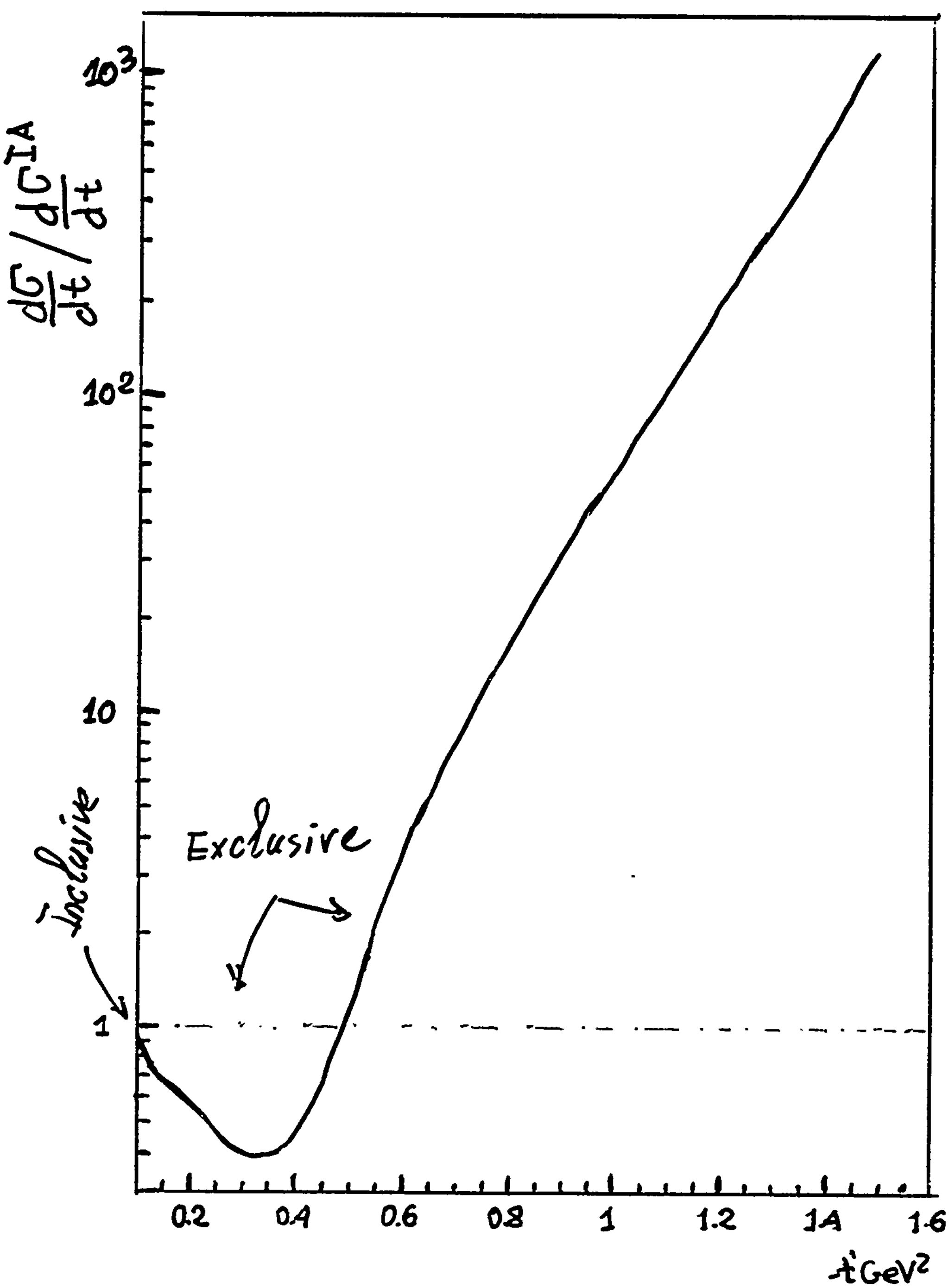

$\frac{d\sigma}{dt} / \frac{d\sigma^{IA}}{dt}$
10^3
10^2
10
1
Inclusive
Exclusive
0.2
0.4
0.6
0.8
1
1.2
1.4
1.6
t GeV²

5

- why ^4He ?

+

$\Rightarrow$ ^4He spherical nucleus without Quadrupol form factor

2. Diffractive electroproduction of vector mesons off the deuteron, ^4He

— Kinematics

the life time τ of a virtual photon with q in a hadron configuration $|n\rangle$ with mass M_n

$$\Rightarrow \quad \tau = \frac{1}{E_n - q_0} \simeq \frac{2q}{(M_n^2 + Q^2)} \simeq \frac{1}{2 m_N x}$$

$M_n^2 \sim Q^2$

$$\tau >> 2R$$

$$\Rightarrow \qquad t_{min} = - \frac{(M_x^2 + Q^2)}{s^2} m_t^2 \,, \quad s = (q + P_A)$$

$$- \frac{t_{min} r_t^2}{3} << 1$$

state X will produced without disturbing target much, not much suppression of formfactor of target nucleus

– at the considered kinematical situation the hadronic configuration of the final state is a result of a coherent superposition of hadronic fluctuation of the photon that satisfy $-\frac{t_{min} r_t^2}{3} \ll 1$.

– the use of completeness over diffractive produced intermediate hadronic states allows to express the result via quarks and gluons, similar to Deep Inelastic Inclusive processes.

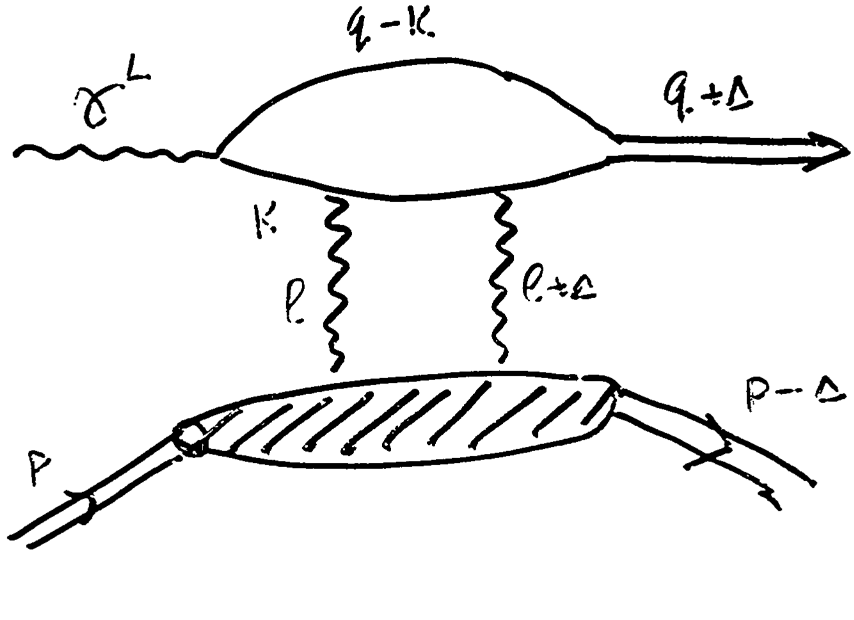

$$A = \Psi^{\gamma^* \to q\bar{q}} \otimes A(q\bar{q}T) \otimes \Psi^{q\bar{q} \to V}$$

- in calculation of $A(q\bar{q}T)$ we use the cross section of small size $q\bar{q}$ configuration interaction with target

$$\sigma_{q\bar{q}T}(b^2) = \frac{\pi^2}{3}\left[b^2 \alpha_s(Q^2) \times G_T(x, Q^2)\right]$$

Blattel, Baym
Frankfurt, Strikm
Phys. Rev. Let
71 (1993) 8:

$$A \sim \int b^2 \times G_T(x, b^2) \Psi^{\gamma_L^*}(z, b)\, \Psi_V(z, b)\, d^2b\, dz$$

Brodsky et a
Phys. Rev. D5?
1994, 3

$$\left.\frac{d\sigma^L_{\gamma^* N \to VN}}{dt}\right|_{t=0} = \frac{12\pi^2 \Gamma_{V \to e^+e^-} M_V \alpha_s^2(Q) \eta_V^2 T_V(Q^2)^2}{\alpha_{em} Q^6 N_c^2} \times$$

$$\times \left| x\, G_T(x, Q^2) + \frac{i\pi}{2} \frac{d}{d\ln x} x\, G_T(x, Q^2) \right|^2$$

why longitudinal photons

$$\Psi^{\gamma_L^*} \sim z(1-z)\,Q\,K_0\left(Qb\sqrt{z(1-z)}\right)$$

$$\Psi^{\gamma_T^*} \sim \frac{\partial}{\partial b_\mu} K_0\left(Qb\sqrt{z(1-z)}\right)$$

where

$$\eta_v \equiv \frac{1}{2} \frac{\int \frac{dz}{z(1-z)} \phi_v(z)}{\int dz\, \phi_v(z)}$$

$$I_v(Q^2) = \frac{\int_0^1 \frac{dz}{z(1-z)} \int_0^{Q^2} d^2k_\perp \frac{Q^4}{\left[Q^2 + \frac{k_\perp^2 + m^2}{z(1-z)}\right]^2} \psi_v(z, k_\perp)}{\int_0^1 \frac{dz}{z(1-z)} \int_0^{Q^2} d^2k_\perp\, \psi_v(z, k_\perp)}$$

⇒ t dependence ⇐

- t dependence of the amplitude characterizing the target, and it should be universal for all hard diffractive processes off same target

$$G^2_{T2g}(t) \sim \exp(Bt) \qquad B \simeq 4-5G$$

⇒ Calculating production off nuclei ⇐

- One have to deal with parton density in the nucleus (deuteron, ^4He).

I) One can construct them within eikonal picture, where nuclear effects generating through rescattering of $q\bar{q}$ off target nucleons.

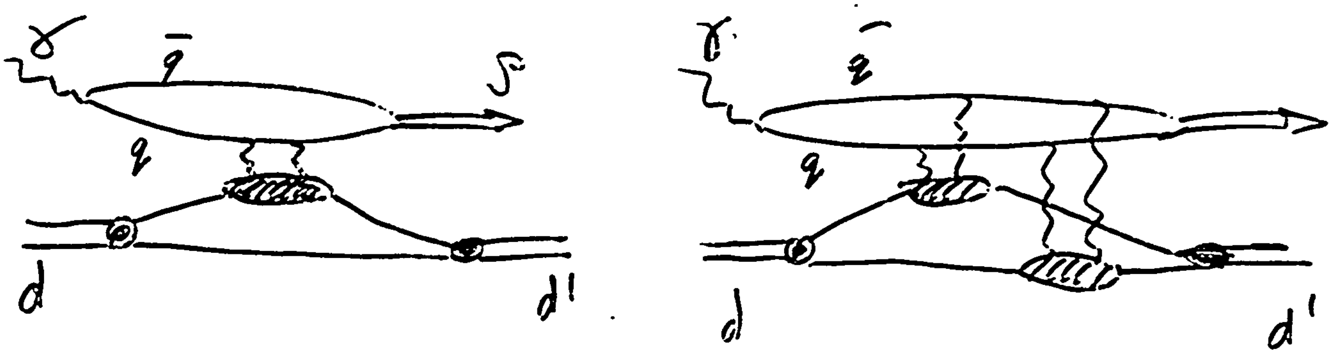

II) and within picture, which do not reduce to eikonal series of rescatt

for example

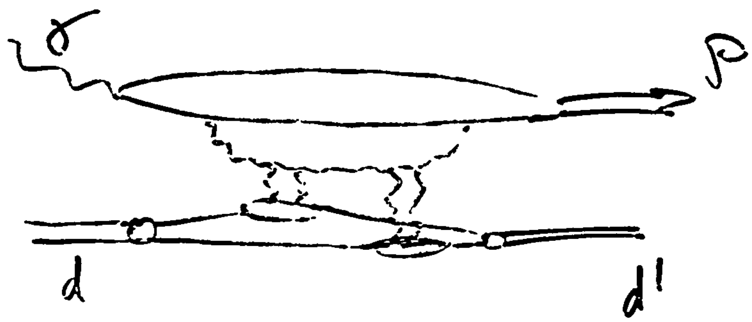

- in considered model of calculations we are neglected contribution by these diagrams

- One reason is that at $t=0$, nuclear effects very small for light nucleus, and at fixed x they even decrease with increasing Q^2

- So we started at kinematics where no nuclear effects (shadowing) at $t=0$

and further nuclear effects generat[illegible]
by eikonal picture of rescatterings
moving to larger -t.

⇒ Eikonal Picture of rescatterings ⇐

⇒ For $\gamma^{*L} + d \to V + d'$

$$\frac{d\sigma}{dt} = \frac{4}{16\pi}\left[F_c^2\left(\frac{t}{4}\right) + F_Q^2\left(\frac{t}{4}\right)\right]\left|f^{\gamma^* N \to VN}(t)\right|^2 -$$

$$- \frac{2}{16\pi}\left[S_c F_c\left(\frac{t}{4}\right) - \frac{1}{\sqrt{2}} S_Q F_Q\left(\frac{t}{4}\right)\right] f^{\gamma^* N \to VN}(t) \quad f^{\gamma^* N \to q\bar{q}N}\left(\frac{t}{4}\right.$$

$$+ \frac{1}{4 \times 16\pi}\left[S_c^2 + 2 S_Q^2\right]\left|f^{\gamma^* N \to q\bar{q}N \to VN}\left(\frac{t}{4}\right)\right|^2$$

$$f^{\gamma^* N \to VN} \sim \int d^2b\, \Psi_{\gamma_L^*}(b)\, \Psi_V(b)\, \sigma_{q\bar{q}N}(b)$$

$$f^{\gamma^* N \to q\bar{q}N \to VN} \sim \int d^2b\, \Psi_{\gamma_L^*}(b)\, \Psi_V(b)\, \sigma^2_{q\bar{q}N}(b)$$

15/11/95 18.11

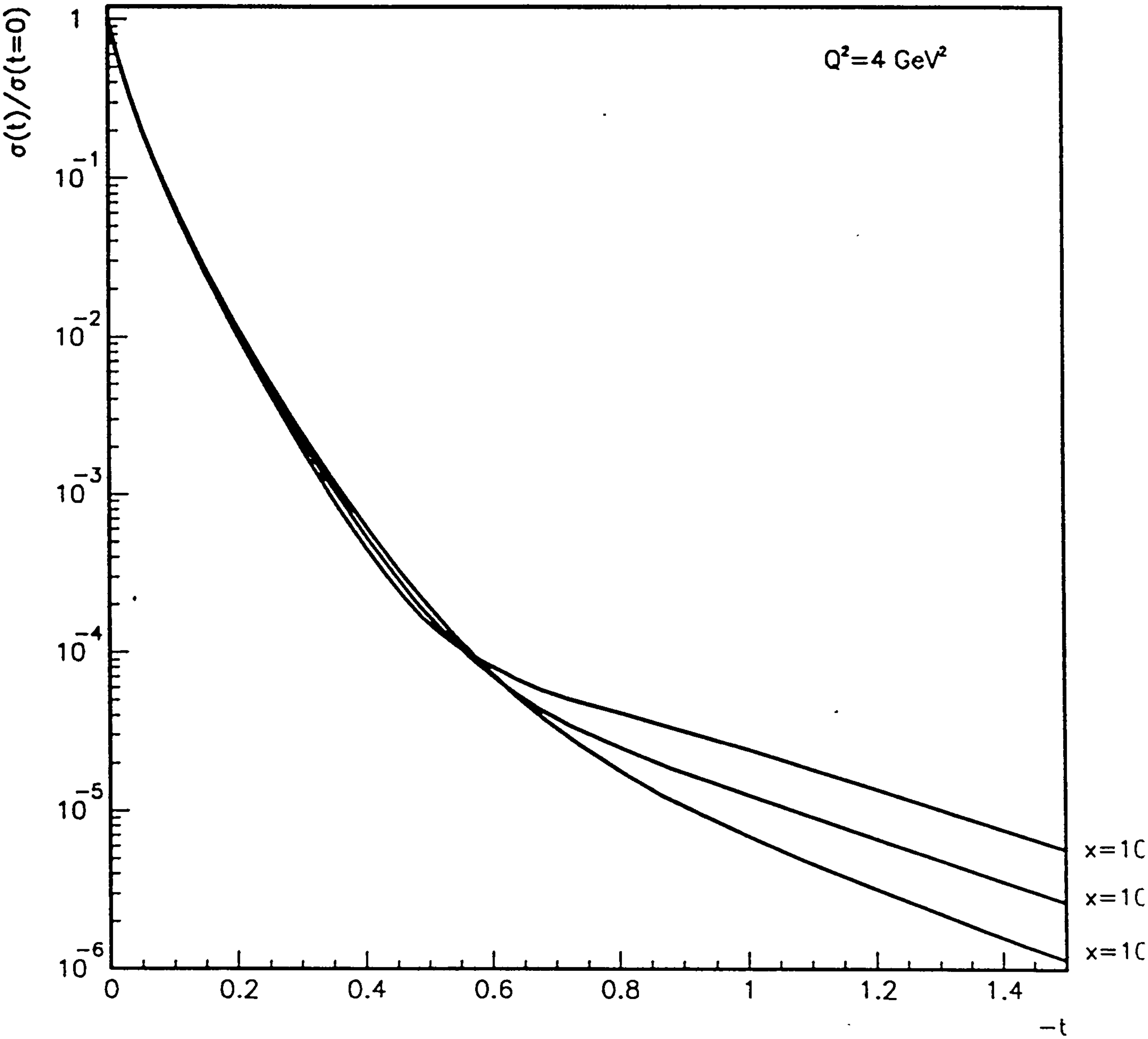

$\sigma(t)/\sigma(t=0)$
Q^2=4 GeV^2
1
10^{-1}
10^{-2}
10^{-3}
10^{-4}
10^{-5}
10^{-6}
0
0.2
0.4
0.6
0.8
1
1.2
1.4
$-t$
x=1C
x=1C
x=1C

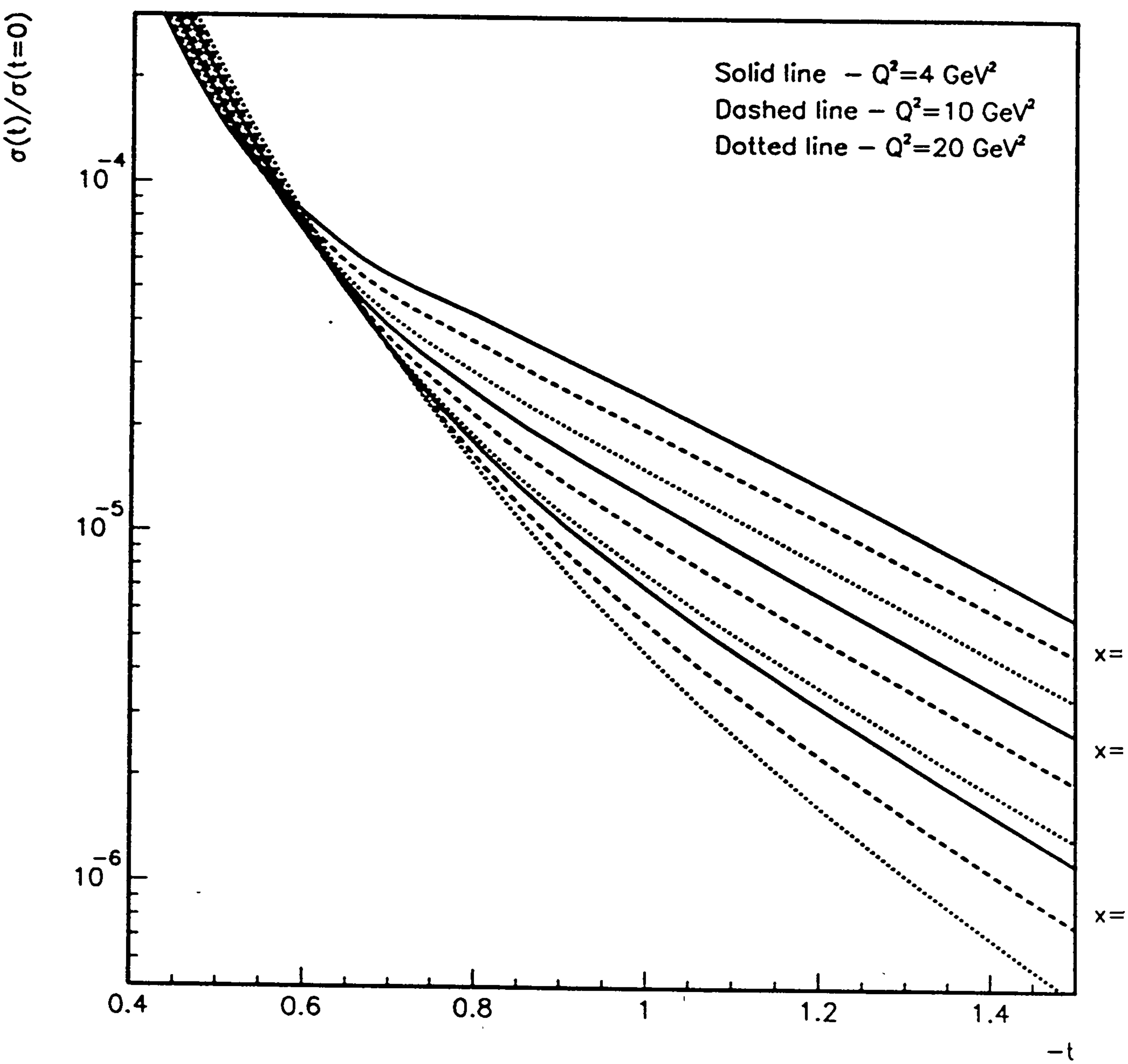

Solid line – Q^2=4 GeV^2
Dashed line – Q^2=10 GeV^2
Dotted line – Q^2=20 GeV^2
$\sigma(t)/\sigma(t=0)$
10^{-4}
10^{-5}
10^{-6}
0.4
0.6
0.8
1
1.2
1.4
$-t$
x=
x=
x=

1

15/11/95 16.53

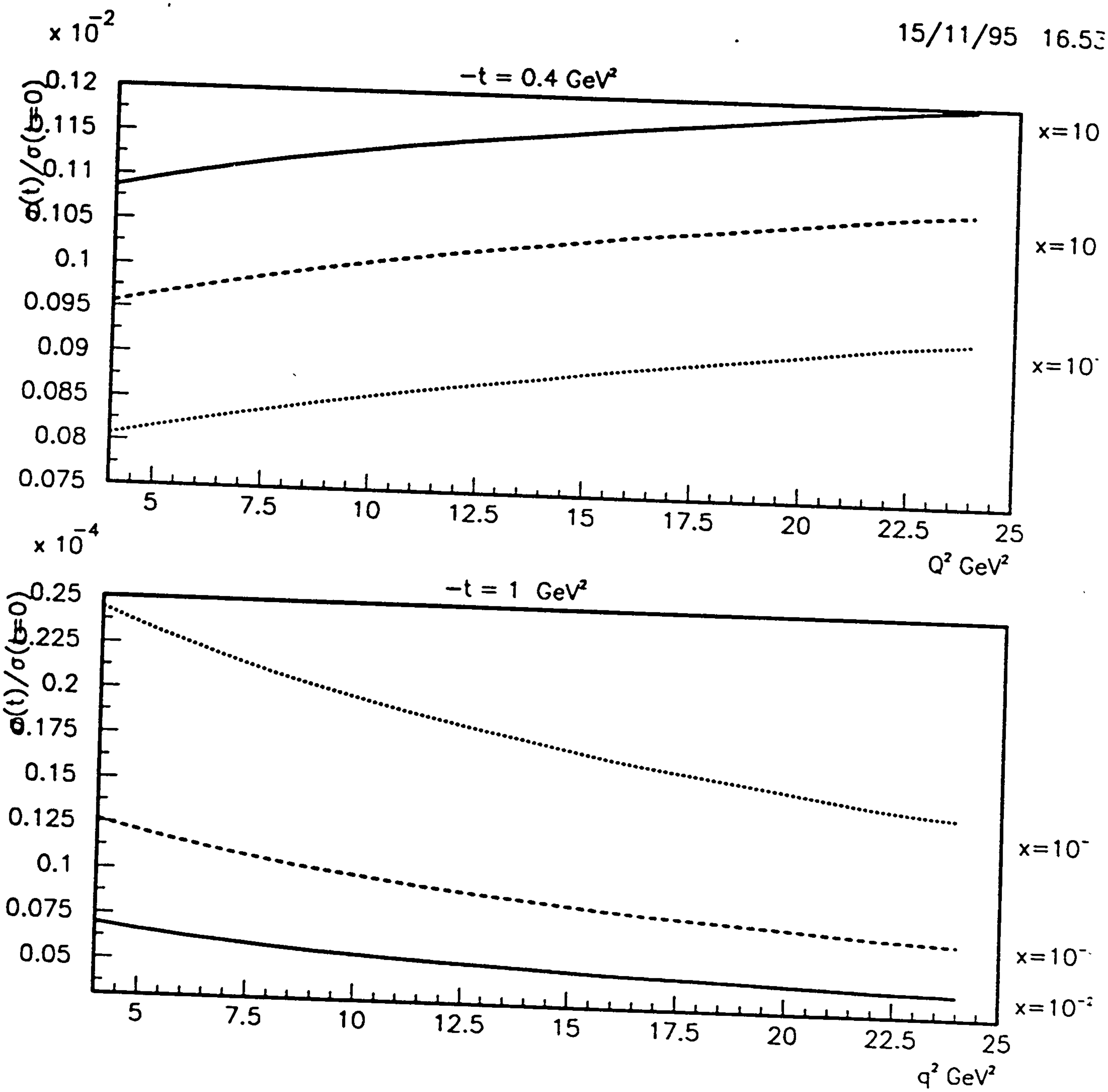

1

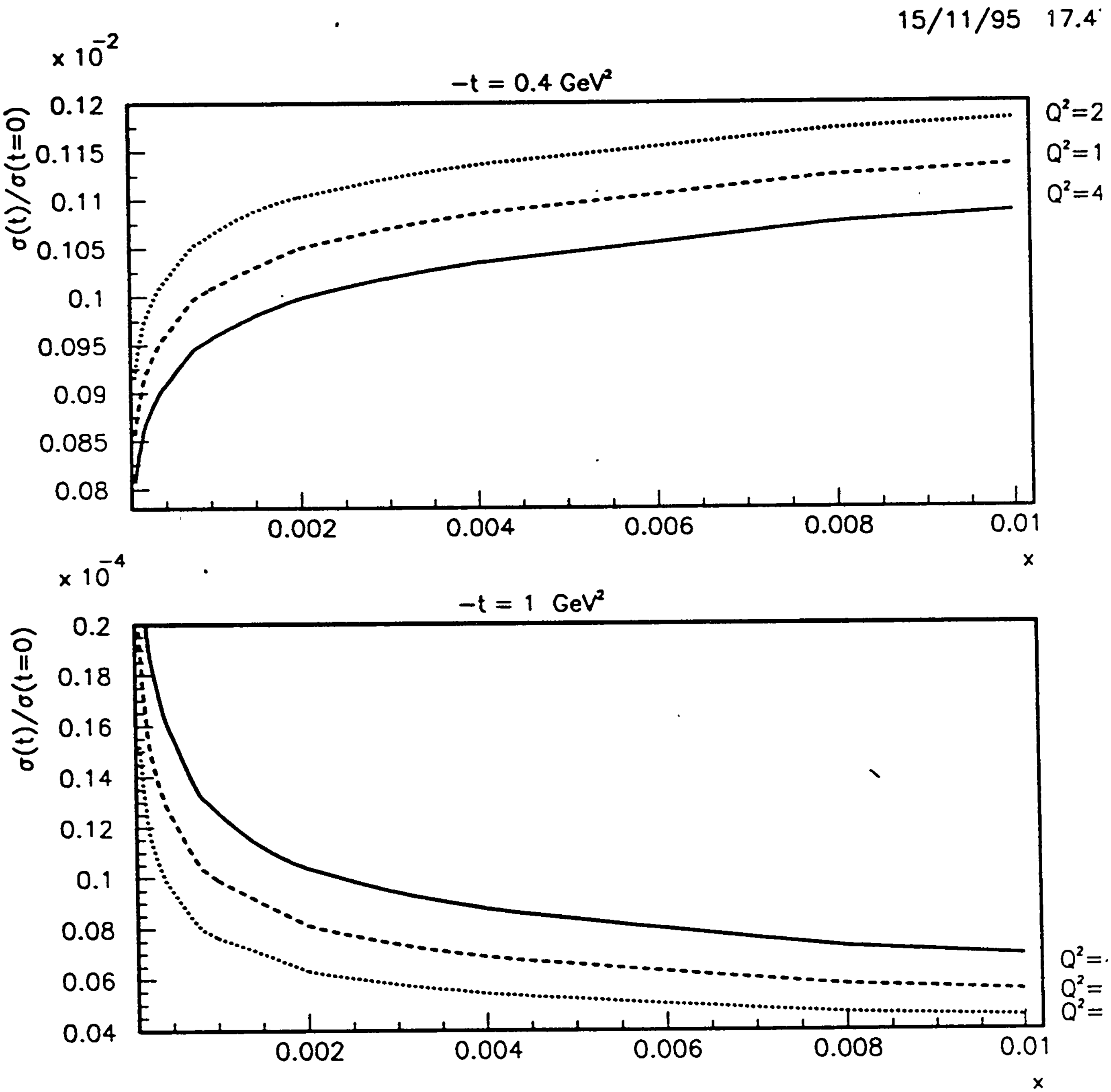
15/11/95 17.4
x 10^-2
−t = 0.4 GeV²
σ(t)/σ(t=0)
0.12
0.115
0.11
0.105
0.1
0.095
0.09
0.085
0.08
0.002
0.004
0.006
0.008
0.01
x
Q²=2
Q²=1
Q²=4
x 10^-4
−t = 1 GeV²
σ(t)/σ(t=0)
0.2
0.18
0.16
0.14
0.12
0.1
0.08
0.06
0.04
0.002
0.004
0.006
0.008
0.01
x
Q²=
Q²=
Q²=

$\Rightarrow$ For $\gamma^{*L} + {}^4He \rightarrow V + {}^4He$

$$\frac{d\sigma}{dt} = \frac{1}{16\pi}\left| 4\sigma^{(1)}\Phi_1(t)\, e^{\frac{B}{2}t} - \frac{3\sigma^{(2)}}{4\pi(\alpha+B)}\, e^{\left(\frac{2B+\alpha}{8}t\right)} + \frac{\sigma^{(3)}}{12\pi^2(\alpha+B)^2}\, e^{\frac{4B+\alpha}{24}t} - \frac{\sigma^{(4)}}{256\pi^3(\alpha+B)^3}\, e^{\frac{B}{8}t} \right|^2$$

where

$$\sigma^{(n)} \sim \int d^2b\, \Psi_{\gamma_L^*}(b)\, \sigma^n_{q\bar{q}N}(b)\, \Psi_V(b)$$

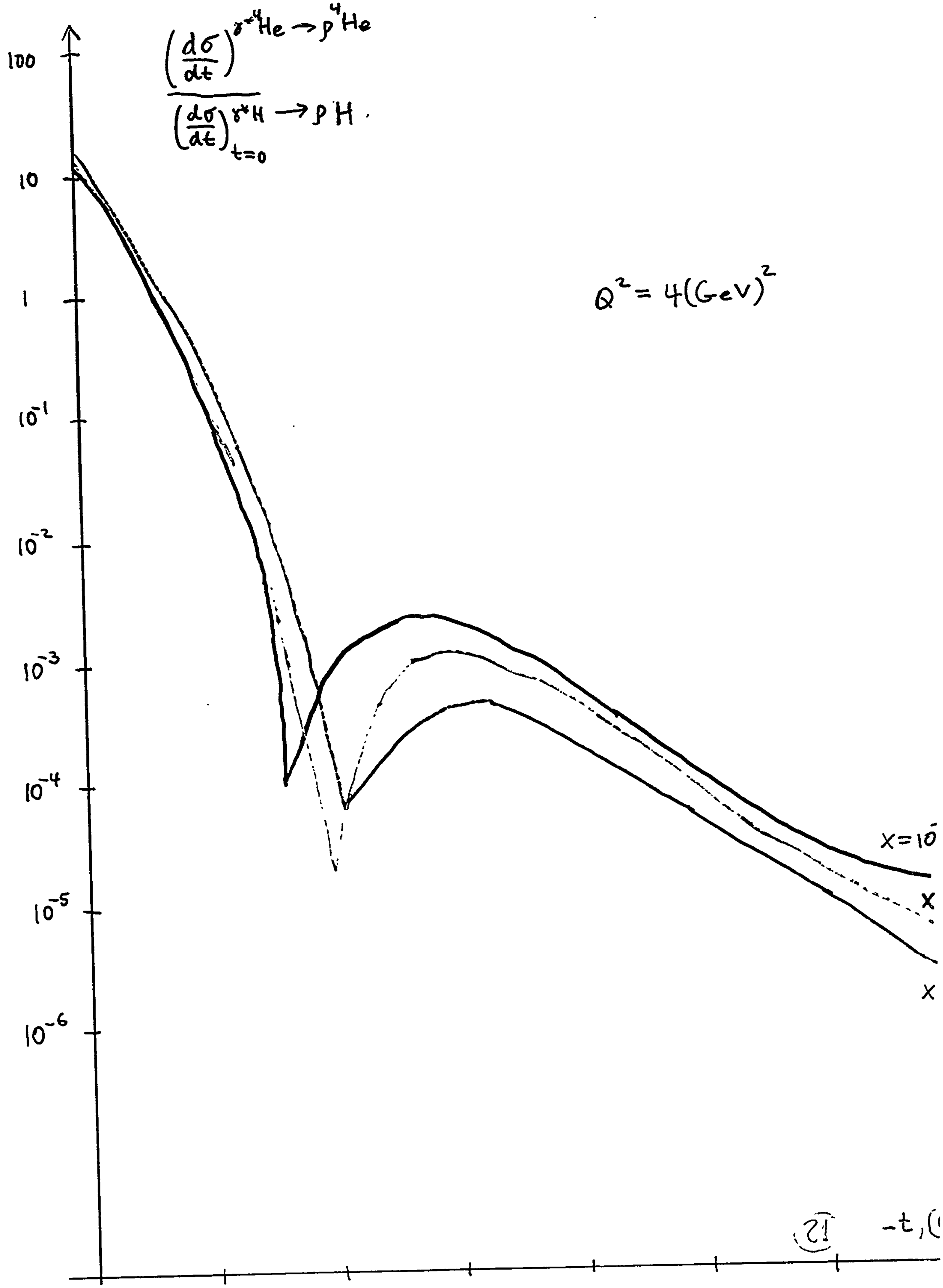

$\dfrac{\left(\frac{d\sigma}{dt}\right)^{\gamma^* {}^4He \to \rho\, {}^4He}}{\left(\frac{d\sigma}{dt}\right)^{\gamma^* H \to \rho H}_{t=0}}$
100
10
1
10^{-1}
10^{-2}
10^{-3}
10^{-4}
10^{-5}
10^{-6}
$Q^2 = 4 (GeV)^2$
x=10
x
x
(21)
-t, (

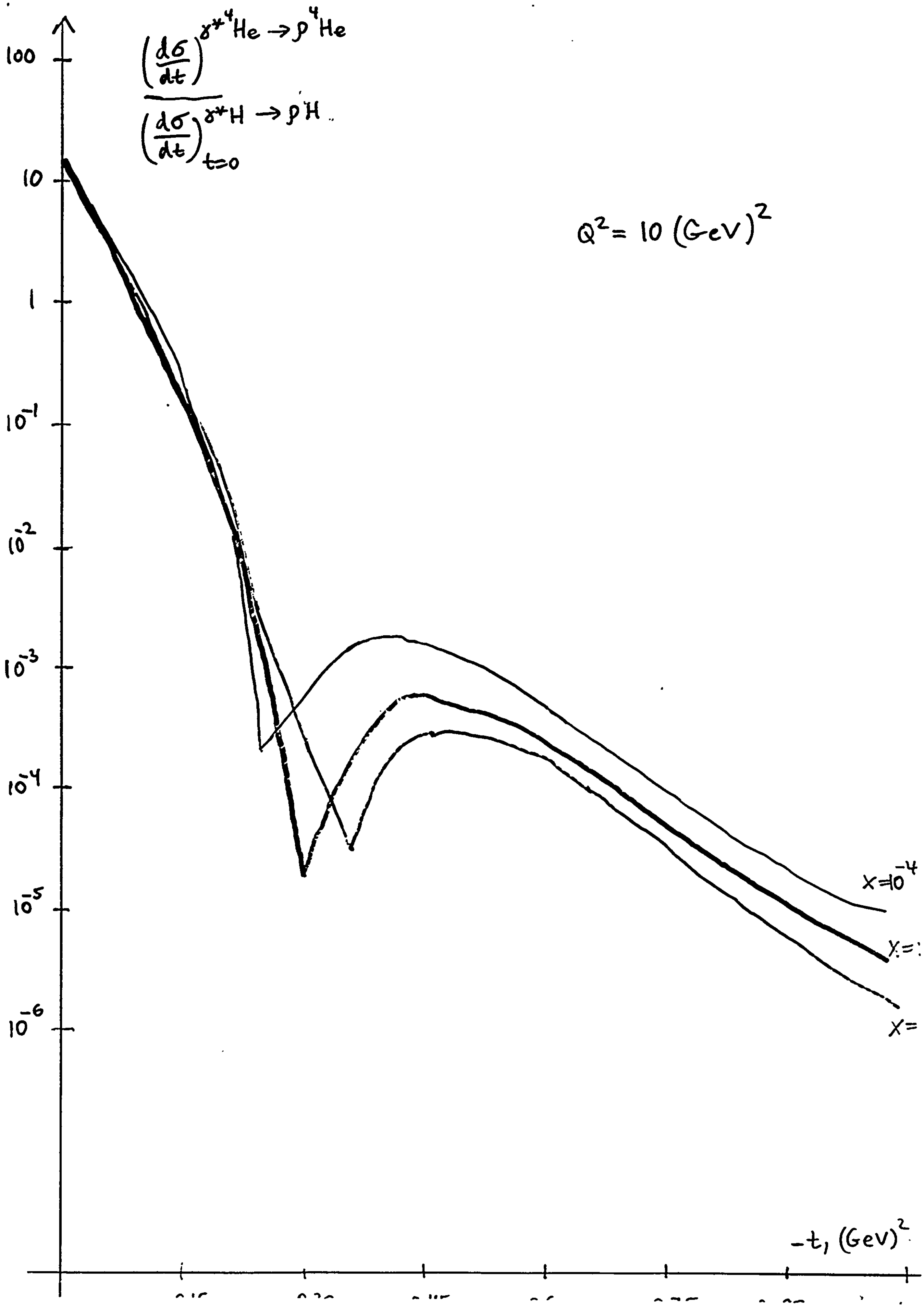

$$\frac{\left(\frac{d\sigma}{dt}\right)^{\gamma^* {}^4He \to \rho\, {}^4He}}{\left(\frac{d\sigma}{dt}\right)^{\gamma^* H \to \rho H}_{t=0}}$$
100
10
1
10^{-1}
10^{-2}
10^{-3}
10^{-4}
10^{-5}
10^{-6}
$Q^2 = 10\ (GeV)^2$
$x = 10^{-4}$
$x =$
$x =$
$-t,\ (GeV)^2$

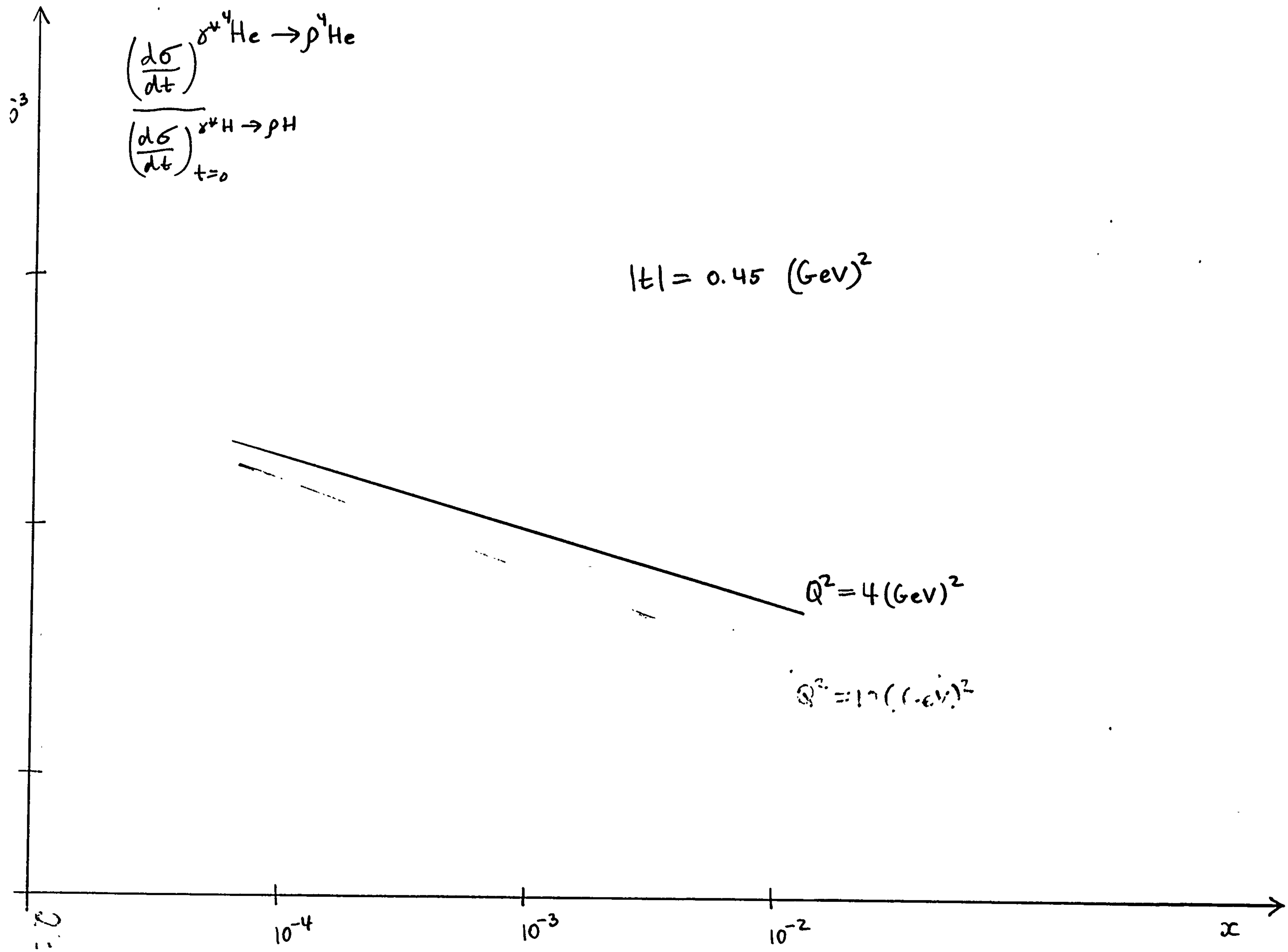

$\dfrac{\left(\frac{d\sigma}{dt}\right)^{\gamma^{*4}He \to \rho^4 He}}{\left(\frac{d\sigma}{dt}\right)^{\gamma^* H \to \rho H}_{t=0}}$
$|t| = 0.45\ (GeV)^2$
$Q^2 = 4 (GeV)^2$
10^{-4}
10^{-3}
10^{-2}
x

A Model of High Parton Densities in PQCD

Raju Venugopalan
INT, Seattle

A Model of High Parton Densities in pQCD.

Raju Venugopalan.
INT, Seattle.

A. Ayala

R. Gavai

J. Jalilian-Marian

* A. Korner

L. McLerran

* H. Weigert.

AN OUTLINE:

* Introduction
* Setting up the problem.
* The classical background field.
  (non-Abelian Weizsäcker-Williams fields)
* Small fluctuations in the classical background field.
  a) Green's functions
  b) The distribution function to $O(\alpha_s^2)$
  c) One loop corrections to the classical NAWW field.
  d) higher orders in perturbation theory.
* Screening mass in a 2-D Euclidean field theory.
* Nuclear Collisions:
  a) The classical background field of two nuclei.
  b) Quantum corrections? The -onium picture.
* Summary

INTRODUCTION:

* Question: Can we compute the "wee" parton distributions in nuclei in the ∞-momentum frame? (McLerran, R.V: PRD 49 2233, 3352 (1994))

* Inspiration: GLR, Mueller-Qin, Mueller.
  ↳ NPB 335, 115 (199

* Experiment:

  1) Initial conditions at RHIC & LHC ($y=0$)
  - understand evolution of Weizsäcker-Williams fields.

  2) DIS: e^- scattering off large nuclei (HERA!)
  - direct test of model's predictions.

* Consider $A \gg 1$ with $\gamma \gg 1$.

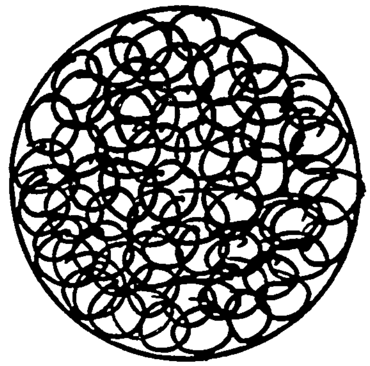

* Large nucleon density $\Rightarrow$ enhanced scale.
  - overcrowding sooner in $A \gg 1$.

* Introduce parameter $\mu^2 \sim A^{1/3}\,\mathrm{fm}^{-2}$

  $\hookrightarrow$ (avg. valence quark color charge squared / area.

* μ^2 proportional to parton density at $x \ll 1$.

* For $\mu^2 \gg \Lambda^2_{QCD}$, $\boxed{\alpha_s(\mu^2) \ll 1}$

  Weak coupling regime!

  (dimensional transmutation.)

SET UP THE PROBLEM

a) $\Delta z_v = \frac{2R}{P} \cdot m$, $\Delta z_g = \frac{1}{xP}$; $\Delta z_v \ll \Delta z_g$

$$\Downarrow$$

$$\boxed{x \ll A^{-1/3}}$$

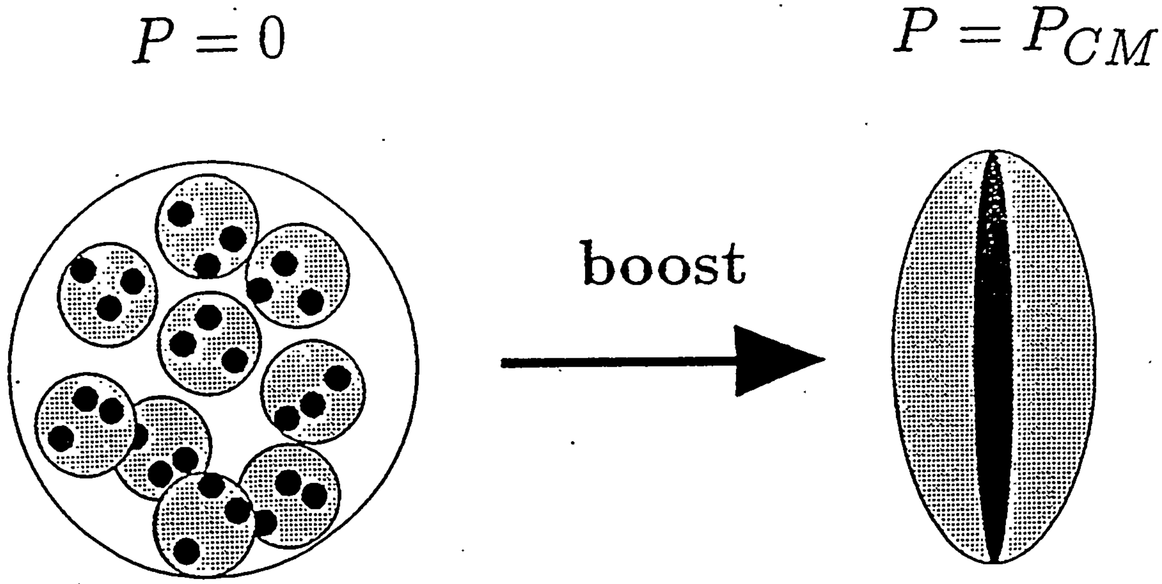

If $x \ll A^{-1/3}$, low x partons see Lorentz contracted valence distribution.

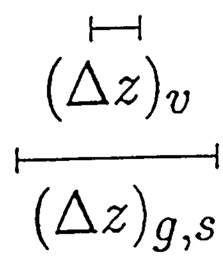

b) For $\alpha_s(\mu^2) \ll 1$,

Small x parton Bremsstrahlung does not change valence quark trajectory $\rightarrow$ "FROZEN" charges.

VALENCE [illegible]: RECOIL-LE[illegible], [illegible]

[illegible]

c) Uniform nuclear matter distributions for $A \gg 1$.

$$\frac{1}{N}\frac{dN}{dr} \sim \frac{1}{R_{nucl.}} \rightarrow 0.$$

slowly varying functions of $x_\perp$.

* PROBLEM: Solve many body problem of $x \ll A^{-1/3}$ parton distributions with external source in ∞-momentum frame.

* SOURCE: Sheet of static valence quarks on Light cone.

$$\boxed{J^{+}_{F,a} = \rho_a(x^+, x_\perp)\,\delta(x^-)}$$

* PROBE: Fock decomposition of nuclear wave function in Light-Cone quantization: (DRELL, YAN – 1970; BRODSKY, LEPAGE – 1980)

$$x\,G(x,Q^2) = \left\langle \int^{Q^2} d^2k_\perp\, dk^+ x\, \delta\!\left(x - \frac{k^+}{P^+}\right) \sum_{\lambda=\pm} a^\dagger_\lambda a_\lambda \right\rangle$$

Parton Density

Number density operator.

* Q.E.D.

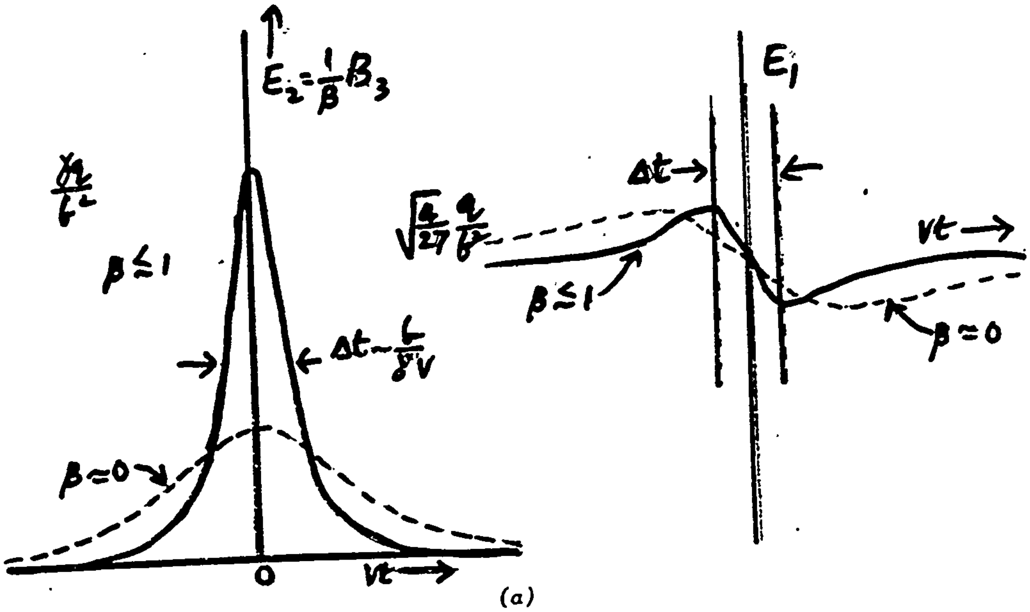

(a)

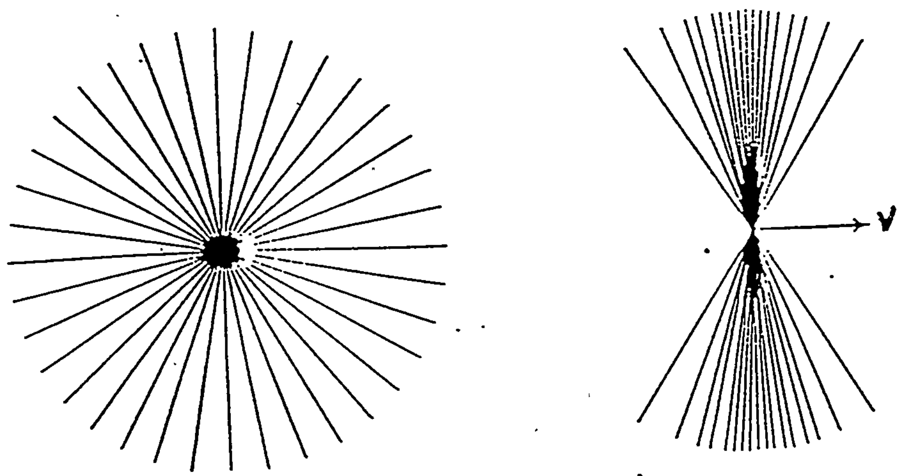

WEIZSÄCKER
WILLIAMS

$$\boxed{\frac{dN}{dk^+ d^2k_\perp} = \frac{\alpha}{\pi^2} \frac{1}{k^+ k_\perp^2}}$$

Light Cone Hamiltonian.

$$\boxed{A^- = 0.}$$

$$P^- \equiv P_0^- + P^-_{int.}$$

$$= \frac{1}{4} F_t^2 + \frac{1}{2} (J_f + D_t \cdot E_t) \frac{1}{(p^+)^2} (J_f + D_t \cdot E_t)$$

$$+ \frac{1}{2} \psi_+^\dagger (m_f - \not{D}_t) \frac{1}{(p^+)} (m_f + \not{D}_t) \psi_+$$

$A_\perp$ and ψ_+ are dynamical fields.

Have used LC- constraint Eqns. to eliminate ψ_- & A_+

$$P_0^- = \frac{1}{2} \left\{ (\vec{\nabla} \times A_t^a)^2 + (\nabla_t \cdot A_t^a)^2 + \frac{1}{2} \psi_+^\dagger (m_f - \not{D}_t) \frac{1}{P^+} (m_f + \not{D}_t) \psi_+ \right.$$

$$P^-_{int.} = \frac{1}{2} \left\{ (J_f^+)^a \frac{1}{(p^+)^2} (\partial_i \partial_- A_i^a) + (\partial_i \partial_- A_i^a) \frac{1}{(p^+)^2} (J_f^a)^a \right\}$$

$(J_f^+)^a$ is the light cone component of fermion current.

PARTON DISTRIBUTIONS IN QCD.

* Return to QCD.....

Recall external source

$$J_a^+ = \rho_a(x^+, x_\perp)\,\delta(x^-)$$

* Compute ground state expectation values

$$Z = \lim_{T\to i\infty} \mathrm{Tr}\left\{ e^{iTP^-} \right\} = \lim_{T \to i\infty} \sum_N \langle N | e^{iTP^-} | N$$

$$= \,?$$

Sum over color labels of external source

* Low x ($\ll A^{-1/3}$) partons resolve grid in 2-D transverse space.

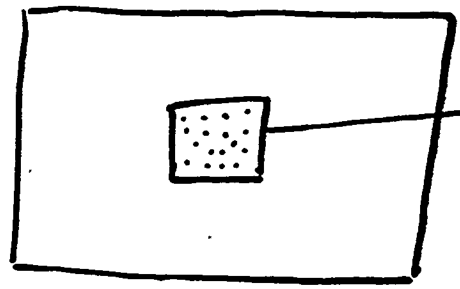

$d^2x_\perp \sim \frac{1}{q_\perp^2}$

$q_\perp$: parton momentum

* If $\quad d^2x_\perp \gg \frac{\pi R^2}{N_{valence}}$ or $q_\perp^2 \ll \frac{N_{valence}}{\pi R^2} \sim A^{1/3}\, fm^{-2}$

then $\quad [Q, Q] \sim Q \ll Q^2$

(Higher dimensional representation of color algebra)

COLOR CHARGE DIST. IS CLASSICAL.

* If total charge in grid $\ll$ max. possible charge,

GAUSSIAN DENSITY OF STATES

$$* \quad \exp\left[-\frac{1}{2\mu^2}\int d^2x_\perp\, \rho^2\right]$$

$\rho \to$ color charge / area.

$\mu^2 \to$ average color charge squared / area

$$\mu^2 = \frac{N_{valence}}{\pi R^2}\langle Q^2\rangle_{1\,quark} \simeq \frac{3A}{\pi A^{2/3}}\cdot\frac{4}{3} = \boxed{1.1\ A^{1/3}\ fm}$$

$$\left(\text{Note: } \langle \rho^a(x_\perp)\,\rho^b(y_\perp)\rangle = \mu^2\delta^{ab}\delta^{(2)}(x_\perp - y_\perp) \atop \langle\rho^a(x)\rangle = 0\right)$$

* <u>PARTITION</u> <u>FUNCTION</u>

$$Z = \int [dA_+\, dA_\perp]\,[d\psi^\dagger d\psi]\,[d\rho]$$

$$* \exp\left[\, i S_{QCD} + ig\int d^4x\, A_+\,\delta(x^-)\,\rho(x^+, x_\perp) - \frac{1}{2\mu^2}\int d^2x_\perp\, \rho^2(0, x_\perp)\right]$$

BACKGROUND FIELD METHOD:

Solutions of equations of motion: $\boxed{D_\mu F^{\mu\nu} = -g J^\nu}$

$A_\perp = 0$

$x^- = 0$

$A_\perp = -\frac{1}{ig} U \nabla_\perp U^\dagger$

$A_+ = A_- = 0.$

pure gauge in 2-D

* $U(x_\perp)$ determined by $\boxed{\vec{\nabla}\cdot(U\vec{\nabla}U^\dagger) = -ig^2\rho(x_\perp)}$

* Compute correlation functions $\langle A_\perp(x_\perp) A_\perp(y_\perp)\rangle$ of background field for arbitrary sources of external charge.

Measure: $\int [dU]\, \det(\vec{\nabla}\cdot\vec{D}) \exp\left[-\frac{1}{\alpha_s^2\mu^2}\int d^2x_\perp \mathrm{Tr}\{\nabla\cdot(U\nabla U^\dagger)\}^2\right]$

Effective coupling
— all orders in $\alpha_s\mu$!

2-D Monte Carlo.

* Gluon distributions in background field:

$$\frac{1}{\pi R^2}\frac{dN}{dx\, d^2k_\perp} = \frac{(N_c^2-1)}{\pi^2}\,\frac{1}{x}\,\frac{1}{\alpha_s}\,\underbrace{H\left(\frac{k_\perp^2}{\alpha_s^2\mu^2}\right)}$$

Correlation functions of Euclide[an] 2-D field theory.

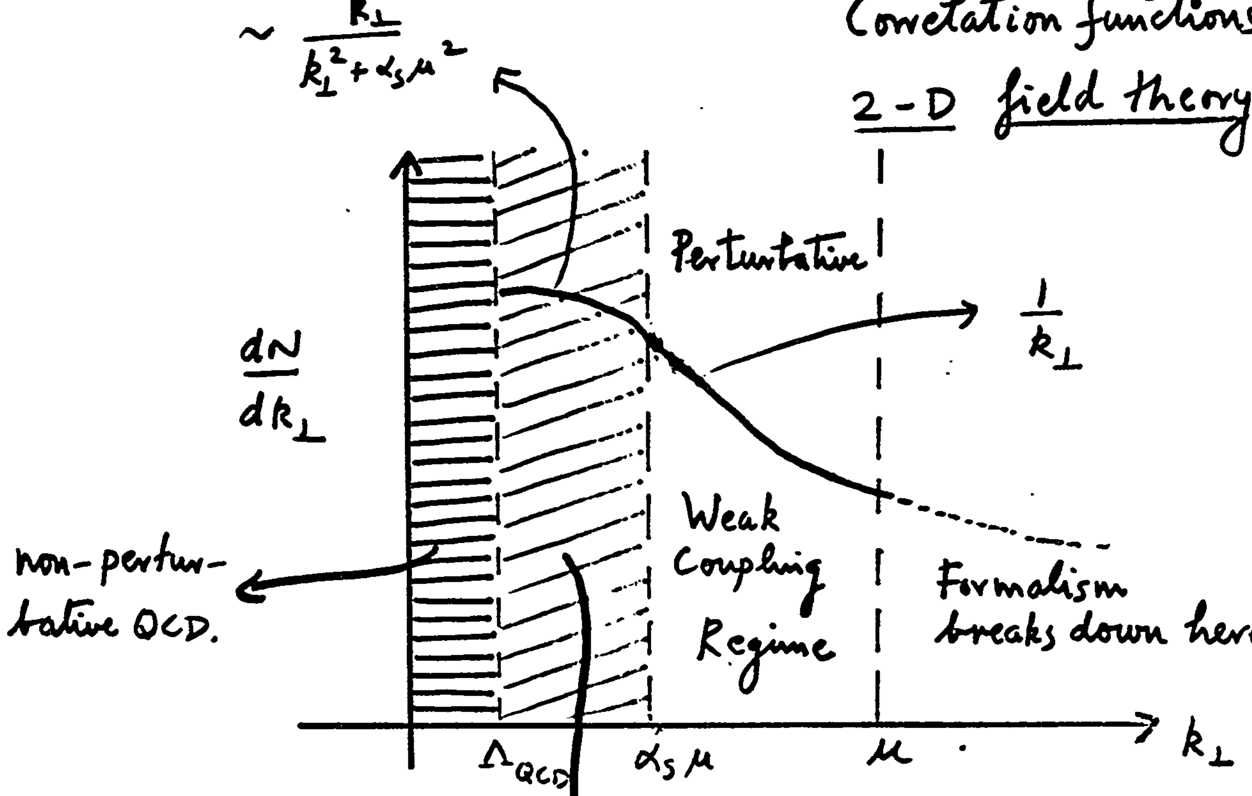

Strong coupling - screening effects : $\frac{dN}{dk_\perp^2} \sim \frac{1}{k_\perp^2+\underbrace{\alpha_s^2\mu}_{\text{"Debye Mass"}}}$

(all orders in $\frac{k_\perp}{\alpha_s\mu}$)

McLerran, RV: PRD 52, 2935 (1995)

* Small Fluctuations Propagator In Non-Abelian Weizsäcker-Williams Fields.

* Generic small fluctuations propagator:

$$G(x,y) = \sum_\lambda \frac{\delta\phi_\lambda(x)\,\delta\phi_\lambda^\dagger(y)}{\lambda}$$

* In light cone gauge, $(A^+=0)$

$$D^2(B)\,\delta A^\mu - D^\mu(B)\,D(B)\cdot\delta A = -2\,\underbrace{\delta(x^-)}_{\text{from source.}}\,\alpha^i(x_\perp)\times\delta A_i$$

using $\boxed{A^\mu = B^\mu + \delta A^\mu}$

and $\boxed{\delta A^-(x^-=0) = 0}$ → fix residual gauge freedom.

* Look at "+" component: →

$$\partial^+\delta A^- - D(A)\,\delta A_i = -2\,\theta(x^-)\,\alpha_i\times\delta A_i\Big|_{x^-=0} + h(x^+, x_\perp)$$

$$\Downarrow$$

Fields are singular at $x^- = \pm\infty$!

INT-50-78.
to appear in PRD.

* SOLUTION:

a) Work in $A^- = 0$ gauge.

Solutions well behaved $\rightarrow$ construct small fluctuations propagator.

$$\Downarrow$$

b) Gauge transform small fluctuation fields back to $A^+ = 0$ gauge.

$$\Downarrow$$

c) Gauge transformation singular in $\frac{1}{\partial^-}\ \frac{1}{\partial^+}$.

From boundary conditions (fix residual gauge freedom).

$$\frac{1}{\partial^-} \rightarrow \frac{1}{i k^-} \rightarrow \frac{1}{i\left(k^- + \frac{i\epsilon}{k^+}\right)}$$ Leibbrandt-Mandelstam.

$$\frac{1}{\partial^+} \rightarrow \frac{1}{i k^+} \rightarrow \frac{\left(e^{i k^+ x^-} - 1\right)}{i k^+}$$ well defined for $k^+ \rightarrow 0$.

$$\Downarrow$$

d) Obtain small fluctuations propagator in $A^+ = 0$ gauge

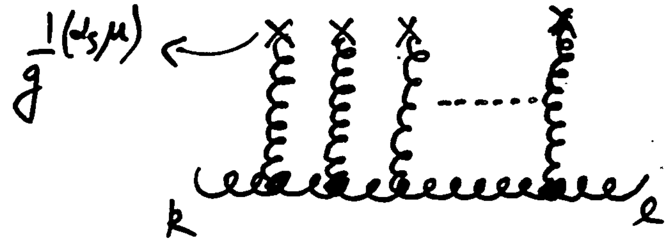

$$\langle G_{ij}^{ab}(k,\ell)\rangle_\rho = (2\pi)\,\delta(k^- - \ell^-)\,(2\pi)^2\,\delta^{(2)}(k_\perp - \ell_\perp) \ast D_{ij}^{ab}(k,\ell)$$

$$\boxed{D_{ij}^{ab} = D^{ab}_{\substack{--\\ ij}} + D^{ab}_{\substack{++\\ ij}} + D^{ab}_{\substack{+-\\ ij}} + D^{ab}_{\substack{-+\\ ij}}}$$

$$D^{ab}_{--} = -\delta^{ab}\left\{ \theta(k^-)\frac{1}{\ell^2}\left[\frac{1}{\ell^+ - k^+ + i\epsilon}\left(\delta_{ij} + \frac{k_i k_j(\ell^+ - k^+)}{k^- k^+ \ell^+}\right) + 2\pi i\,\delta(k^+)\frac{k_i k_j}{k^- \ell^+}\right] + k,\ell \to -\ell,-k\right\}$$

$$D^{ab}_{++} = \int \frac{d^2 p_\perp}{(2\pi)^2}\,\Gamma^{ab}(p_\perp - k_\perp)\left\{\theta(k^-)\frac{1}{p_\perp^2 - 2k^-k^+ - i\epsilon} \ast \left[\frac{1}{k^+ - \ell^+}\left(\delta_{ij} + \frac{p_i p_j}{k^- k^+ \ell^+}(k^+ - \ell^+)\right) + 2\pi i\,\delta(\ell^+)\frac{p_i p_j}{k^- k^+}\right] + k,\ell \to -\ell,-k\right\}$$

$$D^{ab}_{+-} = i\,2k^-\,\theta(k^-)\frac{1}{\ell^2}\int\frac{d^2p_\perp}{(2\pi)^2}\,\Gamma^{ab}(p_\perp - k_\perp)\frac{1}{p_\perp^2 - 2k^-k^+ - i\epsilon} \ast \left[\delta_{ij} - \frac{k_i k_j}{k^-\ell^+} - \frac{p_i p_j}{k^- k^+} + \frac{p_i k_j\, p_\perp\cdot k_\perp}{k^- k^+ k^- \ell^+}\right]$$

$$D^{ab}_{\substack{-+\\ ij}} = D^{ba}_{\substack{+-\\ ji}}(-\ell^-, -k^-)$$

$$\Gamma^{ab}(x_\perp - y_\perp) = 2\left\langle \mathrm{Tr}\, U^\dagger(x_\perp)\tau^a U(x_\perp) U^\dagger(y_\perp)\tau^b U(y_\perp)\right\rangle_\rho$$

ONE LOOP CORRECTIONS TO CLASSICAL FIELD

* Can write the two point fn to all orders:

$$\langle A A \rangle = \langle A_{cl} \rangle \langle A_{cl} \rangle + \langle A_{qu} A_{qu} \rangle$$

$$A_{cl}^{(0)} + A_{cl}^{(1)} + \cdots\cdots$$

* $A_{cl}^{(0)} \equiv$  $\frac{1}{g}(\alpha_s \mu)^n$

(Note : Weizsäcker–Williams : 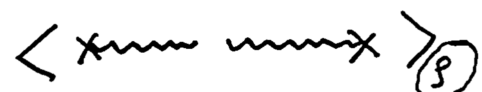

$\frac{1}{g}(\alpha_s \mu)^n \qquad \frac{1}{g}(\alpha_s \mu)^n$

* $A_{cl}^{(1)} \equiv$ 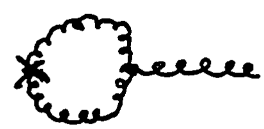

$=$ 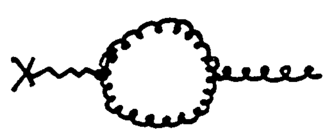 $+$ 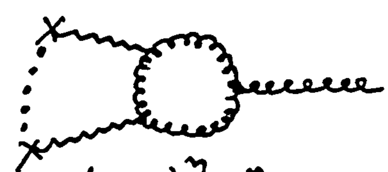

$\frac{1}{g}(\alpha_s \mu) \cdot g \cdot g \qquad \frac{1}{g^n}(\alpha_s \mu)^n \cdot g^n \cdot g$

* Again, expand $A^\mu = B^\mu + \delta A^\mu$

Keeping terms quadratic in δA, can write

$$D_\mu F^{\mu\nu} = g\, J^\nu \quad \equiv$$

$$- \quad \partial_- \partial^+ B^-_a - (D_i \partial^+ B^i)_a = g\, j^+_a + g \langle J^+_a \rangle$$

$$(D_i D^i B^-)_a - (D_i \partial^- B^i)_a + (D_+ \partial^+ B^-)_a = 0$$

$$(D_j D^j B^i)_a - (D_j \partial^i B^j)_a + (D_+ \partial^+ B^i)_a - (\partial_- D^i B^-)_a = 0$$

* Only term to survive is

$$j^+_a(x) = f_{abc} \langle \delta A^i_b(x)\, \partial^+ \delta A^i_c(x) \rangle$$

$$= i f_{abc} \lim_{y \to x} \frac{\partial}{\partial y^-} \boxed{G^{ii}_{bc}(x,y)}$$

Small fluctuations propagator!

(to appear in PRD)

*

$$g\, \tilde{j}^{+}_{a}(p) = \Pi^{+i}_{ab}(p)\, A^{i(0)}_{b}(p)$$

with

$$\Pi^{+i}_{ab}(p) = g^2 p^+ p^i \left(\frac{5\,\Gamma(-\omega)}{16\pi^2} \right) \delta_{ab}$$

* Recover standard expression for "$+i$" components of polarization tensor in light cone gauge!

*

$$B^-(x) = 0$$

$$B^i(x) = \theta(x^-)\,\alpha^i_R(x_\perp)$$

$$\text{I.}\ \alpha^i_R(x) = \frac{i}{g_R}\, U(x_\perp)\,\nabla^i U^\dagger(x_\perp)\,.$$

where $g_R^2 = Z_3\, g^2\,, \quad Z_3 = \left(1 + \dfrac{11 g^2}{16\pi^2(1-\omega)} \right)$

$$\Rightarrow B^i(x) = Z_3^{-1/2}\, A^{i(0)}(x)$$

(A.J, J.M, L.M, R.V – to appear, PRD)

* Quantum Corrections To Distribution Fn.

$$\frac{dN}{d^3k} = \frac{i\,2k^+}{(2\pi)^3} \lim_{k^+\to l^+} \int \frac{dk^-}{2\pi} \int \frac{dl^-}{2\pi} \left\langle D_{ii}^{aa}(k,l) \right\rangle$$

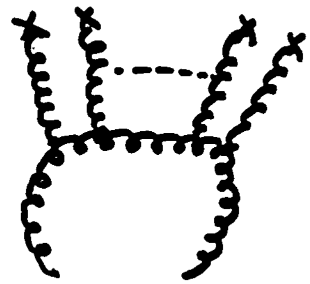

k   k

* Leading contribution.

$$\text{WC} \rightarrow (2\pi)^2 \frac{\alpha_s^2 \mu^2 N_c}{p_\perp^4}$$

$$\frac{1}{\pi R^2} \frac{dN}{dx\, d^2k_\perp} = \frac{8(N_c^2-1)}{(2\pi)^4} \frac{1}{x} \int \frac{d^2p_\perp}{(2\pi)^2} \Pi(p_\perp - k_\perp) \left[1 - \frac{(p_\perp \cdot k_\perp)^2}{p_\perp^2 k_\perp^2} \right] * \ln\left(\frac{1}{x}\right)$$

* In weak coupling, $(\alpha_s \mu \le p_\perp)$

$$\boxed{\frac{1}{\pi R^2} \frac{dN}{dx\, d^2k_\perp} = N_c (N_c^2-1) \frac{\alpha_s^2 \mu^2}{x\, k_\perp^2} \frac{2}{\pi^3} \left(\ln\left(\frac{k_\perp}{\alpha_s \mu}\right) + \frac{1}{2} \right) * \ln\left(\frac{1}{x}\right)}$$

See also A. Mueller, NPB 335.

Higher Orders In Perturbation Theory.

* Sum ladders:

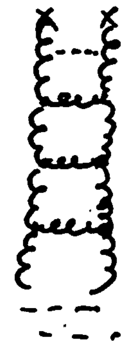

$$\frac{1}{x}\left[1 + c_1 \ln(x) + \frac{c_1^2}{2!}\ln^2 x + \dots\right] \qquad ?$$

SATURATION

* Relation of Lipatov ansatz to previous result?

$$\frac{1}{\hat{t}} \rightarrow \frac{1}{\hat{t}} \exp\left[\alpha_s N_c \ln\left(\frac{q_\perp^2}{m^2}\right) \ln\left(-\frac{\hat{s}}{\hat{t}}\right)\right]$$

* How does the infrared behaviour ($\Lambda_{QCD} \ll p_\perp \ll \alpha_s u$) influence saturation? (A. White)

* PARTON DISTRIBUTIONS AS CORRELATION FN'S OF 2-D EUCLIDEAN FIELD THEORY

* Product of classical fields:

$$\langle \alpha_\perp(x_\perp)\alpha_\perp(y_\perp)\rangle_\rho = \mathrm{Tr}\int [d\rho] \left(-\frac{1}{ig} U(x_\perp)\nabla_\perp U^\dagger(x_\perp)\right)_\rho * \frac{\left(-\frac{1}{ig} U\nabla U^\dagger(y_\perp)\right)_\rho \exp\left[-\frac{1}{2\mu^2}\int d^2x_\perp\, \rho^2(x_\perp)\right]}{\int[d\rho]\exp\left[-\frac{1}{2\mu^2}\int d^2x_\perp\, \rho^2(x_\perp)\right]}$$

$$\alpha_\perp = -\frac{1}{ig} U(x_\perp)\nabla_\perp U^\dagger(x_\perp) \;;\quad \nabla_\perp\cdot(U\nabla_\perp U^\dagger) = -ig^2\rho(x_\perp)$$

*

strong coupling: $k_\perp < \alpha_s\mu$

weak coupling: $k_\perp > \alpha_s\mu$ (Weizsäcker - Williams)

* Solve strong coupling problem (all orders in $\frac{\alpha_s\mu}{k_\perp}$) on the Lattice.

(in progress - with Rajiv Gavai)

* Screening mass ? $m = \# \alpha_s \mu$.

* <u>Multi-dimensional Monte-Carlo</u>:

Lattice algorithm: $SU(2)$, $31 \otimes 31$.

$$Z = \int \prod_{x,a} d\rho^a(x) \prod_x du(x) \exp\Big[-\sum_{x,a} \rho^a(x)\rho^a(x) + \lambda \left(D^a + 2g^2\mu a \rho^a(x)\right)^2 \Big]$$

$$D^a_\tau = i \sum_k D^a_k \tau^a = \sum_k \Big[u(x_\perp)u^\dagger(x+a\hat{e}_k) + u(x_\perp)u^\dagger(x_\perp - a\hat{e}_k) - u(x+a\hat{e}_k)u^\dagger(x_\perp) - u(x-a\hat{e}_k)u^\dagger(x_\perp) \Big] + O(a^4)$$

Obtain correlators of $\frac{u\nabla_i u^\dagger}{-ig}$ in limit $\lambda \to \infty$

* <u>Conjugate Gradient</u>:

$$F = \sum_{x,a}^{3} L^a(x) L^a(x) + \sum (uu^\dagger - 1)^2$$

$$\tau^a L^a(x) = \sum_k \operatorname{Im}\left\{ u(x)u^\dagger(x+a\hat{e}_k) + u(x)u^\dagger(x-a\hat{e}_k) \right\} + \sqrt{2}\, g^2\mu a\, \rho(x_\perp).$$

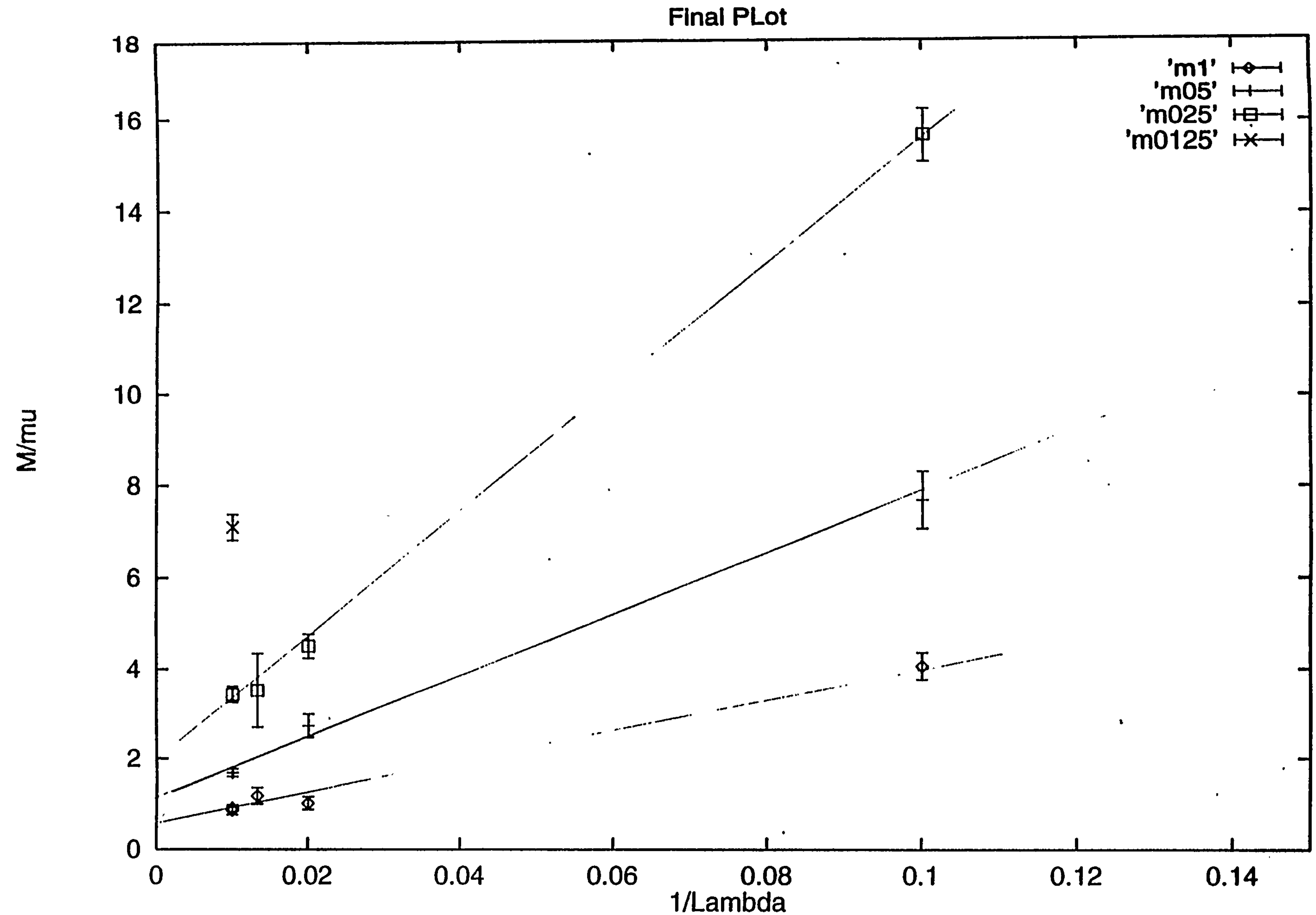
Final PLot
'm1'
'm05'
'm025'
'm0125'
M/mu
1/Lambda
0
2
4
6
8
10
12
14
16
18
0.02
0.04
0.06
0.08
0.1
0.12
0.14

a = 0.025

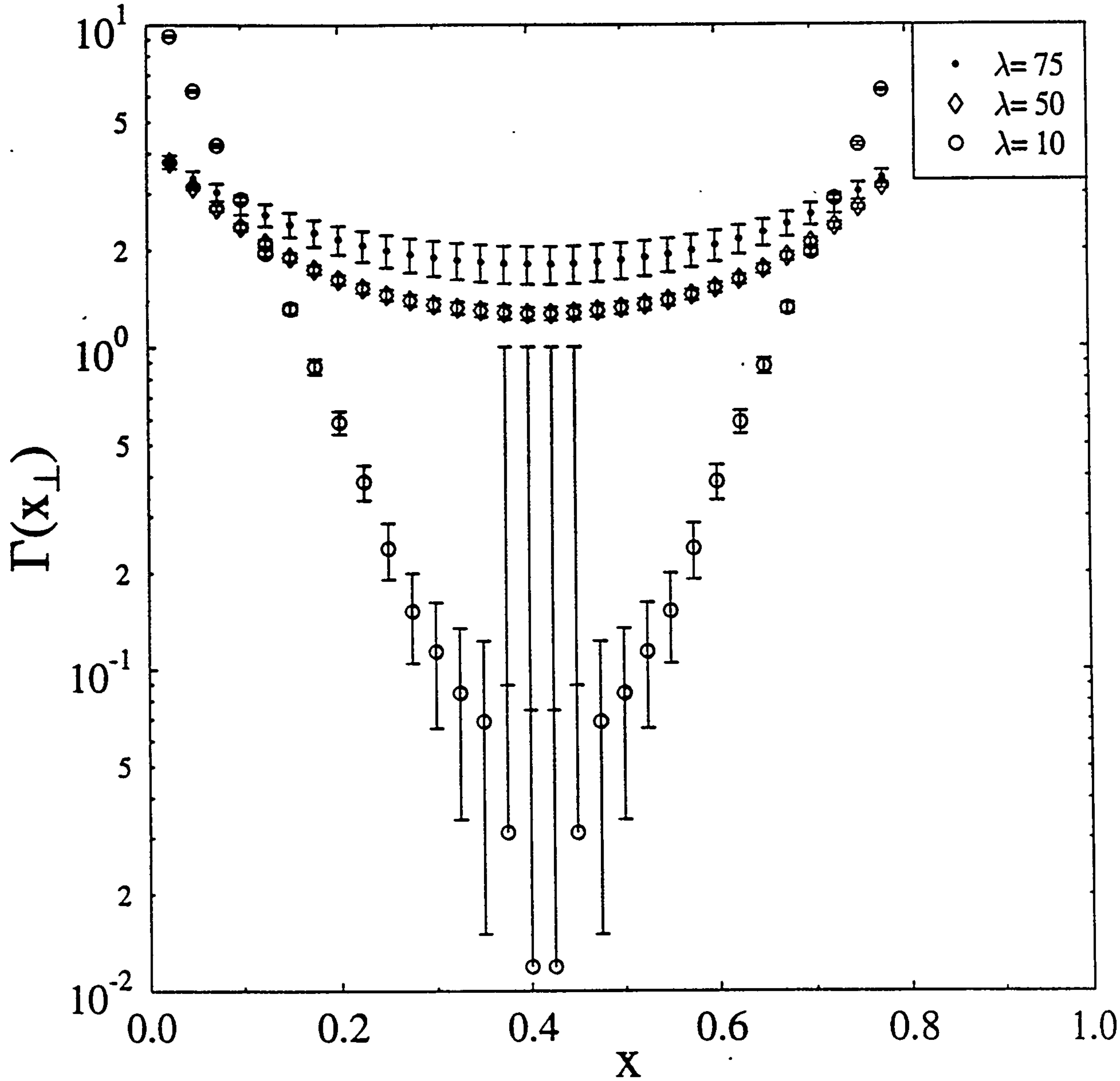

10^1
5
2
10^0
5
2
10^{-1}
5
2
10^{-2}
$\Gamma(x_\perp)$
0.0
0.2
0.4
0.6
0.8
1.0
x
$\lambda = 75$
$\lambda = 50$
$\lambda = 10$

Gluon Production for Weizsäcker-Williams Field in Nucleus–Nucleus Collisions

Heribert Weigert
University of Minnesota

Gluon Production

from

Weizsäcker-Williams Fields

in

Nucleus-Nucleus Collisions

A. Kovner   L. McLerran   H. Weigert

- assumptions & scales
- from single nucleus to colliding nuclei

  equations & boundary conditions for classical gluon fields
- asymptotics $\longrightarrow$ gluon distribution functions
- perturbative solutions
- conclusions

Introduction: Theoretical approaches to heavy ion collisions

- omit early stages   assume initial condition

  - typical example: hydrodynamics (local thermal equi

soft processes
equilibrium ?

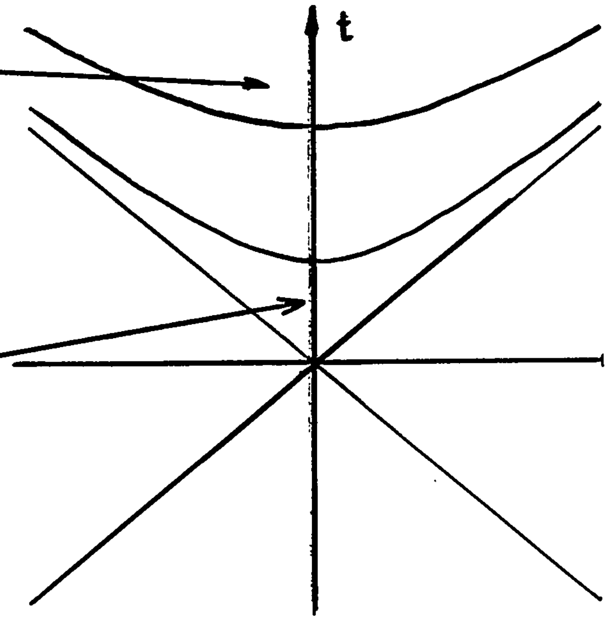

hard processes

- towards earlier stages:

  - parton cascade   (K. Geiger, B. Müller)

    - input: q & g distributions (experiment)
    - assumptions: nuclei = incoherent classical partic
    - aimed at: early stages
      hard scattering signals

Basic assumptions

small x gluons

x

valence quarks

gluons (sea quarks)

eikonalization of valence quarks in b.g. of small x gluons

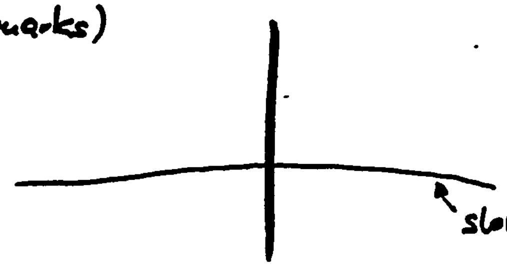

slowly varying gluon fields

transverse scales: large nuclei

$$\mu^2 := \frac{\#\,\text{partons}^2}{\text{unit area}^2} \sim A^{1/3}$$

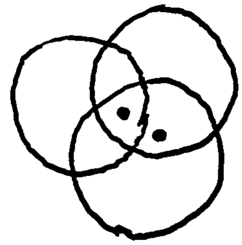

$\Delta x \ll 1\,\text{fm}$

classical uncorrelated color charges ρ

$$\int D[\rho]\; e^{-\frac{\rho}{2\mu}} + \mathcal{L}[\rho, A]$$

coupling to small x gauge potentials

$$\boxed{\frac{\delta}{\delta A_\mu(x)}\,\mathcal{L}[\rho, A] = J^\mu[A] = U[A](x, z(x))\; J(z(x))\; U[A](z(x), x)}$$

$\delta(x^-)\,\rho(x_\perp)$

Classical gluon fields

large numbers $\longrightarrow$ classical fields

$$[D_\mu[A], F^{\mu\nu}[A]] = J^\mu[A] \longrightarrow A$$

□ expansion parameter $(\alpha_s \mu)^2$

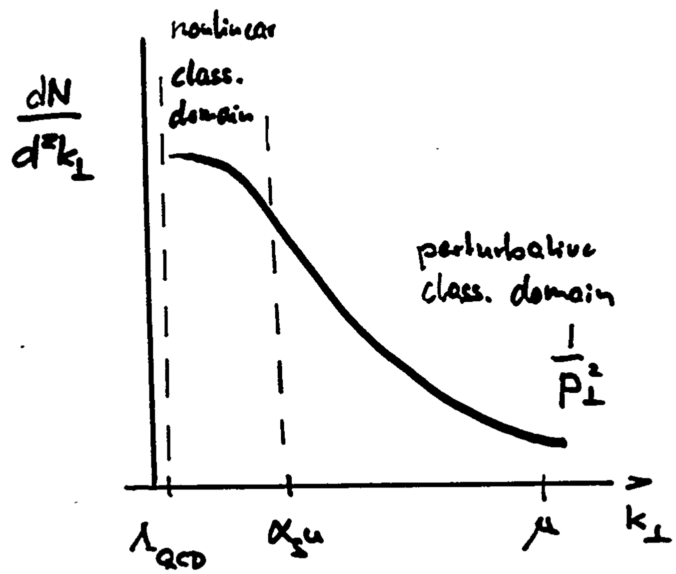

single nucleus

The single nucleus field:

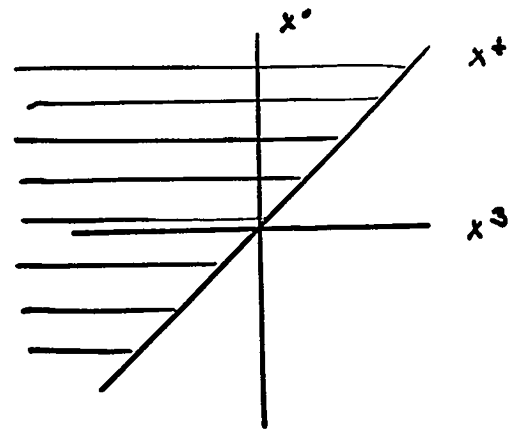

$A^+ = 0 \quad A^- = 0$

$A^i = \theta(x^-)\,\alpha^i(x_\perp)$
$i = 1,2$

eq. of motion

$$\boxed{\begin{array}{c} F^{ij} = 0 \\ \partial_i \alpha^i = g \cdot \rho \end{array}}$$

solution

$$\boxed{\begin{aligned} \alpha_i &= -\frac{1}{ig} U(x_\perp)\,\partial_i\,U^{-1}(x_\perp) \\ &= -g\,\partial^i \left[\frac{1}{\nabla_\perp^2}\rho\right](x_\perp) + O(g^2) \end{aligned}}$$

A_μ pure gauge almost everywhere

physics in discontinuity

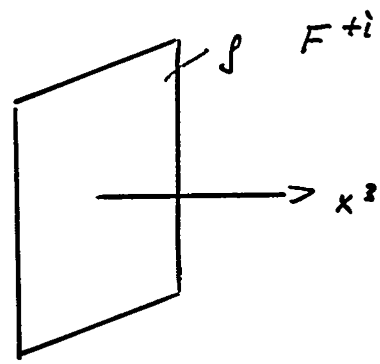

$$\frac{1}{\pi R^2}\,\frac{dN}{dx\,d^2k_\perp} = \frac{N_c^2 - 1}{\pi^2}\,\frac{1}{x}\,\frac{1}{\alpha_s}\,H\left(\frac{k_\perp^2}{(\alpha_s \mu)^2}\right)$$

Two colliding nuclei:

$$[D_\mu, F^{\mu\nu}] = \underbrace{J_1^\nu[A]}_{\sim\delta(x^-)\rho_1(x_\perp)} + \underbrace{J_2^\nu[A]}_{\sim\delta(x^+)\rho_2(x_\perp)}$$

□ before collision

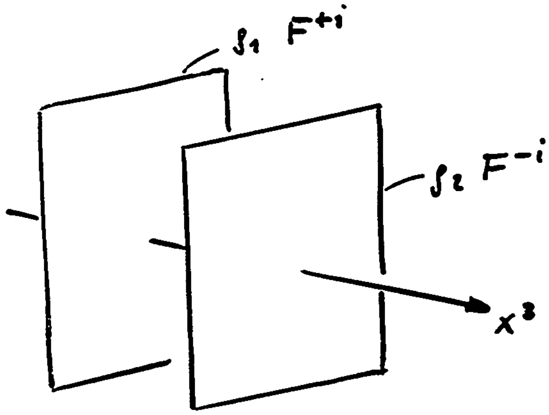

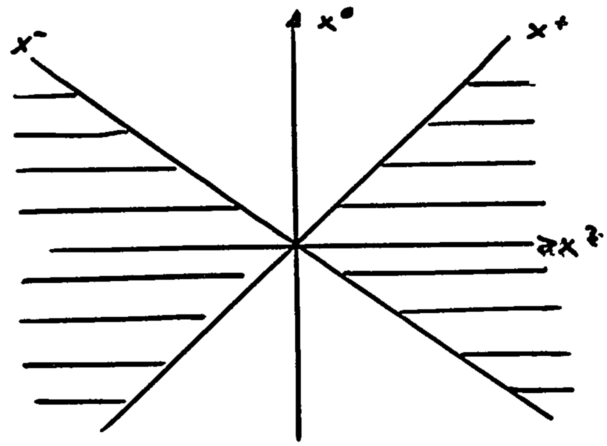

$$\partial^i \alpha_m(x_\perp) = \rho(x_\perp) \qquad \alpha_m^i(x_\perp) = -\frac{1}{ig} U_m(x_\perp)\partial^i U_m$$

□ after the collision no y dependence

$$A^+ = x^+ \alpha(\tau, x_\perp) \qquad A^- = -x^- \alpha(\tau, x_\perp) \qquad A^i = \alpha_\perp(\tau, x_\perp)$$

▶ equations in forward wedge:

$$\frac{1}{\tau^3}\partial_\tau \tau^3 \partial_\tau \alpha + [D_i, [D^i, \alpha]] = 0$$

$$\frac{1}{\tau}[D_i, \partial_\tau \alpha_\perp^i] + ig\tau[\alpha, \partial_\tau \alpha] = 0$$

$$\frac{1}{\tau}\partial_\tau \tau \partial_\tau \alpha_\perp^i - ig\tau^2[\alpha, [D^i, \alpha]] + [D_j, F^{ji}] = 0$$

▶ matching conditions:

$$\nu = i \qquad \alpha_\perp^i\Big|_{\tau=0} = \alpha_1^i + \alpha_2^i \qquad \nu = \pm \qquad \alpha\Big|_{\tau=0} = -\frac{1}{ig}[\alpha_{1i}, \alpha_2^i]$$

The asymptotic limit

- $\tau \to \infty \longrightarrow$ dissipation of energy density $\longrightarrow$ small $F^{\mu\nu}$

$$A_\mu = V(x_\perp)\left[\underset{\text{small}}{\underbrace{\varepsilon_\mu}} - \frac{1}{ig}\partial_\mu\right]V^{-1}(x_\perp)$$

- Y.M. equations linearize

$$\varepsilon^{\pm} = \pm x^{\pm}\int\frac{d^2k_\perp}{(2\pi)^2}\frac{1}{\sqrt{2\omega}}\left\{a_1(k_\perp)\frac{e^{i(k_\perp x_\perp - \omega t)}}{\tau^{3/2}} + c.c\right\}$$

$$\varepsilon^{i} = \int\frac{d^2k_\perp}{(2\pi)^2}\frac{\varepsilon^{ij}k_j/\omega}{\sqrt{2\omega}}\left\{a_2(k_\perp)\frac{e^{i(k_\perp x_\perp - \omega t)}}{\tau^{1/2}} + c.c.\right\}$$

- 2 indep. amplitudes a_1, a_2 !

Perturbative solutions 1: expansion in ρ

- initial conditions:

$$\partial^i \alpha^i_m = \partial^i \left\{ -\frac{1}{ig} U_m(x_\perp) \partial^i U_m^{-1}(x_\perp) \right\} = g\,\rho(x_\perp)$$

$$\longrightarrow \quad \alpha^i_m = \alpha^i_{m\,(1)} + \alpha^i_{m\,(2)} + \ldots$$

feeds into
$$\begin{cases} \alpha^i_\perp \Big|_{\tau=0} = \alpha^i_1 + \alpha^i_2 & \text{starts at } \mathcal{O}(\rho) \\ \alpha \Big|_{\tau=0} = \frac{ig}{2}\left[\alpha^i_1, \alpha^i_2\right] & \text{starts at } \mathcal{O}(\rho^2) \end{cases}$$

- change the gauge

$$\partial^i V(x_\perp)\left[\alpha^i_\perp - \frac{1}{ig}\partial^i\right] V^{-1}(x_\perp)\Big|_{\tau=0} \stackrel{!}{=} 0$$

$$\longrightarrow \begin{cases} \varepsilon^i := V(x_\perp)\left[\alpha^i_\perp - \frac{1}{ig}\partial^i\right] V^{-1}(x_\perp) \\ \varepsilon := V(x_\perp)\,\alpha\, V^{-1}(x_\perp) \\ \text{boundary conditions !} \end{cases}$$

□ lowest order equations: $(n) = (1), (2), (3)$

$$\frac{1}{\tau^3}\partial_\tau \tau^3 \partial_\tau \; \mathcal{E}_{(n)} - \nabla_\perp^2 \mathcal{E}_{(n)} = 0$$

$$\partial_\tau \partial^i \varepsilon^i_{(n)} = 0$$

$$\frac{1}{\tau}\partial_\tau \tau \partial_\tau \varepsilon^i_{(n)} - (\delta^{ij}\nabla_\perp^2 - \partial^i\partial^j)\varepsilon^j_{(n)} = 0$$

$$\longrightarrow \quad \varepsilon^i =: \epsilon^{ij}\partial^j \chi$$

□ final version:

$$\left(\frac{1}{\tau^3}\partial_\tau \tau^3 \partial_\tau - \nabla_\perp^2\right) \mathcal{E}_{(n)} = 0$$

$$\left(\frac{1}{\tau}\partial_\tau \tau \, \partial_\tau - \nabla_\perp^2\right) \chi_{(n)} = 0$$

□ with boundary conditions

• first order: $\mathcal{E}_{(1)}\big|_{\tau=0} = \chi_{(1)}\big|_{\tau=0} \equiv 0$

• second order: $\mathcal{E}_{(2)}\big|_{\tau=0} = \frac{ig}{2}\delta^{ij}\left[\partial^i \frac{1}{\nabla_\perp^2}\rho_1, \partial^j \frac{1}{\nabla_\perp^2}\rho_2\right]$

$$\chi_{(2)}\big|_{\tau=0} = -ig\,\epsilon^{ij}\left[\partial^i \frac{1}{\nabla_\perp^2}\rho_1, \partial^j \frac{1}{\nabla_\perp^2}\rho_2\right]$$

Perturbative solutions 2: distribution functions

$$\mathcal{E}_{(2)}(\tau, x_\perp) \xrightarrow{\tau\to\infty} \int \frac{d^2k_\perp}{(2\pi)^2} \frac{1}{(\omega\tau)^{3/2}} \left\{ \boxed{a^a_{\mathcal{E}}} e^{ik_\perp x_\perp - i\omega\tau} + c.c. \right\}$$

$$\chi_{(2)}(\tau, x_\perp) \xrightarrow{\tau\to\infty} \int \frac{d^2k_\perp}{(2\pi)^2} \frac{1}{(\omega\tau)^{\frac{1}{2}}} \left\{ \boxed{a^a_{\chi}} e^{ik_\perp x_\perp - i\omega\tau} + c.c. \right\}$$

initial conditions

- distribution funktion:

$$\frac{d^3N}{dy\, d^2k_\perp} \sim S_\perp \frac{g^2}{k_\perp^2} \left[\delta^{ij}\delta^{kl} + \varepsilon^{ij}\varepsilon^{kl}\right] \int d^2x_\perp\, e^{-ik_\perp x_\perp} \cdot$$

$$\cdot\, \mathrm{tr} \left\langle \left[\partial^i \frac{1}{\nabla_\perp^2}\rho_1, \partial^j \frac{1}{\nabla_\perp^2}\rho_2\right](x_\perp) \left[\partial^k \frac{1}{\nabla_\perp^2}\rho_1, \partial^l \frac{1}{\nabla_\perp^2}\rho_2\right] \right\rangle_{\rho_1, \rho_2}$$

$$= S_\perp C_{N_c} \frac{g^6 \mu^4}{k_\perp^4} \ln \frac{k_\perp^2}{(\alpha_s \mu)^2}$$

Conclusion

pert. factorization

□ $$N(k_\perp) \sim \int d^2p_\perp \; \underbrace{N_1(p_\perp)\; N_2(k_\perp - p_\perp)}_{\frac{\alpha_s \mu^2}{p_\perp^2}} \; \underbrace{\sigma}_{\frac{\alpha_s}{k_\perp^2}}$$

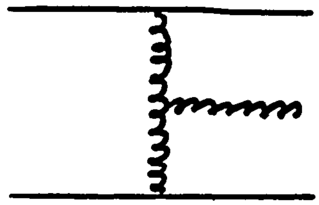

□ scaling

$$N_{total} = \int d^2k_\perp \frac{d^3N}{dy\, d^2k_\perp} \sim S_\perp \mu^2 \sim A^{\frac{2}{3}+\frac{1}{3}}$$

$$N_{pert} = \int_{k_\perp \geq p_\perp \gg \alpha\mu} d^2k_\perp \frac{d^3N}{dy\, d^2k_\perp} \sim S_\perp \mu^4 \sim A^{4/3}$$

□ Wishlist

- Lipatov enhancement — quantum corrections / evolution equations
- nonpert classical fields

Montecarlo simulations / mean fields

Summary Talk

Sean Gavin
Brookhaven National Laboragtory

S. Gavin
BNL

CAN HERA ANSWER HARD QUESTIONS AT RHIC ?

HOW ARE HARD INTERACTIONS IMPORTANT ?

I. HARD PROBES: *use hard processes to have controled probe of dense medium*

HARD PROBES	RHIC USE	SCALE
1) DRELL YAN	Background for thermals	$M_{\mu^+\mu^-}$
2) DIRECT PHOTONS	— " —	$p_T(\gamma)$
3) CHARM (Z. Lin)	— " —	m_T (Ch
4) JETS (Miklos)	Jet quenching ? parton interactions with HOT & COLD matter	p_T (jet
5) J/ψ, ψ', Υ	color screening ? color OCTET interactions with matter ?	$M_{Q\bar{Q}}$

II. MINIJET THERMALI~~ZATION~~TION:

DOES HARD SCALE BECOME
TYPICAL → SOFT ?

SUGGESTIONS:

1) MINIJET PRODUCTION COPIOUS AT RHIC & LHC
Kajantie; Mueller & Blaizot; ....

2) HIGH PARTON DENSITY PROVIDES NEW SMALLER SCALE $p_0 \sim (dN/dy)^{1/2}$

Venugopalan, Kovner, Weigert

3) • HERA real γ vs γ^* transition not abrupt -- maybe $p_0 < 1$ GeV (Ritz)
• GRV gets low x rise from low p_0 (Muel

HERA: HOW DOES THIS WORK IN eA ?
DOES SHADOWING KEEP HARD STUFF HARD

Mueller, Sterman, Qiu, Gyulassy

NUCLEAR EFFECTS IN HARD PROCESSES

- PARTON DISTRIBUTIONS **DIFFERENT** IN NUCLEI

FNAL E665 JaRyan
SMC
...

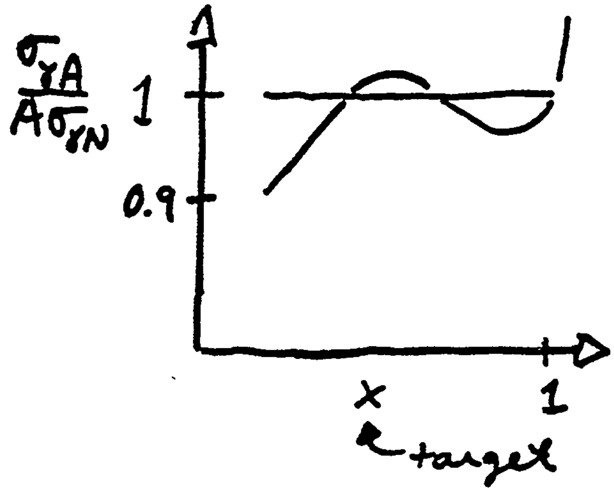

SMALL x:

KINEMATICS SELECT LONG WAVELENGTH PARTONS

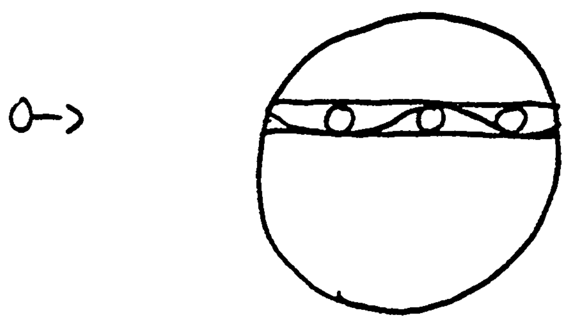

$\lambda = \frac{1}{xP}$

SMALL EFFECT IN μ Xe BUT BIG IN Au+Au

MULTIPLE PARTON SCATTERING

DRELL YAN
CERN NA10
FNAL E772

J/ψ NA3

Υ E772

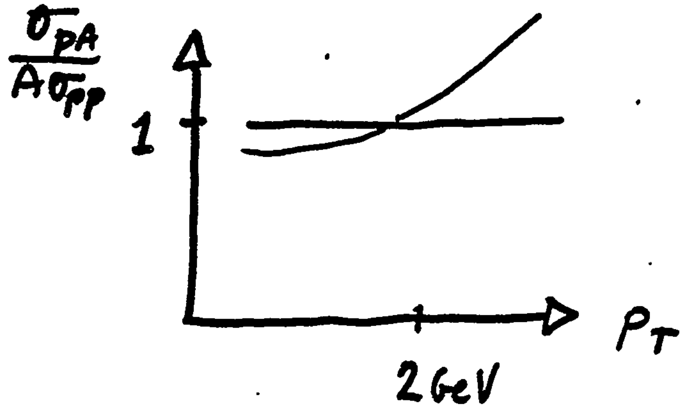

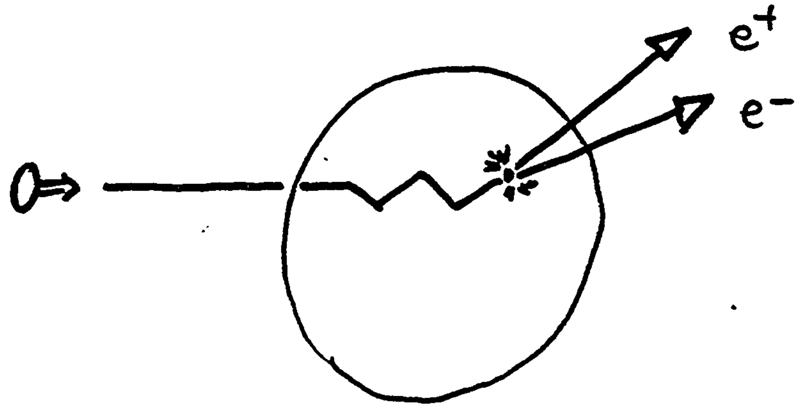

$$\Delta p_T^2 = k_0 A^{1/3}$$

EXPERIMENTS:

DRELL YAN	$k_0 = (0.24\ \text{GeV})^2$	initial + final sta
J/ψ	$k_0 = (0.36\ \text{GeV})^2$	
Υ	$k_0 = (0.51\ \text{GeV})^2$	

- **WHY IS** $k_\psi \approx \frac{1}{2} \times k_\Upsilon$??
- **WHAT HAPPENS IN SHADOWING REGION ?**

PROOF: E772 $\langle p_T^2 \rangle$ vs. A

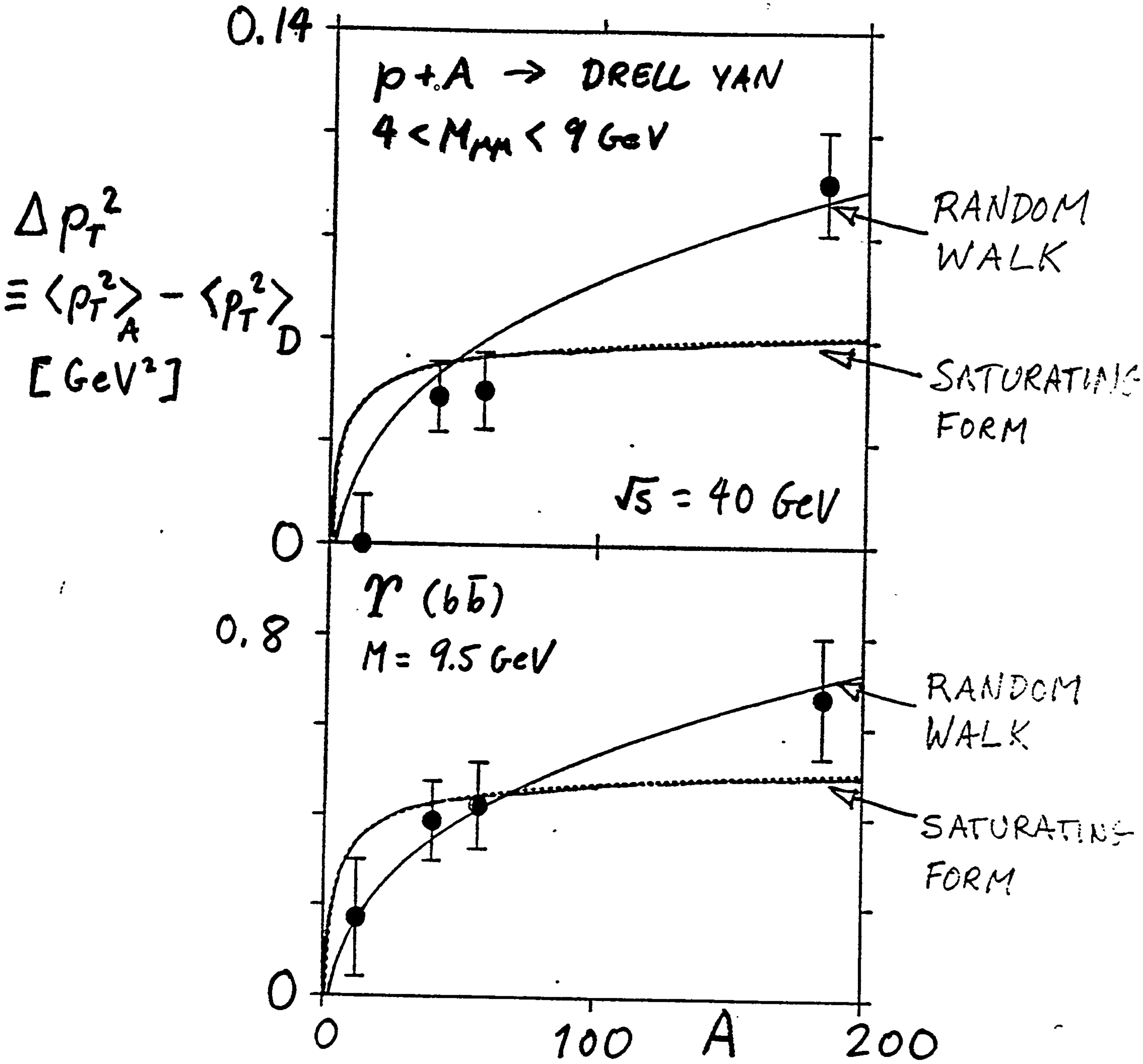

▶ RANDOM WALK WORKS $\Delta p_T^2 \approx K^2 (A^{1/3} - 1)$

Better than SATURATING Form $\propto 1 - A^{-1/3}$ [Satz]

▶ $K_m^2 \sim 2 K_{\perp}^2$ LARGE! Q^2 DEPENDENCE ? TEST DRELL YAN

LEPTON + NUCLEUS EVIDENCE ?

DEEP INELASTIC
ℓA SCATTERING:

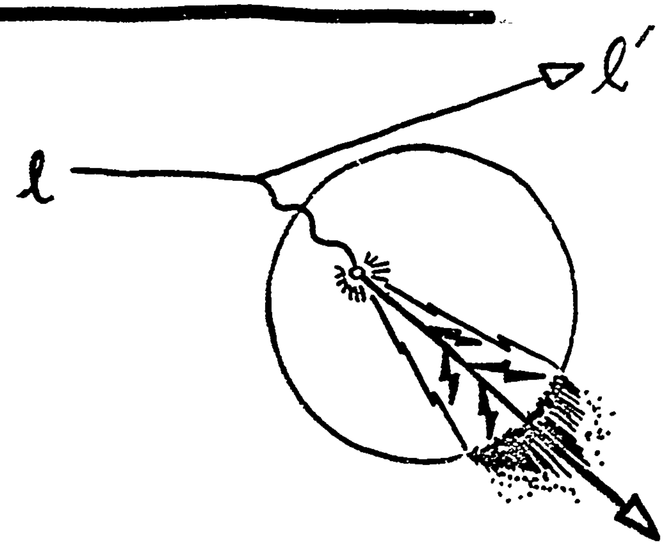

EXPECT **QUARK JET** TO LOSE ENERGY

Gyulassy & Plümer; Bialas et al.
X.N. Wang et al.

- MOST DATA CONSISTENT WITH NO EFFECT (with S-1
- LOW QUARK ENERGY ν **INTERESTING** but **INCONCLUSIVE** -- E665, NMC Disagree

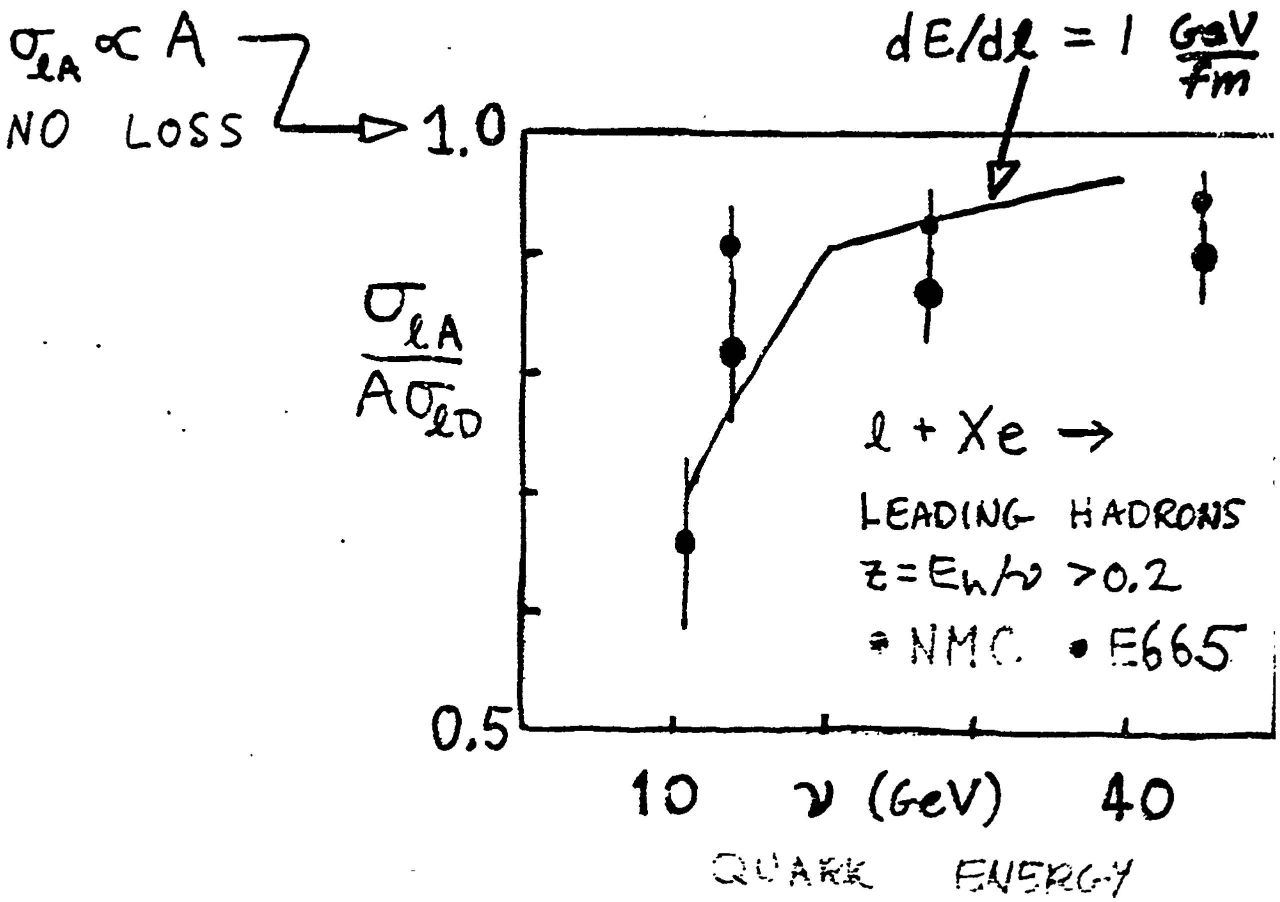

HIGH x_F DEPLETION

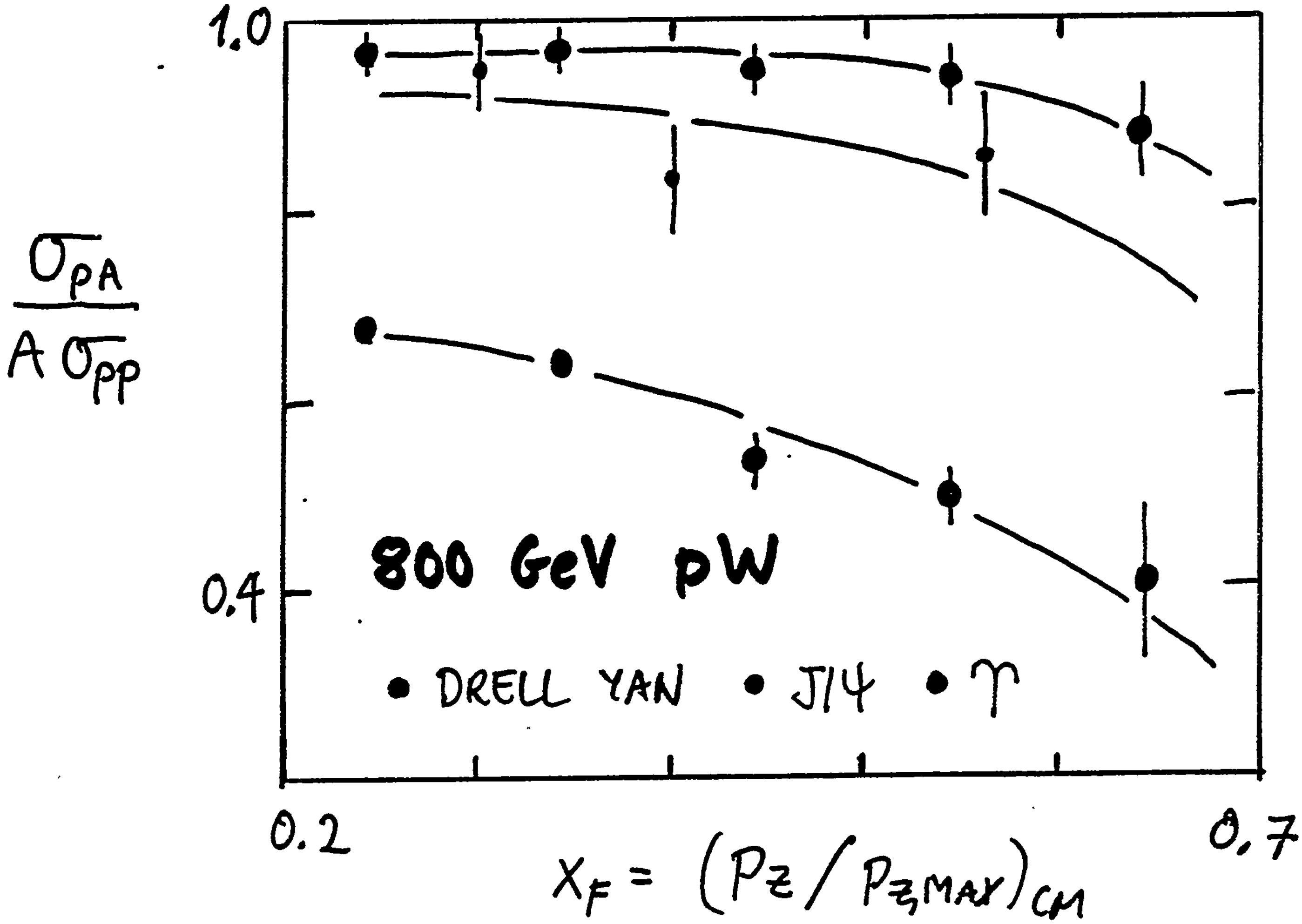

IS THIS ENERGY LOSS ? Milane & S.G.

SHADOWING ?

OR WHAT ?!!

DEPLETION FROM ENERGY LOSS

PROJECTILE PARTON'S MOMENTUM FRACTION x_0 **REDUCED** BY **INITIAL STATE INTERACTIONS** S.G. & J. MILANA

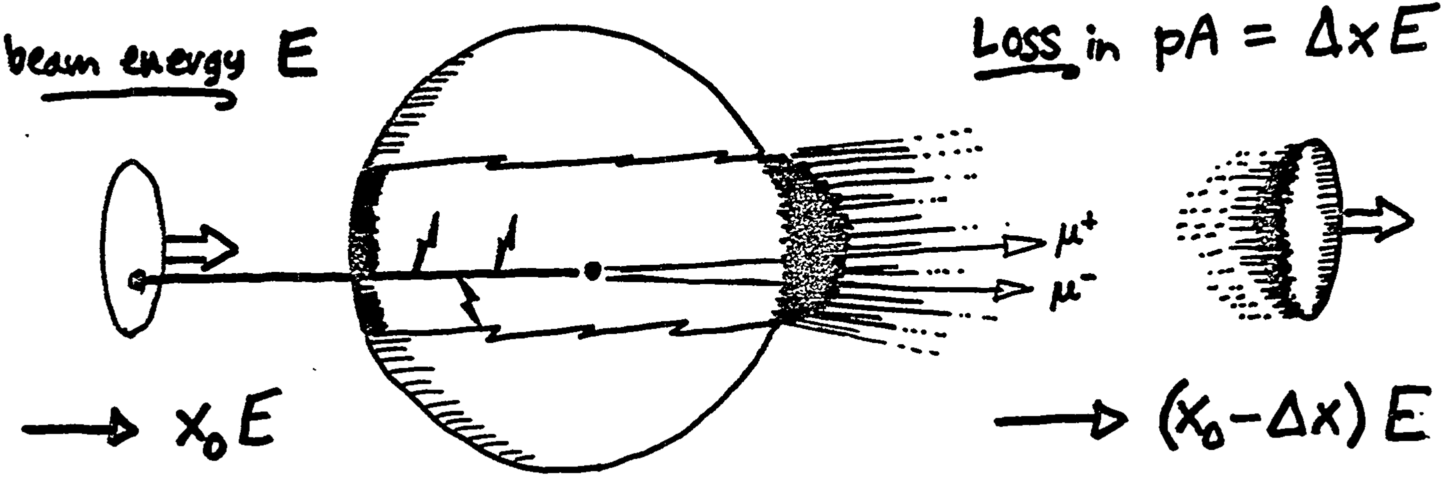

SMALL LOSS near $x_F = 1 \Rightarrow$ **BIG DEPLETION**

$$\frac{\sigma_{pA \to \mu^+\mu^-}}{A\, \sigma_{pp \to \mu^+\mu^-}} \sim \frac{q(x+\Delta x)}{q(x)} \sim \left(1 - \frac{\Delta x}{1-x}\right)^3 \xrightarrow[x \to 1]{} 0$$

- NEED HIGHER $X_0 = X + \Delta X$ in pA FOR FIXED FINAL X
- E772 FIT FOR $\Delta x \sim 0.012$

WORKS IF $dE/dz \sim E\,\Delta x/L \sim 1.5$ GeV/fm **REASONABL**

INITIAL + FINAL STATE OCTET ENERGY LOSS
CONSISTENT WITH ψ, ψ' & Υ DATA

$\Delta x / x \sim \kappa\, C_i\, Q^{-2} A^{1/3}$ **MAGIC FORMULA**

ENERGY LOSS CONFUSION!

- WHERE'S THE EFFECT IN eA ?

- Busza: **UNIVERSAL** EFFECT FOR ALL HADRONS
  -- HOW DOES THIS FIT IN ?

- CAN WE UNDERSTAND ΔE **THEORETICALLY** ?
  Paigné et Al.
  THIS YEAR'S : $\Delta E \propto \langle p_T^2 \rangle L \propto A^{2/3}$

  - x_F SHIFT EMPIRICALLY $\propto A^{1/3}$
  - x_F SHIFT **SMALLER** FOR Υ (vs. J/ψ)
    CONTRADICTS $\langle p_T^2 \rangle_\Upsilon > \langle p_T^2 \rangle_\psi$

- **IF WE KNEW GLUON SHADOWING, COULD DISENTANGLE COMPETING EFFECTS**

WHAT CAN WE LEARN FROM HERA?

COLLIDER MODE:

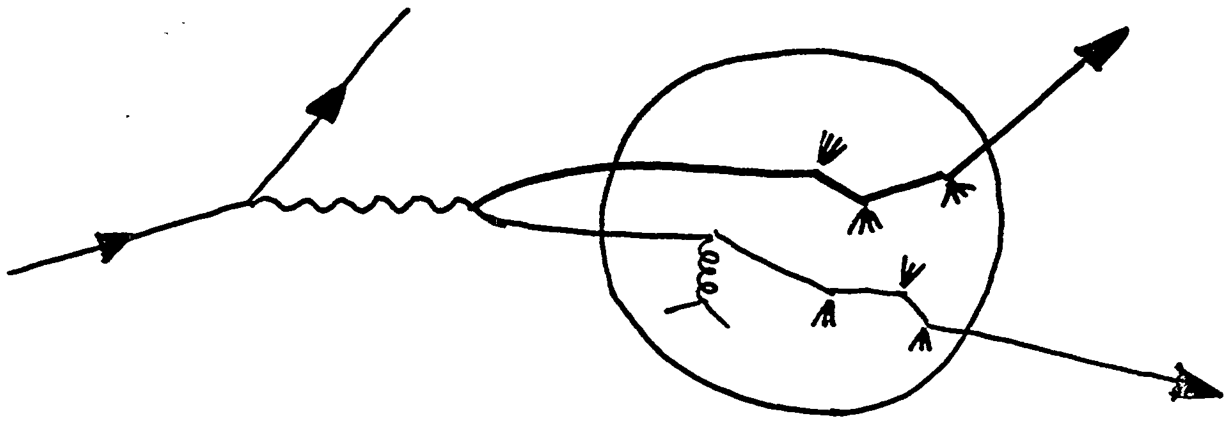

PARTON DISTRIBUTIONS IN NUCLEI AT WEE X

$$27.6 \text{ GeV } e \quad + \quad 820 \times \frac{Z}{A} \sim 410 \text{ GeV} \begin{cases} \text{H} \\ \text{C} \\ \text{S} \end{cases}$$

$x \sim 10^{-3}$ DOWN TO 5×10^{-5}

- SMALL x INTERESTING! SATURATION REGION
- RELEVANT TO MINIJETS AT LHC

RHIC $\quad x = \frac{2p_T}{\sqrt{s}} = \frac{2\,(1\,\text{GeV})}{200\,\text{GeV}} \sim 10^{-2} \quad$ at $y = 0$

LHC $\quad x = \frac{2\,(1\,\text{GeV})}{5.600\,\text{GeV}} \sim 3 \times 10^{-4}$

SATURATION: SCATTERING OF A NUCLEAR DISK

$$\frac{\sigma_{\gamma A}}{A\,\sigma_{\gamma p}} \sim \frac{A^{2/3}}{A} \sim A^{-1/3}$$

JETS **EASY** TO MEASURE IN COLLIDER (Ritz)

ACOPLANARITY → MULTIPLE SCATTERING

$$\Delta k_T^{\,2} \propto A^{1/3}$$

LEADING PARTICLE DEPENDENCE ? $\pi, \bar{p}$

ENERGY LOSS ? IN COLLIDER ?!

NEED SHIFT $\nu + \underbrace{\Delta\nu}_{\text{LOSS}}$ COMPARABLE TO ν

$\Delta\nu \sim 10$ GeV TOO SMALL UNLESS

NEAR KINEMATIC LIMIT : $\mathcal{D} \sim (1-z)^N$; $z = \frac{E_h}{\nu}$

$$\frac{\mathcal{D}_A}{A\mathcal{D}_N} \sim \frac{(1-(z+\Delta z))^N}{(1-z)^N} \sim 1 - N\underbrace{\frac{\Delta z}{1-z}}_{\text{BIG AS } z \to 1}$$